

ISSN 0386-5878  
Technical Report  
of PWRI No.4172

**PROCEEDINGS OF  
THE 25<sup>th</sup> U.S. – JAPAN  
BRIGDE ENGINEERING WORKSHOP**

Tsukuba, Japan  
October 19, 20 and 21, 2009

CENTER FOR ADVANCED ENGINEERING STRUCTURAL ASSESSMENT AND RESEARCH  
PUBLIC WORKS RESEARCH INSTITUTE  
Incorporated Administrative Agency

1-6, Minamihara, Tsukuba-shi, Ibaraki-ken, 305-8516 Japan

Opinions, findings, conclusions and recommendations expressed in the papers contained in this publication are those of the author(s).

Copyright © (2010) by P.W.R.I.

All rights reserved. No part of this book may be reproduced by any means, nor transmitted, nor translated into a machine language without the written permission of the Chief Executive of P.W.R.I.

この報告書は、独立行政法人土木研究所理事長の承認を得て刊行したものである。したがって、本報告書の全部又は一部の転載、複製は、独立行政法人土木研究所理事長の文書による承認を得ずしてこれを行ってはならない。

# PROCEEDINGS OF THE 25<sup>th</sup> U.S. – JAPAN BRIGDE ENGINEERING WORKSHOP

By

Editor: Masahiro Shirato

**Synopsis:**

The proceeding documents the results of the 25<sup>th</sup> U.S. – Japan Bridge Engineering Workshop which was held at Tsukuba, Japan, on October 19, 20, and 21, 2009, as a part of the activities of the Panel on Wind and Seismic Effects, UJNR. The Workshop was organized by Task Committee G “Transportation System” (U.S. side chair: Dr. W. Philip Yen, FHWA, Japan side chair: Mr. Atsushi Yoshioka, CAESAR, PWRI) of the Panel.

**Key Words: Bridge, Design, Construction, Maintenance, Seismic, UJNR**

Page Left Blank

## PREFACE

The 25<sup>th</sup> US-Japan Bridge Engineering Workshop is a continuation of a series of technical interchanges between the United States and Japan on all topics related to bridge engineering. This series of workshops has been conducted under the auspices of Task Committee “G” of the US-Japan Panel on Wind and Seismic Effects, which is one of the 18 panels making up the United States-Japan Cooperative Program in Natural Resources (UJNR). The previous workshops are indicated below.

1 <sup>st</sup>	February 20-23, 1984	Tsukuba Science City, <i>Japan</i>
2 <sup>nd</sup>	August 19-20, 1985	San Francisco, California, <i>United States</i>
3 <sup>rd</sup>	May 8-9, 1987	Tsukuba Science City, <i>Japan</i>
4 <sup>th</sup>	May 11-12, 1988	San Diego, California, <i>United States</i>
5 <sup>th</sup>	May 9-10, 1989	Tsukuba Science City, <i>Japan</i>
6 <sup>th</sup>	May 7-8, 1990	Lake Tahoe, Nevada, <i>United States</i>
7 <sup>th</sup>	May 8-9, 1991	Tsukuba Science City, <i>Japan</i>
8 <sup>th</sup>	May 11-12, 1992	Chicago, Illinois, <i>United States</i>
9 <sup>th</sup>	May 10-11, 1993	Tsukuba Science City, <i>Japan</i>
10 <sup>th</sup>	May 10-11, 1994	Lake Tahoe, Nevada, <i>United States</i>
11 <sup>th</sup>	May 30-31, 1995	Tsukuba Science City, <i>Japan</i>
12 <sup>th</sup>	October 29-30, 1996	Buffalo, New York, <i>United States</i>
13 <sup>th</sup>	October 2-3, 1997	Tsukuba Science City, <i>Japan</i>
14 <sup>th</sup>	November 3-4, 1998	Pittsburgh, Pennsylvania, <i>United States</i>
15 <sup>th</sup>	November 9-10, 1999	Tsukuba Science City, <i>Japan</i>
16 <sup>th</sup>	October 2-4, 2000	South Lake Tahoe, Nevada, <i>United States</i>
17 <sup>th</sup>	November 12-14, 2001	Tsukuba Science City, <i>Japan</i>
18 <sup>th</sup>	October 22-24, 2002	St. Louis, Missouri, <i>United States</i>
19 <sup>th</sup>	October 27-29, 2003	Tsukuba Science City, <i>Japan</i>
20 <sup>th</sup>	October 4-6, 2004	Washington, DC, <i>United States</i>
21 <sup>st</sup>	October 3-5, 2005	Tsukuba Science City, <i>Japan</i>
22 <sup>nd</sup>	October 23-25, 2006	Seattle, Washington, <i>United States</i>
23 <sup>rd</sup>	November 5-7, 2007	Tsukuba Science City, <i>Japan</i>
24 <sup>th</sup>	September 22-27, 2008	Minneapolis, Minnesota, <i>United States</i>
25 <sup>th</sup>	October 19-21, 2009	Tsukuba Science City, <i>Japan</i>

The steering committee for the 25<sup>th</sup> US-Japan Bridge Engineering Workshop consisted of Atsushi Yoshioka, Phillip Yen, David Sanders, and Masahiro Shirato.

The workshop was held at the NILIM and the CAESAR, PWRI, in Tsukuba, Japan. The 2-1/2 day workshop focused on: 1) Earthquake Case Histories, 2) Inspection and Management, 3) Accelerated Bridge Construction, 4) Remedial Work & Partial Replacement, 5) Maintenance 6) Seismic Performance Evaluation, and 7) Seismic Retrofit. Thirteen participants from the US and twenty-eight participants from Japan attended the workshop who were arranged by both T/C chairs in terms of the focused themes. The papers contained within this proceeding are the papers that were presented at the workshop (17 papers from the Japan side and 12 papers from the US side).

In addition to the workshop, there was a bridge study held after the workshop, October 22-23, 2009, visiting bridge sites:

- Accelerated bridge construction, Ton-ya machi viaduct
- Seismic Retrofit, Tsuboyama viaduct and Miwatari bridge
- Construction of integral abutment jointless bridge, Okegawa Bridge
- Construction site of corrugated-steel web prestressed concrete bridge, Ura Takao Bridge
- Construction site of narrow-two-box-girder bridge, Minami Asakawa Bridge,
- Maintenance for Kisogawa Oh-hashii Bridge

in the Kanto and Chubu regions.

Editor: Masahiro Shirato, PhD, Senior Researcher, Bridges and Structures Research Group, Center for Advanced Engineering Structural Assessment and Research (CAESAR), Public Works Research Institute (PWRI)

**TABLE OF CONTENTS**  
**25<sup>th</sup> US-Japan Bridge Engineering Workshop**  
**Tsukuba, Ibaragi October 19 to 21, 2009**

**PREFACE**

**TABLE OF CONTENTS**

**WORKSHOP PROGRAM .....1**

**SESSION 1: Earthquake Case Histories .....9**

**1-1** Seismic Performance Evaluation of Seismic Retrofitted Steel Arch Bridge That Affected by 2007 Niigata-ken Chuetsu-oki Earthquake ..... 11  
By Junichi Sakai and Shigeki Unjoh

**1-2** Analyses of Damaged Bridge by Ground Displacement During Niigata-ken Chuetsu-oki Earthquake .....19  
By Takao Okada and Shigeki Unjoh

**1-3** Torsional Effects on Seismic Performance of Square vs. Circular RC Bridge Columns .....27  
By DJ Belarbi and S. Suriya Prakash

**1-4** Experimental Study on the Seismic Response of Bridge Columns Using E-Defense .....41  
By Kazuhiko Kawashima, Tomohiro Sasaki, and Koichi Kajiwara

**1-5** Evaluation of the Seismic Performance of Bridge Reinforced Concrete Columns Under Combined Actions Using Shake Table .....55  
By David Sanders and Juan G. Arias-Acosta

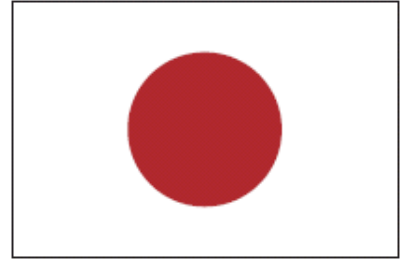
**SESSION 2: Inspection and Management .....65**

**2-1** Analysis of Periodic Inspection Results of Highway Bridges in Japan .....67  
By Koichi Ikuta, Takashi Tamakoshi, and Masanori Okubo

2-2	Bridge Inspection and Management in California	79
	By <u>Barton Newton</u>	
2-3	Measures for Strategic Preventive Bridge Management of Tokyo Metropolitan Government	87
	By <u>Taro Awamoto</u> and Sentaro Takagi	
2-4	Instrumentation and Monitoring of I35W St. > Anthony Falls Bridge	97
	By <u>Catherine French</u> , Carol Shield, Henryk Stolarski, Brock Hedegaard, and Ben Jilk	
2-5	Study for Bridge Renewal and Repair by Osaka Municipal Government	111
	By <u>Shinsuke Yumoto</u> , Tetsuya Yokota, and Yasutomo Komatsu	
<b>SESSION 3: Accelerated Bridge Construction</b>		<b>119</b>
3-1	Seismic Performance and Structural Details of Precast Segmental Concrete Bridge Columns	121
	By <u>Jun-ichi Hoshikuma</u> , Shigeki Unjoh, and Junichi Sakai	
3-2	Accelerated Constructions of the Viaducts on the Second Keihan Expressway	131
	By <u>Yoshihiko Taira</u> , Hirotsugu Mizuno, Kei Muroda, and Akio Kasuga	
3-3	New FHWA Seismic Hazard Mitigation Studies for Highway Bridges	141
	By <u>W. Phillip Yen</u>	
3-4	Overview of the Development Process and Effects of the UFO Method	147
	By <u>Yuji Mishima</u> , Yukio Katsuta, and Tomoaki Tsuji	
<b>SESSION 4: Remedial Work &amp; Partial Replacement</b>		<b>161</b>
4-1	Experimental Study on the Time Dependent Flexural Behavior of Prestressed Reinforced Concrete Beams	163
	By <u>Hiroshi Watanabe</u> , Hirohisa Koga, Hisashi Aoyama, and Yuuki Takeuchi	
4-2	Overnight Delivery - NJDOT Rapid Bridge Replacement	173
	By <u>X. Hannah Cheng</u> and Harry A. Capers, Jr	

<b>4-3</b>	Effect of Reducing Strains by SFRC Pavement on Ohira Viaduct . . . . .	185
	By <u>Takayoshi Kodama</u> , Mamoru Kagata, Shigeo Higashi, Kiyoshi Itoh, and Yatsuhiro Ichinose	
<b>4-4</b>	Rapid Bridge Repair / Rehabilitation in Washington State . . . . .	197
	By <u>Jugesh Kapur</u>	
<b>SESSION 5: Maintenance</b> . . . . .		<b>209</b>
<b>5-1</b>	Development of an Expansion Device for Cold Regions . . . . .	211
	By <u>Shinya Omote</u> , Hiroshi Mitamura, and Hiroaki Nishi	
<b>5-2</b>	Fatigue and Corrosion in Concrete Decks with Asphalt Surfacing . . . . .	219
	By <u>Yoshiki Tanaka</u> , Jun Murakoshi, and Yuko Nagaya	
<b>5-3</b>	Replacing The Suspender Ropes of a Tied Arch Bridge Using Suspension Bridge Methods . . . . .	233
	By <u>Barney T. Martin</u> and Blaise A. Blabac	
<b>5-4</b>	Suspension Bridge Cables: 200 Years of Empiricism, Analysis and Management . . . . .	247
	By <u>Bojidar Yanev</u>	
<b>SESSION 6: Seismic Performance Evaluation</b> . . . . .		<b>263</b>
<b>6-1</b>	Dynamic Response Analysis of Bridge Under Seismic Loading Including Collision . . . . .	265
	By <u>Eiki Yamaguchi</u> , Atsumi Ryuen, Keita Yamada, and Ryo Okamoto	
<b>6-2</b>	Effects of Near-Fault Vertical Accelerations on Highway Bridge Columns . . . . .	275
	By <u>Sashi Kunnath</u> and Huiling Zhao	
<b>6-3</b>	Seismic Design of Multi Span Continuous RIGID-FRAME Bridge with Prestressed Concrete Box Girder . . . . .	285
	By <u>Chiaki Nagao</u> , Yasushi Kamihigashi, Akio Kasuga, and Kenichi Nakatsumi	

<b>SESSION 7: Seismic Retrofit</b>	<b>295</b>
<b>7-1</b> Seismic Retrofit Study of CABLE-STAYED Bridge on TOKYO-GAIKAN EXPRESSWAY	297
By <u>Tsutomu Yoshioka</u> , Yoshinori Kawahira, and Kouichirou Shitou	
<b>7-2</b> Repair of High Shear Standard Reinforced Concrete Bridge Columns Using Cfrp	311
By <u>M. "Saïid" Saïidi</u> and Ashkan Vosooghi	
<b>7-3</b> Seismic Retrofit Techniques for Reinforced Concrete Bridge Columns with Combination of FRP Sheet and Steel Jacketing	321
By <u>Guangfeng Zhang</u> , Shigeki Unjoh, Jun-ichi Hoshikum, and Junichi Sakai	
<b>7-4</b> Development and Refinement of Illinois' Earthquake Resisting System Strategy	331
By <u>Daniel H. Tobias</u> , James M. LaFave, Chad E. Hodel, Larry A. Fahnestock, William M. Kramer, Joshua S. Steelman, Patrik D. Claussen, Kevin L. Riechers, and Mark D. Shaffer	
<b>RESOLUTIONS</b>	<b>345</b>
<b>APPENDIX 1 : JAPAN PARTICIPANTS</b>	<b>349</b>
Resume of Japan Participants	
<b>APPENDIX 2 : US PARTICIPANTS</b>	<b>357</b>
Resume of U.S. Participants	



**25<sup>th</sup> US-Japan  
Bridge Engineering Workshop  
Workshop Program**

Page Left Blank

# **25th U.S.-JAPAN BRIDGE ENGINEERING WORKSHOP**

## **PWRI, Tsukuba, Japan, October 19, 20 and 21, 2009**

---

### **October 19, Monday - Day 1 Workshop**

#### **Conference Hall**

#### **9:00 to 9:30 Opening Session**

**Moderators: Masahiro Shirato and David Sanders**

Welcome Remarks: Tadahiko Sakamoto (Chief Executive, PWRI)

Remarks: W. Phillip Yen (Chairman for the U.S.A Side)

Remarks: Atsushi Yoshioka (Chairman for the Japan Side)

#### **9:30 to 9:55 Quarter Century Anniversary Special Session 1**

**Moderator: Atsushi Yoshioka**

#### **Speaker:**

Koichi Yokoyama on behalf of the Japanese Delegation

#### **10:20 to 12:00 Session 1: Earthquake Case Histories**

**Moderators: Jun-ichi Hoshikuma and W. Phillip Yen**

Seismic Performance Evaluation of Seismic Retrofitted Steel Arch Bridge That Affected  
by 2007 Niigata-ken Chuetsu-oki Earthquake

By Junichi Sakai and Shigeki Unjoh

Analyses of Damaged Bridge by Ground Displacement During Niigata-ken Chuetsu-oki  
Earthquake

By Takao Okada and Shigeki Unjoh

Torsional Effects on Seismic Performance of Square vs. Circular RC Bridge Columns

By DJ Belarbi and S. Suriya Prakash

Experimental Study on the Seismic Response of Bridge Columns Using E-Defense

By Kazuhiko Kawashima, Tomohiro Sasaki, and Koichi Kajiwara

Evaluation of the Seismic Performance of Bridge Reinforced Concrete Columns Under  
Combined Actions Using Shake Table

By David Sanders and Juan G. Arias-Acosta

#### **12:00 to 12:20 Group Photograph at the Entrance of NILIM Main Building**

**13:20 to 14:50 Lab Tours in PWRI & NILIM**

1. Demolished Bridge Samples
2. Research on Seismic Engineering
3. Research on Maintenance

**15:10 to 16:50 Session 2: Inspection and Management**

**Moderators: Shoichi Nakatani and Bojidar Yanev**

Analysis of Periodic Inspection Results of Highway Bridges in Japan

By Koichi Ikuta, Takashi Tamakoshi, and Masanori Okubo

Bridge Inspection and Management in California

By Barton Newton

Measures for Strategic Preventive Bridge Management of Tokyo Metropolitan Government

By Taro Awamoto and Sentaro Takagi

Instrumentation and Monitoring of I35W St. > Anthony Falls Bridge

By Catherine French, Carol Shield, Henryk Stolarski, Brock Hedegaard,  
and Ben Jilk

Study for Bridge Renewal and Repair by Osaka Municipal Government

By Shinsuke Yumoto, Tetsuya Yokota, and Yasutomo Komatsu

## **October 20, Tuesday - Day 2 Workshop**

### **Conference Hall**

#### **9:00 to 10:20 Session 3: Accelerated Bridge Construction**

**Moderators: Jun Murakoshi and Jugesh Kapur**

Seismic Performance and Structural Details of Precast Segmental Concrete Bridge Columns

By Jun-ichi Hoshikuma, Shigeki Unjoh, and Junichi Sakai

Accelerated Constructions of the Viaducts on the Second Keihan Expressway

By Yoshihiko Taira, Hirotsugu Mizuno, Kei Muroda, and Akio Kasuga

New FHWA Seismic Hazard Mitigation Studies for Highway Bridges

By W. Phillip Yen

Overview of the Development Process and Effects of the UFO Method

By Yuji Mishima, Yukio Katsuta, and Tomoaki Tsuji

#### **10:40 to 12:00 Session 4: Remedial Work & Partial Replacement**

**Moderators: Taku Hanai and "Saiid" Saiidi**

Experimental Study on the Time Dependent Flexural Behavior of Prestressed  
Reinforced Concrete Beams

By Hiroshi Watanabe, Hirohisa Koga, Hisashi Aoyama, and Yuuki Takeuchi

Overnight Delivery - NJDOT Rapid Bridge Replacement

By X. Hannah Cheng and Harry A. Capers, Jr

Effect of Reducing Strains by SFRC Pavement on Ohira Viaduct

By Takayoshi Kodama, Mamoru Kagata, Shigeo Higashi, Kiyoshi Itoh, and  
Yatsuhiro Ichinose

Rapid Bridge Repair / Rehabilitation in Washington State

By Jugesh Kapur

#### **13:20 to 14:40 Breakout Session (Conference Hall)**

Group A Seismic Engineering

Moderators: Shigeki Unjoh and David Sanders

Group B Inspection, Evaluation, and Remedial Work (CAESAR Board  
Room)

Moderators: Masahiro Shirato and W. Phillip Yen

**15:00 to 16:20 Session 5: Maintenance**

**Moderators: Takashi Tamakoshi and Hannah Cheng**

Development of an Expansion Device for Cold Regions

By Shinya Omote, Hiroshi Mitamura, and Hiroaki Nishi

Fatigue and Corrosion in Concrete Decks with Asphalt Surfacing

By Yoshiki Tanaka, Jun Murakoshi, and Yuko Nagaya

Replacing The Suspender Ropes of a Tied Arch Bridge Using Suspension Bridge Methods

By Barney T. Martin and Blaise A. Blabac

Suspension Bridge Cables: 200 Years of Empiricism, Analysis and Management

By Bojidar Yanev

**October 21, Tuesday - Day 3 Workshop  
Conference Hall**

**9:00 to 9:25 Quarter Century Anniversary Special Session 2**

**Moderator: W. Phillip Yen**

**Speaker:**

Manos Maragakis on behalf of the US Delegation

**9:25 to 10:25 Session 6: Seismic Performance Evaluation**

**Moderators: Junichi Sakai and Barney T. Martin**

Dynamic Response Analysis of Bridge Under Seismic Loading Including collision

By Eiki Yamaguchi, Atsumi Ryuen, Keita Yamada, and Ryo Okamoto

Effects of Near-Fault Vertical Accelerations on Highway Bridge Columns

By Sashi Kunnath and Huiling Zhao

Seismic Design of Multi Span Continuous RIGID-FRAME Bridge with Prestressed  
Concrete Box Girder

By Chiaki Nagao, Yasushi Kamihigashi, Akio Kasuga, and Kenichi Nakatsumi

**10:45to 12:05 Session 7: Seismic Retrofit**

**Moderators: Yoshiki Tanaka and Catherine French**

Seismic Retrofit Study of CABLE-STAYED Bridge on TOKYO-GAIKAN EXPRESSWAY

By Tsutomu Yoshioka, Yoshinori Kawahira, and Kouichirou Shitou

Repair of High Shear Standard Reinforced Concrete Bridge Columns Using Cfrp

By M. "Saiid" Saiidi and Ashkan Vosooghi

Seismic Retrofit Techniques for Reinforced Concrete Bridge Columns with Combination of  
FRP Sheet and Steel Jacketing

By Guangfeng Zhang, Shigeki Unjoh, Jun-ichi Hoshikum, and Junichi Sakai

Development and Refinement of Illinois' Earthquake Resisting System Strategy

By Daniel H. Tobias, Jerome F. Hajjar, Ralph E. Anderson,

James M. LaFave, Chad E. Hodel, Larry A. Fahnestock, William M. Kramer,

Joshua S. Steelman, Patrik D. Claussen, Kevin L. Riechers, and Mark D. Shaffer

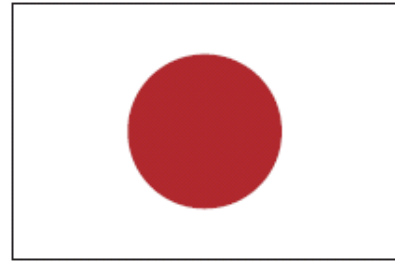
**12:10 to 12:30 Closing Session**

**Moderators: Masahiro Shirato and David Sanders**

Settlement of Resolution

Remarks: W. Phillip Yen (Chairman for the U.S.A Side)

Closing Remarks: Atsushi Yoshioka (Chairman for the Japan Side)



# **25<sup>th</sup> US-Japan Bridge Engineering Workshop**

## **Session 1**

### **Earthquake Case Histories**

Seismic Performance Evaluation of Seismic Retrofitted Steel Arch Bridge That Affected  
by 2007 Niigata-ken Chuetsu-oki Earthquake

By Junichi Sakai and Shigeki Unjoh

Analyses of Damaged Bridge by Ground Displacement During Niigata-ken Chuetsu-oki  
Earthquake

By Takao Okada and Shigeki Unjoh

Torsional Effects on Seismic Performance of Square vs. Circular RC Bridge Columns

By DJ Belarbi and S. Suriya Prakash

Experimental Study on the Seismic Response of Bridge Columns Using E-Defense

By Kazuhiko Kawashima, Tomohiro Sasaki, and Koichi Kajiwara

Evaluation of the Seismic Performance of Bridge Reinforced Concrete Columns Under  
Combined Actions Using Shake Table

By David Sanders and Juan G. Arias-Acosta

Page Left Blank

# **SEISMIC PERFORMANCE EVALUATION OF SEISMIC RETROFITTED STEEL ARCH BRIDGE THAT AFFECTED BY 2007 NIIGATA-KEN CHUETSU-OKI EARTHQUAKE**

Junichi Sakai<sup>1</sup> and Shigeki Unjoh<sup>2</sup>

## **Abstract**

A supported deck steel arch bridge that had been retrofitted after the 1995 Hyogo-Ken Nanbu, Japan, earthquake was affected by strong ground shaking during the 2007 Niigata-Ken Chuetsu-Okii, Japan, earthquake. The bridge suffered minor damage by the earthquake and no structural damage of the main members was observed. To evaluate the seismic response during the earthquake and the effect of seismic retrofit, a series of dynamic analyses was conducted. The results underscored the strengthening of the arch springing by the seismic retrofit worked to prevent the serious damage.

## **Introduction**

The Niigata-Ken Chuetsu-Okii (Chuetsu offshore), Japan, earthquake occurred on July 16th, 2007 in the northwest Niigata region. The JMA magnitude was 6.8, and the moment magnitude was 6.6. The VI upper of the JMA intensity was observed in the Niigata and Nagano prefectures. The nuclear power plant was affected by the earthquake and some severe damage due to land slide was reported (NILIM, PWRI and BRI, 2008). There was no report of severely damaged bridges by the earthquake. Some damage of bearings and settlement of ground at bridge approaches, which were often observed in the past earthquakes, were reported. Additionally, movement of abutment, which was constructed on soft soil, was also reported (Okada and Unjoh, 2009).

Among the bridges that were affected by the earthquake, some bridges had already been retrofitted and no severe damage was observed (Unjoh et al., 2008). Although no instrumentation was provided to the bridges, it would be good examples to evaluate the effect of seismic retrofit of bridges.

In this research, a series of dynamic analyses was conducted for a steel arch bridge that had been retrofitted to evaluate the seismic response of a seismically retrofitted bridge and the effect of the seismic retrofit.

## **Bridge Analyzed and Damage Due to Earthquake**

Photo 1 and Figure 1 show the bridge analyzed. This is a supported deck steel arch bridge. The bridge was constructed in 1965, and the design lateral seismic

---

<sup>1</sup> Senior Researcher, Bridge and Structural Technology Research Group, Center for Advanced Engineering Structural Assessment and Research, PWRI, Japan

<sup>2</sup> Research Coordinator for Earthquake Disaster Prevention, Research Center for Disaster Risk Management, NILIM, Japan

coefficient of 0.2 was used in the original design. The bridge carries two lanes of traffic and the width is 7.5 m. The total length of the bridge, including approaches, is 197 m. The main span is 120 m and the arch rise is 23m. Two single gerber spans are used for the approaches.



**Photo 1 Bridge analyzed**

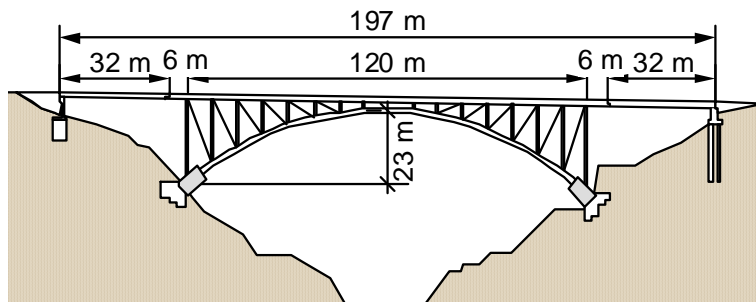


**Figure 1 Bridge analyzed**

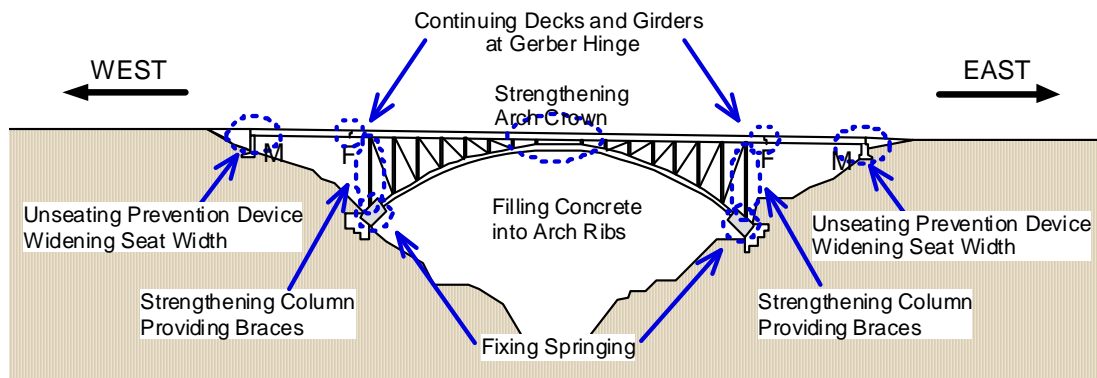


**Figure 2 Seismic retrofit**

The abutments are gravity type and wall type, and the spread foundations and pile foundation are used. Two pinned bearings were used to support the main span. The arch rib is the box type cross section with 1.5 m - height and 0.75 m- width, and the

thickness of the steel plate of the ribs for the crown region is 19mm for upper and lower plates and 10 mm for side plates, and that for the springing region is 25 mm for upper and lower plates and 10 mm for side plates.

The seismic retrofit work was conducted in 2000 and 2001 considering the Level 2 ground motion. Behavior after yielding of the steel members was considered in the retrofit design. As shown in Figure 2, the items listed below were conducted as the seismic retrofit:

1. Fixing the pinned bearings at the both springings,
2. Filling the light-weight concrete into the arch rib,
3. Fixing the gerber bearings to have the bridge continuous,
4. Strengthening the arch crown,
5. Strengthening the bottom of the end columns,
6. Placing the braces for the end columns, and
7. Providing the unseating prevention devices.

The damage investigation reported that evidences of the pounding between the girder and the abutment were observed at the deck end. It was reported that buckling occurred at the gusset plates of lateral beams of the arch rib, but no severe damage of the main structural members was found (Unjoh, et al. 2008).

### **Analytical Model and Conditions**

To simulate the seismic response during the 2007 Niigata-Ken Chuetsu-Oki earthquake and to evaluate the effects of the seismic retrofit to the bridges, a series of dynamic analyses was conducted for two models; one is a model for as-built bridge (As-built model), and the other is a model for the retrofitted bridge (Retrofitted model).

Although premature buckling of arch ribs was estimated to occur for the as-built bridge, nonlinear behavior after buckling was not considered in the analyses. Thus, the members of the arch rib were idealized as elastic beam elements. Other structural members were also modeled as elastic elements.

Since buckling of the members of the arch ribs were not expected but the yielding of the members were expected for the Retrofitted model, nonlinear behavior was idealized by nonlinear beam elements with the bilinear hysteretic model. The effect of variation of axial force to the arch ribs was not considered, and the effect of the axial force due to gravity load was only included in the analyses. Nonlinear behavior of the members of the main girder and supporting columns were also considered.

Table 1 compares the allowable bending moments of members at the arch springing and the arch crown. The buckling moment is shown for the allowable moment for the As-built model, and the yielding moment is shown for the Retrofitted model. The buckling moments at the crown were 5860 kNm and 2382 kNm for the longitudinal and transverse directions, respectively for the As-built model, and the

allowable moment increased to 11508 kNm and 6137 kNm for the Retrofitted model because of the infilled concrete.

Table 2 summarizes the results from the eigen-value analyses, and Figure 3 shows the mode shapes for the dominant modes for the longitudinal and transverse directions. The deformation in the transverse direction is dominant in the 1st mode. The natural period of the 1st mode for the As-built model is 1.6 seconds, and it decreases to 1.16 seconds due to increment of the stiffness of the arch rib due to infilled concrete.

**Table 1 Moment capacity of arch rib (kNm)**

	Arch Crown		Springing	
	LG	TR	LG	TR
As-Built	5860	2382	6661	2229
Retrofitted	11508	6137	14836	7148

**Table 2 Results from eigen-value analyses**

Mode	As-built			Retrofitted		
	Natural Period (sec)	Effective Mass Ratio (%)		Natural Period (sec)	Effective Mass ratio	
		LG	TR		LG	TR
1	1.596	0	79.4	1.159	0	66.2
2	0.839	0	0	0.757	51.6	0
3	0.780	54.9	0	0.575	0	0
4	0.479	0	4.8	0.505	0	0
5	0.423	0	0	0.475	0	0

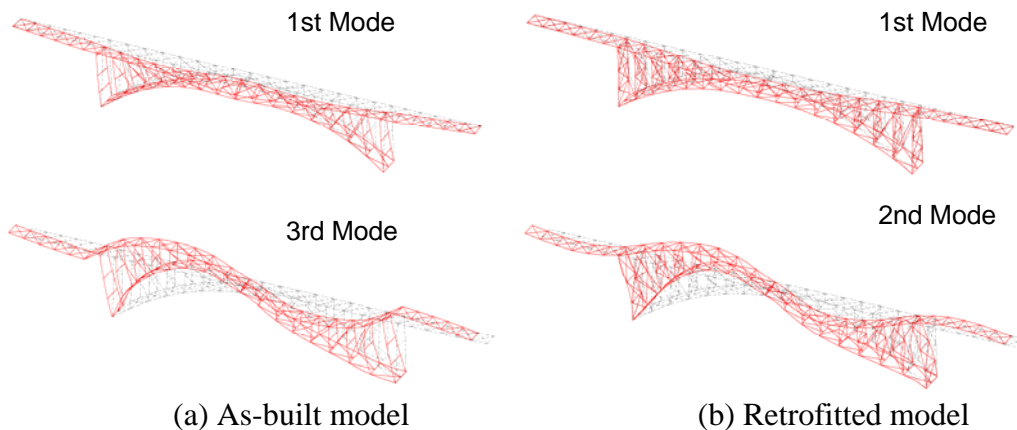


**Figure 3 Mode shapes**

For the dynamic analyses, records obtained near the bridge during the 2007 earthquake were used, and three dimensional analyses were conducted considering two horizontal and one vertical ground motions. The input ground motions and their response spectra are shown in Figure 4. The design spectra of Japanese design

specifications for highway bridges (Japan Road Association, 2002) are shown here for comparison. The peak ground accelerations are  $5.95 \text{ m/sec}^2$ ,  $5.61 \text{ m/sec}^2$  and  $4.52 \text{ m/sec}^2$ , respectively. The horizontal records have peaks over  $20 \text{ m/sec}^2$  at around 0.25 seconds in natural period, which is larger than the design spectra, while the spectra between 0.5 seconds and 1 second in natural periods are smaller than the design spectra. The spectrum of the transverse direction has similar or even larger intensity than the design spectra around the natural period of the 1st mode while that of the longitudinal direction has smaller intensity.

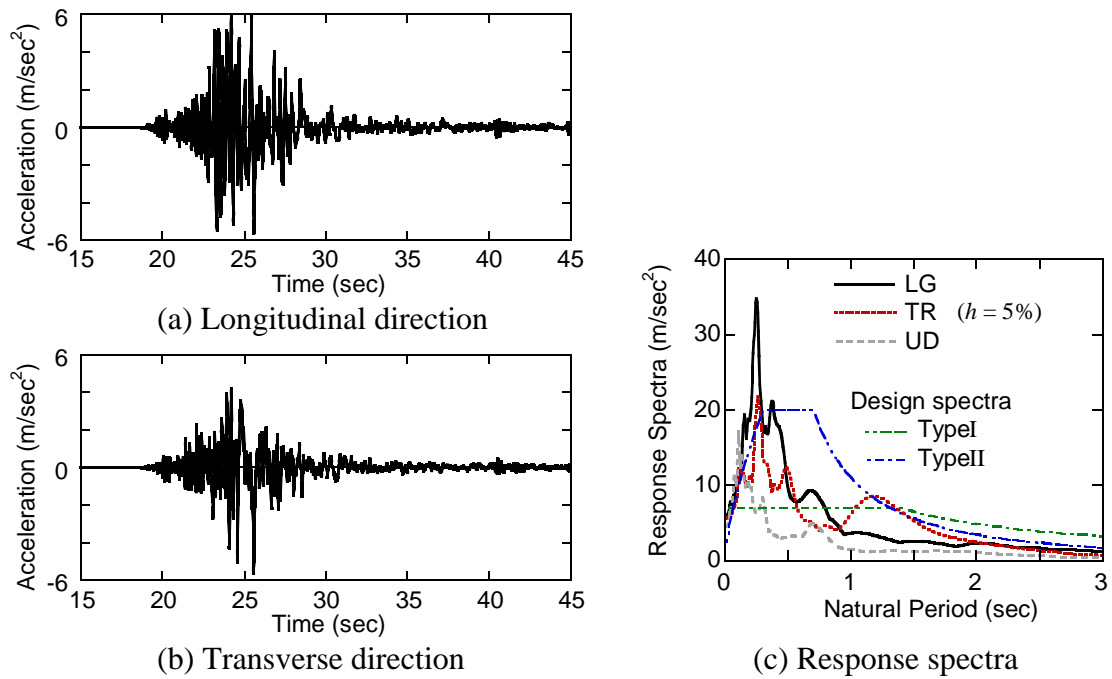


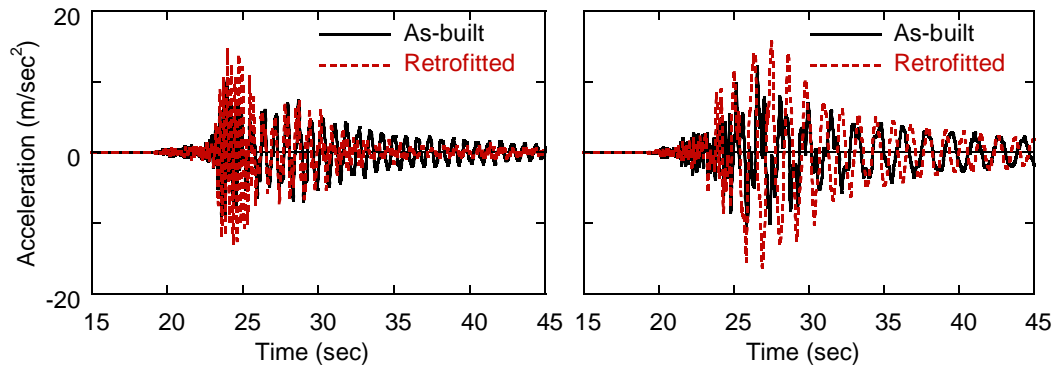
**Figure 4 Input Ground Motions**

### Evaluation of Effects of Seismic Retrofit

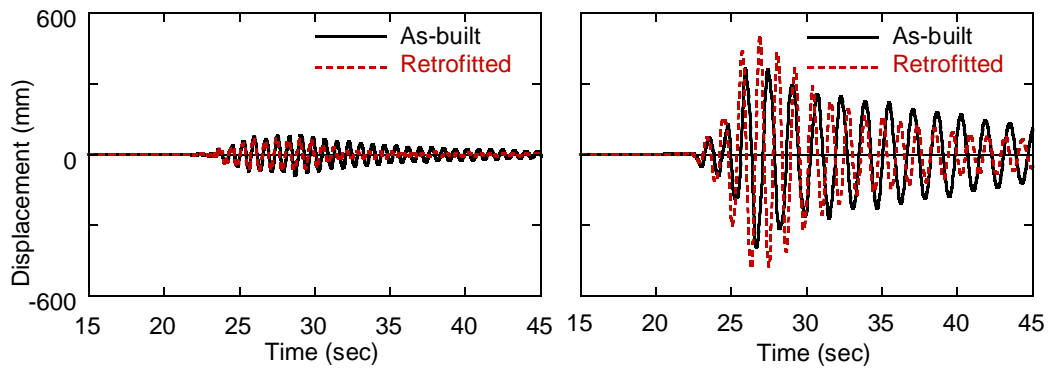
**Figure 5** compares the response acceleration and displacement time histories at the arch crown between the As-built model and the Retrofitted model. **Figure 6** shows the deformation mode when the maximum response occurred for each direction. Based on the results for the Retrofitted model, the lateral displacements over 70 mm and 500 mm are estimated to occur in the longitudinal and transverse directions, respectively, during the 2007 earthquake. Response acceleration increases by about 30% due to strengthening of the bridge.

**Figure 7** compares the allowable moment and the response moment. The response moment is compared to the buckling moment for the As-built model, while that is compared to the yielding moment for the Retrofitted model. Based on the results for the Retrofitted model, large bending moment occurs at the arch springings and the crown, and the response bending moment at the crown is close to the yielding moment.

At the springings, the response moments are about 75% and 65% of the yielding moment for the longitudinal and transverse directions, respectively.



(a) Longitudinal direction (b) Transverse direction  
(1) Response acceleration

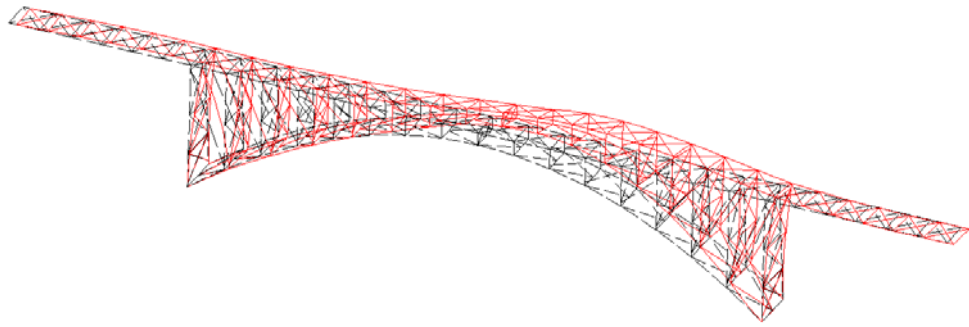


(a) Longitudinal direction (b) Transverse direction  
(2) Response displacement

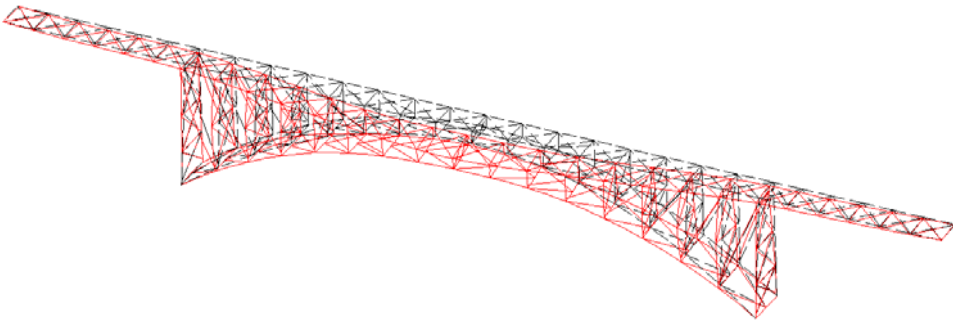
**Figure 5 Response of deck at arch crown**

For the As-built model, response bending moment exceeds by 40% the buckling moment at the arch crown. The response force at the bearings of the arch springings are estimated to be about 10 times larger than the horizontal and vertical capacity of the bearings, and thus it is estimated that the bearings suffer serious damage.

Based on the analytical results, the bearings of the arch springings could suffer serious damage, which affects the structural stability of the arch bridge. The arch rib could also suffer some damage at the arch crown. The responses for the Retrofitted model do not exceed the elastic limit states, and this matches observed damage.



(a) Maximum response displacement in longitudinal direction (= 27.46 seconds)



(b) Maximum response displacement in transverse direction (= 26.89 seconds)

**Figure 6 Deformation modes of retrofitted model**

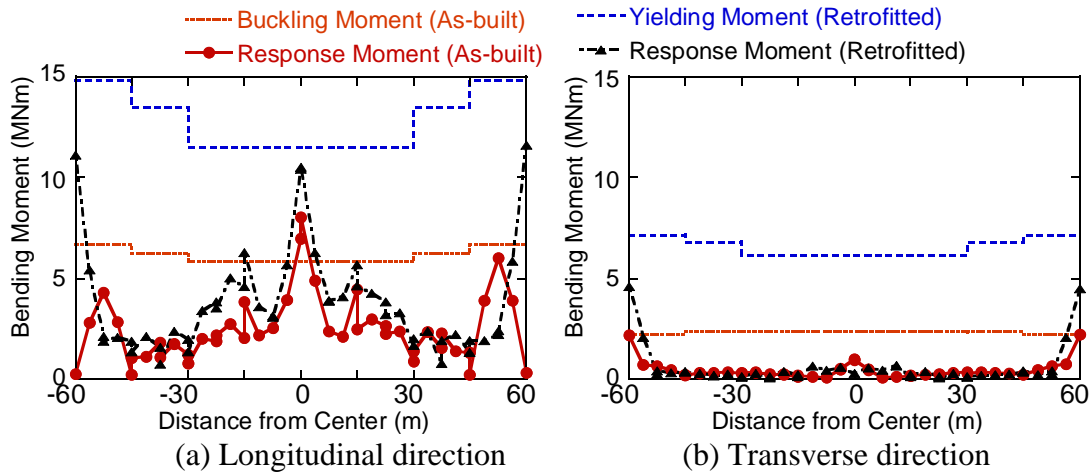


**Figure 7 Maximum response moment at arch rib**

## Conclusions

A series of dynamic analyses was conducted for a steel arch bridge that had been retrofitted to evaluate the seismic response of a seismically retrofitted arch bridge and the effect of the seismic retrofit. Below are the conclusions determined from the study:

1. The lateral displacements over 70 mm and 500 mm are estimated to occur in

longitudinal and transverse directions, respectively, during the 2007 earthquake.

2. The response bending moment at the crown is close to the yielding moment. At the springings, the response moments are about 75% and 65% of the yielding moment for longitudinal and transverse directions, respectively. The responses for the retrofitted bridge do not exceed the elastic limit states, and this matches observed damage.
3. Without the seismic retrofit, the response bending moment exceeds the buckling moment at the arch crown, and the response force at the bearings of the arch springings are estimated to be about 10 times larger than the horizontal and vertical capacity of the bearings. The analyses underscored that the bearings could suffer serious damage, which affects the structural stability of the arch bridge.

### **Acknowledgments**

The authors would like to acknowledge the Hokuriku Regional Development Bureau and the Nagaoka National Highway Office, MILT, for providing the documents and materials on the bridge analyzed. The authors also appreciate the Research Center for Disaster Risk Management, NILIM, for providing the ground motion records.

### **References**

- Japan Road Association (2002). *Specifications for highway bridges. Part V Seismic design*, Japan.
- NILIM, PWRI and BRI (2008). "Report on damage to infrastructures and buildings by the 2007 Niigata-ken Chuetsu-oki earthquake." *Technical Note of PWRI*, No. 4086. (in Japanese)
- Okada, T. and Unjoh, S. (2009). "Analyses of damaged bridge by ground displacement during Niigata-ken Chuetsu-oki earthquake." *Proc. of 25th US-Japan Bridge Engineering Workshop*, Tsukuba, Japan.
- Unjoh, S., Sugimoto, T., Sakai, J. and Okada, T. (2008). "Damage of bridge structures during recent earthquakes and the effectiveness of seismic retrofit." *Proc. of 40th Joint Meeting US-Japan Panel on Wind and Seismic Effects UJNR*, Gaithersburg, USA.

# ANALYSES OF DAMAGED BRIDGE BY GROUND DISPLACEMENT DURING NIIGATA-KEN CHUETSU-OKI EARTHQUAKE

Takao Okada<sup>1</sup> and Shigeki Unjoh<sup>2</sup>

## Abstract

A 3-span continuous girder bridge supported by rubber bearings to disperse seismic lateral forces was affected by 2007 Niigata-ken Chuetsu-oki earthquake. The bridge pier columns and abutment walls were not damaged. However, all pier and abutment foundations moved with the ground displacement and some cracks were found at the pile heads of both abutments. This paper presents the preliminary damage analyses of the bridge to simulate the effect of the earthquake.

## Introduction

The Niigata-ken Chuetsu-oki earthquake occurred on July 16, 2007. The magnitude was 6.8 and the JMA intensity was VI upper. The depth was about 17km. The damage was serious and a number of houses were affected. Nuclear power plant was also affected by the earthquake. In the case of bridge structures, the similar damages were found with those caused by the past earthquakes including damage to bearing supports, parapet walls of abutments, and settlements of backfill soils behind the abutments. Some bridges supported by rubber bearings were affected during the earthquake. The damage of the bridges was not serious but unprecedented. The residual displacement was found at the rubber bearings because of the ground displacement resulting in the movement of substructures.

This paper presents the damage of the bridge and analyses to evaluate the effect of strong ground motion and ground displacement caused by this earthquake.

## Overview of the Bridge and the Damages

The bridge analyzed in this study is located as shown in **Fig. 1**. The bridge is about 20km away from the epicenter. The bridge was designed based on the Specifications for highway bridges (March 2002) and was constructed in 2005 to overpass the river as shown in **Fig. 2**. The bridge length is about 150m (47.6m +55m + 45.2m). The superstructure is 3-span continuous curved steel box girder. The substructures are RC columns with a wall type section and supported by the cast-in-place RC pile foundations. The ground consists mainly of soft silt and clay including thin sandy layers causing liquefaction. The ground type for seismic design is classified in TYPE III. The pile lengths are 55 ~ 70 m and the pile diameter is 1.5m. Bearings are rubber bearings to disperse seismic lateral forces in all direction. Two

---

<sup>1</sup> Researcher, Center for Advanced Engineering Structural Assessment and Research, PWRI

<sup>2</sup> Research Coordinator for Earthquake Disaster Prevention, Research Center for Disaster Risk Management, NILIM

bearings are settled on each pier and abutment. The stoppers are installed at both abutments in transverse direction to bridge axis. Formed cement soil structures were used behind both abutments to decrease the earth pressure to abutments. Box culvert structures are located behind the formed cement soil structures as shown in **Fig. 3**.

During the earthquake, the bridge columns and abutment walls were not damaged, but some movements of foundations of all piers and abutments were found as shown in **Fig. 4**. A2 abutment moved longitudinally by 45cm toward the river. A1 abutment moved transversely by 16cm. The superstructure rotated clockwise. **Fig. 5** shows the residual displacements observed at the rubber bearings. **Fig. 6** shows the joint gap closure between the superstructure and A2 abutment. A1 abutment, P1 column and P2 column settled by 3~4 cm. The backfill soils behind abutments settled by 25 ~ 40 cm as shown in **Fig. 3**. Some cracks at the pile heads of A1 and A2 abutment were found by core drilling investigation.

After the earthquake, the bridge was repaired and retrofitted seismically. The foundation of A2 abutment was retrofitted by adding the number of cast-in-place RC piles. The rubber bearing were restored by jacking up the superstructure and by pushing the superstructure horizontally. The parapet wall of A2 abutment was removed and reconstructed to restore the expansion joints and the design gap between the end of superstructure and abutment.

### **Dynamic Analysis**

Nonlinear dynamic analyses were performed to simulate the dynamic behavior during the earthquake and to figure out the effect of the inertia force caused by the strong ground motion. The analytical model used was a simple beam spring-mass system which was commonly used in the usual seismic design. The superstructure was modeled by the elastic beam elements. The rubber bearings on both abutments and columns were modeled by the linear spring elements. The columns were modeled by elastic beam elements and nonlinear spring elements for plastic hinges. The foundations of each substructure were modeled by the linear spring elements. Equivalent damping ratio used in the analysis was assumed as **Table 1**.

The acceleration strong motion records were obtained by the seismometer of Kashiwazaki interchange which was located nearby the bridge as shown in **Fig. 1**. The accelerations of three directions were used as input ground motion to perform the dynamic analyses. The records were observed in north-south direction and east-west direction. The input accelerations are transformed in the direction of the bridge axis and transverse of the bridge axis. **Fig. 7** shows the input accelerations and the acceleration spectra. The natural period of the bridge is 1.25 seconds. The value of the accelerations is slightly smaller than the standard acceleration for Type II earthquake design ground motion in the range of fundamental natural period of this bridge.

**Table 2** shows the comparison of the maximum value obtained through the analysis and the design allowable value of each structural member. The result shows that the piers are within the elastic range and the displacement of rubber bearings are

smaller than the design allowable displacement. The analysis estimated that the bridge was not damaged by the inertia force by the earthquake. Since no damage was found to the pier columns and abutment walls, the analytical result accords with the observed situation of the bridge.

### **Pushover Analysis to Simulate the Bridge Movement**

There is a possibility that the movement of foundations were caused by the soft soil and liquefaction-induced ground flow. Through the investigation, it was clarified the displacement of each substructure and residual displacement of rubber bearings as shown in **Fig. 4** and **Fig. 5**. To simulate the behavior of the bridge caused by the ground displacement, the pushover analysis considering the observed displacement of each substructure was performed.

The analytical model was the same with the dynamic analysis. The observed displacement of each substructure was input to each footing of substructures to simulate the bridge movement and the residual displacement of rubber bearings. **Fig. 8** and **Table 3** show the comparison of the analytical and the observed displacements. The bridge movement and the residual displacement of the rubber bearings are simulated well. The analytical results of directions of the A1 and P1 movement were slightly different from the observed ones. In this analytical model, the contact of the superstructure with parapets of abutments was not modeled. Therefore it might affect the difference. In fact, the superstructure contacted with both parapets and the superstructure was limited to move and turn around as shown in **Fig. 6**.

### **Conclusion**

This paper presented the preliminary analyses of the bridge behavior during the 2007 Niigata-ken chuetu-oki earthquake. The following conclusions may be deduced:

1. The damage was not serious but the residual displacements were found at substructures and rubber bearings which were caused by the ground displacement.
2. The dynamic analysis estimated that the bridge was not affected by the strong ground motion. The pushover analysis considering the observed displacement of each substructure simulated the bridge movement and the residual displacement of rubber bearings well.

In future study, it is needed to clarify the reason why the ground displacement occurred. Moreover, it is necessary to consider whether rigid or elastic bearing supports are better on the soft ground conditions including sandy layers causing liquefaction.

## Acknowledgments

The authors would like to acknowledge the Hokuriku Regional Development Bureau and the Nagaoka National Highway Office, MILT, for providing the documents and materials on the bridge analyzed. The authors also appreciate East Nippon Highway Company, for providing the ground motion records.

## References

Japan Road Association (2003). Specifications for highway bridges. Part V Seismic design, Japan.

Public Works Research Institute (2008). 'Report on Damage to Infrastructures and Buildings by the 2007 Niigata-ken Chuetsu-oki Earthquake' Technical Note of Public Works Research Institute, No4086, Japan

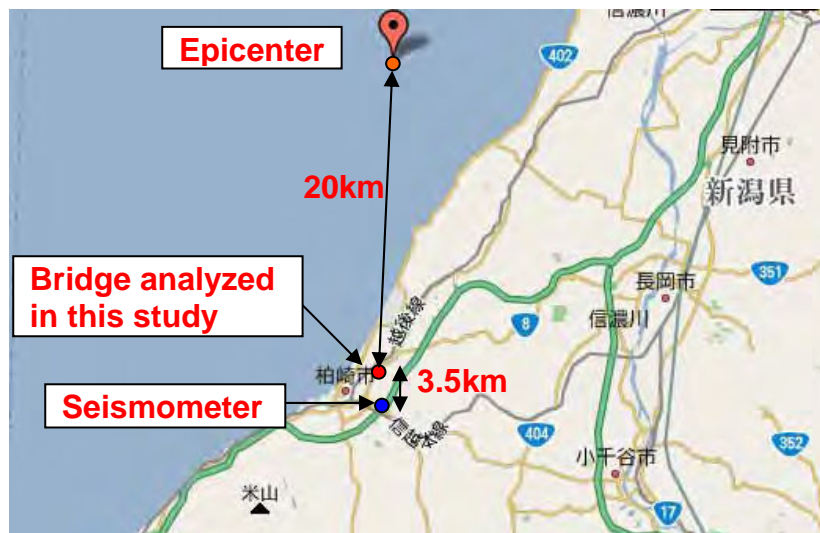


**Fig. 1** Location of the bridge analyzed



**Fig. 2** Overview of the bridge supported by rubber bearings

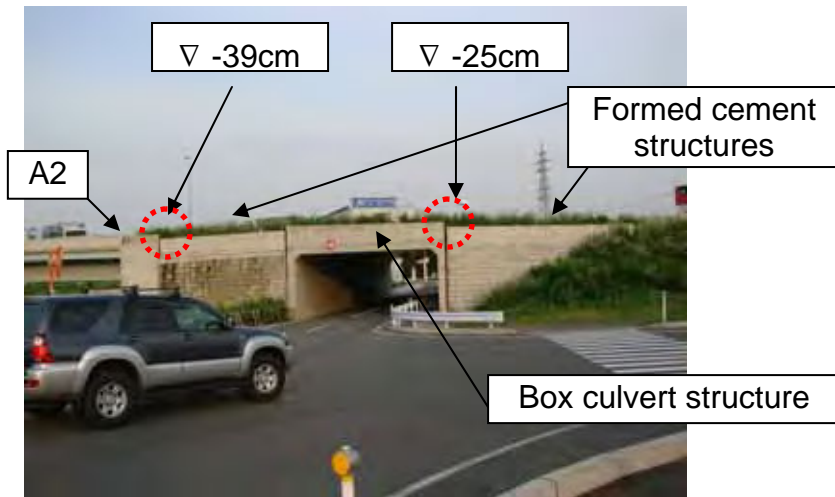


**Fig. 3** Box culvert structure nearby A2 abutment

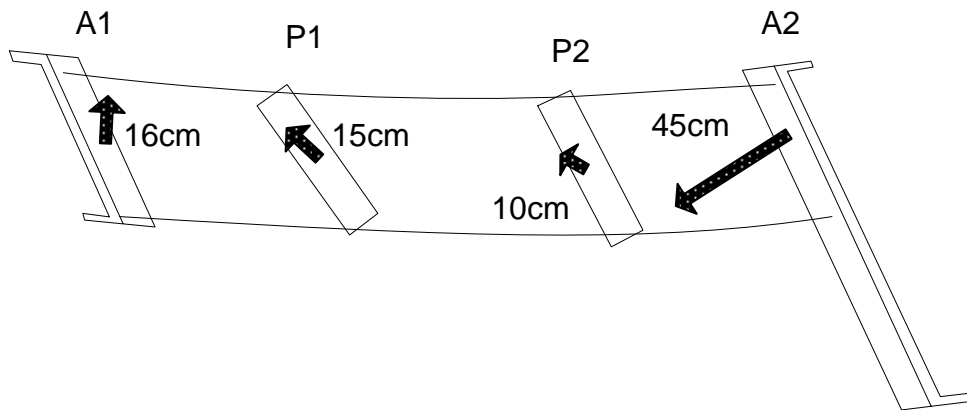


**Fig. 4** Horizontal movement of A1, P1, P2 and A2

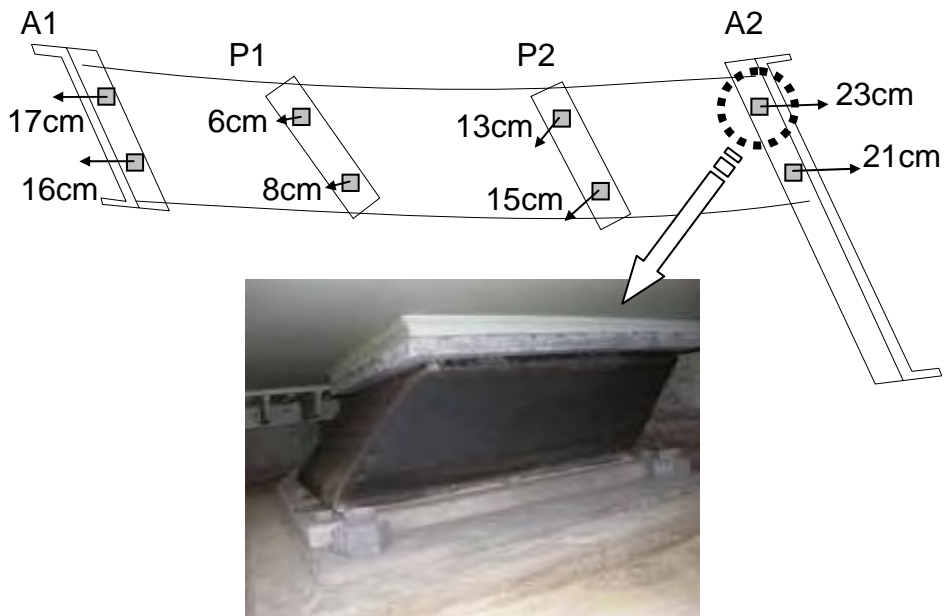


**Fig. 5** Residual displacement of rubber bearings



**Fig. 6 Clogging of expansion joint**

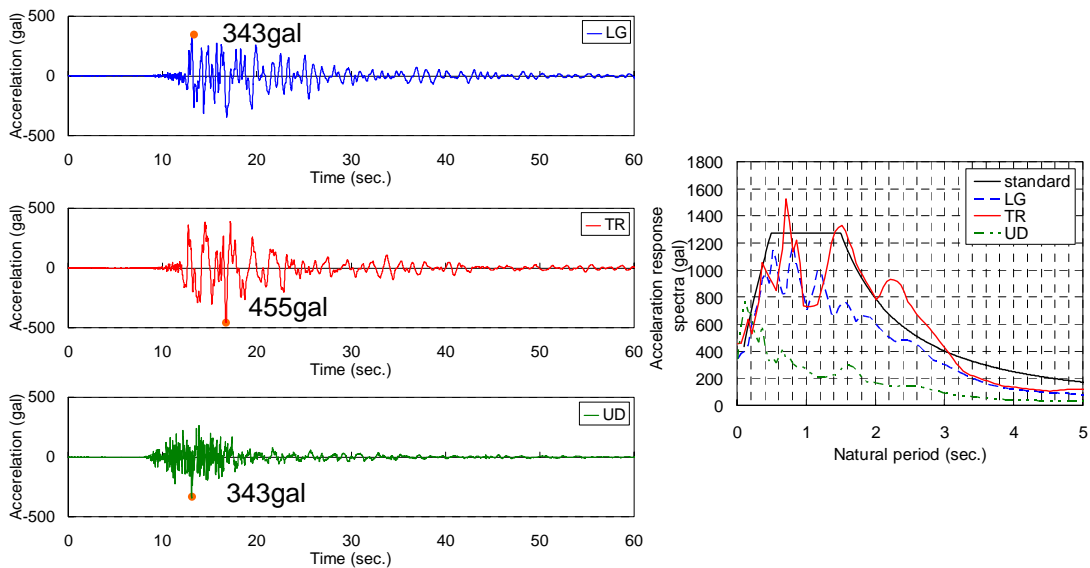


**Fig. 7 Input accelerations and acceleration response spectra**

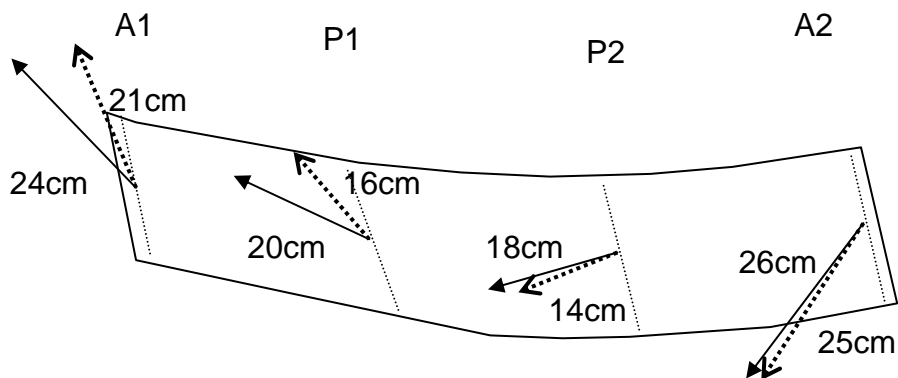


**Fig. 8 Comparison of displacement of superstructures**  
 Analysis : .....→      Observed data : ———→

**Table 1 Equivalent damping ratio for each structural element**

Structural members	Super-structure	RC (except plastic hinge)	Plastic hinge of P1 and P2	Rubber bearing	Foundation
Damping ratio	0.02	0.05	0.02	0.04	0.2

**Table 2 Result of dynamic analysis**

Rubber bearings			
Displacement		Analysis result (m)	Allowable value (m)
A1	longitudinal axis	0.28	0.58
	transverse axis	-	
P1	longitudinal axis	0.20	0.5
	Transverse axis	0.15	
P2	longitudinal axis	0.20	0.48
	transverse axis	0.17	
A2	longitudinal axis	0.30	0.51
	transverse axis	-	
Piers			
Ductility of plastic hinge		Analysis result	Allowable value ( $\mu$ a)
P1	longitudinal axis	0.81	4.3
	transverse axis	0.26	3.3
P2	longitudinal axis	0.84	4.2
	transverse axis	0.24	3.2
Shear stress		Analysis result (kN)	Allowable value (kN)
P1	longitudinal axis	7845	203044
	transverse axis	7854	27488
P2	longitudinal axis	8075	20344
	transverse axis	7137	27488

**Table 3 Comparison of the residual displacement of rubber bearings**

Residual displacement of rubber bearings		Analysis result (mm)		Observed value (mm)	
		G1	G2	G1	G2
A1	longitudinal axis	150	150	170	160
	transverse axis	-	-	0	0
P1	longitudinal axis	7	21	60	80
	Transverse axis	-5	-16	-10	-20
P2	longitudinal axis	11	36	80	110
	transverse axis	-64	-76	-100	-100
A2	longitudinal axis	-246	-247	-230	-210
	transverse axis	-	-	10	10

blank

# TORSIONAL EFFECTS ON SEISMIC PERFORMANCE OF SQUARE vs. CIRCULAR RC BRIDGE COLUMNS

A. Belarbi<sup>1</sup>, Q. Li<sup>2</sup>, and S. Suriya Prakash<sup>3</sup>

## Abstract

Reinforced concrete (RC) bridge columns could be subjected to combined flexural, axial, shear, and torsional loading during earthquake excitations. This combination of seismic loading can result in complex flexural and shear failure of bridge columns. Several researchers have investigated and proposed various models for predicting seismic performance; however, knowledge of the interaction between flexure, shear, and torsion in RC bridge columns is still limited. An experimental study is being conducted at Missouri S&T to understand the behavior of circular and square RC columns under combined loading including torsion. The main variable being considered is the ratio of torsion-to-bending moment (T/M). The differences in behavior between RC columns of square and circular cross section under combined loading are discussed in this paper. The main difference between the behavior of circular and square sections under combined loadings including torsion is related to confinement characteristics due to transverse reinforcement arrangement as well as warping effect in square cross sections due to torsion. In particular, the effect of cross-sectional shape on hysteretic torsional and flexural response, damage distribution, and ductility characteristics under combined flexure and torsional moments are discussed.

## Introduction

RC bridge columns can be subjected to multi-directional ground motions which result in the combination of axial force, shearing force, flexural and torsional moments. The addition of significant torsion is more likely in skewed or horizontally curved bridges, bridges with unequal spans or column heights, and bridges with outrigger bents. In addition, structural constraints due to a rigid decking, movement of joints, abutment restraints, and soil conditions also lead to combined loading effects. This combination of seismic loading can result in complex flexural and shear failure of bridge columns. Moreover, the cross-sectional details also affect the seismic behavior of RC bridge columns, such as damage distribution and ductility characteristics. The effect of cross section on the behavior of RC columns under combined loading including torsion is investigated. Test results of four square and four circular columns under cyclic flexure and shear, pure cyclic torsion, and combined cyclic flexure and shear and torsion are presented and discussed.

---

<sup>1</sup>Distinguished Professor, <sup>2,3</sup> PhD Candidate, Missouri University of Science & Technology, USA.

## **Previous Research**

Several experimental studies have been performed to investigate the behavior of columns under bending and shearing with and without axial compression. There are rational and accurate models available for analyzing the interaction between axial compression and flexure for columns. Park and Ang (1985), Priestly and Benzoni (1996), Priestly et al. (1998) and Lehman et al. (1998) have all investigated and proposed various models for predicting the seismic response under flexure. However, knowledge of the interaction between flexural and torsional moments in behavior of RC bridge columns is limited. Few researchers have investigated the effects of combined loading on the seismic performance of bridge columns. The effect of combined flexure and torsion with compression has also not been studied intensively, and most of the tests were focused on static monotonic loads. Otsuka et al. (2004) conducted cyclic loading tests on nine rectangular RC columns under pure torsion, flexure and shear and different ratios of combined flexural and torsional moments. The authors found that the hysteresis loop of torsion was significantly affected by the spacing of the transverse reinforcement. Tirasit and Kawashima (2005) tested reinforced concrete columns under combined cyclic flexure and torsion with three different rotation-to-drift ratios and formulated a nonlinear torsional hysteretic model. The authors concluded that the flexural capacity of reinforced concrete columns decreases as the rotation-drift ratio increases and the damage tends to occur above the flexural plastic hinge region. Recently, Belarbi et al. (2008) presented a state of the art report on behavior of RC columns under combined loadings and scope for further research. They found that the effect of degradation of concrete strength in the presence of shear and torsional loads and confinement of core concrete due to transverse reinforcement significantly affected the ultimate strength of concrete sections under combined loading. They also suggested developing simplified constitutive models to incorporate softening and confinement effects. Prakash and Belarbi (2009) reported test results of several circular columns under combined loadings with different spiral ratios and T/M ratios. They reported that the effects of combined loading decrease the flexural and torsional capacity and affect the failure modes and deformation characteristics. They also concluded that the transverse reinforcement which might be adequate from the flexural design point of view could be inadequate under the presence of torsional loadings.

## **Research Significance**

A review of previous literature revealed that there have been few studies reporting on the behavior of RC circular and square columns under combined loading. The effect of cross-sectional shape on the interaction between flexure and torsional moment in the presence of axial compression has not been investigated adequately. The seismic behavior of circular and square columns is significantly different under combined loading due to the transverse reinforcement configurations and its effect on confinement of concrete, variation of shear stress flow, and warping effect. For circular columns, the spirals provide significant confinement to the core concrete which could result in higher strength. In addition, the locking and unlocking effect of the spiral significantly affects the behavior of circular columns due to their winding and unwinding action during cyclic loading. The spirals when unlocked during torsional loads cause significant spalling due to the reduced confinement effect on the concrete core. On the other hand, the locking effect of the spirals contributes more to the confinement of the concrete core resulting in higher strength and deformational

capacity. However, for the square column, the efficiency of transverse reinforcement is somewhat lesser in confining the core concrete compared to circular columns. And there is no effect of locking and unlocking of transverse reinforcement. Thus, the behavior of circular and square columns needs to be clearly understood to avoid brittle failure modes under combined loading. In addition, shear stress flow due to combined torsional moment and shear force on the square and circular section causes difference in damage distribution and ductility characteristics. The results from the current study will provide useful contributions to establishing rational interaction diagrams for circular and square sections under combined loading and outline differences in behavior between the two models. The above information is essential to develop equations for interaction surfaces and design guidelines for circular and square RC columns subject to combined loading including torsion.

### **Experimental Program**

#### **Specimen Details**

Half-scale test specimens were designed to be representative of typical existing bridge columns. Circular specimen dimensions and reinforcement layout are shown in Figure 1(a) and (c). Each of the circular RC column specimens had a diameter of 610 mm. and a clear concrete cover of 25 mm. Sectional details of square columns are shown in Figure 1 (b) and (d), which had a width of 550 mm and clear concrete cover of 38 mm. All these specimens were fabricated in the High Bay Structures Laboratory at Missouri University of Science and Technology (Missouri S&T). Both the circular and square columns had the same aspect ratio ( $H/D=6$ ). The total height of the circular column was 4.5 m. with an effective height of 3.66m measured from the top of the footing to the centerline of the applied forces; the total height of the square columns was 4.2 m with an effective height of 3.35 m.

Table 1 Mechanical Properties of Concrete and Steel used in Columns

PROPERTY	CIRCULAR COLUMNS				SQUARE COLUMNS			
	H/D(6)- T/M(0)	H/D(3)- T/M( $\infty$ )	H/D(6)- T/M(0.2)	H/D(6)- T/M(0.4)	H/B(6)- T/M(0)	H/B(6)- T/M( $\infty$ )	H/B(6)- T/M(0.2)	H/B(6)- T/M(0.4)
Compressive Strength ( $f'_c$ , MPa)	33.4	28.0	41.2	41.2	36.27	34.63	40.5	40.43
Modulus of Rupture ( $f_{cr}$ , MPa)	3.52	3.42	3.86	3.93	3.73	3.57	3.68	3.64
Spiral Reinforcement Ratio (%)	0.73	1.32	1.32	1.32	1.32	1.32	1.32	1.32
Transverse Yield Strength ( $f_{ly}$ , MPa)	450				454			
Longitudinal Yield Strength ( $f_{ly}$ , MPa)	457				512			

Typically, the axial load due to the superstructure dead load to bridge columns varies between 5% and 10% of the capacity of the columns. Therefore, an axial load equivalent to 7% of the concrete capacity of the columns for both circular and square columns was applied during testing. For circular columns, twelve No.8 bars (25 mm diameter) were designed as the longitudinal reinforcement. The longitudinal

reinforcement ratio was 2.1% for all the circular specimens. Spiral reinforcement was designed as No.4 bars (12.5 mm diameter) with the pitch of 70 mm to obtain transverse reinforcement ratios of 1.32%. For square columns, four No.9 bars (28 mm diameter) and eight No.8 bars (25 mm diameter) were employed as the longitudinal reinforcement providing a longitudinal reinforcement ratio of 2.13% similar to the circular columns. To achieve better confinement of the core concrete, rectangular and octagonal No.3 rebars were used as transverse reinforcement with spacing of 83 mm. This resulted in a transverse reinforcement ratio of 1.32% similar to circular columns. In order to compare the seismic performance of square and circular columns, the cross sectional dimension were chosen in a way such that both the square and circular columns would have equal flexural and torsional capacities with similar longitudinal and transverse reinforcement ratio. Columns under combined loadings were tested under T/M ratios of 0.2 and 0.4. The reinforcement details of the test specimens are given in Table 1.

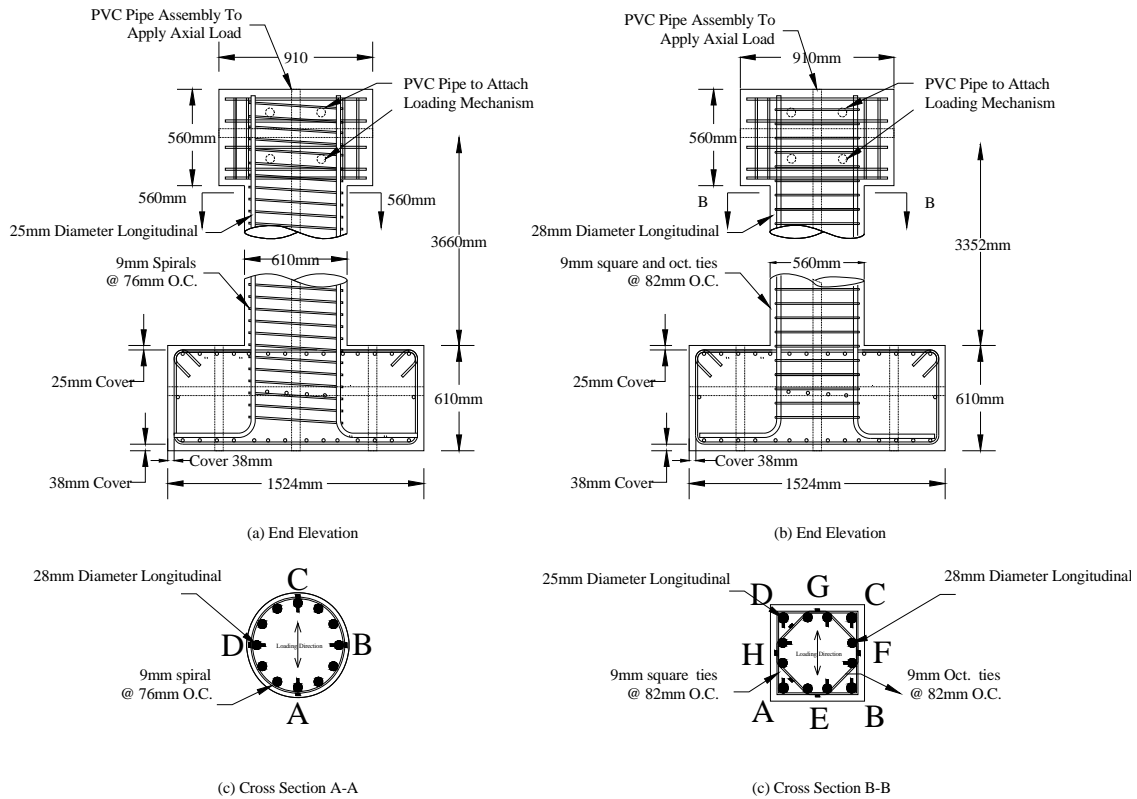


Figure 1 Circular and Square Column Sectional Details

### Material Properties

The concrete was supplied by a local Ready Mix Plant with requested 28-day design cylinder compressive strength of 34.5 MPa. Deformed bars were used in all specimens. The design yield strengths of transverse and longitudinal reinforcement are supposed to be 415 MPa. Standard tests for concrete compressive strength, modulus of rupture, and tension tests on steel coupons were conducted. The actual material properties of the circular and square columns on the day of the testing are given in Table 1.

### Test Setup and Instrumentation

The axial load was applied by a hydraulic jack on top of the columns which transferred the load to the column via seven un-bonded high-strength pre-stressed steel strands. The strands all ran through a duct which was made of PVC tube in the center of the column and anchored to a steel plate underneath the test specimen. A target 7% axial load ratio was applied to simulate the dead load on the column in a bridge. Cyclic torsion, uniaxial flexure and shear, and combined flexure and shear and torsion were generated by controlling the two horizontal servo-controlled hydraulic actuators shown diagrammatically in Figure 2. Cyclic flexure and shear load were generated by applying equal forces in the same direction with the two actuators. Pure torsion was created by driving equal but opposite directional forces with the two actuators. Combined cyclic torsion and flexural moments were generated by applying different forces/displacements with each actuator. The ratio of the imposing flexural moment to torsional moment was controlled by maintaining the ratio of the forces or displacements in the two actuators. A number of instruments were used to measure the applied loads, deformations, and internal strains. The axial load in the un-bonded pre-stressed steel strands was measured by a load cell between the hydraulic jack and the top of the load stub. Two load cells were installed in the horizontal hydraulic actuators to measure the applied force. Electric strain gages were attached to the surface of the longitudinal and transverse reinforcement to measure strains in order to study the deformation of reinforcement under different loading conditions. The strain gauges were mounted at different heights along the whole column in various patterns based on different loading conditions.

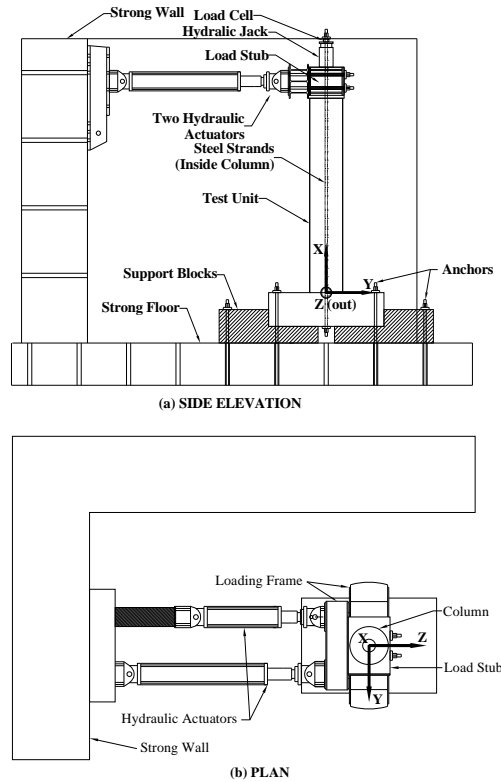


Figure 2 Test Setup

### Loading Protocol

Experimental testing was conducted in load control mode for all columns under flexure and shear, and combined flexure, shear and torsion loading conditions until the first yielding of the longitudinal bars. The load was applied in load control mode for circular columns at intervals of 25%, 50%, 75%, and 100% of the predicted yielding of the first longitudinal bar ( $F_y$ ). The horizontal displacement corresponding to yielding of the first longitudinal bar was defined as displacement ductility one ( $\mu_\Delta=1$ ). The circular column under pure torsion was loaded in load control mode at intervals of 25%, 50%, 75%, and 100% of the estimated yielding of the first spiral ( $T_y$ ). The rotation corresponding to yielding of the first spiral was defined as twist ductility one ( $\mu_\theta=1$ ). For square columns, the load control mode was imposed at intervals of every 10% of the predicted yielding of the first longitudinal bar ( $F_y$ ) under flexure and shear and combined flexure, shear and torsion loading conditions. The square column under pure torsion was loaded at 10% intervals of the predicted yielding of the first transverse bar ( $T_y$ ). More loading steps prior to yielding were implemented in the square column testing to obtain more data for establishing the influence of torsion on curvature of columns under flexure. After the first yield, the tests were performed in displacement control mode until the ultimate failure of the specimens at specific levels of ductility, meanwhile controlling the desired T/M ratios at the same time. Three cycles of loading were performed at each ductility level. The imposed pattern of three cycles was intended to give an indication of degradation characteristics. The loadings were applied along the direction A-C for the circular columns as shown in Figure 1c. The loading along the direction A-C and C-A are defined as positive and negative cycles, respectively. Similarly, for the square columns, the loadings were applied along the direction A-D as shown in Figure 1d. The loading along the direction D-A and A-D are defined as positive and negative cycles, respectively

### Test Results and Discussions

#### Columns under Flexure and Shear

Circular Column: The column tested under flexure and shear began exhibiting flexural cracks near the bottom on side A and side C after cyclically loading the column to 50% of  $F_y$ . These cracks continued to grow and new cracks appeared on both sides of the column as higher levels of ductility were reached. The cover concrete started spalling at a drift of about 3.2%. Spacers were attached between the actuators and the column and the displacement was applied only in the A-C direction after ductility eight. The failure mode of the specimen began with the formation of a flexural plastic hinge at the base of the column, followed by core degradation, and finally by the buckling of longitudinal bars on the compression side at a drift of about 12.7%. The flexural hysteresis is shown in Figure 3 up to ductility level of eight. The flexural resistance was stable between 3% and 12.7% drift with nearly a constant flexural strength of 232.8 kN. During the last cycle of loading, a longitudinal bar started buckling while unloading, as shown in Figure 4c. The yielding zone of the longitudinal bars was about 610 mm from the base of the column. Longitudinal bars on sides 'A' and 'C' both reached the yield strain at the predicted ductility level one. The spirals remained elastic until a ductility level of six, after which they yielded. Soon after cracking and spalling at the location of the spiral gages, the spiral gages became non-functional.

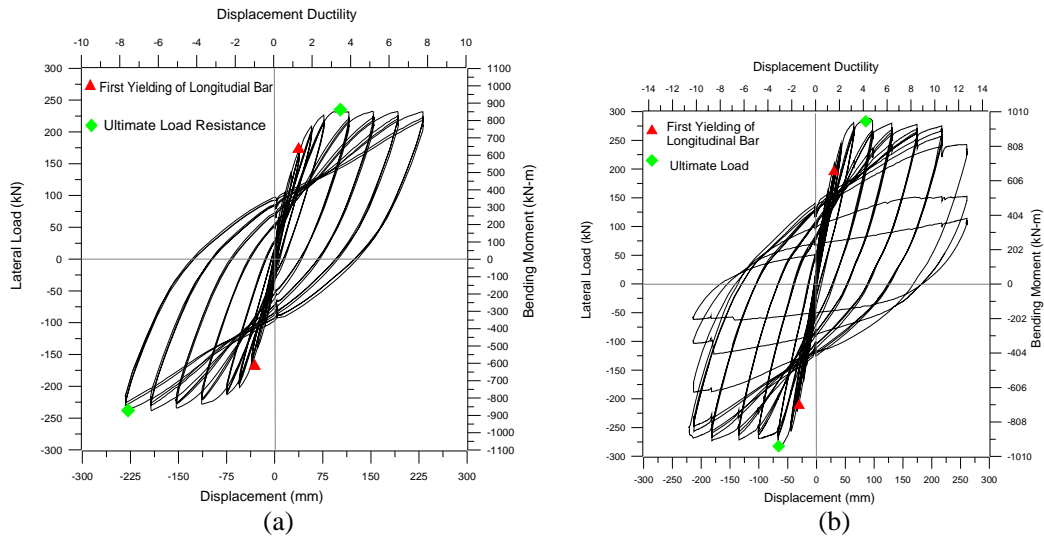
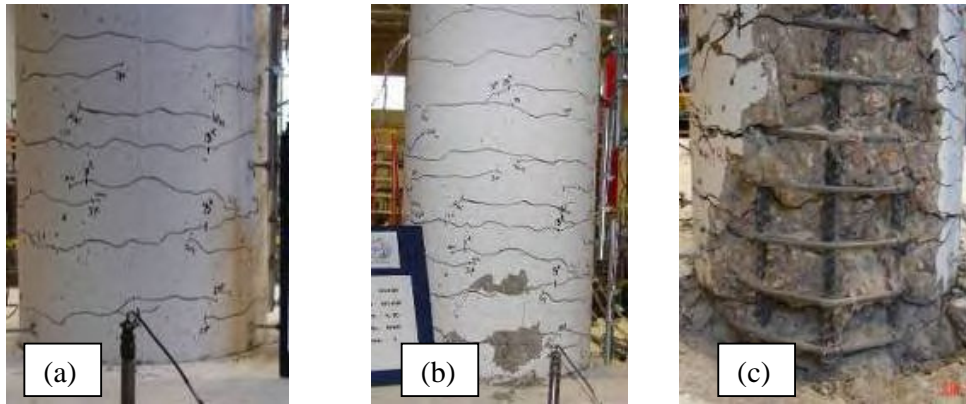
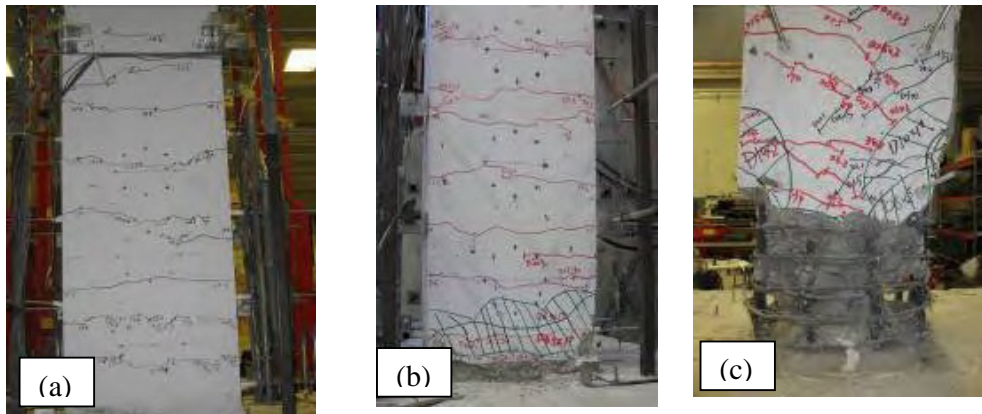


Figure 3 Hysteresis Curves under Flexure and Shear (a) Circular and (b) Square



(1) Circular Columns



(2) Square Columns

Figure 4 Failure Modes of Columns under Flexure and Shear at (a) Longitudinal Bar Yield, (b) Ultimate, and (c) Final failure

**Square Column:** The flexural hysteresis of the square column is shown in Figure 3b. The column tested under flexure and shear started to show flexural cracking near the bottom 400 mm above the footing on side AB and side CD after cyclically loading the

column to 40% of  $F_y$ . These cracks continued to develop and new cracks appeared on each side of the column in higher position with increasing levels of ductility. Subsequently, the cover concrete started to spall at a drift of about 2% when the column was loaded to ductility three. Application of ductility levels higher than ten were limited by the actuator stroke capacity. After this point, the displacements applied in the A-D direction (Negative) were limited to a smaller value of 210 mm. During the last cycle of ductility 12, almost all the longitudinal bars buckled while unloading as shown in Figure 4c. The yielding zone of the longitudinal bars was about 600 mm from the base of the column. Longitudinal bars on sides 'AB' and 'CD' both reached the yield strain at the predicted ductility level one. The square and octagonal transverse reinforcement remained elastic until a ductility level of eight, after which they yielded. The failure mode of the column began with the formation of a flexural plastic hinge with 580 mm height from the base of the column, followed by core concrete degradation due to crushing of concrete. The column finally failed by the buckling and breaking of longitudinal bars and rupturing of transverse bars on the compression side at a drift of about 8%. The progressing damage of the square column is shown in Figure 4.

### **Columns under Cyclic Pure Torsion**

In practice, pure torsion is rarely present in structural members. It usually occurs in combination with other actions often flexure and shear forces. And, understanding the behavior of members subjected to pure torsion is necessary for generalizing the analysis of a structural member under combined loadings. However, only very few studies have been reported on the behavior of RC circular and square sections under pure torsion.

**Circular Column:** The torsional strength of a member depends mainly on the amount of transverse and longitudinal reinforcement, the sectional dimensions, and the concrete strength. In the post peak behavior, dowel action of longitudinal bars is also reported to significantly affect the load resistance at higher cycles of loading (Belarbi et al., 2008). The torsional hysteresis curve of the column tested under pure torsion is shown in Figure 5a. Under pure torsional loading, significant diagonal cracks started developing near mid-height on the column at lower levels of ductility (Figure 5a). The cracks lengthened when the applied torsion was increased. The progressing damage of the specimen is shown in Figure 6a. Soon after the yielding of spirals, spalling was observed. The angle of diagonal cracks was about 40 degrees relative to the cross section (horizontal) of the column. The post cracking stiffness was found to decrease proportionally with increase in the cycles of loading. The locking and unlocking effect of the spirals was observed in the negative and positive loading cycles. During the positive cycles of twisting, the spirals were unlocked which helped to cause significant spalling and reduced the confinement effect on the concrete core. On the other hand, during the negative cycles of loading, the spirals underwent locking and contributed more to the confinement of the concrete core. This effect is reflected in the unsymmetric nature of the observed hysteresis loop at higher levels of loading (Figure 5a). At higher ductility levels, the load resistance on the negative cycles was higher than that under positive cycles of loading due to the added confinement generated by the locking effect of the spirals. Though, the concrete cover spalled along the entire length of the column, significant spalling led to the formation of a torsional plastic hinge near mid-height of the column (Figure 6c). The

damage pattern of the column under pure torsion was significantly different from that of column under flexure and shear.

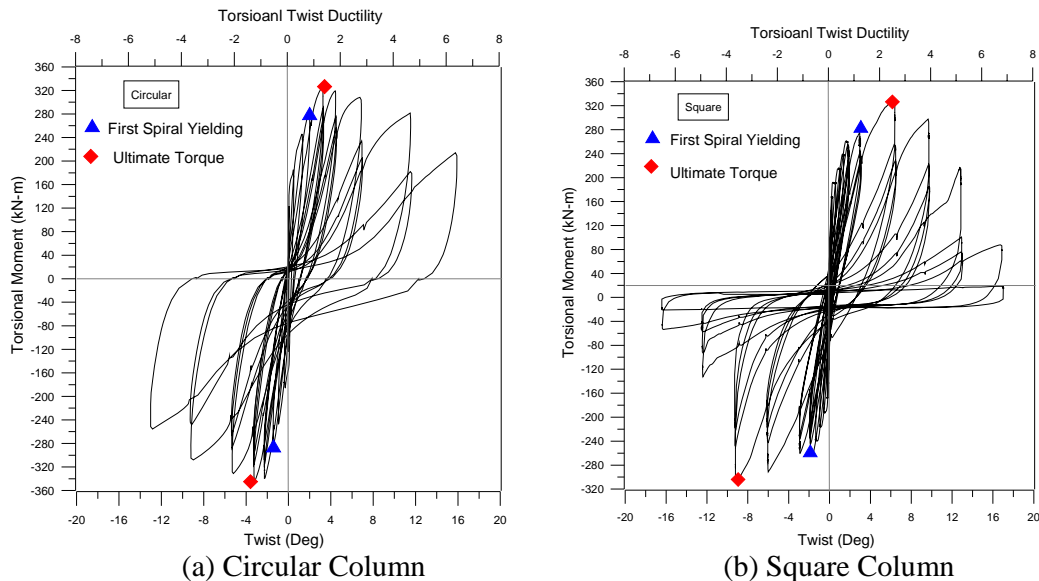
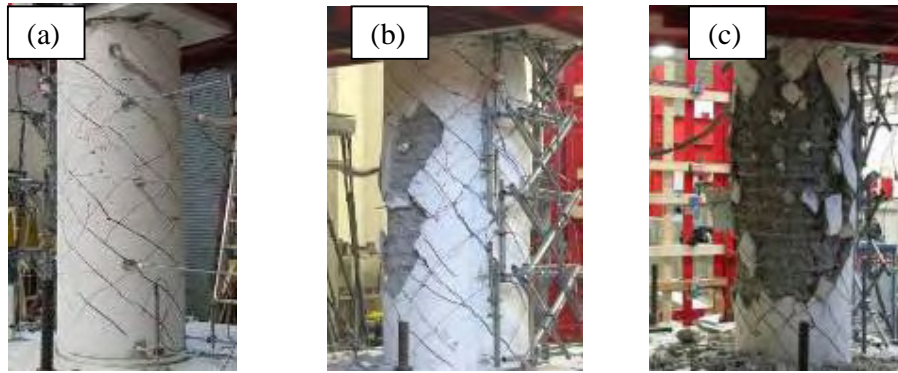
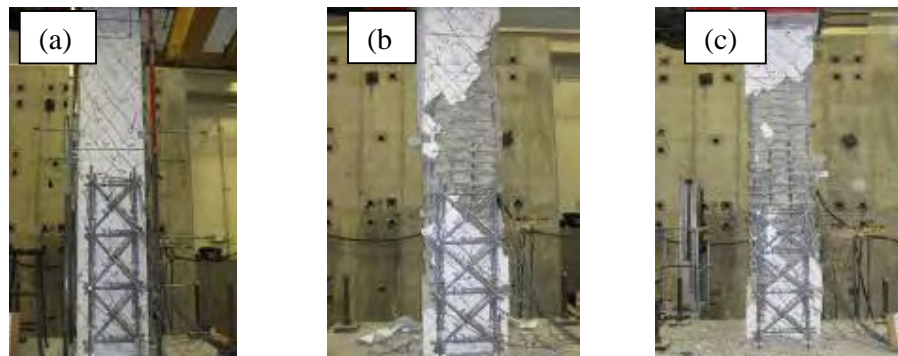


Figure 5 Torsional Hysteresis under Pure Torsion

**Square Column:** The torsional moment-twist hysteresis response of the column is shown in Figure 5b. The torsional moment -twist curves are approximately linear up to cracking torsional moment and thereafter become nonlinear with a decrease in the torsional stiffness. The post cracking stiffness decreased proportionally with increase in the cycles of loading. The torsional resistance increased significantly due to the longitudinal reinforcement contribution at higher load levels. Finally, the square and octagonal ties were broken in the plastic hinge zone. Under pure torsional loading, significant shear cracks started developing near mid-height on the column at lower levels of 60%  $T_y$ . The cracks developed in length and width when the applied torsional moment was increased. The diagonal cracks continued to form at an inclination of 40 to 42 degrees relative to the cross section (horizontal) of the column as the test progressed. Concrete spalling occurred at ductility one and the spalling region appeared along the column from bottom to top when the torsion loading reached ductility eight. At higher levels of loading, a plastic hinge formed near mid-height of the column due to significant concrete spalling. The damage pattern of column under pure torsion was significantly different from that of column under flexure and shear, which was concentrated near the middle of the column height instead of the typical flexural plastic hinge zone within one column cross sectional dimension from the base of the column. Typical damage progress of the columns with square and circular cross section under pure torsion is shown in Figure 6.



(1) Circular Column



(2) Square Column

Figure 6 Damage of Column under Pure Torsion at (a) Yield (b) Peak Torsional moment and (c) Overall Failure

### **Columns under Cyclic Combined Flexure, Shear, and Torsion**

Two circular and two square columns with transverse reinforcement ratio of 1.32% were tested under combined flexure, shear and torsion by maintaining T/M ratios of 0.2 and 0.4. The results from tests on columns under flexure and shear and pure torsion were used as the benchmarks for analyzing the behavior of specimens under combined flexure, shear, and torsion.

**Circular Columns:** For the two columns tested under combined flexure and torsion, flexural cracks first appeared near the bottom of the column. The angle of the cracks became more inclined at increasing heights above the top of the footing with increasing cycles of loading and depending on the amount of T/M ratio. In all the columns, side 'A' of the column exhibited less damage compared to side 'C'. The main reason for this is that side 'A' always experienced smaller displacements compared to side 'C' while applying the combined loading. In general, there are three failure modes possible under combined flexure, shear, and torsion for the concrete member reinforced with longitudinal and transverse reinforcement: completely under reinforced (longitudinal and transverse steel yield), partially over reinforced (only longitudinal steel yields or only transverse reinforcement yields), and completely over-reinforced (concrete crushing before steel yields). The flexural and torsional hysteresis behaviors of the column are shown in Figure 7 and Figure 8. The un-symmetric nature of the flexural envelopes under combined flexure and torsion is due to both the locking and unlocking effect and the fact that one face is subjected to

higher shearing stresses because the components of shear stresses from flexure and torsion are additive resulting in more damage and leading to less load resistance. In all columns under combined flexure and torsion, failure started due to severe combinations of shear and flexural cracks leading to progressive spalling of the concrete cover. The columns under combined loadings finally failed due to severe core degradation followed by buckling of longitudinal bars on side 'C'. The typical damage of circular column under combined flexure and torsional moments is shown in Figure 9.

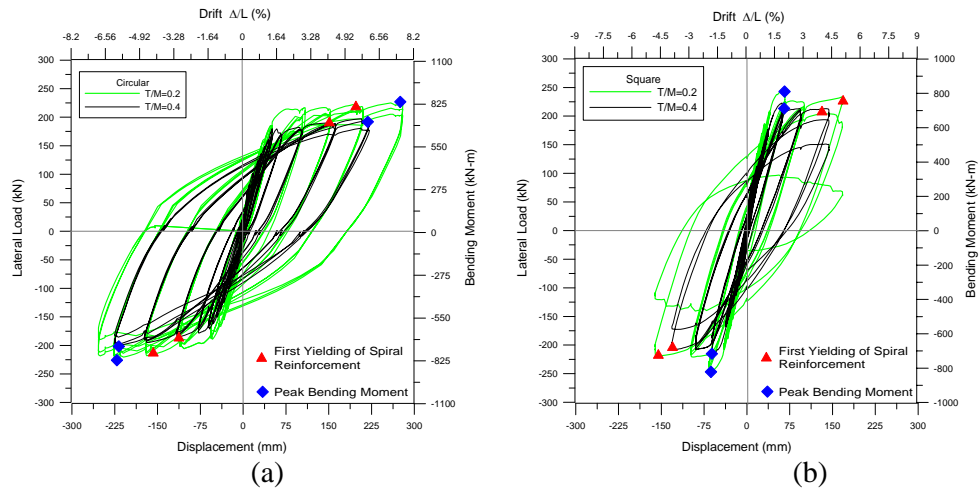


Figure 7 Comparison of Flexural Hysteresis Behavior under Combined Loading  
(a) Circular and (b) Square

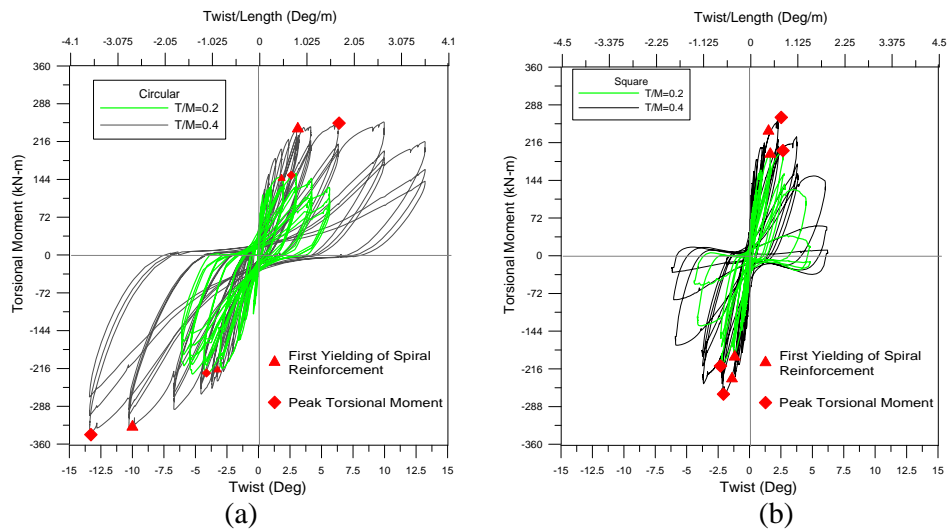
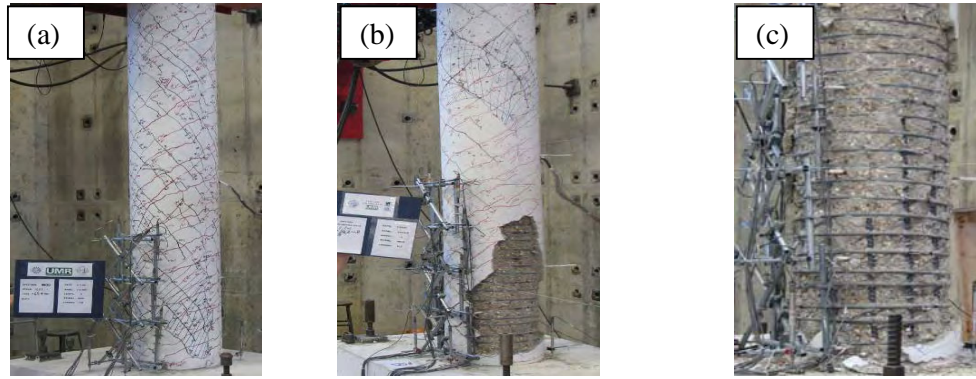
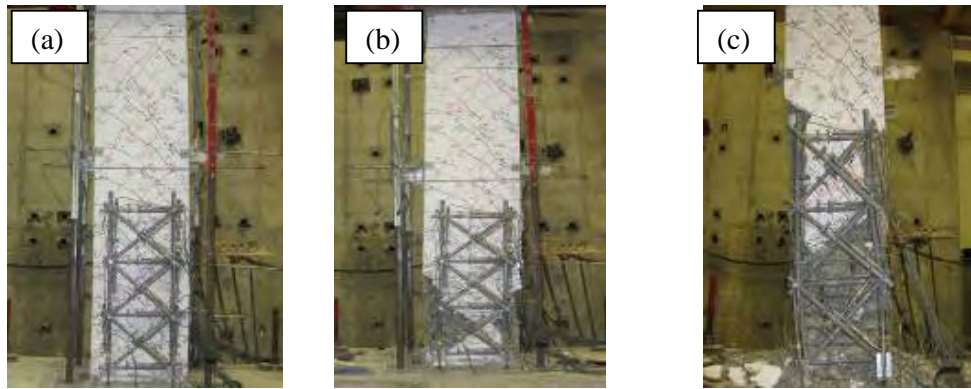


Figure 8 Comparison of Torsional Hysteresis Behavior under Combined Loading (a) Circular and (b) Square



(a) Circular Column at T/M=0.4



(a) Square Column at T/M=0.4

Figure 9 Comparison of Damages under Combined Loading at (a) Longitudinal Reinforcement Yield (b) Peak Torsional moment and (c) Overall Failure

**Square Columns:** For the two columns tested under combined flexure and torsion, flexural cracks first appeared near the bottom of the column at 40% of the yield strength, which is a smaller load level compared to the flexure and shear and pure torsion columns. The flexural and torsional hysteresis behaviors of the column are shown in Figure 7 and Figure 8. Strength and stiffness degradation were observed with increases in the loading cycles at each ductility level for the first two cycles, but less significant difference is seen between the curves of the second and third loading cycles. This indicates that the deterioration of the column capacities is substantial in the first loading cycle. It is clearly shown that due to the effect of combined loading, torsional and flexural strength reduces considerably according to the applied T/M ratio as observed in the circular columns. The flexural and torsional capacities as compared to the pure flexure and torsion tests were indeed found to decrease due to the effect of combined loading in this column. With increasing torsional and flexural moments, the angle of the cracks became more inclined at increasing heights above the top of the footing with increasing cycles of loading. The side 'BC' of the column exhibited more damage compared to side 'AD' in the column under combined flexure and torsion. The main reason for this is that side 'BC' always experienced larger shear stress compared to side 'AD' while applying the combined loading. The sequence and severity of damage of concrete and reinforcement lead to three different possible failure modes under combined flexure, shear and torsion as above for circular columns. Core degradation was observed up to a higher level of 1100 mm from the

base of the column as compared to 560 mm for flexure and shear loading. This shows that the flexure and shear plastic hinge location changes due to the effect of torsion. However, the specific location of the plastic hinge should depend on the ratio of applied T/M ratio. The location of the plastic hinge shifted to higher location with increasing T/M ratios. Failure of the columns under combined loading, started due to severe combinations of shear and flexural cracks. The column finally failed due to buckling of longitudinal bars on side 'AB' and 'CD'. Typical damage characteristics and failure sequence of the columns under combined flexure and torsion is shown in Figure 9.

### **Effect of Cross Section Shape on Flexure-Torsion Interaction**

Interaction diagrams between flexural and torsional moments are shown in Figure 10. The locking and unlocking effect of the spiral was significant in circular columns. It can be observed that in circular columns, the torsional strength was reached first and then flexural strength, while the square columns reached their torsional and flexural strength simultaneously. However, the failure sequence in all the specimens were in the order of flexural cracking, followed by shear cracking, longitudinal bar yielding, spalling of concrete cover, spiral yielding and then final failure by buckling of longitudinal bars after severe core degradation. It should be noted that the T/M ratio was close to the desired loading ratio in all the specimens till peak torsional moment. Soon after reaching the peak torsional strength, it was not possible to maintain the desired loading ratio as torsional strength was degrading much faster. Further, experimental research is in progress on behavior of square columns at Missouri S&T. Additional test results at different T/M ratios and further analysis would provide valuable information on the effect of warping and its significance on the torsion and flexural moment interaction diagrams.

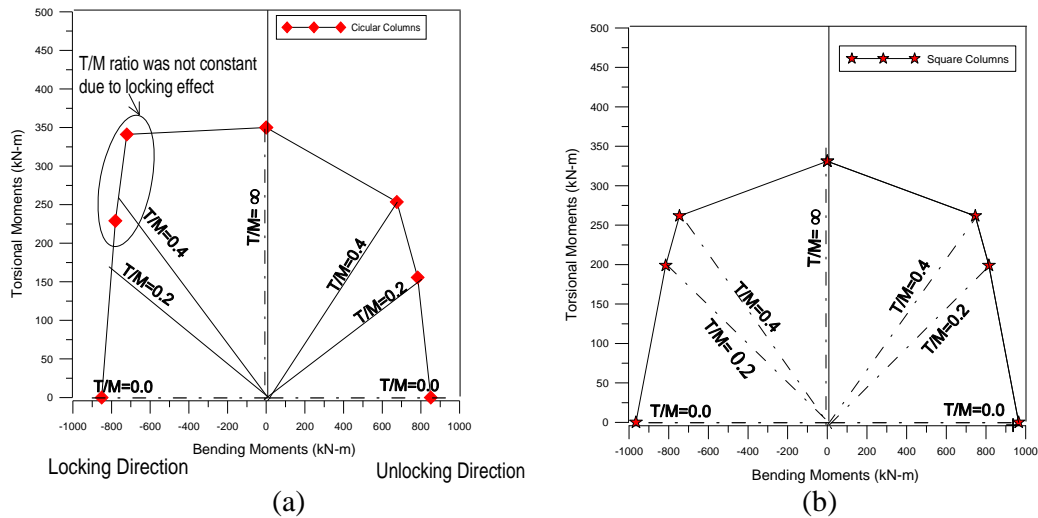


Figure 10 Torsion and Bending Interaction at Peak Torque (a) Circular and (b) Square

### **Summary and Concluding Remarks**

An experimental study on the effect of combined cyclic flexure and torsion on the behavior of circular and square reinforced concrete columns was presented. Based on

the test results presented in this paper, the following conclusions can be drawn:

- 1) The failure of the circular and square columns under pure torsion was caused by significant diagonal shear cracking leading to the formation of a torsional plastic hinge at middle height of the column. The concrete cover spalled along the full height of the column.
- 2) The existence of torsion altered the damage patterns of reinforced concrete columns under combined loading. Due to the presence of high shear stresses from shear force and torsional moment, the inclined crack developed significantly resulting in early spalling of concrete cover even before the ultimate shear was attained.
- 3) The square and octagonal transverse reinforcement for square columns provided confinement to the core concrete similar to the spiral reinforcement for circular columns. This ensured that the square column under flexure and shear obtained nearly the same strength as circular columns. However, their influence on confinement of concrete core under combined loading needs to be investigated further.
- 4) The ultimate lateral load and displacement capacity of the columns deteriorates with increasing levels of torsion. Similarly, the decrease of T/M ratio resulted in the deterioration of the torsional moment and the ultimate twist capacity.
- 5) The locking and unlocking effect of spiral reinforcement significantly affected the failure modes of circular columns under combined torsional and bending moments.

## **References**

1. Belarbi, A.; Prakash, S.S.; and Silva, P. (2008), "Flexure-Shear-Torsion Interaction of RC Bridge Columns," Paper No. 6, *Proceedings of the Concrete Bridge Conference*, St Louis, MO.
2. Lehman, D.E., Calderone, A.J. and Moehle, J.P. (1998), "Behavior and Design of Slender Columns Subjected to Lateral Loading", *Proceedings of Sixth U.S. National Conference on Earthquake Engineering*, EERI, Oakland, California. 1998.
3. Otsuka, H. Takeshita, E., Yabuki, W. Wang, Y., Yoshimura, T. and Tsunomoto, M. (2004), "Study on the Seismic Performance of Reinforced Concrete Columns Subjected to Torsional Moment, Bending Moment and Axial Force", *13<sup>th</sup> World Conference on Earthquake Engineering*, Vancouver, Canada, Paper No. 393, 2004.
4. Park, Y.J. and Ang, A.H.S. (1985), "Mechanistic Seismic Damage Model for Reinforced Concrete", *ASCE Journal of Structural Engineering*, V. 111, 1985, pp. 722-739.
5. Prakash, S.S. and Belarbi, A. (2009), "Bending-shear-torsion interaction features of RC circular bridge columns-An experimental study", Special Publication-SP 265, Paper No. SP-20, ACI Publications, Symposium in honor of Prof. Hsu (in press).
6. Priestly, M.J.N and Benzoni, G. (1996), "Seismic Performance of Circular Columns with Low Longitudinal Reinforcement Ratios", *ACI Structural Journal*, V. 93, No. 4, 1996, pp. 474-485.
7. Priestly, M.J.N, Seible, F., and Calvi, G.M. (1996), "Seismic Design and Retrofit of Bridges", John Wiley and Sons, Inc., New York, 1996, pp. 686.
8. Tirasit, P., Kawashima, K., and Watanabe, G. (2005), "An Experimental Study on the Performance of RC columns Subjected to Cyclic Flexural Torsional Loading", *Second International Conference on Urban Earthquake Engineering*, Tokyo, Japan, pp. 357-364.

## EXPERIMENTAL STUDY ON THE SEISMIC RESPONSE OF BRIDGE COLUMNS USING E-DEFENSE

Kazuhiko Kawashima<sup>1</sup>, Tomohiro Sasaki<sup>2</sup>, and Koichi Kajiwara<sup>3</sup>

### Abstract

This paper presents preliminary results of a large scale shake table experiment for studying the failure mechanism of three reinforced concrete bridge columns; a typical flexural dominant column in the 1970s (C1-1), a typical shear failure dominant column in the 1970s (C1-2) and a typical column designed in accordance with the current design code (C1-5). They were 7.5 m tall 1.8-2.0m diameter circular reinforced concrete columns. They were subjected to a near-field ground motion recorded during the 1995 Kobe, Japan earthquake. Preliminary results on the experiment and analytical correlation are presented.

### Introduction

Bridges are a vital component of transportation facilities; however it is known that bridges are vulnerable to the seismic effect. Bridges suffered extensive damage in past earthquakes such as 1989 Loma Prieta earthquake, 1994 Northridge earthquake, 1995 Kobe earthquake, 1999 Chi Chi earthquake, 1999 Bolu earthquake and 2008 Wenchuan earthquake. A large scale bridge experimental program was initiated in 2005 in the National Research Institute for Earth Science and Disaster Prevention (NIED), Japan as one of the three US-Japan cooperative research programs based on NEES and E-Defense collaboration. In the bridge program, it was originally proposed to conduct experiments on two model types; 1) component models and 2) system models. They are called hereinafter as C1 experiment and C2 experiment, respectively (Nakashima 2008).

The objective of the C1 experiment is to clarify the failure mechanism of reinforced concrete columns using models with as large section as possible. On the other hand, C2 experiment was proposed to clarify the system failure mechanism of a bridge consisting of decks, columns, abutments, bearings, expansion joints and unseating prevention devices.

C1 experiment was conducted for two typical reinforced concrete columns which failed during the 1995 Kobe earthquake (C1-1 and C1-2 experiments) and a typical reinforced concrete column designed in accordance with the current design requirements (C1-5 experiment). This paper shows preliminary results of the experiment and analysis on three C1 columns.

---

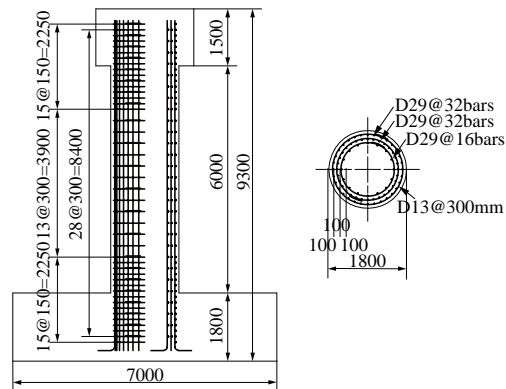
<sup>1</sup> Professor, Department of Civil Engineering, Tokyo Institute of Technology

<sup>2</sup> Graduate Student, Department of Civil Engineering, Tokyo Institute of Technology

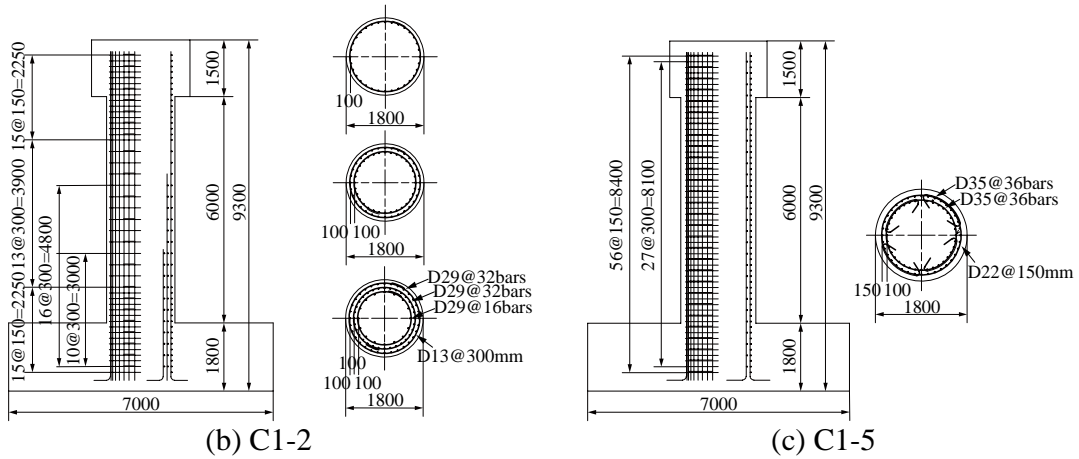
<sup>3</sup> Senior Researcher, National Research Institute for Earth Science and Disaster Prevention



**Photo 1** C1 on E-Defense



(a) C1-1



(b) C1-2

(c) C1-5

**Fig. 1** C1 column models

### Column Models

Photo 1 shows the experimental setup of three columns using E-Defense (Kawashima et al. 2009). Two simply supported decks were set on the column and on the two steel end supports. A catch frame was set under the lateral beam of the column to prevent collapse of the column when it was excessively damaged. Tributary mass to the

column by two decks including four weights was 307 t and 215 t in the longitudinal and transverse directions, respectively. The tributary mass was increased by 21 % from 307 t to 372 t in a part of C1-5 excitation.

Three full-size reinforced concrete columns as shown in Fig. 1 were constructed for the experiment. Columns used for C1-1, C1-2 and C1-5 experiments, which are called hereinafter as C1-1, C1-2 and C1-5, respectively, are 7.5 m tall reinforced concrete columns with a diameter of 1.8 m in C1-1 and C1-2 and 2 m in C1-5. C1-1 and C1-2 are typical columns which were built in the 1970s based on a combination of the static lateral force method and the working stress design in accordance with the 1964 Design Specifications of Steel Road Bridges, Japan Road Association. Since it was a common practice prior to 1980 to terminate longitudinal bars at mid-heights, the inner and center longitudinal bars were cut off at 1.86 m and 3.86 m from the column base, respectively. The cut-off heights were determined by extending a length equivalent to a lap splicing length  $l_{ls}$  (about 30 times bar diameter) from the height where longitudinal bars became unnecessary based on the moment distribution. On the other hand, longitudinal bars were not cut-off in C1-1. C1-1 and C1-2 had the same shape, heights, bar arrangement and properties except the cut-off. As a consequence, C1-1 failed in flexure while C1-2 failed in shear, as will be described later. The shear failure due to cut-off was one of the major sources of the extensive damage of bridges in the 1995 Kobe earthquake (Kawashima and Unjoh 1997). Combination of the lateral seismic coefficient of 0.23 and the vertical seismic coefficient of +/-0.11 (upward and downward seismic force) was assumed in the design of C1-1 and C1-2.

Deformed 13 mm diameter circular ties were provided at 300 mm interval, except the outer ties at the top 1.15m zone and the base 0.95 m zone where they were provided at 150mm interval in C1-1. Ties were only lap spliced with 30 times the bar diameter. Lap splice was a common practice by the mid 1980s. The longitudinal and tie bars had a nominal strength of 345 MPa (SD345), and the design concrete strength was 27 MPa. The longitudinal reinforcement ratio  $P_l$  was 2.02 % and the volumetric tie reinforcement ratio  $\rho_s$  was 0.32 % except the top 1.15 m and base 0.95m zones where  $\rho_s$  was 0.42% in C1-1.  $P_l$  and  $\rho_s$  varied depending on the zones in C1-2; 2.02 % and 0.42 % at the base 0.95 m zone, 2.02 % and 0.32 % between 0.95 m and 1.86 m, 1.62 % and 0.21 % between 1.86 m and 3.86 m, 0.81 % and 0.11 % between 3.86 m and 4.85 m, and 0.81 % and 0.21 % at the top 1.15 m zone, respectively.

On the other hand C1-5 was designed in accordance with the 2002 JRA Design Specifications of Highway Bridges (JRA 2002). Sixty four deformed 35mm diameter longitudinal bars were provided in two layers. Deformed 22 mm diameter circular ties were set at 150 mm and 300 mm interval in the outer and inner longitudinal bars, respectively. The ties were developed in the core concrete using 135 degree bent hooks after lap spliced with 40 times the bar diameter. The nominal strength of longitudinal and tie bars and the design concrete strength were the same with those in C1-1 and C1-2

columns. The longitudinal reinforcement ratio  $P_l$  was 2.19 % and the volumetric tie reinforcement ratio  $\rho_s$  was 0.92 %

Evaluation of the seismic performance of C1-1 and C1-5 in the longitudinal direction based on the 2002 JRA code is as follows: Because the design response acceleration  $S_A$  is  $17.16 \text{ m/s}^2$  for both C1-1 and C1-5, the yield displacement  $u_y$  and ultimate displacement  $u_u$  are 0.046 m and 0.099 m in C1-1 and 0.045 m and 0.231 m in C1-5. The design displacement  $u_d$  is evaluated from  $u_y$  and  $u_u$  as

$$u_d = u_y + \frac{u_u - u_y}{\alpha} \quad (1)$$

in which  $\alpha$  depends on the type of ground motion (near-field or middle field ground motion) and the importance of the bridge. Assuming  $\alpha$  is 1.5 for a combination of the near-field ground motion category and the important bridges category, the design displacement  $u_d$  is 0.081 m in C1-1 and 0.169 m in C1-5.

On the other hand, the displacement demand  $u$  is 0.328 m in C1-1 and 0.168 m in C1-5 because the force reduction factor is 1.58 and 2.56 respectively. Consequently, C1-1 and C1-5 were evaluated to be unsafe and safe, respectively based on the current design code.

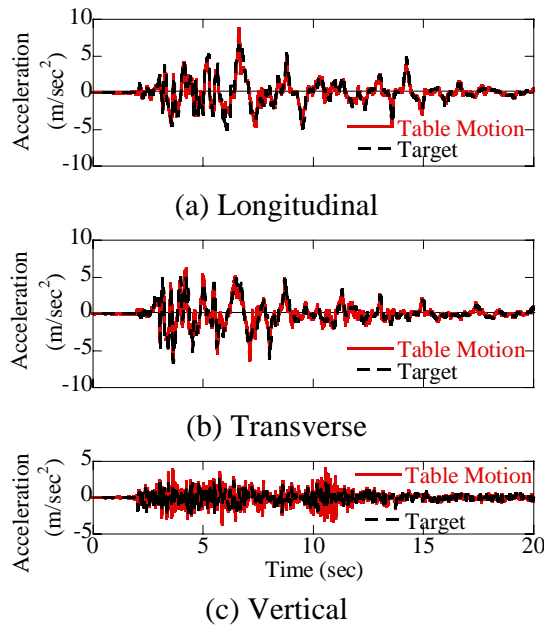


**Fig. 2** 100% E-Takatori ground motion (C1-5(1)-1 excitation)

Three columns were excited using a near-field ground motion as shown in Fig. 2 which was recorded at the JR Takatori Station during the 1995 Kobe earthquake. It was one of the most influential ground motions to structures. However duration was short. Taking account of the soil structure interaction, a ground motion with 80% the original intensity of JR Takatori record was imposed as a command to the table in the experiment. This ground motion is called hereinafter as the 100 % E-Takatori ground motion. Excitation was repeated to clarify the seismic performance of the columns when they were subjected to near-field ground motions with longer duration and/or stronger intensity. Only C1-5 was excited using 125 % E-Takatori ground motion with 21 % increased deck mass to study the seismic performance under a stronger ground motion than the JR-Takatori Station ground motion.

### Seismic Performance of C1-1 and C1-5

#### Progress of failure

C1-1 was subjected to the 100 % E-Takatori ground motion twice. Photo 2 shows the progress of failure at the plastic hinge on the SW surface where damage was most extensive. NS and EW direction correspond to the transverse and longitudinal directions, respectively, of the model. During the first excitation (C1-1-1 excitation), at least two outer longitudinal bars from S to W locally buckled between the ties at 200 mm and 500 mm from the base. During the second excitation (C1-1-2 excitation), both the covering and core concrete suffered extensive damage between the base and 0.7 m from the base on the SW surface. Three ties from the base completely separated at the lap splices. Eleven outer and three center longitudinal bars locally buckled between ties at 50 mm and 500 mm from the base.



(a) C1-1-1 excitation (8.35s)



(b) C1-1-2 excitation (7.71s)

**Photo 2** Progress of damage of C1-1

On the other hand, C1-5 was subjected to the 100% E-Takatori ground motion twice (C1-5(1)-1 and C1-5(1)-2 excitations). After the mass was increased by 21 % from 307 t to 372 t, C1-5 was subjected to the 100% E-Takatori ground motion once (C1-5(2)

excitation). Then C1-5 was subjected to the 125% E-Takatori ground motion twice (C1-5(3)-1 and C1-5(3)-2 excitations).

Photo 3 shows the progress of failure of C1-5 at the plastic hinge during C1-5(1)-1, C1-5(2) and C1-5(3)-2 excitations. During C1-5(1)-1 excitation, only a few flexural cracks with the maximum width of 1mm occurred around the column at the plastic hinge. Therefore it is noted that the seismic performance is enhanced in C1-5 than C1-1 under the first 100% E-Takatori excitation. The damage progressed during C1-5(2) excitation such that the covering concrete spalled off at the 500 mm base zone from WSW to SSW. During C1-5(3)-2 excitation, the failure extensively progressed. The core concrete crashed due to repeated compression, and blocks of crashed core concrete spilled out from the steel cages like explosion. Such a failure was never seen in the past quasi-static cyclic or hybrid loading experiments. Because the maximum aggregate size was 20 mm, the concrete blocks after crashed can be as small as 20-40 mm. Because the gaps of longitudinal bars and circular ties were 132 mm and 128 mm, respectively, it was possible for the blocks of crashed core concrete to move out from the steel cages. Furthermore twelve outer longitudinal bars and nineteen inner longitudinal bars locally buckled on SW and NE-E surfaces. The 135 degree bent hooks developed in the core concrete still existed in the original position although the core concrete around the hooks suffered extensive damage.



(a) C1-5(2) excitation (8.80s)



(b) C1-5(3)-2 excitation (7.17s)

**Photo 3** Progress of damage of C1-5

### **Response displacement and moment capacity**

Figs. 3 and 4 show the response displacement at the top of C1-1 and C1-5, respectively, in the principal response direction (nearly SW-NE direction). The peak displacement of C1-1 was 0.179 m (2.4 % drift) during C1-1-1 excitation while the peak displacement of C1-5 was 0.084 m (1.1 % drift) during C1-5(1)-1 excitation. Because the ultimate displacement in accordance with JRA 2002 code was 0.100 m and 0.235 m in C1-1 and C1-5, respectively, the above peak response displacements corresponded to 179 % and 36 % the ultimate displacement in C1-1 and C1-5, respectively.

Figs. 5 and 6 show the moment at the column base vs. lateral displacement at the column top hysteresees of C1-1 and C1-5, respectively, in the principal response direction. The computed moment vs. lateral displacement relations based on the 2002 JRA code are also shown here for comparison. The moment capacity of C1-1 during C1-1-2 excitation was 13.41 MNm which deteriorated by 19 % from the moment capacity during C1-1-1 excitation of 16.47 MNm. On the other hand, the moment capacity of C1-5 column progressed from 19.82 MNm during C1-5(1)-1 excitation to 20.14 MNm and 24.85 MNm during the C1-5(2) and C1-5(3)-2 excitations, respectively. However since the moment capacity of C1-5 during the C1-5(3)-1 excitation was 25.54 MNm, the moment capacity of C1-5 deteriorated by 3% during C1-5(3)-2 excitation. The computed moment capacities are close to the experimental values in both C1-1 and C1-5, however the computed ultimate displacement are very conservative compared to the experiment.

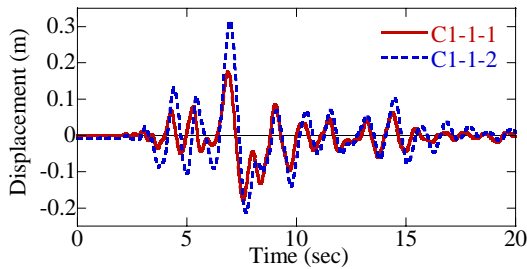


**Fig. 3** Response displacement at the top of C1-1 in the principle response direction

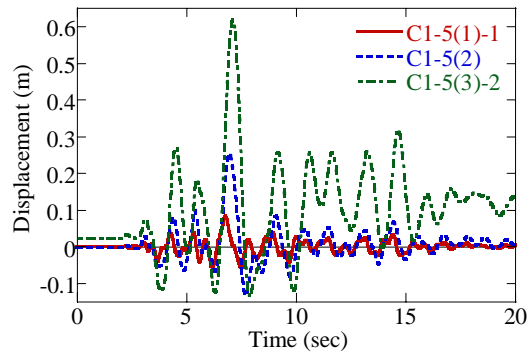


**Fig. 4** Response displacement at the top of C1-5 in the principle response direction

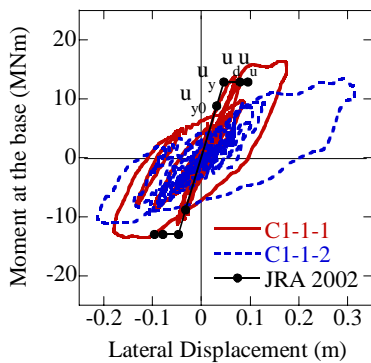


**Fig. 5** Moment at the base vs. lateral displacement of the top hysteresis of C1-1 in the principle response direction

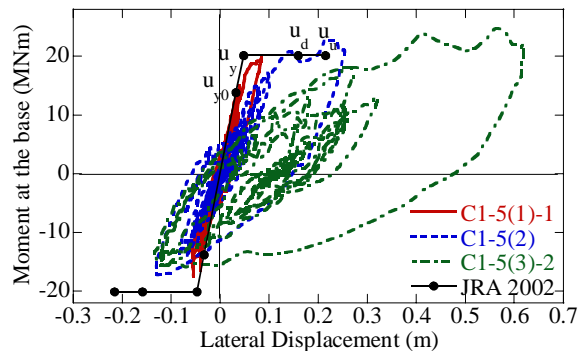


**Fig. 6** Moment at the base vs. lateral displacement of the top hysteresis of C1-5 in the principle response direction



(a) NW



(b) SE

(1) 6.50s



(a) NW



(b) SE

(2) 6.87s

**Photo 4** Progress of damage of C1-2

### Seismic Performance of C1-2

#### Progress of failure

Photo 4 shows the progress of failure of C1-2 on NW and SE surfaces. A horizontal crack first developed at 4.10s along NW to E surface, and it progressed to a shear crack at 4.33 s. Another horizontal crack developed at 4.60s along W to SE surface, and it extended to at least two diagonal cracks at 4.87s. Among two diagonal cracks developed at 4.33 s, a crack on NW surface extended to W surface, and the other crack on SE surface extended to S at 5.37s. The core concrete started to crush due to shear, and the blocks of crushed core concrete started to move out from the inside of the column near the upper cut-off on N and NW surfaces at 6.04 s. The same but more extensive failure occurred on S and SW surfaces at 6.504 s. The blocks of crushed core concrete progressively moved out from steel cages associated with the column response in the SW direction.

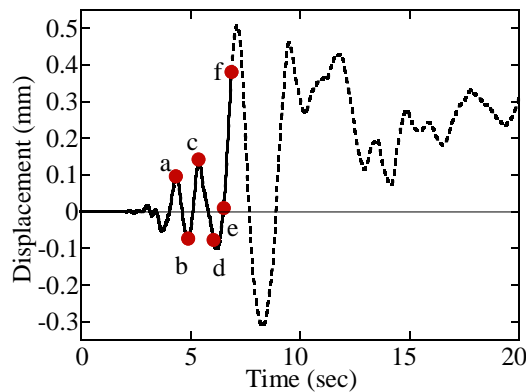
At 6.87 s, the bottom of lateral beam hit with the upper surface of catch frame due

to excessive response displacement. Three circular tie bars completely separated at their lap splice and the longitudinal bars deformed in the outward direction. Extensive failure of core concrete and deformation of longitudinal bars progressed on W, NW, N, NE and E surfaces.

It should be noted in the above process that the failure of core concrete was extensive and a large numbers of blocks of crashed core concrete as well as deformed longitudinal bars moved out from inside of the column during very short time (less than 3 s). It was like an explosion.

### Response and shear capacity

Fig. 7 shows response displacement of C1-2 in the principal response direction. As described above, since bottom of the lateral beam hit with the upper surface of catch frame at 6.87 s, the column response after 6.87 s was affected by this contact. Without the catch frame, the column possibly overturned. Therefore the response displacement after this contact is plotted by dotted line in Fig. 7. At 7.125 s, right after the contact, the column response displacement reached its peak of 439.2 mm and 253.0 mm in the longitudinal and transverse directions, respectively. Residual drifts of 204.5 mm and 343.2 mm were developed after the excitation.



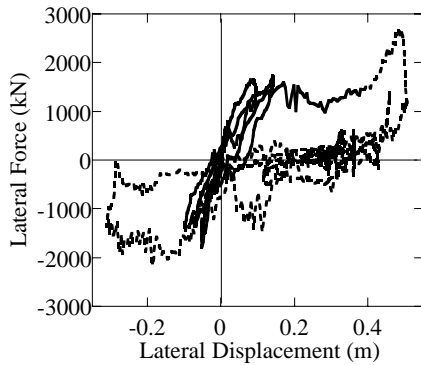
**Fig. 7** Response displacement at the top C1-2 in the principle response direction

Fig. 8 shows the lateral force at the upper cut-off vs. lateral displacement at the column top hysteresis in the principal response direction. The hysteresis after the contact of the column with the catch frame is plotted by dotted line. The shear capacity of the column  $F_s$  was evaluated based on the truss theory (Priestly 1996).

The shear stress at the upper cut-off vs. the lateral displacement at the column top relation was evaluated as shown in Fig. 9, in which  $\tau_c$  is normalized in terms of  $\alpha_c$  and  $\alpha_{pl}$  defined as

$$\alpha_c = \left(\frac{24}{f_c}\right)^{-1/3} ; \alpha_{pl} = \left(\frac{0.012}{p_l}\right)^{-1/3} \quad (2)$$

In Fig. 9, shear stress evaluated for two 1.68m tall 400mm diameter scaled model columns with different shear vs. flexure strength ratio is included for comparison (Sasaki et al. 2008).  $\tau_c / \alpha_c \alpha_{pl}$  of C1-2 is 0.68 MPa which is 15% larger than the value evaluated based on the shear equation (0.59 MPa) by Kono et al (Kono et al. 1996).



**Fig. 8** Lateral force at upper cut-off vs. lateral displacement at the column top hysteresis in the principle response direction

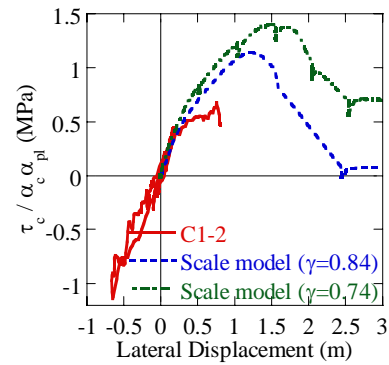


**Fig. 9** Shear stress of concrete

### Analytical Correlation for C1-5

Analytical correlation for C1-5 during C1-5(2) and C1-5(3)-2 excitations is shown here. The column was idealized by a 3D discrete analytical model including  $P - \Delta$  effect as shown in Fig. 10. The column was idealized by fiber elements. A section was divided into 400 fibers.

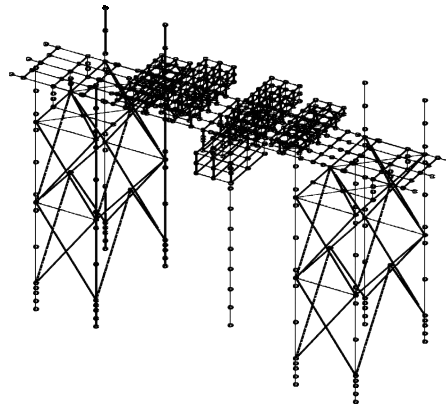
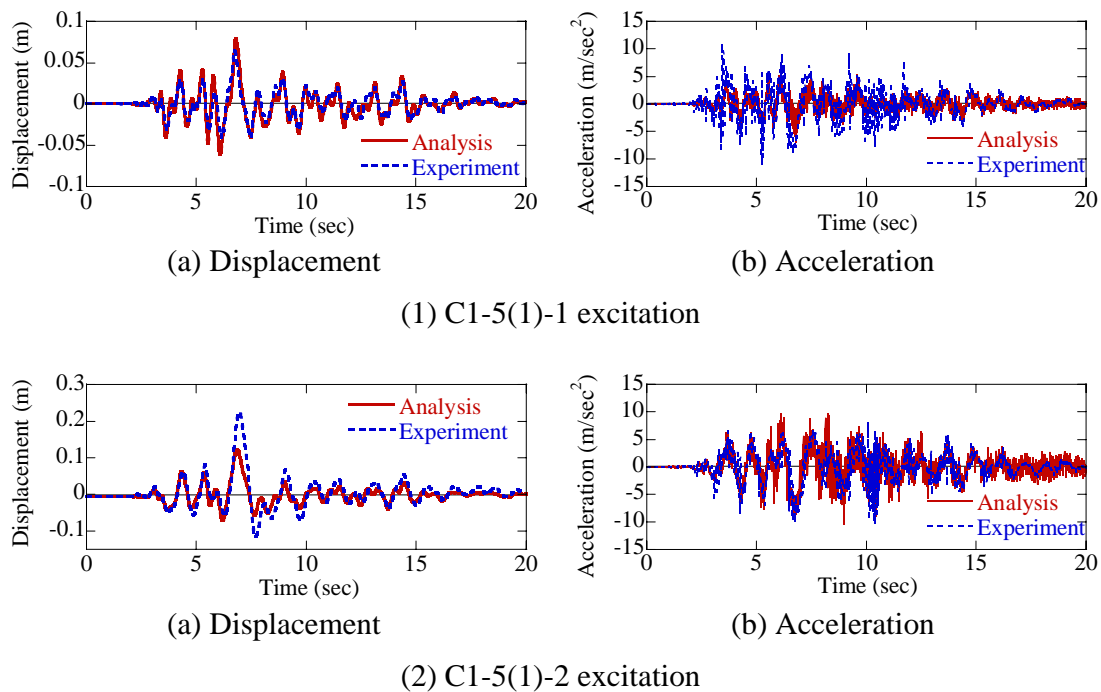


**Fig. 10** Analytical model

The stress vs. strain constitutive model of confined concrete is assumed based on

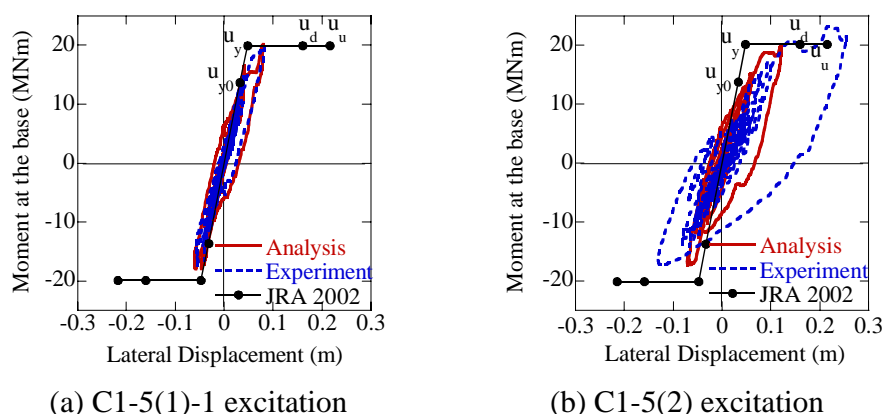
Hoshikuma et al (1997) and Sakai and Kawashima (2006). The Modified Menegotto-Pinto model was used to idealize the stress vs. strain relation of longitudinal bars (Menegotto and Pinto 1973, Sakai and Kawashima 2003).

Fig. 11 shows the analytical correlation on the response displacements at the top of the column in the principal direction during C1-5(1)-1 and C1-5(2) excitations. Fig. 12 compares the measured and computed moment at the base vs. lateral displacement at the column top hysteresses during the two excitations. Because nonlinear hysteretic response was still limited during C1-5(1)-1 excitation, the computed response displacement and moment vs. lateral displacement hysteresses are quite in good agreement with the experimental results, however as C1-5 suffered more damage, the accuracy of analytical prediction decreases.



**Fig. 11** Analytical correlation for the response displacement and acceleration at the column top in the principle response direction

Consequently, it is required to develop an analytical model that can predict the response of the columns until collapse for realizing reliable performance based seismic design.



**Fig. 12** Moment vs. lateral displacement at the column top in the principle response direction

### Conclusions

A preliminary result on a series of shake table experiment and analysis to three full-size reinforced concrete columns was presented. Based on the results presented herein, the following tentative conclusions may be deduced;

1) C1-1 which is a typical column in the 1970s suffered extensive damage under C1-1-1 excitation. The progress of damage during C1-1-2 excitation was extensive even though it was anticipated before the experiment that damage would not progress unless the intensity of second excitation was much larger than that of the first excitation. This resulted from the extensive deterioration of the lateral confinement due to separation of ties at the lap splices. It is highly possible that columns without sufficient lateral confinement have a similar progress of damage during a long-duration near-field ground motion or strong aftershocks.

2) C1-5 which is a typical column in accordance with the current design criteria suffered only a few numbers of horizontal cracks with the maximum width of 1 mm under C1-5 (1)-1 excitation. The ultimate drift was 2.9 % which was 2.2 times larger than that of C1-1. Consequently, enhancement of the seismic performance of C1-5 compared to C1-1 is obvious. However the progress of failure of C1-5 was extensive when it was subjected to 25 % stronger excitation under 21% added mass (C1-5(3) excitations). Blocks of crashed core concrete spilled out like explosion from the steel cages. The seismic performance of C1-5 subjected to longer duration near-field ground motion has to be carefully evaluated.

3) C1-2 failed in shear at the upper cut-off. As soon as circular ties at the upper cut-off yielded, a small diagonal cracks developed. As they extended to several major diagonal cracks, C1-2 completely failed in shear within less than 2.5 s since the initiation of a couple of small diagonal cracks. Concrete blocks crashed by shear and deformed

longitudinal bars extensively moved out from the inside of column.

4) The lateral confinement in the flexure dominant columns is not uniform around the ties as it is currently assumed in design. More importantly, the lateral confinement of multi layered ties is very complex. Strains of ties are not similar among the multi-layered ties, and they are related to the degree of constraint exerted for preventing local buckling of longitudinal bars. Strains are generally larger in the outer ties than the inner ties. This implies that the lateral confinement by Eq. (2) can be overestimated.

5) Computed response for the flexure dominant columns is satisfactory while response undergoes the moderate nonlinear range, however accuracy of the analytical prediction deteriorates once the columns undergo the strong nonlinear range. An analytical model which can predict response of the columns until failure should be developed for enhancing the reliability of the performance based seismic design.

### **Acknowledgments**

The C1 experiment was conducted based on the extensive support of over 70 personnel in the Overview Committee (Chair, Professor Emeritus Hirokazu Iemura, Kyoto University), Executing Committee of Large-scale Bridge Experimental Program (Chair, Professor Kazuhiko Kawashima, Tokyo Institute of Technology), Analytical Correlation WG (Chair, Dr. Shigeki Unjoh, Public Works Research Institute), Measurements WG (Chair, Professor Yoshikazu Takahashi, Kyoto University), Dampers & Bearings WG (Chair, Dr. Masaaki Yabe, Chodai) and Blind Analysis WG (Chair, Professor Hiroshi Mutsuyoshi, Saitama University). Their strong support is greatly appreciated. Invaluable support and encouragement of Professor Stephen Mahin, University of California, Berkeley and Professor Ian Buckle, University of Nevada, Reno are greatly appreciated.

### **References**

- Nakashima, M., Kawashima, K., Ukon, H. and Kajiwara, K. (2008), "Shake table experimental project on the seismic performance of bridges using E-Defense," S17-02-010 (CD-ROM), 14 WCEE, Beijing, China.
- Hoshikuma, J., Kawashima, K., Nagaya, K. and Taylor, A.W. (1997), "Stress-strain model for confined reinforced concrete in bridge piers," *Journal of Structural Engineering*, ASCE, 123(5), 624-633.
- Kawashima, K. Sasaki, T., Kajiwara, K., Ukon, H., Unjoh, S., Sakai, J., Takahashi, Y., Kosa, K., and Yabe, M. (2009), "Seismic performance of a flexural failure type reinforced concrete bridge column based on E-Defense excitation," *Proc. JSCE*, A, Invited paper, 1-19, JSCE.
- Kawashima, K. and Unjoh, S. (1997), "The damage of highway bridges in the 1995

- Hyogo-ken nanbu earthquake and its impact on Japanese seismic design,” *Journal of Earthquake Engineering*, 1(3), 505-542.
- Kono, H., Watanabe, H. and Kikumori, Y. (1996), “Shear strength of large RC beams,” Technical Note, 3426, Public Works Research Institute, Tsukuba, Japan.
- Priestley, M.N.J., Seible, F. and Calvi, G.M. (1996), “Seismic design and retrofit of bridges,” John Wiley & Sons, New York, USA.
- Menegotto, M. and Pinto, P.E. (1973), “Method of analysis for cyclically loaded R.C. plane frames including changes in geometry and non-elastic behavior of elements under combined normalized force and bending,” *Proc. IABSE Symposium on Resistance and Ultimate Deformability of Structures Acted on by Well Defined Repeated Loadings*, 15-22.
- Sakai, J. and Kawashima, K. (2003), “Modification of the Giuffre, Menegotto and Pinto model for unloading and reloading paths with small strain variations,” *Journal of Structural Mechanics and Earthquake Engineering*, JSCE, 738/I-64, 159-169.
- Sakai, J. and Kawashima, K. (2006), “Unloading and reloading stress-strain model for confined concrete,” *Journal of Structural Engineering*, ASCE, 132 (1), 112-122.
- Sasaki, T., Kurita, H., and Kawashima, K. (2008), “Seismic performance of RC bridge columns with termination of main reinforcement with inadequate development,” S17-02-009 (CD-ROM), 14WCEE, Beijing, China.

# EVALUATION OF THE SEISMIC PERFORMANCE OF BRIDGE REINFORCED CONCRETE COLUMNS UNDER COMBINED ACTIONS USING SHAKE TABLE

Juan G. Arias-Acosta<sup>1</sup> and David H. Sanders<sup>2</sup>

## Abstract

Combined actions (axial, shear, bending and torsion) can have significant effects on the force and deformation capacity of reinforced concrete bridge columns (RCC); these load combinations can result in unexpected large deformations and extensive damage that can seriously affect the seismic performance of bridges. To study the impact of different loadings combinations on both circular and non-circular sections (double interlocking spirals), eight large-scale cantilever-type RCC specimens will be tested on the bidirectional shake table facility at University of Nevada, Reno (UNR). As part of the study, an inertial loading system named Bidirectional Mass Rig was developed to allow shake table testing of single RCC under biaxial ground motions. Two sets of circular and interlocking RCC will be subjected to different levels of biaxial, torsion and vertical loads through real time earthquake motions. The performance of the specimens will be assessed in terms of strength, deformation, and failure mode.

## Introduction

During moderate to large earthquakes, reinforced concrete bridge columns are subjected to combinations of actions and deformations, caused by spatially-complex earthquake ground motions, structural configurations and the interaction between input and response characteristics. As a result, the seismic behavior of RCC will be seriously affected, and that in turn influences the performance of bridges as essential components of transportation systems. In addition, current analysis methods, behavior theories and design practices do not take into consideration the full range of interactions, due to the scarcity of experimental data and a lack of behavioral understanding.

In order to address the complex behavior of bridge members under combined loadings and its impact on system response, a comprehensive project sponsored by the National Science Foundation was established in 2006. This project includes researchers from six institutions, and the objectives are to develop a fundamental knowledge of the impact of combined actions on column performance and their implications on system response through analytical and experimental research.

The work at UNR focuses on the development of refined analysis and shaking table tests of cantilever-type scale models of bridge columns subjected to different levels of biaxial, torsion and vertical loads through real time earthquake motions. The performance of the specimens will be assessed in terms of strength, deformation, energy dissipation and failure mode. These results will be used to validate analytical tools, developing new inelastic models for RCC under combined loadings and to propose new design methodologies. This paper highlights some of the preliminary work underway at UNR.

---

<sup>1</sup> Graduate Student, Dept. of Civil & Environmental Engineering, Univ. of Nevada, Reno, NV89557, USA

<sup>2</sup> Professor, Dept. of Civil & Environmental Engineering, Univ. of Nevada, Reno, NV89557, USA

## **Specimen Details**

Two sets of specimens of circular and double interlocking columns were constructed using current bridge design details typical of bridges in California in accordance with the *Seismic Design Criteria* (CALTRANS, 2006). The structural configuration selected was similar to previous columns tested at UNR (Laplace *et al.*, 1999 and Correal *et al.*, 2004). For circular columns the scaling factor selected was 1/3. The diameter of the specimens was 406 mm (16 in) and the height 1830 mm (72 in), thus the aspect ratio was 4.5, which allows for flexural dominated behavior. The columns were reinforced with 20 No.4 (D13) deformed longitudinal bars, distributed uniformly around the perimeter and fully developed with 90 degree hooks in the footing. This resulted in a longitudinal reinforcement ratio of 2%. The confinement consisted of a continuous spiral made from galvanized steel wire with a diameter of 6.25 mm (0.25 in) and a pitch of 38 mm (1.5 in). The clear cover was set to 19 mm (0.75 in) and the resulting volumetric ratio of the spiral reinforcement was 0.92%. Details of circular specimens are shown in Fig. 1.

For double interlocking columns a scale factor of 1/4 was used. Consequently, the height was 1830 mm (72 in) and the width in the short side was 305 mm (12 in), while that in the long dimension was 445 mm (17.5 in). The longitudinal reinforcement consisted of 32 No. 3 (D10) deformed bars, spaced evenly in two circular patterns and fully developed in the footing. The resulting reinforcement ratio was 2%, while the volumetric ratio of the spiral reinforcement was 1.0%. The confinement for each of the circular sections consisted of a continuous spiral made from galvanized steel wire with a diameter of 4.9 mm (0.192 in) and a pitch of 25 mm (1.0 in). The clear cover was set to 13 mm (0.5 in). Details of the interlocking specimens are shown in Fig. 2.

The design compressive strength of the concrete was set as 30 MPa (4.5 ksi), while the nominal yielding strength of the steel was 447 MPa (64 ksi) for deformed bars and 420 MPa (60 ksi) for steel wire. Table 1 shows the real properties of steel and concrete based on coupons and cylinders tests. The superstructure mass was defined as 356 kN (80 kips), which is equivalent to an axial load of 8% of  $A_g f'_c$ .

## **Experimental Test Setup**

As part of the project a new inertial loading system was developed at UNR to test single cantilever-type columns on shake table under biaxial excitations. The aim of the test setup is to have a supporting structure that carries safely the vertical component of the inertial mass (superstructure weight) but allows transfer the inertial forces from the structure to the specimen. A similar structure that allows dynamic excitation in one direction was developed at UNR ten years ago (Laplace, 1999).

The new system is composed by a 3D four columns frame and a platform that sets on ball bearings located at the top of the columns. The platform is connected to the RCC specimen through links in two perpendicular directions, which transfer shear and torsion but not axial load (Fig. 3a). Additional mass is set on the platform to simulate the weight of a portion of the bridge superstructure and this can be distributed in an asymmetric configuration to induce torsion in the system. In addition, a safety system was designed to catch the platform in the event of large displacements or specimen collapse.

**Table 1: Material properties**

Days	Concrete Compressive Strength [MPa]			
	Circular		Interlocking	
	Footing	Column	Footing	Column
28	33	28	36	27

Steel Properties	No.3	No.4	W2.9	W5.0
Yield stress [MPa]	423	448	400	400
Yield strain	0.0022	0.0023	0.0024	0.0024
Strain at hardening	0.012	0.0075	N.A	N.A
Peak stress [MPa]	653	712	541	541
Strain at peak	0.124	0.115	0.115	0.126
Fracture stress [MPa]	561	687	537	484
Fracture strain	0.195	0.151	0.154	0.138

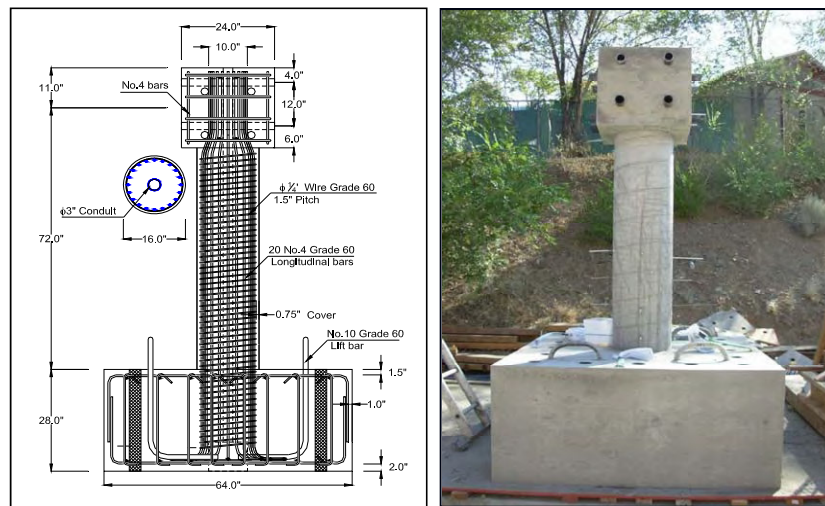


**Figure 1: Geometric configuration and reinforcement for circular RCC\*.**

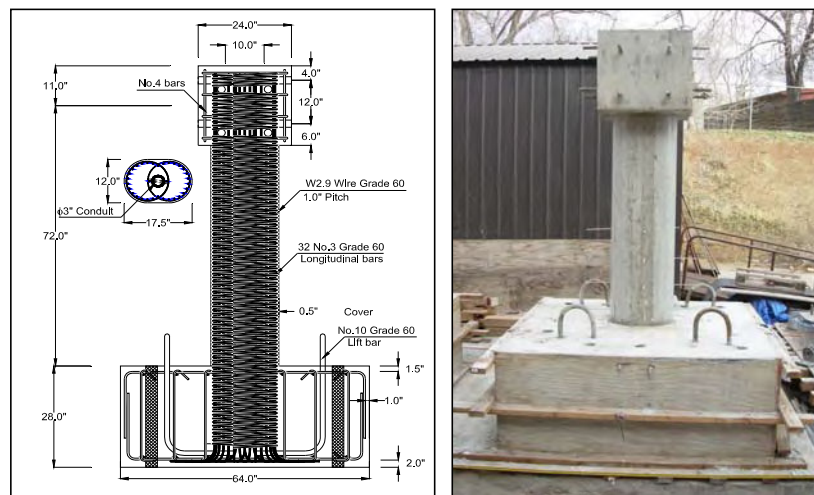


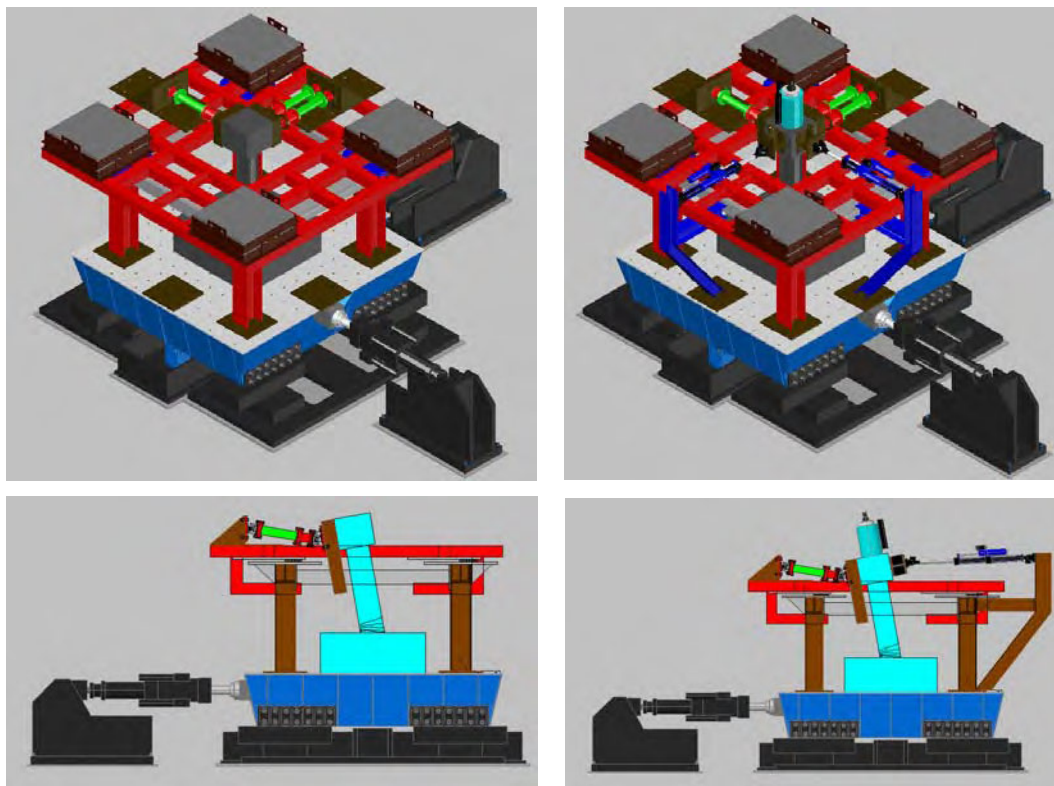
**Figure 2: Geometric configuration and reinforcement for double interlocking RCC\*.**

\* Unit conversion 1 in = 25.4 mm.

The axial load is applied directly to the specimen through a center-hole ram equipped with a servo-valve. The ram is connected to the specimen throughout an unbonded prestressed bar placed in an ungrouted conduit at the middle of the column and anchored at the footing. It is important to note that the main purpose of the prestressed bar is to induce the required level of axial load in the columns rather than increases its displacement capacity as has been found in other studies (Sakai *et al.*, 2006).

Since the designed system does not induce secondary moments (PD-effects) in the specimen and the unbonded prestressed bar inside the column would generate restoring lateral forces, additional dynamic actuators will be located at the top of the specimen to induce the equivalent force to have PD effects and to compensate the restoring force throughout hybrid simulation (Fig. 3b).

In view of the complexity of the system in terms of the active control of dynamic actuators, the test program was divided in two phases. At the beginning a set of two circular and two interlocking columns will be tested without any axial load or PD effects. A second phase will incorporate all the effects.



a: Without axial load. b: With axial load (prestressed bar + actuators)

**Figure 3 - Inertial loading system (Bidirectional Mass Rig).**

### **Analytical Investigation**

Analytical models were developed to anticipate the seismic performance of the specimens and to determine the appropriate input loadings to be used during the tests. Time history inelastic

analysis have been performed using OpenSees (Mazzoni *et al.*,2006). Analytical models of single cantilever-type columns with lumped mass as well as models of the specimens including the inertial loading system were studied under different levels of earthquake excitations and mass distribution to determine limit states in the behavior of the columns during the tests.

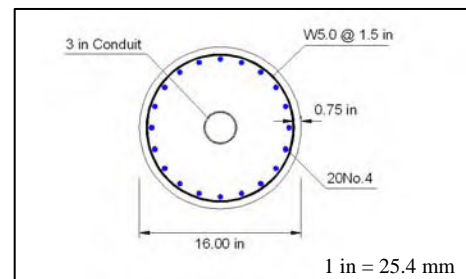
The biaxial flexural behavior of the columns was simulated using a distributed plasticity model throughout uniaxial fiber elements (element inelastic beam-column in OpenSees). The stress-strain properties of the unconfined and confined concrete were simulated using the Mander’s model (Mander *et al.*, 1988). For that, the actual strength of the concrete measured from cylinders at 28 days was used. Likewise, the longitudinal reinforcing steel was idealized using the uniaxial steel material model developed by Chang and Mander (1994). The actual stress-strain backbone curve measured from coupons was used as the input parameter for the steel material model. Also, the reinforcement slippage was included in the models in the form of additional rotation at the plastic hinge location.

Since inelastic fiber models for torsion are still under development (Mullapudi *et al.*, 2008), a reduction factor of 20% the elastic torsional stiffness (GJ) was used to take in account the torsional cracking of the concrete in agreement with the *Seismic Design Criteria* (CALTRANS, 2006).

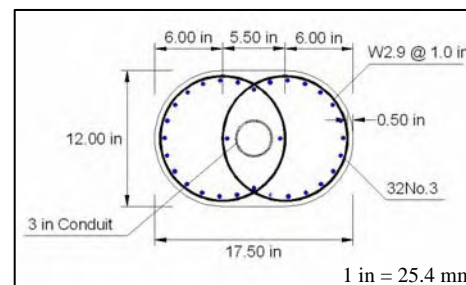
To estimate the lateral load and displacement capacities of the specimens moment-curvature analysis were performed. Table 2 summarizes the capacities of the circular and interlocking columns. Once the capacity was estimated, a series of nonlinear time history analysis were conducted to select the input motion to be simulated in the shake table test. As was mentioned before, five cases of mass distribution were studied to determine the largest torsional demand on the specimen.

**Table 2: Lateral load capacities of the specimens**

Circular Columns P=0	
Properties	Radial
$\phi_y$	0.00034
My (kN-m)	177
$\phi_u$	0.00584
Mu (kN-m)	223
$\mu\Delta$	8.29
Vu (kN)	122



Interlocking Columns P=0		
Properties	Short dimension	Long dimension
$\phi_y$	0.0004	0.0003
My (kN-m)	158	229
$\phi_u$	0.00742	0.00431
Mu (kN-m)	177	253
$\mu\Delta$	11.5	9.3
Vu (kN)	98	138



## Ground motions

The two horizontal components of the 1940 Imperial Valley earthquake (El Centro), the 1994 Northridge earthquake, the 1992 Petrolia at Mendocino earthquake and the 1995 Hyogo-ken Nanbu earthquake (Kobe) were used as the input motions. The earthquake records for Northridge and Petrolia were scaled to have a hazard level of 2% of exceedence in 50 years (Zhang and Xu, 2008). The amplitude of the records was increased until the maximum capacity of the analytical model was achieved. Also, the time axis of the input motions was compressed to account for the specimen scale factor. Factors of 0.58 and 0.5 were used for circular and interlocking specimens, respectively.

From the dynamic analysis, it was found that the record Petrolia at Mendocino and Sylmar at Northridge amplified by factors of 2.0 and 1.8, will induce the maximum displacement ductility demand on the circular and double interlocking specimens without exceeding the shake table capacity. The maximum accelerations imposed in both horizontal directions were 0.9g and 1.2g, for Petrolia and 1.1g and 1.5g for Sylmar ground motion.

## Column C1 – Experimental Results

The first circular specimen (C1) was tested under the two components of the Petrolia earthquake. For this test no axial load was applied, and also the distribution of the mass was symmetric to induce low torsion. The column was subjected to multiple motions, increasing the amplitude in subsequent runs. Small increments (10% to 20% of the real earthquake) were initially applied to determine elastic properties and the effective yielding, after that, the amplitude of the records was successively increased until failure. Signals of white noise were applied to the model to measure the change in period and damping ratio between runs. Table 3 summarizes the measured response of the column during the test.

**Table 3: Measured Response of Specimen C1**

Earthquake		Accel. in X (g)	Accel. in Y (g)	Rel. disp. in X (mm)	Rel disp. in Y (mm)	Force in X (kN)	Force in Y (kN)
0.1xPET	MAX	0.105	0.050	10.83	6.26	42.43	24.72
	MIN	-0.086	-0.049	-10.33	-6.86	-52.18	-25.93
0.2xPET	MAX	0.191	0.106	13.55	22.46	68.83	45.57
	MIN	-0.185	-0.104	-18.15	-23.27	-95.58	-40.65
0.4xPET	MAX	0.363	0.255	-20.33	-11.67	99.45	56.01
	MIN	-0.444	-0.238	24.98	9.81	-115.69	-57.96
0.6xPET	MAX	0.455	0.337	-20.64	-12.81	93.34	50.33
	MIN	-0.588	-0.381	24.97	9.32	-103.29	-49.70
0.8xPET	MAX	0.590	0.466	36.25	12.91	111.65	49.23
	MIN	-0.667	-0.456	-29.43	-17.67	-82.56	-58.14
1.0xPET	MAX	0.692	0.607	38.39	48.38	121.39	48.41
	MIN	-0.737	-0.570	-97.04	-15.73	-65.64	-66.46
1.2xPET	MAX	0.806	0.752	61.38	21.40	123.72	44.27
	MIN	-0.808	-0.656	-47.59	-28.66	-67.80	-70.47
1.4xPET	MAX	0.887	0.863	74.08	25.83	125.73	45.71
	MIN	-0.868	-0.762	-56.22	-34.41	-66.53	-73.43
1.6xPET	MAX	0.981	1.039	86.97	30.17	127.03	45.14
	MIN	-0.939	-0.876	-65.48	-40.09	-67.50	-73.95
1.8xPET	MAX	1.098	1.175	-59.48	156.00	124.16	49.24
	MIN	-0.993	-0.965	-316.66	32.81	-71.81	-74.40

The behavior of the specimen was controlled by the biaxial effect of bending, with horizontal cracks distributed on the height of the specimen, as well as some inclined cracks at the plastic hinge zone.

The first yielding was observed during 0.2xPET, after this motion, horizontal cracks spreaded out from the bottom of the column until the motion 1.0xPET, where the concrete cover at the south side spalled out. The maximum force was recorded at 1.6xPET, at this stage most of the transverse reinforcement was exposed. Finally the failure of the column was observed at 1.8xPET, at this stage some of the longitudinal bars undergone buckling and large degradation of the concrete core was observed. Figure 4 shows the final damage state of the column, while figure 5 shows the displacement history and the hysteretic behavior of the specimen in longitudinal direction (X). On the same plot is shown the predicted behavior using the analytical model.

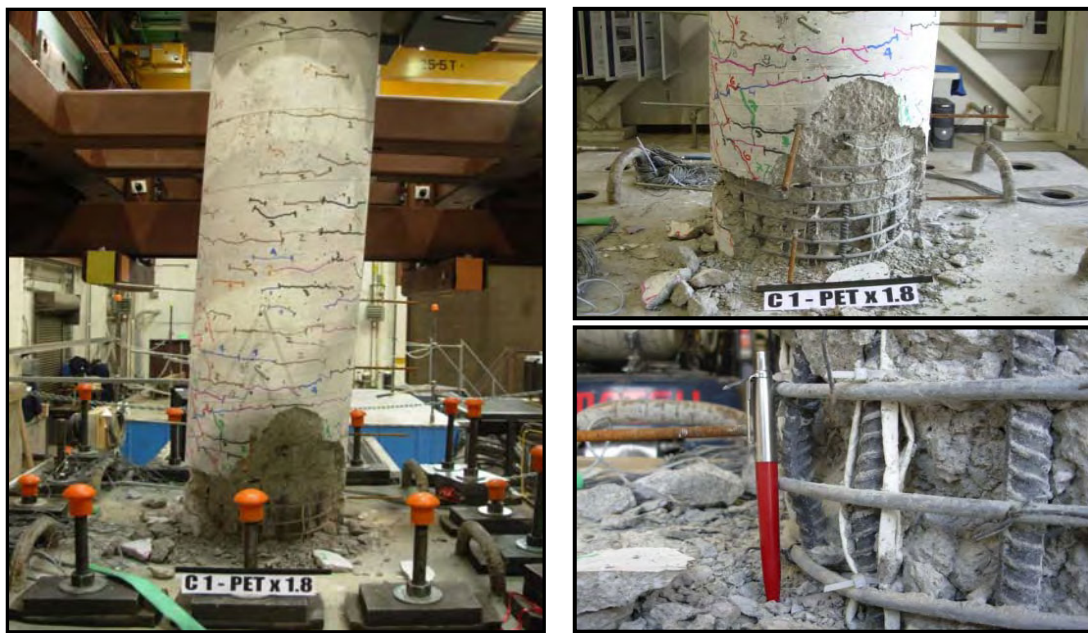


Figure 4 – Specimen C1 after failure

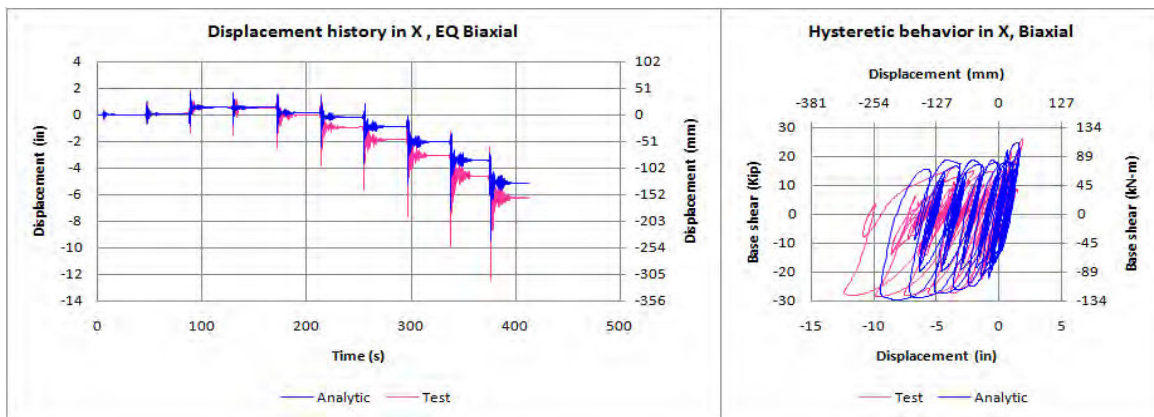


Figure 5– Displacement history and hysteresis for specimen C1

## **Concluding Remarks**

The new inertial mass system to be used on bidirectional shake table tests at UNR represent a significant advance in the simulation of single RCC under simultaneous loads induced by real time earthquake motions. One of the most important characteristics of this system is that it allows the interaction between bending and torsion with or without axial load.

The analytical model used to simulate the seismic performance of the specimen and the inertial mass system as shown in Fig.4 predicted the answer reasonably well in terms of relative displacement and hysteretic behavior.

Preliminary analytical and experimental results found at UNR and by researchers from other institutions involved in the project have shown that the interaction between loads have a significant effect in the capacity of reinforced concrete bridge columns under seismic loads. These results are being used to develop analytical tools and new inelastic models for reinforced concrete columns that in turn will assist in the development of new design methodologies.

## **Acknowledgements**

The research presented in this paper was founded by The National Science Foundation under Grant No.EMS – 0530737. The assistance of Ian Buckle, Patrick Laplace, Chad Lyttle and the staff of the Large Scale Structural Laboratory at University of Nevada Reno is gratefully acknowledged.

## **References**

ACI Committee 318 (2008), "Building Code Requirements for Structural Concrete (ACI 318-08) and Commentary." American Concrete Institute, Farmington Hills, Michigan, USA, 465 pp.

California Department of Transportation. (2006) "Bridge Design Specifications." Engineering Service Center, Earthquake Engineering Branch, California, USA, 250 pp.

Chang, G. and Mander, J. (1994). "Seismic Energy Based Fatigue Damage Analysis of Bridge Columns: Part I – Evaluation of Seismic capacity." NCEER Technical Report 94-0006.

Correal, J.F., Saiidi, M.S., and Sanders, D.H. (2004). "Seismic Performance of RC Bridge Columns Reinforced with Interlocking Spirals." Report No. CCEER-04-6, Center for Civil Engineering Earthquake Research, Department of Civil Engineering, University of Nevada-Reno, USA, 438 pp.

Zhang, J. and Xu, S.Y. (2008). " Seismic Response Simulations of Bridges Considering Shear-Flexural Interaction of Columns. " Proceedings of the 6th National Seismic Conference on Bridges & Highways, Paper No. P29, Charleston, South Carolina, USA.

Mander J.B., Priestley, M.J.N. and Park, R. (1988). "Theoretical Stress-Strain Model for Confined Concrete." Journal of Structural Eng. 114 (8), pp 1804-1826.

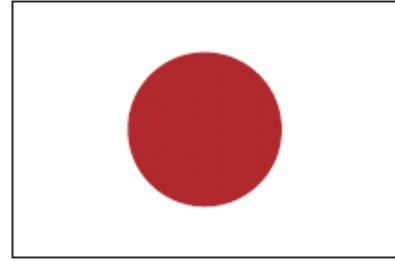
Laplace, P., Sanders, D.H., and Saiidi, M.S. (1999). "Shake Table Testing of Flexure Dominated Reinforced Concrete Bridge Columns." Report No. CCEER-99-13, Center for Civil Engineering Earthquake Research, Department of Civil Engineering, University of Nevada-Reno, USA, 438 pp.

Mazzoni, S., McKenna, F., Scott, M., and Fenves, G.L. "Open System for Earthquake Engineering Simulation (OpenSees), 2006." User manual, version 1.7.3, Pacific Earthquake Engineering Research Center, University of California, Berkeley, California, USA, <http://opensees.berkeley.edu/OpenSees/manuals/usermanual/index.html>.

Mullapudi, T.R., Ayoub, S. and Belarbi, A. (2008). "Effect of Coupled Shear-Bending Deformations on the Behavior of RC Highway Structures Subjected to Extreme Seismic Loading." Proceedings of the 6th National Seismic Conference on Bridges & Highways, Paper No. P19, Charleston, South Carolina, USA.

Sakai, J., Jeong H. and Mahin, S.A. (2006). "Reinforced Concrete Bridge Columns that Re-Center Following Earthquakes." Proceedings of the 8th U.S. National Conference on Earthquake Engineering, Paper No. 1421, San Francisco, CA.

blank



# 25<sup>th</sup> US-Japan Bridge Engineering Workshop

## Session 2

### Inspection and Management

Analysis of Periodic Inspection Results of Highway Bridges in Japan

By Koichi Ikuta, Takashi Tamakoshi, and Masanori Okubo

Bridge Inspection and Management in California

By Barton Newton

Measures for Strategic Preventive Bridge Management of Tokyo Metropolitan Government

By Taro Awamoto and Sentaro Takagi

Instrumentation and Monitoring of I35W St. > Anthony Falls Bridge

By Catherine French, Carol Shield, Henryk Stolarski, Brock Hedegaard,  
and Ben Jilk

Study for Bridge Renewal and Repair by Osaka Municipal Government

By Shinsuke Yumoto, Tetsuya Yokota, and Yasutomo Komatsu

Page Left Blank

# ANALYSIS OF PERIODIC INSPECTION RESULTS OF HIGHWAY BRIDGES IN JAPAN

Takashi TAMAKOSHI<sup>1</sup>, Masanori OKUBO<sup>2</sup>, Koichi IKUTA<sup>3</sup>

## Abstract

Analyses of initial inspection results, relationship between age and damage, progress of damage, and fatigue damage were conducted using periodic inspection results as a part of the research on rational periodic inspection method to grasp conditions of nationwide bridges from the uniform point of view efficiently.

## Background

In Japan, under limited budget and stuff according to social and economical change that low fertility and aging are in progress, to maintain service level of its huge road network strategically and efficiently is required. For this, prevention maintenance that countermeasures are conducted at the early stage before the abnormalities become serious, not the countermeasures like symptomatic treatment for remarkable damages, is needed, and strategic and rational management that contributes on reducing life cycle cost for long time considering whole road asset is also needed. Furthermore, it comes important to maintain roads over the nation as network.

Under this background, paying attention to bridge inspection which is the most basic action to get information needed for bridge maintenance, analyses of periodic inspection results were conducted as a part of the research about the rational periodic inspection method to grasp conditions of nationwide bridges from an uniform point of view efficiently.

## State of bridge inspection in Japan

Bridges operated by MILT are inspected with periodic inspection manual, which was revised on March 2004 from that edited on July 1988 to conduct inspection more efficiently with the new findings in maintenance and inspection results.

### 1) Frequency of inspection

For inspection frequency, initial inspection should be done within 2 years after the bridge is opened to the traffic, after that the bridge should be inspected every 5 years.

---

<sup>1</sup> Head, Bridge and Structures Division, Road Department, NILIM, Japan

<sup>2</sup> Senior Researcher, Bridge and Structures Division, Road Department, NILIM, Japan

<sup>3</sup> Researcher, Bridge and Structures Division, Road Department, NILIM, Japan

Initial inspection is aimed to increase durability and to reduce life cycle cost by taking measure at early stage against initial defects which appear within several years after opening to the traffic. The initial inspection results are meaningful as the initial data for various maintenance works like repair and reinforce within the service life of the bridge.

## 2) Method of periodic inspection

The method of periodic inspection has basically followed the precedent: the method to evaluate every member considering every usual kinds of damage by close visual inspection.

This is the result of the judge that this inspection method is the most rational and indispensable considering economy at this point to detect partial damage and to grasp the progress of serious damage which develops extremely rapidly at some parts in the point of view of keeping structural safety of the bridges, preventing damage for a third person, realizing preventive maintenance by detecting the indication of damage at early stage. That is, considering the limit of staff and budget, there are some places to examine to use distant view or to introduce advanced technical skills like non-destructive inspection methods, but many serious damages to affect the safety of bridges like short of sectional area in steel members by crack or corrosion are difficult to detect by distant view, and the rational methods to cover the risk of missing those damages have not been established.

## 3) Evaluation of inspection results

Two types of evaluation of inspection results were introduced when the periodic inspection manual was revised on 2004: “evaluation of degree of damage”- it is a record of facts of degree of damages, and “judgment of countermeasure”- it is a first diagnosis about function of bridge and structure by proper engineers.

Information which is grasped by inspection like damages and aging is not only indispensable to inferring cause and to evaluating performance, but also used for future estimation or trend analysis. Information should be objective data based on an uniform standard.

On the other hand, evaluation and diagnosis by engineer with technical knowledge accompanied with inspection are dispensable to various damages and their effects' being measured. It is very important for administrator to decision-make properly about need for traffic regulation and countermeasure like repair and rehabilitation gasping the performance of bridges from inspection. For this, it is important to get not only facts of

kind of each damage and degree of their development, but also damage's effect to bridge's performance and view about response that should be done from the damage's effect. For example, some fatigue cracks of steel members develop rapidly to dangerous state of the bridge even if the crack is small when it is detected.

For "evaluation of degree of damage", every parts is evaluated in the divided unit of each member because the evaluation is the basic data for investigation for rationalization of future inspection. Damages detected at periodic inspection are evaluated at every element and at every degree of damage, and the classification means objective facts indicating the degree of damage. The classification of degree of damage is shown in Table.1. Damages are evaluated to the classification of "a", "b", "c", "d", and "e" by degree of damage, and "a" is the least serious and "e" is the most serious.

Table 1. Classification of degree of damage

Evaluation division	Degree of damage
a	Small
b	↓
c	
d	↓
e	

For "judgment of countermeasure", on the other hand, the unit of member with some sizes, like main girder or pier, is evaluated because "judgment of countermeasure" is qualitative evaluation which can be called an advice for administrator about countermeasure in relation to performance of the bridge. The classification of evaluation is shown in Table.2.

Table. 2 The classification of evaluation at judgment of countermeasure

Evaluation division	Content of evaluation
A	Damage is not confirmed or little, so repair is dispensable.
B	Repair is needed according to the situation.
C	Repair is needed immediately.
E 1	Emergency response is needed for structure safety.
E 2	Emergency response is needed for other reason.
M	Response through maintenance construction work is necessary.
S	Detailed investigation is necessary.

**Analysis of periodic inspection results**

Various kinds of analysis of the periodic inspection results were conducted for improvement of periodic inspection because one round of periodic inspection had almost

finished.

### 1) Analysis of initial inspection results

Damages were detected in most of bridges in first inspection. The number of bridges as the objects of first inspection was 198, which were within 2 years after opening to the traffic and after construction completed, and damages were detected in 193 bridges (97%). The most detected damage was deterioration of rust-proof performance and corrosion in steel members and crack, leakage and isolated lime in concrete members. Abnormality of anchorage zone of PC member and abnormality of performance of bearing were detected as the serious damage to affect performance of bridge.

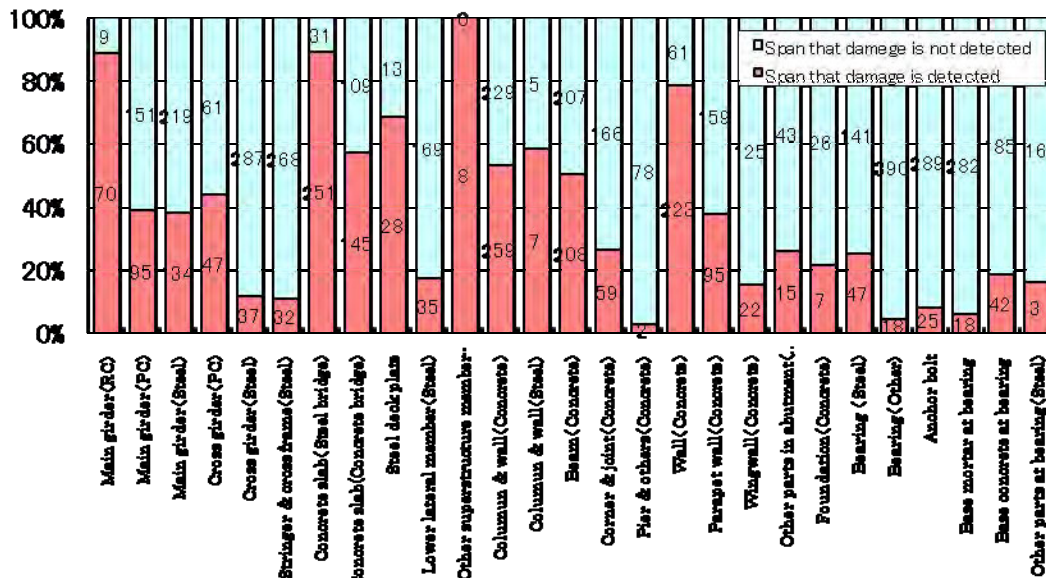


Fig.1 Initial inspection results (main members)

### 2) Relationship between age and damage

As a whole, the rate of abnormality seems to increase in accordance with age. Fig.2 shows states of damage in periodic inspection results at age after opening to the traffic. Bridges' deterioration characteristic has huge variation because it depends on bridge's structure and environment, and it can be inferred that degree of deterioration and damage of each bridge differ. However, as a whole, the trend that the rate of abnormality increases in accordance with age is notable.

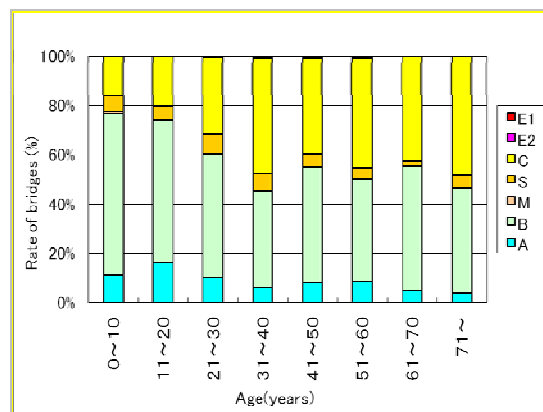


Fig.2 The rate of bridges in classification of measure

3) Analysis about progress of damages

① Crack at concrete members (part)

Among the relationships between age and degree of various kinds of damage, the example of crack at concrete main girder is shown in Fig.3, and the example of abutment is shown in Fig.4. The transitions of main girder and abutment are different. On the other hand, it can be inferred that when crack generated even at main girder, the crack certainly progresses within 5 years.

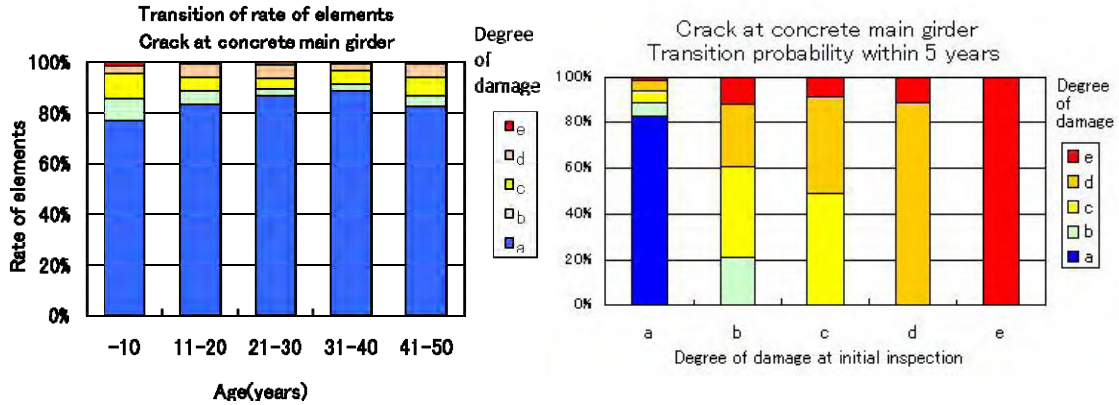


Fig.3 Relationship between age and degree of damage (crack at concrete main girder)

② Crack at concrete members (environment)

The transition of two periodic inspection results was analyzed classifying chloride damage area and other area to grasp the effect of environment regardless age. The result is shown in Fig.5. Markov transition probability based on Fig.5 is shown in Fig.6. It is recognized that the deterioration speed in is a little faster chloride damage area when degree of damage is light.

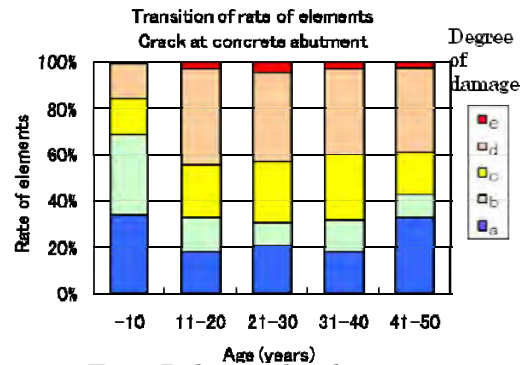


Fig.4 Relationship between age and degree of damage (crack at concrete abutment)

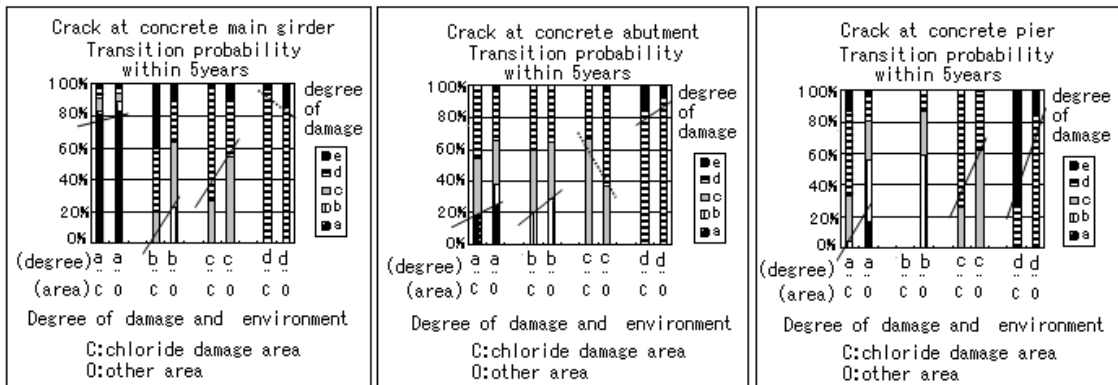


Fig. 5 Transition probability of generation of crack at concrete members

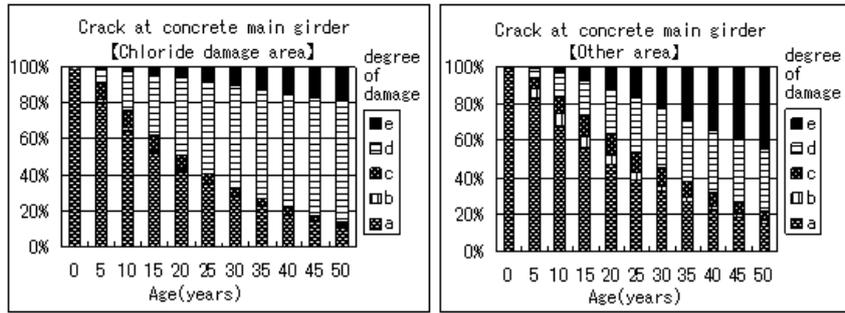


Fig.6 Markov transition probability of crack at concrete main girders

③ Crack at concrete members(structural type, crack pattern)

Age and state of crack generation at PC post-tensioned hollow slab bridge and PC post-tensioned T section girder bridge are shown in Fig.7 and Fig.8.

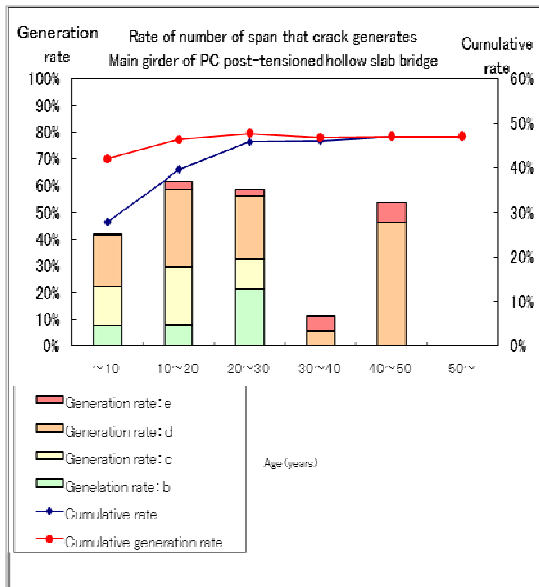


Fig.7 Age and state of crack generation (PC post-tensioned hollow slab bridge)

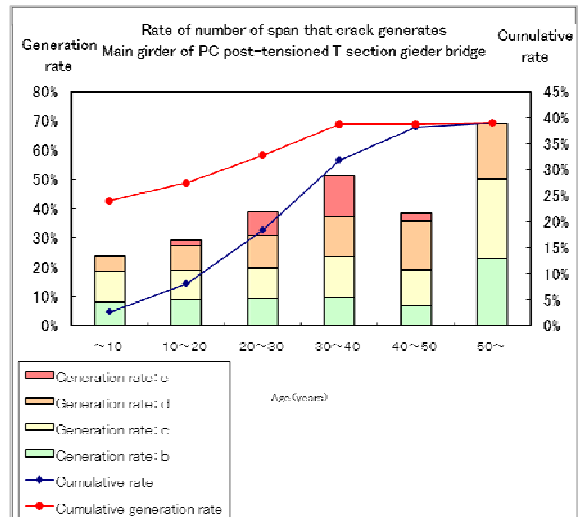


Fig.8 Age and state of crack generation (PC post-tensioned T section girder bridge)

For PC post-tensioned T section girders, age and state of crack generation in each pattern whose generation rate is high is shown in from Fig.9 to Fig.12

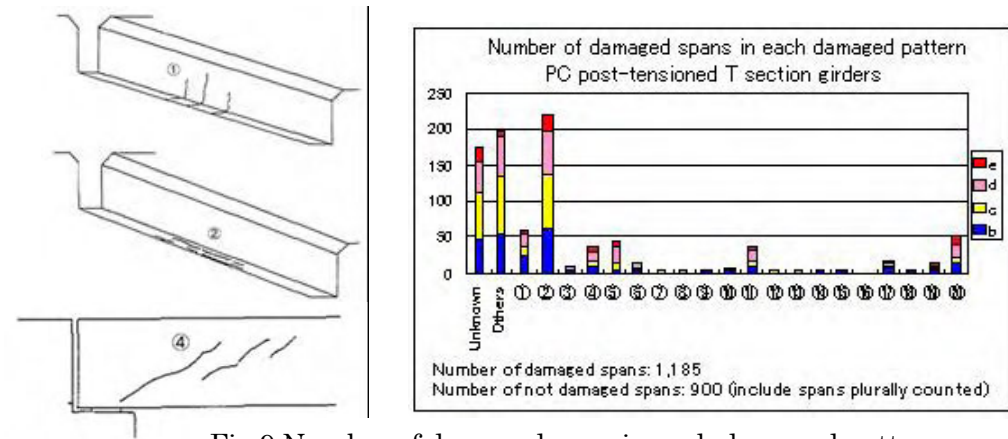


Fig.9 Number of damaged span in each damaged pattern (PC post-tensioned T section girder bridge)

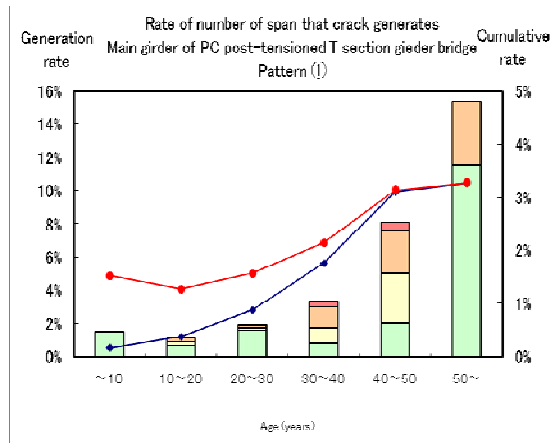


Fig.10 Age of PC post-tensioned T-section girder bridges and state of crack generation (Pattern①)

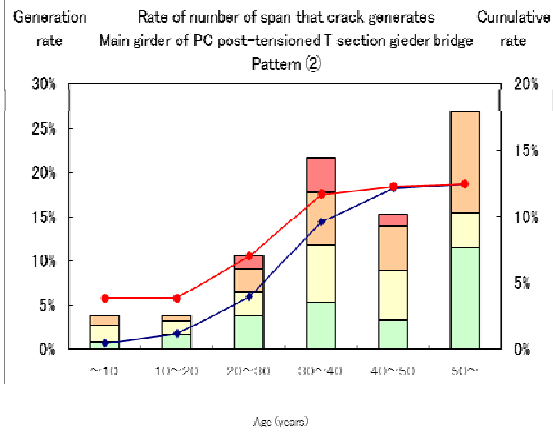


Fig.11 Age of PC post-tensioned T-section girder bridges and state of crack generation (Pattern②)

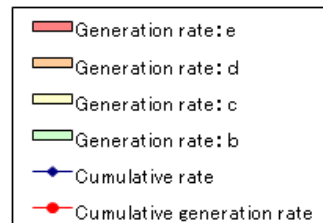
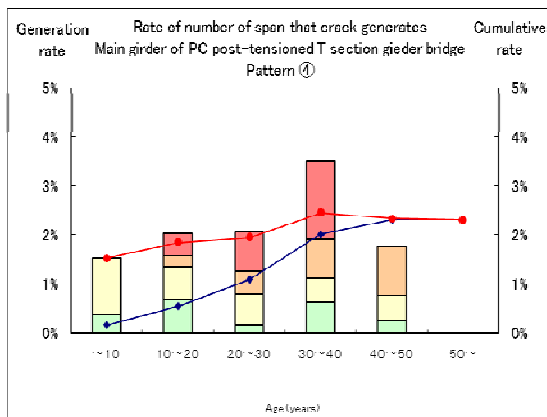


Fig.12 Age of PC post-tensioned T-section girder bridges and state of crack generation (Pattern④)

④ Corrosion at steel girder (difference of material)

Transition probability about corrosion at steel girder also calculated at general painting system and heavy-duty painting system. The result is shown in Fig.13.

The trend is that the speed of development at general painting system is quicker than that of heavy-duty painting system for small damage, but the difference is not notable for large damage.

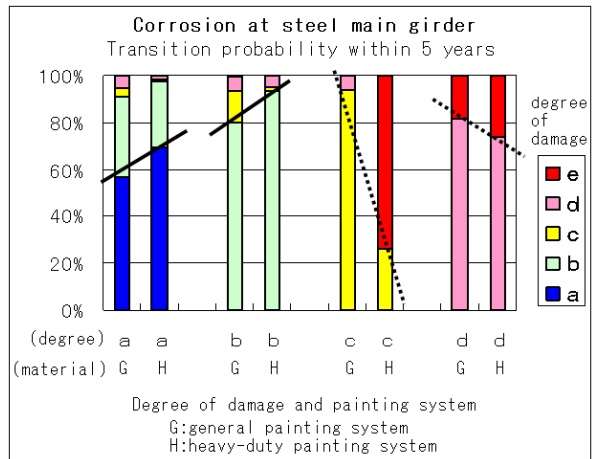


Fig.13 transition probability of corrosion at steel main girders

4) Analysis about fatigue

In the crack of steel member, the relationship of fatigue damage, age, and cumulative traffic volume was analyzed. The results of steel plate girder bridges and steel box girder bridges are shown in Fig.14, and the results of steel truss bridge are shown in Fig.15. The trend is recognized that the rate of generation of crack increases when the age gets more than 30 years, and cumulative large vehicle volume gets 250 thousand vehicles·year in steel plate girder bridges and steel box girder bridges, and that the rate of generation of crack increases when the age gets more than 30 years in steel truss bridges.

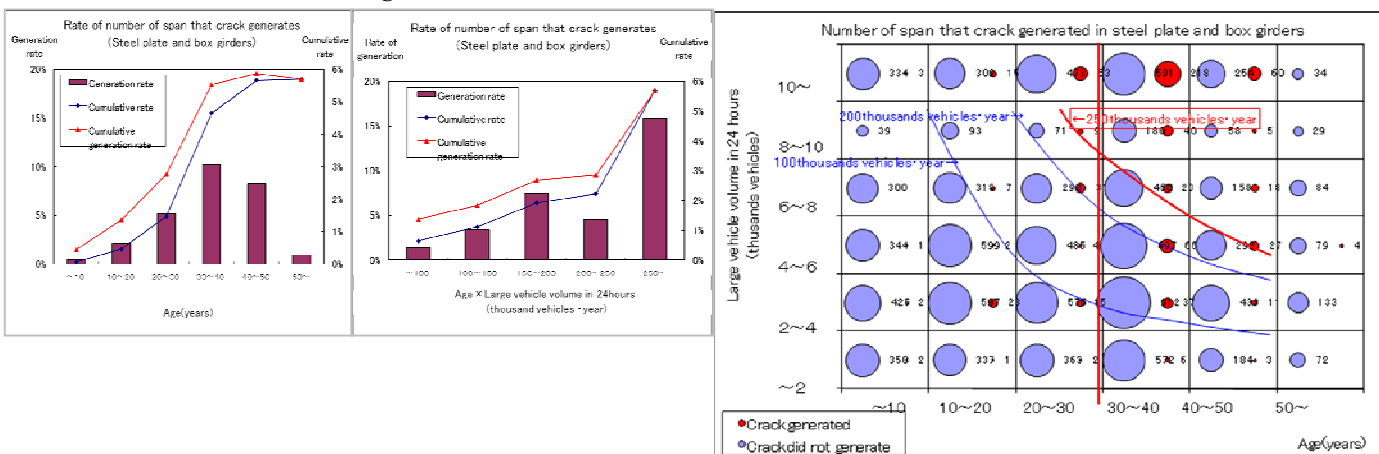


Fig.14 Rate of number of span that crack generates (Steel plate and box girder bridges)

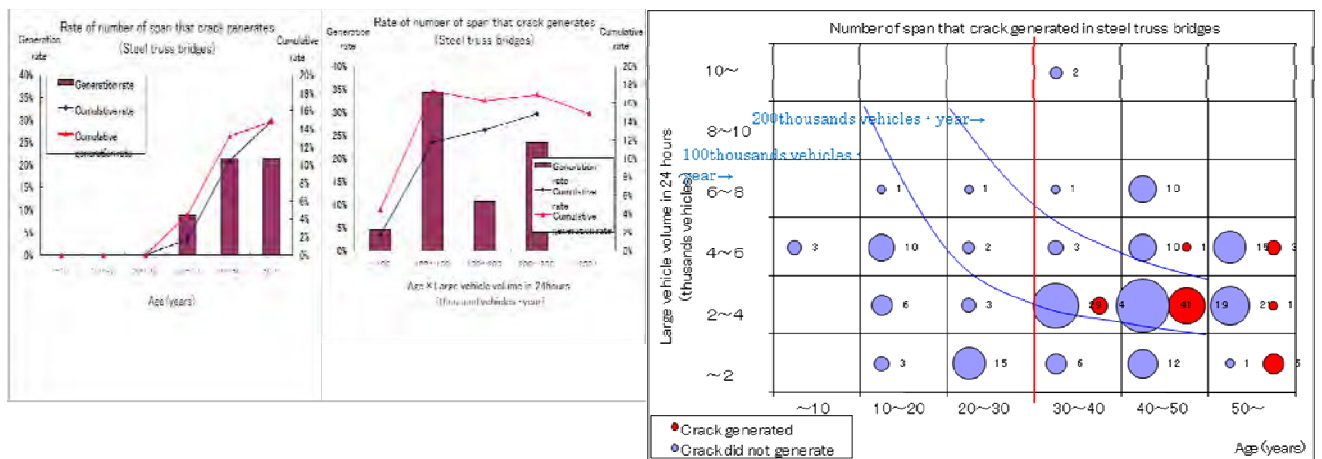


Fig.15 Rate of number of span that crack generates (Steel plate and box girder bridges)

The results about RC slab are shown in Fig.16. It could not be seen the damage's significant relationship with age and traffic volume. The damages might include the damage except for fatigue.

For fatigue damage of RC slab, damage progress patterns are being analyzed including states of leakage and isolated lime with crack. The result of analysis of crack patterns is shown in Fig.17

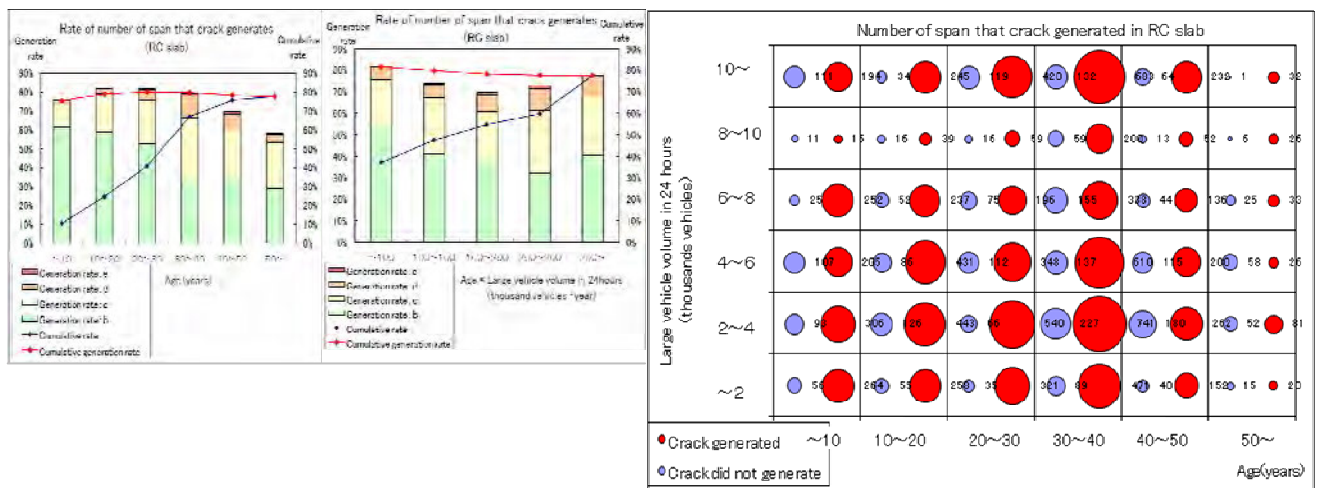


Fig.16 Rate of number of span that crack generates (RC slab)

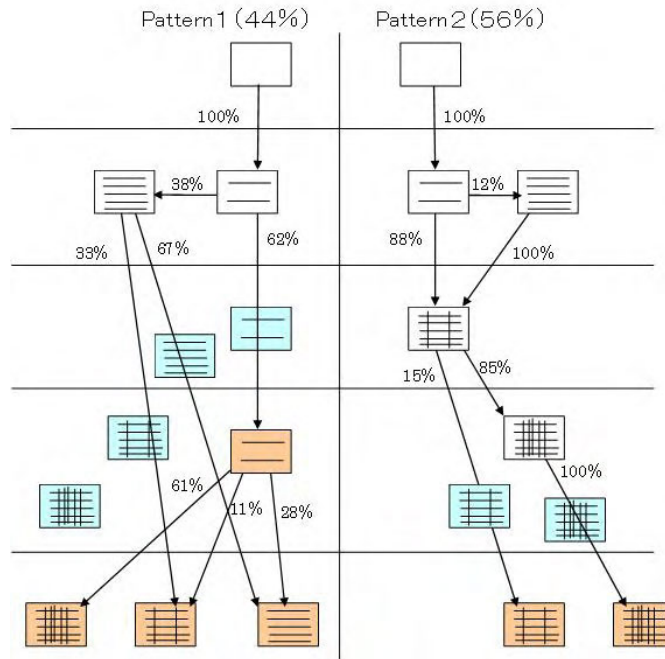


Fig.17 Analysis of crack patterns of RC slab

5) The relationship of degree of damage and classification of measure

The relationship of degree of damage and classification of measure in the case of crack at concrete main girder is shown in Fig.18. Both evaluations are not coincident. It can be inferred that engineers evaluate in classification of measure considering the bridge's unique condition like environment.

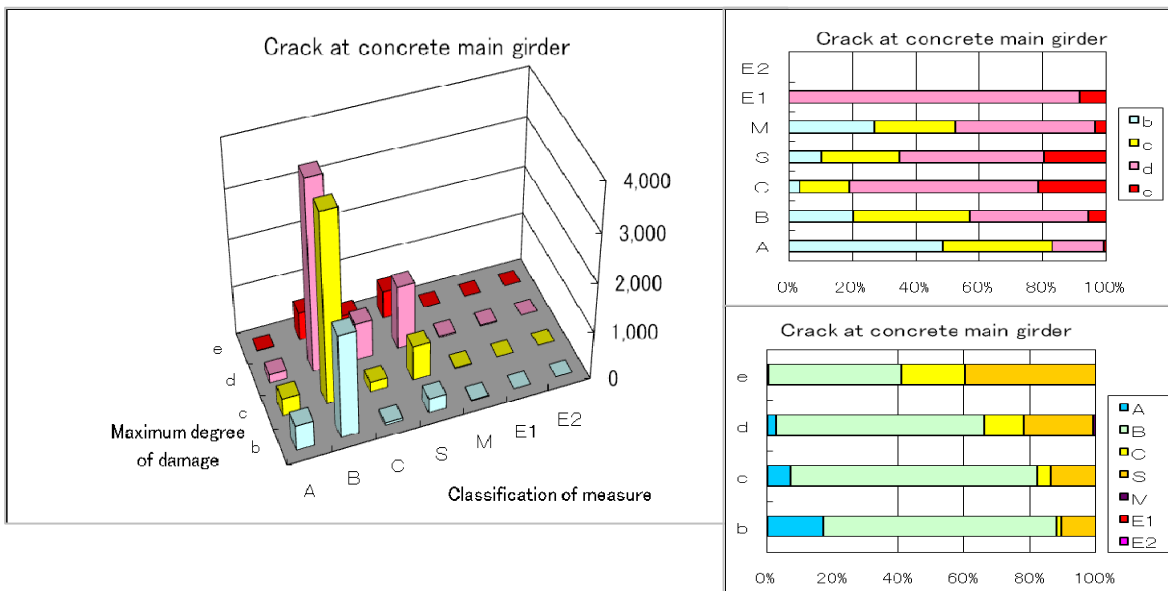


Fig.18 The relationship of degree of damage and classification of measure (crack at concrete main girder)

## Summary

Periodic inspection data has been analyzed to rationalize periodic inspection to get basic data in maintenance strategy and to grasp state of bridges for prevention of emergent accident and timely countermeasure like preventive maintenance.

The followings can be mentioned as findings from this analysis:

- 1) It is highly possible that there is a limitation to model deterioration characteristic because progress of deterioration is related to various factors such as construction environment, traffic condition, structural characteristic of whole bridge and every member.
- 2) Therefore, it can be referred that inspection method and frequency should be optimized according to not only common conditions such as structural characteristic and traffic but also individual part or member of the same bridge.
- 3) Degree of damage as “Objective fact” used for deterioration prediction and statistical analysis not always corresponds with evaluation based on performance of the bridge. Both of them are needed for maintenance.
- 4) Evaluation based on performance of the bridge should be considered each viewpoint of damage risk, emergency, preventive maintenance and so on for proper countermeasure.

Analyses of inspection results will be continued for an establishment of the rational bridge inspection system.

blank

# **BRIDGE INSPECTION & MANAGEMENT IN CALIFORNIA**

Barton J. Newton, PE<sup>1</sup>

## **Abstract**

This paper provides an overview of the California Department of Transportation (Caltrans) Bridge Management Program including inspection and investigations; special investigations including NDE/NDT technology; data management; prioritization and programming decision making; accomplishing bridge maintenance work; rehabilitation and replacement programs; and measuring performance.

## **Introduction**

California – the Golden State - boasts a growing, diverse population of 38 million people. For more than 50 years, California has embodied a spirit of innovation and entrepreneurship that has given birth to new technologies and industries while building the eighth largest economy in the world.

The backbone of the economic miracle that is California has been the construction, operation and maintenance of the finest highway system in the world. Caltrans is helping propel California's economic engine by spearheading \$9.5 billion worth of construction work that is supporting more than 170,000 jobs in this state.

Today, that system of highways and bridges safely and reliably carries millions of people and dependably delivers commerce to and from every corner of the state, the nation and the world. Not only is the work we are doing in California important to economic recovery, it's critical to America's economic strength in the worldwide economy as products that flow into and out of this country rely on a fully-functional nationwide transportation system. What we all do in the transportation business is important.

The California Department of Transportation is responsible for maintaining more than 15,000 centerline miles (50,000 lanes miles) of pavement and 12,600 bridges on the state highway system.

Taking care of its bridge inventory has been a critical part of California's success in making sure its transportation program continues to deliver reliable service year after year. In 1927, state leaders initiated a study to determine and document the condition, safe load carrying limits and other restrictions of each public bridge in the state and to develop progress reports with work recommendations. Out of that effort was born California's bridge inspection and maintenance program.

---

<sup>1</sup>State Bridge Maintenance Engineer, State of California Department of Transportation (Caltrans)

## **Inventory**

The California Department of Transportation, as the owner and operator of the state highway system, is responsible for the protection and preservation of the state's bridge inventory which has an estimated replacement value of more than \$52 billion.

California's bridge inventory is aging with about two-thirds of structures on the state highway system having been built between 1950 and 1980. Approximately 92% of California's state highway bridges are concrete, 7% steel with timber and composite materials comprising the remainder. Concrete box girders are the most common bridge type.

## **Bridge Program Goals**

California's bridge inspection and maintenance program has five goals:

1. To ensure the safety of the traveling public as required by Federal and State Law.
2. To manage the bridge assets to an agreed level of service.
3. To collect inventory and condition data
4. To recommend needed repairs, rehabilitation and/ or replacement
5. To determine safe load carrying capacity of each structure.

## **Structure Maintenance & Investigations**

As part of the Caltrans Division of Maintenance, the Structure Maintenance & Investigations (SM&I) organization is charged with ensuring the structural integrity of the 12,600 state highway bridge inventory and 12,500 bridges owned by local government agencies.

The SM&I staff performs bridge inspections and engineering investigations in accordance with federal regulations, makes repair work recommendations; investigates hydraulic problems and scour potential; determines the safe load carrying capacity of all bridges; reviews and approves encroachment permits and air space lease proposals for state-owned structures; manages the State's bridge funding programs; delivers plans specifications and estimates for maintenance and rehabilitation on state-owned bridge projects; and coordinates the protective coating work on more than 800 steel state-owned highway bridges. SM&I is also the Department lead responsible for responding to any type of bridge related emergency including earthquakes, floods, over height vehicles, and tanker fires.

There are over 180 bridge engineers, structural steel technicians and support staff in six offices within SM&I. Those offices are listed below.

1. The Executive Office located in Sacramento.
2. The Office of Structure Investigations, North located in Sacramento is responsible for performing bridge inspections of all types on State and Locally-owned structures in the upper 49 counties of the State.
3. The Office of Structure Investigations, South located in Los Angeles is responsible for performing bridge inspections of all types on State and

Locally-owned structures in the lower 9 counties of the State and maintenance repair design of state owned bridges in the southern part of the State.

4. The Office of Toll Bridge Investigations located in Oakland is responsible for the inspection, maintenance repair design and general custodianship of the major toll bridges in San Francisco bay area.
5. The Office Specialty Investigations and Bridge Management located in Sacramento is responsible for the special Fracture Critical and Underwater Investigations for specified bridges statewide. It also manages the Statewide Bridge Preservation Program (Capital Funded) and the Statewide Bridge Maintenance Program, and is responsible for the data management for all bridges in the state.
6. The Office of Structural Design and Analysis is located in Sacramento and provides design services for bridge repair projects, establishes the safe load carrying capacity for all bridges and reviews encroachment and transportation permits. In addition, hydrologic and hydraulic evaluations and investigations are also performed for all existing bridges over waterways by this office.

### **Inspection**

The foundation of the bridge inspection program is grounded on the requirements of the National Bridge Inspection Standards (US Code of Federal Regulations 23 CFR 650). California uses element level inspection protocols, visual and non-destructive testing techniques to assess the condition of each bridge on regular intervals between two to five years. The interval is based on the minimum federal requirements as well as a risk assessment of each bridge that considers type, actual condition, and redundancy of the structure and the judgment of the inspector.

Ensuring the safety and reliability of California's bridges is achieved through an ongoing effort of routine, fracture critical and underwater inspections performed by licensed engineers and specially trained structural steel inspectors. Federal regulations require that routine inspections be conducted every two to four years, fracture critical inspections every two years and underwater inspections every five years.

#### **Routine Inspections**

During routine inspections, inspectors who are licensed engineers look for any signs of distress that could compromise the structural integrity of a bridge. These inspectors assess the structural condition of the bridge, looking for any indications of potential problems. They examine the bridge deck – the riding surface- looking for cracks or other signs of distress. The inspectors, drawing on their expertise, can tell if cracks are superficial or signal something more serious. The conditions are documented, monitored, and repairs recommended if necessary. Inspectors also may order additional investigation if needed, such as NDE techniques or taking core samples of the concrete deck in for testing to the Caltrans laboratory to document and determine the extent of cracking etc.

The same process is followed on the superstructure—the structural members that support the deck. The Inspectors, relying on their knowledge and expertise and

using their trained eyes to identify any signs of distress. They will climb piers and use sophisticated equipment to access structural members of the bridge. Again, conditions are documented and repairs recommended as needed.

Finally, inspectors examine the surround areas and the substructure—the foundation of the bridge—looking for any signs of deterioration. As with the deck and superstructure, conditions of the substructure are documented and repairs recommended in a bridge inspection report.

### Fracture Critical Inspections

A nine member team of engineers and structural steel inspectors is responsible for inspecting more than 1,000 state and local agency steel structures. A fracture critical bridge has a steel member whose failure could cause a portion of or the entire bridge to collapse. The I-35 West Bridge that collapsed in 2007 in Minnesota was a fracture critical bridge.

All areas of fracture critical bridges are required to be inspected visually, within arms reach, every 2 years with the aid of lift equipment or an under bridge inspection truck to place the inspector within arms reach of the fracture critical element. Many times fracture critical inspections utilize non-destructive testing equipment to help find cracks in critical members that can be invisible to the naked eye.

### Underwater Inspections

Caltrans employs a full commercial certified underwater inspection team to perform bridge inspections and to respond to emergencies such as ship collisions with bridges.

SM&I's 11-member Underwater Inspection Team is responsible for ensuring the structural integrity of the supporting piers for more than 530 bridges including major bay crossings like the San Francisco-Oakland Bay, the Richmond-San Rafael and the San Diego-Coronado bridges. Inspectors look for any damage and scouring of bridge piers.

Underwater inspections of bridge piers are conducted in waterways from the Pacific Ocean and the state's major rivers to the California Aqueduct. These underwater inspections are designed to detect any loss of strength or the potential of scouring on bridge piers below the water surface.

### Non-Destructive Testing

Safety is enhanced through these inspections and by “rating” bridge components, such as the deck, superstructure, and substructure, and by the use of non-destructive evaluation (NDE) methods and other advanced technologies. Visual inspection is the primary method and technique used to perform bridge inspections in California. Type, location, accessibility, and condition of a bridge, as well as type of inspection, are some of the factors that determine what methods of inspection practices are used. When problems are detected, or during the inspection of critical areas, more advanced NDE tools are employed. On occasion, destructive tests are conducted to evaluate specific areas or materials of concern, or to help identify appropriate corrective work.

The inspection team utilize many NDE methods for steel structures such as liquid penetrant testing (PT), ultrasonics (UT), eddy current (EC), radiography (RT) and magnetic particle testing, strain gauging, acoustic emission (AE), and x-ray technology.

Methods utilized during inspections of concrete structures include impact echo, infrared thermography, ground penetrating radar, and strain gauges for concrete structures and elements.

### **Load Ratings and Transportation Permits**

The Bridge Ratings and Analysis Branch are responsible for establishing the safe load carrying capacity for all bridges and reviewing all overweight transport permits.

The unit completed 126 load rating analyses during the 2008/09 Fiscal Year, reviewed nearly 200 extra legal truck loads weighing more than 250,000 pounds. More than a third of these loads were more than 800,000 pounds. They also successfully routed one super load of more than one million pounds and four super loads of nearly one million pounds. All five loads were transformers.

The four loads of nearly one million pounds were manufactured in Southeast Asia, shipped to the Port of San Diego and transported to a storage facility in El Centro. The transformer weighting more than one million pounds was brought by rail from Houston to Fontana in San Bernardino County. The transformer was transported over California's road network to the Mexico/California border for eventual delivery to a new natural gas power plant in Rosarito, Mexico that will supply power to Tijuana and San Diego.

### **Bridge Data and Management**

SM&I serves as the repository of data and information about every state and local agency bridge in the state. This information includes a historical record of the condition of each bridge on the state highway and local road networks, including all the as-built engineering plans and all completed bridge inspection reports. Bridge inspection reports are prepared following each inspection. These inspection reports provide a living history of each structure. Our library of information contains more than one million documents and gives engineers easy access to the entire structural history of each bridge in California

Bridge needs arise from the deterioration of bridge components, vulnerabilities to scour and seismic forces, changing safety standards and emergencies/accidents involving bridges.

Bridge Inspection Reports serve as the basis for initiating repairs in a timely and cost effective manner to ensure that each bridge is safe and well maintained.

Caltrans uses the AASHTOWare Pontis Bridge Management System and other tools to help evaluate the needs and prioritize repairs to maximize the benefit of available preservation dollars. Caltrans employs a life cycle cost analysis approach to compare alternatives at the project level.

Caltrans has recently begun a movement to a utility based benefit cost analysis approach that can combine physical condition and risk into a single utility that can be objectively compared across bridges.

### **Bridge Maintenance Design**

There are four maintenance design units in SM&I, two in Sacramento and one each in Los Angeles and Oakland. A total of 32 design engineers and structural design technicians are responsible for delivering plans, specifications and estimates for a variety of bridge deck, superstructure and substructure structure preservation and repair projects.

The projects include methacrylate deck treatments and polyester overlays, joint seals, bridge rail repairs and foundation protection work. During the 2008/09 fiscal year, SM&I designers delivered engineering plans for more than \$135 million to repair 983 bridges around the state.

### **Research**

SM&I is actively involved in advancing the science of engineering to extend the service life and reliability of the state's bridges. In conjunction with the Caltrans Division of Research and Innovation, SM&I is involved in a variety of structural research efforts including the effectiveness of deck rehabilitation strategies and the use of sonar imaging to validate the structural integrity of bridge piers.

### **Preserving the Bridge Inventory**

California has an ambitious bridge preservation program designed to extend the reliable, productive service of the state's bridges. The preservation effort is comprised of three main components: Caltrans inspection and maintenance crews, major maintenance contract projects and the State Highway Operation and Protection Program (SHOPP).

Work recommendations are generated from information collected through bridge inspections. The work recommendations are addressed by the bridge crews or programmed into projects to fix joint seals, methacrylate deck crack sealing, bearing replacements, painting, polyester concrete overlays and replacing approach slabs.

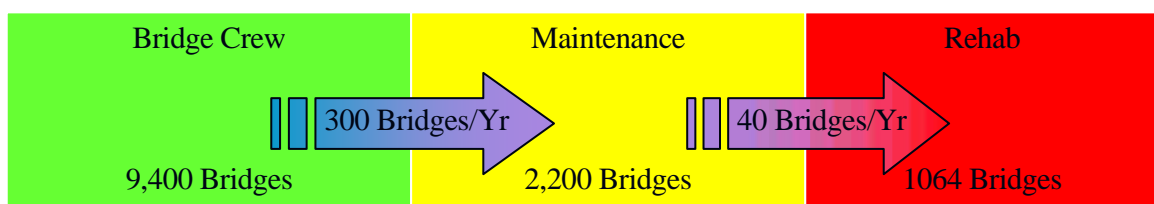
Projects are prioritized to address the most pressing needs first to ensure continued reliability of the system. Peer reviews are conducted by SM&I engineering staff on all bridge replacement and major repair project exceeding \$4 million to make sure that the recommended repair strategy is the best engineering and most cost effective alternative.

Caltrans invests \$67 million annually for inspection, bridge maintenance and bridge painting crews. The inspection effort is augmented by bridge maintenance crews performing minor repairs such as filling potholes on bridge decks and repairing minor bridge rail damage. They also respond to emergencies such as filling holes in a bridge deck to restore traffic service on a temporary basis until a permanent repair can be completed.

Bridge Paint crews are responsible for painting more than 800 steel bridges around the state. There are permanent painting crews assigned to some of the large Bay crossings such as the San Francisco-Bay Bridge. There also are general crews responsible for painting the other steel bridges up and down the state.

Caltrans is investing an additional \$93 million annually for major maintenance contract projects. These projects are designed to protect the bridges and extend their service life. Approximately 23% of California’s bridge inventory, 2,844 bridges, have major maintenance repair work recommendations pending.

Bridges like all physical assets will deteriorate over time and require maintenance, rehabilitation or replacement. The graphic below depicts the rate of progression of bridges from good (green) to fair (yellow) to poor condition (red).



The wear and tear of highway traffic, weather, and movement cause approximately 300 bridges to change from good to fair condition and another 40 bridges change from needing maintenance work to needing rehabilitation.

Caltrans bridge preservation approach is a three prong attack that strives to counteract deterioration:

1. Bridge crews employed by Caltrans address minor preservation very quickly to keep bridges in the green.
2. Major maintenance contracts are required when the scope of the work exceeds what the crews can do.
3. Major maintenance contracts are designed to delay or prevent the progression into the costly red rehabilitation/replacement area.

Major rehabilitation or replacement is required to address the bridges in the red area.

### Measuring performance

The United States government uses inspection data compiled by Caltrans engineers to calculate a complex formula called the sufficiency rating to determine federal bridge program funding eligibility. The sufficiency rating combines the condition and functional adequacy data collected on every bridge into a single aggregate number. Sufficiency rating values range from 0 (low) to 100 (high). If the sufficiency rating on a bridge is 50 or less and it is designated as “structurally deficient” or “functionally obsolete” the bridge qualifies for federal replacement funding. A low sufficiency rating number does not necessarily mean that the bridge is in need of repair.

Caltrans identifies prudent repair and rehabilitation projects taking into consideration many factors that may not be fully captured by these federal designations and ratings. For example, none of the federal designations or ratings take into consideration the need for seismic strengthening. Caltrans relies on the recommendations from its field assessments and analyses to develop repair projects. These repairs may be minor and assigned to Caltrans maintenance crews or they may be more involved and require further analysis or planning studies to determine the appropriate course of action. Caltrans utilizes bridge management system software tools that can forecast deterioration and conduct life cycle cost analyses along with multi-disciplinary peer reviews to develop our ultimate projects. Project decisions are made on a bridge-by-bridge basis.

Crews are measured on their ability to retire identified work within specified time frames. The Caltrans Five Year Maintenance Plan tracks the number of bridges requiring maintenance contracts and the SHOPP measures the number of distressed bridges with rehabilitation or replacement needs.

### **Emergency response**

Structures Maintenance and Investigations (SM&I) is the lead engineering responder to all emergencies involving existing state highway structures.

Operating from its three offices: Sacramento (North), Oakland (Toll Bridges), and Los Angeles (South), SM&I engineers are responsible for all matters involving the structural integrity of any highway structure damaged in natural disasters, accidents such as high load hits or other incidents. In the event of a disaster, the official damage report is prepared, stamped and signed by a licensed civil engineer at SM&I. The damage report is included in the Caltrans Bridge management database (SMART), which is maintained by SM&I.

Damage information is shared with the California Office of Emergency Services, which has responsibility for directing the statewide response to all disasters in the Golden State and the Caltrans Division of Maintenance which coordinates the response of maintenance forces around the state.

SM&I engineers have been at the forefront in responding to some of the most noteworthy natural disasters in the past 20 years including the 1989 Loma Prieta and 1994 Northridge earthquakes, the 2008 collapse of the MacArthur Maze connector ramp in Oakland due to a tanker truck fire and the collision of an oil tanker into the protective sheathing around one of the San Francisco-Oakland Bay Bridge's piers that resulted in one of the worst environmental catastrophes in state history.

# MEASURES FOR STRATEGIC PREVENTIVE BRIDGE MANAGEMENT OF TOKYO METROPOLITAN GOVERNMENT

\* Taro Awamoto<sup>1</sup>  
Sentaro Takagi<sup>2</sup>

## Abstract

Tokyo Metropolitan Government (TMG), Bureau of Construction has done periodic bridge inspection and has been corrective bridge maintenance. As aging bridge is increase, the possibility that serious accident is high. Finance limitation demand the peak project cost cut and reduce of total cost. Therefore we changed maintenance management strategy from corrective to preventive. We adopted New Public Management type Asset management. We developed some mechanism, which is deterioration model, social benefit, project prioritization method, and computer systems. Finally we planned “Long-Term Bridge Management Plan”. This paper reports our measures for strategic preventive bridge management of TMG.

## Introduction

TMG, Bureau of Construction, manages approximately 1,250 road bridges. Many bridges constructed in two periods. First period is reconstruction period from Great Kanto earthquake damage on 1923. Second period is high economic growth period from middle 1950s to early 1970s. (figure 1). For number of bridge, 52 percent are Reinforced concrete bridges or Prestressed concrete bridges, and 40 percent are Steel bridges. Whereas for area, only 12 percent is Reinforced concrete or Prestressed concrete and 56 percent is Steel (figure 2).

Bureau of Construction developed periodic bridge inspection every five years from 1987. The method is direct sight inspection as much as possible. Inspection contents are thirty one, which is corrosion, fatigue of steel girder, crack of concrete, and so on. Bridge health index is decided two steps. First, the condition of bridge is graded five ranks from ‘a’ to ‘e’ for member unit. Second, total bridge health index is graded five ranks from ‘A’ to ‘E’ for span unit and bridge unit, with used two index durability and safety. The deterioration of bridge progressed certainly, by the result of bridge inspection from 1987 to 2002. The rank C and D, which is required to rehabilitation, is increase (figure 3). The cause of steel girder bridge damage and deterioration is below. First is corrosion and deterioration of painting. Second is deformation caused by bearing has not work normally or foundation have moved. Third is fatigue damage by repeated heavy load. The damages of concrete bridge are confirmed fall of filling deck slab, free lime, and crack.

Bridge maintenance was corrective, when damage and deterioration was found, bridge took appropriate measures. TMG constructed many bridges in the 1960s, high economic growth period. We envisage the peak of bridge replacement cost is early 2030s, so that huge budget is need. Supposed from present TMG budget, increase of

---

<sup>1</sup> Senior Staff Member, Bureau of Construction, Tokyo Metropolitan Government

<sup>2</sup> Profession Director, Bureau of Construction, Tokyo Metropolitan Government

bridge management budget is not much expected. We need to try to decrease peak cost of bridge replacement and total bridge management cost. As bridge is aging, damage and deterioration is rapidly extended, it is difficult to the inspector find damage and deterioration. Thus, in the case of too late finding damage and deterioration to practice corrective measure, serious accident can occur. The I-35W bridge collapse in Minneapolis, Minnesota in the United States, 2007. In Japan, steel truss diagonal member broke on two bridges, Kisogawa Ohashi Bridge on National Road 23 and Honjo-Ohashi Bridge on National Road 7. Existent bridge is lack of usability and safety. It is not satisfy present design standard. Remaining this condition, the possibility of fatigue damage is high. A surrounded environment changed with progress of technique. Asset management methodology developed and tried to introduce on business in many countries. As the result of high level study, the technique of new material and new method of construction developed. Therefore the measure to long-life bridge without block traffic flow, is enable.

On a basis of the change of these situations, TMG change management strategy to preventive maintenance with asset management methodology. We decide try to decrease peak cost of bridge replacement, to reduction total bridge management cost, and to keep safety traffic. For important bridges, replacement of bridge is not executed because the replacement cost of these bridges is much cost needed. To satisfy present design and to make long-life bridges, maintenance cost decrease by performance based design. This paper reports present condition of measures of TMG.

### **Asset Management**

Asset management means generally the businesses which manage property substitute for owner and investor. The term used to use securities firm and real estate agent.

Recently, in the United States and other countries, Asset management methodology was introduced to operation and maintenance of infrastructure. FHWA created an office of Asset management in 1999. Now, Asset management is accepted among many agencies in the United States. In Japan, some local government are working on introduce of Asset management.

Japanese Asset Management method is two types. One type is LCC type, to try minimum life cycle cost and another type is New Public Management (NPM) type, to try maximum difference between value and cost (JSCE(2005)). NPM type is the advanced LCC type, to progressively and for invests. As we know, in Japan, local governments except TMG have introduced LCC type Asset management. Only TMG is introduced NPM type Asset management.

New Public Management is the movement to achieve public efficiency and progress of quality of work, by widely introduced private enterprise management style. The goal of the NPM type Asset management of TMG is, the government as agent of Tokyo metropolitan citizens, uses their tax efficiency to road infrastructure, and return effective and efficient public service to citizen or user. More specifically, the result of public investment, entrusted use of citizen tax, to maximum the effect tax payer received. Bureau of Construction make investment project plan to difference between benefit occurred from bridge exist and project cost.

## **Deterioration Model**

On preventive maintenance management, evaluate future condition of each bridge by deterioration forecasting and make plan which can execute appropriate measure on best timing is need.

We set original deterioration curve from past twenty decades bridge inspection data collection, calculated last bridge life length. The deterioration curve is calculated life-cycle analysis and non linear regression analysis. In the beginnings, we tried to set standard deterioration curve, with use linear curve as general deterioration curve calculation method. But there are almost no data the most danger health index 'E', we judged this linear curve do not mirror real deterioration and changed our policy to the above method.

The process of deterioration curve set is below. First, we divided bridge inspection data into twenty types by combination of three elements, member, material, and damage. And calculate the time to reach next rank by life-cycle analysis. Second, we made four alternative curve types, exponential convex curve type, linear curve type, second polynomial curve type, and third concave curve type. Each bridge deterioration curve is decided by select the most nearly curve type compared with the result of the life-cycle analysis (figure 4).

## **Social Benefit**

The achievement of NPM type Asset management of TMG is to maximize the difference between benefit Tokyo citizens receive and project cost. The benefit is imaginary profit, and we call social benefit it. Cost benefit analysis, which is used in economic and civil field, supply that the measurement method of some benefit. Setting on each benefit contents, we focused that the variations in traffic flow with project operation. We reasoned that the benefit Tokyo people received is difference benefit of With: the project is operated, and of Without: the project is not operated. We set five benefit contents, drive time shortening, driving cost reduction, comfort driving, environment load reduction, and traffic accident reduction.

Drive time shortening is based on the Cost Benefit Analysis manual (MLIT(2003)). We suppose drive time is increase because of traffic jam and diversion traffic by road construction. We estimate the difference of drive time with measure construction and without.

Drive cost reduction is also based on the same Cost Benefit Analysis manual. The target contents is except concerned with drive time, of the cost reduction by drive condition is improved. We estimated the cost, gas, grease, tire, maintenance, and depreciation.

Comfort driving is well ride and well handling operation. We can quantitative estimate the effect of improvement of road condition. The method is Willingness To Pay (WTP). WTP is the amount people would be willing to pay for the value. We estimated WTP by Contingent Valuation Method (CVM). We did a paper survey of 10,000 people lives in Tokyo in 2005, and estimated amount for good road condition.

Environment load reduction contents are air pollution, traffic noise, landscape, ecosystem, and energy. Executing our project, roadside environment is improved. We estimated five contents. CO<sub>2</sub>, NO<sub>x</sub>, PM, and traffic tremble was estimated by past

literature and existent data. Traffic noise was estimated by survey.

Traffic accident reduction is estimated three contents. One is human damage cost about driver, people in the car with driver, and pedestrian. Second is object damage cost about vehicle and construction that occurred damage by traffic accident. Third is variation in damages cost by traffic concentration.

### **Project Prioritization**

Project prioritization is decided by evaluation of the best combination of each bridge project. Index of project priority is Net Present Value (NPV). NPV is investment index, private enterprise use of project feasibility research. We define the best investment plan is not only obtain to minimum of project cost, but also achieve  $NPV > 0$  and obtain to maximum of the difference between benefit and cost. We developed loop program to decide project prioritization. This program can select the best project combination to maximum of NPV for 30 years. The project combination is calculated to prevent traffic concentration, by construction site with traffic restriction is close to each other.

### **Asset Management System**

We programmed application software which realized our plan, started operation of the asset management system in 2007. The system is consisted of calculation server, database server, web server, and firewall system. Server OS is Windows 2000 server and database soft is oracle engine. The functions of the system are database area and calculation area. By utilize accumulated data, the system can calculate various programs, deterioration prediction, project prioritization, and so on.

### **Long-Term Bridge Management Plan**

We made “Long-Term Bridge Management Plan” in 2009 with our asset management methodology. We predicted deterioration of bridge and decided the adequate timing for measures in every bridge. Each measure, concrete deck exchange to steel deck, steel girder to tied, and so on, set according to health index. The standard costs of each measure refer latest rehabilitation technique. We evaluated Life Cycle Cost (LCC) both corrective maintenance and preventive maintenance, and compared two. Finally, we decided project prioritization and finished this planning.

This plan is all the bridges is divided into three maintenance types; long-life, general and replacement. The measure to existent bridge, for earthquake and over loading, is also included.

The number of Long-life type maintenance bridge, is 212: high social value bridge, and the bridge that rehabilitation is difficult for the construction is serious affect to traffic. Kachidoki Bashi Bridge, Eitai bashi Bridge, and Kiyosu Bashi Bridge, they are nominated national important heritage, is included. For the Long-life type bridge, measure to obtain the lifetime more than 100 years by utilized new technology is executed.

### **Effects**

Executing this plan produces five effects: cost, benefit, environment, safety, and accountability.

First is the project peak cost cut and reduction of total project cost. The peak cost is cut by long-life measure is executed. The effect of the total project cost reduction is expected 1,100 billion yen (1,200 million dollars, if one dollar is 90yen), the total cost is 1,600 billion yen (1,800 million dollars) on corrective maintenance and the total cost is 500 billion yen (600 million dollars) on preventive maintenance based on this plan (figure 5).

Secondly, the best project combination plan can achieve to maximum of the difference between benefit and cost. We try to minimum of construction cost and device the combination of construction project. We keep road safety and save the benefit Tokyo citizens received.

The third is reduction of the load to environment. CO<sub>2</sub> emission is reduced by the life of bridge become long. Bridge replacement is decrease, quantity of used material becomes less, and the operation time of construction machine is decrease. When the bridge management strategy is change from corrective maintenance to preventive maintenance, CO<sub>2</sub> emission in thirty years is reduced 1,120 thousand ton, from 1,590 thousand ton to 470 thousand ton. For evaluating CO<sub>2</sub> emission, we adopted released unit as much as possible. We evaluated the emission data in each bridge, used the emission data of construction machine. The data is released from Japan Science Committee Engineering and Center for Advanced Engineering Structural Assessment and Research.

The fourth is save the road safety and secure. We can considerably loss the risk by the lack of safety. Because we estimate bridge condition by inspection, predict deterioration and damage, and execute preventive measures. The safety of bridge is secured by the measures for long-life bridge. Because executing the measure for over-load and earthquake can improve durability of bridge.

The Final effect is progress of accountability. We execute the project which based on the plan utilized with the asset management system, we can account about planning process and project assessment for Tokyo citizens.

## **Conclusion**

This paper reported about the TMG measure for bridge management; try to change management strategy from corrective maintenance to preventive maintenance.

“Long-term bridge management plan” have planned with developed Asset management system. The purpose is bridge replacement peak cut, reduction of total project cost, and save road safety. Some issues remain to steadily executing this plan: secure the project organization system, reconfirm project cost, training in-house engineers, and improving bridge inspection.

TMG forward preventive maintenance steadily, realizes effective and efficient bridge management for Tokyo citizens, and keeps road safety and secure.

## **References**

JSCE(2005), Challenge to Introduction of Asset Management, Gihodoshuppan, Tokyo,

pp.35-40 (in Japanese)

Ministry of Land, Infrastructure, Transportation, and Tourism (MLIT) (2003), Cost Benefit Analysis manual (in Japanese)

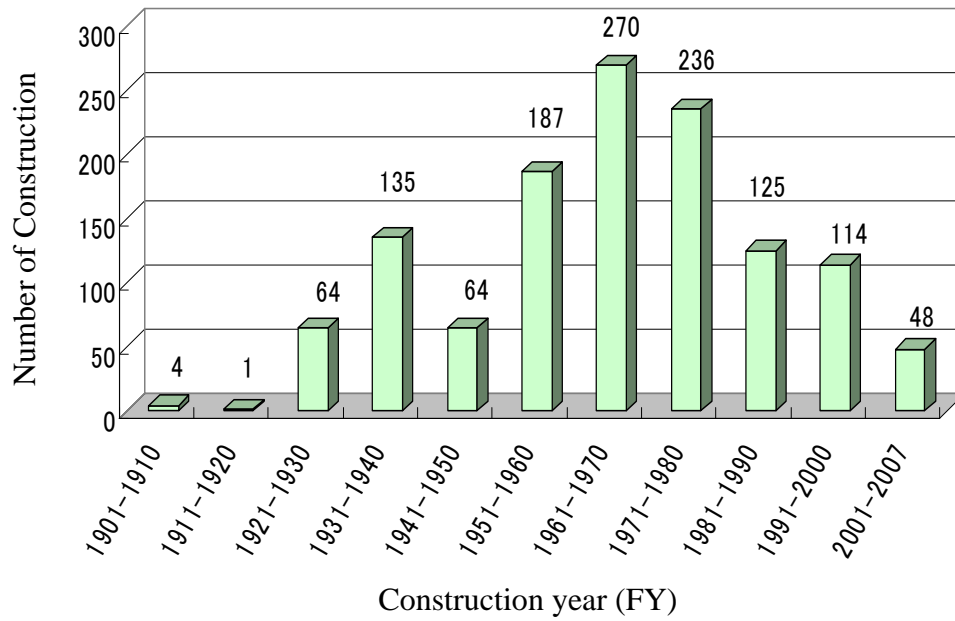


Figure 1: Distribution bridge construction year of TMG

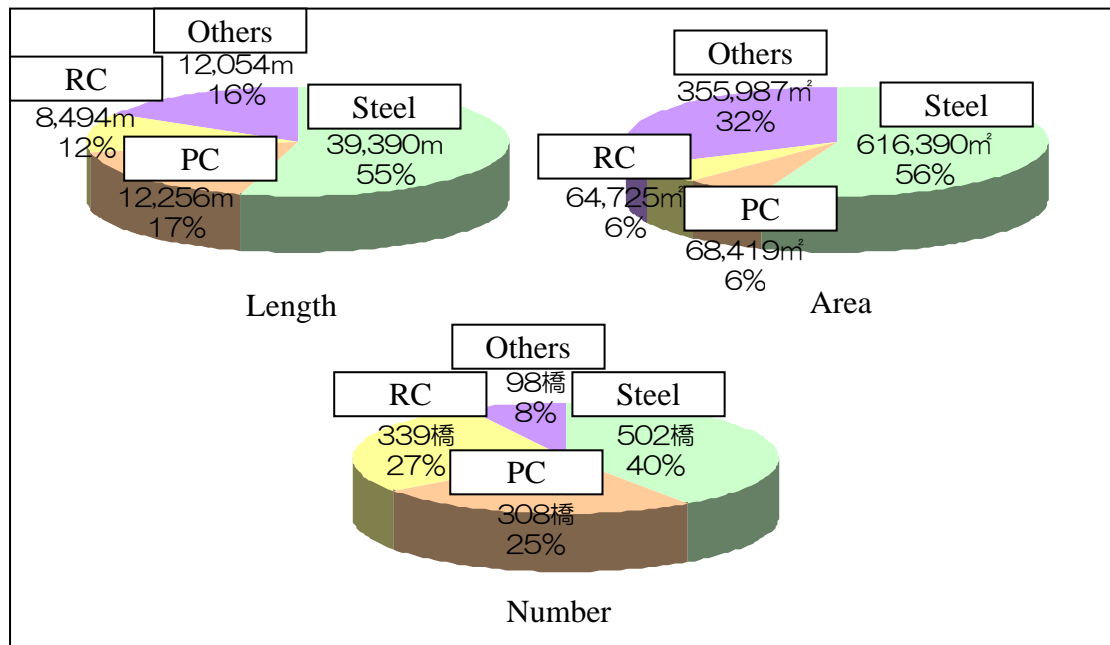


Figure 2: classification by material of TMG bridge

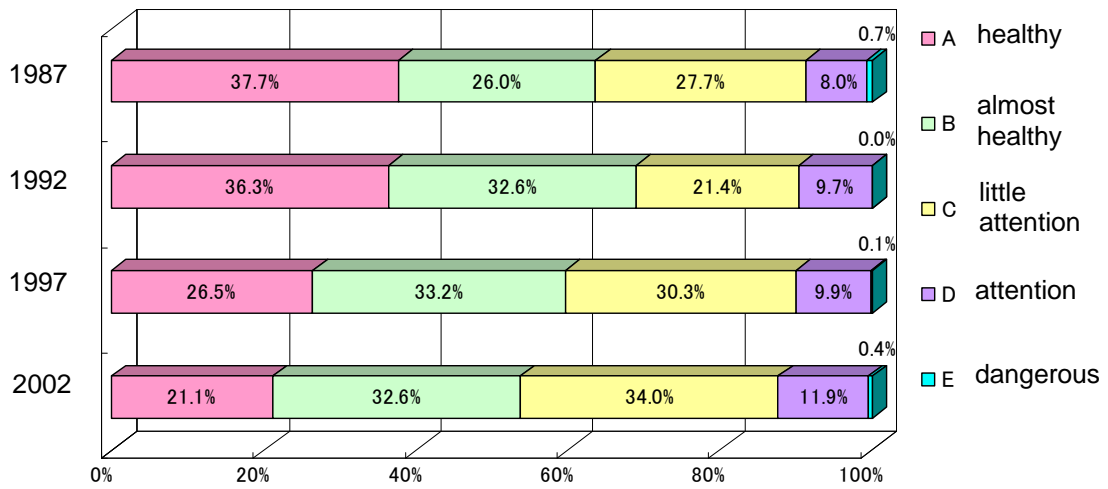


Figure 3: Progress of Bridge Health Index

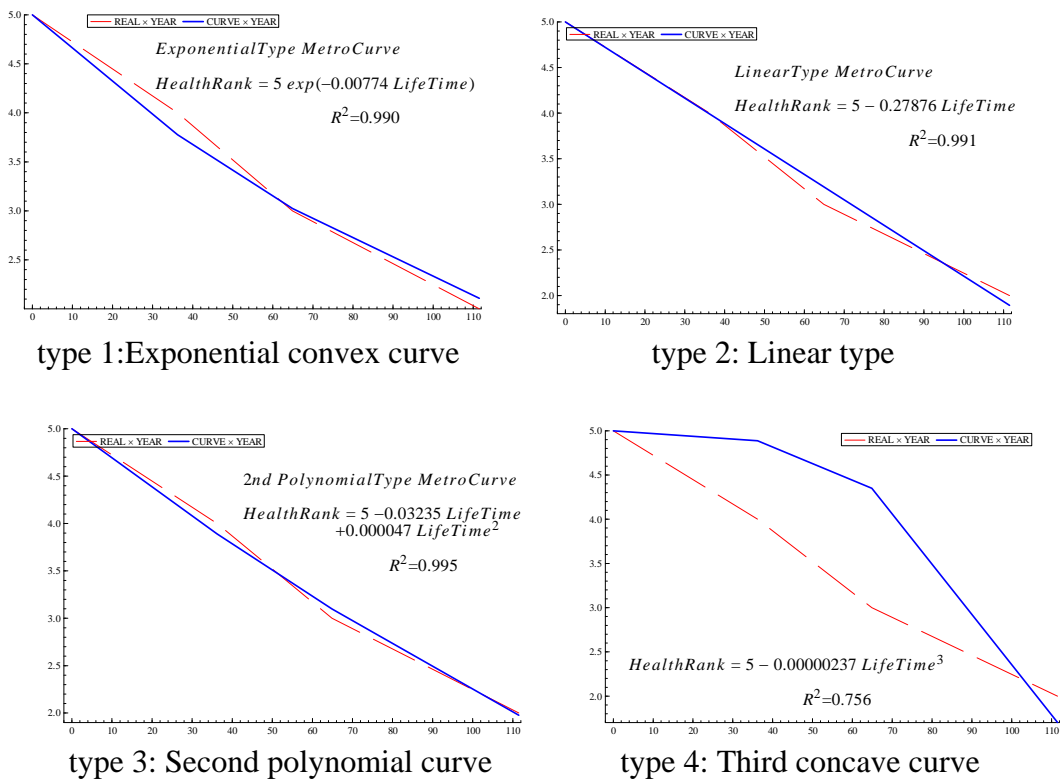


Figure 4: four alternative deterioration curve types

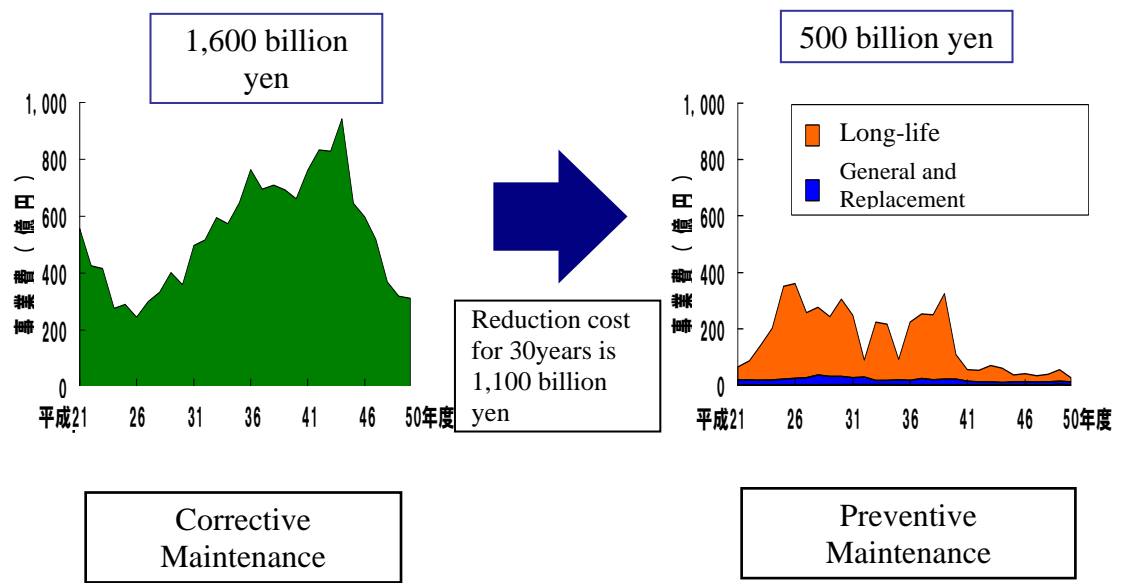


Figure 5: Project cost compared preventive and corrective

blank

## INSTRUMENTATION AND MONITORING OF I35W ST. ANTHONY FALLS BRIDGE

Catherine French<sup>1</sup>, Carol Shield<sup>1</sup>, Henryk Stolarski<sup>1</sup>, Brock Hedegaard<sup>2</sup>, Ben Jilk<sup>3</sup>

### Abstract

The I35W St. Anthony Falls Bridge, constructed to replace the steel truss bridge that collapsed in 2007, contains over 500 instruments to monitor the structural behavior. Numerical models of the bridge are being developed and calibrated to the collected data obtained during truck load testing and environmental loading. The data obtained over the first few years of monitoring will be correlated with the calibrated models and used to develop the baseline bridge behavior. This information will be used to develop a system to monitor and interpret the long-term behavior of the bridge. This paper describes the instrumentation, preliminary results from the data and model calibration, and plan for developing the long-term monitoring capabilities.

### Introduction

The I35W St. Anthony Falls Bridge, constructed to replace the steel truss bridge that collapsed in 2007, consists of two parallel bridges to carry northbound and southbound traffic. The four-span bridges consist of prestressed concrete box girders. Three of the spans were fabricated with cast-in-place concrete. The fourth span, the river span (i.e., Span 2), was fabricated with match-cast precast segmental construction. To accelerate the construction of the replacement bridge, the design-build approach was used. The proposal from the design-build team of Flatiron-Manson in conjunction with Figg Bridge Engineers featured the incorporation of a “smart-bridge” system. This system included instruments to monitor the structural behavior of the bridge, as well as instruments to control the anti-icing and lighting systems. Photographs of the bridge nearing completion of construction are shown in Figure 1. Figure 2 shows elevation views of the bridge which indicate the primary instrumented sections of the bridge and the variation in the cross-sectional shape of the boxes along the length of the bridge.

The University of Minnesota (UMN) is involved in the collection and interpretation of the data obtained from the more than 500 sensors installed within the bridge as part of the “smart-bridge” system. In addition to using the information obtained to better understand the behavior of prestressed concrete box girder bridges, the UMN researchers are developing a system which can be used by the Minnesota Department of Transportation to conduct long-term monitoring of the bridge.

---

<sup>1</sup> Professor, Dept. of Civil Engineering, University of Minnesota, Mpls., MN

<sup>2</sup> Graduate Research Asst., Dept. of Civil Engineering, University of Minnesota, Mpls., MN

<sup>3</sup> Engineer, Minnesota Department of Transportation, MN

## **Description of Instrumentation**

This section contains a brief description of the types of sensors installed in the bridge followed by the quantities of each instrument in parentheses. Sensors include a CorSenSys system (4), an example of which is shown in Figure 3, to monitor the corrosion susceptibility of the reinforcement within the deck. Information from this system can be used to determine when the deck needs to be resurfaced to prevent the chlorides from reaching the reinforcement layer and initiating corrosion. Additional instrumentation includes: strain gages to measure the deformations of the bridge (24 resistive, 195 vibrating wire [VW], 12 fiber optic); accelerometers to measure the vibrations of the bridge and to relate those measurements to structural deformations if possible (26); linear potentiometers to measure displacements of the expansion joints in the structure (12), and thermistors to measure the thermal gradients through the bridge cross section (243, including the thermistors associated with the VW gages). The vibrating wire strain gages and thermistor data are recorded statically at four to twenty-four times per day; whereas the accelerometer, resistive gage, and linear potentiometer data are recorded at up to 200 Hz continuously during the day, and then processed daily to save a shorter period of data coincident with the VW data, and the asynchronous major events of the day.

The strain, temperature, and vibration measuring systems in the bridge are distributed in several sections throughout each span of the bridge. A few sections are more heavily instrumented in order to investigate more detailed response which can be compared to the limited set of information obtained in the other sections of the bridge. The exterior box of the southbound (SB) river span (Span 2) contains three different types of systems (i.e., VW and fiber optic strain gages and accelerometers) that provide some redundancy and enable the evaluation of the relative effectiveness of the three different types of systems for consideration in future bridge monitoring implementations. Examples of the more heavily instrumented sections are shown in Figures 4 through 6.

Figure 4 shows the cross section of the SB bridge at midspan of Span 2 which has the largest number of VW gages. The gages oriented in the longitudinal direction, shown as solid circles in the figure, enable the measure of the longitudinal curvatures at midspan and the distribution of the strains across the top flange of the bridge. Pairs of transverse gages, shown as solid rectangles, are located to investigate the transverse curvatures at five locations across that section. The open circles in the figure indicate locations of additional sets of thermistors, with the numbers in the circles indicating the number of thermistors through the thickness at each location.

Figure 5 shows the SOFO (fiber optic) sensors which were located in Span 2 of the SB exterior box. These twelve gages were oriented in pairs at six locations distributed along the length of the span. Whereas VW strain gages have very short gage lengths (i.e., ~6 in. [~150mm]), the SOFO gages measure strains over 13 ft [4m] gage lengths. The sets of SOFO gages are expected to provide information on the overall curvature across the span which may be used to determine the deflections of the SB river span.

Accelerometers are located below the deck near midspan of each of the boxes. In the exterior box of SB Span 2, 14 accelerometers can be reconfigured in different orientations at different locations. Figure 6 shows the typical location of the accelerometers below the center of the deck (in all spans) and attached near the corner of the flange in Span 2 (i.e., typical configuration of 13 of the 14 accelerometers in Span 2). The accelerometers were attached near the corner of the flange to better measure the overall dynamics of the span without the influence of the local deck vibrations. The 13 accelerometers in Span 2 are currently distributed fairly uniformly along the length, with one gage at midspan of the deck to replicate the configuration in the other spans.

### **Truck Load Tests**

Prior to opening the bridge to traffic, a series of static and dynamic truck load tests were conducted on the evenings of September 14 and 17, 2008. The loads were provided by a series of eight heavily loaded sand trucks which were carefully weighed and measured before the tests. The vehicles each weighed approximately the same and had a combined weight of approximately 400 kips (1,800 kN). The trucks were positioned in a series of different pre-established configurations on the bridge. For the static tests, the trucks were stationed at each of the pre-established locations long enough to typically capture three readings. Several of these tests were also repeated over the course of the evening as time permitted. One of the configurations (ST I) is shown in Figure 7, for which case the eight trucks were positioned across the width of the bridge.

These tests provided valuable information used to calibrate numerical models of the bridge subjected to known loads at known locations. This information also provided a “baseline” for the measured behavior of the bridge. If desired, future truck tests could be conducted to compare the results to the initial baseline tests.

### **Finite Element Method (FEM) Model**

Finite element models were developed to provide means to interpret the data obtained from the bridge. The most current FEM model was created in ABAQUS using continuum (solid) quadratic 20-node elements with reduced integration. The benefits of the solid elements included the ability to accurately model the geometry of the complex cross-sectional shape and to simulate the thermal gradient through the section (node by node). The scope of the initial model was limited to the continuous three-span section of the southbound bridge, as shown in Figure 8, where most of the instrumentation was located. Boundary conditions were chosen to approximate the physical constraints on the bridge including Piers 2 and 3 (assumed fixed at the base and pinned at the top), with longitudinal expansion joints modeled at Abutment 1 and Pier 4. To model the steel and prestress present in the bridge, all post-tensioning tendons (with the exception of the draped external tendons) were approximated as shells embedded in the top and bottom flanges. Mild steel was assumed to be uniformly distributed throughout the section by adjusting the modulus of elasticity of the concrete to account for the additional stiffness introduced by the reinforcement.

All of the concrete in the FEM model was assumed to be normal-weight concrete. The specified material properties for the cast-in-place and precast concrete were initially used. Studies are currently underway at the University of Minnesota using concrete samples obtained from the bridge during construction to investigate the measured material properties of the bridge including modulus of elasticity, creep, shrinkage, and coefficient of thermal expansion. The results of these studies may be used to further refine the numerical models.

### **Calibration of FEM Model**

The results of the truck load tests were used to calibrate the FEM model. The results of the FEM model were compared to the measured data for the various configurations and positions of the static truck tests. Figure 9 shows the longitudinal strains and deformed configuration of the midspan cross section of SB Span 2 (magnified 2500 times) with loading to simulate truck orientation ST I (as shown in Fig. 7). Figure 10 shows the longitudinal mechanical strains obtained from the FEM model at the top of the deck and 6 in (150mm) below the top of the deck, relative to the VW strain gages assumed to be embedded at 6 in. (150mm) below the top of the deck. From the figure, it is evident that the trends in the measured data are similar to those obtained from the FEM model. The measured data better matched the FEM model results predicted to occur slightly lower in the section (e.g., at 7 in. [180mm] below the top of the deck). Differences between the measurements and the model may be attributed to sources including differences in the as-built and assumed cross section of the structure (e.g., the deck thickness was estimated to vary by approximately 1in.), and potential errors associated with the as-built locations of the sensors embedded within the structure.

In addition to calibrating the FEM model with the truck load tests, studies are underway to calibrate the model with the measured results due to environmental effects including the effect of the thermal gradient on the structure. Figure 11 shows thermal gradients measured through the cross section of the bridge obtained at four times over an 18 hour period. The effect of solar radiation has a dramatic effect on the thermal gradient through the section particularly in the April to late June time frame.

Following calibration, the FEM model can be used to investigate potential damage scenarios and how they might manifest themselves in the measured data.

### **Effects due to Temperature**

To illustrate the effects of temperature on the response of the bridge, the measured strains obtained at the top and bottom of the box section near midspan of SB Span 2 are shown in Figure 12 over a twelve hour period during the course of one of the truck tests. Note that the strain values in the plot were arbitrarily zeroed on September 1, 2008; it is the changes in strain that can be determined from the plot that are of importance. The peaks in the plot represent the strains when the load was positioned locally with respect to the instrumentation. It should be emphasized that the truck tests took place over the course of an evening, from approximately 5:00 pm to 5:00 am, so the effects of the solar radiation should have been minimized. From the

figure, however, the temperature variation during that time frame can be noted by the change in the readings of the bridge when it was unloaded. From this figure it is evident that the trucks caused a maximum local strain change of approximately  $20\mu\epsilon$  in the top gage readings.

Figure 13 shows the data from the same strain gages (i.e., in the top and bottom of the box section near midspan of SB Span 2) that were measured four times a day (i.e., midnight, 6:00 am, noon and 6:00 pm) over a ten month period (arbitrarily zeroed on September 1, 2008). As evident in the figure, the daily changes in total strain of the top gages ( $\sim 100\mu\epsilon$ ) due to the thermal gradient and temperature changes were nearly five times the magnitudes of those obtained during the truck load test with the eight trucks stationed across the bridge at this section (i.e.,  $\sim 20\mu\epsilon$ ). The seasonal changes in total strain were more than  $500\mu\epsilon$  for the same gages.

Besides having a significant effect on the strain measurements, the temperature changes also appear to affect other bridge properties including the modal frequencies. Preliminary data obtained from the accelerometer at midspan of Span 2 was used to determine the modal frequencies. To obtain this data, input averaging of 20 points was used on the dynamic data collected at 200 Hz over an approximately half hour period to obtain greater resolution in the frequencies in the 0 to 5 Hz range where the structural frequencies were expected to reside. The resulting Fast Fourier Transform (FFT) applied to the data showed three strong peaks at approximately 0.8 Hz, 1.5 Hz, and 2.3 Hz as shown in Figure 14, which compared reasonably well with the data obtained from the FEM model. In the FEM model, the frequencies around 0.8 Hz and 1.5 Hz represented bending modes, while the mode at 2.3 Hz was associated with a torsional mode. The FFTs were then applied to the data bimonthly, to investigate the consistency in the three noted frequencies over time. Figure 15 shows a sample of these results. The variation of the modal frequencies for the first mode is shown compared with the bridge temperature at the time of measurements. Data obtained for the other modes showed similar variations with respect to temperature. It appears that there is some correlation between temperature and bridge modal frequencies. As the temperature increased, all modal frequencies were observed to decrease. Further studies regarding this behavior are currently underway.

### **Plan for Development of Long-Term Monitoring System**

The data obtained over the first few years of monitoring the I35W St. Anthony Falls Bridge will provide a “baseline” that describes what is considered “normal” behavior of the bridge; however using the baseline data to establish absolute maximum and minimum bounds on the expected behavior of the bridge is not sufficient to identify abnormal behavior. As evident in the discussion of the measured data above, the environmental effects (i.e., temperatures and thermal gradients) have a significant impact on the bridge response. As noted in Figures 12 and 13 showing the top longitudinal strain data measured near midspan of SB Span 2, the thermal effects were observed to be approximately 25 times larger than the effect of eight fully loaded sand trucks stationed across midspan of the SB bridge. In order to provide a useful long-term bridge monitoring system, it is important to be able to discern the

relationship between the thermal effects and the behavior of the bridge. The desire is to provide a range of “moving” bounds that are related to the range of expected results associated with the measured thermal gradients. The FEM model which has been calibrated to both the truck load data and the data associated with thermal effects will serve as a useful tool in this regard. Any changes in expected behavior outside of the “moving” bounds will provide a means to signal when the response of the bridge may need further investigation or when maintenance needs to be performed.

One of the challenges is that no “turn-key” system for monitoring bridges such as this exists. The monitoring system has to be created where the inputs from the bridge (i.e., measured temperature distributions and expected traffic loads) can be combined with other information (e.g., measured strains) to identify anomalies in behavior. In order to provide a range of “moving” bounds, the calibrated FEM model will be used to establish relationships between the thermal gradient effects and the expected responses from the sensor data. As an example, a “look-up” table may be developed that could correlate the measured data obtained from the thermistors to the measured data from the other types of sensors (e.g., strain gages and linear potentiometers).

Figure 16 shows a schematic that illustrates the plan for the structural monitoring system under development. In the schematic, the raw *data* from the multiple dynamic and static acquisition systems is collected and *analyzed* or processed. The outputs of the processed data are then considered either *model input* (e.g., thermal effects) or *response* (i.e., measured responses of the bridge associated with the measured model inputs). The *model input* is used to determine *expected response* (e.g., expected bridge curvatures, deflections, etc.), by means of a “*passive*” or “*active model*.” A “look-up” table, as described above, is an example of a “*passive*” *model*. An example of an “*active*” *model* would be a study with the calibrated FEM model to investigate an intermittent load test of the bridge. The *expected responses* from the *active* or *passive models* would be *compared* to the measured “*response*” of the bridge. The system would then *output* the results of the comparison to the bridge management engineer. Example outputs include notifications when the measured *responses* are out of range of the *expected responses* which may warrant further examination.

The system will also be designed to notify the bridge management engineer when any problems are encountered with the data collection system, such that steps may be readily taken to avoid the loss of information. One of the challenges with the large volume of data collected with the system is the large amount of storage required to retain data. The system under development will be designed to cull the collected data to maintain sufficient information to ensure gradual changes in behavior are documented without causing overwhelming long-term storage demands.

## **Summary**

A long-term structural monitoring system is being developed by the UMN for the I35W St. Anthony Falls Bridge. This structure contains over 500 instruments which includes sensors to monitor corrosion susceptibility, accelerations, strains, and movements at the piers and abutments. Numerical models of the bridge have been developed and calibrated to the collected data obtained from truck load tests, while studies are currently underway to calibrate the model to environmental (thermal) loading. The data obtained over the first few years of monitoring will be correlated with the calibrated models and used to develop the baseline bridge behavior. Because the thermal effects have such a significant impact on the response of the bridge, one of the challenges in developing the long-term structural monitoring system is the creation of “moving bounds” to distinguish when the response of the bridge is out of the expected range. The long-term monitoring system is being designed as a tool for bridge management engineers to investigate when the response of the bridge requires further evaluation and when maintenance may need to be performed.

## **Acknowledgments**

This research is sponsored by the Minnesota Department of Transportation (Mn/DOT). The views expressed herein are those of the authors and do not necessarily reflect those of the sponsors.

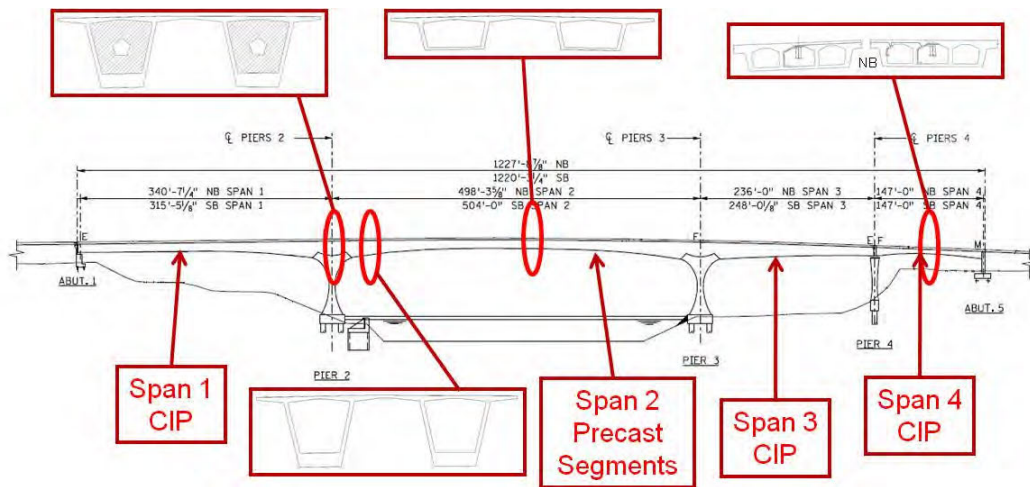
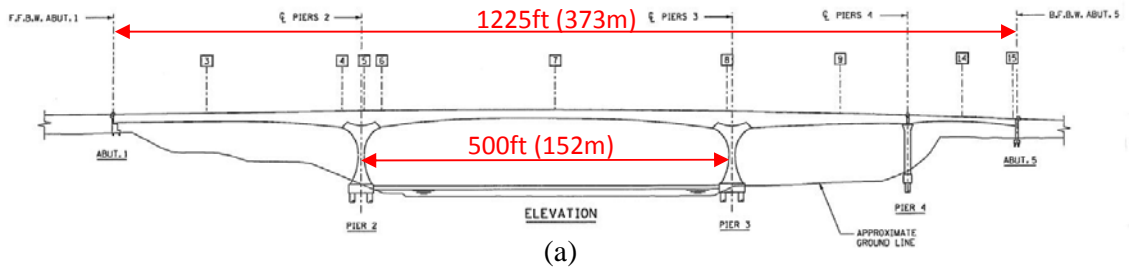
## **Unit Conversion**

1 in. = 25.4 mm

1 k = 4.448 kN



FIGURE 1: PHOTOS OF THE I35W ST. ANTHONY FALLS BRIDGE DURING CONSTRUCTION



(b)

FIGURE 2: ELEVATION VIEWS INDICATING (a) INSTRUMENTED LOCATIONS AND (b) CROSS-SECTIONAL SHAPES ALONG THE BRIDGE



FIGURE 3: EXAMPLE OF CORSENSYS CORROSION SENSOR INSTALLATION

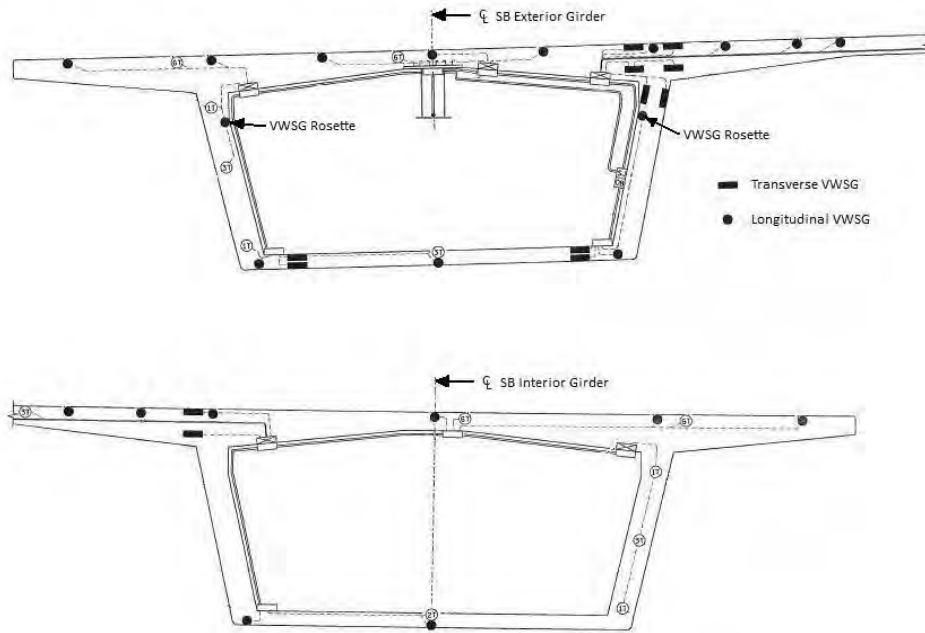


FIGURE 4: VIBRATING WIRE STRAIN GAGE LAYOUT FOR MIDSPAN OF SPAN 2 OF SOUTHBOUND BRIDGE (LOCATION 7SB)

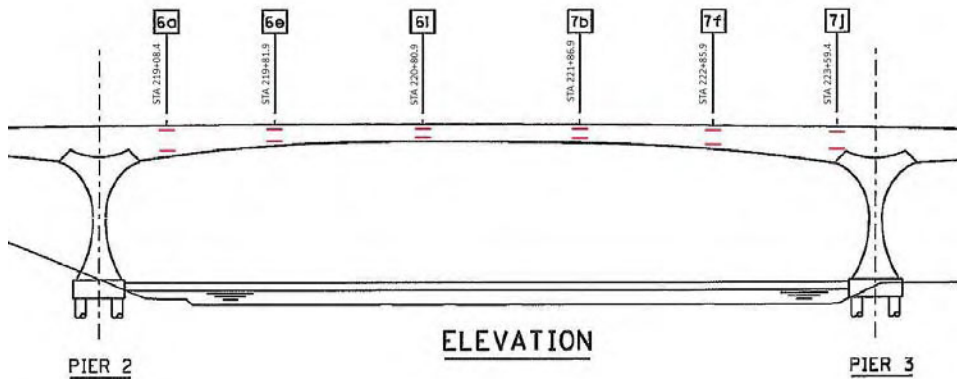


FIGURE 5: SOFO SENSOR LOCATIONS ALONG LENGTH OF SPAN 2 OF SOUTHBOUND BRIDGE EXTERIOR BOX

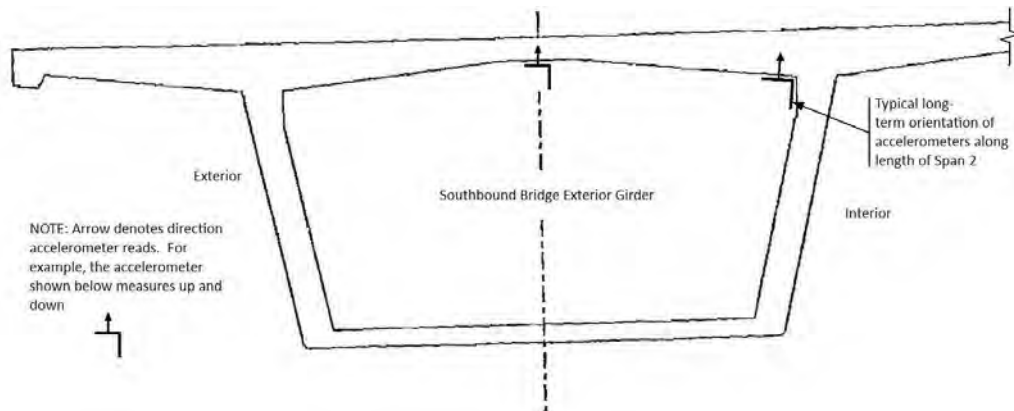


FIGURE 6: ACCELEROMETER LAYOUT IN THE SOUTHBOUND BRIDGE

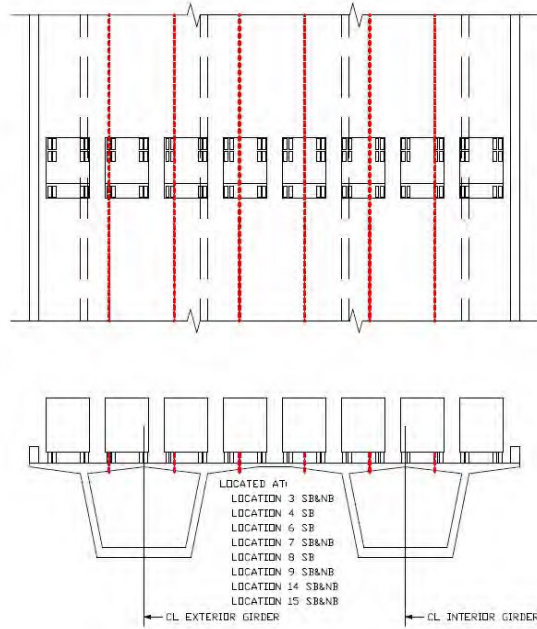


FIGURE 7: TRUCK ORIENTATION ST I

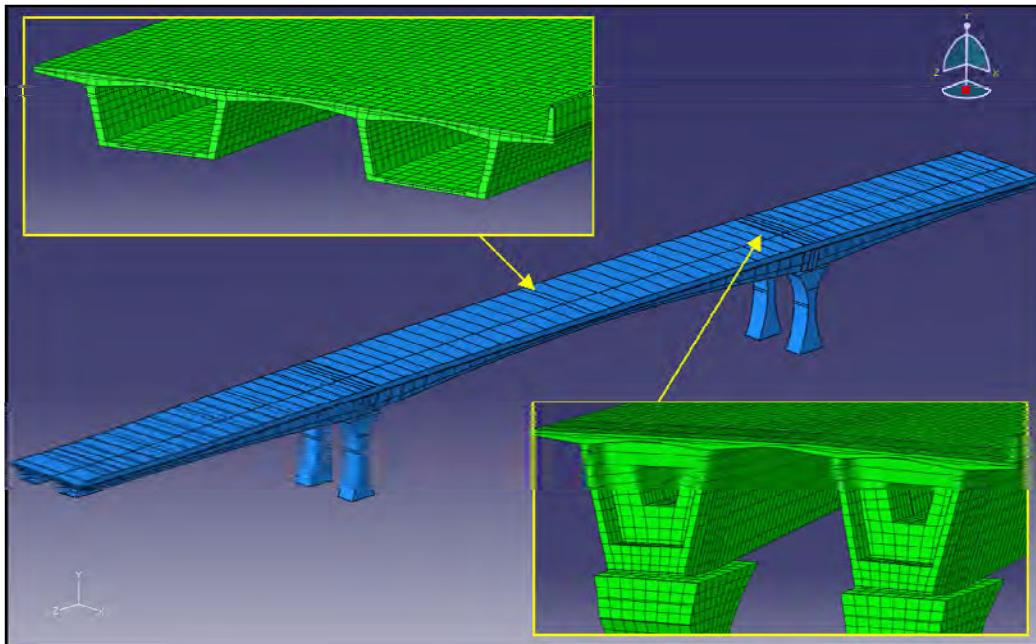


FIGURE 8: FINITE ELEMENT MODEL OF I35W ST. ANTHONY FALLS BRIDGE

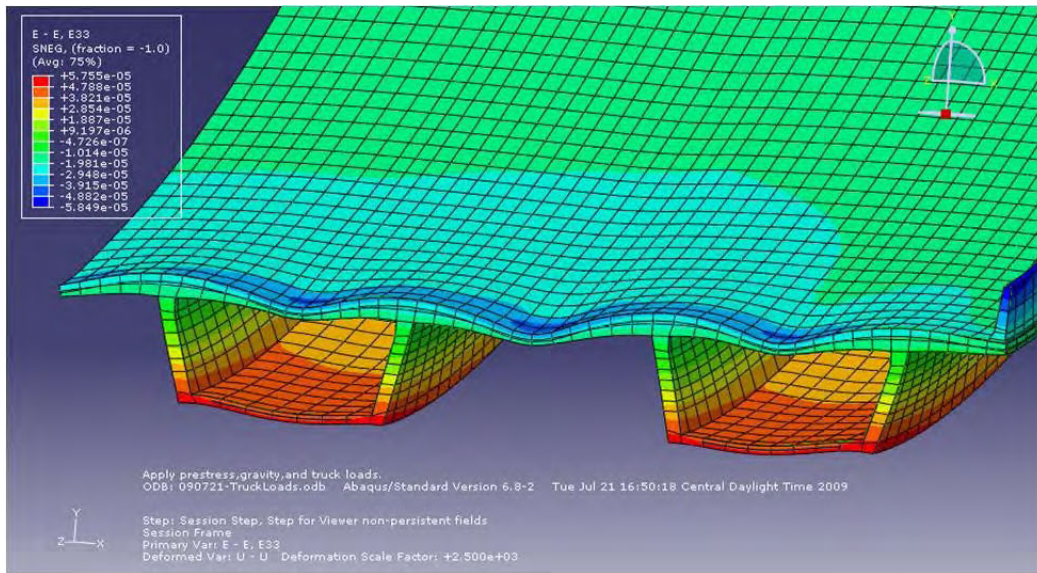


FIGURE 9: LONGITUDINAL STRAINS AT MIDSPAN OF SPAN 2 UNDER TRUCK TEST STI-7SB (DEFORMATIONS MAGNIFIED BY 2500)

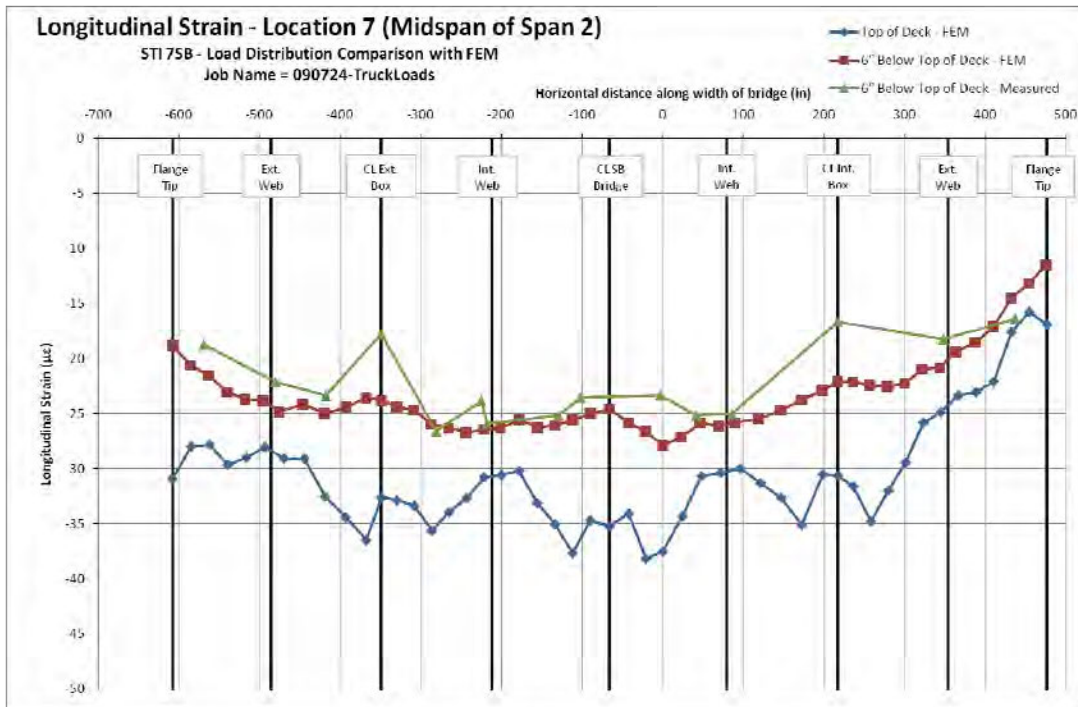


FIGURE 10: LONGITUDINAL MECHANICAL STRAINS ACROSS SECTION (MIDSPAN OF SB SPAN 2)

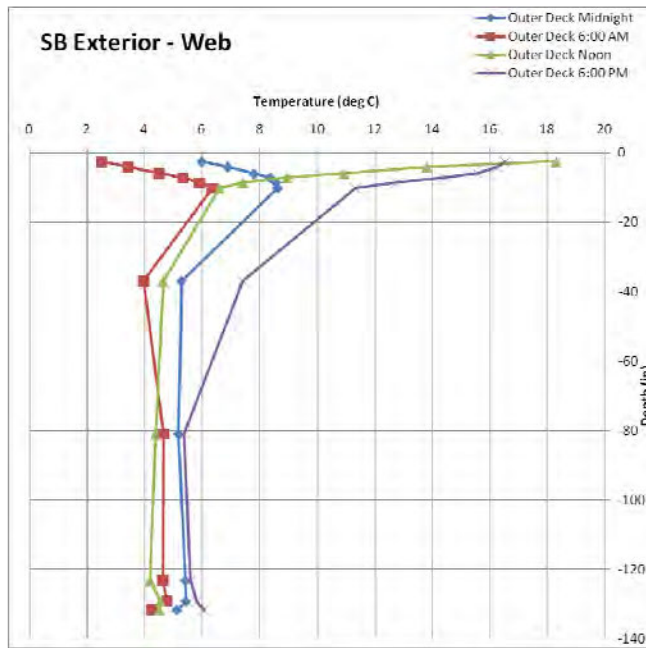


FIGURE 11: MEASURED THERMAL GRADIENTS THROUGH THE SECTION DEPTH OF WEB (MIDSPAN OF SB SPAN 2) 4/9/2009

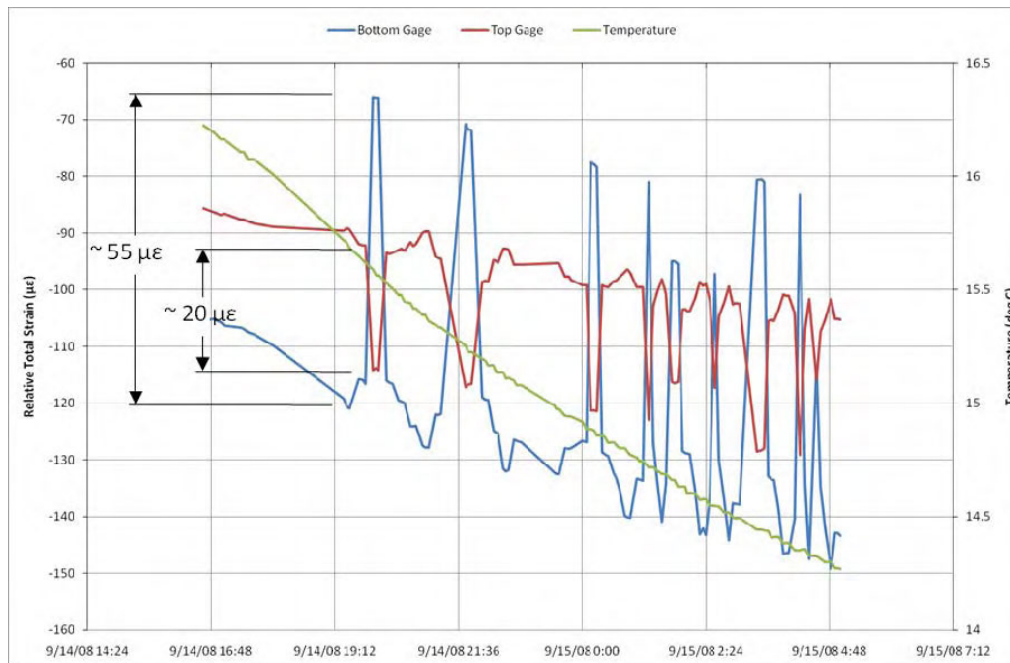


FIGURE 12: MEASURED TOP AND BOTTOM TOTAL STRAINS (MIDSPAN OF SB SPAN 2) AND TEMPERATURE VARIATION VS. TIME DURING TRUCK TESTS

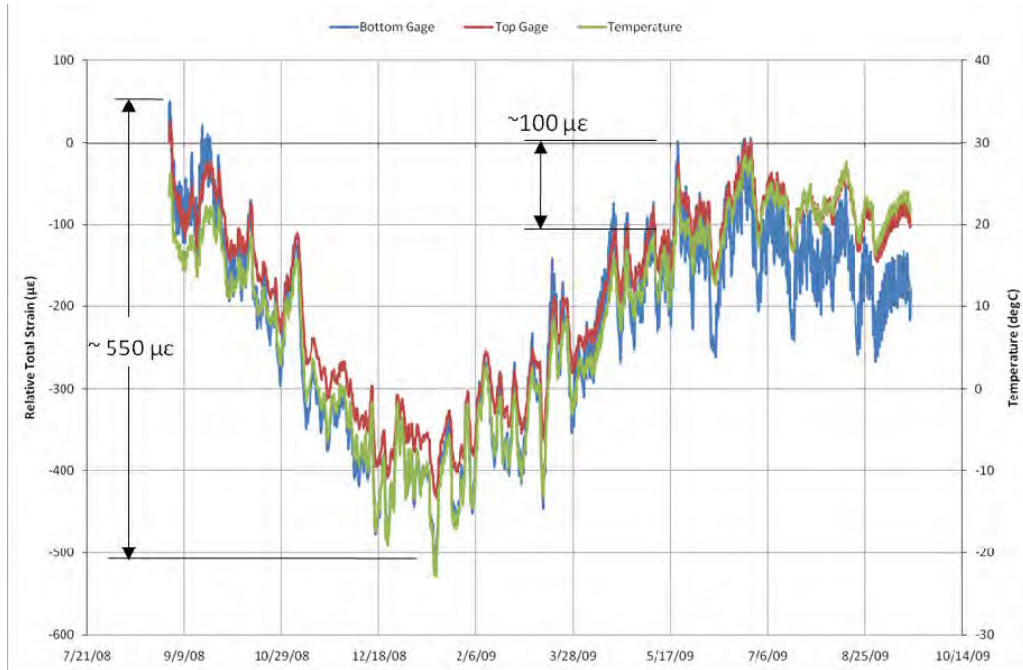


FIGURE 13: MEASURED TOP AND BOTTOM TOTAL STRAINS (MIDSPAN OF SB SPAN 2) VS. TIME (OVER 12 MONTH PERIOD)

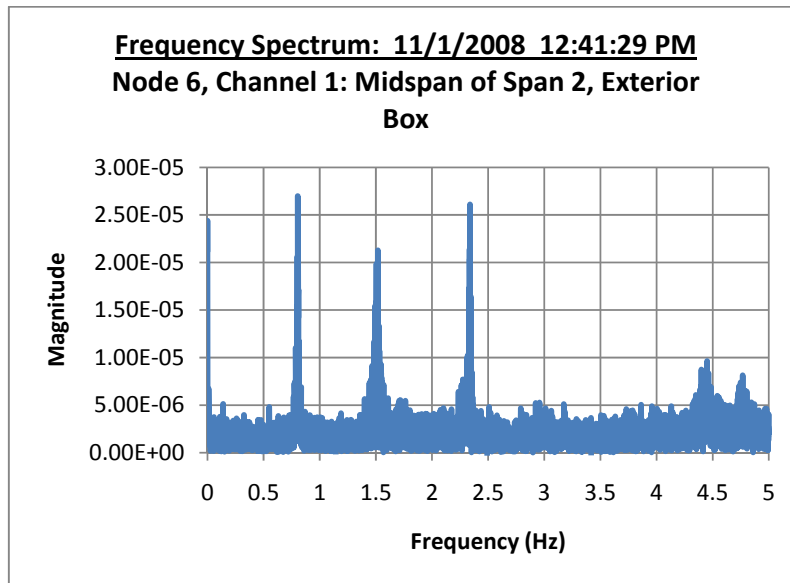


FIGURE 14: MODAL FREQUENCIES OF SPAN 2 ON 5/9/2009

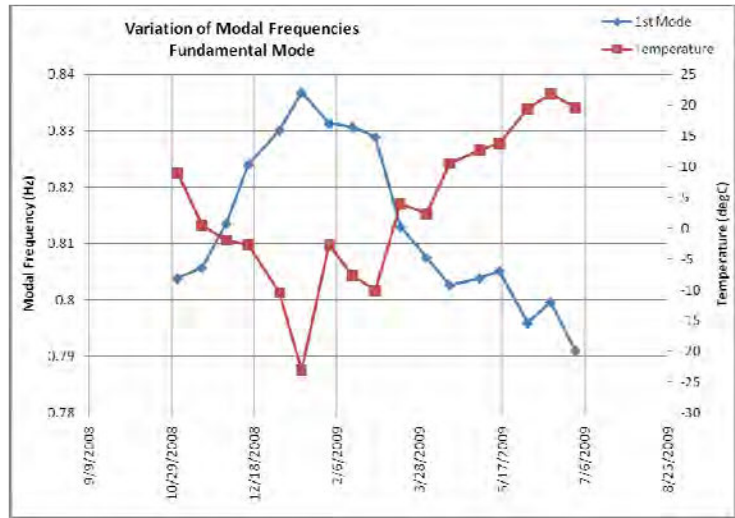


FIGURE 15: MODAL FREQUENCIES OF SPAN 2 (OVER EIGHT MONTH PERIOD)

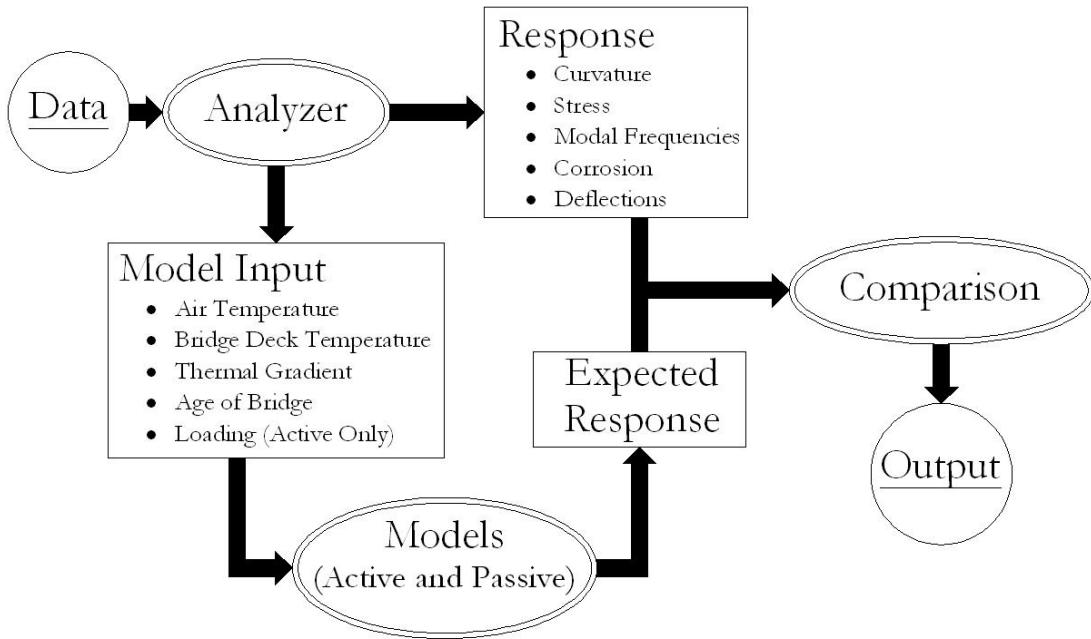


FIGURE 16: SCHEMATIC FOR DEVELOPMENT OF STRUCTURAL MONITORING SYSTEM

## Study for Bridge Renewal and Repair by Osaka Municipal Government

Shinsuke Yumoto<sup>1</sup>  
Tetsuya Yokota<sup>2</sup>  
Yasutomo Komatsu<sup>3</sup>

### Abstract

There are 764 bridges which managed by Osaka Municipal Government (incl. about 100 old bridges that over 70 years old)

Although many old bridges will be 100 years old in coming 30 years, to replace the all old bridges within 30 years is impossible when consider the financial pressure in Osaka city. Therefore, it provided the replacement plan refereed to the Study Group.

Specifically, Osaka Municipal Government created the own Replacement Judgment Policy through the Evaluation of Health Assessment by bridge inspection and Evaluation of Functionality by structure collation. This is the report of the Judgment Process.

### Introduction

Osaka is the second big city next to Tokyo where has an area of about 222 km<sup>2</sup>, population is about 2,600,000 that is the metropolis in the western part of Japan (Fig.1).

There are many bridges which loved by citizens such as Tenjinbashi-Bridge, Tenmabashi-Bridge and Naniwa-Bridge (Naniwa major three bridges). Osaka is called “Naniwa Happyaku-Ya-Bashi” whereas Tokyo is called “Edo Happyaku-Ya-Cho”.

Osaka Municipal Government is managing about 764 bridges (Bridges Area is about 720,000m<sup>2</sup> (2009.1st. Apr.), including Consecutive viaducts (such as Midosuji to have traffic density more than 100,000 per day) (Photo. 1), long bridges over the vast river, well known bridges (Photo. 2), and many kinds of bridges.

On the other hands, many bridges were constructed during the First City Planning Stage, started from 1921, the ratio of old bridges which over 50 years old



Fig.1 Location of Osaka

<sup>1</sup> Public Works Bureau, Osaka Municipal Government, Osaka, Japan

<sup>2</sup> Public Works Bureau, Osaka Municipal Government, Osaka, Japan

<sup>3</sup> Public Works Bureau, Osaka Municipal Government, Osaka, Japan

holds about 20% of all bridges. Compared with about 6% of the Japanese average, it indicates that how the aging of the bridge progress in Osaka city. Furthermore, about 100 bridges will become 100 years old in coming 30 years (Fig.2). To provide of the maintenance principle for these old bridges becomes the urgent important problem.

Osaka Municipal Government is considering maintenance and the replacement plan with the Study Group on the Bridge Maintenance and Renewal of the Osaka Municipal Government from 2007. This is the report of the maintenance process of the old bridges through this examination.

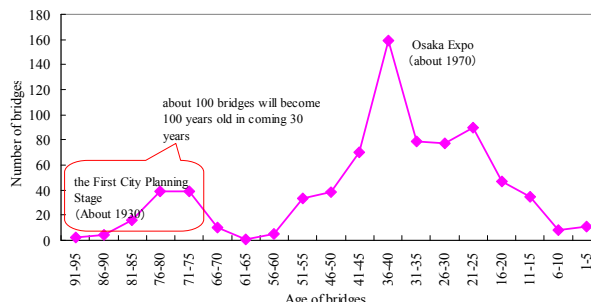


Fig.2 Distribution of the Number of Bridges (As of Apr.1, 2008)



Photo 1 Shinmido Viaducts



Photo 2 Naniwa Bridge

### The background of the examination

Recently, Osaka Municipal Government is very severe financial status. Although it controlled to build the new bridge and replacement such as reconstruction costs or the earthquake proof construction, cost reduction by new maintenance technique is demanded. It because that the conventional expense measure was insufficient. (Fig.3)

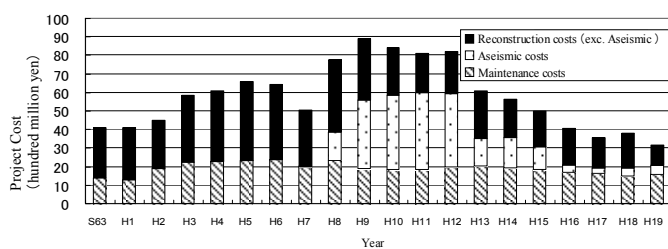


Fig 3 The Process of the Bridge Business Expense

Osaka Municipal Office has started to operate the Bridge Maintenance System (OBMS) since 2005. OBMS was developed from 2003 which introduced technique of the asset management.

Although Osaka Municipal Office is basis on the bridge prolongation by the

prevention maintenance, it found out that replacing the minimum percentage of bridge is very important. Therefore, it required classify bridges into prolongation and replacement to consider the maintenance and the replacement plan for old bridges. Next contents are explaining the process of Replacement judgment.

**Replacement judgment policy of old bridges**

As an object of 100 super old bridges older than 70 years old which constructed before WWR II (except the bridges which have replacement or removal plan), Osaka city had made the 1st selection for bridges which necessary the detail analysis through the Replacement judgment matrix. Then, evaluated general evaluation based on LCC analysis and selected bridges which are necessity renewal or not (Fig.4).

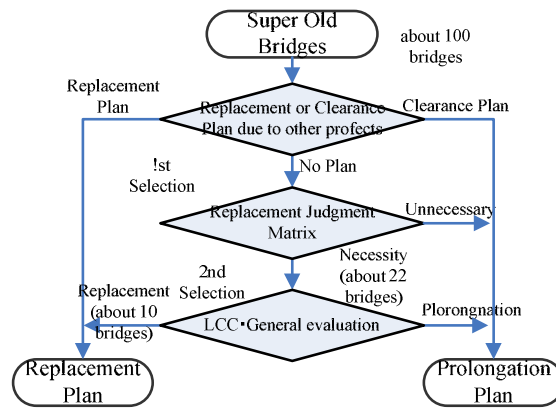


Fig.4 Diagram of Replacement Plan

**Replacement judgment matrix**

**(1) Evaluation method**

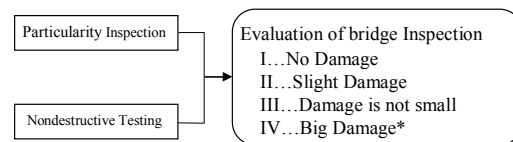
It is common way to consider the maintenance plan based on the result of by the bridge inspection when made the plan for maintenance plan.

However, the judgment on the bridge replacement only on the basis of the bridge health assessment may lead to wrong decisions. This is caused by the view of the fact that the old bridges built before the World War II were designed using different codes from now with respect to loads, earthquake-resistant design and river conditions and do not correspond to the present design codes.

For the reason, the final decision of replacement of old bridge was judged to use evaluation both 1.Evaluation of Health assessment and 2.Evaluation of Functionality.

**(2) Evaluation of Health assessment (by bridge inspection)**

As for the evaluation of health assessment, Osaka city evaluated it on the basis of future deterioration progress based on particularity inspection (nearness viewing) and the result of Nondestructive testing (Fig.5).



\* Problem bridges based on the strength of concrete and carbonation in the slabs, bridge piers and abutments.

Fig.5 Evaluation of Health Assessment

About the Nondestructive testing, it is the quantitative evaluate which cannot to

confirm by viewing kind of the measurement of the neutralization depth and the salt content and concrete strength testing. It could be anticipate the precision improvement of the evaluation of health assessment.

Furthermore, I-III was judged to use status index<sup>1)</sup> by National Institute for Land and Infrastructure Management as trial. Evaluation IV that the damage was the most remarkable defined it that concrete strength deteriorated remarkably.

**(3) Evaluation of Functionality (by Structure collation)**

The functional evaluation was instituted whether load resistance, seismic resistance and river conditions could take adjustment for a current standard (Fig. 6). The river conditions are impediment ratio of river flow, standard diameter length and the height under the girder.

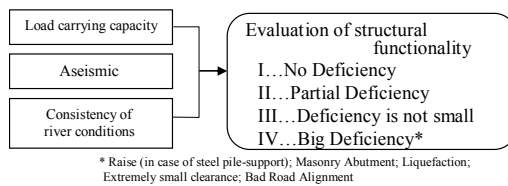


Fig.6 Evaluation of Functionality

About the bridge which road linear shapes extremely bad were evaluated IV as the bridge that lack of function was remarkable such as pilling-stones abutment (Photo.3), the liquefaction ground, the bridge which raises a figure (Photo 4) and the bridge that a girder soaks in water at the time of rise of the river.



Photo3 E.g. of Masonry Abutment



Photo4 Raising Bridge Floor Bottom by a Steel Beam.

**(4) Extraction result of bridge renewal examination**

The bridges divided into to two groups “The bridges for prolongation” and “The bridges to be replaced” through the result of both evaluation of Health assessment and Functionality. Fig.7 is shown that the Replacement judgment matrix.<sup>2)</sup>

According to the result of the replacement judgment matrix, the bridges which did not satisfy a current

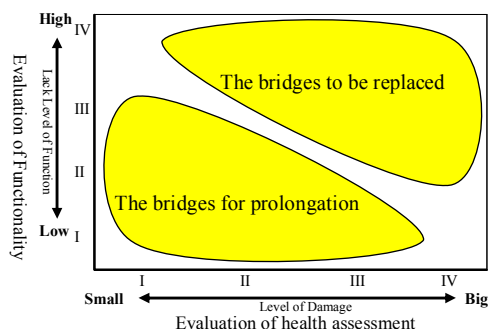


Fig.7 Replacement Judgment Matrix

standard were chosen as the bridges renewal examination which should have examined reconstructs in future despite of the soundness was no problems in inspection. The standard is changing with the times, so that old bridge does not adapt the current standard properly. On the other hand, many of old bridges which kept soundness enough even now were confirmed.

From these results, there is a limit to judge the condition of the bridge from only a check result by the viewing. It means that admitted it is necessary to examine a characteristic each bridges in detail when makes an important decision for replace and so on.

### General evaluation based on LCC Analysis

The economical evaluation was assessed by LCC of the next 50 years which based on the result of replacement and prolongation analysis in the replacement detail judgments (2nd selection) of super old bridges.(Fig.8) In addition, it were judged whether necessity the replacement or not which basis of the consistency of higher plan. The next expression is shown the detail of LCC.

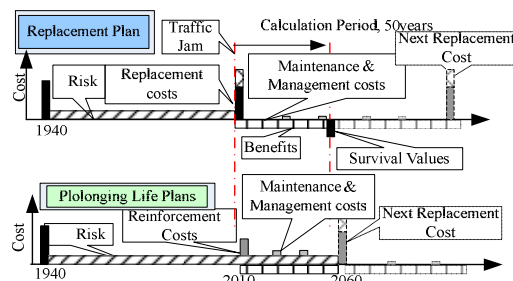


Fig.8 Idea of Life Cycle

$$LCC = [\text{Replacement Costs}] \text{ or } [\text{Reinforcement (Improvement) Costs}] + [\text{Maintenance \& Management Costs}] + [\text{Traffic congestion losses due to construction}] + [\text{Risks}] - [\text{Benefits}] - [\text{Survival Values}]$$

While Replacement costs and Maintenance & Management costs are evaluation objects normally, Risks, Benefits and Survival values were appropriated as costs in this examination, then, the replacement bridges are judged objective and quantitatively.

[Replacement costs] was calculated based on structural calculation and Maintenance & Management costs. In the case of reconstruct, as those old bridges are still usable even after 50 years, [Survival values] is to be considered. Additionally, traffic regulation is required when renewal the bridges, therefore, [Traffic congestion losses due to construction] need to be considered. Traffic congestion loss was calculated by carrying out traffic estimation using traffic network assignment of all area of Osaka City, then calculated 3 benefits such as traffic time, traffic costs and loss of traffic accident basis on the current situation and discrepancy of traffic regulation.

As for [Reinforcement & Improvement costs], it calculated to consider the seismic reinforcements, the necessity of the anti-vehicle upsizing measure and reinforcement structures. In the case of the shiftlessness, it assumed that appropriated the amount of damage when an earthquake occurred as [Risk]. It is attributed to be

damaged at the time of an earthquake.

[Benefits] was appropriated it when the function of the bridge improved in both case of renewal and reinforcements and improvements.

**The case of Test Calculation**

Fig.9 is shown the examples that the result of LCC analysis of the bridges which chosen prolongation or reconstructed. As comparison, in case of minimum maintenance and management of LCC was shown without reconstruct and prolongation measure (the following "Shiftlessness plan"). The most suitable plan of LCC ratio is 1.0. The cost of reconstruct is subtracted for survival value.

A bridge is the Gerber girder bridge which has the wooden posts of about 80 years. Although the girder had rose, it required the foundation reinforcement in the result of the seismic verification. However, according to the LCC analysis, the reconstruct plan is economical rather than foundation reinforcement. In shiftlessness plan, the earthquake damage were occurred sort of traffic suspension or the recovery costs, besides the amount of damage by stops of the production activity will increase.

B bridge is the arch bridge, seismic is secured, used about 80 years. While the project of the water transportation activation is promoted by the Water Metropolis Revival Plan, there is few girder bottom room of the bridge it becomes the obstruction of the water transportation, so that the water transportation loss was appropriated. This is caused by the girder bottom room was not secured by the refinement construction work or reconstruct plan in Shiftlessness plan.

	A Bridge	B bridge
	Gerber girder bridge, Wooden posts	Arch Bridge
Present Condition	Wooden Posts in Liquefaction Ground, Less seismic	No rooms under the girder, obstruction of the water transportation
Prolongation Plan	Pier, Basic reinforcement	Floor reinforcement
Replacement Plan	Steel Flooring Bridge	Arch Bridge
Shiftlessness plan	Damage from Earthquakes	Only repair

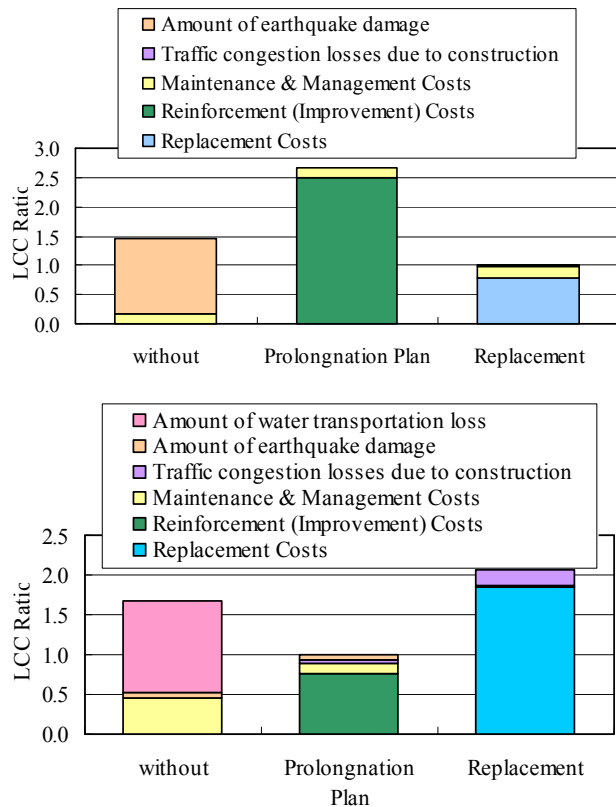


Fig.9 Result of LCC Analysis

As a result of having evaluated LCC or consistency with the higher plan in object bridges, it is judged the prolongation plan is the most suitable plan through the refinement construction work of the upper side of the bridge. Moreover, reconstruct plan were assumed as the same type of now, because of the well known bridges have historical values.

## Conclusion

Osaka city is considering the maintenance and the replacement plan of the old Bridges based on a basic policy. Fig.10 is shows the result of these examinations

(1) As the result of the 1st selection by Replacement judgment matrix, about 20 bridges were selected as an object of replacement judgment from about 100 old bridges except bridges which were to be rebuilding by other plans.

(2) As the result of the 2nd selection by LCC analysis, about 10 bridges were selected after the 1st selection.

(3) To other object of reconstruct bridges is to be trying for the precision improvement of the project plan based on the enforcement of the close inspection of the local condition and the detailed design in future including valuable in the history of civil technology (Photo.5,6) and so on. Osaka city will also examine how manage these bridges in the future.

As regards to the plan theory of LCC analysis when consider the reinforcements or replacements, it investigated with various way<sup>3)4)5)</sup>. This examination was important to provide the maintenance plan of bridges on the basis of the results of the past studies.

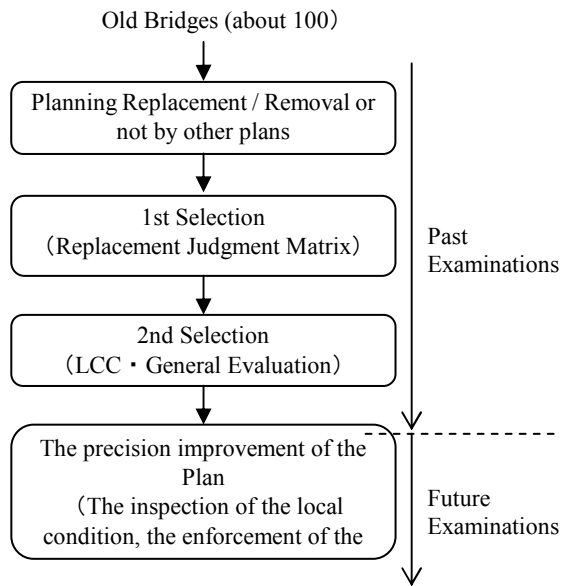


Fig.10 Schedule of Examinations

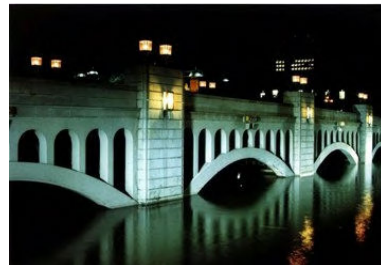


Photo 5 Suisho Bridge (Well-known Bridge)



Photo 6 Honmachi Bridge (Oldest Bridge built in 1913)

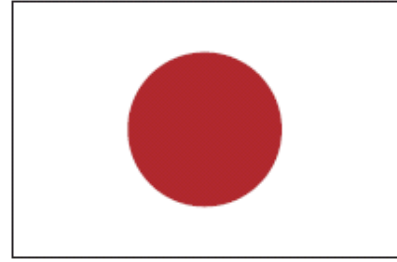
## **Acknowledgments**

This is the report that explaining the basic concepts regarding the project on the reconstruct of old and historical bridges. Thanks to the well-preserved drawings, documents of summary of works and records of works on the bridges built before the World War II, the project has been promoted quite smoothly. Thus, the effort and tradition of the bridge engineers of the Osaka Municipal Office must be highly respected. The importance of the succession of the important documents and information to the next generations is becoming more and more important.

Finally, we would like to take this opportunity to express their appreciation to the member of the Study Group on the Bridge Maintenance and Renewal of the Osaka Municipal Government for their precious opinions and advice., Chairperson: Mr. E.Watanabe (Emeritus of Kyoto University), Committee: Mr. H. Furuta(Professor of Kansai University) and Ms. M.Tanaka (Assistant Professor of Osaka Industrial University).

## **References**

- 1) Hiratsuka, Tamakoshi, Takeda, Tateyama, Study for general evaluation index of Road Bridges (61st Annual Meeting of JSCE 2006.9)
- 2) Yokota, Komatsu, Nagahashi, Replacement Plan of Old Bridges by Osaka Municipal Government (Bridges and Foundation, 2008.8)
- 3) Kaito, Abe, Kumon, Fujino, Bridge management based on minimization of total cost considering its stock value (Proceedings of Structural Engineering 2001.3)
- 4) Yamaguchi, Ito, Miki, Ichikawa, Life Cycle Cost evaluation of highway bridges considering social influence (Proceedings of Structural Engineering 2001.3)
- 5) Sato, Yoshida, Masumoto, Kanaji, Prioritization of seismic retrofit for road bridges based on the concept of Life Cycle Cost (Proceedings of JSCE 2005.3)



# **25<sup>th</sup> US-Japan Bridge Engineering Workshop**

## **Session 3**

### **Accelerated Bridge Construction**

Seismic Performance and Structural Details of Precast Segmental Concrete Bridge Columns

By Jun-ichi Hoshikuma, Shigeki Unjoh, and Junichi Sakai

Accelerated Constructions of the Viaducts on the Second Keihan Expressway

By Yoshihiko Taira, Hirotugu Mizuno, Kei Muroda, and Akio Kasuga

New FHWA Seismic Hazard Mitigation Studies for Highway Bridges

By W. Phillip Yen

Overview of the Development Process and Effects of the UFO Method

By Yuji Mishima, Yukio Katsuta, and Tomoaki Tsuji

Page Left Blank

# SEISMIC PERFORMANCE AND STRUCTURAL DETAILS OF PRECAST SEGMENTAL CONCRETE BRIDGE COLUMNS

Jun-ichi Hoshikuma<sup>1</sup>, Shigeki Unjoh<sup>2</sup>, Junichi Sakai<sup>3</sup>

## **Abstract**

The precast segmental concrete bridge column would be one of the options for the accelerated bridge constructions because the construction period at site can be shortened due to no need of formwork, placement and curing of concrete. Thus, those columns are expected to be applied for the bridges for overpass crossings in urban areas to minimize the effect on existing traffic. Additionally, high quality of the concrete members would be ensured because the concrete segments are fabricated at factories. This paper briefly introduces the state-of-practice of the segmental concrete bridge columns in Japan. Furthermore, recent research activities in PWRI for the precast segmental concrete bridge columns are summarized.

## **Introduction**

With a background of the generalization of the performance-based design concept into practices, the applications of new materials, new designs, and new structures have initiated to be actively employed with necessary performance verifications. The precast segmental bridge columns are one of such new applications, and effectively use the combination of high strength materials including steels and concrete. The precast segments are fabricated at factory, so that the precast segmental bridge columns can be easily achieved to have better-quality. Therefore, the precast segmental bridge columns are expected to improve the constructionability at sites and shorten the construction period.

Public Works Research Institute conducted 2-years joint research program for the development of the new precast segmental concrete bridge columns with three private construction companies. In the research program, three types of structural details of precast segmental concrete bridge columns were proposed and the failure mechanism of the proposed columns was investigated through a series of shake table test. Based on the experimental studies, the limit states for the required seismic performance are discussed in this paper. Structural details for those columns were also introduced.

---

<sup>1</sup> Chief Researcher, Center for Advanced Engineering Structural Assessment and Research, Public Works Research Institute (PWRI)

<sup>2</sup> Research Coordinator for Earthquake Disaster Prevention, Research Center for Disaster Risk Management, National Institute for Land and Infrastructure Management (NILIM)

<sup>3</sup> Senior Researcher, Center for Advanced Engineering Structural Assessment and Research, Public Works Research Institute (PWRI)

## Structural Concept of Precast Segmental Bridge Columns

**Figure 1** shows the outline of the precast segmental bridge columns which have been designed and constructed in the past in Japan. The precast segments are produced at factory and transported to the construction site. These segments are piled up at the site and connected each other through the steel bars, to be a column. It would be an important advantage to shorten the construction period at the site because of no need of formwork, placement and curing of concrete. Therefore, the precast segmental bridge system would be expected to be applied for overpass crossings in the urban areas in order to decrease the traffic jamming and then to minimize the effect on existing traffic.

Structural details of the conventional precast segmental bridge columns are shown in **Figure 2**. There are two types of the precast segmental columns. The precast PC columns are built with the segments connected through the high strength steel bars columns, as illustrated on the left side section in **Figure 2**. Each segment is post-tensioned by all high strength steel bars, to integrate with column structure. After post-tensioning, the following segment is piled up on the lower segment and the high strength steel bars are installed into the section through the ducts. These bars are coupled with the lower high strength steel bars and the grout is injected to the duct to be bonded. Details of the segment connection are shown in **Figure 3**. These processes are repeated up to the column height.

On the other hand, the precast RC columns are built with the segments connected basically through the nominal strength steel bar, as illustrated on the right side section in **Figure 2**. A few high-strength steel bars are installed and minimum post-tension required for setup of the segment is applied to these bars. The steel bars are coupled and grouted with the same procedure as the precast PC column.

Construction samples of the precast segmental concrete columns or piles are shown in **Photos 1** and **2**. **Photo 1** shows connection of the precast segmental PC piles with the cast-in-place footing. **Photos 2** shows the precast RC oval column constructed very close to existing bridge column.

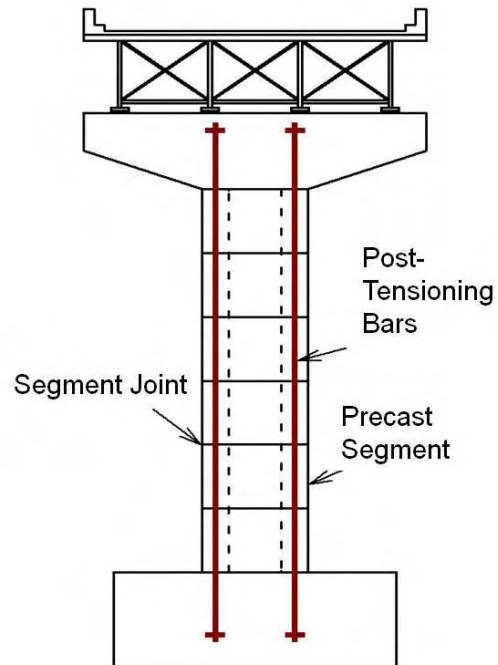


**Figure 1** Illustration of Precast Segmental Concrete Columns

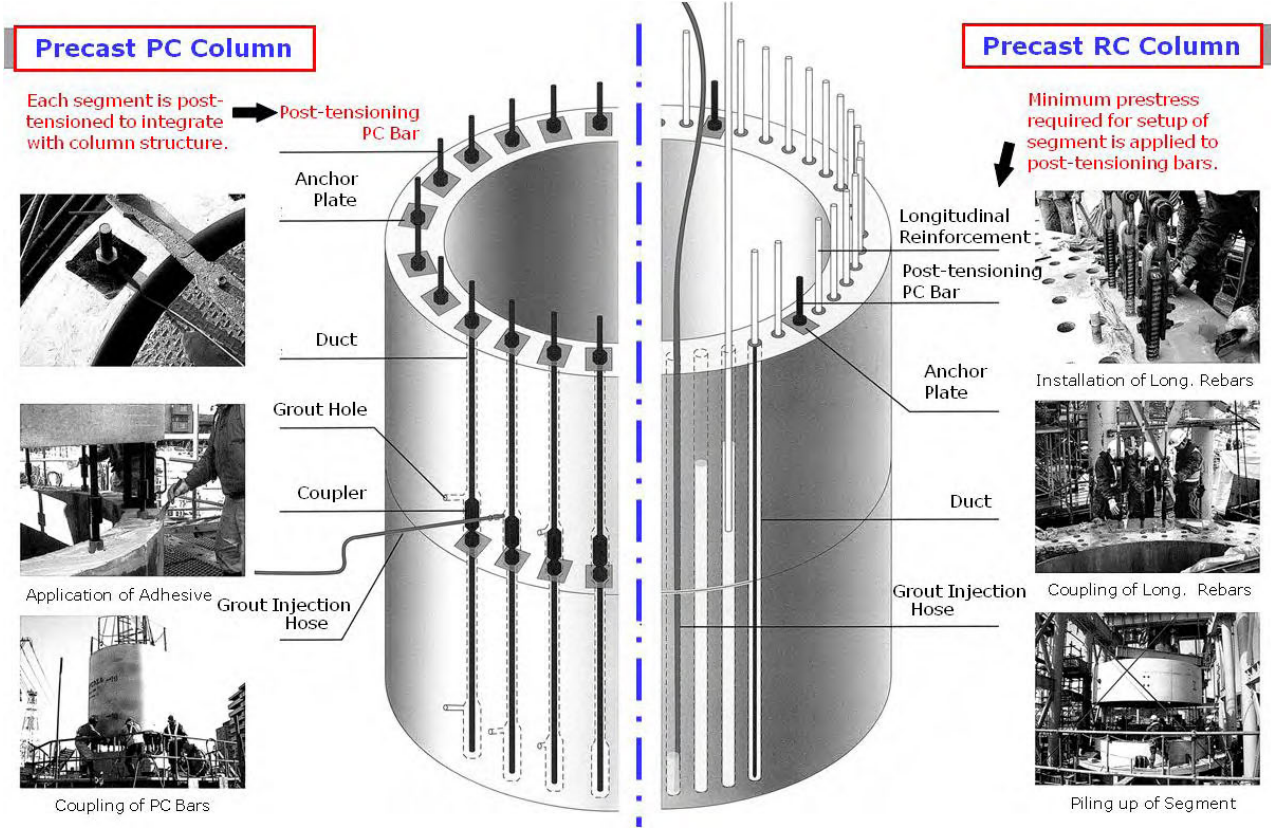


**Figure 2** Concepts of Connection Details in Conventional Precast Segmental Concrete Columns

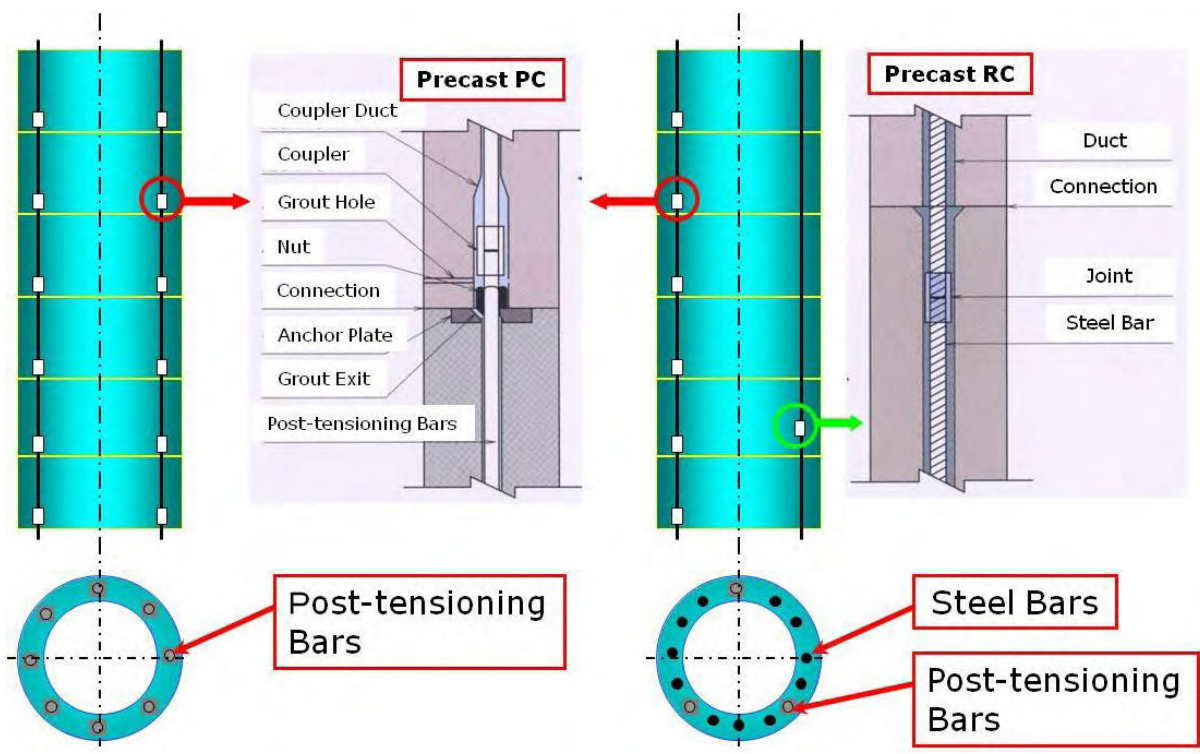


**Figure 3** Connection Details of Steel Bars in Segment

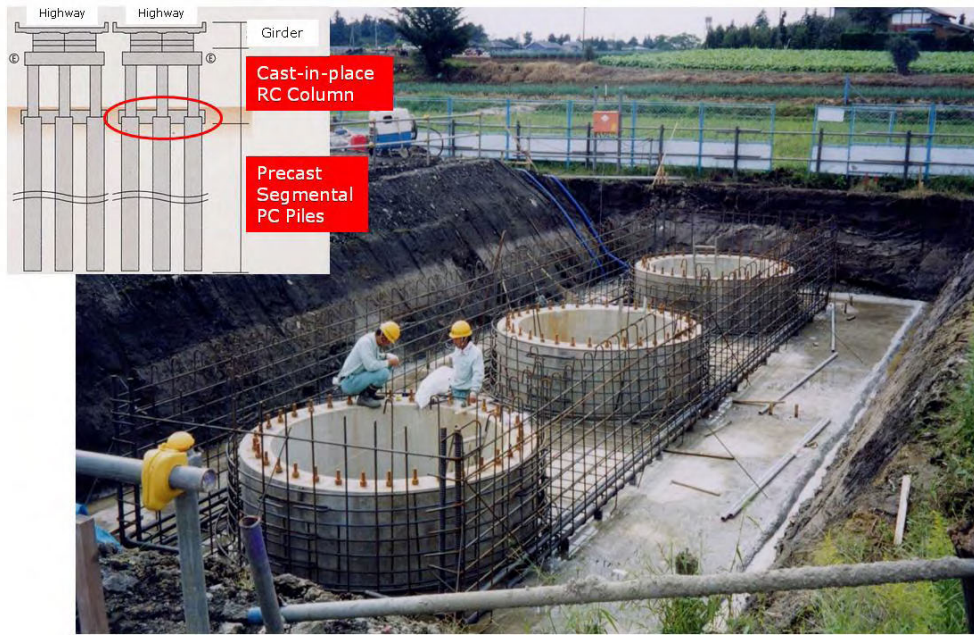


**Photo 1** Connection of Precast Segmental PC Piles with Cast-in-place Footing

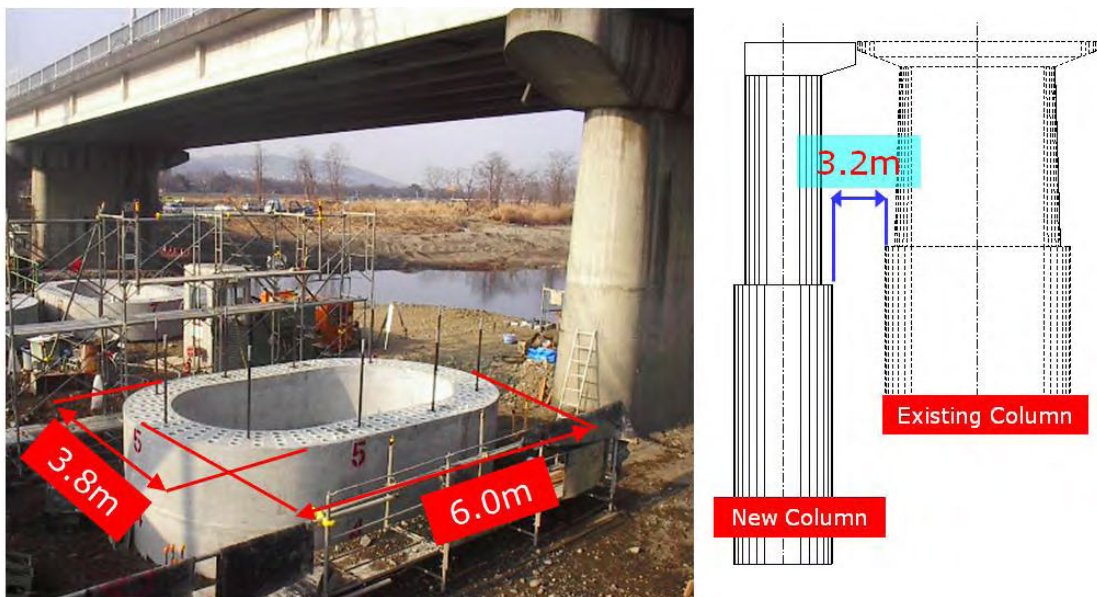


**Photo 2** Precast RC Oval Column Constructed Very Close to Existing Column

### **Recent Research Activities for Precast Segmental Bridge Columns in PWRI**

PWRI conducted the joint research program on the new precast segmental concrete columns with 3 private companies including Kajima Co., Sumitomo Mitsui Construction Co., Ltd., and P.S. Mitsubishi Construction Co., Ltd. Three types of the precast segmental concrete column details were proposed. Research issues were to

obtain the data on the failure mechanism, the strength and ductility performance, and the dynamic behavior of proposed precast segmental bridge columns, and to develop the design method including the limit states to achieve necessary seismic performance, detailed design methods for segments, joints, PC cables, bending–shear resistance evaluation, and construction methods. In the joint research program, a series of cyclic loading tests, shaking table tests, and analytical studies were made to develop the seismic design guidelines for the proposed precast segmental concrete columns.

Structural concepts of the proposed precast segmental concrete columns are shown in **Figures 4 to 6**. The structural details and properties are described in the followings. **Figure 4** shows the outline of the precast PC column proposed by Kajima Co. The segments are piled up at the site, and each segment has the outer and inner steel pipes. Outer steel piles are embedded in the segment when it is produced at factory, and inner steel pipe are installed at the site between the segments. The inner steel pipe is to resist against the shear force acted the joints of segments as a shear key. After the piling up of all segments for columns, the vertical tensioning force is applied for segments by post-tensioning bars through the inner pipes, in which the those bars work as longitudinal steel.

Sumitomo Mitsui Construction Co., Ltd proposed the precast segmental PC hybrid columns as shown in **Figure 5**. The segments are piled up at the site. Each segment is made of combination of inside steel shell and outside concrete. Inside steel shells of the segments are connected by steel bolts. After the piling up of all segments for column, vertical tensioning is applied for segments by external post-tensioning bars. At the joints between segments, shear keys are provided at the edge of steel shell and concrete mortar is placed between the segments outside concrete. Therefore, vertical axial force by dead load and live load is carried by inside steel shell but the earthquake force is carried by steel shells, bolts, and outside concrete. Shear force acted at the joints is carried by the shear keys of steel shell. Steel shells and bolts, and PC cables works as longitudinal steel. The bolts are designed to be firstly yielded when the deformation is exceeding the elastic limit and then the steel shells are not expected to be damaged. It is an important concept for this column that the yielded bolts can be replaceable after the earthquake and then the columns can be easily recovered to the original performance.

**Figure 6** illustrates the precast RC column proposed by P.S. Mitsubishi Construction Co., Ltd. The concrete segments are piled up at the site with a few temporally post-tensioning bars. Those bars are provided not for tensioning as longitudinal steel but for just construction to assure the quality of the joint connection between segments by resin. After piling up of all segments, mild longitudinal steel bars are inserted into the ducts, which are pre-grouted with the mortar from the top to the bottom of the column. The columns are made of segments but the design concept is the same as nominal reinforced concrete column. Since the longitudinal steel bars are placed inside the sheathe of segments, so the confinement effect to prevent the buckling of longitudinal bars is much higher than the nominal reinforced concrete columns which is confined by the cover concrete and lateral steel bars.

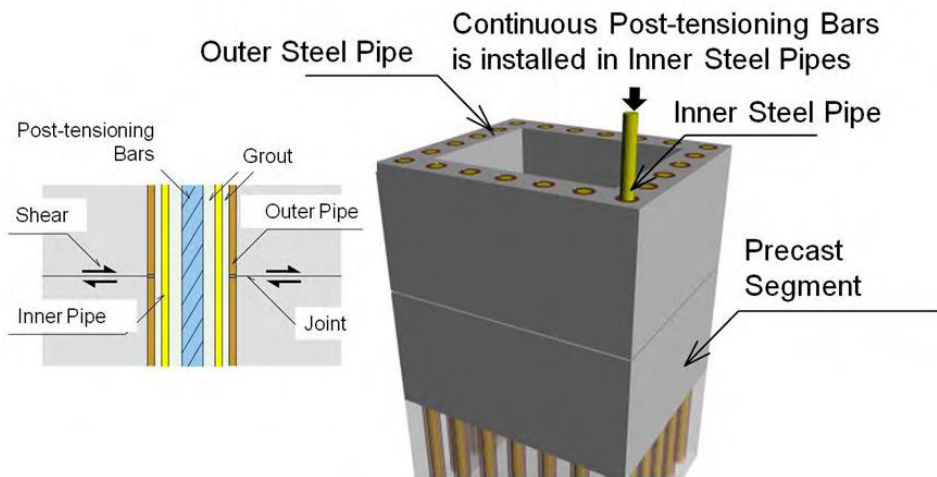


**Figure 4** Precast Segmental Prestressed Columns Proposed by Kajima Co., Ltd.

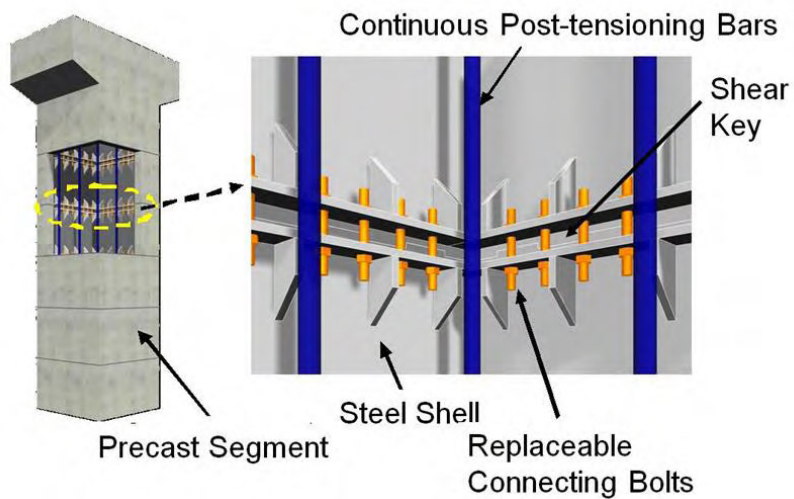


**Figure 5** Precast Segmental Hybrid Columns Proposed by Sumitomo Mitsui Co., Ltd.

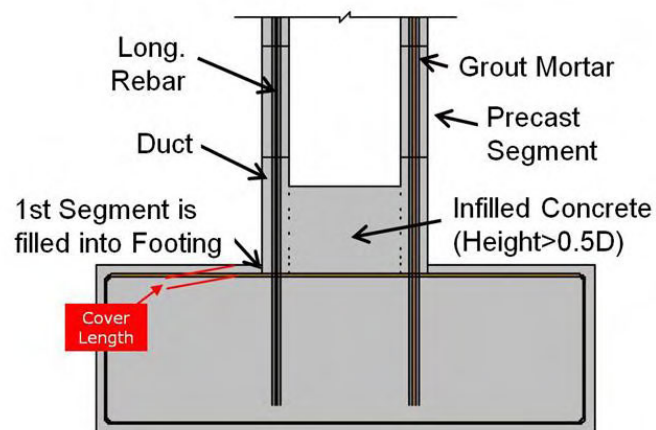


**Figure 6** Precast Segmental RC Columns Proposed by P.S. Mitsubishi Co., Ltd.

## Limit States of Precast Segmental Bridge Columns

### General Concepts of Limit States

It should be essential to determine the limit state for each seismic performance level, to develop the seismic design method. In Design Specifications for Highway Bridges issued by Japan Road Association, three seismic performance levels are specified for intensities of design ground motions and importance of the bridges. The limit states are determined based on the required seismic performance, which are described in terms of the safety, serviceability and repairability. The schematic image of the limit state for the conventional reinforced concrete bridge column is shown in **Figure 7**.

For the seismic performance level 1, it is required to ensure the normal functions of bridges after an earthquake, which means the mechanical properties of the structural members should behave within the elastic ranges. For each structural member, the stress induced by an earthquake shall not exceed its allowable stress. For the seismic performance level 2, it is required to ensure the serviceability and repairability after an earthquake. As the limit state, the structural members in which the nonlinear behavior is allowed deform beyond elastic range but within a range of easy functional recovery. For the seismic performance level 3, it is required to ensure the structural safety during an earthquake. Since neither serviceability nor repairability is required, structural members in which the nonlinear behavior is allowed deform within the ultimate ductility capacity.

### Limit States for Proposed Precast Segmental Concrete Bridge Columns

The limit states for the precast segmental concrete bridge columns shown in **Figures 4, 5 and 6** are determined considering the structural properties and nonlinear behavior of each structure. For the seismic performance level 1, the limit states of the precast segmental structures are determined to be same to a conventional reinforced concrete column. For each structural member, the stress induced by an earthquake shall not exceed its allowable stress.

The limit states for the seismic performance levels 2 and 3 are determined based on the nonlinear behavior of each structure, which are introduced in details below.

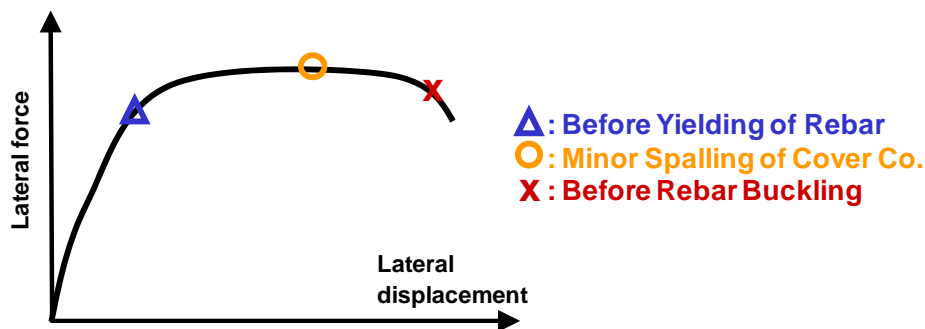


**Figure 7** Limit states for Conventional Reinforced Concrete Columns

### ***Limit States for Precast Prestressed Concrete Bridge Column***

Because no mild longitudinal reinforcement is provided in the precast prestressed concrete bridge column, the yielding of the post-tensioning steel bar is the important limit state. Once the yielding of the post-tensioning steel bar occur, it is difficult to recover the required functions. Based on these properties of the structure, the limit states shall be determined as shown in **Figure 8**.

For the seismic performance level 2, the yielding of the post-tensioning steel bar is determined as the limit state to ensure the serviceability and reparability. **Figure 9** shows the force-displacement hysteresis and the failure mode obtained from the shake table tests for the precast prestressed columns during the design level earthquake ground motion. The post-tensioning steel bars remained in the elastic range and minor spalling of cover concrete was observed. Although the column model performed well beyond the yielding of the post-tensioning steel bars in the shake table test, the range beyond this point is not considered in the seismic design of the precast prestressed concrete bridge for safety consideration. Thus, the limit state for the seismic performance levels 3 should be determined beyond the yielding of the post-tensioning steel bars. Further research may be needed for consideration of the behavior after yielding of the post-tensioning steel bars.

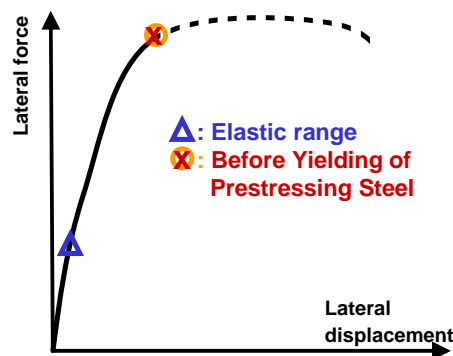


**Figure 8** Limit states of precast prestressed concrete columns

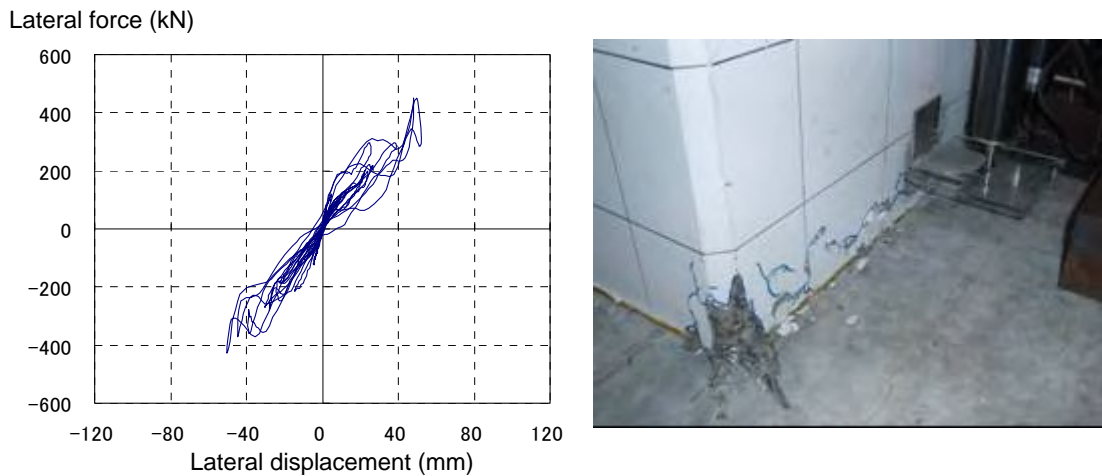


**Figure 9** Seismic Response and Failure Mode after Design Ground Motion Level Test for Precast Prestressed Column

### Limit States of Precast Hybrid Bridge Column

The schematic image of the limit states of the precast hybrid bridge column is shown in **Figure 10**. Since the key feature of this column is the reparability by replacement of the connecting bolts, the limit states of the seismic performance level 3 should be determined to be same as those of the seismic performance level 2. The replaceable limit of the connecting bolts is determined as the limit state for the seismic performance level 2. The allowable strain of the bolts is estimate to be 2% based on the low-cycle fatigue tests and the shake table tests. The other structural members should remain in the elastic range. **Figure 11** shows the force-displacement hysteresis and the failure mode obtained from the shake table tests during the design level earthquake ground motion. The results from as-built series (case 1) and post-repair series (case 2) are compared. After the design level tests in the post-repair series, the response displacement was still smaller than the design displacement while about 2% strain was induced in the connecting bolts and minor spalling of cover concrete was observed.

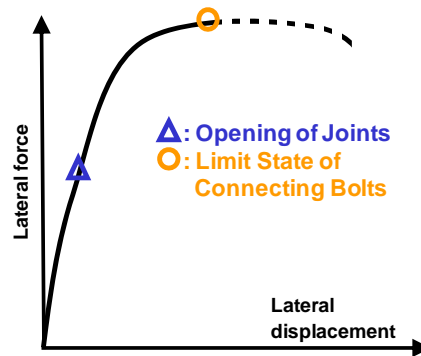


**Figure 10** Limit states of precast hybrid concrete columns

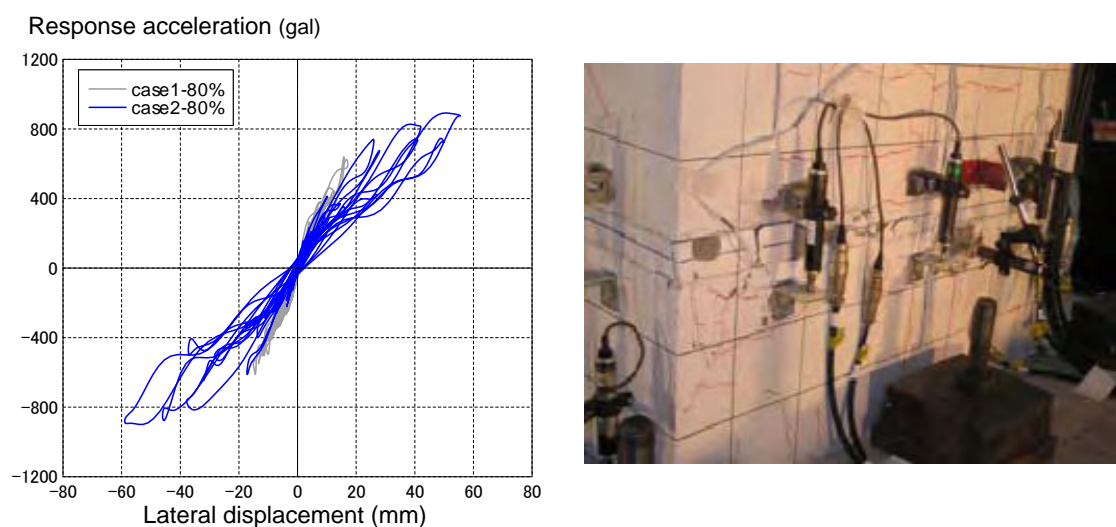


**Figure 11** Seismic Response and Failure Mode after Design Ground Motion Level Test in Post-repair Series for Precast Hybrid Column

### ***Limit States of Precast Reinforced Concrete Bridge Column***

It was confirmed that the nonlinear behavior of the precast reinforced concrete bridge column was similar or even better than the conventional reinforced concrete bridge column because the longitudinal reinforcing bars inserted into the mortar-grouted ducts have better performance on anti-buckling. The limit states of this column can be determined to be the same as those of the conventional reinforced concrete columns, which is shown in **Figure 7**. **Figure 12** shows the force-displacement hysteresis and the failure mode obtained from the shake table tests during the design level earthquake ground motion. Only flexural cracks were observed, and the stable hysteresis loop was obtained.

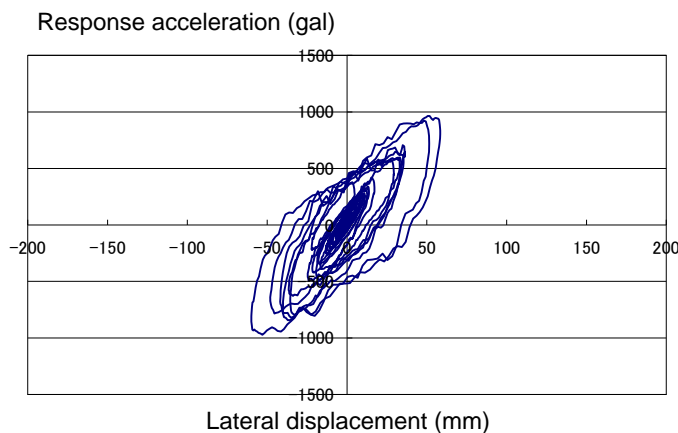


**Figure 12** Seismic Response and Failure Mode after Design Ground Motion Level Test for Precast Reinforced Concrete Column

### **Conclusions**

This paper introduces the state-of-practice of the conventional segmental concrete bridge columns in Japan. Also, recent research works for the development of the new precast segmental concrete columns were introduced in this paper. Design Guidelines for the seismic effect of the precast segmental concrete columns is scheduled to be published in 2010. The seismic performance and the seismic limit states of the precast segmental columns will be described in the guidelines based on discussion of the test results. Furthermore, connection design details of those columns will be specified.

### **Acknowledgments**

Some illustrations and photos of the structural details of the precast segmental concrete bridge columns in this paper were provided by PC-WELL Method Association, Kajima Co., Sumitomo Mitsui Construction Co., Ltd., and P.S. Mitsubishi Construction Co., Ltd. Author would like to appreciate their contribution for the paper.

## **Accelerated Constructions of the Viaducts on the Second Keihan Expressway**

Yoshihiko Taira<sup>1</sup>  
Hirotugu Mizuno<sup>2</sup>  
Kei Muroda<sup>3</sup>  
Akio Kasuga<sup>4</sup>

### **Abstract**

The Second Keihan Expressway located between Kyoto and Osaka has been constructed as a bypass of the existing national route. Since the expressway is located in the suburban residential area, cost saving, accelerated construction, environmental protection for the surrounding residential area as well as improving the safety were required for the construction of the expressway. To meet these requirements, unique rationalized construction methods were applied for the different site conditions in two viaduct projects, the viaducts in Nasu-dukuri Area and in Aoyama Area.

This paper describes these new erection methods.

### **1. Introduction**

The Second Keihan Expressway linking Kyoto and Osaka has been constructed as a bypass of the existing national route (Fig.-1). Since the expressway passes the suburban residential area, accelerated construction and reduction of the environmental impact during construction as well as improving the safety etc. are required for the construction of the expressway. To meet these requirements, two kinds of rationalized construction methods were newly developed and applied in two viaducts in Nasu-dukuri Area and in Aoyama Area, which are suitable for their own site conditions.

In Nasu-dukuri Area, since some degrees of construction area could be used in the construction site, the areas were used as casting yard and a unique U-shaped precast girders were adopted. It was not as the conventional erection method that uses multi-number of small precast segments divided longitudinally. It was possible to have some casting yard along the viaduct and to transport the segment from the casting yard to the below area of the viaduct. The erection method was called “U girder lifting erection” in which site-fabricated U-shaped precast girders were used.

On the other hand in the viaduct in Aoyama Area, it was impossible to have enough construction yard around the viaduct, and also it was impossible to use the area under the superstructures due to the topographical conditions. The segments were fabricated at the concrete factory and transported to the site. The

---

<sup>1</sup>Senior Structural Engineer, Sumitomo Mitsui Construction,

<sup>2</sup>Manager, Naniwa National Highway Office, MLIT,

<sup>3</sup>Senior Structural Engineer, SMC, <sup>4</sup>Chief Engineer, SMC

girder was divided into several segments longitudinally and the already completed deck surface was used as the assembling yard of the segments. The transported segments were lifted up, put on the deck and jointed as a girder. Then the girder was transported on the deck to the newly erecting span with the erection girder. This erection method is called “Span-by-span erection with rear assembly system”.

In both viaducts, accelerated construction could be achieved by developing the conventional erection methods, which are suitable for their own construction conditions. It could shorten the erection cycle and could also save the construction cost.

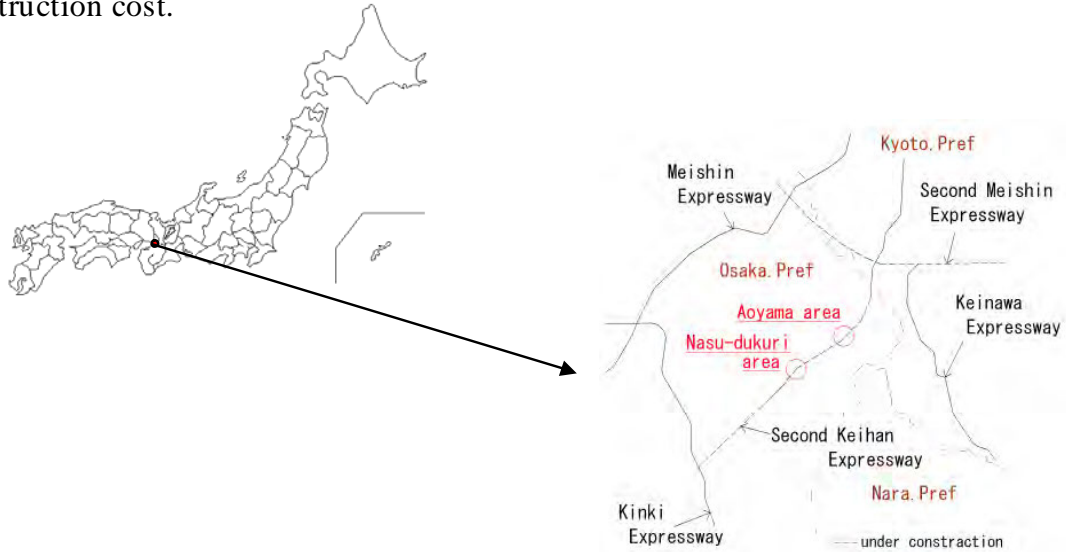


Fig.-1 The Second Keihan Expressway,

## 2. Project summary

### 2.1 General features

General views of the viaducts are shown in Fig.-2 and Fig.-3, and the cross sections of the girders are shown in Fig.-4 and a Fig.-5, respectively. The project summary and the viaduct properties are also shown in Table-1. The configurations of these two viaducts such as width, total length, span length and the structural type are quite similar. The design-built biddings were applied, and the construction methods were proposed by the contractor.

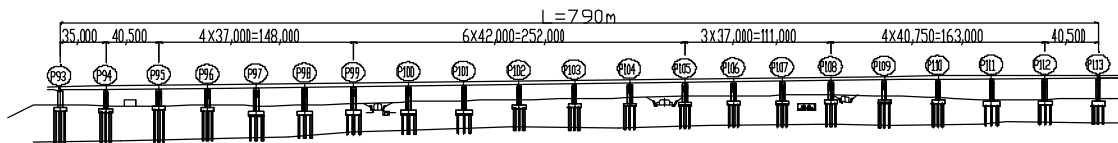


Fig.-2 Nasu-dukuri Viaduct

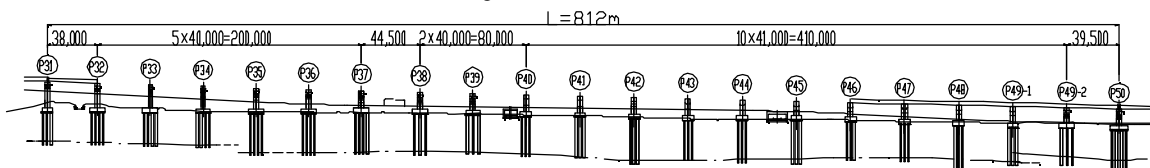


Fig.-3 Aoyama Viaduct

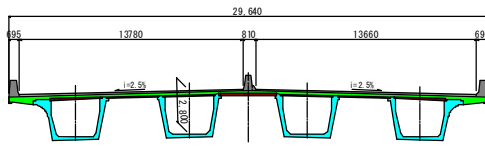


Fig.-4 Cross section of Nasu-dukuri Viaduct

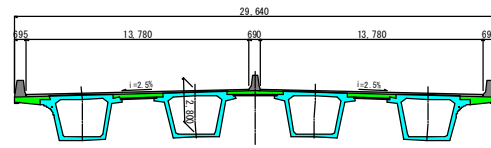


Fig.-5 Cross section of Aoyama Viaduct

Table-1 Project outlines and properties

Project	Nasu-dukuri Viaduct	Aoyama Viaduct
Profile	(20,2@2,2@7)spans prestressed concrete viaduct	20 spans prestressed concrete viaduct
Period	Mar.2007-Mar.2009	Sept.2007-Dec.2009
Length	790m	812m
Spans	37m, 40.75m, 42m	40m, 41m
Effective Width	2@13.780m	13.780m, 13.660m
Alignment	R=1950-A=650-R=∞	R=∞-A=500
Vertical Alignment	1.240%-0.300%	2.966%-2.366%
Horizontal Alignment	2.500%	2.500%

## 2.2 Requirements for the projects

During construction periods in both projects, following requirements were imposed.

1) Each construction period is about two years. However, considering the time for the detail design and other preparation work, only 18 months were remained as the direct construction periods. Therefore, strong time reduction was required.

2) Both viaducts are located in the quiet residential area, especially in Aoyama Area. Therefore, the environmental impact had to be strongly reduced.

## 3. Construction of the viaduct in Nasu-dukuri Area

### 3.1 Outline of the erection method

In Nasu-dukuri they could use some degrees of construction yard at the site and precast girders were selected. After fabrication the precast girder, the girder was transported to the erected span and lifted using erection girder. The U-shaped girder with no upper slab was first applied in Furukawa viaduct on the New Meishin Expressway (2002)<sup>1)</sup>. This erection method is called “U girder lifting erection method” (Fig.-6).

The procedures of the U girder lifting erection are shown in Fig.-7. Maximum weight of a U girder is 2,400kN, and the girder was lifted with the erection girder.

Since the precast girders were lifted near the supports of the erection girder on the piers, the bending moment acting on the erection girder could be quite small. Furthermore, applying the U-shaped girder without upper slab could also reduce the weight of the erection girder. As results, the bending moment acting on the erection girder could be reduced up to 1/6 compared with the conventional span-by-span erection, and the erection girder could be lightened drastically (Fig.-7, 8 and Table-2).

The following effects to the surrounding area could be expected.

- 1) Noises and vibrations caused by the construction work can be reduced since the girders are fabricated at the fixed fabrication yard in the site.
- 2) No need to use the large trailers to pass the existing residential area for transporting the precast segments.

The standard construction cycle of the superstructures is shown in Table-3. In Nasu-dukuri Area, no stockyard was built for the U girder. This could be achieved by that the casting cycle of four girders were set to be equal to their erection cycle. In order to achieve the cycle, four casting beds were used, and two sets of lifting girders were used in order to achieve the two weeks erection cycle of four girders per span.

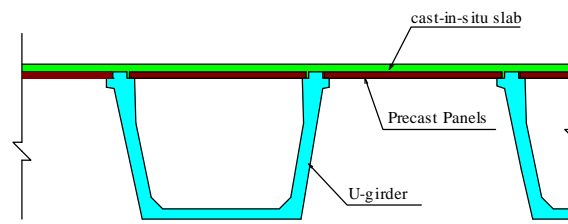


Fig.-6 Girders and slab structures in Nasu-dukuri Viaduct

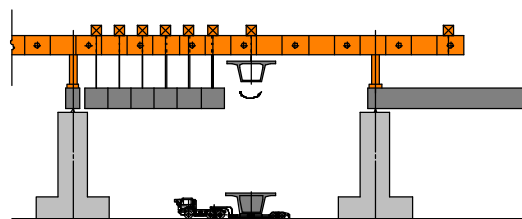


Fig.-7 Conventional span-by-span erection

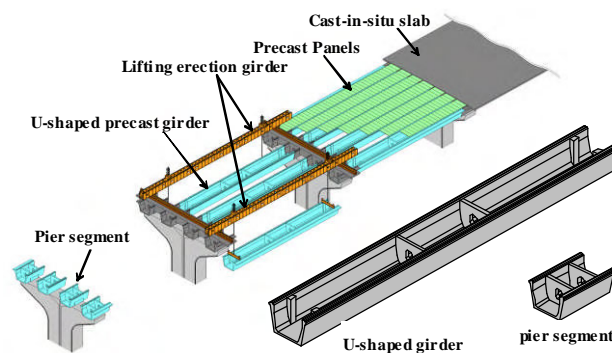


Fig.-8 Overview of the U-shaped girder lifting erection

Table-2 Erection methods and the bending moments of the erection girder

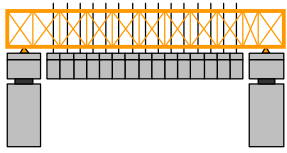
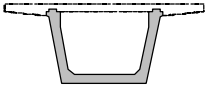
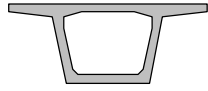
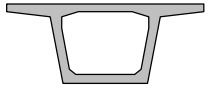
Erection Method	U-shaped girder lifting	Box girder lifting	Conventional span by span
			
Cross Section at Erection	U-girder 	Box girder 	Box girder 
Max Bending Moment in Erection girder	4100 kNm 18%	6800 kNm 30%	23000 kNm 100%

Table-3 Construction cycle of Nasu-dukuri Viaduct

	1	2	3	4	5	6	7	8	9	10	11	12
U-girder1	T	E	J	C	S							
U-girder2		T	E	J	C	S						
U-girder3						T	E	J	C	S		
U-girder4							T	E	J	C	S	
erection girder	Er											Er

T : Transportation E : Erection J : joint concreting  
C : Curing S : Stressing Er : Erection Girder Equipment

### 3.2 Fabrication and erection of the U girder

Considering the limited construction area and the way to transport the construction materials as well as the construction cycle work, four sets of casting bed were arranged in line longitudinally along the viaduct (Photo-1).

The U girders were transported from the casting bed to the erecting span with a large trailer (Photo-2). Photo-3 shows the erection of the U girder. Since large tensile stresses occur near the lifting points inside the webs during lifting, the vertical prestressing and the additional reinforcement were arranged for the local stress. Prior to the fabrication, a mockup test was conducted to confirm the stress and the safety during erection.

After lifting the girder, the girder was moved horizontally and transversally to the fixed location, following that the U girder No.2 was lifted by another erection girder. The U girder No.2 was then moved also horizontally and transversally (Photo-4).

150 mm closure joints were placed at both ends of the girder and the pier segments. After placing concrete, each girder was externally prestressed and then the lifting devices were released.

Segments No. 3 and No. 4 were also constructed as the same ways and the construction of one span was completed.



Photo-1 Casting yard



Photo-2 Transportation of the U-girder



Photo-3 Erection of the U-girder



Photo-4 Transversal movement of the girder

### 3.3 Construction of slab

For the construction of the slab, precast and prestressed panels were placed on the webs of the U girder. These panels are used as structural components as well as for the formwork, and the re-bars were assembled on them. For the thermal stress and the stress caused by the deformation of the girder due to the influence of the concreting in the adjacent slab, as well as shrinkage and creep effects. Expansive admixture was used as well as additional reinforcement designed through the thermal stress analysis (Photo-5, 6).



Photo-5 Precast panels



Photo-6 Cast-in-situ slab

## **4. Construction of the viaduct in Aoyama Area**

### 4.1 Outline of the erection method

Since it was impossible to have the casting yard near the construction site and it was difficult to use the area below the superstructures in Aoyama Area, existing concrete factory was utilized as the fabrication yard for the precast segments of the girder. After the factory-fabricated precast segments were transported from the factory to the construction site, the segments are then lifted and assembled on the already constructed deck surface as an assembling yard. This erection method is called “the span-by-span erection with rear assembly system”. The core segment without some length of overhang slab could save the weight of the girder (Fig.-9). Compared with the viaduct in Nasu-dukuri Area, transversal movement devices were used in order to reduce the number of erection girder, and the cost of the construction girder was reduced substantially.

Construction procedures of the erection method is shown in Fig.-10 as followed, and the standard construction cycle of the superstructures is shown in Table-4.

- 1) Segments of the girder No.1 are put and jointed together on the already constructed deck surface. The assembled girder is transported toward the erection girder along the deck surface and erected with the erection girder. The weight of a girder is about 3,500kN.
- 2) The girder No.1 is horizontally and transversally moved by the devices and then tensioned. The following girder No.2 is also assembled, transported and erected from the rear span continuously.
- 3) After the girder No.3 and the girder No.4 are erected in sequence and all the four girders are erected, precast panels are placed and the erection girder is moved toward the next span.
- 4) Slab concrete is placed.

In Aoyama Area, transporting the segments, lift up to the deck surface and joining were performed in one day, and the transportation, erection and transversal movement on the next day, while the segments of the next girder were transported to the site in 2 days later. Joining work of the next girder was performed concurrently at the rear assembling yard while the installation and tensioning were performed in the erecting span. As results, the construction cycle in one span of four girders took two weeks and was achieved as the same as that in Nasu-dukuri Area.

Compared with the conventional span-by-span erection method, this erection method with one set of erection girder could construct 1/2-1/3 faster by the number of days. In other words, 2 to 3 sets of erection girder would be needed to have the same erection speed in the conventional erection method (Fig.-11).

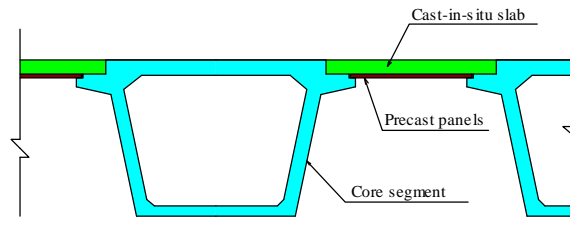


Fig.-9 Girders and slab structures in Aoyama Viaduct

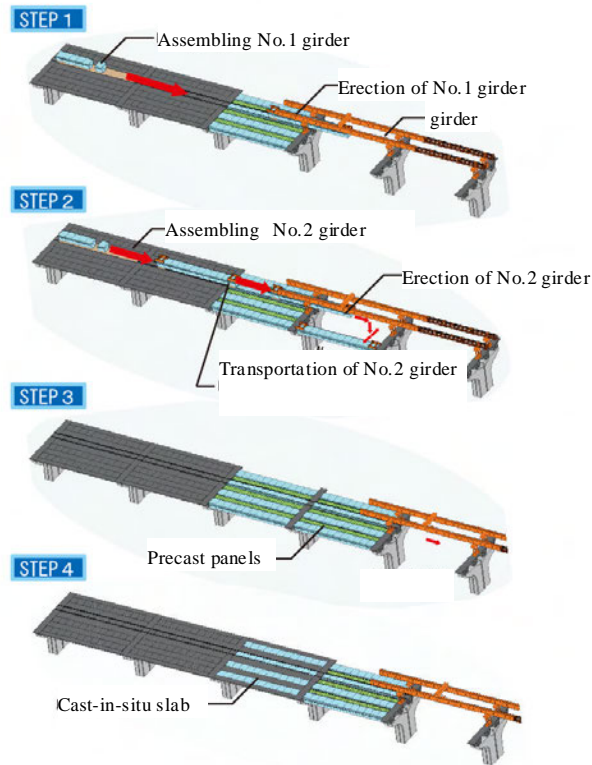


Fig.-10 Overview of the span-by-span erection with rear segment assembly system

Table-4 Construction cycle of Aoyama Viaduct

	1	2	3	4	5	6	7	8	9	10	11	12
main girder 1		E	J	S	Er							
main girder 2			E	J	S	Er						
main girder 3				E	J	S	Er		J	S	Er	
main girder 4					E	J	S	Er				
erection girder	Er											Er

E : Erection J : joint concreting  
S : Stressing Er : Erection Girder Equipment

#### 4.2 Assembly and erection of the segments

13 numbers of segments were transported from the factory with trailers. The segments were placed on the deck surface with a crane, jointed together as a girder (Photo-7). Then the girder was prestressed and put on the carriers.

Devices for transversal movement were installed at the upper part of both ends of the girder, and the girder was transported toward the erecting span (Photo-8). Since the weight of the girder and the devices reaches about 3,500kN

and they were transported on one of four existing girders, the stress of the girder due to the loading was verified and additional prestressing tendons were arranged.

After the girder was transported toward the erecting span, the girder was hung by the crane installed on the erection girder (Photo-9). The devices for transversal movement were installed on the rail on the pier segments, and the devices with the girder were moved transversally to the fixed location (Photo-10).

As the same as the viaduct in Nasu-dukuri Area, 150 mm closure joints were placed at both ends of the girder and the pier segments, supported with the transversal movement devices. After placing concrete, each girder was externally prestressed and then the supporting devices were released.



Photo-7 Assembling the segments



Photo-8 Transportation of the girder



Photo-9 Erection of the girder



Photo-10 Transversal movement of the girder

#### 4.3 Construction of slab

Precast panels were placed between the top of the girders (Photo-11), and re-bars assembly and concrete placing were conducted (Photo-12).

By using precast panels with labor saving, the slab could be constructed at the same days of the erection of four girders in next span. These procedures were quite effective ways to achieve the required construction cycles.



Photo-11 Precast panels



Photo-12 Cast-in-situ slab

### **5. Afterword**

It has been considered that the conventional span-by-span erection using conventional multi precast segments is suitable for the construction of the large-scaled continuous urban viaduct project for the cost saving, achieving the high quality and for the accelerated construction. However, in the urban viaduct projects, there might be some severe site conditions as mentioned. In such cases, the construction methods adopted newly developed in the viaducts in Nasudukuri Area and Aoyama Area on the Second Keihan Expressway can be the good solutions in different site conditions. In both projects, the rate of construction speed of  $2,400\text{m}^2$  per month were both achieved.

### **Reference**

- 1) Ikeda S., Ikeda H., Mizuguchi K., Muroda K., and Taira Y.: Design and Construction of Furukawa Viaduct, Proceedings of the 1<sup>st</sup> fib Congress, Osaka, 2002

## **New FHWA Seismic Hazard Mitigation Studies for Highway Bridges**

W. Phillip Yen, PhD, PE<sup>1</sup>

### **Abstract**

Earthquakes are inevitable events in our living environment. Each large magnitude earthquake located around urban area created devastated destruction of our infrastructures, including the transportation system, and claimed vast human fatalities. Since 1992, FHWA has initiated three major research projects in the seismic hazard mitigation, they are Seismic Vulnerability Study for Existing and New Highway Constructions, Seismic Vulnerability of Highway System, and the SAFETEA-LU Seismic Research Program.

This paper describes the Federal Highway Administration's (FHWA) new seismic research program to mitigate earthquake loss of highway infrastructures. This program consisted with two major research studies started in 2007 (five-year plan), the first is FHWA/MCEER project, titled, Innovative Technologies and Their Applications to Enhance the Seismic Performance of Highway Bridges, and the second one is FHWA/ UNR project, titled, Improving the Seismic Resilience of the Federal-Aid Highway System.

### **Introduction**

Surface transportation is a vital component of our society. Our highways link airports, train stations, harbors, manufacturing plants, farms office and residences. This transportation network must continue functioning during and after a natural hazard such as an n earthquake so that the lifelines of our society may be restored as soon as possible. Of all the components of the surface transportation system bridges are the most vulnerable to earthquake damage.

About 65 percent of the approximate 600,000 bridges in the U.S. were constructed prior to 1971 with little or no consideration given to seismic resistance. Recent earthquakes such as Loma Prieta, CA in 1989, Northridge, CA in 1994 and Kobe, Japan in 1995 & Chi-Chi Earthquake, Taiwan in 1999, have demonstrated the need to find new ways to build earthquake-resistant bridges and highways, and to retrofit existing bridges.

Recognizing the shortcomings evident in both existing bridges and design

---

<sup>1</sup> Program Manager, Seismic Hazard Mitigation, Office of Infrastructure, R&D Federal Highway Administration, 6300 Georgetown Pike, McLean, VA 20121 Email address: [Wen-huei.Yen@fhwa.dot.gov](mailto:Wen-huei.Yen@fhwa.dot.gov)

specifications, the Federal Highway Administration (FHWA) initiated several comprehensive seismic research studies on bridges and highways since 1992. As a result, a new seismic retrofitting manual, consisting of two parts (bridges and other highway structures), was completed and published. A new comprehensive seismic design recommendation was also published under the seismic vulnerability studies.

Furthermore, FHWA also published the research products in seismic retrofitting of truss bridges, seismic isolation manual and Risks from Earthquake Damage to Roadway System (REDARS). To implement these technologies into our Federal-Aid transportation system with limited resource, cost-effective and practical methods such as accelerated bridge construction, are also essential to successfully improve the seismic safety.

Under the new Transportation Authorization SAFETEA-LU, FHWA is working with Multi-disciplinary Center of Earthquake Engineering Research (MCEER) of New York State University at Buffalo and University of Nevada at Reno (UNR) to initiate two major seismic research studies and started in 2007. The following are the summary of these two new studies:

### **Seismic Research Study 1 (with MCEER): The Innovative Technologies and Their Applications to Enhance the Seismic Performance of Highway Bridges**

The objective of this study is to improve the seismic resistance of our highway system, by developing new innovative technologies and their applications, by developing cost-effective methods for implementing design and retrofitting technologies, and by refining and expanding applicability.

This project is to increase the mobility and safety of our surface transportation system as the FHWA envisions reducing the construction/ maintenance time of new and existing highway structures. Applying accelerated bridge construction technology to high seismicity area requires more advanced connection detail to accommodate the large ground motions. Innovative technologies and their applications are continuously sought to refine and expand their applicability to enhance the seismic performance of our surface transportation system.

The major tasks of this study are:

#### **Developing Detailed Technology to Apply Accelerated Bridge Construction (ABC) in Seismic Regions**

This task is to develop implementable seismic design guidelines applicable to the bridges located in the seismic regions. The focus of this task is on prefabricated reinforced concrete, segmentally constructed highway bridges of short to medium span length. A technical monograph for the bridge system is expected from this study. In addition, a separate subtask is set up to develop recommended design guidelines with design examples for practical applications.

### Innovative Seismic Protection Technologies

In this task, innovative technologies will be explored that can enhance the seismic performances of precast R.C. Bridges with emphasis given to ABC. This task will include subtask study on:

- Design Guidelines and Demonstration of Roller Isolation Bearings,
- Lifetime Performance of Bridges with Seismic Protective System,
- Bridge Information Modeling for Seismic Aspects of Accelerated Bridge Engineering
- Development of Structural Fuse Concept for Bridges
- And Down-Scaled Bridge Pier Testing

### **Seismic Study 2 (with UNR): Improving the Seismic Resilience of the Federal-Aid Highway System**

#### Background

Today *life-safety* is no longer the sole requirement for the successful design of a highway system for a major earthquake. *Resilience* is now expected by the traveling public as an integral component of any design strategy, so as to ensure rapid recovery and minimal impact on the socio-economic fabric of modern society. This realization has led to the concept of *performance-based seismic design* which is a relatively new development in the design and construction of civil infrastructure. Nevertheless substantial progress has been made in this area, particularly with respect to the performance of individual components of the built environment, such as buildings and bridges. But the real potential for performance-based design comes when these concepts are applied to systems and subsystems of the infrastructure, such as transportation networks, subject to both service load conditions and extreme events.

Since 1993, the FHWA has been researching methodologies for seismic risk analysis (SRA) under its seismic research program. The result of this effort has been the development of an earthquake loss estimation software tool called REDARS, which is now being used in pilot projects by several State Departments of Transportation. REDARS has been specifically developed for assessing the performance of highway systems taking into account the inter-connectedness of the network and vulnerability of bridges to seismic loads.

Performance measures calculated by REDARS include congestion and delay times. These measures allow system-level performance criteria to be specified for earthquakes of various sizes, such as maximum permissible traffic delay times and minimum restoration times. Accordingly the resilience of a highway system may be defined and measured in quantitative terms, such as the time it takes to restore the system's pre-earthquake capacity, as illustrated in figure 1. In doing so, financial and

societal incentives can be developed that will improve resilience and at the same time reduce risk to life and property.

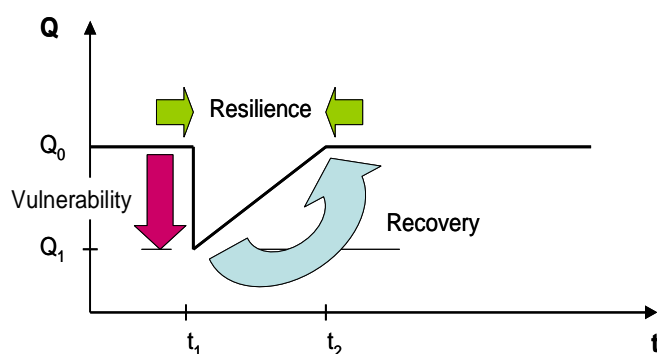


**Figure 1. System resilience, after Bruneau (Buckle and Lee, 2006).**

Whereas REDARS is the result of a decade-long period of development, and recently shown to adequately replicate the performance of the highway system in the San Fernando Valley following the 1995 Northridge earthquake, there is still much to be done to enable the methodology to be used with confidence and be widely applicable. REDARS has been developed with the expectation that new and more sophisticated modules will be developed overtime, in order to improve its accuracy and expand its range of application. This is considered a critical step in the drive towards quantifying the resilience of the highway system.

For example, lessons learned from recent large earthquakes, such as the 1999 Chi-Chi earthquake in Taiwan, have indicated the importance near-fault effects on bridge response. At the FHWA/NCEER Workshop on the National Representation of Seismic Ground Motion for New and Existing Highway Facilities held in San Francisco in May 1997, a consensus was reached that a response spectrum alone is not an adequate representation of near-fault ground motion characteristics, because it does not adequately represent the demand for the high rate of energy absorption imposed by near-fault pulses. This is especially true for high ground motion levels that drive structures into the non-linear range, invalidating linear elastic assumptions on which the elastic response spectrum is based. Near-fault ground motions are different from ordinary ground motions in that they often contain strong coherent dynamic long period pulses and permanent ground displacements. The dynamic motions are dominated by a large long period pulse of motion that occurs on the horizontal component perpendicular to the strike of the fault, caused by rupture directivity effects. Near fault recordings from recent earthquakes, such as Chi-Chi earthquake, indicate that this pulse is a narrow band pulse whose period increases with magnitude, as expected from analysis.

Many cities on the West Coast of the U.S. are located in near-fault environments and this should be taken into account when studying the resilience of highway systems on the West Coast in particular. Thus bridge fragility functions are required that include near-fault effects for inclusion in loss-estimation models such as REDARS. In addition practical recommendations are required for the design of highway bridges subject to near-fault effects.

The objective of this project is to study the resilience of highway systems with a view to improving the performance of these systems subject to major earthquakes. A comprehensive assessment tool to measure highway resilience shall be developed by improving current loss estimation technologies, such as REDARS; factors affecting system resilience will be identified such as damage-tolerant bridge structures and network redundancy; design aids for curved bridges and those structures in near-fault regions will be developed; new technologies will be developed for improving the seismic performance of bridges; methodologies and technologies developed herein will be implemented in REDARS to the extent practical; and outreach to improve seismic safety will be conducted.

The following are the major tasks of this study:

*REDARS Customization for Resilience Studies*

This task shall implement those upgrades for resilience studies that will focus on improving computation and display of important parameters for characterizing resilience.

*Characterizations of Seismic Hazards for Near-Fault Bridges*

This task will work on Ground Motions including Effects of Rupture Directivity and Surface Fault Rupture Hazards to improve its characterization of surface fault-rupture displacements with a focus on faults as a single straight line.

*Seismic Response of Horizontally-Curved Highway Bridges*

This task is to perform a comprehensive study of the seismic response of horizontally-curved highway bridges. A set of seismic design guidelines for this type of bridge shall be developed.

*Near-Fault Bridge Study*

This task is to develop recommendations for procedures that can be readily used to design bridges in the vicinity of faults and improve public safety throughout the United States.

*Fragility Function for Curved, Near-Fault and other Bridges.*

This task will focus on the development of fragility functions for both curved bridge and near-fault bridges, and other bridges.

**Concluding Remarks**

Risk mitigation methods to reduce earthquake losses need a great effort for development and implementation. The most difficulty with mitigating earthquake hazards is that earthquakes come without any notice. There is no way to accurately predict when an earthquake will occur, nor what its magnitude will be. Earthquakes

are devastating, often resulting in a great number of deaths, injuries and extensive infrastructure damage. Losses will occur in just one or two minutes. Systematic approaches to evaluating earthquake risks, including direct and indirect losses such as economic impact, have become an important issue in our engineering community.

The above two studies focus on (1) The Innovative Technologies and Their Applications to Enhance the Seismic Performance, and (2) Improving the Seismic Resilience of the Federal-Aid Highway System. These two studies will produce many practical recommendations for bridge design in accelerated bridge construction arena, and advance the current design guidelines of curved and near-fault bridges. The study will enhance the previously developed REDARS program with more meaningful and accurate fragility functions to estimate the earthquake losses.

**Reference:**

FHWA Congressional Seismic Research Studies under the SAFETEA-LU Program.

# OVERVIEW OF THE DEVELOPMENT PROCESS AND EFFECTS OF THE UFO METHOD (ACCELERATED CONSTRUCTION METHOD FOR OVERPASSES)

Yuji Mishima<sup>1</sup>, Yukio Katsuta<sup>2</sup>, and Tomoaki Tsuji<sup>3</sup>

## **Abstract**

Traffic congestion at intersections is a serious problem in urban Japan because it causes economic loss and environmental degradation. Shorter construction periods and minimal traffic restrictions are needed to prevent further congestion during the construction of overpasses. The Uni-Fly-Over (UFO) method was developed to achieve dramatically shorter construction periods through structural rationalization for foundations. This paper describes projects for which the UFO method has been used to reduce construction time, explains the method's advantages such as its mitigation of environmental degradation, and outlines a review on the technical issues that had to be overcome to develop steel spread foundations.

## **Introduction**

According to a recent survey conducted by the Ministry of Land, Infrastructure, Transport and Tourism (MLIT), there are over 2,000 intersections throughout Japan that are in need of a solution to the problem of traffic congestion. This indicates that the mitigation of traffic congestion at intersections and railroad crossings is a key issue in realizing an improvement in urban road functions.

Although overpass of intersections is an extremely effective technique for alleviating traffic congestion, the construction of a grade-separated junction in areas suffering from congestion creates further congestion due to the traffic restrictions that must be enforced during the work or aggravates the roadside environment as a result of the noise and vibrations generated in the course of the work.

Given this, there is a growing social need for an accelerated construction technology that will reduce the economic loss that results from traffic restrictions and avoid environmental deterioration by shortening the construction period for overpasses.

The UFO method was developed in 1989 by Hitachi Zosen Corporation to provide an engineering solution to society's demands for a technology that would accelerate the construction of an overpass with a spread foundation. This method has been applied in the construction of three bridges to date. The greatest advantage of this method is the considerable reduction in local construction time it offers by enabling the use of lightweight, prefabricated steel members in the construction of the foundations, which has been a very time-consuming task until now.

This paper describes the development concept and characteristics of the UFO

---

<sup>1</sup> Manager, Infrastructure Technology Development Dept., Hitachi Zosen Corporation, Japan

<sup>2</sup> Manager, Bridge Construction Dept., Hitachi Zosen Corporation, Japan

<sup>3</sup> Assistant Manager, Bridge Design Dept., Hitachi Zosen Corporation, Japan

method and explains its advantages by looking at actual cases in which the method has been applied. The paper also outlines a review made of the technical problems involved in the development of the steel spread foundation, one of the characteristic features of the UFO method, based on some case studies.

### **Development Concept**

The principal purpose of developing the UFO method was to reduce the local construction time for overpasses—including the construction of the superstructure, substructure, and foundations—and to minimize the period of time for which traffic restrictions are imposed. Its development involved the study of conventional problems and their potential solutions. Once that had been done, a method that satisfied the following conditions was realized:

- 1) Earthwork and concreting work, which are both time-consuming activities performed at the work site, should be minimized.
- 2) Members should be prefabricated and a structure that reduces the construction time at the work site should be used.
- 3) Structural rationalization and downsizing should be carried out with respect to the foundation structure, whose construction takes place mainly at the work site and is very time-consuming.
- 4) The retaining wall at the approach should be constructed at the same time as the overpass.
- 5) The members should be erected using readily available machines, and members that can be erected without the use of special equipment should be used to ensure the universality of the method.

Originally intended for use in the construction of spread foundations that are laid on the bearing layer about 5 m underground, the UFO method was developed to satisfy the above-mentioned five conditions. The aim was to achieve a substantial reduction in the local construction time of over 50% compared with conventional methods. An accelerated construction method for pile foundations that was intended for deeper bearing layer was developed jointly by PWRI and Hitachi Zosen. Known as the Uni-Anchor System, it provides a rational combination of steel pier and pile foundations, as shown in Fig. 1. (PWRI. 2005; Mishima et al., 2005)

### **Characteristics of UFO Method**

Fig. 2 provides a structural overview of the UFO method that was developed based on the above-mentioned concept. The structural features are as follows:

#### **1) Continuous steel rigid-frame box-girder bridge with steel deck and integrated superstructure and substructure**

To facilitate quicker construction work, the superstructure and substructure are constructed using prefabricated steel piers and box girders with steel deck. An integrated rigid-frame structure is employed for the superstructure and substructure to

provide enhanced earthquake resistance. As this structure also eliminates the need for bearings and expansion joints, it also provides a smoother ride for vehicles and saving in maintenance costs.

## **2) Steel spread foundations**

As the superstructure and substructure of a conventional overpass are made of a concrete structure with a substantial dead load, larger foundations are inevitably required. This not only necessitates an extension of the work period, but also an enlargement of the work yard, which ultimately means that strict traffic restrictions have to be imposed for the roads at and around the construction site.

The UFO method offers a reduction in weight because the use of steel members for the superstructure and substructure results in the foundations being subjected to a smaller load, enabling prefabricated steel members to be used for the foundation structure. More specifically, a foundation structure built using the UFO method consists of steel members—namely, supporting beams and connecting beam—laid out in a grid pattern with a thin reinforced concrete slab laid underneath them, as shown in Fig. 2. The load from the superstructure and substructure is efficiently dispersed into the ground from the steel members arranged in a grid pattern via the footing. Fig. 3 compares the reaction dispersion mechanism for the UFO method with that of a conventional method. As shown in this figure, the spread foundation is divided into two types: continuous footing along the bridge axis (hereinafter, “continuous footing”), which is a series of steel footings installed between piers along the bridge axis; and isolated footing along the bridge axis (hereinafter, “isolated footing”), which is a single steel footing installed for each bridge pier along the bridge axis. Continuous footing is generally employed when the bearing capacity of ground is relatively low and a large foundation would be required if isolated footing were used. It is also used if it is necessary to disperse the subgrade reaction into the ground as a result of the interaction between the foundations and any underground buried objects. On the other hand, isolated footing is generally employed if any underground buried objects present has no impact on the foundations and the bearing capacity of ground is relatively high.

As mentioned earlier, the UFO method makes use of prefabricated members for almost all the members of both the superstructure and substructure and compact members for the foundation structure. It therefore realizes a significant reduction in the work period and the size of the work yard compared with conventional methods.

## **3) On-site construction method**

The basic method for erecting steel members involves the use of truck cranes, which are economic, versatile, and highly mobile. Use of this erection method enables the following to be achieved: a reduction in the size of the work yard, the cyclic erection of members using the dividing strip as the work yard, and the simultaneous construction of approach section (retaining wall).

The Harada Viaduct is shown in Fig. 4 as an example of the standard procedure employed with the UFO method. As the figure shows, the procedure involves ground excavation for installation of a pier foundation and construction of the concrete slab. This is followed by the cyclic erection of the foundation members, bridge piers, and

the superstructure, in this order. After the erection of the side spans has been completed, the central spans are erected in the direction of the intersection, and finally upper spans are set in place directly above the intersection. Since the degree of precision achieved in the fabrication of the steel members has a great impact on the degree of precision achieved in their erection, the finished quality of the members needs to be strictly controlled by temporary assembly in a fabrication shop, as shown in Fig. 5.

### **UFO Method Case Studies**

#### **1) Kitahanada Overpass**

Conditions at the construction site for the Kitahanada Intersection (located in Sakai city, Osaka prefecture) were extremely challenging because the area in which it is located is home to a major intersection and the Kitahanada subway station. To achieve an uninterrupted traffic flow at this junction, Osaka Prefecture began a project to construct what would become known as the Kitahanada Overpass in 1994, and construction work was completed in 1996. The UFO method was employed for this project so as to realize a considerable reduction in construction time and minimize the impact of the overpass on the subway station structure.

The overpass is a 15-span continuous steel rigid-frame box-girder bridge with steel deck, as shown in Fig. 6. When the structural composition of the overpass was first planned, a design had to be devised that would ensure that the bridge construction would have no impact on the subway station structure. This was necessary because when the subway station was constructed, no consideration had been given to the possible addition of any extra load. Specifically, the steel spread foundation was buried underground and lightweight EPS (expanded polystyrene) was used as backfill to make the weight of the excavated soil equal to the weight of the bridge structure. To ensure an even dispersion of the subgrade reaction, a continuous footing was also employed for the steel spread foundation, based on which the bridge pier intervals were determined. In addition, the soil under the bridge piers was improved to achieve uniform bearing capacity of ground.

Since this was the first time that a foundation structure had ever been built using the UFO method, a 1:10 scale model, as shown in Fig. 7, was produced to conduct loading tests. These tests confirmed its safety with respect to the subway station building.

Thanks to the UFO method, the superstructure and substructure were completed in just 12 months. It was estimated that had a conventional method been taken, it would have taken 27 months to build a rigid-frame bridge comprising 2-span continuous non-composite steel I-girder and 3-span continuous steel box girder with steel deck as the superstructure and a pile foundation as the substructure. This means that a reduction ratio of over 50% was achieved. (Hayakawa et al., 1997)

#### **2) Harada Viaduct**

The Shikoku Regional Development Bureau of the MLIT decided to employ an accelerated construction method in the construction of a viaduct over the Harada

intersection (Marugame City, Kagawa Prefecture) to mitigate traffic congestion and prevent traffic accidents. In selecting the construction method during the development of the basic plan, the Shikoku Regional Development Bureau chose to review 12 accelerated construction methods that might be suitable, comparing them on the basis of construction period, cost, and constructability. Following this review, the UFO method was adopted as the standard method because it had a proven track record and received high evaluations overall. Tenders were invited in 2003 for the construction of a viaduct over the Harada intersection, and the tenderers were screened using the comprehensive evaluation method for which the main evaluation items were the construction fee and how few days the project could be completed in. The project was successfully completed in 2004. Fig. 8 shows the erection work and the completed viaduct.

The viaduct is a 7-span continuous steel rigid-frame box-girder bridge with steel deck, as shown in Fig. 9. Because a bearing layer with an N value of 30 or more was found at a depth of 3 to 8 m from the ground surface of the site, it was possible to use fewer bridge piers in the plan for the viaduct's structural composition than were required for the Kitahanada Overpass, which had extremely challenging ground conditions. Soil improvement was also conducted to reduce the amount of earth that would need to be excavated, which eventually helped to minimize the number of on-site construction days required. Continuous footing was used since a uniform distribution of reaction in the improved soil was needed for the steel spread foundation.

With construction of the superstructure and substructure completed in just 250 days, the UFO method achieved a 60% reduction in the on-site construction period, as shown in Table 1. In contrast, it was estimated that had a conventional construction method been used, it would have taken 630 days to construct a hollow PC slab bridge and a simple composite steel I-girder bridge as the superstructure and an RC bridge pier and RC spread foundation as the substructure and foundation. This reduction in the construction period meant that the method was also able to reduce the traffic restriction period by 40%.

To assess the economic efficiency of the method, the time lost as a result of congestion during the traffic restriction period and the time gained as a result of the early opening of the roads were calculated in monetary terms, the results of which were then evaluated together with the construction cost (see Fig. 10). This revealed that using the UFO method is about 20% more expensive than the conventional method, but about 2% more advantageous in terms of a comprehensive evaluation of losses arising from congestion and gains from the early opening. Further advantages are known to be gained from the use of the UFO method, including the prevention of the environmental degradation, which cannot be valued in monetary terms and a reduction in losses from disruption to goods distribution. (Yamada et al., 2005)

### **3) Tonyamachi Overpass**

In 2007, the Kanto Regional Development Bureau of the MLIT invited tenders for a project to construct a viaduct over the Tonya intersection (located in Utsunomiya City, Tochigi Prefecture) to mitigate traffic congestion at the intersection point.

Executed as a package contract for the design and construction of the overpass, the project involved large-scale construction work over a length of road totaling 1,190 m in length that included the construction of an elevated bridge and approach as well as road improvements to the section under the intersection. A joint venture in which we, Hitachi Zosen Corporation, participated won the contract because our proposal offered an on-site construction period that would, thanks to the use of the UFO method for the construction of the overpass, be 50% shorter than the employer's requirement and because our bid price was the lowest of the three joint ventures who participated in the tender. The project is currently underway, with completion scheduled for March 2010.

The overpass is a 3-span continuous steel rigid-frame box-girder bridge with steel deck as shown in Fig. 11. The dimensions of the bridge and the retaining wall were determined in such a way as to achieve a good balance between the construction cost and a reduction in the construction period. In addition, isolated footing, rather than continuous footing, was used for the steel spread foundation because, unlike for the Kitahanada Overpass or the Harada Viaduct, underground buried objects had no impact on the work, the bridge length was short, and the supporting ground had sufficient strength. This rationalization allowed us to plan for a reduction in the standard on-site construction period set by the employer of over 50%.

## **Technical Review of Steel Spread Foundations**

### **1) Outline**

The greatest advantage of the UFO method is its ability to significantly reduce the on-site construction period and the size of the work yard by employing a steel spread foundation composed of prefabricated members that are both lightweight and compact. The use of such a steel spread foundation was unprecedented, and the greatest challenge posed by the application of this method was to ensure its safety.

There are two types of steel spread foundation used in the UFO method: continuous footing and isolated footing. Which of these methods is employed depends on the bearing capacity of ground and the conditions of any underground buried objects, as earlier mentioned.

Reviews conducted of these two types of footing are outlined in the following sections using the Harada Viaduct and Tonyamachi Overpass Bridge as case studies, with a particular focus placed on safety.

### **2) Continuous footing**

If a spread foundation is being considered for use as a rigid foundation, as is conventionally done for a reinforced concrete footing, its safety should be verified against the Specifications for Highway Bridges (Japan Road Association, 2002), and the footing should then be designed to be thick enough to be verified as a rigid entity in accordance with the said specifications. If a footing is confirmed to be thick enough as a rigid body, this means that the equations for calculating the bearing capacity of ground or subgrade reaction as specified by the Specifications for Highway Bridges are determined based on the assumption that the footing in question is a rigid body. The type of spread foundation used for the Kitahanada Overpass and the Harada Viaduct

was a continuous footing both along the bridge axis and in the direction perpendicular to the bridge axis. For the direction perpendicular to the bridge axis, the rigidity of the foundation as a rigid body can be maintained because of a shorter footing span. For the direction along the bridge axis, however, since the footing span is 14 to 21 m, it is not rational either in terms of structure or construction for the footing to have sufficient thickness as a rigid body. Therefore, it was necessary to consider the continuous footing as an elastic foundation and to check the stability in terms of bearing capacity, toppling, and sliding by taking into account the uneven distribution of the reaction from the superstructure and substructure. Typical safety check methods include loading tests using a scale model, as in the case of the Kitahanada Overpass, and finite element analysis. The finite element analysis used for the Harada Viaduct is explained below to serve as an example.

For the Harada Viaduct project, both the local ground and the steel foundation members determined relative to external forces during the design stage were modeled for review using three-dimensional finite element analysis, which can accurately consider the impact of the three-dimensional ground supporting the spread foundation, as shown in Fig. 12. For a conventional type of spread foundation, only a test load equivalent to the load that would occur in the event of a Level 1 earthquake is used due to the behavioral characteristics of the foundations in the event of a major earthquake. But since no behavioral characteristics for a steel spread foundation have been identified yet, the load that would occur in the event of a Level 2 earthquake was used for the safety check to err on the side of caution.

The distribution of the level of vertical stress on the ground is shown in Fig. 13 as an example of the analytical results. This figure indicates that no stress in excess of the allowable value was exerted on the ground and that stress was generally dispersed across all of the ground at a depth of 6 to 7 m. The results for toppling and sliding also revealed no problems.

In conclusion, the safety of steel spread foundations was verified using three-dimensional finite element analysis, which takes into account the three-dimensionality of the ground.

### **3) Isolated footing**

If the ground strength is relatively high and underground buried objects do not cause any major problems, isolated footing that is compact and easy to construct serves best, as was the case with the Tonyamachi Overpass (Fig. 11). However, for an isolated footing, steel spread foundation members are cantilevered along the bridge axis, which eventually causes a concentration of the reaction just under the bridge pier if the footing rigidity is low. Therefore, it is necessary to provide steel members with a level of rigidity that is as high as that of a conventional spread foundation so that the reaction force of the superstructure and substructure acts uniformly on the ground.

As has already been mentioned, the required rigidity for a spread foundation is specified in the Specifications for Highway Bridges. However, the provisions in these specifications are meant for conventional spread foundations, which are made of

reinforced concrete of high rigidity. As such these specifications cannot be applied directly for lightweight, relatively flexible foundations such as foundations made of steel members and thin concrete slabs, as used in the UFO method. For a steel spread foundation, therefore, it was necessary to verify whether the steel foundation members, whose cross section had been determined in the design stage according to the external forces to which they would be subjected, possessed the required rigidity.

As a result, three-dimensional finite element analysis was used to verify this, as was the case with the Harada Viaduct. Given that the subject for analysis was an isolated footing, a partial model was used, as shown in Fig. 14. To be on the safe side, the loads to be checked included those that would occur in the event of Level 2 earthquake. The section forces of the pier base, which were calculated from a separately conducted dynamic analysis, were applied to the end of the model as a boundary section force.

The rigidity of the steel spread foundation was evaluated based on an existing research paper (Iijima, 1981) that served as the basis for the rigidity judgment adopted in the Specifications for Highway Bridges. More specifically, attention was paid to the level of subgrade reaction intensity, and the difference between the subgrade reaction intensity ( $P_{\text{mean}}$ ) for a spread foundation as a rigid body and the maximum subgrade reaction intensity ( $P_{\text{max}}$ ) for a steel spread foundation was expressed as a ratio to  $P_{\text{mean}}$  (see Fig. 15). This ratio is taken as the dispersivity of reaction. If the allowable level of this dispersivity is within  $\pm 20\%$ , the foundation should be taken as a rigid body.

As an example of this result, the distribution of the subgrade reaction in the event of a Level 2 earthquake in the direction perpendicular to the bridge axis is shown in Fig. 16. As the figure shows, the dispersivity of the subgrade reaction is within the allowable limits. This confirms that steel spread foundations have sufficient rigidity.

Highly precise results may be obtained from a rigidity evaluation of a steel spread foundation if finite element analysis is used, but considering the time and money it would take to carry out such an analysis every time one was necessary, a simplified evaluation equation would be of great benefit for the actual design work.

## **Conclusion**

This paper presents an outline of how the UFO method, an accelerated construction method used to mitigate congestion at intersection points, was developed and introduces some projects for which the method was applied. The projects for which the UFO method was applied turned out to be successful in terms of the intended goal of achieving a significant reduction in the construction period, despite differences in their on-site conditions.

The following points summarize the conclusions of this paper.

- 1) The UFO method can be successfully used to reduce the on-site construction period by over 50% compared with conventional methods, although the actual reduction varies according to the local conditions.
- 2) A reduction in the on-site construction period will produce various other advantages, including a reduction in the traffic restriction period and

- mitigation of the negative impact on the environment.
- 3) The UFO method uses two types of spread foundation: continuous footing, which is a series of steel footings along the bridge axis, and isolated footing, which is a single steel footing along the bridge axis. A significant reduction in the on-site construction period can be achieved by selecting the type of foundation suited to the bearing capacity of ground and the conditions of any underground buried objects.
  - 4) Loading tests with a scale model or 3D FE analysis with a local ground model have verified that steel spread foundations are safe in the event of a Level 2 earthquake.

## References

- Hayakawa, Kitaya, Yamashita, Beppu, Shiomi, and Wakita: “Design of the Kitahanada Overpass—Built using a Spread Foundation Immediately Above the Subway Station Building,” *Bridge and Foundation Engineering*, Vol. 31, No. 1, Jan. 1997. In Japanese.
- Iijima: “Footing Thickness,” *Bridge and Foundation Engineering*, Vol. 15, No. 5, 1981. In Japanese.
- Japan Road Association: “Specifications for Highway Bridges and their Explanation,” March 2002
- Mishima, Tahara, Wakabayashi, Sasaya, Fukui, and Takeguchi: “Experimental Study of Connection between Steel Bridge Pier and Foundation,” *Bridge and Foundation Engineering*, Vol. 41, No. 11, Nov. 2007. In Japanese.
- Public Works Research Institute, Hitachi Zosen Corporation, and Fujita Corporation: “Joint Research Report on the Development of a Technique to Reduce the On-road Construction Period for an Overpass Project,” Joint Research Report No. 334, March 2005. In Japanese.
- Yamada, Toyosaki, Takeuchi, Mishima, Tahara and Ishiyama: “Design and Construction of the Harada Viaduct—Overpass of an Intersection using an Accelerated Construction Method,” *Bridge and Foundation Engineering*, Vol. 39, No. 9, Sept. 2005. In Japanese.

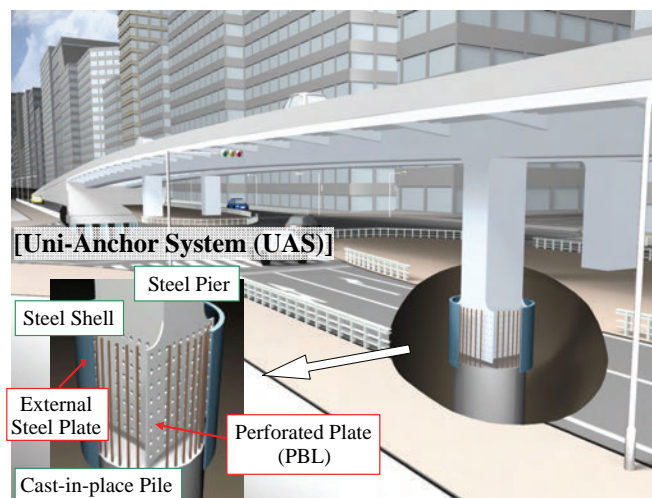


Fig. 1 Structural Overview of the Uni-Anchor System

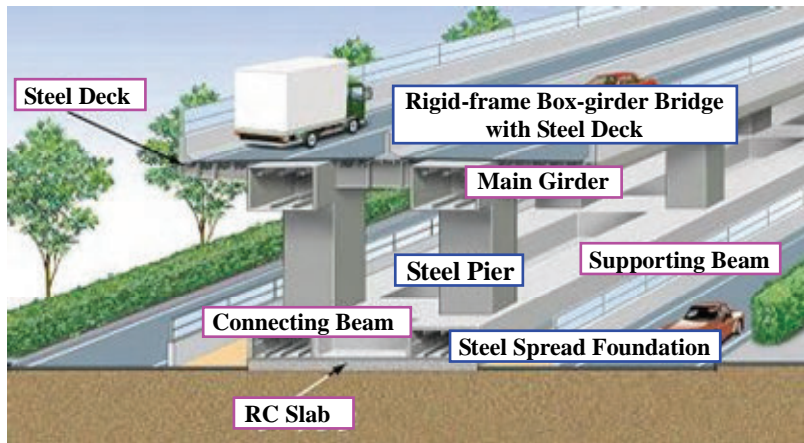


Fig. 2 Structural Overview of the UFO Method

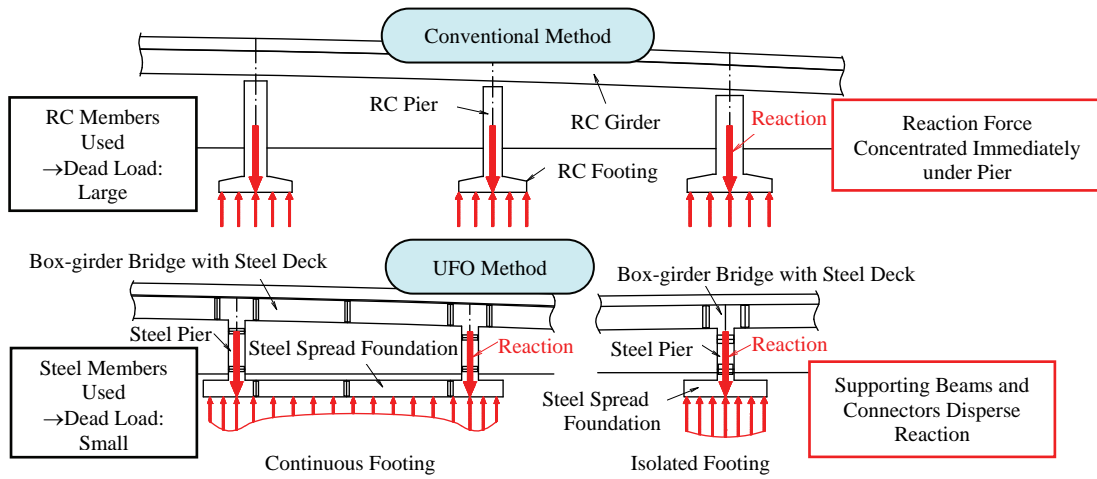


Fig. 3 Comparison of Reaction Dispersion Mechanisms

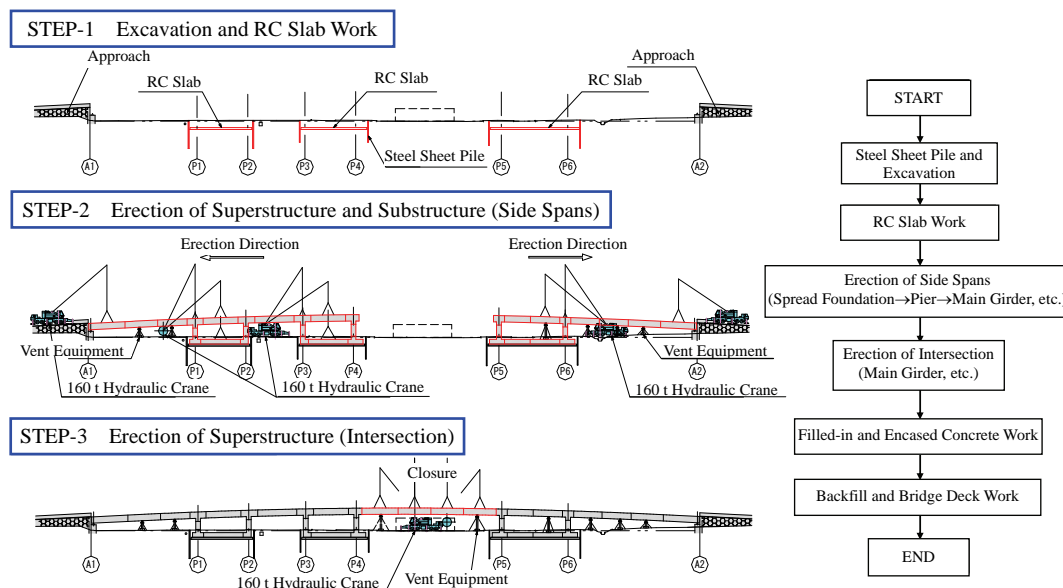


Fig. 4 Standard Construction Procedure (Harada Viaduct)





Steel Spread Foundation  
(Continuous Footing)



Full View of the Completed Viaduct

Fig. 8 Erection Work and Full View of the Harada Viaduct

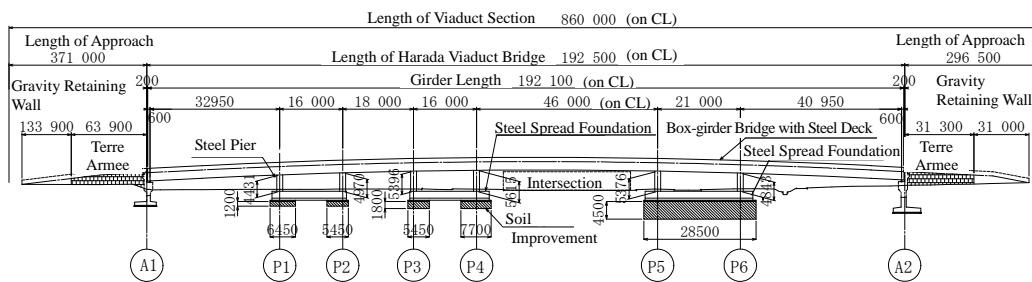


Fig. 9 Construction Plan for the Harada Viaduct

Table 1 Comparison of Construction and Traffic Restrictions Period

Month		1	2	3	4	5	6	7	8	9	10	11	12	13	14	15	16	17	18	19	20	21	22	23	24	25	26
Work Period for Entire Project	Conventional method	750 Days (25 Months)																									
	UFO Method	450 Days (15 Months)															Saving of 300 Days (40% Reduction)										
Work Period for Overpass	Conventional method	630 Days (21 Months)																									
	UFO Method	250 Days (8.3 Months)								Saving of 380 Days (60% Reduction)																	
Overpass Work Traffic Restrictions	Conventional method	315 Days (10.5 Months)																									
	UFO Method	185 Days (6.2 Months)						Saving of 130 Days (40% Reduction)																			

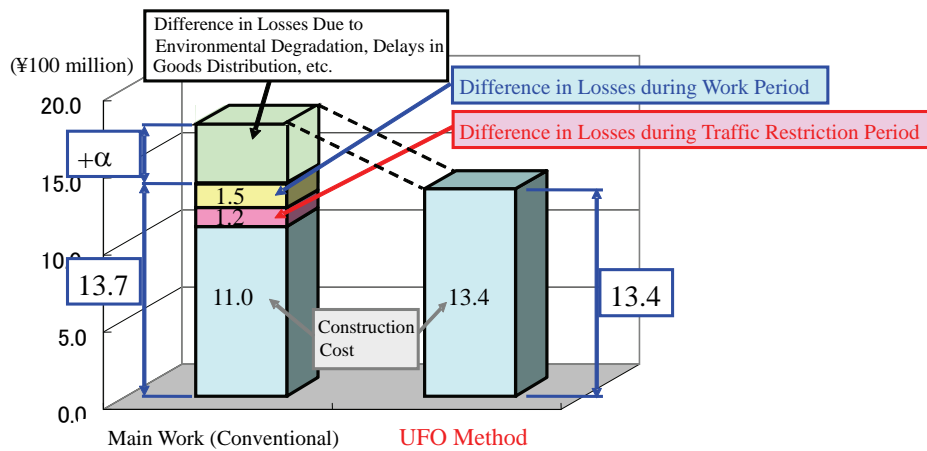


Fig. 10 Economic Benefits of the UFO Method (Evaluated by MLIT)

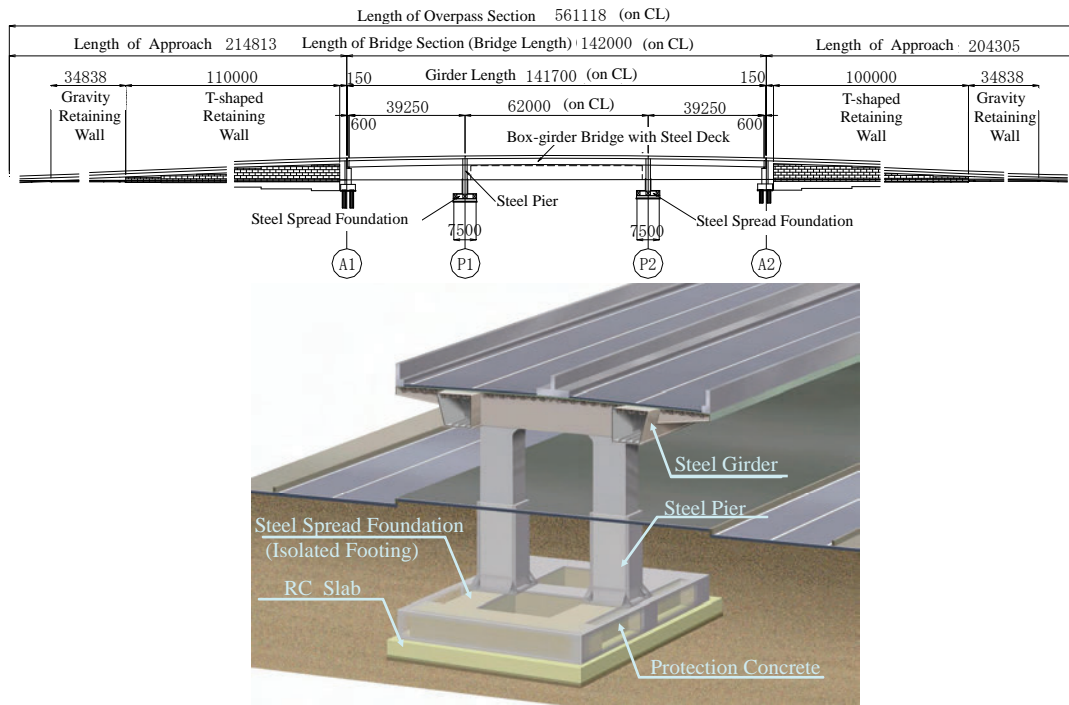


Fig. 11 Structural Overview of the Tonyamachi Overpass

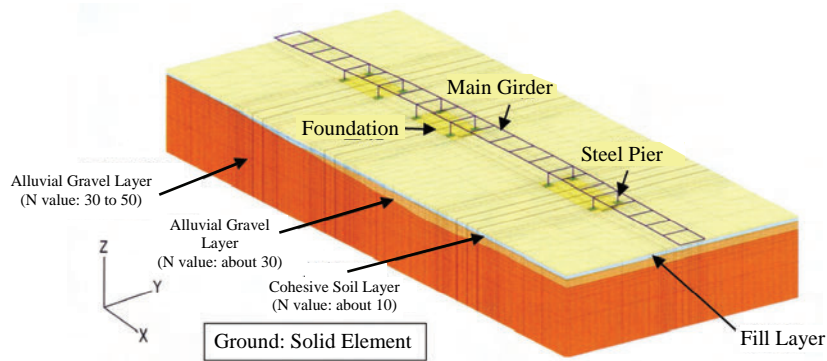


Fig. 12 Three-dimensional FE Model (Harada Viaduct)

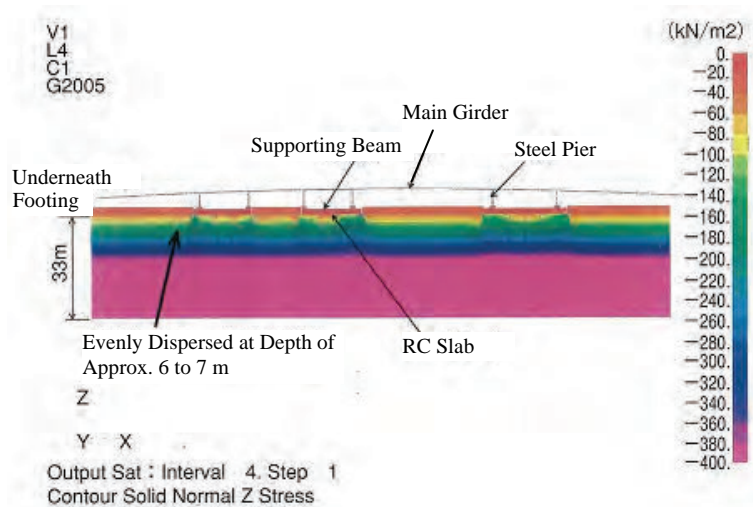


Fig. 13 Example of Analysis Result (Subgrade Reaction Distribution)

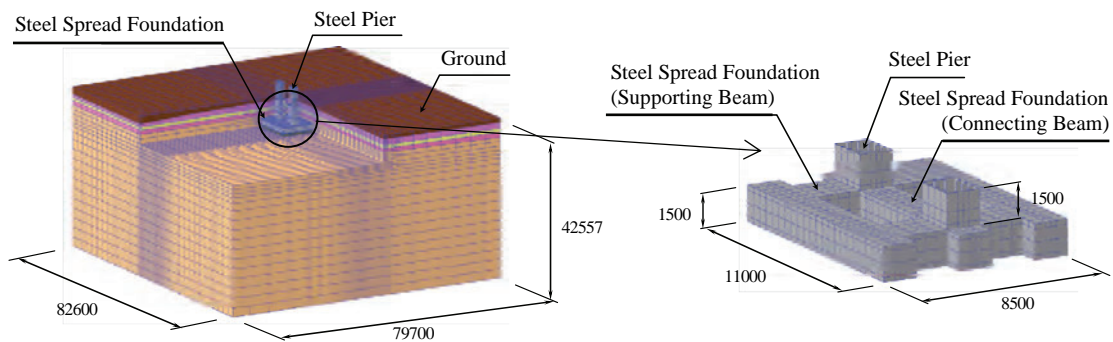
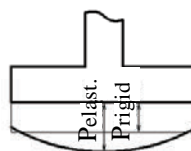


Fig. 14 Three-dimensional FE Model (Tonyamachi Overpass)

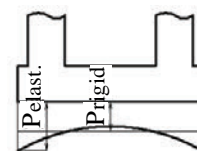
Dispersivity of Subgrade Reaction 
$$\bar{P} = \frac{P_{\text{elast.}} - P_{\text{rigid}}}{P_{\text{rigid}}} \leq \pm 20\%$$

$P_{\text{elast.}}$ : Subgrade Reaction Intensity of Steel Spread Foundation as an Elastic Body

$P_{\text{rigid}}$ : Subgrade Reaction Intensity of the Footing as a Rigid Body

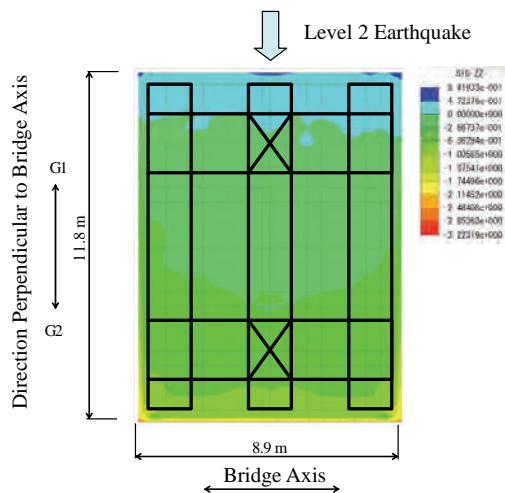


Bridge axis direction

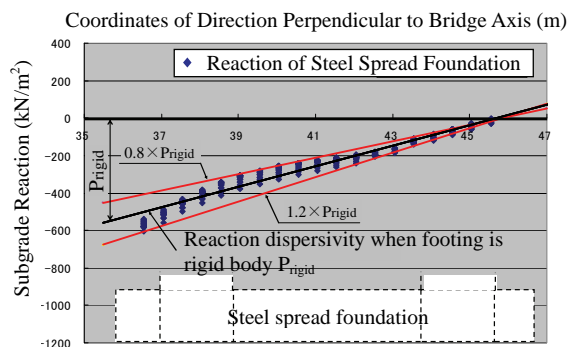


Direction perpendicular to bridge axis

Fig. 15 Judgment of Rigidity Body

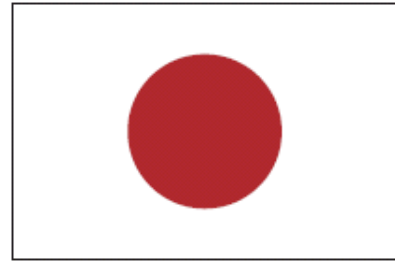


(a) Subgrade Reaction Contour



(b) Subgrade Reaction Distribution

Fig. 16 Example Judgment Result for Footing Rigidity



# 25<sup>th</sup> US-Japan Bridge Engineering Workshop

## Session 4

### Remedial Work & Partial Replacement

Experimental Study on the Time Dependent Flexural Behavior of Prestressed  
Reinforced Concrete Beams

By Hiroshi Watanabe, Hirohisa Koga, Hisashi Aoyama, and Yuuki Takeuchi

Overnight Delivery - NJDOT Rapid Bridge Replacement

By X. Hannah Cheng and Harry A. Capers, Jr

Effect of Reducing Strains by SFRC Pavement on Ohira Viaduct

By Takayoshi Kodama, Mamoru Kagata, Shigeo Higashi, Kiyoshi Itoh, and  
Yatsuhiro Ichinose

Rapid Bridge Repair / Rehabilitation in Washington State

By Jugesh Kapur

Page Left Blank

# **Experimental study on the time dependent flexural behavior of prestressed reinforced concrete beams**

H.Watanabe<sup>1</sup>, H.Koga<sup>1</sup>, H.Aoyama<sup>2</sup>, Y.Takeuchi<sup>2</sup>

## **ABSTRACT**

For prestressed reinforced concrete structures, cracking is allowed at the serviceability limit, and the crack width should be controlled by deformed reinforcing bars and prestressing forces. There are many research results relating to the flexural crack widths in RC beams; however it is not clear in PRC beams especially the effect of creep and drying shrinkage on their crack width. Experimental study using PRC, RC and PC beams are carried out to investigate it. In this paper deformation and crack widths of PRC beams under the sustained flexural load will be discussed with the data of creep and drying shrinkage of concrete without reinforcement.

## **INTRODUCTION**

In prestressed reinforced concrete bridges, cracking is allowed at the serviceability limit and the crack width should be controlled by arrangement of de-formed reinforcing bars and prestressing forces. PRC bridges increases in number recently while most prestressed concrete road bridges in Japan were designed to avoid cracking in design load combinations.

In PRC bridges, crack control is important to as-sure durability. However long-term behavior of crack width in PRC beams, especially the effect of creep and drying shrinkage, is not clear.

In this paper, cracking, deformation and crack widths of PRC beams under the sustained flexural load will be discussed with the data of creep and drying shrinkage of concrete without reinforcement.

## **EXPERIMENTAL PROCEDURE**

Dimensions of test beams are shown in Figure 1 and Table 1. Span length of each beam is 3000mm.

Beam A1 was designed as fully prestressed concrete member; there is no compressive/tensile stress at the concrete surface with design load in this test, 27.5kN m (1.0Md). Beam B1, B2 and C2 were designed as PRC members and prestressing force of these beams were decreased. Beam D1 and D2 were designed as RC members.

Diameter of re-bars was selected as tensile stress of longitudinal reinforcements in beam B2, C2 and D2 would be approximately 200MPa with 2.0Md bending

---

<sup>1</sup> Senior Researcher, Center for Advanced Engineering Structural Assessment and Research, PWRI

<sup>2</sup> Former Interchange Researcher, Advanced Engineering Structural Assessment and Research, PWRI

moment.

Prestressing tendons and steel reinforcing bars were in compliance with JIS. Prestressing force was introduced after 10 days from casting. Properties of prestressing tendons, tensile longitudinal reinforcement and concrete are shown in Table 2 and Table 3.

Sustained load test started approximately 28 days after casting. Test beams were set upside down on support steel H-beams and flexural load was introduced by four prestressing tendons placed near both ends of beams (Fig. 2). Sustained flexural load was checked and adjusted at least once a month.

Displacement at the mid-span of test beams, strain of prestressing steel, re-bars and concrete were monitored with strain gauges. Deformation of beams was measured with contact strain gauge that

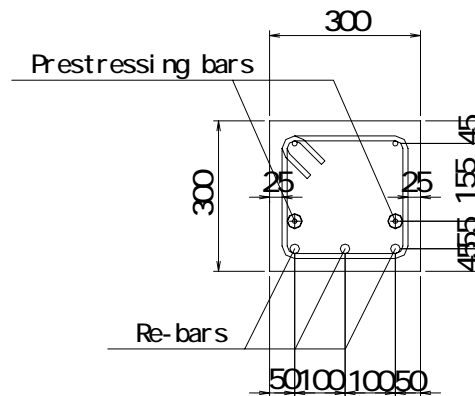


Figure 1. Section of test beams.

Table 1. Test beams.

Beam	A1	B1 B2	- C2	D1 D2
Prestressing bars*	2-17mm	2-13mm	2-9.2mm	-
Re-bars*	2-10mm	3-16mm	3-19mm	3-22mm
Prestressing force	272kN	159kN	80kN	-
k**	100%	58%	29%	0%
Sustained load***	1.0Md (A1, B1 and D1) 2.0Md (B2, C2 and D2)			
Tension stress of Re-bars (MPa)	1.6	38.0	-	110.8
Tensile stress of concrete surface (MPa)	-	222.0	219.0	210.8
	0.0	2.1	-	4.8
	-	7.5	8.7	9.8

\* Diameter of prestressing bars/re-bars

\*\*  $k = M_0 / M_d$ ,  $M_0$  is the bending moment with which there is no stress at concrete surface in tension side.

\*\*\* 1.0Md = 27.5kN m in this test. Sustained loads in beam B2, C2 and D2 were adjusted to control maximum tensile stress in tensile longitudinal reinforcement (200MPa).

Table 2. Properties of prestressing bars and rebars.

Beam Specimen	Diameter	E Modulus	Yield Strength
<Prestressing bars>			
A1	17mm	200GPa	1061MPa
B1, B2	13mm	201GPa	1055MPa
C2	9.2mm	200GPa	1262MPa
<Re-bars>			
A1	10mm	187GPa	369MPa
B1, B2	16mm	188GPa	365MPa
C2	19mm	185GPa	379MPa
D1, D2	22mm	186GPa	386MPa

Table 3. Properties of concrete

Water cement ratio	49%
Compressive strength	39.7MPa
E Modulus	28.6GPa
Tensile strength	3.22MPa

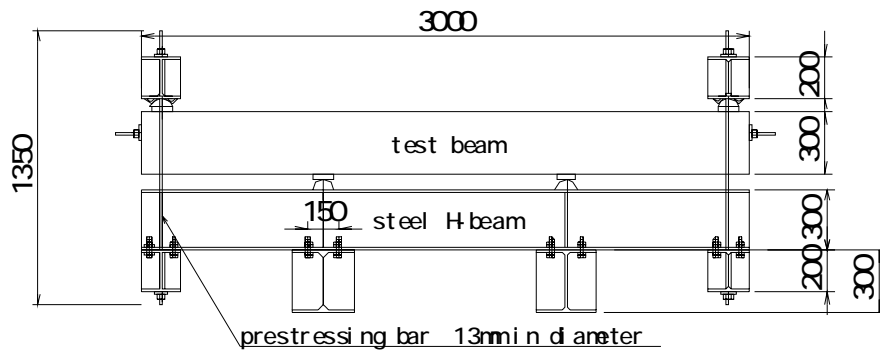


Figure 2. Arrangement for sustained load test (dimensions in mm)

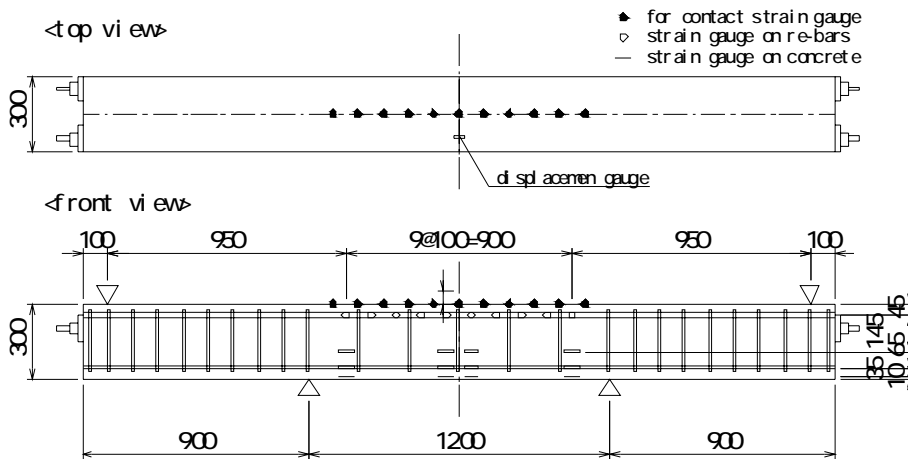


Figure 3. Positions of strain gauges and points for measurement (dimensions in mm).

has 100mm base length and in cracked area measured values are taken as the change of crack width. This measurement was carried out once a month. Positions of strain gauges and points for measurement are shown in Figure 3.

Table 4. Drying shrinkage of concrete

Days after casting	28	62	91	227	413
Strain $\times 10^{-6}$	97	156	216	348	402

Drying started 4days after casting.

Table 5. Creep coefficient

Days after introducing prestressing force	22	64	201	386
coefficient	0.73	1.04	1.60	1.84

Drying shrinkage of concrete was measured at center of  $300 \times 300 \times 1200$ mm concrete specimen (Table 4). Creep coefficients were measured with  $300 \times 300 \times 3600$ mm concrete specimens with 483kN prestressing force (Table 5).

## **TEST RESULTS**

### *Cracking of beams*

Cracking maps after one year loading are shown in Figure 4. Nine or ten cracks were observed on the surface of beam B2, C2, D1 and D2 at the start of sustained load test. The numbers of cracks have not changed through the test. Five cracks were observed on the surface of beam B1 after 60days loading while no crack was observed

at the beginning of test. The number of cracks in beam B1 has not changed after cracking was observed.

In beam B2, C2, D1 and D2, average crack spacing in each beam is fit to the calculation result proposed in JSCE standard specification that is based on an assumption that tensile stress in concrete is negligible. On the other hand, in beam B1, number of crack is less than that of B2, C2 and D2.

No crack was observed on the surface of beam A1.

*Deflection of beams*

Mid-span deflections of test beams are shown in Figure 5. Deflection of beam B2, C2 and D2 has been increased approximately 0.5mm under sustained flexural load and deflection of beam D1 in-creases approximately 0.4mm.

Beam A1 and B1 have no bending crack at the beginning of sustained load test and deflections of these beams are almost same. However, deflection of beam B1 has increased through the sustained load test while deflection of beam A1 has not been in-creased significantly.

*Crack width*

Maximum crack widths of test beams are shown in Figure 6. Crack widths increased in first 6 months and then show some decreasing.

The reason of this is not clear, but temperature change can affect. Maximum crack widths of beam B2, C2 and D2 loaded to have almost the same tensile stress in tensile longitudinal reinforcement have

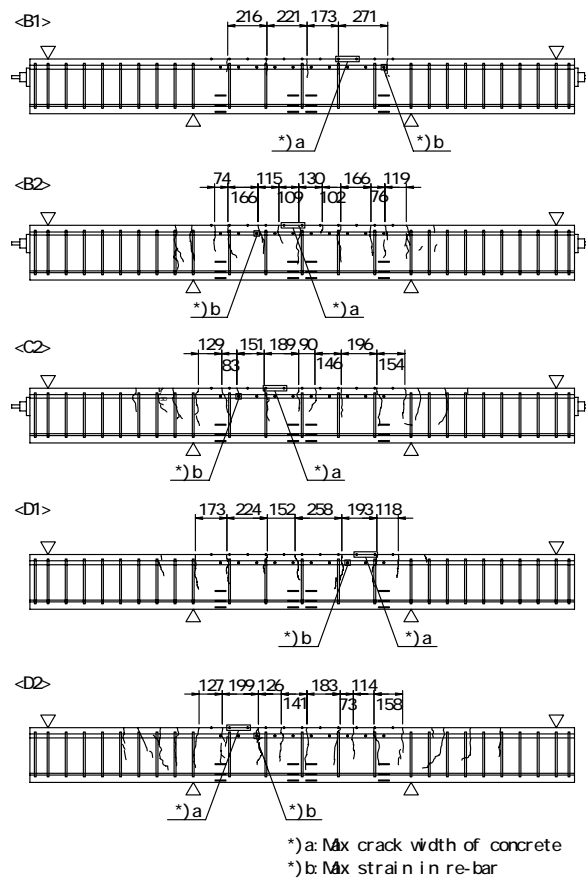


Figure 4. Cracking maps after one sustained load test.

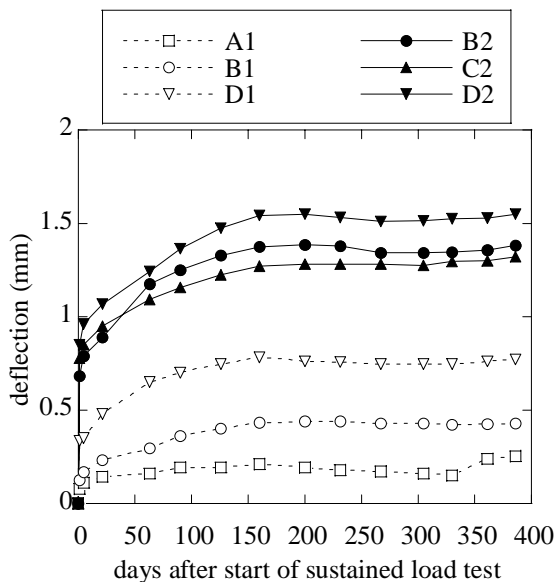


Figure 5 Change of the mid-span deflection of each beam.

been increased approximately 0.1mm through sustained flexural test. The effect of prestressing force to the long-term behavior of crack width is not clear.

Maximum crack widths of beam D1 on which the half of D2 bending moment was applied has been increased approximately 0.07mm.

While there is no crack in beam B1 when the sustained load test was started, changing of measured lengths with the contact strain gauge are calculated and maximum crack width has been increased approximately 0.04mm.

Measured crack widths in beam B2 are shown in Figure 7. Increased crack widths in sustained load test have been different in each measured point. However, there are relatively bigger cracks and smaller cracks on the surface of beam B2 and this tendency has been kept through test period.

*Strain of concrete and tensile longitudinal reinforcement*

Strain at concrete surface in four sections and strain of tensile longitudinal reinforcement in ten sections are monitored through the test. In

Figure 8, average values of these data in beam B1 and B2. In Figure 8, results of linear regression analysis with strain of concrete are shown.

In beam B2, compressive strain of concrete has increased approximately  $900 \times 10^{-6}$  and strain of tensile longitudinal reinforcement has increased approximately  $500 \times 10^{-6}$  through sustained load test. Change of strain of tensile longitudinal reinforcement corresponds with change of regression line calculated with strain of concrete. Also in beam C2, D1 and D2, strain of section looks to be proportional to the distance from the neutral axis.

In beam B1, when sustained load test started, strain of tensile longitudinal reinforcement is almost zero as there was no crack in beam B1 and tension force was

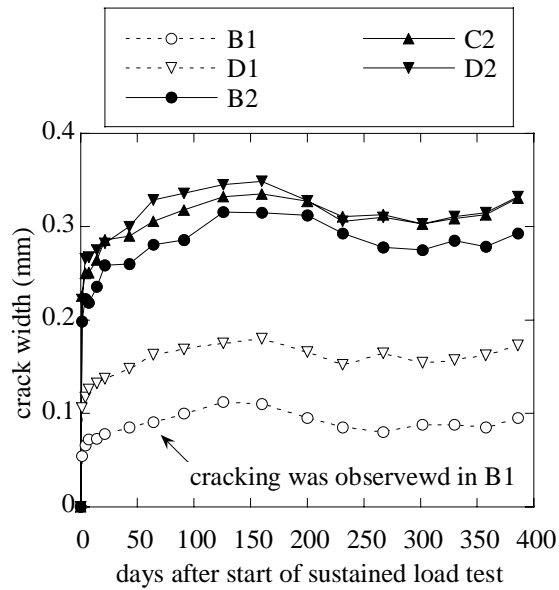


Figure 6. Change of the maximum crack width of each beam.

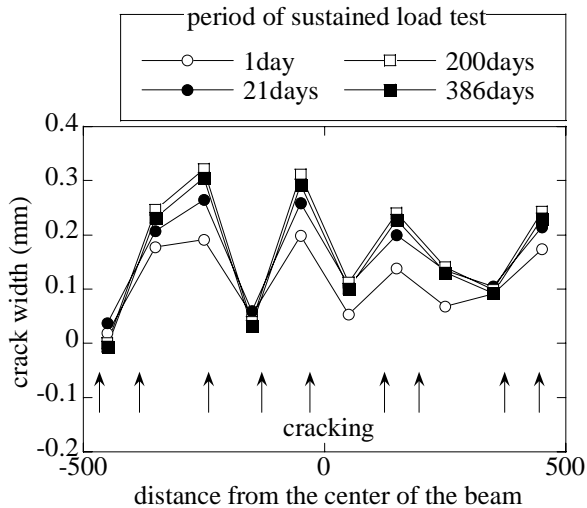


Figure 7. Change of the distance (crack width) on the tension side concrete surface of beam B2.

mainly sustained by concrete. Strain of tensile longitudinal reinforcement in beam B1, however, has been increased with time. This should be the effect of cracking and decrease of tension force shared by concrete in tension area.

From the data of strain of concrete and tensile longitudinal reinforcement, deflection of each beam was calculated as curvature and shown in Figure 9. Change of curvature is in good accordance with mid-span deflection shown in Figure 5.

*Distribution of strain in tensile longitudinal reinforcement*

From the difference of numbers of crack, crack widths and strain in tensile longitudinal reinforcements between beam B1 and B2, effect of tension stiffening would be different in two beams. To discuss it, distribution and change of strain of tensile longitudinal reinforcement where equal bending moment is loaded are shown in Figure 10.

In beam B1, strain of tensile longitudinal reinforcement was uniform when sustained load test was started and this uniformity was kept before cracking while strain of reinforcement

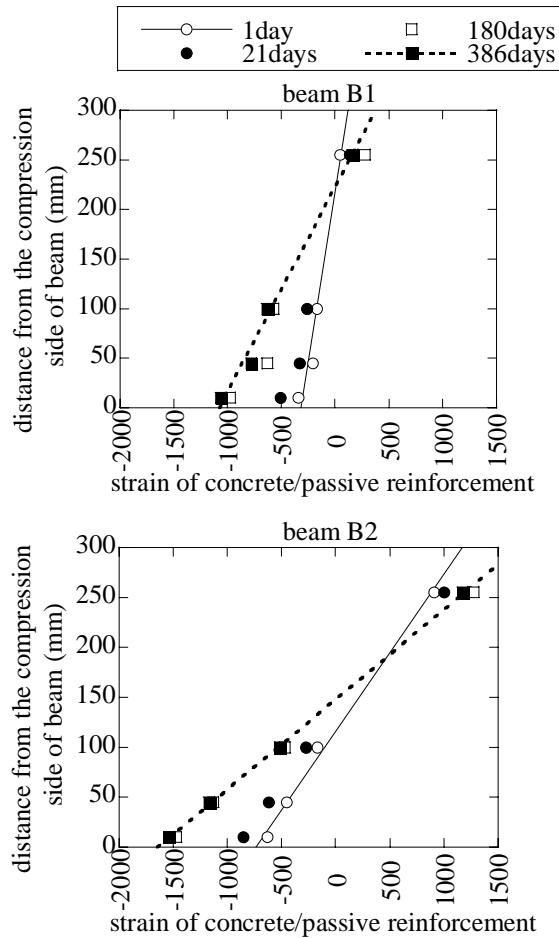


Figure 8. Change of the distance (crack width) on the tension side concrete surface of beam B2.

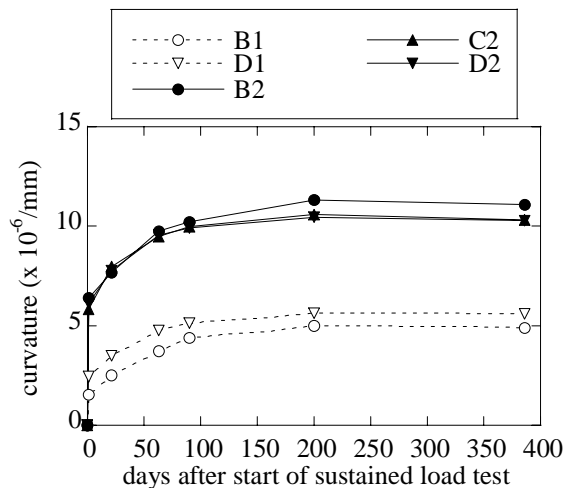


Figure 9. Change of mid-span curvature calculated with the data of strain gauges on concrete and tensile longitudinal reinforcement.

increased with time. After cracking, strain of reinforcement has increased more in the area near bending crack.

Cracks in B1 were observed after 60 days loading and the tensile creep can affect the cracking. Tensile strength of concrete is known to become smaller when loading rate is small. In B1, tensile stress of concrete under the sustained flexural load is closet to the tensile strength of concrete.

In beam B2, there is no newly cracking under the sustained load and change of strain of tensile longitudinal reinforcement under the sustained load is al-most same in each strain gauge. In beam C2 and D2 under 2.0Md sustained load, also in beam D1 under 1.0Md sustained load, strain of tensile longitudinal reinforcement changed alike. Bond between concrete and tensile longitudinal reinforcement has not changed in these beams.

*The effect of drying shrinkage of concrete*

One of the beam specimen, arrangement of reinforcements is the same as B1 and B2, has been placed upside-down on steel H-beam without prestressing force and sustained load. Drying shrink-age of this test beam is shown in Figure 11. Progress of drying shrinkage in three monitored point of this test beam is similar to that of plain concrete shown in Table 3.

Drying shrinkage of plain concrete after through the period of sustained load

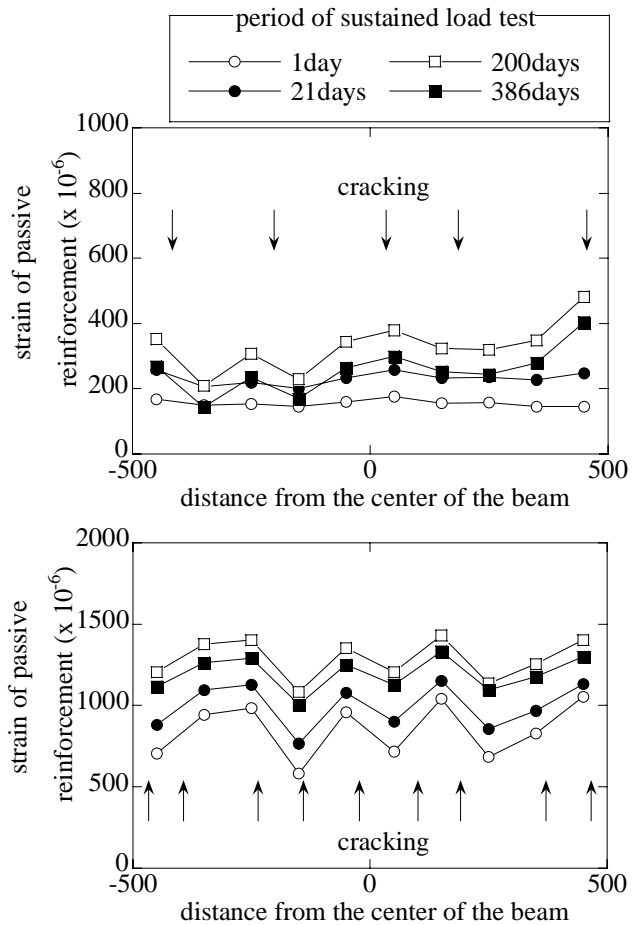


Figure 10. Distribution of strain of tensile longitudinal reinforcement.

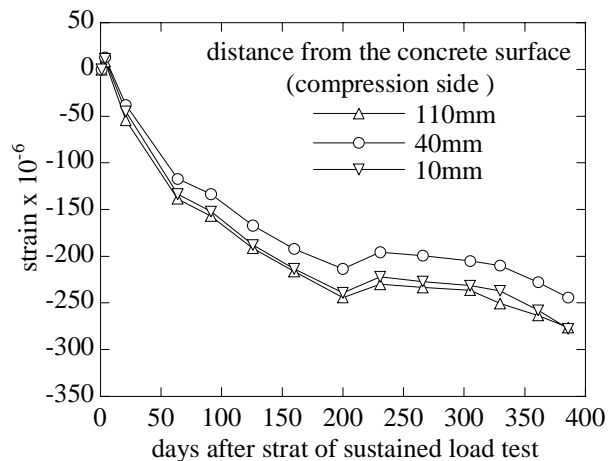


Figure 11. Strain of concrete in the test beam that is not loaded.

test is  $305 \times 10^{-6}$  (Table 3) and maximum space between cracks in beam B2, C2 and D2 is 199mm (Fig. 4). Increase of crack width caused by drying shrinkage is estimated to be approximately 0.06mm. However, this calculation result is half of actual crack widening in beams under 2.0Md sustained load (Fig. 6). Crack widening under sustained load test, therefore, can not be explained by drying shrinkage only.

### **COMPARISON WITH PROPOSED ESTIMATION METHOD FOR CRACK WIDTHS**

In JSCE (Japan Society of Civil Engineer) standard specification for concrete structure, examination for flexural crack width should be done with Equation 1 and given permissible crack width. In other specifications for PRC bridges, framework of examination method is similar.

$$w = 1.1k_1k_2k_3 \left\{ 4c + 0.7(c_s - \phi) \right\} \left( \frac{\sigma_{se}}{E_s} + \varepsilon'_{csd} \right) \quad (1)$$

where,  $k_1, k_2, k_3$  = constant values to take into account the effect of surface geometry of reinforcement, concrete quality and multiple layers of tensile reinforcement on crack width;  $c$  = concrete cover(mm);  $c_s$  = center to center distance of tensile reinforcement (mm);  $\phi$  = diameter of tensile reinforcement (mm);  $\varepsilon'_{csd}$  = compressive strain for evaluation of increment of crack width due to shrinkage and creep of concrete;  $\sigma_{se}$  = increment of stress of reinforcement from the state in which concrete stress at the portion of reinforcement is zero  $N/mm^2$ .

However, the value of  $\varepsilon'_{csd}$  for designing PRC bridge has not been established yet. To compare with proposed design values as  $\varepsilon'_{csd}$ ,  $\varepsilon'_{csd}$  in each beam is calculated with maximum crack width and increase of tensile longitudinal reinforcement in each beam and shown in Figure 12, as calculated value of  $w$  in Equation 1 virtually shows maximum crack width.

Calculated values of  $\varepsilon'_{csd}$  after one year sustained load test range are bigger than proposed value,  $150 \times 10^{-6}$  by JSCE in beam C2, D1 and D2. Calculated values of  $\varepsilon'_{csd}$  is smaller in PRC beam than RC beam. However the cause of this tendency is not clear.

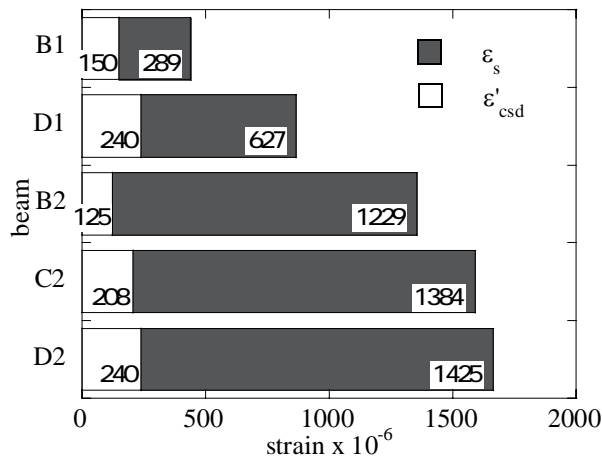


Figure 12. Calculated values of  $\varepsilon'_{csd}$  and  $\varepsilon_s$  after 390 days sustained load test.

## **CONCLUSIONS**

Increase of the mid-span deflection and bending crack width are observed in beams under sustained flexural load and prestressing force dose not affect the rate of it when tensile strain of tensile longitudinal reinforcement is same.

Strain of concrete and tensile longitudinal reinforcement in beams under sustained flexural load has been proportional to the distance from the neutral axis generally.

Bond between concrete and tensile longitudinal reinforcement has not been affected significantly by sustained flexural load.  
Compressive strain for evaluation of increment of crack width due to shrinkage and creep of concrete ( $\epsilon'_{csd}$ ) was bigger than proposed value by JSCE in some test beams.

## **References**

JSCE (2002) Standard specifications for concrete structures-2002 “Structural Performance Verification”

blank

## **OVERNIGHT DELIVERY – NEW JERSEY DOT RAPID BRIDGE REPLACEMENT**

Xiaohua H. Cheng<sup>1</sup> and Harry A. Capers, Jr.<sup>2</sup>

### **Abstract**

The aging highway bridge infrastructure in the US is being subjected to increasing traffic volumes, structural deficiency and functional obsolete. They must be continuously renewed while accommodating traffic flow. This paper demonstrates application of prefabrication technology where traffic control issues demanded rapid construction and decision making risk of total facility shutdown. It shows an example supporting the FHWA's Accelerated Bridge Construction Decision Making Framework. Using the lessons learned from previous experience with the emergency repair/replacement, the Rt.1 reconstruction project involved replacing superstructures of two bridges with prefabricated components installed in 59-hour time window over a weekend. The experience becomes standard practice of "Hyperbuild".

### **Introduction**

The aging highway bridge infrastructure in the United States is being subjected to increasing traffic volumes, structural deficiency and functional obsolete. They must be continuously renewed while accommodating traffic flow. The traveling public is demanding that the rehabilitation and replacement be done more quickly to reduce congestion and improve safety. Conventional bridge reconstruction is typically on the critical path because of the sequential labor-intensive processes of completing the foundation, the substructure, the superstructure components, railings, and other accessories. Prefabricated bridge systems can allow components to be fabricated off-site and moved into place quickly while maintaining traffic flow. Depending on the specific site conditions, the use of prefabricated bridge systems can minimize traffic disruption, improve work-zone safety, minimize impact to the environment, improve constructability, increase quality, and lower life-cycle costs. New Jersey Department of Transportation (NJDOT) clearly demonstrated the truth of these statements with their approach to replacement of the superstructures of two structurally deficient bridges carrying a freeway section of US Rt.1 through the Capital City of Trenton.

The project involved completely replacing three superstructures of two bridges with new ones designed for a 75 year life, made off site and installed over three weekend shutdowns of 59 hours each. The design and construction of this project learned lessons from the past experience of two emergency repair/replacement projects. A project of this magnitude would typically take the Department approximately 2 years to design and construct as a traditional deck replacement and bridge rehabilitation

---

<sup>1</sup> Senior Engineer, Bureau of Structural Engineering, New Jersey Department of Transportation (NJDOT), Trenton, NJ 08625, USA

<sup>2</sup> Vice President, Arora and Associates, P.C., Lawrenceville, NJ 08648, USA

project. The project approach saved more than 22 months and an estimated design and construction cost, including delay-related user costs in excess of \$2M. The results? An extremely happy motoring public, bridge owner and contractor.

This paper will outline the application of prefab technology on the project where traffic control issues demanded rapid bridge construction techniques. The paper will also demonstrate a past project where decision makers took the risk of total facility shutdown to allow for rapid emergency repair/replacement as lessons learned for this project.

### **Needs for Accelerated Bridge Construction**

Bridge engineers have successfully used accelerated bridge construction (ABC) practices for many years around the globe. Our good fortune in this country to experience continued growth has also had the result of developing a greater dependence on our transportation infrastructure and less tolerance to interruptions caused by taking lanes out of service for routine maintenance. With the advent of high performance materials and emerging advanced technologies, the FHWA is attempting to provide leadership in meeting the public's expectations as illustrated in their Vision and Mission Statements. They identified three "Vital Few" important items to be focused on by the agency, those being Safety, Congestion Mitigation, and Environmental Stewardship and Streamlining.

In focusing on these priorities and goals the FHWA has led to the recommendation for modular prefabricated construction, among other things. The concept of prefabricated bridge elements and systems (PBES) is being researched as well as applied and put to use in building bridges as illustrated in the FHWA Decision-making Framework (FHWA, 2005)

To obtain information about technologies being used in other industrialized countries, a scanning tour of five countries was made in April 2004 (Ralls et. al, 2005). The overall objectives of the scanning tour were to identify international uses of prefabricated bridge elements and systems and to identify decision processes, design methodologies, construction techniques, costs, and maintenance and inspection issues associated with use of the technology. The prefab bridge elements and systems consisted of foundations, abutments, piers or columns, pier caps, beams or girders, and decks. Bridges with span lengths in the range of 20 to 140 feet (6 to 43m) were the major focus, although longer spans were of interest if a large amount of innovative prefabrication was used.

The focus areas of the study were, therefore, prefabricated bridge systems that

- Minimize traffic disruption,
- Improve work zone safety,
- Minimize environmental impact,
- Improve constructability,
- Increase quality, and
- Lower life-cycle costs.

During the tour, it was observed that precast deck panels were used on steel beams to produce both composite and non-composite members. The use of full depth prefabricated concrete decks reduces construction time by eliminating the need to provide cast-in-place concrete. Composite action was developed through the use of studs located in pockets in the concrete deck slab. In addition, use of innovative equipment, e.g. self-propelled modular transporters (SPMTs) were observed. These provided a means to accelerate bridge construction using a factory produced product for the state bridge owners.

According to the Year 2006 National Bridge Inventory (NBI), New Jersey has nearly 6,500 highway bridges (2,580 NJDOT bridges). About 35% are structurally deficient and functionally obsolete. The average age is close to 50 years old, while 52.5 years old for steel bridges. The most projects under plan, design, and construction are rehab and replacement related. Furthermore, New Jersey is the most highly urbanized and densely populated state in the US. Therefore, rapid bridge construction for both new and old bridges using prefab elements and systems is extremely vital in New Jersey.

In 2004 NJDOT established “Hyperbuild” program for accelerated roadway and bridge constructions. The term “Hyperbuild” was coined by the NJDOT Commissioner Jack Lettiere. Hyperbuild projects acknowledge the tremendous need to minimize traffic impacts for all of the previously mentioned reasons and recognize the potential savings of millions of dollars in design, construction, and road user costs that could be realized. The Commissioner’s vision was to reduce the time from initiation of design to the opening of the finished project to traffic (“project end date”) and require roads be functional while constructing, by utilizing innovative methods of design and procurement for certain types of projects. Such projects have to have a well-defined scope and, if possible, require *limited* right-of-way acquisition, utility relocations and environmental impacts. With the past experience of rapid emergency replacement of I-295 project, the US Rt.1 Freeway reconstruction became the first “Hyperbuild” project. These two projects will be presented in the following sections, respectively.

### **Rapid Emergency Bridge Replacement**

#### ***Creek Road Over I-295 Bridge Emergency Repair/Replacement***

In May 30, 2002, a tractor trailer traveling along I-295 South struck the overpass for Creek Road over I-295 in Bellmawr, Camden County, New Jersey near the border of Gloucester County (NJDOT, 2002a). The location is very sensitive because the estimated ADT in that area of I-295 is 80,000-120,000. The impact of the oversized and over height piece of earth-moving equipment that the tractor-trailer was carrying shattered the fascia beam and the fifth interior beam causing serious damage and potential catastrophic failure of the overpass (**Figure 1**). The overpass was a two simple span bridge having eight prestressed concrete girders and was classified structurally deficient (SD) and functionally obsolete (FO) with the permit

underclearance of 13'-9" (4.19m) per the inspection prior to the accident, while NJDOT currently requires 16'-6" (5.03m) underclearance for bridge design.

After initial inspection by the NJDOT bridge staff, the overpass was found to be structurally unsound requiring closure of the both I-295 mainline and Creek Road until temporary repairs could be made. The bridge was strengthened with a new, reinforced beam that was installed from the top of the bridge deck (strongback). Options to repair the bridge from under the deck were evaluated, but ultimately rejected, because they would have further restricted the bridge's maximum height safety requirements. The mainline of Route I-295 was reopened after the installation of a temporary support beam, but replacement of a portion of the deck and structural members down to the abutments was required before Creek Road could be reopened.



**Figure 1** Exposed Prestressing Strands of Damaged Interior and Fascia Girder of Creek Road Overpass Bridge

Creek Road overpass is a major route supporting commercial and emergency services for the City of Bellmawr and any traffic diversions on Creek Road or from I-295 onto surrounding network roads would cause unacceptable abnormally heavy traffic in those areas. Such conditions constituted an emergency in the region and it was determined by the Governor's office that damage to the overpass required immediate repairs on an emergency basis.

The Governor’s declaration of an emergency allowed the department’s structural engineers to quickly search various proprietary prefabricated bridge systems to rapidly put the bridge back into service (McGreevy, 2002; NJDOT, 2002b). The chosen strategy was to advertise for a superstructure system consists of a prefabricated composite concrete deck and stringer unit usually produced for simple spans manufactured by a supplier.

Several stipulations were that the systems would be designed in accordance with current American Association of State Highway and Transportation Official’s Bridge Design Standards (AASHTO), would utilize weathering steel, concrete with corrosion inhibitors (high performance concrete (HPC)) to increase service life and would provide a shallower superstructure depth than existed prior to the accident.

The permanent replacement was made utilizing “Inverset” deck panels (**Figure 2**). The panels provided are cast inverted in forms suspended from the support girders and when turned upright the decks are precompressed which should provide for increased durability. Panels come in lengths up to about 100 feet (30.48m) (86.5’ (26.37m) for this bridge) with widths usually in the 8 to 12-foot (2.44 to 3.66m) range. Stringer spacing of the panels was arranged to permit the construction of new bearing seats under the existing bridge between existing stringers prior to demolition of the damaged superstructure. It should be noted that these bearing seats were also prefabricated to minimize construction time on site. Spacing the stringers to allow this construction of the bridge bearing seats also resulted in closer spacing allowing for a 9-inch (0.23m) increase in vertical underclearance.

Upon completion of off-site fabrication and delivery on site, required modifications to the bearings, staged demolition of existing structure, erection of the new modular panels (four units) was performed on successive weekend night shutdowns, tremendously minimizing traffic impacts to the interstate I-295 and Creek Road (**Figure 3**). Besides replacement of the damaged span, the other existing span was repaired on concrete spalls and previous minor collision impact.

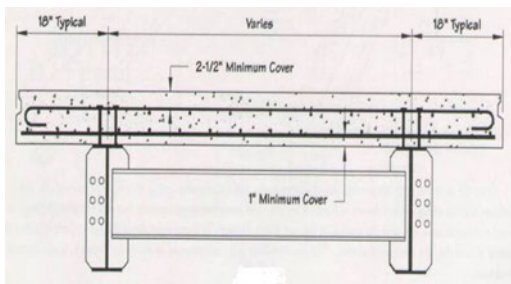


**Figure 2** Prefabricated “Inverset” Deck Panel (Modular Deck-Girder Unit)

**Figure 3** Night Time Erection of Modular Deck Panels Over I-295

### ***Rt.70 Friendship Creek Bridge Emergency Replacement***

The Rt.70 Friendship Creek Bridge was a concrete encased steel girder bridge with concrete gravity abutments at both ends. On July 12, 2004, 13 inches of rain fell in a 12 hour period in the area that was equivalent to a 1,000 year event storm. The storm caused that six dams were breached and the bridge collapsed with abutment failure on July 13, 2004 in the early morning due to scour. The State Police and NJDOT closed the road and established the detour for local traffic. A temporary bridge was built using prefabricated steel truss and the road opened to traffic on July 19, 2004 (**Figure 4**). It was followed by a new bridge construction including new abutments and new superstructures. The replaced superstructure is of precast concrete box beams with asphalt overlay. The replacement substructures is PZ steel sheeting with pipe piles bearing support and tiebacks. The first half of the replacement bridge completed on September 9, 2004 and the full bridge opened to traffic in October, 2004 (**Figure 4**).



**Figure 4** Temporary Bridge and Replacement Bridge Using Prefabricated system and Components

### **US Rt.1 Freeway Bridge Reconstruction Project**

Each day the US Route 1 carries more than 50,000 vehicles through the City of Trenton, the capital of the State of New Jersey. The US Rt. 1 serves as a vital link to adjacent Pennsylvania and is a heavily traveled land service route for those communities along the Northeast Corridor between New York City and Philadelphia. Just north of the City of Trenton in Lawrence Township, Rt. 1 divides into two Routes, Rt.1 Business which carries local traffic to points in the city and Rt. 1 Freeway which was intended to provide faster access to downtown Trenton, the State Government Offices, and the crossing of the Delaware River between Trenton of New Jersey and Morrisville of Pennsylvania.

The freeway section configuration of the highway was constructed on embankment and provides for two lanes of traffic in each direction divided by a Jersey Barrier along its entire length creating significant challenges for maintenance of traffic for any work performed within its limits. However, three bridge decks on the Route 1

Freeway mainline, one at the Olden Avenue Connector and two at Mulberry Street, had deteriorated to the point where they were in need of constant maintenance. Both bridges (3 superstructures) were single-span simply supported steel girder bridges built in 1953 with skew of 56 degrees and 10 degrees, respectively. Although the steel girders and bearings were repainted in 2000, the inspection report and evaluation revealed and classified the superstructures as structurally deficient due to poor condition of concrete decks and bearings (**Figure 5**; **Figure 6**). The deteriorations included large concrete spalls of decks with exposed rebars, patch spalls, fine transverse and map cracks underneath decks, steel girder and stiffener buckling due to prior collision impact, undermined concrete pedestals and rusted anchor bolts of bearings.



**Figure 5** Deteriorated Decks of the Route 1 Bridge over the Olden Avenue Connector      **Figure 6** Deteriorated Pedestal of Bearings

In 2005 the replacement of these three bridge superstructures was undertaken in one project that was to become the NJDOT’s first “Hyperbuild” project. The three bridges in the project were actually located at two points along the mainline of US Rt.1 separated by approximately a half mile. The Rt. 1 Bridge over the Olden Avenue Connector is a highly-skewed steel girder bridge with concrete deck (**Figure 5**). The 35.0-ft (10.67m) wide single-span bridge has a span of 86.8-ft (26.46m) and carries 2-lanes of traffic. The Rt. 1 Bridge over Mulberry Street consists of two parallel bridge superstructures on a common abutment with a median barrier separating each direction of traffic. The 82.2-ft (25.05m) wide bridge has a 60.0-ft (18.29m) long single-span and carries 4-lane of traffic over Mulberry Street.

Preliminary review of the sites of these deficient bridges indicated that they met the criteria of “Hyperbuild”. Several prefabrication options were considered for rehabilitation of these bridges based on the past emergency repair experience and availability of precast products (capers, 2005; 2006). Using the lessons learned during the previous emergency repairs of the Creek Road Bridge over I-295, NJDOT’s structural engineers concluded that a similar approach of using prefabricated superstructure modular panels for the rapid replacement of these bad decks would be an effective strategy due to the very limiting project site space and significant need for rapid project development/design and construction. Use of SPMTs for an entire prefab

bridge superstructure system was not an option due to the limited site space to accommodate either the prefeb units or the SPMT equipment.

Each superstructure was designed using 5 full-length modular segments of varying width, each with two Grade 50W steel girders and a 9-inch (229mm) thick composite concrete “Inverset” deck system. The 86.8-ft (26.46m) long bridge span over Olden Avenue utilized W36x182 girders, and the 60-ft (18.29m) long bridge spans over Mulberry Street utilized W30x99 girders. Segments sizes considered the transportability and erection restrictions associated with urban nature of the project site. All new structures were designed for 75 year design life.

The 15 modular segments were designed and fabricated in Schuylerville, New York, assembled at the plant to verify field tolerances, and trucked to an airport parking lot near the bridge (**Figure 7**). The segments were required to be on site 24 hours prior to the start of demolition of the existing bridge. The contract specified high performance concrete (HPC) to be used for all concrete on the job.



**Figure 7** Prefabricated Modular Segment in Transportation

The construction was planned to occur using only weekends to shut down mainline traffic to minimize disruption along the corridor. Each of the 3 superstructures was allowed a 59-hour window commencing Friday evening (7:00pm) with all activities off the roadway and both lanes re-opened before the morning rush (6:00am) on Monday. If this window was exceeded, a Lane Occupancy Charge would be assessed, up to \$10,000 per day.

As is typical on NJDOT projects, incentives and disincentives) were included on this project to encourage the contractor to minimize onsite construction time even further than 59 hours per bridge. For the bridge over the Olden Avenue Connector, an incentive (or disincentive) of \$1,500 per hour was specified if the work was completed in less (or more) than 59 hours, not to exceed a maximum of \$27,000. For each structure over Mulberry Street, an incentive (or disincentive) of \$2,000 per hour was specified if the work was completed early (or late), not to exceed \$36,000.

Liquidated damages were also specified. The contractor would be charged \$4,200 per day if the bridges weren't substantially completed by the specified completion date in the contract, and an additional \$900 per day if all work was not completed within 3 months following that.

The engineer's estimate for this project was \$3.8M. The low bid of \$3.5M was 8% or \$297,000 less than the engineer's estimate. There were 5 bidders on this project. The second lowest bid was 10% higher than the low bid.

The Rt. 1 Bridge over the Olden Avenue Connector was replaced during a weekend closure in August 2005. The Rt. 1 Southbound Bridge over Mulberry Street was replaced during a weekend closure in September 2005, followed by the Rt. 1 Northbound Bridge over Mulberry Street during a weekend closure in October 2005. Design and construction of such bridges would have taken 22 months using conventional methods.

**Olden Avenue Bridge** The Route 1 Bridge over the Olden Avenue Connector was closed at 7 p.m. on a Friday in August 2005, and traffic was rerouted onto a 5-mile detour. The bridge was demolished in place using conventional methods. The existing abutments were repaired and new bearing seats were constructed. The prefabricated superstructure was then erected during nighttime. The longitudinal joints between superstructure segments were then sealed, and the expansion joints at the ends of the span were completed. The cast-in-place (CIP) parapets were connected to the outside segments with bars in threaded inserts.

**Mulberry Street Bridge** The Rt. 1 Southbound and Northbound bridges over Mulberry Street were closed at 7 p.m. on a Friday in September and October 2005, respectively, and traffic was rerouted onto a 5-mile detour for Southbound Mulberry, while off- and on-ramps were used for Northbound Mulberry. The construction methods and time required to replace these bridges were similar to the bridge over the Olden Avenue Connector. Parapets were cast-in-place (CIP) concrete and median barriers were precast. The typical construction time frame was as follows.

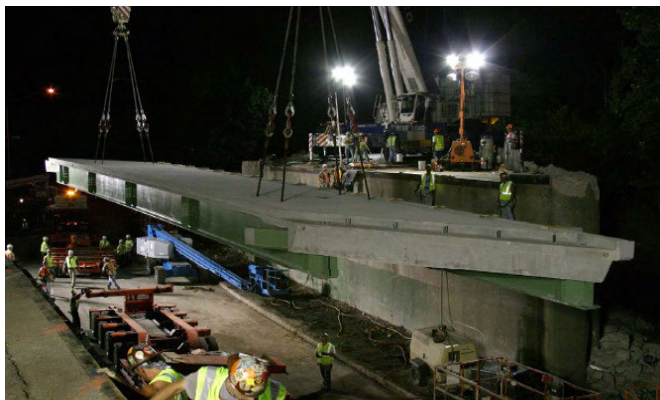
- Weekend closure: Friday 7:00 pm to Monday 6:00 am
- New bearing pedestal installation: prior to and during the project
- Demolition and removal of old structure: Friday/Saturday (**Figure 8(a)**)
- Bearing and expansion joint replacement: Saturday
- Prefab modular bridge unit erection: Saturday night (**Figure 8(b)**; **Figure 8(c)**)
- Bridge installation completion: Sunday morning (**Figure 8(d)**)
- CIP parapets and prefab median barriers: Sunday
- Cleaning and Reopen: Monday early morning



(a) Demolition/Removal of Existing Structure



(b) Initiation of Erection of Route 1 Southbound Bridge over Mulberry Street



(c) Erection of Prefabricated Modular Segment



(d) Erection of Final Deck Panel of Route 1 Southbound Bridge over Mulberry Street

### **Figure 8** Reconstruction of Two US Rt.1 Freeway Bridges

All three bridges were opened in less than the required 59 hours. The bridge over the Olden Avenue Connector was opened in 56 hours, the bridge over Southbound Mulberry was opened in 51 hours, and the bridge over Northbound Mulberry was opened in 54.5 hours. With all three bridges opened well before Monday morning rush hour, the contractor earned an \$18,500 incentive.

### **Summary**

Each of the 3 bridge superstructures in the New Jersey DOT's first "Hyperbuild" project was replaced over a weekend, during a total of 6 days in 3 consecutive months. The replacements were completed in significantly less than the 22 months required for conventional design and construction, and they were completed under budget. The design and construction savings, including delay-related user costs, are in excess of \$2M.

Each bridge is expected to see a 75-100 year service life due to the quality of its prefabricated superstructure, the use of high performance concrete, and the attention given to connection details. Conventionally constructed bridges have an average minimum 50-year life in New Jersey.

There are a large number of such bridges to repair and rehabilitate in New Jersey. The experience of Rt.1 Freeway reconstruction set a good example for the future work and became standard practice of "Hyperbuild" projects. The project clearly demonstrated the benefits that can be reaped by applying accelerated construction strategies: less construction time, increase work zone safety, less maintenance, more durability, higher quality, reduce user cost and life-cycle cost, and minimize traffic disruption and environmental impact. And of course, an extremely happy motoring public! In the mean time, NJDOT looks forward to more and more innovative and cost-effective prefabricated products that can be selected for the future projects.

## References

1. Capers, H. (2005) *Hyperbuild! Rapid Bridge Construction Techniques in New Jersey*, Transportation Research Board 6th International Bridge Engineering Conference, Boston, MA, July, 2005
2. Capers, H., Lopez, J., Lewis, R. and Nassif (2003), H., *Applying The Principals Of Get In, Get Out, And Stay Out Designing And Detailing Of Highway Structures For Rapid Construction In New Jersey*, 2003 NYC Bridge Conference, New York, NY, August, 2003
3. Federal Highway Administration (FHWA) (2005), *Framework for Prefabricated Bridge Elements and Systems (PBME) Decision-Making*, Dec., 2005
4. McGreevey, E. James, Governor, *Executive Order #28*, State Of New Jersey, Trenton, NJ
5. New Jersey Department of Transportation, News Release, *Creek Road Bridge Repairs Move Forward to Allow Reopening on Monday Morning*, Trenton, NJ, June 5, 2002
6. New Jersey Department of Transportation, News Release, *Creek Road Bridge Over I-295 Damaged in Afternoon Accident*, Trenton, NJ, May 30, 2002
7. Ralls, Tang, Bhidé, Brecto, Calvert, Capers, Dorgan, Matsumoto, Napier, Nickas, Russell (2005), *Prefabricated Bridge Elements and Systems in Japan and Europe*, Washington, D.C., March, 2005
8. Roads and Bridges Magazine, November, *Hyperbuild Project*, Scranton Gillette Communications, Inc. Arlington Heights, II, November, 2005

## Effect of reducing strains by SFRC pavement on Ohira Viaduct

Takayoshi Kodama<sup>1</sup>, Mamoru Kagata, Shigeo Higashi, Kiyoshi Itoh, Yatsuhiko Ichinose

### **Abstract**

Fatigue damage of orthotropic steel bridge decks owing to increasing traffic volumes and higher wheel loads have been reported. Steel fiber reinforced concrete (SFRC) pavement holds promise as a countermeasure for improving the fatigue durability of existing orthotropic steel decks. Static loading tests using a 200 kN dump truck were conducted on the orthotropic steel deck of the Ohira Viaduct. This paper reports the results of strains measurement before and after construction of the SFRC pavement, which show a marked effect in terms of reducing local strains in the steel deck.

### **Introduction**

There have been numerous reports of fatigue-induced damage and cracking concerning orthotropic steel deck bridges used by heavy vehicles. The reported crack occurrences were in the welds between transverse ribs and longitudinal ribs, the welds between longitudinal ribs and deck plates, the welds between neighboring longitudinal ribs, etc. Rare instances of cracks that originate in the vicinity of a deck plate and run through that deck plate, as well as road surface subsidence [1, 2], also have been reported, raising the possibility of traffic accidents and making this an important issue to be addressed.

A number of studies have been conducted on how to prevent such fatigue damage, including the use of highly rigid steel fiber reinforced concrete (hereafter, SFRC) for the pavement of the steel deck to inhibit local deformation of the steel deck, and the reduction of local stress to improve fatigue durability. SFRC pavement was used a long time ago by the Nagoya Expressway Public Corporation [3] as a way to prevent pavement damage of ramps with a steep longitudinal gradient, tollgates, etc. More recently, as a fatigue countermeasure for steel decks, SFRC pavement was applied through a new method using epoxy resin adhesive instead of conventional stud dowels for the joints between the SFRC and deck plate, in the section of National Highway 357 forming the lower level of Yokohama Bay Bridge [4, 5], Shonan-Ohashi Bridge [6, 7], and the Metropolitan Expressway [8].

The Ohira Viaduct, an orthotropic steel deck bridge currently in service in Oyama, Tochigi Prefecture, features SFRC pavement as part of various fatigue countermeasures. In the present study, we used this location to run truck-loading tests on old-type asphalt pavement and new-type SFRC pavement as shown in Fig.1 and Fig.2. These tests revealed the effectiveness of SFRC pavement in reducing stress on the steel deck, as reported below.

---

<sup>1</sup> Manager, Technology Department, KAJIMA ROAD.,LTD

**Influence of an overlay material**

First of all, the result of researching the adhesion of an adhesive and fresh concrete is shown below.

**(1) Three type of overlay materials used for the experiment**

It was compared with the adhesion from the difference of overlay materials (cement paste, mortar and concrete) to hardening base concrete. The used mixture proportions of base concrete are shown in Table 1. The used cement paste as overlay material was made into 47% that is the same water cement ratio as the concrete shown in Table 1. The used cement mortar as overlay material was used as water cement ratio 0.47 of cement paste, and three kinds of sand-cement ratio such as 0.1, 0.5, and 2.39 were added. Furthermore, overlay concrete that had sand-total aggregate ratio from 40% to 49% was also used. The examination was executed after 7 days from producing the test cores. 0.7kg per 1square-meter of epoxy-adhesives were applied. The time interval from spraying the adhesives to overlaying the fresh concrete was made into 1 hour so that it might achieve the same conditions as real construction.

Table 1 Mixture proportions of concrete

Gmax (mm)	W/C (%)	s/a (%)	Unit contents(kg/m <sup>3</sup> )				Ad Cx%
			W	C	S	G	
20	47.0	44.4	157	334	797	1030	0.7

Gmax means the maximum size of aggregates. Small size figure of s means the volume of sands and a means the volume of aggregates. Cx% means the content percentage of admixture to cements.

The test result of bonding strength by different overlay materials is shown in Fig.1. The bonding strength of cement paste and the mortar of 0.1 and 0.5 is a small value, and they had exfoliated in the bonding interface. With the mortar of 2.39 and concrete, it had excellent bonding strength and the position of rupture was mostly inside the mortar or concrete. From the result of this bonding test, it is thought that existence of aggregate is indispensable in bonding with adhesives and fresh concrete. Aggregates bonded with adhesives first, paste up firmly, and it is thought that concrete hardens and unifies after that. Fig. 2 shows the bonding strength in the case of sand-total aggregate ratio in the range between 40% and 49%. In this range, bonding strength was almost the same. Therefore, it is thought that there is almost no influence that the rate of fine aggregate has to bonding strength.

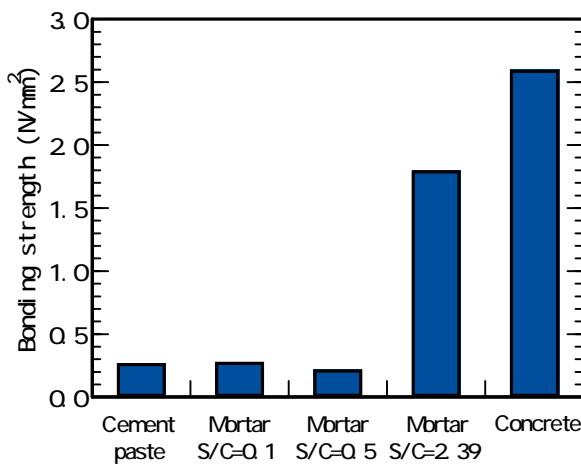


Fig. 1 Bonding strength of cement paste and mortar

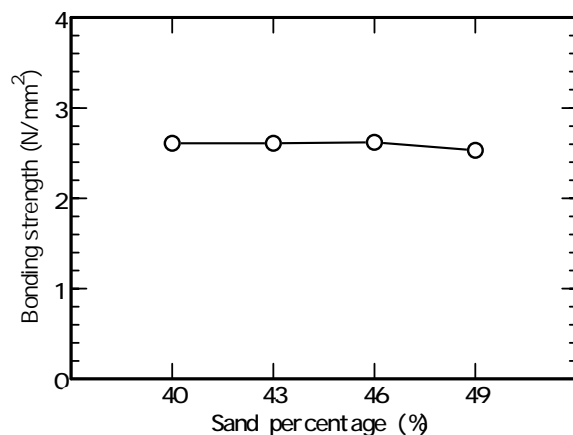


Fig. 2 Relationship of sand percentage and bonding

**(2)Various intensity of the BONDED concrete by EPOXY ADHESIVE AGENT**

Next, the strength property in the case of putting it with the adhesives is shown. The used mixture proportion of concrete is shown in Table 1. The cylinder specimen with diameter of 100mm and height of 200mm was used for the tests of compressive strength and shear strength. The height of base concrete and overlay concrete was 100mm in 200mm high. The speed of loading in shear test was controlled by displacement to be set to 1mm per 1 minute. The specimen used for the bending test was 100mm in height, 100mm in width, and 400mm in length, and the base concrete was set to the lower layer. 0.7kg per 1square-meter was sprayed on base concrete, and fresh concrete was placed 5 hours after the application. The examination was executed after 14 days from placing the concrete.

The results of strength test are shown in Fig.3. The bonding strength of bonded specimen was equivalent to a body of base concrete and overlay concrete. Moreover, there was no exfoliation at interface between base concrete and overlay concrete. Shear strength of bonded specimen is equivalent to base concrete and overlay concrete, and the rupture position is inside of the overlay concrete. It is thought that this was destroyed in concrete because interfacial bonding strengths of the adhesive and the overlay concrete are larger than tensile strength of overlay concrete. Sufficient adhesion to shear stress was checked. It was shown that it is equivalent to a body of base concrete and overlay concrete in compressive strength, and the adhesion by adhesives is absolutely excellent.

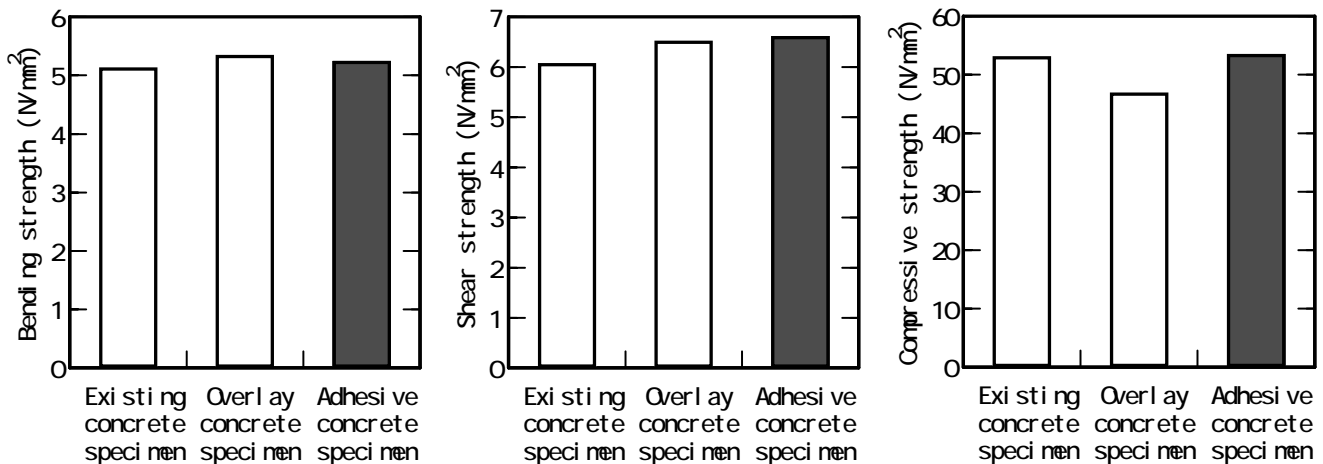


Fig. 3 Strengths of adhesive bonded specimen

**Outline of Ohira Viaduct and SFRC paving**

The Ohira Viaduct is a road bridge on National Highway 50 consisting of 31 spans and measuring 987 m. The bridge's two inbound (Takasaki-bound) lanes were completed in 1983, and its two outbound lanes, which run parallel with the inbound lanes, were opened to traffic in 2005. The bridge has independent superstructures for the inbound lanes and outbound lanes, but common piers support these. The Ohira Viaduct was paved with SFRC over a length of 213 m, consisting of one 3-span continuous 2-box girder and two simple plate box girders of the steel deck with U-ribs of the inbound lanes. The part of the bridge that was selected for measurement in the present study consisted of a 3-span continuous steel deck 2-box girder spanning piers

3 to 6 of the inbound lanes (Takasaki-bound). The deck plates are 12 mm thick, the U-ribs are 320 mm wide, 200 mm high, 6 mm thick, and have an effective span of 40 m, 56 m, and 50 m, respectively. The bridge has been in service for longer than 20 years and the steel deck welds directly under the path of the truck wheels, for example the welds between the deck plates and U-ribs show signs of fatigue damage. As part of the fatigue countermeasures, it was decided to use SFRC paving to reduce local stress in the various parts of the steel deck. The SFRC paving application was split in two along the width direction. Stud dowels with a diameter of 9 mm and height of 30 mm were placed at 300 mm intervals in double rows along the length of the work area (in parallel with the bridge axis) and along the work area joints (at right angles with the bridge axis). The adhesive used was high-durability epoxy resin adhesive that was shown not to lose bond strength under water-immersed wheel load fatigue testing [9], applied at 1.4 kg/m<sup>2</sup> (Photo.1). Further, the adhesive was used not only for the bond between the deck plate and SFRC, but also as the bond for the joint faces of SFRC-SFRC construction joints and the SFRC-expansion joint interface.

As the two inbound lanes could be closed to traffic for a period of approximately 1.5 months only, high-early-strength concrete was used for the SFRC. Concrete with design compressive strength of 29.4 N/mm<sup>2</sup>, 20 kg/m<sup>3</sup> of expansive agent, and 120 kg/m<sup>3</sup> of 30 mm steel fibers were used. To ensure stiffness after cracking under negative bending moment in the SFRC paving directly above the web of the main box girder, a 100 mm mesh CRFP (carbon fiber) grid with a width of 1.0 m was placed at the center of the main girder web at a depth giving a bottom cover of 30 mm (Photo.2). The CFRP grid that was used had a cross section of 39.2 mm<sup>2</sup> and tensile strength of 1400 N/mm<sup>2</sup>.

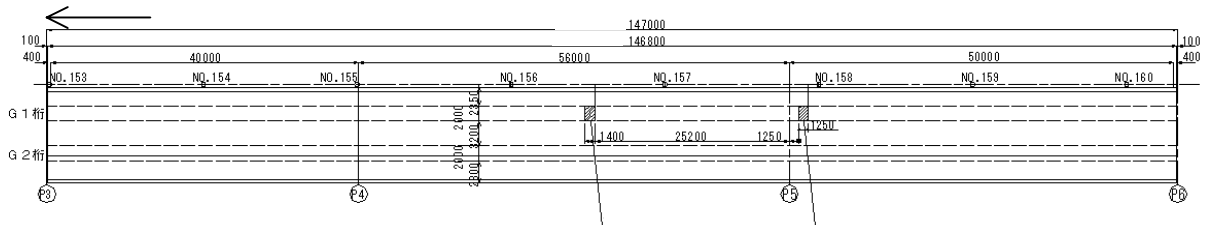


Fig.4 shows a top plan view

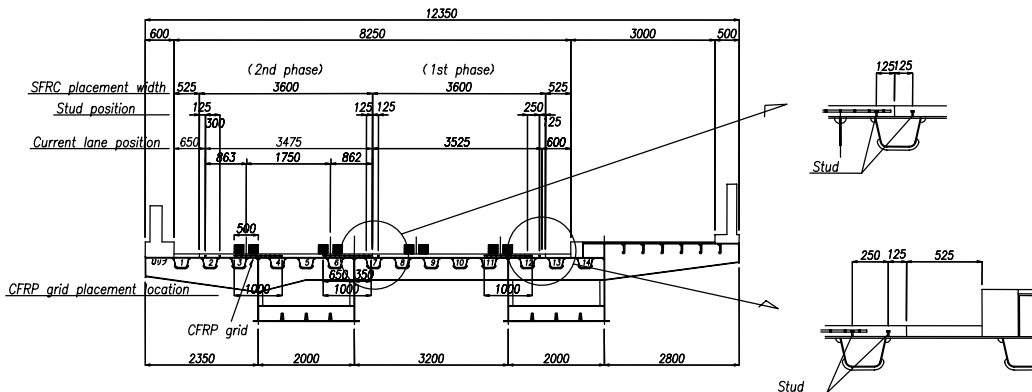


Fig.5 a cross-section of the bridge section selected for measurement.



Photo.1 Adhesive and Stud Dowels



Photo.2 CFRP Grid Placement



Photo.3 Applying epoxy adhesives



Photo.4 SFRC Placement

### **Structural Considerations of SFRC**

The main aspects considered are SFRC and the width of the CFRP grid were considered outlined below. Regarding the thickness of the SFRC, three cases were considered, namely the same thickness as the asphalt pavement (75 mm), greater thickness than the asphalt pavement (100 mm), and a two-layer pavement (SFRC thickness of 45 mm + surface asphalt thickness of 30 mm), conducting comparisons in terms of economic efficiency, workability, and maintainability. In the end, SFRC with the same thickness of 75 mm as the existing asphalt pavement was selected. Regarding the CRFP grids and stud dowels for reinforcing the SFRC, two models, the SFRC directly over main girder model and the one bridge portion model were examined using finite-element analysis. The degree of stress generated in SFRC varies according to the steel deck structure, including main girder placement, transverse rib interval, and U-rib interval, and the degree of stress generated by live load, heat of cement hydration, etc., was obtained with the bridge part model modeling the Ohira Viaduct.

The effectiveness of CFRP grids for limiting the crack width in SFRC was confirmed as a result, and 1.0 m above the main girder was selected as the installation range. With regard to warping of the pavement owing to heat of cement hydration, drying shrinkage, etc., adhesive was judged to be a sufficient countermeasure and the use of stud dowels was deemed unnecessary. However, as the long-term durability of adhesive in the actual bridge was not ascertained, it was decided to use stud dowels only at the edges of the SFRC to prevent the infiltration of water, etc., in case of peeling

off of the adhesive layer. Further, with regard to the future maintenance and repair of the SFRC pavement, the height of the stud dowels was set to 30 mm (special-order product) and the bottom cover of the grid to 30 mm, in order to support a pavement cutting depth of approximately 30 mm.

**Outline of Fatigue Damage of Ohira Viaduct**

In 2005 and 2006, the steel deck part using U-ribs was inspected and repaired. As a result, fatigue damage was found to have occurred in numerous locations, including the fillet welded joints between the deck plate directly under the truck wheels and the U-rib (Type A), and the fillet welded joints between the deck plate and vertical stiffeners (Type C). Figure.6 shows a schematic diagram of the different types of fatigue damage, and Table 2 lists the number of fatigue damage locations in each span. An example of fatigue damage in the Ohira Viaduct is also shown in Photo.5. As can be seen in this photograph, the crack in the weld between the deck plate and the U-rib changes direction and progresses into the U-rib, and a stop hole is provided at the tip of the crack.

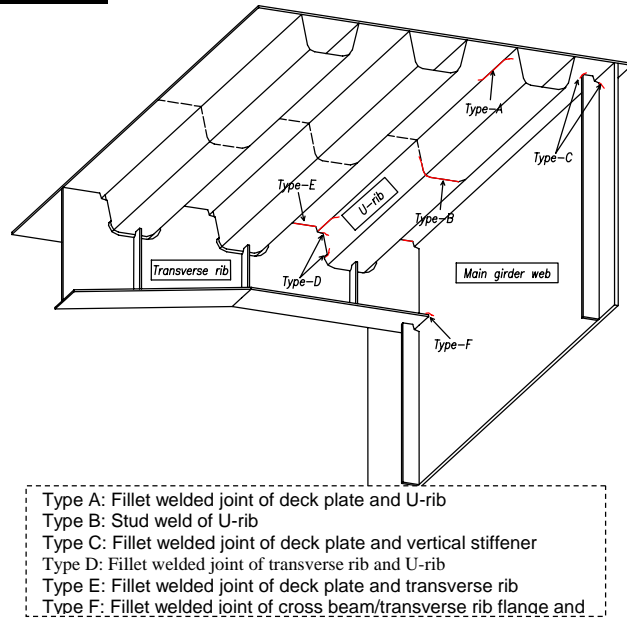


Fig.6 Schematic Diagram of Types of Fatigue Damage

Table 2 Fatigue Damage Locations in Each Span

Section	Superstructure type	Type-A	Type-B	Type-C	Type-D	Type-E	Type-F	Total
P3-P4	3-span continuous box girder	31	0	15	5	0	0	51
P4-P5		42	0	27	19	2	0	90
P5-P6		26	0	3	10	2	0	41
P10-P11	Simple steel plate girder	7	4	8	0	2	0	21
P13-P14	Simple steel plate girder	8	1	1	2	0	0	12
Total		114	5	54	36	6	0	215

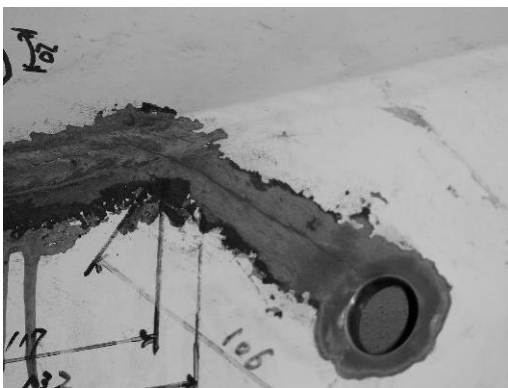


Photo.5 Example of Fatigue Crack at Ohira Viaduct

**Measurement Plan and Measurement Contents**

**(1) Outline of measurements**

SFRC pavement can be applied to reduce deformation of the deck plates of the steel deck and improve load distribution, thereby diminishing strain localized around weld areas, in other words local strains. In this study, strain gauges were attached, mainly to

the welds of deck plates, but also to transverse ribs and U-ribs, in order to ascertain the effect of SFRC pavement in terms for the reduction of local stress on the steel deck. As the strain reduction effect of SFRC pavement was predicted to differ between strain gauge attachment location 1 at approximately the middle point between piers P4 and P5, where the bridge's vertical deflection is comparatively large, and strain gauge attachment location 2 near intermediate support P5, where vertical deflection is comparatively small, it was decided to perform measurements at these two locations.

The measurement target was the box girder on the overtaking lane side (median strip side), and survey lines a to f were selected, taking into consideration the positions of the wheel tracks and U-ribs. It was assumed that the right wheels would travel over survey lines a to e, and the left wheels over survey line f. The positions of the survey lines are shown in Fig.7.

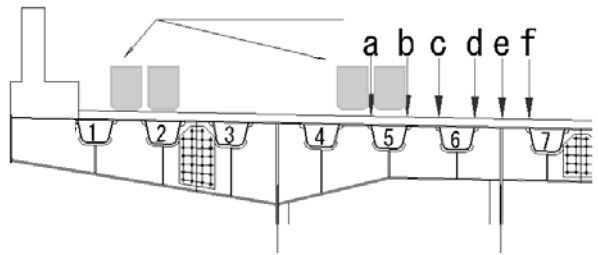


Fig.7 Position of Truck Loading Survey Lines

**(2) Loading test case**

Three-axle trucks with two single wheels at the front and four double wheels at the rear end were used for the loading test. The gross weight of each truck was adjusted to be approximately 200 kN. Fig.8 shows the details of the front wheels, front-rear wheels, and rear-rear wheels. Regarding the loading of the double tires on the rear axes, loading was done so that the centerline of the double tires coincided with the survey line. As shown in Fig.8, the loading position of the front wheels in the width direction is 45 mm retracted from the position of the external wheels. Therefore, the front wheels pass directly over the middle of the U-ribs, as the positions of the double tires of the rear wheels span exactly the survey lines. To clarify the loads of the trucks that were used, the axle loads of the trucks were measured at the time of the asphalt pavement and after SFRC application. The measurement results are listed below.

- 1) Axle load of loaded truck at time of asphalt
  - Total weight: 222.0 kN
  - Front wheel axle weight: 58.2 kN
  - Front-rear wheel axle weight: 83.2 kN
  - Rear-rear wheel axle weight: 72.8 kN
- 2) Axle load of loaded truck during SFRC work
  - Total weight: 222.3 kN
  - Front wheel axle weight: 56.4 kN
  - Front-rear wheel axle weight: 87.0 kN
  - Rear-rear wheel axle weight: 73.3 kN

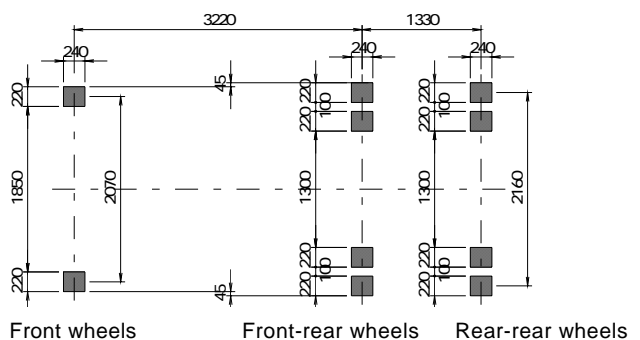


Fig.8 Details of Truck Wheel Placement and Contact Area

The differences between the two types of truck were judged to be small, and the measurement data was sorted under the assumption that trucks of the same weight were loaded, without taking into consideration axle weight differences.

### **(3) Measurement schedule**

Measurements were performed twice, during asphalt pavement prior to removal (before reinforcement), and about one week following SFRC placement (after reinforcement), in order to determine the efficiency of SFRC pavement for strain reduction in the steel deck.

The measurement dates and the average temperature data of the Utsunomiya Local Meteorological Observatory and Oyama are listed below.

- 1) During asphalt pavement: 2 October 2007, 19.1°C, cloudy
- 2) During SFRC pavement: 30 October 2007, 16.1°C, cloudy
- 3) During SFRC pavement: 11 November 2007, 14.3°C, cloudy

### **(4) Positions of measurement strain gauges**

Strain gauges were used mainly to measure the strain in the deck plates in the box girders. As shown in Fig.9, the strains along the bridge axis of the deck plates and the axis orthogonal to the bridge axis were measured in the vicinity of the transverse ribs (D-D section) and transverse rib span center (E-E section). At the intersection of the transverse rib and U-rib, a 3-axis rosette gauge was used, taking into consideration the fact that the principal stress direction is unknown, as shown in the lower right part of the same figure. Regarding the organization of the strain data, the values of the strain gauges on axis 1 and axis 2 were used as is, and for axis 3, the principal strain values were used. Table 3 shows the measuring equipment that was used. For the strain gauges at the scallop locations, a gauge length of 3 mm was attached at a position 5 mm from the weld toe, as shown in Fig.10.

Table3 Used of Measuring Equipment

	Equipment Name	Usage Location
Strain gauge	1-axis strain gauge : FLA-3-11-10LTSA	Steel beam
	2-axis strain gauge : FCA-3-11-10LTSA	Steel beam
	3-axis strain gauge : FRA-3-11-10LTSA	Transverse rib
Data logger	TDS-303	
Switch box	ASW-50C	

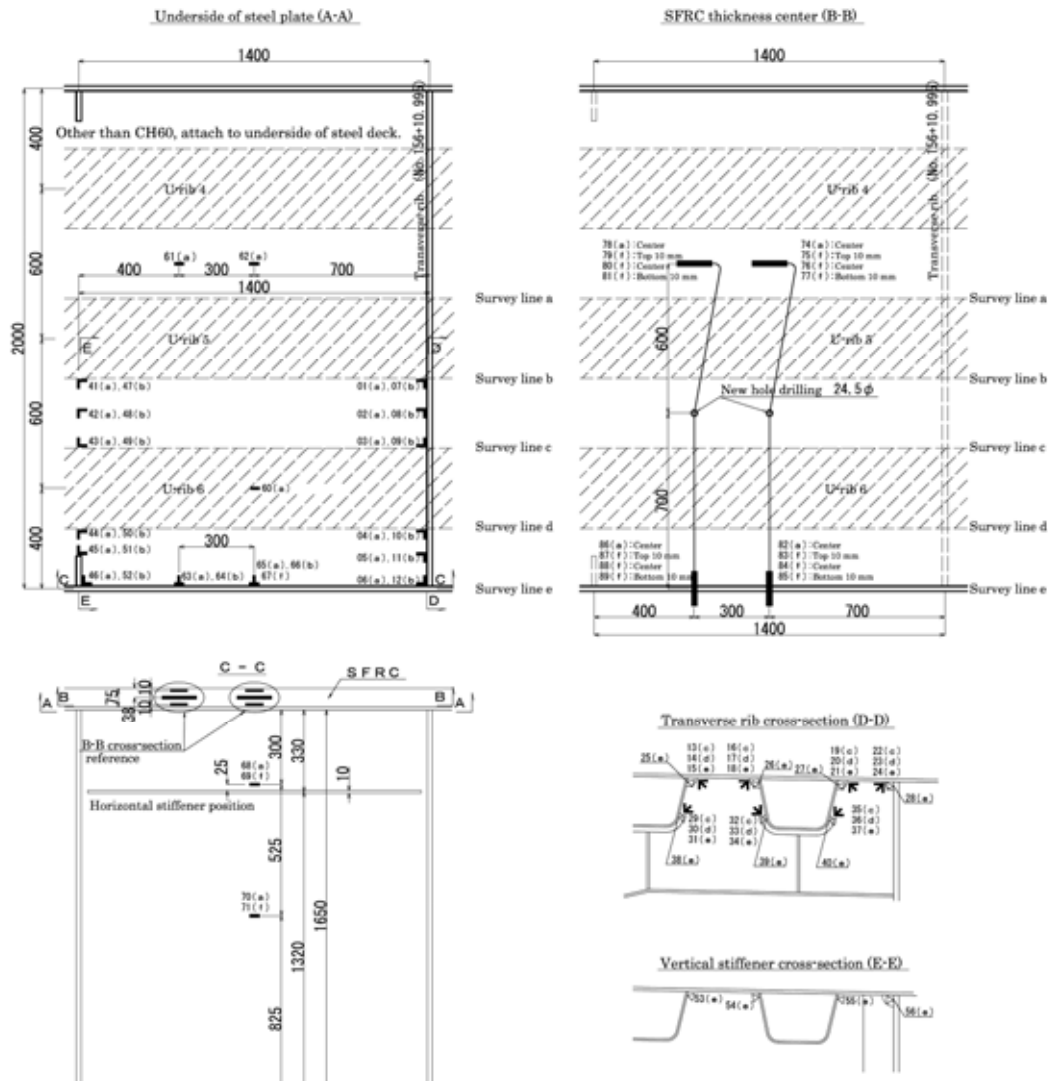
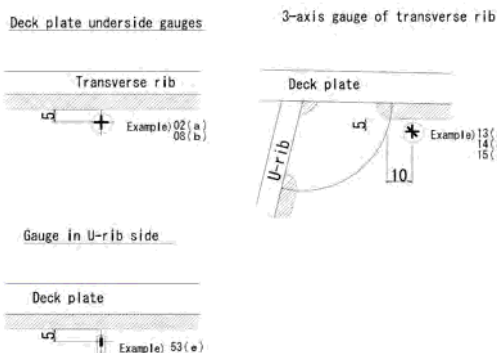


Fig.9 Gauge Positions and Gauge Numbers



Notes

1. Meaning of characters in ( )
  - (a) : Strain gauge in bridge axis direction
  - (b) : Strain gauge in direction at right angle to bridge axis
  - (c) : Strain gauge in horizontal direction
  - (d) : Strain gauge in 45 direction
  - (e) : Strain gauge in vertical direction
  - (f) : Thermocouple
2. The gauge No. at gauge attachment position 2 are incremented by 100 compared to the No. of attachment position (for organization simplicity).

Fig.10 Scallop Position Gauges

## **Works**

At the attached steel plate on the steel-deck plate, removal of the existing asphalt pavement by hands were executed paying attention to the position of bolts based on preliminary-survey results. In this case, the breaker that had an even edge so that damage may not be given to the steel deck plates was used. Much attention was paid especially so that damage might not be done to the bolt that was binding the attached steel plate tight. After removal of the existing asphalt pavement, the water jet machine stripped off all the water-resistant layers that remained on the deck plate.

As grinding processing in the deck plate to secure an excellent adhesion, the rust and foreign substances was removed by using two or more sets of shot blasting apparatuses. Small-sized apparatuses (0.35m in width) were used for the corner of steel deck plates, while large-sized apparatuses (1.0m in width) were used for the central part. In both sized apparatuses the density of shot blasting using steel balls of 1.4 mm in diameter was controlled by 300kg /m<sup>2</sup>. Application of epoxy resin adhesive started by 30 minutes before placing of SFRC and the speed of application was accommodated to the placing of SFRC.

Concrete with high-early-strength Portland cement and expansive admixture was manufactured in ready-mixed concrete plant and transported with agitator vehicles to the site. The steel fiber was put in the agitator car with the special device set up on the site, and mixed with concrete. The expansive admixture was used in order to reduce cracking due to drying shrinkage. After slump test and test for air content of the manufactured fresh SFRC samples was conducted to check the quality, the SFRC was discharged.

The SFRC was placed and compacted with a finisher. The SFRC was cured with plastic sheets for one day after placing and sprayed water for the following four days.

## **Measurement and observations**

To clarify the strain reducing effect of SFRC pavement, the results of comparisons before and after SFRC reinforcement at the strain gauges near deck plates, and comparisons before and after SFRC reinforcement, in other words at the time of the asphalt pavement and at the time of the SFRC pavement (hereafter, before and after SFRC reinforcement), at the strain gauges at the cross beams were compiled and sorted. The results are shown in Figure.11. The strain amplitude, which is the difference between the maximum strain and minimum strain during the passage of the trucks used in assessing fatigue durability performance, was used as the strain. The two-digit numbers and three-digit numbers in the strain gauge column indicate mid-span and P5 pier vicinity strain gauge attachment positions, respectively. Regarding the comparisons before and after SFRC reinforcement, the ratio (%) of the value after SFRC reinforcement ( $100 \times \text{value after reinforcement} \div \text{value before reinforcement}$ ) was used, defining the value before SFRC reinforcement as 100, and this numeric value is indicated at the right end of the strain amplitude (bar graph) in Fig.11. Particularly in the case of deck plates (shaded parts in Fig.11), this value was often 10% or lower.

Looking at the strain values of the shaded parts, none of the gauges whose strain amplitude caused by wheel loads was on the order of 400 to 500  $\mu$  (84 to 105N/mm<sup>2</sup>) at the asphalt stage reach 100  $\mu$  (21 N/mm<sup>2</sup>).

Moreover, regarding the welds of the deck plates and transverse ribs (E and F in

Fig.11), there are many gauges with values after SFRC pavement that have dropped to as low as 20% to 30% of the original value, a result showing that SFRC pavement is highly effective in reducing fatigue cracks in the steel deck.

**Conclusions**

SFRC pavement was laid over a length of 213 m consisting of one 3-span continuous 2-box girder and two simple plate box girders of the inbound (Takasaki-bound) lanes of the Ohira Viaduct. Before and after reinforcement of the 3-span continuous 2-box girder that was selected for strain measurement, in other words when the pavement consisted of asphalt and SFRC, respectively, loading tests were performed. Trucks were used as the loads, and the reduction in strain obtained through SFRC pavement prior to opening of the bridge to traffic was investigated. The main findings are summarized below.

- 1) The strain reducing effect at deck plates locations is extremely large, particularly at the welds between deck plates and U-ribs, and in some cases, the strain value was reduced to as little as 1/10th the level following SFRC reinforcement.
- 2) Even at the welds between transverse ribs and U-ribs, the strain value was reduced to between 1/2 and 1/3 as the result of SFRC reinforcement, clearly attesting to the strain reducing effect of SFRC reinforcement, though to a lesser level than at deck plates.

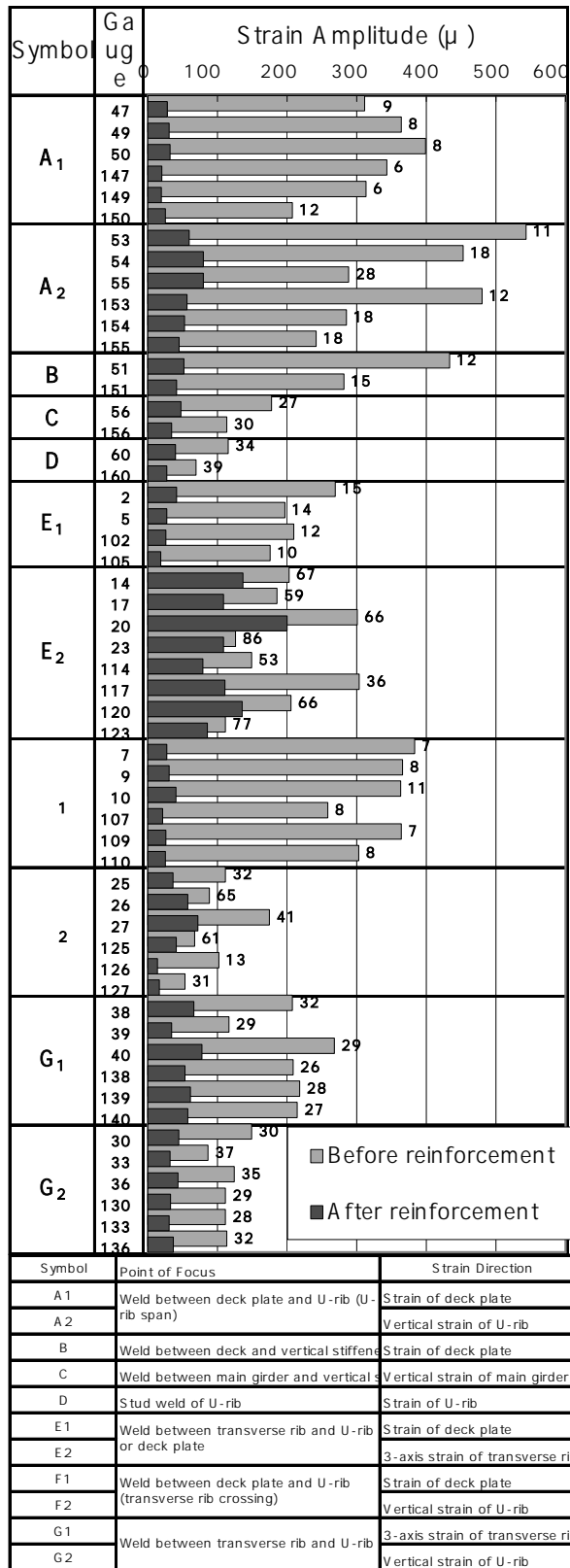


Fig.11 Strain before and after SFRC Reinforcement

## **FINAL REMARKS**

The measurements conducted in the present study were carried out immediately after reinforcement, when the reinforcing effect of SFRC can be expected to be greatest, and a large strain reducing effect believed to contribute to the improvement of fatigue durability of steel decks was observed. Even after the lapse of approximately four months under service following SFRC placement, no cracks were observed at the surface of the SFRC, and the placement of CFRP grids as a countermeasure [10] to prevent cracks in main girder webs is also believed to have an effect, but the occurrence of cracks to some extent in the future is still considered possible. Follow-ups will be done and the effect of the SFRC pavement that was placed this time as a fatigue countermeasure for the steel deck, the persistence of this effect, the durability of the pavement proper, and other aspects will be examined.

## **REFERENCES**

1. Nishikawa, Steel deck surfacing with SFRC—A New Relationship between Steel and Concrete, Bridge and Foundation Engineering, August 2005, pp. 84-87.
2. Yamada, Fatigue Damage of Steel Plate Decks under Heavy Traffic—Cases around Nagoya, Japan Society of Civil Engineers, 10th Symposium on Steel Structures and Bridges. August 2007.
3. Satoh et al., Composite Effect of Steel Deck Surfaced with Steel Fiber Reinforced Concrete Pavement, Steel Structures and Bridges, February 1986, pp. 26-30.
4. Kagata et al., Measures against Fatigue Damage of Steel Decks through SFRC Paving—The Case of Paving Work on National Highway 357's Yokohama Bay Bridge, Steel Structures and Bridges, October 2004, pp. 27-32.
5. Yamada, Fatigue Reducing Effect of SFR Pavement on Steel Decks, 62nd Annual Conference of the Japan Society of Civil Engineers, September 2007.
6. Kikuchi et al., Fatigue Countermeasures for Steel Plate Deck of Shonan-Ohashi Bridge, Japan Society of Civil Engineers, 10th Symposium on Steel Structures and Bridges. August 2007.
7. Kodama et al., Fatigue Countermeasures for Steel Decks using SFRC during In-Service Period, Bridge and Foundation Engineering, November 2006, pp. 30-38.
8. Kogoshi et al., Measurement of Effect of SFRC Reinforcement of Existing Steel Decks of Bridges," 62nd Annual Conference of the Japan Society of Civil Engineers, September 2007.
9. Ono et al., "Water Immersion/Wheel Load Fatigue Test for Steel Deck Surfaced with Steel Fiber Reinforced Concrete, 62nd Annual Conference of the Japan Society of Civil Engineers, September 2007.
10. Hitose et al., A Study on Rebars for Increasing Durability of SFRC Pavement on Steel Plate Decks, 62nd Annual Conference of the Japan Society of Civil Engineers, September 2007.

## **RAPID BRIDGE REPAIR / REHABILITATION IN WASHINGTON STATE**

Jugesh Kapur<sup>1</sup>

### **Abstract**

The Washington State Department of Transportation (WSDOT) used a very cost-effective technique using Carbon Fiber Reinforced Polymer (CFRP) to rehabilitate and strengthen a deteriorated precast concrete bridge. The beams on this bridge had experienced spalling of concrete and corrosion of reinforcement. WSDOT also replaced four, 122 cm movement steel modular joints on an Interstate 90 floating bridge due to fatigue cracking of the transverse center beams in the modular joint. In order to meet the new fatigue resistant design criteria, the new center beams are solid and 2.5cm wider than the center beams in the original modular expansion joint. Both projects were done very efficiently and rapidly without loss of quality.

### **US 2 Ebey Slough Viaduct – Repair with Carbon Fiber Reinforced Polymer (CFRP)**

The Washington State Department of Transportation (WSDOT) has effectively used Carbon Fiber Reinforced Polymer (CFRP) to rehabilitate portions of a deteriorated precast concrete bridge located near Everett, Washington at beginning of highway US 2. Portions of the bridge were repaired in 1999 and 2007 with the final section due to be completed in 2010. CFRP strengthening of vertical load carrying elements is relatively new in the United States even though it is used extensively in Europe and Japan. CFRP strengthening can be a cost-effective alternative to replacement or posting of structurally deficient bridges. Despite its high cost, CFRP possesses high strength and is light in weight. It is also corrosion resistant, easily constructible and has a high fatigue resistance. These qualities make it a favorable material for the rehabilitation of our nation's transportation infrastructure.

### **Existing Bridge**

The Ebey Slough Viaduct was constructed during the late 1960's and opened to traffic in 1968. The bridge carries nearly 35,000 vehicles per day and provides a vital link between western and eastern Washington. The bridge spans a river and slough area that floods every year. The bridge has several different superstructure types and is 11,909 feet (3630 meters) in length with a total of 256 spans.

## **EBEY SLOUGH VIADUCT**

---

<sup>1</sup> State Bridge Engineer, Washington State Dept. of Transportation, Olympia, WA



A significant portion of the bridge, 226 spans – 7,410 feet (2259 meters) has conventionally reinforced precast concrete double tee concrete units, also known as inverted tub units. The concrete unit spans approximately 38 feet (11.6 meters) between piers with each span composed of six superstructure units bolted together transversely through their webs.

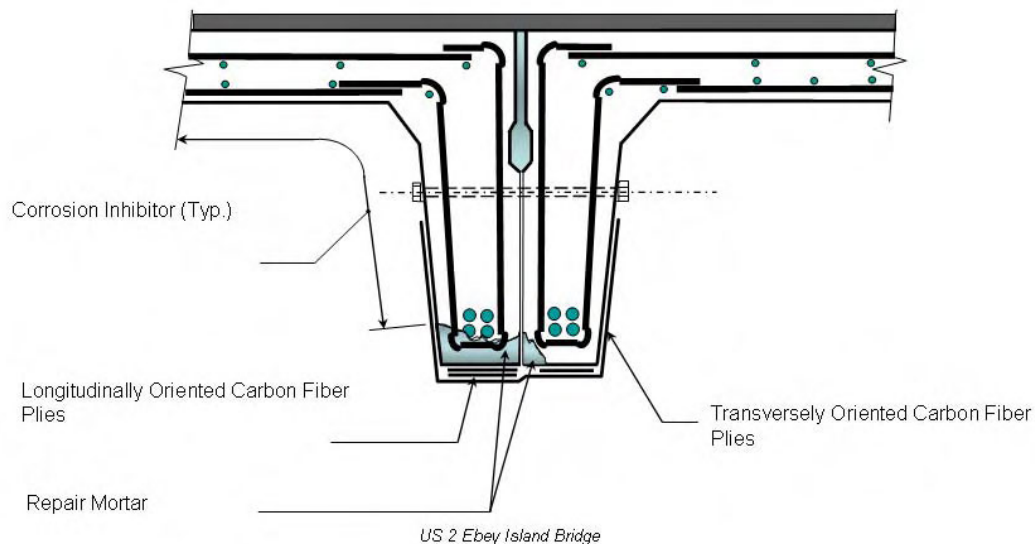
Each individual unit has a bundle of four #11 reinforcing bars at the bottom of each web covered with 1 inch of concrete. The precast concrete units also have grouted keyways between them. Over the years the grout in the keyways had deteriorated allowing water and deicing salt to penetrate between the precast units which caused the main longitudinal steel reinforcing bars to corrode and spall off the concrete cover. Areas of exposed and corroded reinforcing steel are scattered, but mostly predominant in the exterior units.



WSDOT contracted with Construction Technology Laboratories to analyze several randomly obtained core samples with the objective of evaluating the technical feasibility of repairing this structure. An analysis of the concrete core samples determined that structural rehabilitation was feasible.

## **Repair and Rehabilitation Using CFRP**

WSDOT bridge engineers reviewed different options and decided to repair the precast tub units using CFRP. Since the amount of section loss in the steel reinforcing was unknown, the CFRP would make up for the loss. CFRP material properties and applications methods differ from conventional bridge materials and how these



realities affect typical civil structural engineering design philosophies. The carbon fiber has an elastic modulus comparable to that of steel and an ultimate strength that is much greater than that of steel. Carbon does not possess the same ductility. This is different with respect to the traditional ductile concrete and reinforcing steel design philosophy.

CFRP composites have positive attributes including high strength-to-weight ratios. Additionally, the designer is afforded the flexibility of orienting stiffness and strength in the directions required. FRP composites have high resistance to fatigue and corrosion. Compared to other rehabilitation methods, FRP composites minimize handling difficulties and can be installed in limited access situations, often with minimal disruption to traffic.



In spite of these advantages, many perceived technical and institutional barriers still exist to FRP composite usage in the civil engineering arena such as, standardized/codified design criteria is limited and there is a lack of construction specifications available. Durability is another issue. The aerospace industry has conducted extensive durability tests on FRP composites relevant to their needs. Obviously, the applicability of some of these tests to civil engineering applications is

somewhat contentious. Plausible durability tests include resistance to humidity, salt water immersion, alkali, dry heat, fuel, ultraviolet weathering, and freeze/thaw cycling. The questions which need to be definitively answered are: Which of these tests are pertinent and should be required? For what durations should such tests be conducted?

FRP composite costs are perceived to be high. In rationalizing material costs, other factors must be considered: life cycle costs, traffic disruptions, durability, worker safety, and real estate costs associated with wholesale bridge replacement. One important issue was the sequencing under which carbon fiber plies are bonded to load carrying elements. Manufacturers and suppliers of CFRP materials have asserted that the plies can be bonded to structural bending elements of a bridge while that structure is under full traffic. Structural engineers disagree on the effectiveness of strengthening performed under full live load.

The main concern is that imposed live load will subject both the resin bonding agent and the carbon fiber plies to micro-strain during the curing process. Assuming full development of bond to the substrate structural material, the carbon fiber plies will augment the ultimate capacity of the structural bending element. The carbon fiber plies will not participate in resisting future live loads that are less than those that were imposed during the resin curing process. This could have potential long-term durability implications depending upon the condition of the structure before rehabilitation, the live load levels anticipated during bond cure, and the future environment to which the structure will be subjected.

Prior to structural design of the Ebey Viaduct repairs, a field survey was conducted to estimate steel corrosion losses at various locations. Based upon these estimates, a stress-strain compatibility analyses was performed to establish the carbon fiber ply cross sectional area required to regain structural moment capacity. This was done for varying levels of steel reinforcement bar corrosion loss.



Carbon fiber ply application plans specifying carbon fiber ply tensile capacity requirements were developed for each span for the contract documents. Multiple longitudinal plies were required by the design calculations. In areas where very severe spalling had occurred, transversely oriented carbon fiber plies were specified to resist horizontal shear across the existing concrete-to-repair mortar interface.

Epoxy injection of all cracks greater than 0.02" (0.51 mm) wide was required. Concrete surface preparation follows. In addition to removal of spalling concrete, this includes application of passive grout to all exposed steel reinforcement following its sandblasting to a white metal finish.

All existing sharp edges/corners in the concrete are ground smooth. Repair mortar placement follows. Once the repair mortar cures, a primer is applied to the bottoms of all concrete webs to prepare the surfaces for carbon fiber ply bonding. Putty is then used to fill all surface concavities. A resin undercoat is then applied to which the carbon fiber plies are immediately bonded. After the plies are bonded and rolled smooth, a resin overcoat is applied. Sand was broadcast onto the resin overcoat for aesthetic reasons and to provide some level of resistance to ultraviolet degradation.

Performing either repair mortar placement or carbon fiber bonding work under full traffic conditions was ruled out due to the high amount of truck traffic on the structure. A compromise was reached by electing to perform these repairs during either full traffic closure or under restricted traffic conditions. Restricted traffic was defined as only vehicles under 5 tons (4546 kg) at speeds below 25 miles (40 km) per hour. This gave four different combinations that determined how to perform the work on the remainder of the bridge.

### **Pilot Project on eight spans**



WSDOT bridge engineers selected a 304 feet (92.7 meters) long eight span section of the bridge for a pilot project. The objective of this pilot project was to assess the feasibility of rehabilitating all the precast concrete tub units on the entire bridge using advanced composite CFRP materials, both from an economic and a durability perspective. The use of CFRP would provide a way to repair and strengthen the bridge with minimal disruptions to traffic.

The work began in June 1999 and was completed by August 1999. The contract was awarded to Concrete Barrier Incorporated for nearly \$970,000 with 40 days to complete the work. Mitsubishi Chemical supplied the carbon fiber system.

The overall scope of work included setting up a containment and work platform. Removal of the existing ACP overlay to allow repair of deck delaminations and to inspect and repair the longitudinal keyway joints between adjacent concrete units. To repair the grouted keyways, the contractor sawcut 9 inches (23 cm) deep to the mid-depth of the keyways and cleaned and filled the resulting 1 inch wide gap with low modulus epoxy. A new deck membrane and ACP overlay was then placed on the roadway deck side of these eight spans. Upon completion of the overlay repairs, the spalled concrete web surfaces were prepared for placement of repair mortar. After repair mortar placement, carbon fiber plies were bonded to the web bottoms.

Corrosion inhibitor was applied to all exposed surfaces of the precast concrete units to enhance durability. The overall rehabilitation strategy involved the removal of deteriorated concrete adjacent to spalls, blast cleaning of all exposed corroded steel to a white metal condition, epoxy injection of cracks wider than 0.02", repair mortar placement, miscellaneous concrete surface preparation, and bonding of CFRP strips to the web bottoms. Structural design calculations were set up in an automated electronic format to establish the cross sectional CFRP requirements for varying levels of longitudinal steel reinforcement corrosion loss.

The carbon fiber supplier's willingness to be on the jobsite to provide technical guidance and train to the contractor was directly related to the success of the project. The supplier and contractor's work crew had a meeting prior to the carbon fiber application. Previous projects nationally have demonstrated that CFRP can be bonded under full traffic conditions to strengthen bridge superstructures. In order to evaluate several construction staging options, span-specific traffic control requirements with respect to placement of repair mortar and CFRP strip bonding were specified. Two traffic control conditions were imposed during construction: full traffic closure and a restricted traffic condition with vehicle weights limited to five tons at a maximum speed of 25 miles (40 km) per hour. Durability and performance of spans repaired under the two different traffic control scenarios will be examined and taken into consideration in developing a long-term repair strategy for the entire bridge.



Total cost of this initial pilot project was about \$970,000 which equates to about \$106/SF (\$1141/m<sup>2</sup>) of bridge deck area. This cost is 10% or less of the cost of bridge replacement. A breakdown of seven bid items representing approximately 80% of the contract cost shows the removal and replacement of concrete accounted for about 40% of the total with the CFRP application accounted for about 8% of the total cost.



Ten years following construction, all CFRP repaired concrete areas have been inspected with the longitudinal joint repairs and carbon fiber reinforcement performing as originally designed with no visible deterioration. It is anticipated that this repair will provide 25 years or more of service.

### **Phase 2 Project - Rehabilitate 128 spans**

WSDOT bridge engineers identified 136 spans of the tub units for the second phase of the Ebey Slough Viaduct rehabilitation. The project followed the same design as specified in the 1999 pilot project. The contract was awarded to Wilder Construction Company for nearly \$7.9 million with 97 days to complete the work. The work began in April 2007 and was completed by November 2007.

The contract plans specified that all traffic be restricted during the application of the carbon fiber which required the use of the parallel bridge at times to carry both directions of traffic. The contractor was allowed to determine the number of layers of carbon fiber to apply based on the amount of corrosion of the steel reinforcing bars. This provision became a problem during the project since WSDOT review of assumptions made by the contractor did not justify the number of layers of carbon fiber the contractor applied. The total cost of the carbon fiber material was nearly \$1.5 million or 19% of the total project cost.

Two years following construction, all CFRP repaired concrete areas have been inspected with the carbon fiber reinforcement performing as originally designed with no visible deterioration. It is anticipated that this repair will provide 25 years or more of service.

### **Phase 3 Final Project - Rehabilitate 82 spans**

The final 75 spans of the precast concrete tub units for the Ebey Slough Viaduct are scheduled to be rehabilitated in 2010. The project will follow the same design as specified in the 1999 and 2007 projects. This project has a budget of nearly \$31 million. It is anticipated that the actual cost will be substantially less than what is currently budgeted.

The traffic control and construction access will be more difficult than the previous two phases. These bridge spans are over water so the contractor must install work platforms from the existing bridge deck requiring additional lane closures. Connections to the parallel bridge are also more difficult in this area thus the traffic control options will be more complicated.

### **I-90 Homer Hadley Floating Bridge – Replacement of Modular Expansion Joints**

The Interstate 90 “Homer M. Hadley” bridge is the third floating bridge to be constructed across Lake Washington between Mercer Island and Seattle and carries five lanes of traffic (three for westbound and two reversible). This bridge was officially opened on June 4, 1989 and is 5,811 feet (1771 meters) in length with eighteen floating



pontoons. The three westbound lanes have an Average Daily Traffic (ADT) of 60,000 and the two reversible lanes have an ADT of 12,000.

The bridge has transition spans at both ends that allow traffic to move from the approaches to the floating sections and to allow boats to go under the bridge. The longitudinal movement, which represents a combination of wind and wave loading, seasonal water level fluctuations, and thermal variations in the bridge are accomplished through the steel modular expansion joints.

### **ORIGINAL MODULAR EXPANSION JOINTS**



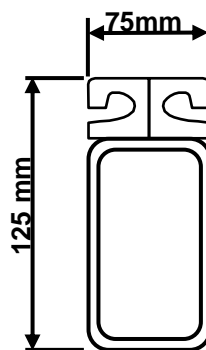
The section of the bridge with the three westbound lanes has two large movement modular joints (48 inch, 122 cm) that are 63 feet (19.2 meters) in length and the section with two reversible lanes has two large movement modular joints (48 inch, 122 cm) that are 40 feet (12.2 meters) in length. Thus there are a total of four of these sizes of joints

on the bridge.

The original modular joints were designed, fabricated, and installed prior to the advent of fatigue-based design and manufacturing criteria for modular expansion joints. The joint manufacturer chose to use a hollow tube shape for the main transverse center beams.

Fatigue cracking initiated in the hollow tube and the welded support bar connection within 18 months after the Homer Hadley Bridge opened to traffic.

WSDOT developed some research projects with the University of Washington to investigate the cause of the cracking. The university performed field measurements of the dynamic wheel loads. The location and extent of the cracks were also carefully monitored. Repairs were made in several instances by welding the cracks but nearly all of these locations cracked again.



### **Fatigue Design of New Modular Expansion Joints**

In November 1990, the pontoons in the parallel original I-90 Lacey V. Murrow floating bridge, which was being rehabilitated at the time, sunk. WSDOT recognized the need to improve on the design of the large movement modular joints during the design of the I-90 Lacey V Murrow replacement.

As part of that effort, WSDOT worked with D.S. Brown, the joints' manufacturer, the German-based Maurer Sohne Company, and University of Innsbruck (Austria) to develop the first generation fatigue resistant design specification for WSDOT. This new design was used on the new Lacey V. Murrow Bridge replacement.

Following the work by WSDOT, there was a substantial amount of interest throughout the United States to improve the fatigue resistance of steel modular expansion joints. The Transportation Research Board (TRB) subsequently funded NCHRP Project 12-40. This project culminated in the publication and release of NCHRP Report 402, which provided comprehensive fatigue-based test and design specifications for modular expansion joints.

To date, all of the modular expansion joints designed and installed based on this new fatigue design criteria are performing well.

### **Project Planning and Design**

A decision was made in 2007 that all four of the 48 inch (122 cm) movement steel modular joints needed to be replaced due to the amount of fatigue cracking in the transverse center beams and the high risk associated with a potential failure. In order to meet the fatigue resistant design criteria, the new center beams are solid and one inch wider than the center beams in the original modular expansion joint.



The replacement of the joints required WSDOT to determine the best way for the joints to be manufactured, delivered and installed. WSDOT developed an initial estimate and plan then had a meeting with the Association of General Contractors (AGC) to review the details.

At the meeting, the AGC and WSDOT discussed some of these details:

1. The amount of time to replace the joints – three weeks for the westbound lanes and 3 weeks for the reversible lanes.
2. The joints should be replaced in two separate closures, one for the westbound lanes and one for the reversible lanes.
3. WSDOT should purchase the joints and advertise the replacement/installation project separately.
4. Make sure the liability issues and warranty issues are understood and addressed.

WSDOT decided to purchase the joints directly from the manufacture and have them shipped to Washington State. These joints would be handed over to the contractor that was given the joint replacement contract. WSDOT supplying the joints would speed up the manufacture and delivery time, eliminate contractor mark-up, reduce contractor risk for acceptance of the joint. Having the joint design prior to the bid will allow WSDOT to fully design the replacement reinforcement and dowels into the block out area. The contractor would then have a better idea of the actual removal-installation details.

### **Project Construction**

The expansion joint contract was awarded to the General Construction Company for \$5.7 million with the final construction cost being \$5.85 million. The 4 modular expansion joints were replaced in two stages.



Stage 1 replaced the two 40 foot long joints located in the reversible lane roadway. All traffic used only the three westbound lanes. The first closure began on May 4, 2009 and was completed on May 16, 2009. The contract allowed 19 days with the contractor completing the work in 12 days. For the first closure, the contract had a provision to pay the contractor an extra \$40,000 for each 24 hour period completed early. Total was not to exceed \$160,000.

The first closure and replacement of the two 40 foot (12.2 meters) long joints allowed the contractor to better understand the work. We thought that the lessons learned during the May work would enhance the contractor's productivity during the more complicated stage 2 closure.

Stage 2 replaced the 63 foot (19.2 meters) long joints located in the westbound lane roadway. All traffic had to use the two reversible lanes. The second closure began on July 5, 2009 and was completed on July 17, 2009. The contract allowed 21 days with the contractor completing the work in 12 days. For the first closure, the

contract had a provision to pay the contractor an extra \$80,000 for each 24 hour period completed early. Total not to exceed \$320,000.



Our Special Provisions required that the contractor submit structural analyses verifying the load carrying capacity of the bridge for the specific cranes that would be used. Given the weight of each joint being installed and the boom radii that would be required to position these joints in their respective blockouts, we realized that the contractor would need some pretty substantial lifting equipment. Additionally, we required that the contractor operate all cranes on a

separate pad and load distribution system designed in accordance with AASHTO LRFD Bridge Design Specifications.

The contractor used a 250-ton (228,000 kg) and a 300-ton (272,000 kg) crane operating on the respective transition spans to install joints on the reversible lane roadway. The contractor used a barge-mounted crane to install the two modular joints on the westbound lane roadway.

The contractor developed a good method to remove the concrete in the header area on both sides of the existing expansion joint and removal of the existing joint. A large concrete saw was used to cut a line across the bridge at the removal limits. Workers then used chipping hammers to remove the concrete.



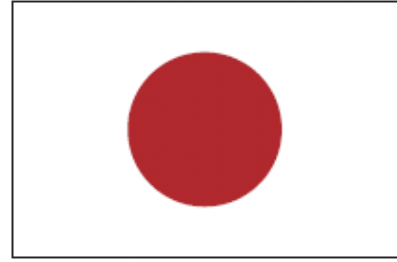
The first of the technical issues was the fact that the overall width of the replacement modular joints was greater than that of the originally installed joints. This created some issues with the traffic barriers. When a new bridge is constructed, blockouts are formed in the concrete deck or edge beam to accommodate the modular expansion joint later on. After the modular joint is installed, the concrete barriers are constructed up to the outside limits of the modular joint with steel embedment for attaching steel sliding cover plates.

Removing and reconstructing the ends of each concrete barrier would have added at least three days to the total construction duration. In lieu of demolishing the ends of the existing concrete barrier it was decided to install all four joints in contracted configurations before expanding them prior to anchorage and concrete placement. The bottoms of the concrete barriers were chipped out to accommodate the edge beam upturns beyond the curb line.



The next technical issue was the gap to set the replacement modular expansion joint in place. The cumulative gap setting is primarily a function of wind and wave motion and water level, not the temperature of the bridge, the floating portion of which is moderated by the temperature of the lake water. It was decided to set reference pins in the roadway slab prior to removal of the existing joints, then to install the replacement joints so that they would have the same cumulative gap setting as the original joints.

The overall project was considered a success. It is anticipated that the lessons learned on this project will be used when WSDOT replaces other large movement bridge expansion joints in the future.



# **25<sup>th</sup> US-Japan Bridge Engineering Workshop**

## **Session 5**

### **Maintenance**

Development of an Expansion Device for Cold Regions

By Shinya Omote, Hiroshi Mitamura, and Hiroaki Nishi

Fatigue and Corrosion in Concrete Decks with Asphalt Surfacing

By Yoshiki Tanaka, Jun Murakoshi, and Yuko Nagaya

Replacing The Suspender Ropes of a Tied Arch Bridge Using Suspension Bridge Methods

By Barney T. Martin and Blaise A. Blabac

Suspension Bridge Cables: 200 Years of Empiricism, Analysis and Management

By Bojidar Yaney

Page Left Blank

# DEVELOPMENT OF AN EXPANSION DEVICE FOR COLD REGIONS

## - TEST INSTALLATION OF AN EXPANSION DEVICE ON A NATIONAL ROUTE 274 INTERCHANGE VIADUCT -

Shinya Omote<sup>1</sup>  
Dr. Ing.Hiroshi Mitamura<sup>2</sup>  
Dr. Ing.Hiroaki Nishi<sup>3</sup>

### **Abstract**

Bridge expansion devices in Hokkaido face severe conditions (including frost/salt damage and impact from snow-removal activities), meaning that they deteriorate and sustain damage faster than other bridge members. As the replacement of damaged expansion devices has increased dramatically in recent years, a model with high fatigue durability and load capacity was developed to reduce future life cycle costs. The expansion device designed for cold regions was installed on a bridge administered by the Sapporo city to examine its workability, load-carrying capacity, waterproof performance and anticorrosive function, as well as to enable on-site verification through data accumulation, including information on the impact of snow-removal activities and stress propagation characteristics under conditions with running vehicles.

### **Introduction**

Bridge expansion devices in cold, snowy regions operate in severe conditions (including frost/salt damage and impact from snow-removal activities), meaning that they deteriorate and sustain damage faster than other bridge members. The replacement frequency of damaged expansion devices has increased dramatically in recent years. This paper presents the results of a study on the development and installation of an expansion device with high fatigue durability and load capacity aimed at reducing future life cycle costs.

### **1 Results of a survey on the conditions of expansion devices**

---

<sup>1</sup>Researcher, Structures Research Team, Public Works Research Institute, Civil Engineering Research Institute for Cold Region

<sup>2</sup> Senior Researcher, Structures Research Team, Public Works Research Institute, Civil Engineering Research Institute for Cold Region

<sup>3</sup> Team Reader, Structures Research Team, Public Works Research Institute, Civil Engineering Research Institute for Cold Region

### 1.1 Survey overview

The targets of the survey were 561 sections with expansion devices and 186 ridges on heavily trafficked major arterial roads around Sapporo, as shown in Fig. 1.1. of these, 136 bridges and 459 sections with expansion devices were on national highways. In the field survey, the damage conditions of bridges and expansion devices were examined mainly through visual observation.

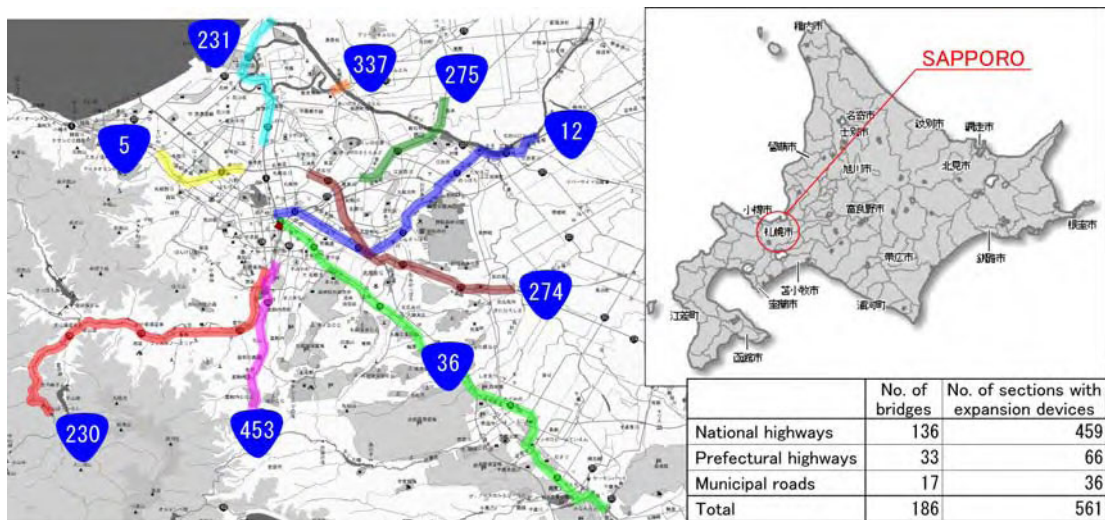


FIG. 1.1 SURVEY LOCATIONS

### 1.2 Status of bridges and existing expansion devices

#### (1) Status of bridges

River bridges accounted for approximately 80% of the total, while the ratios of viaducts and bridges over railways were a little less than 10% each.

#### (2) Status of expansion devices

Figure 1.3 shows the types of target expansion devices, of which 60% were the load-support types, 20% were the no-joint type and the other 20% were the match type.



FIG. 1.3 TYPES OF EXPANSION DEVICE

### 1.3 Age occurrence conditions

Figure 1.6 shows the results of the survey on damage to expansion devices.

#### (1) Load-support type

(a) Unevenness of face plates (Photo 1), insufficient expansion gaps (Photo 2) and cuts made by snowplows (Photo 3) were observed in many cases with the

steel-finger type, and sediment accumulation, clogging and corrosion were found at water cutoff parts. In cases using the beam type, differences in beam level and deformation were observed (Photo 4). At water cutoff parts, blockage of expansion gaps with sediment (Photo 5) and loss of cutoff rubber (Photo 6) were found.

(b) Extrusion of sealing material (Photo 7) was observed in many cases with horizontal simple-installation-type expansion devices made of steel, although there was little damage to their main bodies. In cases with vertical-type devices, deformation (Photo 8), breakage and corrosion of the main bodies were significant, loss of waterproofness was observed and water leakage was severe.

(c) In all cases with the load-support type, scaling of the pavement around expansion devices (Photo 9) and hollowness, scaling and wear of site-placed concrete (Photo 10) were observed. Such damage was significant on the front side in the side facing the direction of traffic.

(2) Match type

(a) Breakage of steel beams (Photo 11) and other serious damage to main units were found in some cases with the beam type. Blockage of water cutoff parts with sediment and loss (Photo 12) and cracking (Photo 13) of cutoff rubber were also observed. In cases with devices made of rubber, peeling of surface rubber was seen.

(b) Scaling of the pavement around expansion devices (Photo 14) and hollowness, scaling and wear (Photo 15) of site-placed concrete were observed in all types.

(3) No-joint type

(a) While the status of internal structures was unknown because the survey was conducted through visual observation only, cracking (Photo 16), loosening, scaling, unevenness, caving and other damage to pavement were observed in the vast majority of cases.

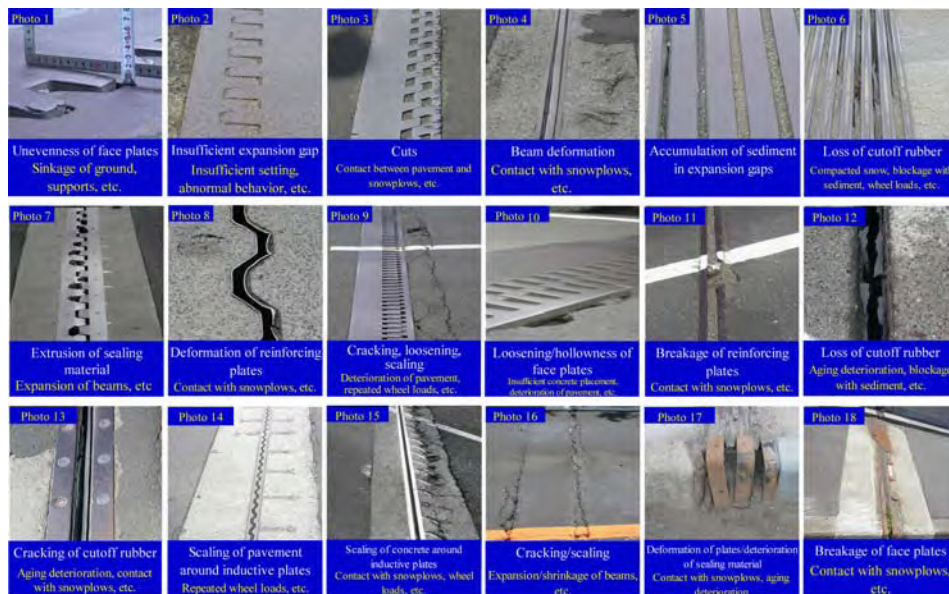


FIG. 1.6 CONDITIONS OF DAMAGE TO EXPANSION DEVICES

(4) Other

- (a) Many cases of curb breakage and edge-plate breakage/deformation (Photo 17) were observed at wheel guard parts, while deterioration and peeling of sealing materials and blockage with sediment were seen at the water cutoff parts of expansion gaps.
- (b) Significant breakage of main units (Photo 18), rusting, corrosion and other serious damage were observed in some parts of sidewalk areas. Scaling and loosening of surrounding pavement and damage to site-placed concrete were also found in all types.

## **2 Estimation of the causes of damage**

Possible causes of damage to expansion devices peculiar to Hokkaido are listed below.

(1) Damage caused by snowplows

Scaling of pavement and concrete around expansion devices was thought to result from contact with snowplows during snow removal work and from fatigue caused by the wheel loads of large vehicles.

(2) Damage caused by sediment and compacted snow

Breakage and loss of cutoff material was thought to result from the transmission of wheel loads to expansion gaps due to blockage with sediment and compacted snow.

(3) Damage caused by insufficient performance at low temperatures

Extrusion and loss of cutoff rubber was thought to be a result of adhesive failure caused by the corrosion of steel materials and insufficient performance at low temperatures.

Scaling and loosening in cases with the no-joint type were thought to be a result of repeated beam expansion and shrinkage due to temperature variations and insufficient load-following capability in the expansion devices themselves.

(4) Damage caused by spreading of antifreeze agent

Rusting of steel material and scaling/wear on concrete were thought to result from aging deterioration and the acceleration of rusting and corrosion from the spreading of antifreeze agent on road surfaces.

## **3 Improvements to expansion devices for cold regions**

### 3.1 Performance requirements in cold-region environments

To satisfy performance requirements in the conditions of cold, snowy regions with wheel loads and aging deterioration, the following considerations are desirable for expansion devices:

- (1) Safety against snowplow-related impact must be ensured.
- (2) The cutoff structure must be strong enough to resist damage from sediment accumulation and compacted snow in expansion gaps where wheel loads are transmitted.
- (3) Resistance to corrosion resulting from the spreading of antifreeze agent, etc. must be improved. Examination of the internal structure of expansion devices Figure 3.1 presents the examined part, and Photo 3.1 shows the improved expansion device.

(4) Installation structure of snowplow inductive plates

To decrease the impact of snowplows, the installation intervals of inductive plates were reduced from 300 to 225 mm. This structure was adopted to control snowplow-related damage and disperse wheel loads.

(5) Installation of dust-proof material and slide plates

To prevent the blockage of expansion gaps with sediment or snow and avoid damage to cutoff materials when wheel loads are transmitted, the entry of sediment was inhibited and the indentation force of compacted snow was supported by placing dust-proof material (polyethylene foam) under face plates and laying slide plates under it. This structure was used to maintain the durability of the elastic sealant used as the cutoff material.

(6) Improvement of anti-corrosion performance

The anti-corrosion performance of expansion devices was improved by spraying Al-Mg (aluminum-magnesium) plasma on the steel materials used (the inside of the main units, the face plates, the sides of the main units on the pavement surface and the inductive plates on the pavement surface). The metal spraying method involves the application of a layer of aluminum/magnesium (95:5) approximately 100 microns thick melted with plasma onto metal surfaces after Type 1 surface preparation. The adhesion of sprayed metals can reach more than four times (around  $7 \text{ N/mm}^2$ ) that of paint. In a combined cycle test, no corrosion was observed even after 6,000 hours (representing more than 100 ordinary years of service), and a self-healing, corrosion-inhibiting effect from the eluted magnesium was observed at cross-cut sections<sup>1)</sup>.

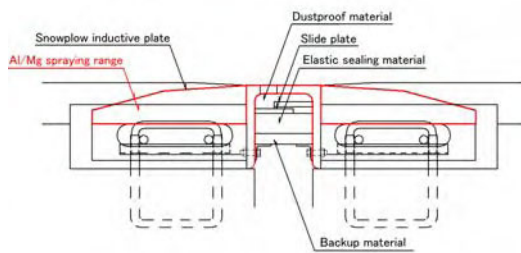


FIG. 3.1 CROSS SECTION OF THE INTERNAL STRUCTURE OF AN EXPANSION DEVICE

PHOTO 3 IMPROVED EXPANSION

**4 Performance evaluation of the improved expansion device for cold regions**

A full-scale specimen was produced for fatigue experiments to evaluate the performance of the improved expansion device. The specimen had a maximum expansion gap and a difference in level with the road surface. A wheel running machine was used for the experiment.

#### 4.1 Running test

##### (1) Purpose

This experiment was conducted to clarify the process of damage to expansion devices, and to confirm and summarize the mechanism behind the transmission of wheel loads to such devices and subsequently to the concrete in the installation section. The results of the transmission mechanism investigation can also be used to clarify the damage process.

##### (2) Wheel running machine overview

In the fatigue experiment, the method of using a crank-type wheel running machine (owned by the Civil Engineering Research Institute for Cold Region) was adopted. This technique has been established as a method of testing fatigue durability acceleration for road bridge slabs. The experiment is currently under way using a machine with rubber tires rather than the conventional iron wheels (as shown in Photos 4.1 and 4.2) to simulate actual running conditions.



PHOTO 4.1 WHEEL RUNNING MACHINE (FULL VIEW)



PHOTO 4.2 WHEEL RUNNING MACHINE

#### 4.2 Running test on an actual bridge

##### (1) Test construction overview

For a running test on an actual bridge, an expansion device for cold regions was installed at the section shown in Fig. 4.1. The bridge was an IC viaduct (957 m in length) constructed in November 1981. The test construction is expected to clarify the impact of snow removal in winter and the stress propagation of actual loads applied by many types of large vehicle, as well as to verify water cutoff and freezing conditions.

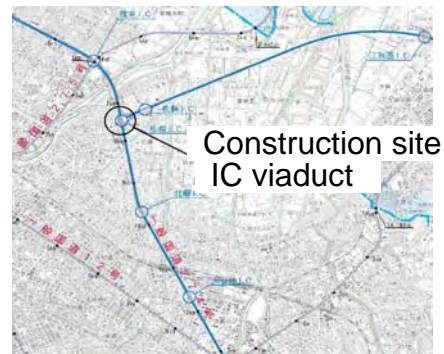


FIG. 4.1 LOCATION OF THE TEST CONSTRUCTION SITE



- 4) Placement of ultra-rapid hardening concrete: Ultra-rapid hardening concrete was placed after installation of the expansion device was complete. The concrete was blended and mixed on site using a jet mixer truck. After placement, a curing time of three hours was observed in principle (Photo 4.6).
- 5) Asphalt pavement: After the ultra-rapid hardening concrete had cured, its top surface was paved with asphalt. While concrete is usually placed up to the installation surface in repair work due to time constraints, asphalt pavement was used in this case in consideration of preventing damage to the surrounding pavement (Photos 4.7 and 4.8).



PHOTO 4.3 CUTTING



PHOTO 4.4 REMOVAL OF EXISTING DEVICE



PHOTO 4.5 INSTALLATION OF NEW DEVICE



PHOTO 4.6 CONCRETE PLACEMENT



PHOTO 4.7 PAVEMENT



PHOTO 4.8 AFTER COMPLETION

### Conclusion

The survey results indicated that the most important points were rust proofing, protection of cutoff material, and snowplow countermeasures. These measures also lengthen service life, not only for expansion devices but also for bridges themselves, and result in higher LCC assessment. In this paper, an improved expansion device and its performance evaluation method were presented in consideration of the above matters. In the future, the authors intend to summarize the experimental data obtained from the wheel running test and the driving test on an actual bridge to confirm the transmission mechanism of wheel loads.

### Reference

- [1] The Plazwire System – a long-term anti-rusting technology involving plasma spraying, Kyushu Electric Power Co., Inc. Research Laboratory

## FATIGUE AND CORROSION IN CONCRETE DECKS WITH ASPHALT SURFACING

Yoshiki Tanaka<sup>1</sup>  
Jun Murakoshi<sup>1</sup>  
Yuko Nagaya<sup>1</sup>

### **Abstract**

In 20th century, a large number of highway bridge concrete decks in U.S. suffered from corrosion due to deicing salt, but those in Japan suffered from fatigue due to cyclic loading of heavy trucks. Lately, significant corrosion of concrete decks due to deicing salt have been reported in Japan, giving rise to further concerns about combined deterioration from fatigue and corrosion in existing bridge decks designed according to old specifications. This paper provides chloride profiles in concrete decks surfaced with asphalt mixtures, which is one of reasons concerning a significant difference in deterioration between both countries. Additionally, with regard to mechanisms of fatigue deterioration of concrete decks, a current result obtained from the truck wheel traveling tests is presented.

### **Introduction**

In 1960s, construction of interstates began in U.S. But spalling due to corrosion frequently appeared on concrete decks in several years since completion. It was caused by a rapid increase in salt use for deicing in those days shown in Fig. 1. In 1970s, the deterioration affects traffic safety, drivability, traffic congestion during repair, and budget, being a major problem. A large number of deficient bridges due to corrosion still remain as current issues in bridge management in U.S.<sup>1</sup>

In Japan, fatigue due to cyclic loading of heavy trucks is major deterioration of concrete decks shown in Fig. 2 to date. Currently, however, attention should be paid not to only fatigue, but also chloride-induced deterioration on the concrete decks, because salt use have been increasing since spike tires were prohibited in 1990s as shown in Fig. 3.<sup>2,3</sup> Figure 4 shows chloride-induced deterioration observed on a bridge deck in Japan the late 1990s. While corrosion due to deicing salt is not often observed in national roads and rural roads, significant corrosion on bridge decks in expressway was reported.<sup>4</sup> In addition, most of existing bridges were built from the mid-1950s to the mid-1970s, having lower potential for fatigue durability than current bridges (Fig. 5, 6). The possibility of combined deterioration from fatigue and corrosion should be taken into account in maintenance of existing highway bridges.

---

<sup>1</sup> Public Works Research Institute, Japan

With respect to the reasons why both countries differ in major deterioration of concrete decks, quantity of salt use, traffic loading including illegal vehicles and asphalt surfacing (newly constructed bridges are almost surfaced with asphalt pavement in Japan) contrast apparently (Fig. 7).<sup>2,3</sup> Chloride ingress from the asphalt surface to concrete decks is probably governed by water. As-built asphalt mixtures should not be expected as waterproofing because of its permeability, whereas it was reported that asphalt surfacing contributed to prevent concrete decks from salt ingress while being imperfect.<sup>3</sup> Additionally water significantly affects fatigue durability of concrete decks.<sup>5</sup> Thus field performance of asphalt surfacing on the decks should be investigated for managing to prevent existing concrete decks from fatigue and corrosion in Japan.

This paper indicates results of field investigations on asphalt surfacing and chloride profiles in decks using two closed bridges; a post-tensioned concrete bridge at coastal area (ATG bridge) and a steel girder bridge with a concrete deck (TYD bridge) subjected to deicing salt. In addition, new results regarding mechanisms of fatigue deterioration in concrete decks are presented for discussing the influence of spalling on fatigue behavior.

### **Field Investigations of Chloride Ingress under Asphalt Surfacing**

Test cores consisting of asphalt mixtures and portland cement concrete of decks were taken from the closed bridges before removing asphalt surfacing (Fig. 8). Content of acid-soluble chloride ions in each slice with 10 mm depth of concrete cores was determined. A percentage of void content of asphalt mixture cores  $V_v$  was determined as described below.

$$V_v = 1 - (\gamma_M / \gamma_{max}) \times 100\% \quad (1)$$

where,  $\gamma_M$  is measured mixture density (= dry weight in air / (wet weight in air - weight in water));  $\gamma_{max}$  is a percentage of the maximum density. The values of  $\gamma_{max}$  were determined using a fragment of the removed asphalt mixtures according to the test method similar to ASTM D 2041.

Water permeability tests of asphalt mixture cores were conducted under a constant pressure of 150 kPa. Water permeability  $k$  was determined from the test results based on Darcy's law as below.

$$k = LQ / (AHT) \quad (2)$$

where,  $Q$  is total discharge (cm<sup>3</sup>);  $H$  is head (cm, =1 500 cm);  $T$  is time (s);  $A$  is area of cores (cm<sup>2</sup>);  $L$  is depth of cores (cm). No leakage of water in 24 hours was defined as impermeable.

In Fig. 9, chloride profiles of cores taken from ATG bridge are shown. The ATG bridge was built at coastal area in 1971, replaced due to corrosion of post-tensioned girders in 2005. No corrosion was observed on the road surface. Curbs were replaced around 1985 for upgrading traffic safety. The thicknesses of asphalt mixtures in the cores ranged from 37 mm to 66 mm. From the figure, it can be seen that chloride contents at the surface of deck concrete were much less than that of a core A-3 taken from the top of curb not covered with asphalt, even though low chloride permeability of prestressed concrete was taken into account. All asphalt cores of ATG bridge were determined as impermeable.

Likewise, results from the investigation of TYD bridge are shown in Fig. 10. The water permeability  $k$  is indicated, no indication of  $k$  means impermeable except a core T-9 untested. Deicing salt was applied on TYD bridge, being somewhat apart from the sea. The thicknesses of asphalt mixtures in the cores ranged from 44 mm to 71 mm. Chloride ingress of deck concrete was definitely observed at a joint between asphalt mixtures (core T-9). Except the joint, much chloride contents were not observed in the concrete of decks. All asphalt cores taken from TYD bridge were not impermeable. Determined permeability ranged from 1 to  $20 \times 10^{-7}$  cm/s except cores near curbs.

Most of asphalt cores taken from existing bridges including 20 bridges investigated previously<sup>3</sup> and the above mentioned ATG and TYD bridges had the void contents  $V_v$  of less than 2%, being determined as impermeable. It was reported that the void contents of asphalt mixtures decreased with increasing the service time.<sup>6</sup> With regard to the decrease in the void content in service, compaction due to traffic loading probably influences. But since impermeable areas were not observed only in loading areas determined by ruts, there must be reasons other than the effect of compacting in service, such as melting due to high temperature in summer and clogging. Although waterproofing was installed on the TYD bridge since 1996, a fact that deicing salt had been applied since the day before the installation indicates that the decks was not prevented from chloride ingress by only waterproofing.

Several routes of chloride-contaminated water from the road surface to decks seem to exist depending on depth of asphalt mixtures, magnitude of compaction, finishing at joints of surfacing, damage level and maintenance level of surfacing (Fig. 11). After chloride-contaminated water reach on the concrete decks, chloride ions penetrate into concrete. Chloride penetration in uncracked concrete is ordinarily expressed by Eq. (3).<sup>7</sup>

$$C(x,t) = C_o \left( 1 - \operatorname{erf} \frac{x}{2\sqrt{D_c t}} \right) \quad (3)$$

where,  $x$  is depth from the surface;  $t$  is time;  $C_o$  is chloride level at the surface of concrete;  $\operatorname{erf}(\ )$  is error function,  $D_c$  is diffusion coefficient of chloride ions in concrete.

As shown in Fig. 12, the diffusion coefficient obtained from ponding tests in salt water significantly differs from that obtained from exposure tests in airborne chloride environment at coast.<sup>8</sup> Consider the diffusion coefficient of top cover concrete in decks, while the condition of bare concrete of curbs corresponds to that of the exposure tests, the condition of concrete decks covered with chloride-contaminated water under asphalt mixtures is probably close to that of the ponding tests indicating rapid chloride penetration. In addition, water ingress accelerates disbonding between asphalt surfacing and concrete, providing a fine soil layer in the boundary. The soil layer keeps the surface of concrete wet for long time, forming the condition closer to the ponding tests.

When chloride ingress continues, chloride level at reinforcing steel bars reach the threshold level initiating corrosion of steel in concrete. Expansion of the steel bars due to

corrosion yields cracking and spalling of concrete as well as asphalt mixtures.

Curve fitting to Eq. (3) using chloride profiles obtained from decks without asphalt surfacing provides two parameters of the boundary chloride level  $C_o$  and the diffusion coefficient  $D_c$ . Then exposure time  $t$  is simply determined as the term from construction. But the chloride profiles obtained from decks surfaced with asphalt mixtures are not available to determine the diffusion coefficient of the decks because the exposure time governed by quality, durability and maintenance level of asphalt surfacing is unknown.

As an attempt, the exposure time is estimated using the diffusion coefficient predicted from Fig. 12. Since water-cement ratios of old structures are not exactly predictable, average values of reinforced concrete and post-tensioned concrete are roughly assumed as 0.55 and 0.43, respectively. Fig. 13 shows the estimated exposure time of the concrete decks under asphalt surfacing. With regard to the results of wet condition, the estimated exposure time of decks on ATG bridge is only 0.2 to 1 year despite the severe chloride environment at coast and the lifetime of 34 years. In cores taken from TYD bridge, obvious chloride profile was obtained from only core T-9 at a joint of asphalt, while deicing salt was applied for long years. The estimated exposure time at T-9 is 8 years. It cannot be determined whether chloride ingress took place after installing a waterproof layer or before.

Consequently, it was found that although both bridges investigated did not had waterproofing at completion, the expected exposure time was much shorter than the service term. The results indicate that the impermeable or low permeable asphalt mixtures contributed to prevent bridge decks from chloride contamination in a manner.

### **Mechanisms of Fatigue in Reinforced Concrete Decks under Traffic Loading**

Concrete spalling due to corrosion on decks influences fatigue durability of concrete decks. Fatigue mechanisms of reinforced concrete decks subjected to cyclic wheel loads have been studied since 1960s. Some types of truck wheel traveling tests for real-size decks were proposed to simulate real fatigue deterioration in 1980s,<sup>9</sup> contributing various research of bridge decks so far. To identify the influence of spalling on fatigue behavior, a new approach focusing on the change of internal stress with crack propagation was attempted in our study using a specimen N for the test (Fig. 14).<sup>10, 11</sup> From the results, at relatively early cycles, arch action consisting of concrete arch rib and steel ties (lower main steel reinforcing bars) was recognized through a truck wheel traveling area, similarly to a shear resistance mechanism of reinforced concrete beams.

As shown in Fig. 15, cracks were observed in a deck specimen after the truck wheel traveling test. For showing one of the behavior indicating arch action, distributions of axial forces acting on a main tensile reinforcement at the center of the deck are shown in Fig. 16, being measured using strain gages. The distribution at 50 cycles shows typical flexural behavior of a slab. As the number of cycles increases, the distributions changed even through the bar, indicating the behavior of the tie bar. The change was recognized at early stage corresponding to the cycles  $N_s$  that an apparent neutral axis calculated using measured strains of upper and lower steel bars turned to increase as shown in Fig. 17.

Similarly, using previous data of 11 specimens,<sup>12</sup> the cycles to the change of the apparent neutral axis  $N_s$  were calculated. The cycles  $N_s$  corresponded to the cycles to the crack density (crack length per area) reaching 90% of the final crack density, ranging from 0.05 to 0.3  $N_f$ ,<sup>9</sup> where  $N_f$  is the cycles to failure. All specimens were designed according to the old specifications in 1964 except a specimen having details of 1972 specifications.

Fig. 18 shows the cycles  $N_s$  of the 11 specimens and the specimen N with the applied load level normalized by  $P_{sx}$ , where  $P_{sx}$  is the reduced punching shear strength<sup>5</sup> considering an equilibrium of forces at failure under cyclic loading. From the figure, it was found that the cycles  $N_s$  related to developing arch action can also be expressed as a kind of fatigue behavior similarly to  $N_f$ .

Fatigue tests in compression using 100 mm dia. cylinders made of the same batch of concrete for the deck specimen N were conducted. A relationship between the measured strain ranges at the initial cycle and the cycles to failure was obtained. From the result, the measured strain ranges of 800 to 1000 microstrains in compression resulted in fatigue failure at several hundred thousands cycles corresponding to the cycles to failure of 0.36 million cycles for the deck specimen N.

During the truck wheel traveling test of specimen N, after arch action was formed, the regions, where the strain ranges measured using embedded gages in concrete exceeded the strain range of 800 microstrains, gradually appeared. The deck specimen shifted into the situation that concrete in the region could fail owing to fatigue in compression.

It is known that an elastic modulus of concrete decreases with cycles in fatigue tests. To estimate the elastic modulus of concrete in the deck specimen N, each share of concrete and main compressive reinforcing bars in the internal compressive resultant force under arch action was calculated using measured strains of upper and lower reinforcing bars as shown in Fig. 19. Subsequently, assuming that the share equals to the ratio of concrete area to steel area considering young's modulus ratio, the elastic modulus of concrete in the internal compression zone of arch action was estimated. The result is shown in Fig. 20. It can be recognized that the elastic modulus of concrete in the compression zone rapidly decreased after developing arch action. The turn to increase of the apparent neutral axis observed after arch action was caused by the increase of strains in the upper main reinforcing bars due to the decrease of elastic modulus of concrete in the compression zone.

From this viewpoint, spalling on decks definitely affects fatigue durability of concrete decks under heavy traffic conditions. In fact, another deck specimen having artificial spalling on the top showed a significant decrease in the cycles to failure ( $N_f = 0.14$  million cycles) when compared with the specimen N.<sup>11</sup>

## **Conclusions**

From our investigations regarding fatigue and corrosion of concrete decks, the following two topics were introduced.

- 1) In several surveys to date, asphalt surfacing often prevented concrete decks from chlorides in a manner regardless of waterproofing. Most of asphalt mixtures covering

old removed bridges were determined as impermeable or low permeable. Asphalt mixtures seems to be getting impermeable relatively early in service, while being imperfect.

- 2) At early stage during the truck wheel traveling tests of full-scale concrete decks, arch action consisting of concrete arch rib and steel ties similarly to a shear resistance mechanism in reinforced concrete beams was recognized through the truck wheel traveling area. Unless arch action is constructed, concrete in decks is out of the range available to be fatigued in compression (Fig. 21). The cycles to arch action are likely to be expressed as a kind of fatigue behavior.

### **Acknowledgments**

The authors thank the many staff members in the Ministry of Land, Infrastructure, and Transport that assisted with the surveys presented in this paper.

### **References**

1. Paul Virmani et al., *Corrosion Cost and Preventive Strategies in the United States*, Federal Highway Administration, FHWA-RD-01-156, March 2002.
2. *Report of Research Committee on Deterioration of Concrete Structures due to Deicing Salt*, Japan Concrete Institute, Tokyo, Japan, Nov. 1999. (in Japanese)
3. Public Works Research Institute, *Investigation on Life Cycle Cost of Concrete Bridges-Deterioration and Maintenance Cost of Concrete Bridge*, Technical Memorandum of PWRI No. 3811, Tsukuba, Japan, March 2001. (in Japanese)
4. Yokoyama, K., Honjo, K., Kuzume, K. and Fujiwara, N., Study on deterioration mechanism of reinforced concrete slabs with steel corrosion in expressway bridges, *Proc. of 6th Symp. on Decks of Highway Bridges*, JSCE, pp.145-150, June 2008. (in Japanese)
5. Matsui, S., Fatigue strength of reinforced concrete slabs of highway bridges by wheel running machine and influence of water on fatigue, *Proc. of JCI*, 9-2, pp.627-632, 1987. (in Japanese)
6. *Q & A on Pavement Technology*, Kensetsu-Tosho, Tokyo, Japan, pp.77-82, 1972 and pp.179-183, 1983. (in Japanese)
7. Sherman, M. R., McDonald, D. B. and Pfeifer, D. W., Durability Aspects of Precast, Prestressed Concrete -Part 1: Historical Review, *PCI Journal*, V. 41, No. 4, pp. 62-74, July-August, 1996.
8. Tanaka, Y., Fujita, M., Cheong, H., Watanabe, H. and Kawano, H., Chloride Permeability of High-Strength Concrete, *Proceedings of fib 2002 Osaka Congress*, pp. 145-154, October 2002.
9. Matsui, S., *Study on fatigue of concrete slabs for highway bridges and its design method*, Thesis, Osaka Univ., Japan, Nov. 1984. (in Japanese)
10. Nagaya, Y., Murakoshi, J. and Tanaka, Y., Behavior of cracks in reinforced concrete decks under cyclic running wheel loads, *Proc. of JCI*, 30-3, pp.907-912, July 2008. (in Japanese)
11. Tanaka, Y., Murakoshi, J. and Nagaya, Y., Influence of Spalling of Upper Cover Concrete on Fatigue Behavior of Concrete Bridge Decks, *Proc. of JCI*, 30-3, pp.913-918, July 2008. (in Japanese)
12. *Experimental study on the fatigue durability of highway bridge slabs*, Technical note of NILIM, No.28, Tsukuba, Japan, March 2002. (in Japanese)
13. *Highway Deicing - Comparing Salt and Calcium Magnesium Acetate*, SR235, TRB, National Research Council, 1991.
14. Bridge inventory data was provided by FHWA in 1999.
15. Shimomura, C., Sakai, Y. and Nakajima, H., Investigation on the real condition of spreading deicer, *Civil Engineering Journal*, 31-5, pp.280-285, May 1989. (in Japanese)

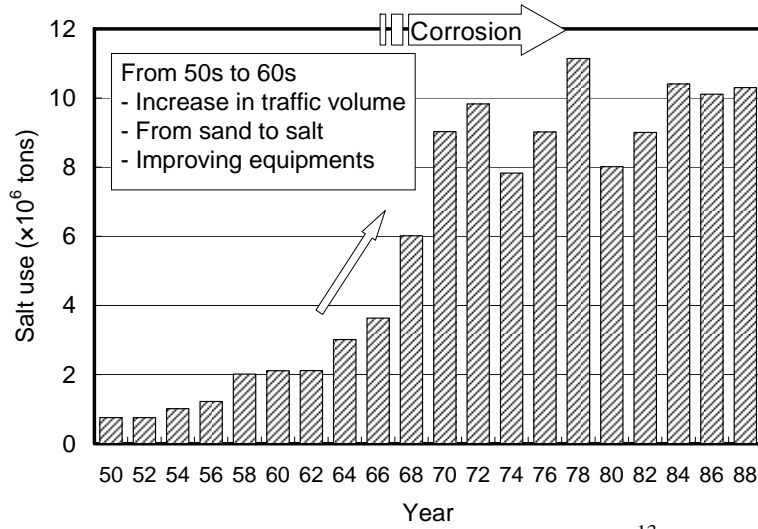
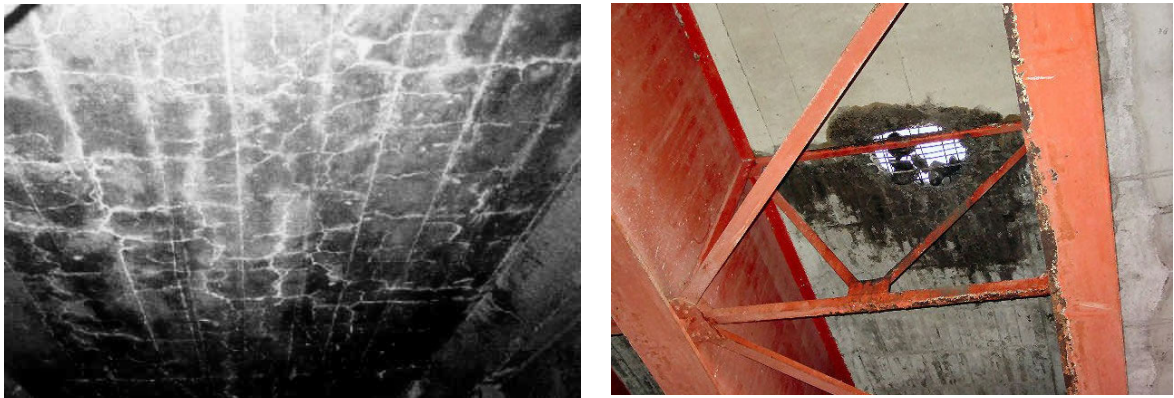


Fig. 1 Trends in deicing salt use in U.S. <sup>13</sup>



(a) Grid cracks (b) Through hole  
Fig. 2 Deterioration due to fatigue in reinforced concrete decks

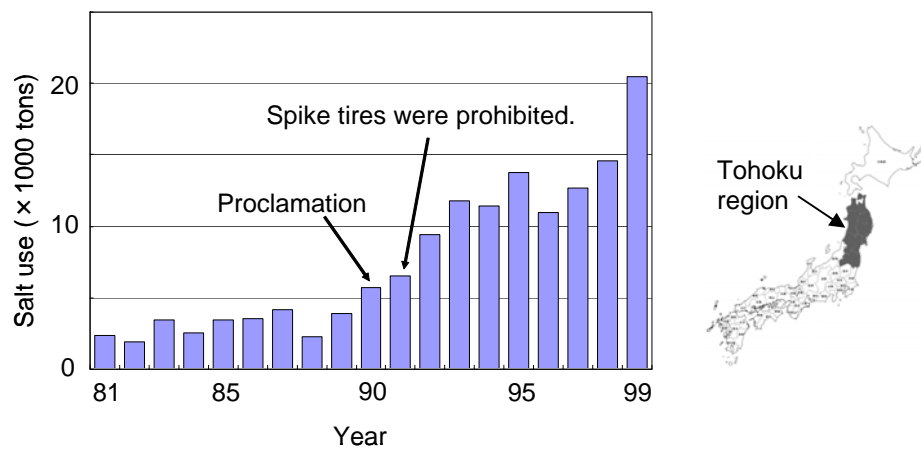


Fig. 3 Trends in deicing salt use in Tohoku region in Japan



Fig. 4 Corrosion of top mat reinforcement due to salt use in reinforced concrete decks  
Both photo shows top of decks after asphalt and spalled concrete cover were removed.

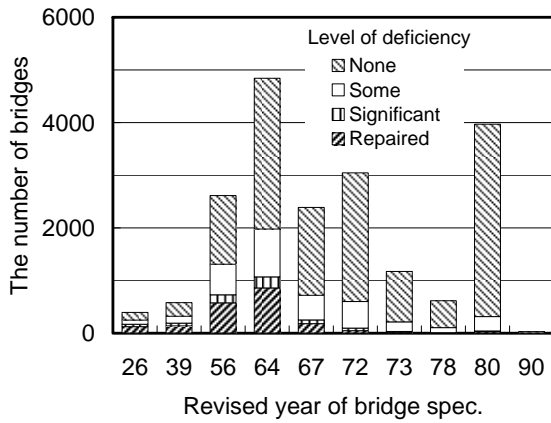


Fig. 5 The number of steel girder bridges classified under the level of deficiency due to fatigue in concrete decks (investigated in 1991)

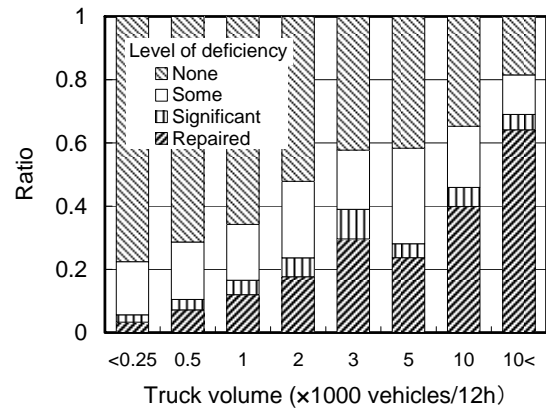


Fig. 6 The influence of traffic volume of large vehicles on fatigue in concrete decks  
The ratio is based on the number of steel girder bridges designed according to highway spec. in 1964. (investigated in 1991)

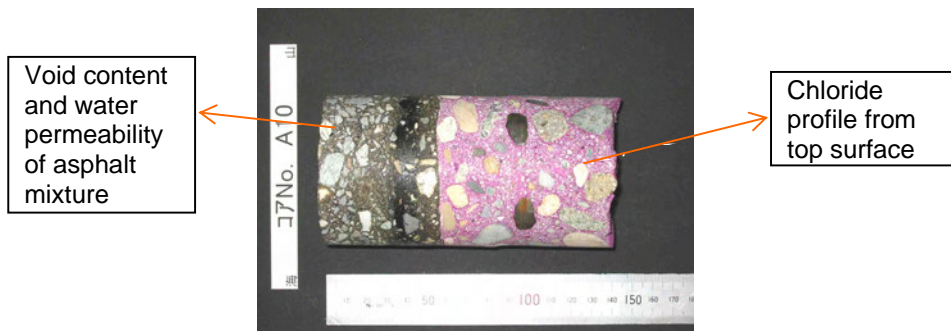
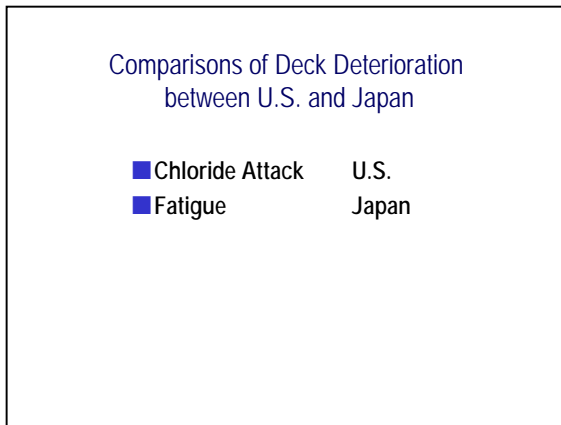
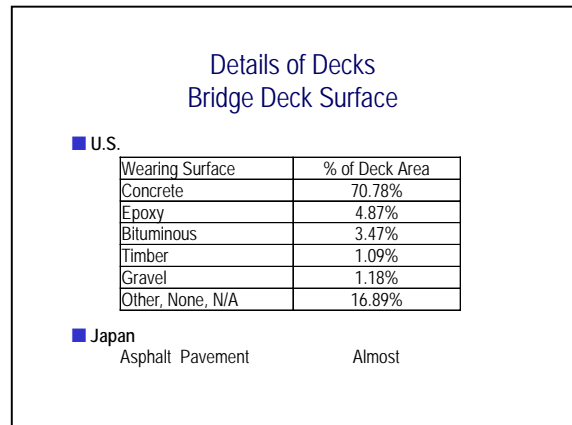


Fig. 8 A core with 70 mm dia. taken from the road surface of a closed prestressed concrete bridge at coastal area and purposes of the core

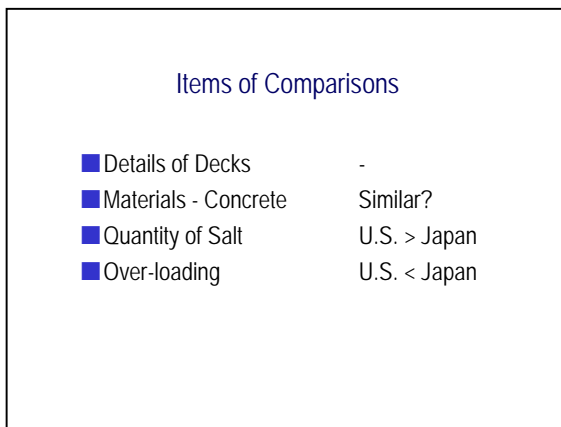
Note: Fig. 7 is shown in next page.



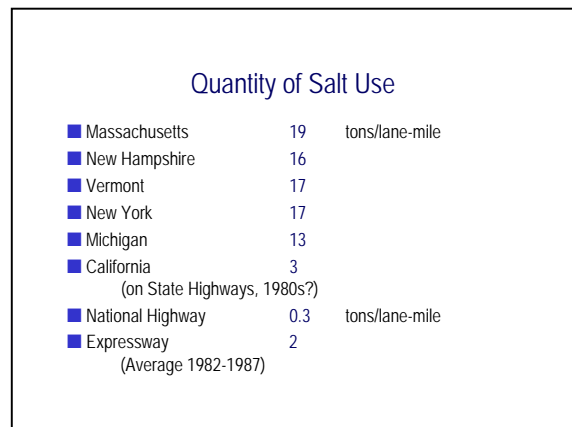
(a) Major problems in concrete bridge decks



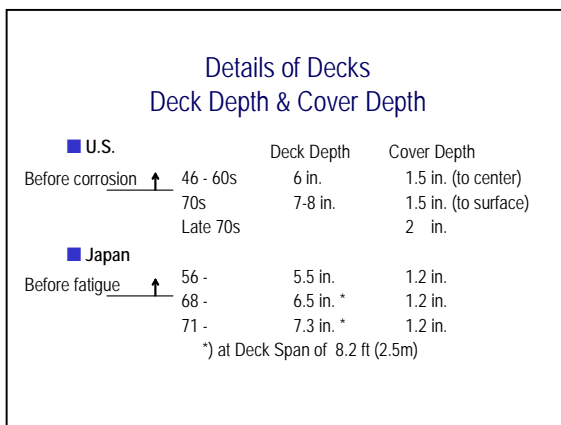
(d) Comparison in surfacing<sup>14</sup>



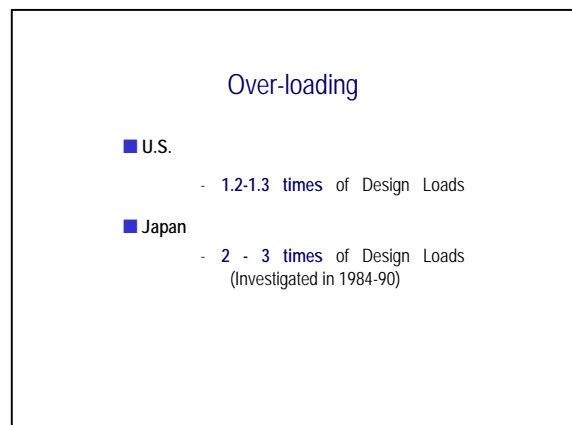
(b) Key items of comparisons



(e) Comparison in salt use<sup>13,15</sup>



(c) Comparisons in details of decks



(f) Comparison in overloading

Fig. 7 Comparisons in deterioration of bridge decks between U.S. and Japan  
(Presented by Y. Tanaka in a breakout session in Reno, 2000)

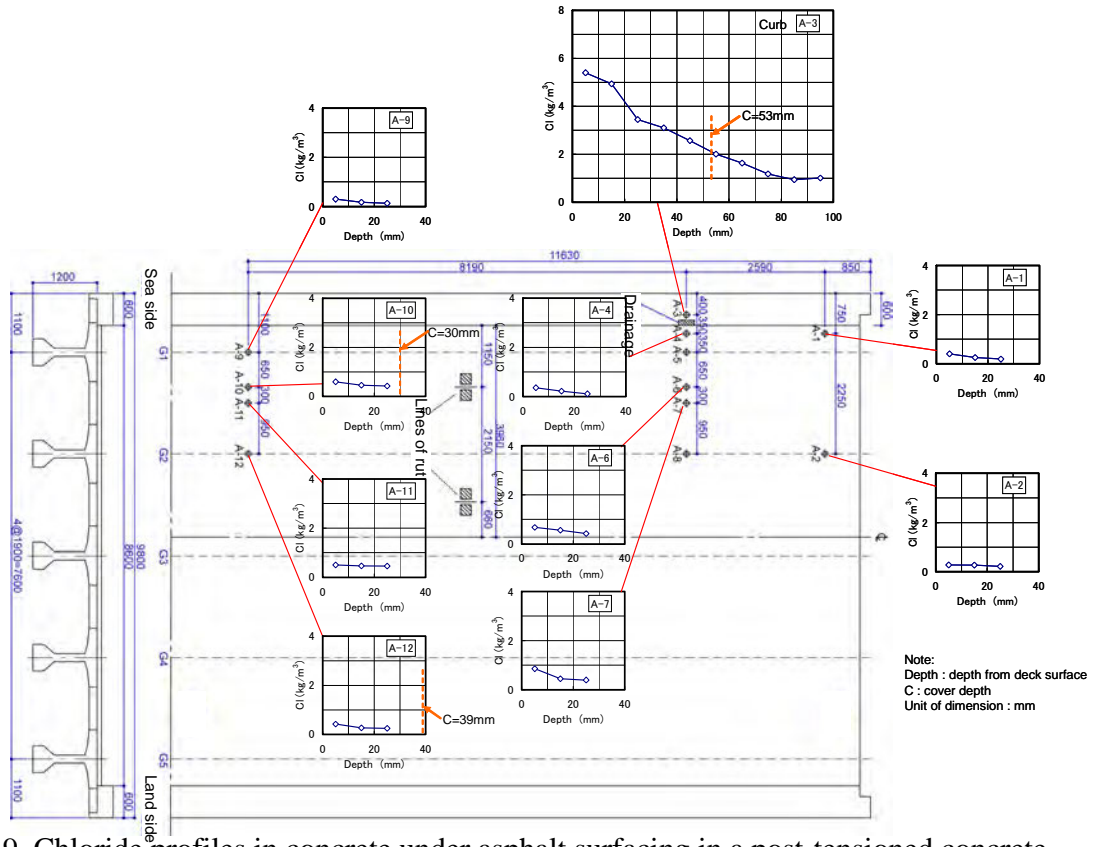


Fig. 9 Chloride profiles in concrete under asphalt surfacing in a post-tensioned concrete bridge exposed at coastal area for 34 years (ATG bridge)

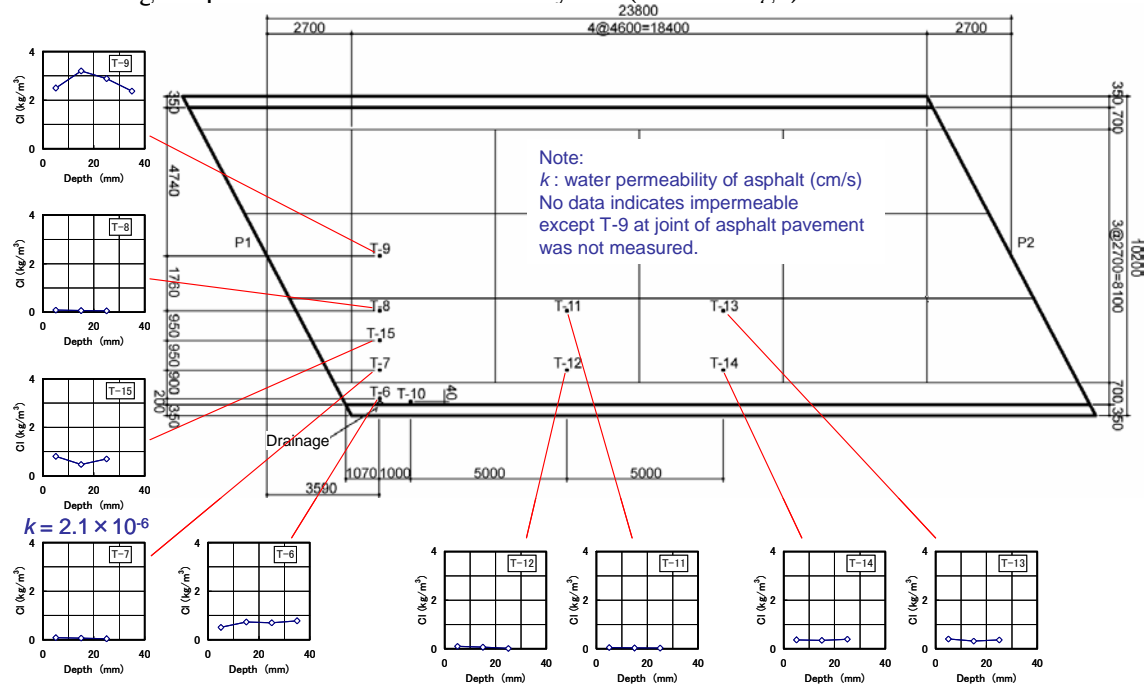


Fig. 10 Chloride profiles in concrete under asphalt surfacing in a concrete deck of a steel girder bridge used for 43 years suffering from deicing salt (TYD bridge)

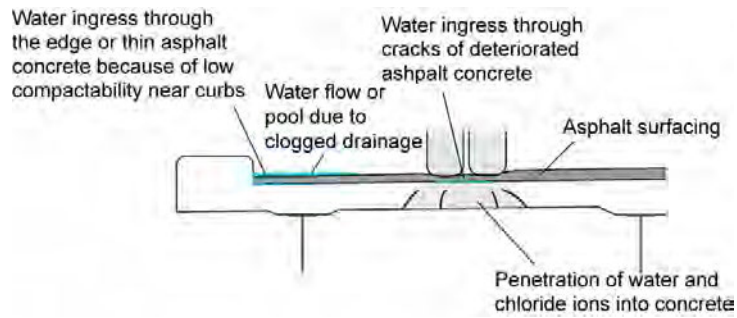


Fig. 11 Routes of chloride ingress to decks surfaced with asphalt mixtures

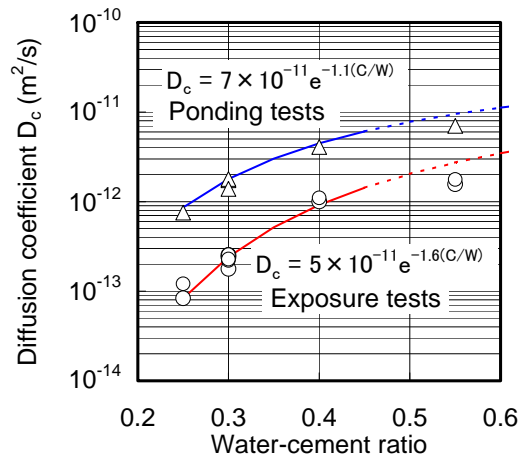


Fig. 12 Difference in diffusion coefficients of chloride ions in concretes between exposure test at coastal area and ponding test in salt water<sup>8</sup>

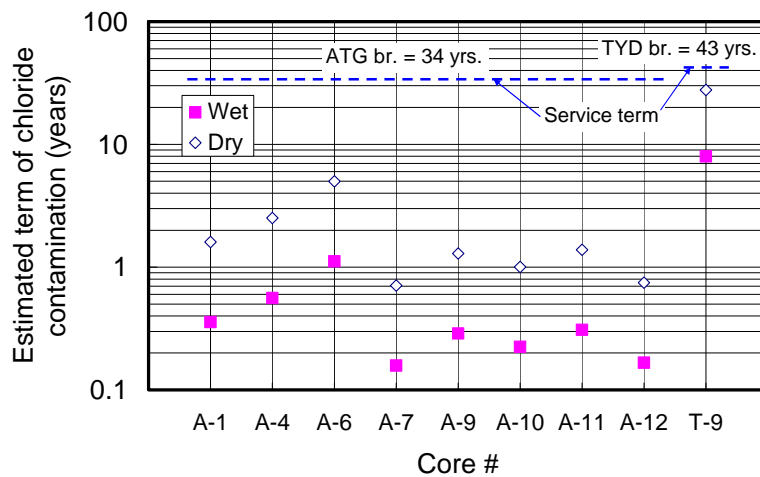


Fig. 13 The estimated terms of chloride contamination at top of decks



Fig. 14 Truck wheel traveling test using real-size concrete decks with 2.8 m x 4.5 m

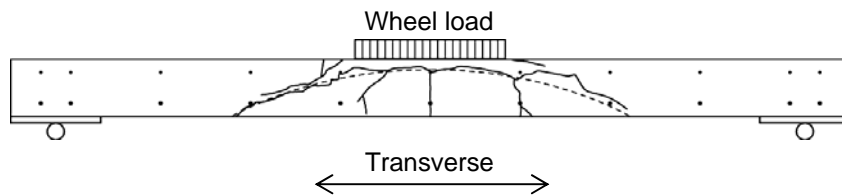


Fig. 15 Cracks in a deck specimen due to cyclic truck wheel loading ( $N_f = 0.36$  million cycles, wheel load = 157 kN)

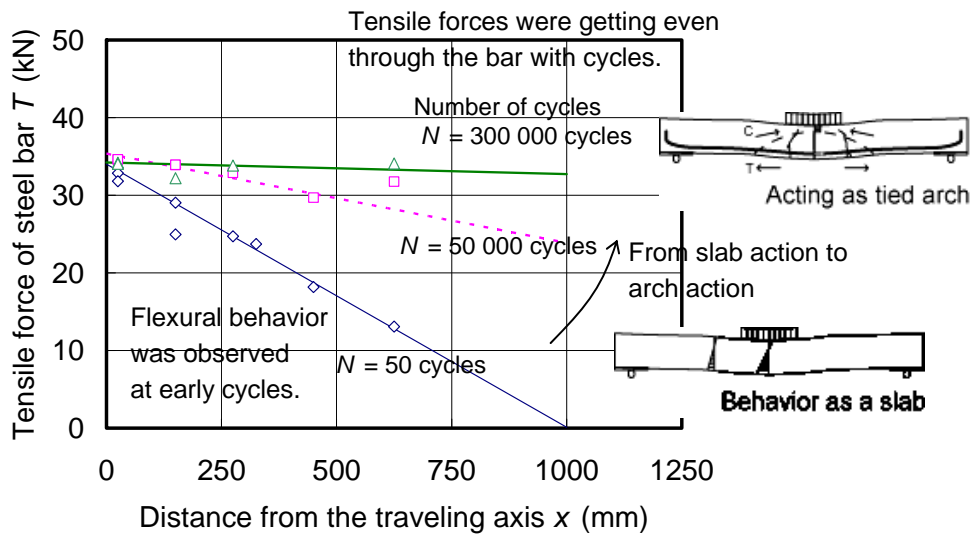


Fig. 16 Distributions of tensile axial force acting on a main reinforcing bar

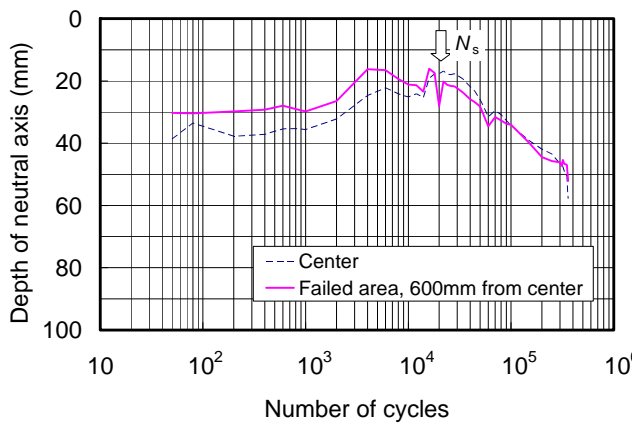


Fig. 17 Relation of depth of the apparent neutral axis from the top surface with cycles

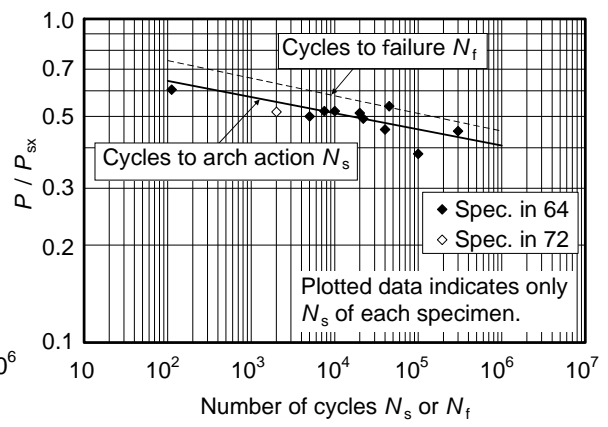


Fig. 18 Relation of loading level with cycles to arch action

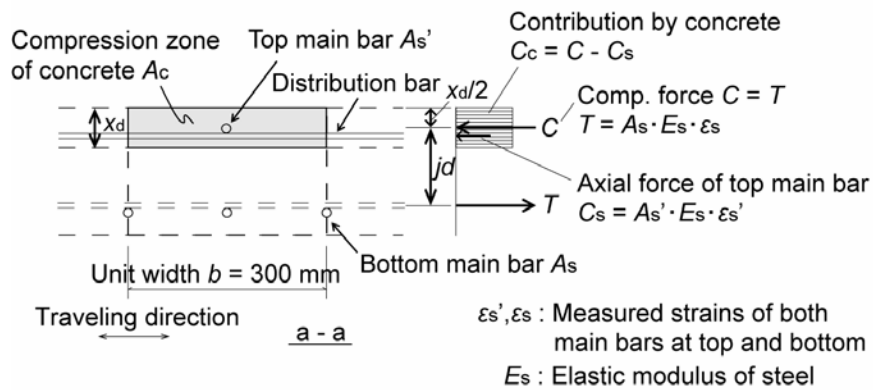
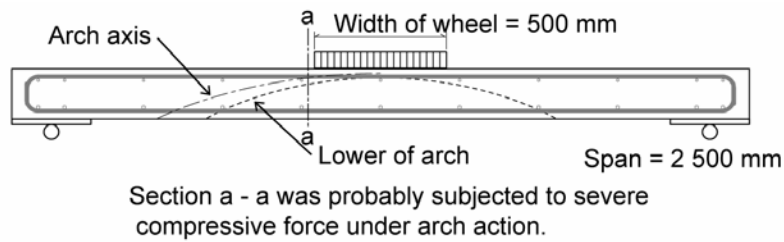


Fig. 19 Schematics of contributions of concrete and a top main steel bar subjected to the internal compressive force under arch action

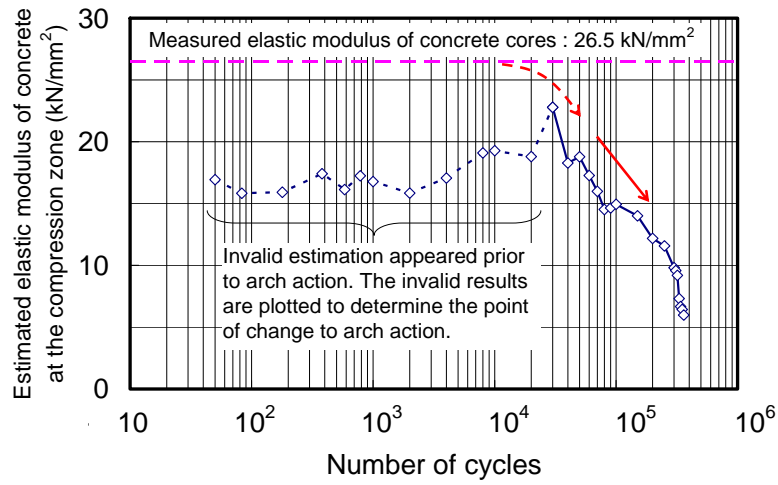


Fig. 20 Decrease in elastic modulus of concrete due to fatigue under arch action

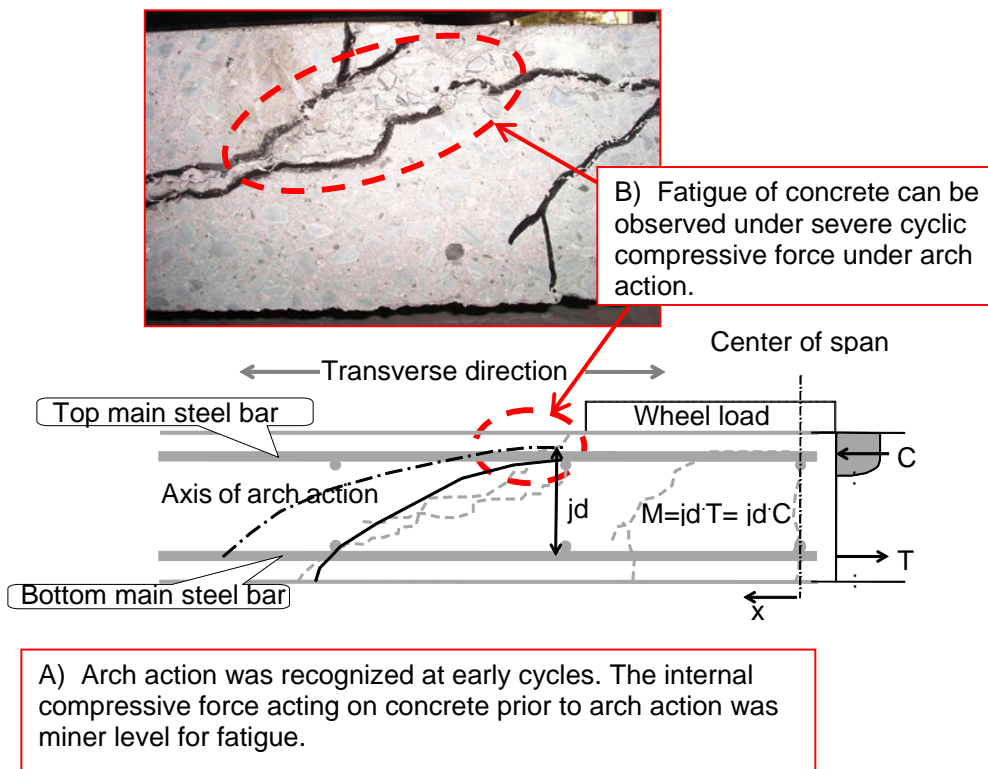


Fig. 21 Arch action and fatigue of concrete in compression

## **REPLACING THE SUSPENDER ROPES OF A TIED ARCH BRIDGE USING SUSPENSION BRIDGE METHODS**

BARNEY T. MARTIN, JR., Ph.D., P.E.<sup>1</sup>, AND BLAISE A. BLABAC, P.E.<sup>2</sup>

### **ABSTRACT:**

The Thaddeus Kosciuszko Bridge consists of twin through-arch structures which span the Mohawk River in the state of New York between the towns of Colonie in Albany County and Halfmoon in Saratoga County. Working with Modjeski and Masters, the contractor for this project proposed an alternative method for the replacement of all 168 suspenders for these bridges utilizing a modified technique previously applied to suspension bridges. One of the most significant benefits of the proposed method was that it allowed the work to be performed under full traffic. This alternative method saved the bridge owner approximately \$5 million by eliminating the complex jacking system and traffic control requirements shown on the original Contract Plans.<sup>1</sup>

### **INTRODUCTION**

The Thaddeus Kosciuszko Bridge consists of twin through-arch structures located in the State of New York which span the Mohawk River between the towns of Colonie in Albany County (on the South) and Halfmoon in Saratoga County (on the North). The bridges were built in 1959 and each carries three lanes of traffic in a single direction on the Northway (Interstate 87) – one bridge is for Northbound traffic and the other for Southbound. The bridges carry a high traffic volume of approximately 110,000 vehicles per day.



**Figure 1 – Northway Twin Arch Bridges (Thaddeus Kosciuszko Bridge), Albany, NY**

---

<sup>1</sup> President, Modjeski and Masters, Inc., Poughkeepsie, New York

<sup>2</sup>Senior Design Engineer, Modjeski and Masters, Inc., Poughkeepsie, New York

In February 2008, a contract was awarded for the replacement of all 168 suspenders on the bridges. The nearly 50-year old suspenders, consisting of 50 mm diameter structural strands, had significant section losses as a result of corrosion caused by an aggressive upstate New York environment. The winning bid price submitted by Piasecki Steel Construction of just under \$12 Million was over \$4 Million less than the Engineer's Estimate. A Value Engineering Proposal submitted by the contractor subsequent to the award saved an additional \$1 Million. Thus, the contractor's alternative method resulted in a combined savings of over \$5 Million.

The cost savings were the result of an innovative approach to replacing the suspenders using an alternative method from that shown on the contract plans. This method substituted the complex jacking and shoring system shown on the plans with a simplified system similar to that used previously on suspender rope replacement projects for suspension bridges. Using this system, the contractor was able to remove and replace the suspenders under full live load. This was a significant improvement over the method shown on the contract plans which required closing the bridge during certain phases of the work resulting in a complex and costly traffic plan that involved a median cross-over to reroute traffic to the adjacent bridge.

### **BRIDGE DESCRIPTION**

The Northway Twin Arch bridges are two-hinged steel arches with a span of 182.9 m between the bearing pins and a rise of 36.6 m relative to the spring line. Each bridge consists of two parallel rectangular arch ribs having a rectangular box cross-section approximately 1.2 m wide by 2.4 m tall, built up of riveted steel plates spaced 15 m center to center. Each bridge carries three 3.6 m lanes with two 1.0 m shoulders, for a total deck width of 12.8 m. The suspended portion of the span has a length of 167.6 m with three approach spans on each end for an overall length of 232.7 m per bridge.

The deck superstructure is suspended from the arches with 50 mm diameter structural strands – one pair of strands supports each end of the intermediate floorbeams. The superstructure of each bridge consists of 21 intermediate floorbeams spaced at 7.62 m on center (22 equal panels). The end floorbeams are connected either directly to the arch (at the fixed end) or attached with a pinned link (at the expansion end). Longitudinal stringers framing into the floorbeams support a reinforced concrete deck (designed as non-composite, although shear connectors were provided for added rigidity). Open steel grid deck is provided between the floorbeams in the shoulder areas to provide drainage.

There are a total of 84 suspenders – the longest of which is over 29.87 m long. The typical suspender has a Type 8 socket on each end – at the top, the socket bears on a transverse beam within the arch box (see Figure 5); and at the bottom, it bears on a stiffened seat angle attached to the web of the floorbeam. The connection is symmetrical about the webs of the transverse beam and floorbeam.

The suspender connection at the crown of the arch is unique. At this location, both suspenders share one large socket which in turn is supported by a pair of U-bolts that straddle a large pin (see Figure 8). The pin is a vestige of an original design

feature of the bridge – it originally functioned as the crown pin for a three-hinged arch. As part of the original design, the bridge was constructed as a three-hinged arch for dead load. Once the deck superstructure was completed, the crown was locked by installing cover plates on the top and bottom of the box section to make this part of the arch continuous. Thus, the bridge was transformed into a two-hinged arch for live loads. Unfortunately, the design made no provision for future replacement of the suspender – the splice plates effectively blocked access to the suspender connection. This made for a more complicated repair at this location, as will be discussed later in this paper.

## **PROJECT BACKGROUND**

In recent years, the condition of the suspender strands had rapidly degraded due to a combination of age and exposure. Salt spray from the adjacent roadway had run down the suspenders over the years, concentrating the damage at the area where the suspender connects to the floorbeam. The suspender strand in the vicinity of the seat angle began to suffer from corrosion related section loss, eventually leading to failure of the individual wires. As the wires began to break, they would splay outward, eventually resulting in a rather dramatic display of deterioration (see Figure 3). In the most extreme cases, section losses of up to 50% were reported. As a result, the decision was made to undertake an immediate replacement of all 168 suspenders on both bridges. Of these, a total of 22 suspenders were identified as requiring emergency replacement.



**Figure 2 – View at Crown of Arch**



**Figure 3 – Photo of Deteriorated Suspender Strand with Broken Wires (After Removal)**

The contract, awarded in February 2008, required the replacement of the 22 worst suspenders prior to the end of November 2008 and complete replacement of all suspenders by November 2009. The contract contained a penalty clause of \$10,000 per day if the contractor did not meet the November 30, 2008 deadline.

Although a temporary support system for the replacement of the suspenders was fully designed and detailed on the contract plans, the contract documents allowed for an alternative lifting scheme to be submitted by the contractor. The contract stipulated that any alternative system would have to meet the specific requirements of the contract, such as load capacity and deflection criteria, and had to be designed and detailed by a licensed Professional Engineer. Furthermore, the alternate system would be subject to review and approval by the NYSDOT.

The winning contractor, Piasecki Steel, hired Modjeski and Masters to prepare the detailed design calculations and working drawings of the alternate structural lifting system. The design was completed in May and accepted by the NYSDOT in June 2008.

The contractor began replacing suspenders in September 2008. In October, as a result of the routine annual inspection of the bridge performed by the NYSDOT, some of the 22 yellow-flagged suspenders were upgraded to a red-flag condition – thus requiring repairs to be completed within 6 weeks. This forced a modification of the already advanced replacement sequence; however, the contractor was able to mobilize additional jacking systems to accommodate the accelerated schedule and the repairs were completed on time – with just 1 day to spare before the November 30<sup>th</sup> deadline!

### **DESCRIPTION OF THE ALTERNATIVE STRUCTURAL LIFTING SYSTEM**

The structural lifting system developed for this project is very similar to those that have been used for the replacement of suspender ropes on suspension bridges. For these structures, the lifting system is designed to perform the following tasks:

1. Temporarily support the floorbeam to allow the suspender to be removed
2. De-tension the existing suspenders
3. Tension the new suspenders

Although similar in concept, some of the features of the suspender system for this bridge structure were quite different from the details found on typical suspension bridges. Due to the unique features of this structure, developing a structural lifting system to allow the completion of all the required repairs presented quite a challenge. Some of these features include:

- Each pair of suspenders supporting the floorbeams of the arch consists of two individual elements, anchored top and bottom. In this case, each suspender could be removed and replaced individually. On most suspension bridges, the suspenders are continuous over the top of the cable, such that both legs of the same rope must be replaced simultaneously. Therefore, when replacing a

suspender rope, both legs of the suspender are typically de-tensioned and tensioned simultaneously.

- The suspenders of this bridge are attached directly to the web of the transverse floorbeams. Unlike suspension bridges, this bridge has no longitudinal stiffening element (truss or girder) that supports the floorbeams. On a suspension bridge, the presence of the stiffening truss typically allows for the installation of separate systems during rope replacement: one to temporarily support the panel point and another to de-tension/tension the suspender ropes. In this case, the structural lifting point had to be located directly on the floorbeam itself and allowed for little space for the attachment of a separate system for suspender removal and installation. Furthermore, the floorbeams required steel repairs, some of which could only be done once the floorbeam was off-loaded and the suspenders were removed.
- Due to the lack of a longitudinal stiffening element, the structure does not provide for a redundant load path to redistribute loads to adjacent panels during the removal of a suspender. Owing to the resulting low inherent stiffness, the ends of the floorbeams are relatively free to deflect during jacking operations. Therefore, the original design contract specified strict limits on the deflection of the floorbeam during the removal and replacement of the suspender: no more than 8 mm of differential downward deflection between any two adjacent floorbeams; and no more than 6 mm of upward deflection of any one floorbeam from its original position. The reasoning provided by the design engineer for the deflection limits was to prevent cracking of the concrete deck as a result of excessive movements of the floorbeam. However, due to the lack of longitudinal stiffness of the deck superstructure, the displacement of the floorbeam as a result of live load exceeds that allowed during jacking (particularly near mid-span where the elastic stretch of the suspenders under the design live load is on the order of 25 mm).

### **ADVANTAGES OF THE ALTERNATIVE SYSTEM**

The method in the value engineering proposal has a number of advantages over the system shown on the original contract plans, such as:

- The system shown on the contract plans relied on transferring load to the adjacent floorbeams (and deteriorated suspenders) with a temporary support beam (see Figure 4). The alternative method uses a completely independent system to support the floorbeams during suspender rope replacement (see Figure 5).
- With the alternative method, there is no change in load path during the removal and replacement of the suspender. The jacking system is attached to both the arch and the floorbeam in a way that is structurally equivalent to the existing suspenders (see Figures 6 and 7).
- The alternative structural lifting system does not require modification of the existing arch cross-section to allow tensioning of the new suspenders. Tensioning of the new strands is accomplished by the same friction clamping system used to de-tension the strands. The stressing method shown on the original contract plans

involved cutting a permanent hole in one of the plates comprising the rib cross section in order to tension the new suspender from within the arch using a special type of top socket.

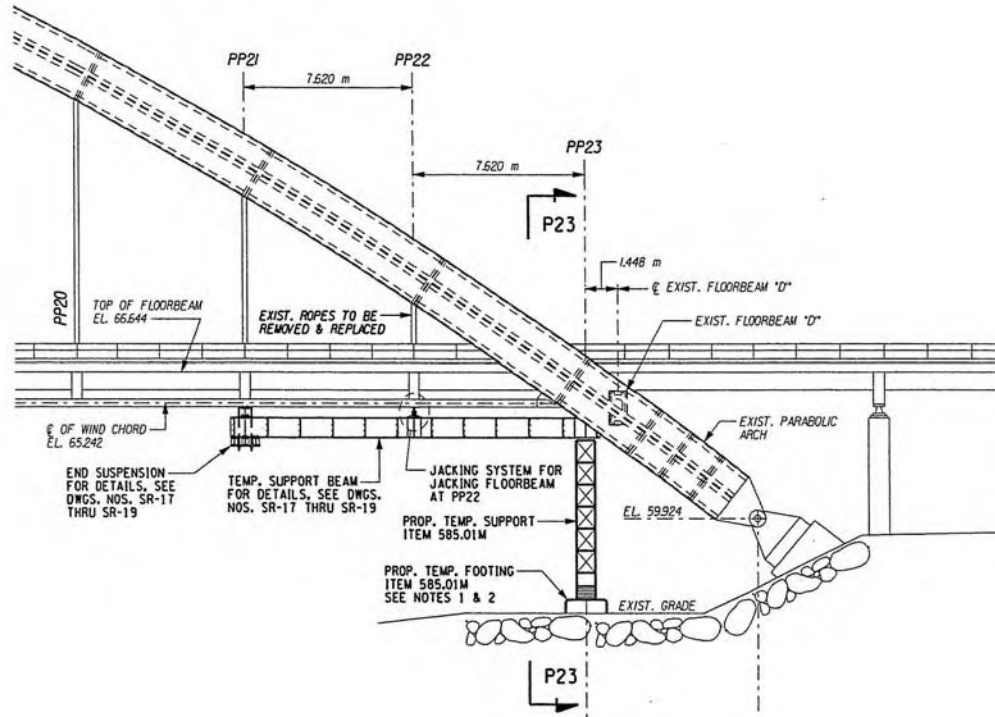


**Figure 4 – Method of Replacing Suspenders in Original Contract Plans.**

- The alternative method allows for suspender rope replacement under full live load. Furthermore, the contractor fabricated the new ropes using the measurements shown on the shop drawings from the original bridge construction, rather than attempting to measure the suspenders in place. This eliminated the complex and costly traffic control procedures required by the contract plans that involved shutting down one bridge at a time and installing cross-over's to re-route traffic to the adjacent bridge.
- The alternative system combines all the functions of the temporary support, detensioning of the existing suspenders and tensioning of the new suspenders in one system. This efficient system has a total weight of only 1.8 tonnes. The system shown on the contract plans utilized a separate means of temporary support, consisting of either beams supported by adjacent suspenders (for intermediate panels) or towers supported at ground level (at end panels). The temporary support beams alone consisted of double W36x300's with a weight of approximately 15.5 tonnes. The temporary support towers had a height of approximately 7.3 m, a capacity of 159 tonnes and required a temporary footing at the edge of the river.
- The contractor was able to complete the replacement of all the suspenders by fabricating 4 identical systems.

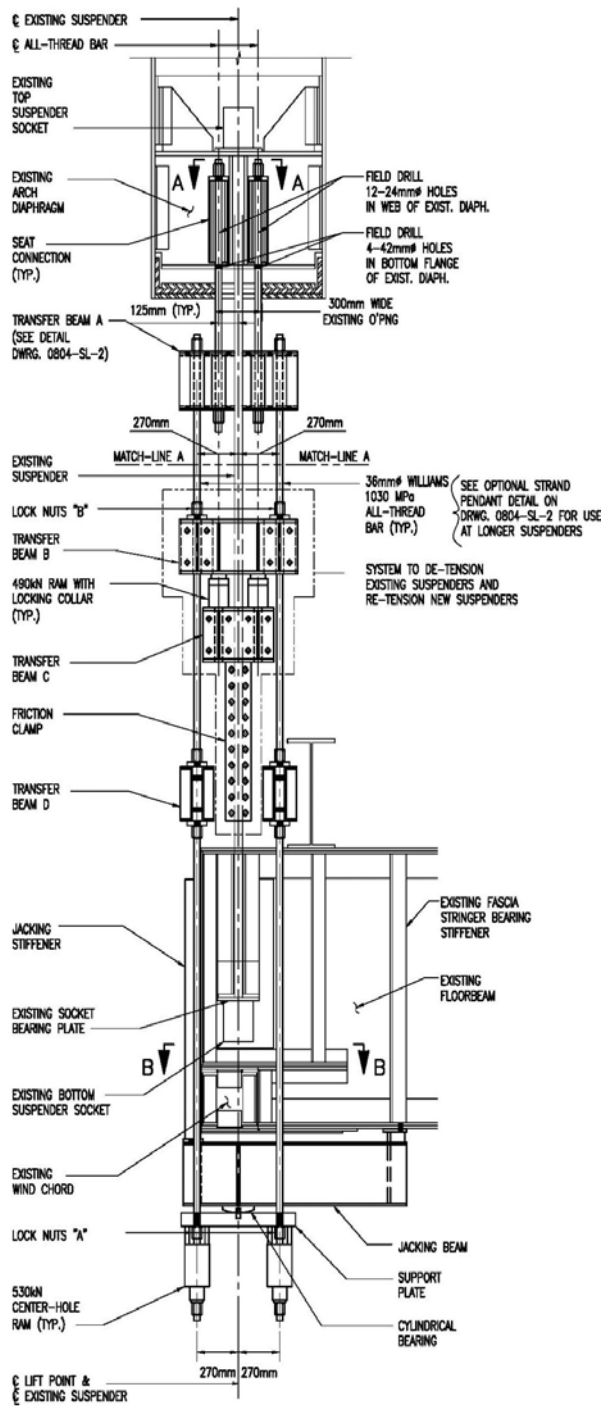


**Figure 5 – Alternate Structural Lift System**



**Figure 6 – Connection at Transverse Beam Inside Arch Box**



**Figure 7 – Structural Lift System Installed at Panel Point 3**

## **FEATURES OF THE ALTERNATIVE SYSTEM**

A thorough description of the features and functions of each element of the alternative jacking system is beyond the length limits of this paper. The following section highlights the details of some of the more unique elements of the alternative system; these are: 1) the friction clamp, 2) the floorbeam steel repairs, and 3) the steel repairs at the arch crown (Panel Point 12).

**FRICITION CLAMP** – Rope removal and installation was performed using a friction clamp, similar to those used on previous suspension bridge suspender rope replacement projects. According to the contract specifications, the clamp had to be load tested to determine the friction factor of the suspender strands for use in the design of the clamp. Due to the proposal to use the friction clamp for the installation of the new ropes, the load test was also required to demonstrate that there would be no damage to the galvanized coating of the suspenders as a result of the applied clamping force.

For this project, it was elected not to use a zinc liner at the contact surface between the clamp and the suspender. Previous experience with installing clamps on wire rope suspenders indicated that there would be no damage to the surface of the ropes. The contractor pointed out that clamping devices are used during the manufacturing of both ropes and strands (as part of the stressing beds used to pretension the strands to remove the initial elastic stretch) which do not utilize zinc liners.

The contractor fabricated two friction clamps for the load test based on a preliminary design performed by Modjeski and Masters (see Figure 8). Assuming a friction coefficient of 0.15, the clamps were designed for the required structural lifting load of 445 kN (per suspender) with a safety factor of 1.5 against slip (ultimate capacity of 668 kN). This resulted in a clamp utilizing 20 – 25 mm diameter A325 bolts fully tensioned to a minimum load of 227 kN each (total clamping force of 4,536 kN, min.). For the initial test, the ram was operated to its maximum capacity (890 kN), but no slip occurred in either clamp. This proved the design was adequate; however, in order to determine the coefficient of friction, it was necessary to determine the load at which slip would occur. Therefore, the test was repeated, removing two bolts each time, until slip was achieved. Slip finally occurred at a load of 890 kNs after eight bolts had been removed (12 bolts remaining). Assuming an average bolt tension of 271kN per bolt (227 kN min., 316 kN, max.) with a total clamping force of 3,256 kN, the actual coefficient of friction coefficient was calculated to be 0.27. This meant that the actual capacity of the clamp was 1,223 kN (ultimate) vs. the required capacity of 445 kN, resulting in a safety factor of 2.75 for the design jacking load.



**Figure 8 – Friction Clamp During Load Test**

Upon the conclusion of the test, the clamps were opened and the rope was visually inspected by NYSDOT personnel. The load test demonstrated that the galvanized coating was in satisfactory condition – there was localized deformation of the coating due to the high bearing stress on the surface of the outer wires, but the integrity of the coating was not compromised.

**FLOORBEAM STEEL REPAIRS** – The original Contract Plans showed three types of steel repairs for the floorbeams: Type 1 involved replacement of the end stiffener angles and plate; Type 2 involved replacement of the vertical stiffener angles at the suspender connection; and Type 3 combined both the Type 1 and Type 2 repairs plus the replacement of an existing fill plate between the vertical stiffener angles and the web. The contract was later modified to include Type 2 repairs at all locations (adding approximately \$700,000 to the cost of the contract). This was prudent given that the only time these repairs could be completed was when the suspenders were removed. An inspection of the existing stiffener angles also revealed that many were in poor condition and the outstanding legs were actually bowed outward (possible due to crevice corrosion at the top and bottom of the stiffener angles). Type 1 repairs could be performed independent of the suspender removal because no off-loading was required.

As a result, it was imperative that the jacking system design accommodate the need to perform steel repairs once the suspenders were removed. In order to accomplish this, the floorbeam would have to be lifted away from the existing suspender connection. However, the most logical location – the bottom flange – was blocked by the presence of the wind chord. Due to the detailing of the wind chord, as well as the deteriorated condition of this member, transferring the floorbeam reaction through this member was not deemed a viable option. Therefore, the decision was made to provide a temporary jacking beam that would effectively bridge over the wind chord by supporting the floorbeam at two points – at the end stiffeners and at the first interior stiffener. (see

Figure 4) A support plate connected to the hanger rods would react against the jacking beam through a simple rocker bearing to ensure equal distribution of the lifting loads to all four hangers. This system required that any Type 1 repairs be performed prior to the installation of the jacking system, as the beam utilized the end angles for support. In cases where no Type 1 repairs were required, the structural capacity of the existing riveted connection of the end angles was compared to the anticipated lifting loads. In fact, it was determined that the rivets were not sufficient and that either the rivets would need to be replaced with new high strength bolts or that additional bolts would need to be added between the existing rivets (the latter option was preferred by the Contractor).

At locations with Type 3 repairs, an additional step was required in the repair process as a result of utilizing the end angles for support of the jacking system. In order to replace the existing fill plate, it needed to be cut into two sections to allow the new end stiffener angles to remain in place while the remainder of the fill plate was removed along with the vertical stiffener angles. This cut had to be performed delicately in order to prevent damaging the existing web. The Contractor employed a core drill to make a series of adjacent holes along the cut line to remove the majority of the plate material. Then a grinder was used to remove any remaining material between the holes and to make a straight edge. A new narrow fill plate was installed along with the new end stiffener angles. Later, when the vertical stiffener angles were removed, the remainder of the fill plate was removed and replaced.

**SUSPENDER REPLACEMENT AND STEEL REPAIRS AT CROWN OF ARCH (PANEL POINT 12)** – The contract plans originally stipulated an extremely tight window for the contractor to remove and replace the suspender strands at Panel Point 12 (crown of arch). The work consisted not only of the replacement of the strand itself, but also involved substantial steel work – the bottom splice plates of the arch first had to be cut to re-establish the original access opening and allow the existing socket to be removed. Once the replacement of the existing suspenders and hardware was complete, the splice plates needed to be reinforced by installing new cover plates. Cutting the access hole involved removing a substantial amount of area from the existing splice plates which maintained the continuity of the arch for live loads. Therefore, the Contract Plans contained an involved procedure that restricted much of the work to take place while the two lanes adjacent to the arch could be closed – a condition that was only allowed during a 6-hour overnight window. The Contractor indicated to the DOT that it was not physically possible to perform all the required repairs in such a limited timeframe (not to mention the difficulty associated with attempting the work at night). Upon further discussion with Modjeski and Mastersn, the restrictions were modified to allow the suspenders to be removed and replaced during one - two-lane closure window and the steel repairs to be performed during a subsequent two-lane closure window. Actual cutting of the splice plates was allowed while maintaining only a single lane closure.

While these work restrictions were ostensibly designed to limit the loads on the arch to account for the reduced splice plate section, a careful review of the procedure on the contract plans showed that the restrictions would not have this effect. In fact, the

procedure indicated that during certain times, lane closures were not required to be maintained at all while the access hole was opened. This fact was confirmed with the NYSDOT and the consultant responsible for the design. Their analysis indicated that the arch would effectively revert back to a two-hinged arch while the repairs were performed and would be adequate for the anticipated live loads. Once it was realized that the burdensome procedure shown on the Plans served no real purpose, it was abandoned in favor of a much simpler method of affecting the repairs.

A repair was developed that allowed all work to proceed without the need for lane closures, except for final torquing of the bolts on one-half of the splice connection (approximately one hour's work, during which a two-lane closure would be required). The jacking system was similar in concept to the other panels on the bridge in that an independent hanger system was used to carry the floorbeam reaction while the existing strands were removed and replaced. The difference at this location was the connection at the arch due to the presence of the original pin in place of the typical transverse beam. In this case, saddle blocks were fabricated that sat on top of the pin which accepted the all-thread hanger rods and transferred the hanger reaction directly through bearing on the top surface of the pin (see Figure 9).

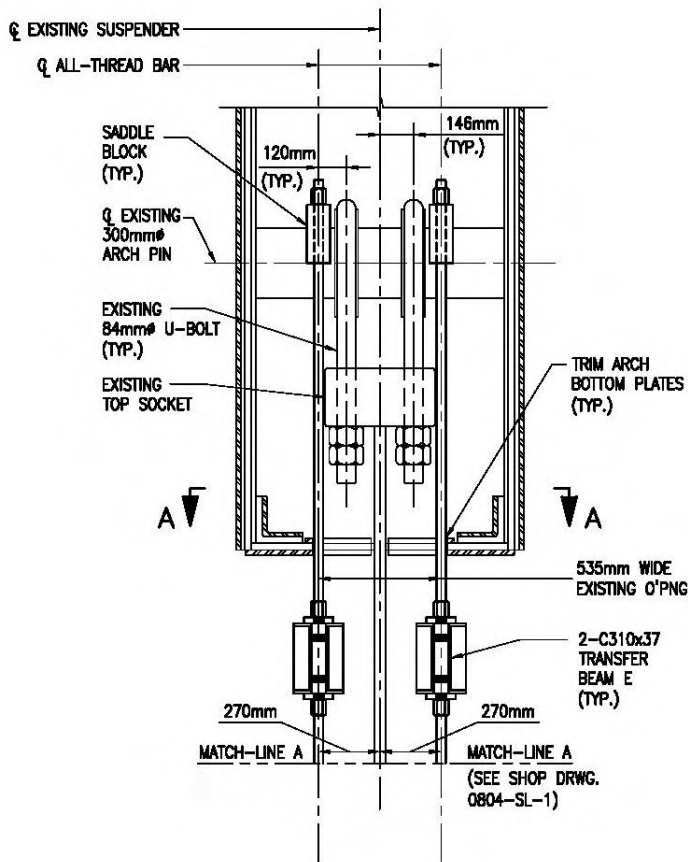
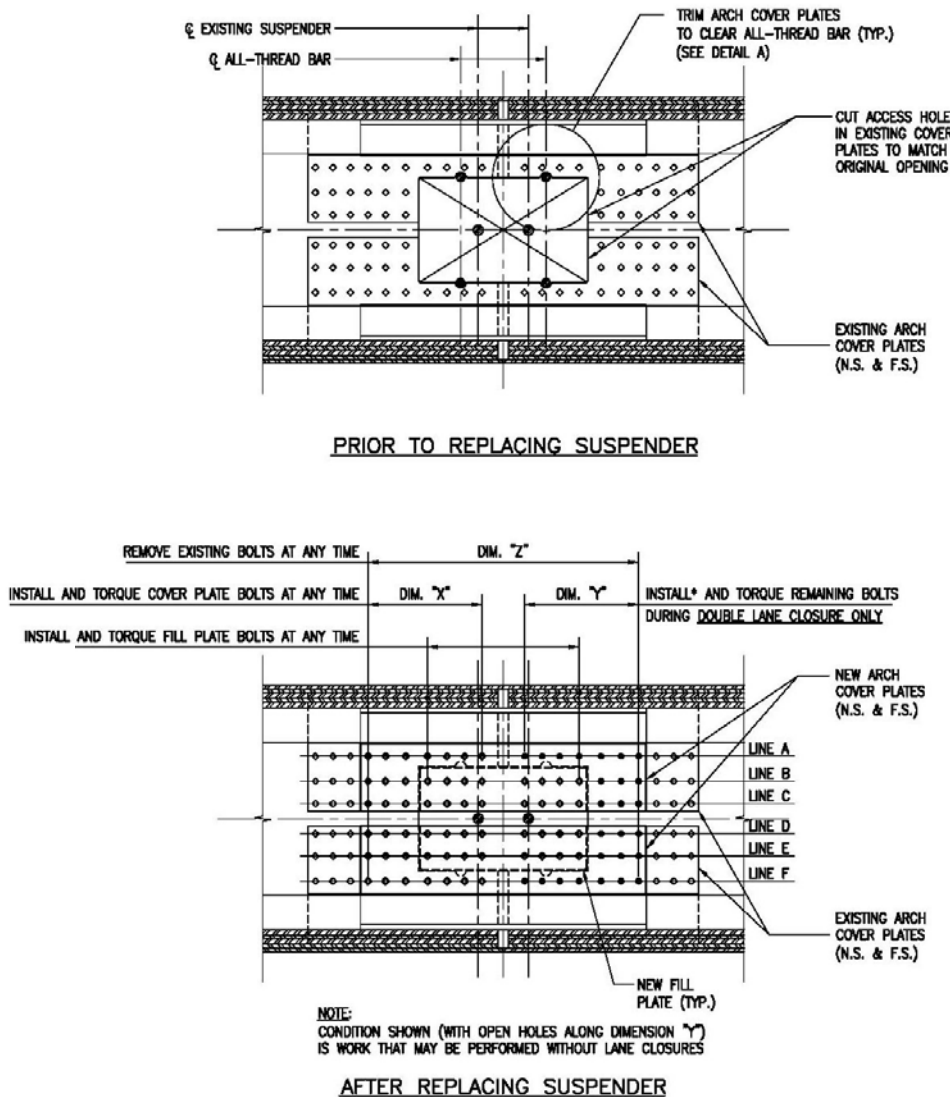


Figure 9 – Cross-Section at Crown of Arch (Panel Point 12)

The tight clearances necessitated some trimming of the edges of the access opening to provide clearance for the hanger rods. The resulting minimum clearance between the new top socket and the hanger rods in the final assembly was only 8 mm. This did not leave much room for error in the installation of the approximately 1.41 tonnes assembly (top socket with a pair of suspenders and bottom sockets). Once the new suspenders, socket and U-bolts were replaced, new cover plates were installed to close the access opening. The cover plates were installed with the bolts torqued on only one side of the splice – final torquing of the remaining bolts was only performed under a two lane closure to minimize the live load stresses on the arch, which are transferred through the splice plates (see Figure 10).



**Figure 10 –Access Opening Repairs at Crown of Arch (Panel Point 12)**

## **CONCLUSION**

A modified method typically used in suspension bridges was proposed as an alternative method for the replacement of the suspenders for twin through-arch bridges which saved the owner, the NYSDOT, over \$5 Million on a roughly \$16 Million project. The alternative structural lifting system was not only less expensive and easier to install than the version shown on the contract plans, but also safer in that it did not impose additional loads on the existing deteriorated suspenders during the replacement process. The system also improved safety and decreased inconvenience to the traveling public by eliminating nightly closures of the individual bridges, which required crossing all traffic over to the adjacent bridge. Even though additional steel repairs have been added to the project, the contractor is on schedule to complete the replacement of all 168 suspenders of both bridges by November 2009.

blank

# SUSPENSION BRIDGE CABLES: 200 YEARS OF EMPIRICISM, ANALYSIS AND MANAGEMENT

Dr. Bojidar Yanev<sup>1</sup>

## **Abstract**

Over the last 200 years suspension bridges have been at the forefront in all aspects of structural engineering, including empirical and theoretical studies, and construction and lifecycle management. Their spans have grown from 50 to 2000 m with designs for 3000 m under consideration. Key elements of modern suspension bridges are their cables. The evolution of suspension cables is examined. The most recent developments in their design, maintenance and inspection are described. Conclusions regarding suspension bridges and engineering structures in general are drawn.

## **Introduction: Empiricism and Theory**

Engineering structures must succeed in three domains: the theoretical, the physical and the social. The operating tools of these domains are abstract analysis, empirical application and economics. Whether successful or not, the required synthesis is particularly spectacular in long-span bridges, among which the suspension ones are the undisputed champions. Suspension bridges using natural fiber ropes have existed since prehistoric times, but their modern history begins with iron chains. The first United States patent for a bridge suspended on iron chains was awarded to James Finley (1762 - 1839), a land-owning judge, in 1808. The patented bridges had a stiffened roadway, designed to carry pedestrians and horse carriages cost-competitively over spans up to 76 m. Judge Finley arrived at his modest but reliable bridges by experiments. His "empirico-inductive" understanding of the suspension structural scheme inspired him to forecast that "something further may be done in the art of bridge building than has yet been accomplished" (Karnakis, 1997, p. 53). Finley appears to have been fully aware of the need for a satisfactory analytical model.

Navier (1785 - 1836) formulated suspension bridge theory in his *Memoire sur les Ponts Suspendus* in 1823. The analysis, design and construction of suspension bridges in France is concisely and comprehensively reviewed in LCPC/SETRA, 1989. In 1827 Navier's extensively analyzed 170 m span at Pont des Invalides, barely completed, had to be dismantled, primarily due to the malfunctioning anchorages. Ever since, analysis and experiment have relentlessly challenged and stimulated the art and science of bridge building. Marc Seguin (1786 - 1875) complained that Navier treated "theoretical notions or mathematical solutions [as] *a priori* admissible" (Karnakis, 1997, p. 269). Nonetheless, further developments, including Seguin's, owe much to the theoretical backing of Navier's *Memoire*.

---

<sup>1</sup>Executive Director, Bridge Inspection & Management, New York City DOT, Adjunct Professor, Columbia University

In the American Railroad and Mechanics Magazine of April 1, 1841, No. 379, Vol. XII, J. Roebling (1806-1869) argued that "the successful introduction of cable bridges into the United States would require the combination of "scientific knowledge and practical judgment of the most eminent Engineers". Roebling proved singularly capable of providing both, along with the organizational abilities required for manufacturing the high strength galvanized cable wires and the procurement of the financial backing his monumental bridges needed. Thus his Brooklyn Bridge in New York City (main span 487 m), completed in 1883 by his son and daughter in law, Washington and Emily Roebling, is carrying more than 80,000 passengers daily in 2009. Billington (1983) concluded that the integration of theory and practice achieved by Roebling and Eiffel (1832 - 1923) elevated structural engineering into an art. One disadvantage of great artistic accomplishments, however is that they do not lend themselves to standardization and mass production. Engineering practice, in contrast, must deliver utility repeatedly, reliably and cost-competitively. This apparent contradiction is demonstrable in bridge design where spans shorter than 150 m are subject to detailed specifications by AASHTO (American Association of State Highway and Transportation Officials), but the longer ones are not. Neither are cable-supported bridges of any length. Thus in the domain of the foremost structural accomplishments, failures and successes jointly advance the state of the art.

### **Failure: the Ultimate Test**

Despite the advances in abstract analysis and controlled testing, failures have the most conspicuous influence on bridge design, construction and management. No planned engineering experiment can match the social and professional impact of an unintended structural collapse. The shock value of the suddenly perceived ignorance and the usually considerable losses add up to a lesson easy to understand and remember by non-professionals. Bridge failures in the United States from 1966 to 2005 are attributed to various respective causes in Fig. 1. Natural hazards (and mostly hydraulic-related ones) dominate this listing as they do in most classifications.

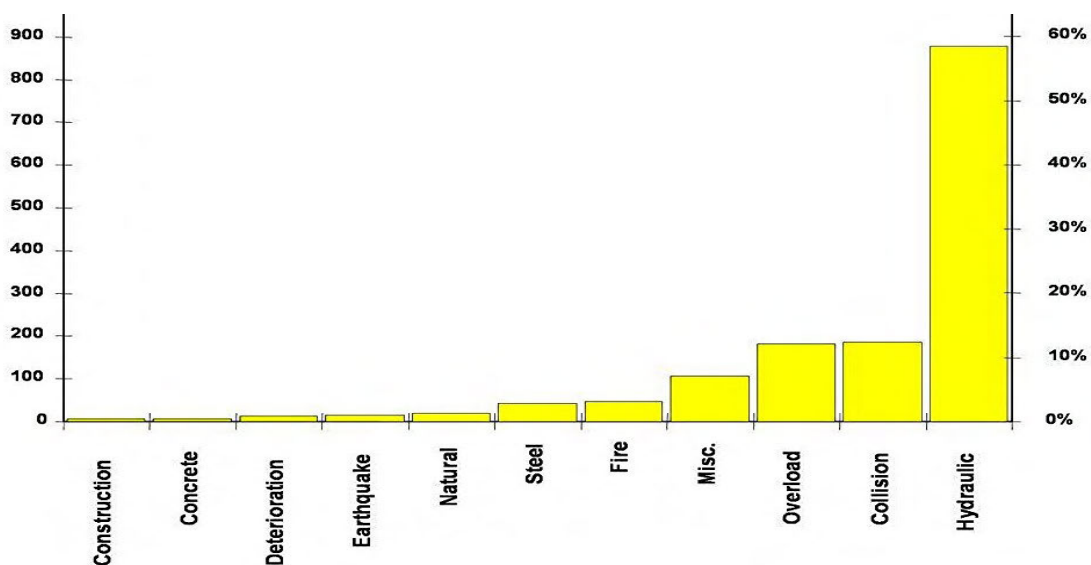


Figure 1. 1502 bridge failures in the USA, 1966 – 2005 (courtesy STV Engineers)

Suspension bridges represent a small portion of the total bridge population, however they are essential to transportation, and at the forefront of engineering innovation. Consequently their failures are critically important not only quantitatively but also qualitatively. H. Petroski (1993) regards failures are inherent in the creative process of bridge design and construction. Citing earlier work by Sibly and Walker in England, he argues that each innovative bridge form is developed by trial and error until its limits are surpassed and spectacular failure occurs. Only then does theory catch up with the practice and fully explains the structural behavior. By this estimate, the still evolving cable-stayed bridges should be viewed with particular concern. A few popular examples may add a historic perspective to this controversial subject.

### **19th Century cable-supported bridges**

Nineteenth Century engineers experimented with both suspension and cable-stay bridges using both ropes and chains. The more complex dynamic behavior of these structures resulted in greater lapses in the designer's knowledge, and hence, the many failures under wind loads, as well as those caused by rushing crowds.

The cable-stayed bridge at Dryburgh collapsed in a gale storm in 1818, 6 months after it was completed. Samuel Brown's Brighton Chain Pier was destroyed by a storm in 1836. The landmark bridge crossing the Menai Straights in England with a main span of 177 m was designed by Thomas Telford (1757 - 1854) and completed in 1826. The bridge chain suspension system never failed, but high winds caused significant damage and repairs were necessary at least twice.

With a main span of 308 m, Charles Ellet's (1810 - 1862) Wheeling suspension bridge over the Ohio River was the world's longest. Ellet had to repair it after it was destroyed by wind in 1854. Roebling later replaced it with his hybrid suspension/stay system. That system created enduring dynamically stable structures without a rigorous theoretical backing. Theoretical advances in the 1920s enhanced suspension bridge analysis. Roebling's semi-empirical hybrid system was stripped of the diagonal stays and the stiffening trusses, ultimately producing the aerodynamically unstable Tacoma bridge.

### **Tacoma Bridge (1940)**

The bridge, in Washington State, was designed by the early proponent of large displacement theory Leon Moiseiff (1872 – 1943), renowned for his contributions at Manhattan Bridge in New York and the Golden Gate in San Francisco. Distinguished by a relatively narrow cross section and longitudinal stiffening girders in lieu of the traditional trusses, it collapsed under wind loads after months in service. The failure is attributed to ignorance of the dynamic phenomenon later recognized as flutter. Yet flutter had already been identified by Von Karman (1940) in research on aircraft wing stability. Thus the ignorance could be perceived as design error. The new Tacoma suspension bridge has a deep stiffening truss. In 1937 Othmar Ammann (1879 – 1966) won an award for the design of the Whitestone Bridge in New York City. Following the collapse of the Tacoma, the very similar Whitestone was stabilized with stiffening

trusses, diagonal stays and a tuned mass damper mid-span. None of these enhancements proved conclusive. They have been removed or are reassessed during a current structural reconfiguration.

### **Silver Bridge (1967)**

The bridge over the Ohio River at Point Pleasant collapsed due to a brittle fracture of an eye-bar of the suspension system. Poor quality control during construction, inability to inspect, ignorance of fatigue behavior and lack of redundancy all contributed to a degree that is still debated. The variety of contributing causes entailed similarly wide ranging responses. The non-redundant 2-eye-bar suspension chain was entirely discredited, leading to the controlled demolition of a similar structure over the Ohio River at St. Mary's, West Virginia. Impressed by the collapse, which took 46 lives, the United States Senate mandated biennial bridge inspections, clearly recognizing that the lack thereof is a management deficiency. The outcome was the National Bridge Inventory (NBI) which currently contains data on more than 600,000 vehicular bridges, 200,000 railroad bridges and more than 100,000 culverts. Fracture-critical details became an important part of the inventory and special provisions were designed for their inspections.

### **Partial failures**

Partial failures, particularly when they appear as near misses are easily overlooked and their lessons are harder to learn. For example, a database developed at Cambridge University blames deterioration for only 3% of the considered bridge failures. Yet deterioration is recognized as widespread. The losses it has caused are vast but not quantifiable, because they rarely include fatalities. As a result, deterioration-related failures are on the rise. They can be traced to neglected maintenance, as well as to the design which did not anticipate such neglect. Since deterioration is a relatively slow process (compared to natural hazards, fractures and losses of stability for example), its effects have been intercepted by inspections and arrested by rehabilitations. Thus partial failures have become increasingly significant. Both Pont de Tancarville and Pont d'Aquitaine in France had their suspension cables replaced without incident following the discovery of breaks caused by corrosion. The original cables had no wrapping and consisted of helical non-galvanized strands. The 4 cables of the Williamsburg Bridge (1903, 488 m main span) in New York City were rehabilitated in the 1990s after a long debate over their viability. The cables, each consisting of 7696 non-galvanized parallel 5 mm wires grouped in 37 strands, were rapidly corroding. During the rehabilitation several strands were re-anchored, many broken wires were spliced, corrosion-inhibiting oil was added and water-proofing was supplied in the form of new wrapping.

Many suspenders and stay-cables have broken, however the effect of these failures has been localized by redundancy. In 1981 one of the diagonal stays of the Brooklyn Bridge broke due to corrosion and killed a pedestrian. All suspenders and stays were subsequently replaced. A suspender broke at the first Bosphorus Bridge in 2004 and a stay cable was burned by lightning at the Rion – Antirion Bridge in 2006,

neither one causing significant traffic interruptions. Suspender and stay replacement is recognized as a periodic necessity. The suspenders of Manhattan Bridge have been replaced at least once and will be replaced again under a pending contract.

### **Overview of failures**

Structural failures in general do not lend themselves to purely quantitative assessments. To the inability to quantify loss of life and other user costs, there are difficulties with evaluating the loss of public and professional confidence. Forensic investigations are post-event efforts to eliminate failure causes. Once identified such causes are perceived as vulnerabilities requiring special treatment. The identification and elimination of vulnerabilities is a perpetual task of management depending on every specific circumstance, however some common characteristics have emerged (also discussed in Yanev, 2007). Failure causes have been classified according to a variety of criteria including the following:

#### *- Event-based*

The classifications of the Cambridge database and Fig. 1, cited earlier are of this type, however they also refer to the structural type and material.

#### *- By the mode of material non-performance*

This classification would identify metal fatigue and fracture, corrosion, corrosion fatigue, ductile failure, residual stress, yield, shear, concrete fatigue, chemical reactivity, temperature, and so on. Although helpful, this classification misses certain vulnerabilities, such as instability. Thus another classification becomes necessary, distinguishing between local and global behavior. Whereas a material failure is by definition local and can lead to global consequences, instability is a global failure which causes local material non-performance.

#### *- "As designed" and "not as designed" modes (Thoft-Christensen and Baker, 1982)*

The failure of the deck truss bridge carrying Rte. I-35-W in Minneapolis on Aug. 1, 2007, caused by overstress of poorly dimensioned gusset plates, is in the "as designed" mode. These are practical failures resulting from poor execution. The failure of the Tacoma bridge, caused by the hitherto unknown flutter is in the "not as designed" mode. Such failures point to theoretical deficiencies.

#### *- According to the bridge life-cycle, e.g. design, construction, maintenance, and operation during which the failure occurs (Yanev, 2007)*

This approach reveals that failures occur when each phase excessively relies on the others, whereas it should have assumed responsibility as if it were critical. For example after the collapse of the bridge over the Schoharie Creek (New York State, 1987) caused by scour, it was concluded that the bridge could have survived if underwater inspections had been more effective, however the collapse could have also been prevented by selecting a longer span with piers out of the channel.

- No failure classification can be entirely independent, and neither are the revealed vulnerabilities. A redundant approach to identifying vulnerabilities by various

partially overlapping criteria has a better chance of capturing all possibilities. New York State for example has established screening procedures for the following vulnerabilities: hydraulic, seismic, overload, steel details, concrete details, collision, sabotage.

- Significant failures are usually caused by combinations of two or more vulnerabilities. In all of the preceding examples, design, construction and maintenance might have intervened to avert the disaster, if they had seen their own role as the most critical. The investigation following the collapse of the Sungsu truss bridge in Seoul in 1994 concluded that the bridge had been "poorly designed, built, maintained and used".

- Significant failures invariably exhibit a discontinuity in the process, in the product or in both. A common one is between experience and theory. This can be expressed as an over-reliance of each on the other or as an ignorance of each about the other. For example, the rationale justifying the use of non-galvanized high strength cable wires on the Williamsburg Bridge was summarized as follows: "If the wires are maintained dry, they do not need zinc coating. If not, it will not save them in the long term." This reasoning may appear sound, yet it lacks both the practical knowledge of life-cycle cable performance and a theoretical model of wire deterioration. The opposite solution would have been correct: wires should have been locally protected by galvanization, whereas the cable should have been globally protected by superior wrapping. As in all discontinuities, the remedy is redundancy.

- Failures can be traced to deficiencies in both the engineered product and the managed process. Thus the gap between theory and practice is matched by an equally detrimental gap between the increasingly diverging professions of engineering and management. The current trend is to rely on engineering competence during the design and construction of the product (in this case the bridge) and to assign the process of its operation to a management, guided primarily by economic considerations. The latter typically minimize initial costs, while shortening the structural life-cycles and increasing the demand for future expenditures.

- Most simplistic and yet inevitable are the failure assessments according to the amount of damage and the responsibility. All structural failures are to some extent attributable to management and this is reflected in the way society reacts to them. The failure of the Silver Bridge was at the origin of the NBI and the biennial bridge inspection program, the partial failure of the Williamsburg bridge led to the re-establishment of the Bridge Division at the New York City Department of Transportation, the numerous failures caused by earthquakes in California and in Japan have influenced the design and construction of bridges worldwide, the collapse of the I-35-W bridge in Minneapolis has stimulated the use of non-destructive structural monitoring techniques. Appropriate as these measures are, they remain reactive, whereas the purpose of engineering management and design is to anticipate. The history of suspension bridge cables offers examples of such anticipation.

## **Suspension bridge cables**

The temporary closure, in 1988, and subsequent rehabilitation of the Williamsburg Bridge attracted much attention to the condition of suspension cables. (That project is currently concluding at a total cost of approximately \$US 1 billion.) The affected structures are among the oldest, largest and historically most significant nationwide. The Cincinnati - Covington Bridge was opened to traffic in 1867, the Brooklyn Bridge - in 1883, Williamsburg - in 1903 and Manhattan - in 1908. Ten major suspension bridges, including Ammann's George Washington (1931 and 1957, 1068 m main span), Verrazano (1964, 1300 m main span), Triborough, Whitestone, Throg's Neck and the East River bridges are in the New York Metropolitan area. During the 1990s the author co-sponsored a comparative survey of these structures along with all respective owners. The resulting report by Columbia University summarized cable conditions, design, construction and maintenance practices. Key findings were presented by Betti and Yanev (1999).

The National Cooperative Highway Research Program (NCHRP) at the Transportation Research Board (TRB) expanded the study to all parallel wire cable-supported bridges nationwide and published NCHRP Report 534 by Mayrbaurl and Camo (2004) of Weidlinger Assoc. The report addressed twenty nine suspension bridges, constructed in North America by the aerial spinning method up to the year 2000 and two (Newport, R.I. and William Preston Lane Jr., MA.) built with shop-fabricated parallel wire strands. The twenty one (shorter) spans supported by helical strand cables were not considered in this study. NCHRP Report 534 recommended further investigation of the behavior of cables under controlled and actual field conditions.

## **Wires: condition, deterioration and failure**

The replacement of suspension chains and eye-bars with parallel wires or helical strands radically improved the *internal redundancy* of suspension cables. The wires in the investigated cables (Williamsburg excepted) are galvanized, have an approximately 5 mm diameter and their strength is around 1515 mPa. In a load-free state, they assume a curvature with roughly 1 m diameter, which indicates their state of bending under working conditions. The non-galvanized wires of the Williamsburg Bridge failed when corrosion reduced their cross-section (Fig. 2 - A and - B). This mode of wire failure is atypical, as well as relatively simple and has not attracted much interest. Failures of non-galvanized helical strands have been reported in detail by Virlogeux (1999) and Kretz et al. (2006), along with the ensuing cable replacements. In contrast, high-strength galvanized wires have proven susceptible to "flat and invert" breaks, and the rarer spiraling breaks (Mayrbaurl and Camo, 2004). Flat breaks are believed to develop as follows:

- The approximately 0.05 mm zinc coating oxidizes and fails over a small areas of the wire surface.
- The exposed steel begins to oxidize, causing surface irregularities, such as pitting and, consequently, stress concentration.

- Cracks develop transversely to the wire surface, further concentrating the stress.
- The cracks propagate at an angle towards the center of the wire until the area is critically reduced and the wire breaks normally to the axis. The sequence raises the following critical questions:

- *Quantifying and qualifying wire corrosion.*

The strength evaluation of a cable is based on visual inspections which, in turn must estimate the state of corrosion. To facilitate these estimates, 4 stages of wire corrosion were described by Hopwood and Havens (1984) as follows:

Stage 1 - Spots of zinc oxidation on the wires;

Stage 2 - Zinc oxidation on the entire wire surface;

Stage 3 - Spots of brown rust covering up to 30% of the surface of a 3 to 6 inch (75 to 150 mm) length of wire;

Stage 4 - Brown rust covering more than 30% of the surface of the 3 to 6 inch length of wire.



Figure 2. Suspension cable wires, z-shaped wrapping wire, and 127 wire strand

Despite the lack of phenomenological backing, this rating system endures, as do all visual inspections. NCHRP Report 534 proposed a model linking the visual findings, classified in the 4 - stage system to an estimate of the number of cracked and broken wires, and ultimately, the cable strength.

- *Does the oxidized zinc contribute the embrittlement of the steel?*

Mayrbaur and Camo (2004) point out that much depends on the further reactions of the resulting zinc oxide (ZnO). Those, in turn depend on the environment and, particularly on the type of humidity. Zinc carbonate ( $ZnCO_3$ ) can form an effective protective film, whereas zinc hydroxide ( $Zn(OH)_2$ ) easily dissolves, leading to the formation of carbonic acid ( $H_2CO_3$ ), which becomes a source of embrittling hydrogen.

- Is there a threshold level of zinc depletion and steel corrosion beyond which cracks begin to occur spontaneously?

To some extent that would depend on the level of stress in the "as-built" cable. Modeling that stress however, besides relying on the uncertain state of the unstressed wires, also depends on their stress level, subject to diverse uncertainties.

#### *Wire stresses*

Suspension cable wires are not in uniaxial tension as is generally assumed in calculating safety factors. High-strength wires are manufactured by the cold-drawn method by extruding them through progressively smaller openings and thus modifying the molecular shape of the original mild steel. Eventually the wires of the desired diameter (roughly 5.1 mm) are dipped in molten zinc for protection against corrosion. The galvanized wires cool off in a permanently curved shape with a diameter of approximately 2 m. Consequently, the wires experience bending stresses in order to conform to the shape of the cable. Mayrbaur and Camo (2004) estimate (based on X-ray diffraction tests) that the straightening produces bending stresses of up to  $\pm 240$  mPa (36 ksi). Eliminating a curvature with radius  $R$  induces in a wire with radius  $r_{wire}$  bending moment  $M$  as follows:

$$M = EI/R \quad (1)$$

The corresponding maximum bending stress  $\sigma$  is:

$$\sigma = M/S = E r_{wire}/R \quad (2)$$

where:  $I = \pi r_{wire}^4 / 4$  is the section moment of inertia.

$S = I / r_{wire}$  is the section modulus.

For  $r_{wire} = 5$  mm and  $R = 2000$  mm in Eq. (2),  $\sigma = 500$  mPa (75 ksi), matching the uniform working stress level for which many suspension cables are designed. Even after many years of service, suspension bridge wires extracted from a cable regain some of their original curvature, testifying to inelastic deformation. Wires invariably crack on the side where straightening has produced tension. Bending is extreme in the traditional anchorages which use sheaves of relatively small diameters. This has been a primary reason for the recent shift, lead by Japan, to prefabricated straight wire strands, originally developed under a U.S. patent (Fig. 2 – F).

#### *Residual stresses*

Residual stresses would be caused by the extrusion process and by the hot-dipping into zinc. The steel surface under the zinc is irregular. Therefore stress concentration and even cracks may exist in the wires before the zinc coating fails.

### **From wires to a cable: condition, deterioration, maintenance and repair**

The knowledge gained from individual wires must be fully used in evaluating the condition of suspension cables. Whereas wire failures have provided understanding of the limits of the material, a cable failure model does not exist and allowing for one to develop spontaneously is not acceptable. Consequently,

physical and statistical, deterministic and probabilistic, analytic and empirical methods are continually developed and combined. All stages of the structural life are closely examined.

#### *Design and construction*

Over the 20th Century parallel wire suspension cables (Fig. 3) evolved as follows:

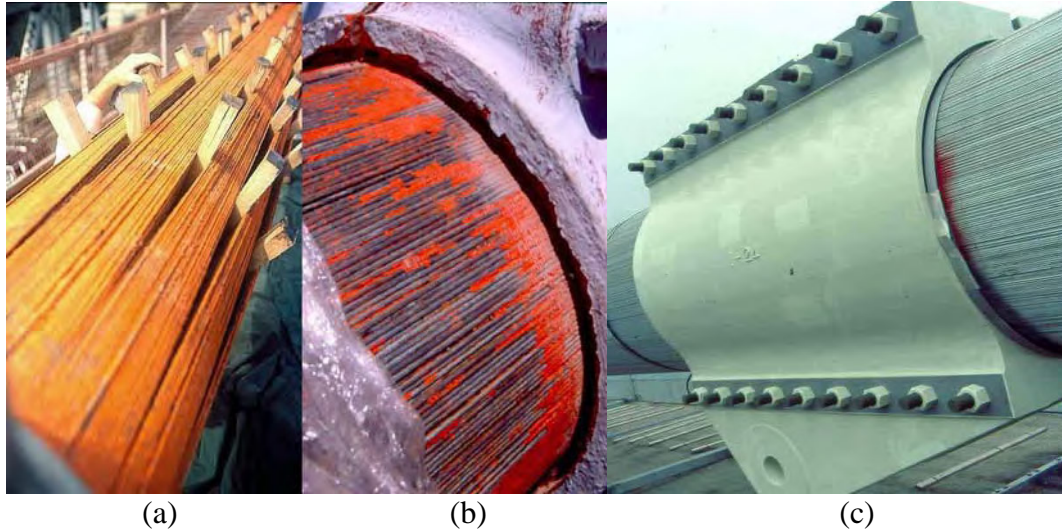


Figure 3. Cables: (a) wedging; (b) cable band with red lead; (c) Akashi – Kaikyo

The number of suspension cables evolved from 2 to 4 and back to 2. Examples of the 4 cable configuration include the East River bridges, the George Washington and the Verrazano in New York City. Notable among the 2 cable bridges are the Ambassador, Macinac (1,158 m), Bay Bridge and Golden Gate (1,280 m). Four cables were originally contemplated at the Akashi-Kaikyo, however the 2 cable cross-section was selected because of its superior aerodynamic properties. The proposed 3,000 m span at the Messina Straights assumes 4 cables. The *global redundancy* of the 4 cable configuration may have saved some bridges from demolition. For his bridge at Oporto, D. Steinman anticipated a second pair of cables carrying added traffic. That modification was completed in the 1990s. At Pont de Tancarville the two original cables were replaced by two pairs, allowing for a future replacement of each pair by a single cable at the original location (Virlogeux, 1999). The two cables of the Storabaelt Bridge in Denmark (1996, main span 1,624 m) were built by the traditional air-spinning method with 18,648 wires of diameter 5.37 mm and minimum strength of  $1,570 \text{ N/mm}^2$  (Fig. 2 - C). The Akashi – Kaikyo (1998, main span 1991 m) cables are built with shop-fabricated parallel wire strands, composed of 127 straight galvanized wires with yield up to  $1800 \text{ N/mm}^2$  (Figs. 2 - D and F, Fig. 3 - c). Each of the two cables have 290 hexagonal strands (Figs. 2 – F and 3 - c).

#### *Suspenders*

Once spaced at roughly 7 m, suspenders are now spaced at about 20 m. The increased distance between suspenders affects primarily their own behavior as well as that of the bridge superstructure. The cables, however are also influenced in at least two ways. The cable bands which improve the behavior of broken wires and the

compaction of the cable are reduced. Consequently they transmit greater concentrated loads to the wires. As the distance between the cable bands increases so does the bending moment introduced by them into the cable.

The traditional corrosion protection of suspenders has been galvanization and paint. Stays are protected in various encasements, primarily cement grout. The limitation of the latter method, however have prompted Japanese designers to use parallel wire suspenders and stays with rubber vulcanization, as at the Akashi - Kaikyo and Tatara Bridges.

#### *Wind loads*

The potential for aerodynamic instability demonstrated by Tacoma and other suspension bridges led to extensive testing of models of all major suspension and cable-stayed bridges in wind tunnels. For the Akashi – Kaikyo Bridge, a 1/100 scale model was tested in a wind tunnel built expressly for that purpose.

The inclined suspenders used on many bridges in Europe, including the record-breaking Humber in Wales (1981, 1,410 m main span) proved even more vulnerable to wind loads and fatigue. After relatively short useful lives, such suspenders were replaced at the Severn and Brotonne bridges while their sockets were modified. Water on the surface of stays was found to modify their aerodynamic response, causing the so-called galloping oscillations. The phenomenon is mitigated by surface obstructions to running water. Dampers are added on longer suspenders and stays.

#### *Clamping length*

The overall stress in cables is estimated by cutting wires and measuring their retraction. That retraction, however is constrained by the friction with adjacent wires and is therefore limited to the so-called *clamping length* of the wires. The clamping length is very important in estimating the contribution of broken wires at longer distances from the fracture points. It is often assumed that tension in a broken wire is restored over the distance of 3 cable bands. Apart from the hypothetical nature of that assumption, it clearly depends on the distance between cable bands and on the level of compaction of the cable. Thus the local condition of the wires must be assessed jointly with the global condition of their totality as a cable.

#### *Safety factor*

This term is somewhat discredited, because of the uncertain assessments of both stress and resistance levels discussed in the preceding section. Nonetheless, the ratio between the ultimate load of the cables at yield and the maximum expected load during its service has declined from over 4 to 2.2. It is argued that 90% of all loads on long-span bridges consist of the relatively constant dead load. Furthermore, the effective stiffness of the cables increases proportionally to the cube of the stress divided by the square of the span length. The formula, attributed to Tischinger and to Ernst, can be written as in Eq. 3.

$$1/E_{ef} = 1/E + (\gamma L)^2 / (12 \sigma^3) \quad (3)$$

where:  $E_{ef}$  - effective modulus of elasticity of the cable;  
 $E$  - modulus of elasticity of the steel;  
 $L$  - span length;  
 $\gamma$  - specific weight of the cable;  
 $\sigma$  - stress in the cable.

Thus longer spans achieve the desired stiffness at the expense of higher stresses in the wires, implying an increased likelihood for "stress-corrosion" and hence a lower tolerance for deterioration.

### *Cable protection*

Cable protection once consisted of linseed oil introduced into the cable voids, a red lead paste coating over the wires, plastic wrapping over the lead, spiral wire wrapping on top and paint over the spiral wire (Fig. 3 – a and b). Because of environmental objections, lead is being substituted by zinc paste. The long-term effects of this modification are yet to be observed, because lead is passive whereas zinc oxidizes. The benefits from the spiral wire wrapping have been disputed and it has been replaced by polyethylene wrapping at some bridges.

On several record-breaking bridges in Japan, such as the Kurushima and Akashi-Kaikyo, managed by the Honshu-Shikoku Bridge Authority, pressurized dry air is injected under the cable wrapping. The system is now under consideration as a rehabilitation feature on older bridges. Z-shaped wires have been used for wrapping, as in Fig. 2 - E.

### *Compaction*

Compaction is a form of cable protection, because it impedes the penetration of water and increases the clamping effect. Air-spinning achieves a relatively uneven compaction of 75%-80%. In a perfectly compact cable all wires except the external ones are in contact with 6 adjacent wires, forming a hexagon. For  $T$  perfectly compacted concentric layers, the net wire to gross cable ratio of areas can be computed as in Eq. 4.

$$2\pi r^2 [3T(T + 1) + 1] / r^2 [(2T + 1)^2 3^{3/2}] \approx 1.211 \times 3/4 \approx 0.907 \quad (4)$$

In cables built by the traditional air-spinning method 80% compaction is realistic, but variations are quite broad.

### **Anchorage**

The anchorages of air-spun cables (Fig. 4 - a) feature three critical transitions:

- From a compacted cable to splaying strands. In this area wires no longer have the benefit of clamping effects and are fully exposed to humidity. As a result entire strands have been lost to corrosion in anchorages, and re-anchorings have been necessary (Fig. 4 - a).

- From strands to eye-bars. The bending over the pins of the eye-bars can cause yield in the wires, but few breaks have been noted in these areas.

- From exposed eye-bars to concrete encasement. Eye-bars corroded significantly at that juncture and have been replaced by new anchoring systems, for example at Manhattan Bridge. Most anchorages (including old ones) are being equipped with de-humidification systems.



Figure 4. Anchorages (a) air-spun cable with re-anchoring; (b) prefabricated cable

### **Uncertainty**

For engineering purposes uncertainty has been separated by ISO (1995) into randomness (for example of natural phenomena), vagueness (as in condition evaluation) and ignorance (of actual conditions). Ang and De Leon (2005) recognize aleatory and epistemic uncertainties, associated with random natural variables and deterministic risk-informed decisions, respectively. In either classification, all types of uncertainties are present in bridge cables. Report NCHRP 534 treats probabilistically the key parameters of the cable model as follows:

#### *Wire condition*

Acoustic emission has been used to detect wire breaks of cables in use. The labor-intensive and intrusive unwrapping and wedging (Fig. 3 - a) remains the only reliable source of information about the condition of the wires. NCHRP 534 proposes methods of projecting the number of wires in each of the four states, based on the limited findings of such inspections. The extrapolations depend on the sizes of the cables and the sample, and the observed conditions.

#### *Cable strength*

NCHRP 534 proposes three models as follows:

*Ductile wire.* Strain increases incrementally. A wire reaching yield carries the corresponding stress until the rest of the wires reach that point and they all fail simultaneously. The cable strength is the average strength of the wires multiplied by their number. This model has a limited application to cables (possibly such as those of the Williamsburg) where loss of section, rather than cracking is critical.

*Brittle wire.* Each wire fails at its tensile strength limit. A step-wise stress-strain diagram results, as the number of wires declines. The model tends to underestimate the cable strength by as much as 20%.

*Limited ductility model.* This more elaborate model recognizes that when the first wire breaks, the force in the remaining wires does not change because the change in the overall strain is negligible. As the ratio of broken to active wires grows, so does the *strain rate*. The process is dynamic.

### **Health monitoring**

Wind tunnel testing has become standard practice on all suspension and cable-stay bridges, however scale models cannot fully simulate the actual structural response. Consequently, dynamic analysis must follow a redundant path, seeking acceptable convergence of analytic and experimental results, as has been the case since the origin of bridge building. The process does not stop with the completion of construction. Monitoring systems collect “real-time” data including dynamic response, stresses, temperatures, traffic weigh in motion, wind velocity.

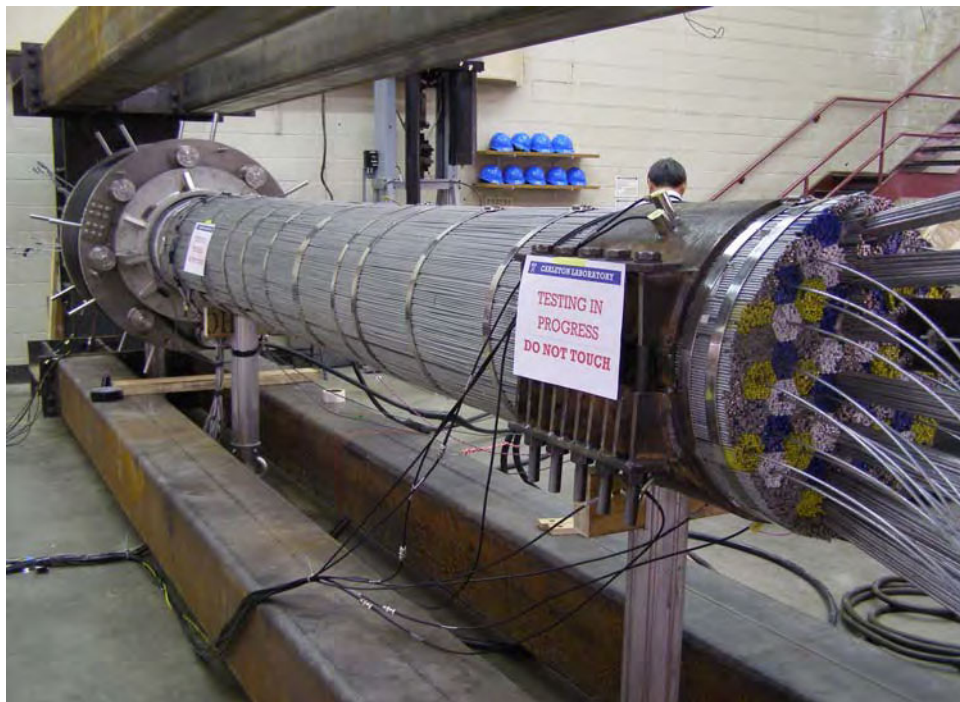


Figure 5. Cable model at Columbia University

New suspension bridges are heavily instrumented with various devices, measuring acceleration, vehicular weight, wind speed, temperature and other environmental and structural parameters. Global positioning systems (GPS) can monitor the movements of large structures with a satisfactory accuracy. Recently Manhattan Bridge was scanned with interferometric radar by IDS Ingeneria of Pisa, Italy and with GPS by Columbia University with closely agreeing results. The time

has come to introduce state of the art instrumentation into the cables and to employ it for their continuous health monitoring. Under a current project sponsored by FHWA, Columbia University researchers are investigating the methods for non-invasive monitoring of cable condition. The research encompasses the testing of a cable model (Fig. 5) under controlled conditions and transferring the monitoring technology to a suspension bridge for field verification. The cable model is instrumented with 76 sensors of different types, placed along three diameters, inclined at 60° angle with respect to each other, so to have a dataset that represents the central conditions for the 6 sectors in which the cross-section is typically subdivided. These sensors measure temperature, relative humidity, pH and corrosion rate. The sensor allocation is shown in Fig. 6. The 16 temperature/relative humidity sensors were evenly spaced along the three diameters in order to have measurements for the temperature and humidity variations inside the entire cross-section. Corrosion rate sensors used different principles to measure corrosion rates: some use Linear Polarization Resistance, some others are Bi-metallic and some others, like the Couple Multiple Array Sensors, measure the number of electrons that flow from anodic to cathodic zones.

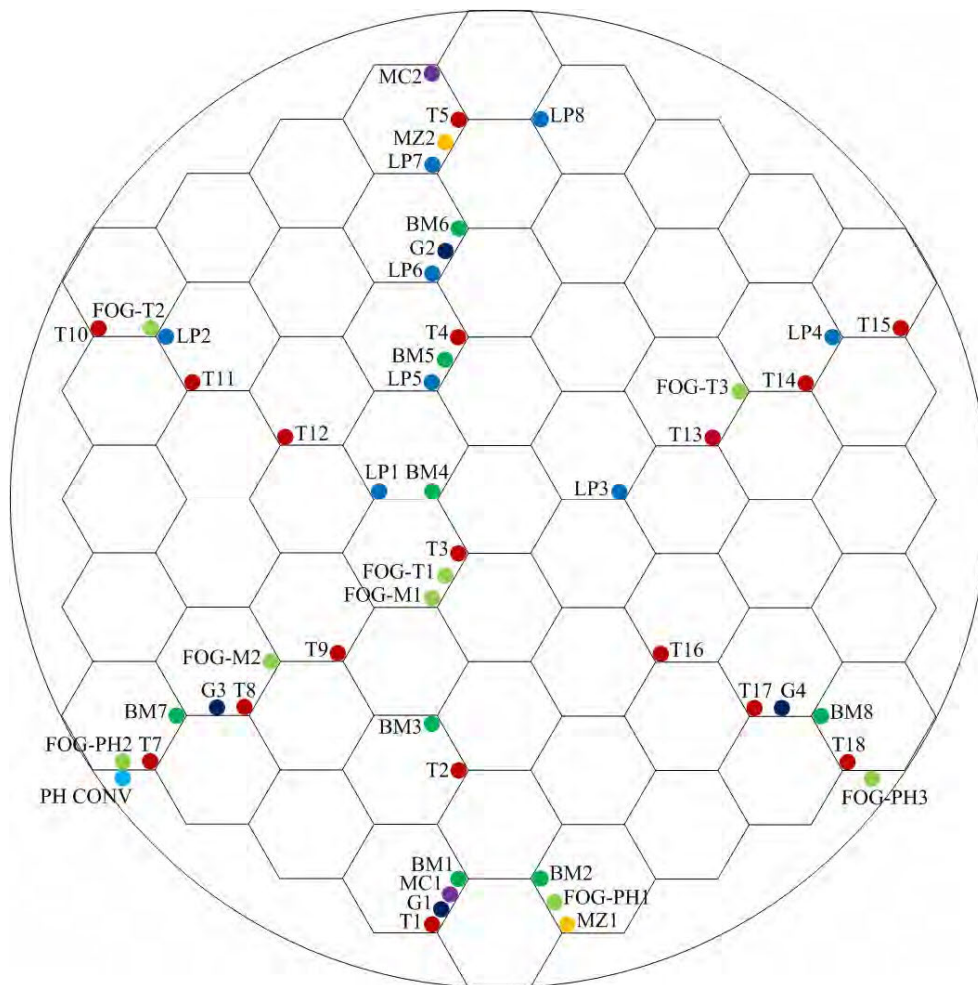


Figure 6. Sensor allocation in the cable model

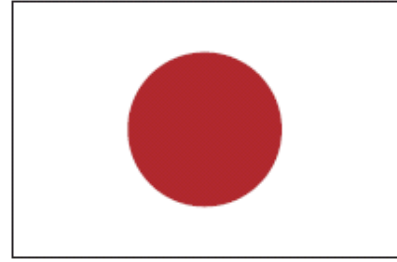
The objective is to identify methods suitable for monitoring the condition of cables without the need to unwrap and wedge them. The instruments selected during the laboratory testing phase will be installed in one of the cables of Manhattan Bridge for field testing in 2010. Thus the design, construction and service of suspension bridges reaches for new levels of theory and application. Once again theory must catch up with practice.

### **Acknowledgment**

The views presented in this article are those of the author and do not express the position of any organization or agency.

### **References**

- Ang, A. H.-S. and D. De Leon (2005) Modeling and Analysis of Uncertainties for Risk-Informed Decisions in Infrastructure Engineering, *Structure and Infrastructure Engineering*, Vol. 1, No. 1, pp. 19 - 31.
- Betti, R. and B. Yanev (1999) Condition of Suspension Bridge Cables, New York Case Study, Paper No. 99-0603, *Transportation Research Record 1654*, National Academy Press, Washington, D.C., pp. 105 - 112.
- Betti, R. et al. (2009) Aging Cables in Suspension Bridges, Proceedings, Aging Infrastructure Workshop, Dept. of Homeland Security, New York.
- Billington, D. P. (1983) **The Tower and the Bridge**, Basic Books, New York.
- Hopwood, T. and J. H. Havens (1984) Corrosion of Cable Suspension Bridges, Kentucky Transportation Research Program, Univ. of Kentucky, Lexington.
- ISO (1995) **Guide to the Expression of Uncertainty in Measurement**, 2nd Ed., International Organization of Standardization, Geneva.
- Karnakis, E. (1997), **Constructing a Bridge**, MIT Press, Cambridge, Mass., USA.
- LCPC/SETRA (1989) Les Ponts Suspendus en France, Laboratoire Central des Ponts et Chaussées, Paris / Service d'Etudes Techniques des Routes et Autoroutes, Bagneux, France.
- Kretz, T. et al. (2006) Rehabilitation and Widening of the Aquitaine Bridge, Conference on Operation of Large Infrastructure Projects, Bridges and Tunnels, IABSE, Copenhagen.
- Mayrbaur, R and S. Camo (2004) Guidelines for Inspection and Strength Evaluation of Suspension Bridge Parallel-Wire Cables, NCHRP Report 534, TRB, Washington, D.C.
- Petroski, H. (1993) Predicting Disaster, *American Scientist*, Vol. 81, Mar. – Apr., pp. 110 - 113.
- Thoft-Christensen, P. and M. J. Baker (1982) **Structural Reliability Theory and Its Applications**, Springer - Verlag, Berlin.
- Virlogeux, M. (1999) Replacement of the Suspension System of the Tancarville Bridge, *Transportation Research Record 1654*, National Academy Press, Washington, D.C., pp. 113 - 120.
- Von Karman, T. and M. A. Biot (1940) **Mathematical Methods in Engineering**, McGraw-Hill, New York.
- Yanev, B. (2007) **Bridge Management**, John Wiley & Sons, Inc, Hoboken, N.J.



# **25<sup>th</sup> US-Japan Bridge Engineering Workshop**

## **Session 6**

### **Seismic Performance Evaluation**

Dynamic Response Analysis of Bridge Under Seismic Loading Including Collision

By Eiki Yamaguchi, Atsumi Ryuen, Keita Yamada, and Ryo Okamoto

Effects of Near-Fault Vertical Accelerations on Highway Bridge Columns

By Sashi Kunnath and Huiling Zhao

Seismic Design of Multi Span Continuous RIGID-FRAME Bridge with Prestressed  
Concrete Box Girder

By Chiaki Nagao, Yasushi Kamihigashi, Akio Kasuga, and Kenichi Nakatsumi

Page Left Blank

# DYNAMIC RESPONSE ANALYSIS OF BRIDGE UNDER SEISMIC LOADING INCLUDING COLLISION

Eiki Yamaguchi<sup>1</sup>, Atsumi Ryuen<sup>2</sup>, Keita Yamada<sup>2</sup>, Ryo Okamoto<sup>2</sup>

## Abstract

In the Mid Niigata Prefecture Earthquake in 2004, the damage of a bridge pier was found mitigated by the collision between a girder and an abutment. Therefore, in the seismic response analysis, it is important to include the effect of the collisions. A simple and practical method of simulating the collision in the analysis is the introduction of a spring where the collision occurs. However, the constant of such a collision spring is yet to be formulated well. In this study, appropriate collision-spring constants are investigated for simulating the collisions between girders and between a girder and an abutment. The response analysis of a bridge under seismic loading is then conducted to see the influence of the collision.

## Introduction

The collision between a bridge girder and an abutment restricts the movement of the girder, which in turn reduces the deformation of a bridge pier, often considerably. This implies that the collision can help mitigate seismic damage of the bridge. In fact, in the aftermath of the Mid Niigata Prefecture Earthquake in 2004 we studied a damaged bridge pier (Photo 1) and concluded that the damage could have been much worse if not for the collision between a bridge girder and an abutment (Kosa et al. 2005). Thus the collision plays an important role in the behavior of a bridge during earthquake, and without including the effect of the collision, the analysis of a bridge behavior during earthquake can be quite misleading.

A simple and practical method of simulating collision in the analysis is the introduction of a spring between two bodies that collide with each other. This spring is called a collision spring and activates only when the two bodies collide with each other; the constant of the collision spring is kept equal to zero when the two bodies are not in contact. The effectiveness of this approach hinges on the behavior of the collision spring. In short, the value of the collision-spring constant is important. Nevertheless, the appropriate value has not been clarified except when the two bodies are identical (Kawashima 1981).

In the present study, the appropriate value of the collision-spring constant between two bodies having different stiffnesses is investigated. The response analysis of a bridge under seismic loading is then conducted to demonstrate the influence of the collision.

---

<sup>1</sup> Professor, Dept. of Civil Engineering, Kyushu Institute of Technology, Kitakyushu

<sup>2</sup> Student, Dept. of Civil Engineering, Kyushu Institute of Technology, Kitakyushu



(a) Overview



(b) View around girder end

Photo 1. Bridge damaged during the Mid Niigata Prefecture Earthquake in 2004.

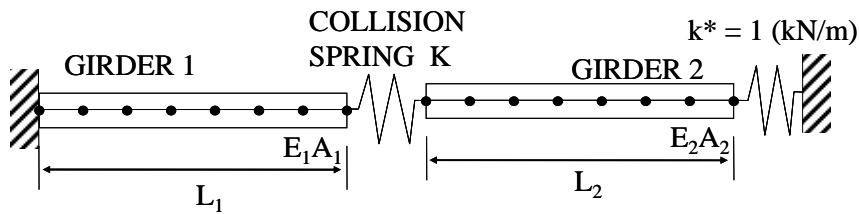


Figure 1. Model A.

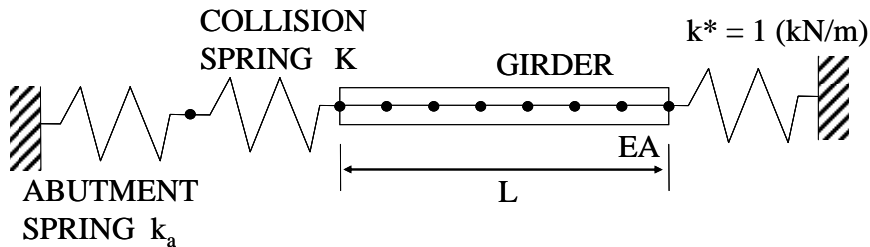


Figure 2. Model B.

### Collision-Spring Constant

#### **Analysis Models**

The analysis models, Models A and B, are shown in Figures 1 and 2. The two models are to study the collisions between two girders and between an abutment and a girder, respectively. The abutment is modeled by a spring and the girder is by beam elements. The spring with a very small spring constant at the right end of the girder is introduced to prevent the free movement of the girder.

The collision spring is placed between the bodies that would collide. The behavior of the collision spring is shown schematically in Figure 3. The relative displacement is the distance between the two bodies. The origin in Figure 3 represents

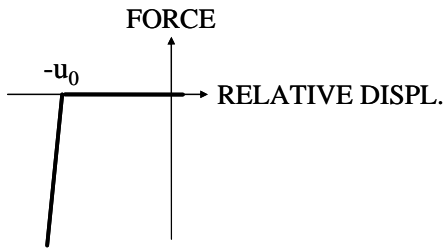


Figure 3. Collision Spring.

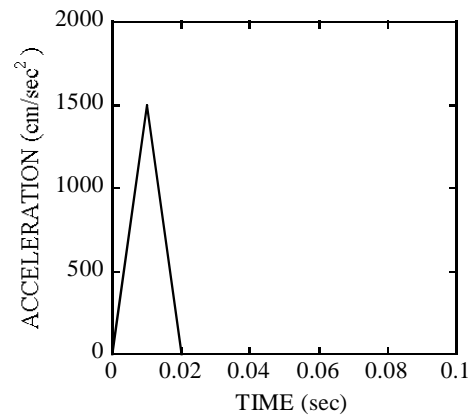


Figure 4. Acceleration.

the initial state. The figure implies that when the relative distance is smaller than  $-u_0$ , the collision spring is activated: its spring constant becomes non-zero, simulating the physical contact of the two bodies. The value  $u_0$  corresponds to the initial gap between the two bodies.

Going through the dimensions of some existing composite girder bridges in Japan, the following values are employed for the present study:

#### Model A

$$E_1 A_1 / L_1 = 5.0 \times 10^5 \text{ kN/m}$$

$$E_2 A_2 / L_2 = 5.0 \times 10^6 \text{ kN/m}$$

#### Model B

$$EA/L = 5.0 \times 10^5, 1.0 \times 10^6, 5.0 \times 10^6 \text{ kN/m}$$

$$k_a = 1.0 \times 10^5, 3.0 \times 10^5, 1.0 \times 10^6, 3.0 \times 10^6, 1.0 \times 10^7, 3.0 \times 10^7, 1.0 \times 10^8, 3.0 \times 10^8 \text{ kN/m}$$

where  $E$  is Young's modulus,  $A$  the cross-sectional area,  $L$  the girder length and  $k_a$  is the stiffness of the abutment.

The initial gaps  $u_0$  between the two girders and between the girder and the abutment are all set equal to 0.15 m. The acceleration shown in Figure 4 is applied in the longitudinal direction for the sake of simplicity. The damping coefficient of the girder is 0.02. Material nonlinearity is not considered. The increment of time for time integration in the present dynamic analysis is  $\Delta t = 1/50000$  sec and 100 beam elements are used for modeling each girder.

## Numerical Results and Discussion

### Model A

The collision spring has been employed to carry out the dynamic response analysis of a bridge that involves collision. Yet the appropriate spring constant, the

slope in the negative region beyond  $-u_0$ , has not been defined well even though it is likely to influence numerical result. To the best of the authors' knowledge, Kawashima's work (1981) is the only one that deals with this issue squarely. He studied the collision of two identical bars and came up with the following proposal:

$$k = nEA/L \quad (1)$$

where  $n$  is the number of elements. To be noted, the usage of the finite element method is presumed and Equation (1) indicates the collision-spring constant may be set equal to the longitudinal stiffness of the element.

This equation can be used right away if the two bodies yield the same  $k$ . But oftentimes that is not the case. The present analysis is one of those cases: two different constants of the collision spring are obtained by Equation (1). Therefore, assuming the two collision springs connected in series, the following formula for the collision-spring constant  $K$  is proposed:

$$K = \frac{1}{\frac{1}{k_1} + \frac{1}{k_2}} = \frac{k_1 k_2}{k_1 + k_2} \quad (2)$$

where  $k_1$  and  $k_2$  are the values obtained by Equation (1) for Girders 1 and 2, respectively.

To investigate the validity of Equation (2), the dynamic analysis of Model A is conducted with various collision-spring constants  $K$  in the range of  $1.0 \times 10^6$  -  $5.0 \times 10^7$  kN/m.

The results are presented in Figure 5. A small collision-spring constant leads to large relative displacement in the negative region: large overlapping of the two bodies occurs, which is a fictitious phenomenon arising from the approximation of the collision behavior in the numerical simulation. The overlapping can be suppressed by using a larger collision-spring constant. But the large collision-spring constant results in a peculiar phenomenon, vibration in the relative speed. Moderate magnitude of the collision-spring constant, not too small and not too large, needs be employed. Judging from the results in Figure 5, it may be realized that the collision-spring constant  $K$  in the range of  $5.0 \times 10^6$  -  $5.0 \times 10^7$  kN/m is acceptable. Since Equation (2) gives  $9.0 \times 10^6$ , this formula can be considered valid for the collision-spring constant between two girders having different stiffnesses.

## Model B

In general, the stiffnesses of the girder and the abutment are not the same and the dynamic behavior of the abutment during earthquake is very different from that of the girder. No good guidelines are available for the collision-spring constant  $K$  between the girder and the abutment.

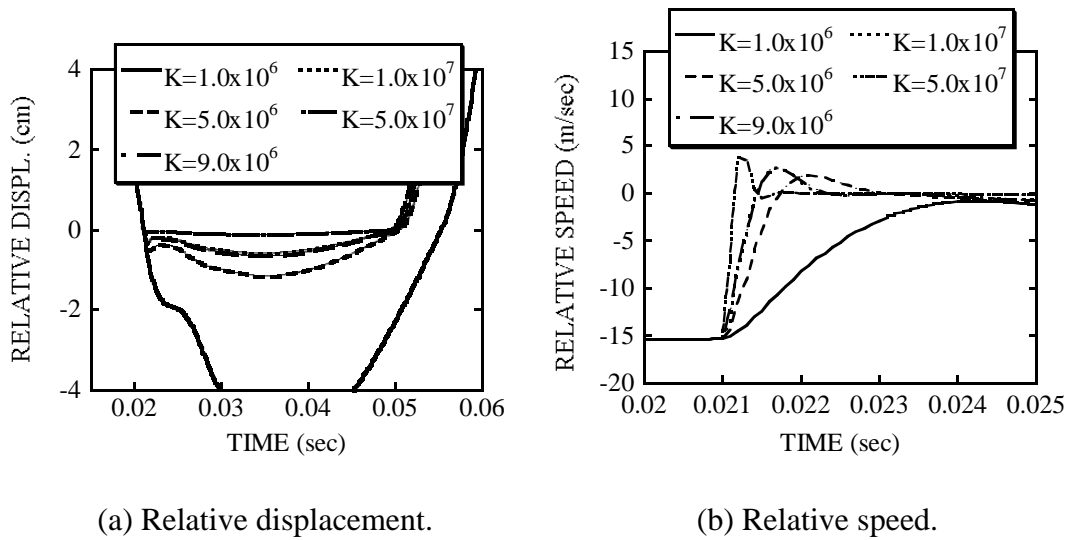


Figure 5. Results of Model A.

Since the dynamic movement of the girder is much bigger, the collision-spring constant may be determined by Equation (1) solely with the girder stiffness. The influence of the abutment on the collision-spring constant is ignored. The collision-spring constant thus obtained is denoted by  $k$ . Referring to the result of Model A, Equation (2) may be used with  $k_1$  computed by Equation (1) with the girder stiffness and  $k_2 = k_a$ . This collision-spring constant is  $K_0$ .

With various values of collision-spring constants, the dynamic response analysis of Model B is conducted. The range of the acceptable collision-spring constants are found through this analysis and shown in Figure 6 as line segments. In this figure,  $k$  and  $K_0$  mentioned in the previous paragraph are also plotted and both are found unacceptable.

It is also noticed in the numerical results that the maximum collision-spring constant  $K_{max}$  in each acceptable range varies almost linearly with  $k_a$  in this double-logarithmic graph of Figure 6. Figure 7 further presents the maximum acceptable collision-spring constants for all the cases, showing that the lines connecting the maximum acceptable collision-spring constants associated with the same values of  $k_1$  are parallel to each other.

Based on these observations, the following formula is constructed:

$$\log K_{max} = \log k_a + \alpha \quad (3)$$

where  $\alpha$  is dependent on  $k_1$  and the regression analysis yields

$$\alpha = -0.945 \times \log k_1 + 11.2 \quad (4)$$

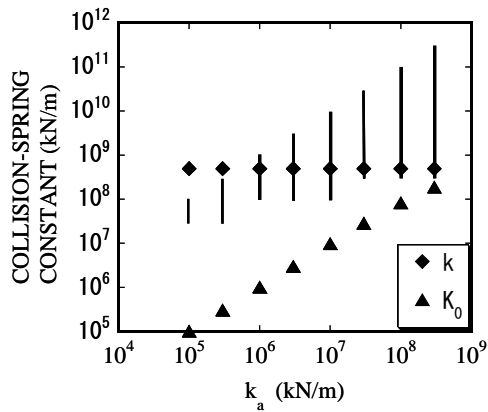


Figure 6. Results of Model B.

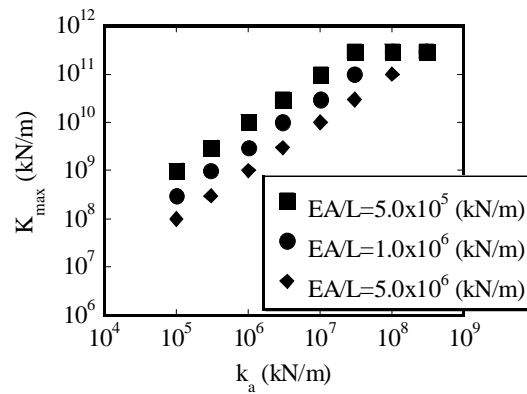


Figure 7. Maximum acceptable collision-spring constants.

Then the following formula may be proposed to estimate the collision-spring constant  $K$ :

$$\log K = \log k_a + 0.9\alpha \quad (5)$$

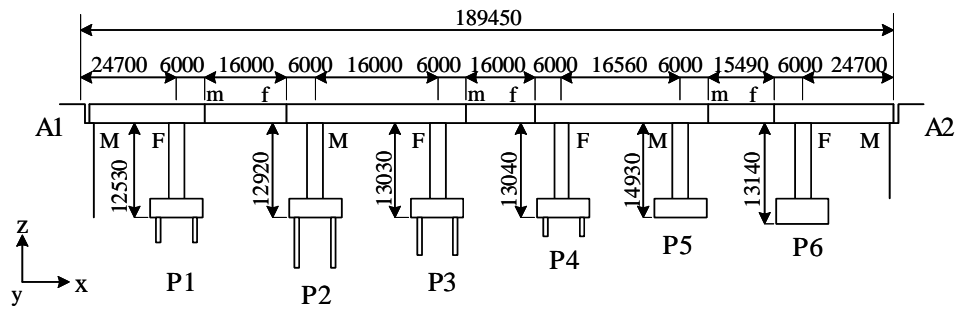
### Response Analysis of Girder Bridge

Referring to an existing bridge, a bridge model is constructed and analyzed. Figure 8 shows the schematic of the bridge: the bridge is a 7-span cantilever girder and the length is 189.45 m. In the figure, M, F, m and f stand for a movable bearing support, a fixed bearing support, a movable hinge and a fixed hinge, respectively. An abutment is assumed at each end of the bridge.

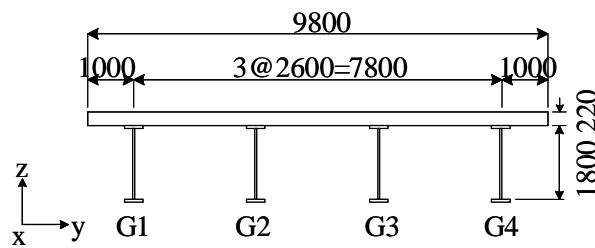
The superstructure is a composite girder with four steel I-shaped girders and a concrete deck. The web plate is constant while the upper-flange width varies from 290 to 490 mm and the upper-flange thickness is from 12 mm to 25 mm; the lower-flange width varies from 200 to 540 mm and the upper-flange thickness from 12 mm to 25 mm. The bridge piers are of a rectangular cross section with 2.2 m  $\times$  10.6 m at the top and 3.6 m  $\times$  13.6 m at the bottom. The nonlinear material behaviors of steel and concrete shown in Figure 9 are assumed with the yield stress of steel  $\sigma_y$  and the compressive strength of concrete  $\sigma_{ck}$  equal to 360N/mm<sup>2</sup> and 21N/mm<sup>2</sup>, respectively. The behavior of the foundation is modeled by springs whose constants are determined by Design Specifications of Highway Bridges (Japan Road Association 2002). The collision-spring constants are determined by the formulas given above.

The seismic wave in the form of acceleration recorded during the Mid Niigata Prefecture Earthquake in 2004 is used in the analysis (Figure 10). The initial gaps are assumed 0.25 m. Two analyses are conducted: one ignores the collision effect and the other includes it.

Figures 11 and 12 summarize the results of the movements of the girders and

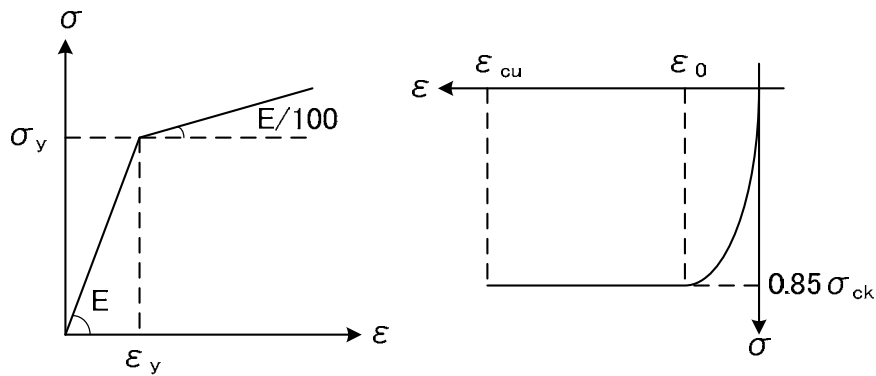


(a) Side view.



(b) Cross section.

Figure 8. Bridge model (Units: mm).



(a) Steel.

(b) Concrete.

Figure 9. Material behavior.

piers. Figure 11 shows the maximum horizontal displacement at four points in the superstructure: the closest point to A1, the mid-span, the closest point to A2 and the point right above P3. Figure 12 presents the maximum horizontal displacements of P1, P3, P4 and P6. It is clearly observed from these figures that the collisions suppress the movement of the bridge, possibly reducing the damages of the piers.

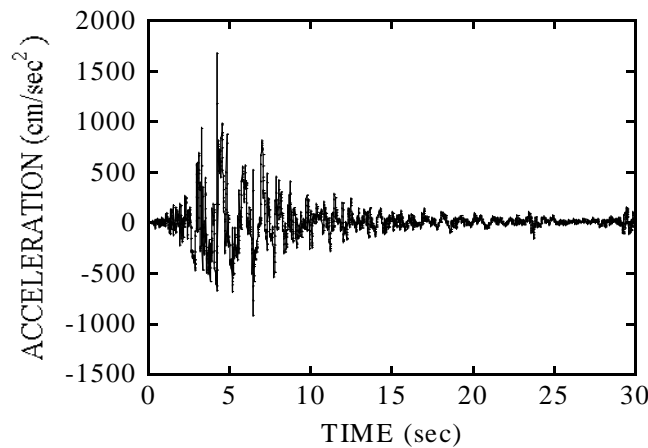


Figure 10. Acceleration recorded during the Mid Niigata Prefecture Earthquake in 2004.

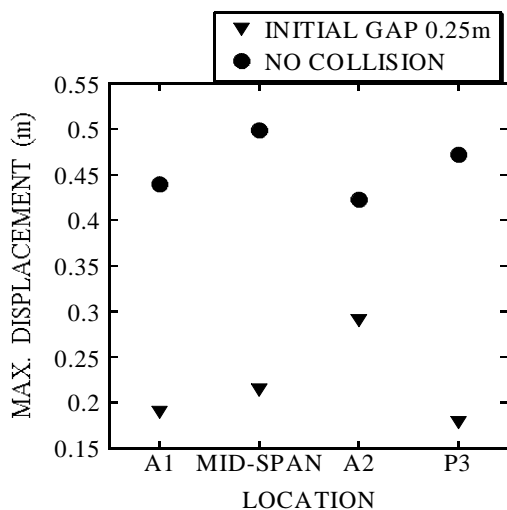


Figure 11. Maximum horizontal displacement of superstructure.

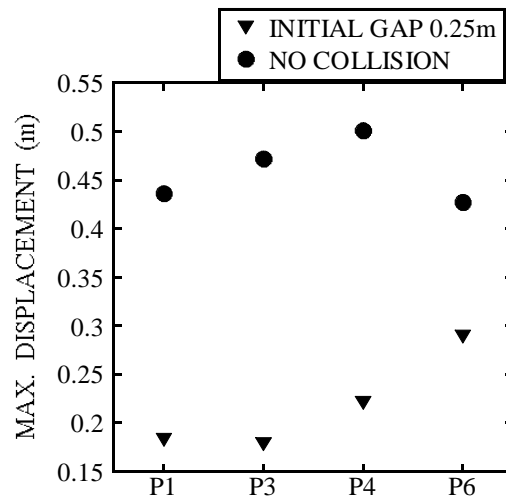


Figure 12. Maximum horizontal displacement of piers.

### **Concluding Remarks**

To include the effect of the collisions, the so-called collision springs are often used. Yet the appropriate constant of the collision spring is not available in the literature except when the two bodies are identical. The present study tackled this issue and, through numerical study, it proposed the formulas for acceptable collision-spring constants between girders and between a girder and an abutment. The dynamic response analysis of a girder bridge was then conducted and the significant influence of the collisions was indeed observed. Therefore, it is crucial to simulate collisions when the dynamic response analysis of a bridge is conducted. To that end, the formulas for acceptable collision-spring constants should be useful.

### **References**

Kawashima, K.: An analytical model of contact and impact in dynamic response analysis, Technical Note, Journal of JSCE, Vol. 308, pp. 123-126, 1981.

Kosa, K., Yamaguchi, E., Inokuma, Y., Tasaki, K.: Investigation and analysis of bridges and other structures damaged during the Mid Niigata Prefecture Earthquake in 2004, Proceedings of the 8th Symposium on Ductility Design Method for Bridges, pp. 35-40, 2005.

Japan Road Association: Design Specifications of Highway Bridges: Part V Seismic Design, Maruzen , Japan, 2002.

blank

# EFFECTS OF NEAR-FAULT VERTICAL ACCELERATIONS ON HIGHWAY BRIDGE COLUMNS

Sashi K. Kunnath<sup>1</sup> and Huiling Zhao<sup>2</sup>

## Abstract

The effects of vertical ground motions on the seismic response of ordinary highway bridges are investigated. Nonlinear simulation models with varying configurations of an existing bridge in California are developed for use in a detailed parametric study. The models are subjected to earthquake motions with and without vertical accelerations. Results indicate that vertical effects lead to significant variations in axial force demand in columns which can result in: fluctuations in moment demands at the face of the bent cap, amplification of moment demands at the girder mid-span, and changes to moment and shear capacity of the column. In the second phase, the effect of vertical motions on shear demand and capacity of bridge columns are examined.

## Introduction

The Seismic Design Criteria (SDC) used by the California Department of Transportation for ordinary standard bridges states that vertical effects should be considered on sites where the peak rock acceleration is expected to be more than 0.6g. However, the procedure to evaluate vertical effects is rather simplistic: a separate equivalent static vertical load analysis should be carried out under a uniformly distributed vertical load of 25% of the dead load applied in the upward and downward directions, respectively (CalTrans 2006).

Recent earthquakes have revealed that the ratio of vertical to horizontal peak ground acceleration can be larger in near-fault records than far-fault records. Hence it has become necessary to reexamine the consequences of vertical motions on typical highway bridges. The characteristics of vertical motions and the effect of vertical accelerations on bridge structures have been investigated by several researchers (Saadeghvaziri and Foutch 1991; Bozorgnia and Niazi 1993; Broekhuizen 1996; Papazoglou and Elnashai 1996; Yu et al. 1997; Gloyd 1997; Collier and Elnashai 2001; Button et al. 2002). Among other findings, these studies conclude that the variation of axial forces due to vertical excitations can influence both the moment and shear capacity of the section and also increase tensile stresses in the deck. An evaluation of the characteristics of response spectra of free-field vertical motions recorded during the 1994 Northridge earthquake by Bozorgnia et al. (2004) found the vertical to horizontal (V/H) response spectral ratios to be strongly dependent on period and site-to-source distance.

---

<sup>1</sup> Professor, Department of Civil and Environmental Engineering, University of California, Davis, CA

<sup>2</sup> Visiting Graduate Student, University of California at Davis & PhD Candidate, Tongji University, China

## Important Characteristics of Vertical Accelerations

A preliminary study of 65 near-fault earthquake records with horizontal PGA greater than 0.5g indicates that:

- The predominant period of the vertical ground motions are smaller than the corresponding horizontal component (Figure 1).
- The ratio of vertical-to-horizontal PGA decreases gradually with increasing fault distance, therefore, the vertical component of ground motions will be more severe for near fault ground motions.

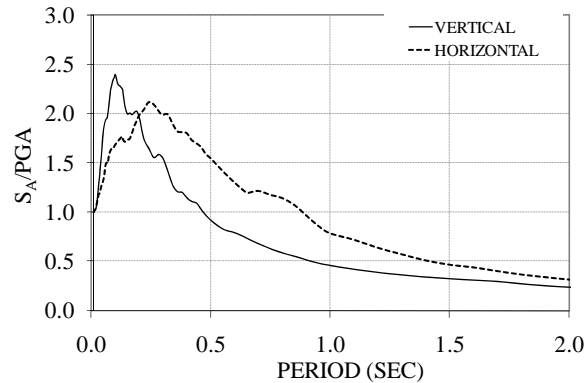


Figure 1: Characteristics of near-fault horizontal and vertical motions

## Summary of Phase I Study

An existing two-span overcrossing was selected to represent a typical ordinary highway bridge in California. The computer model used in the simulations is shown in Figure 2. The superstructure consists of a reinforced concrete box girder supported by two circular columns with a diameter of 1.78 m. The width of the girder was unchanged at  $S = 8.8$  m and the column height was fixed at  $H = 8.5$  m.

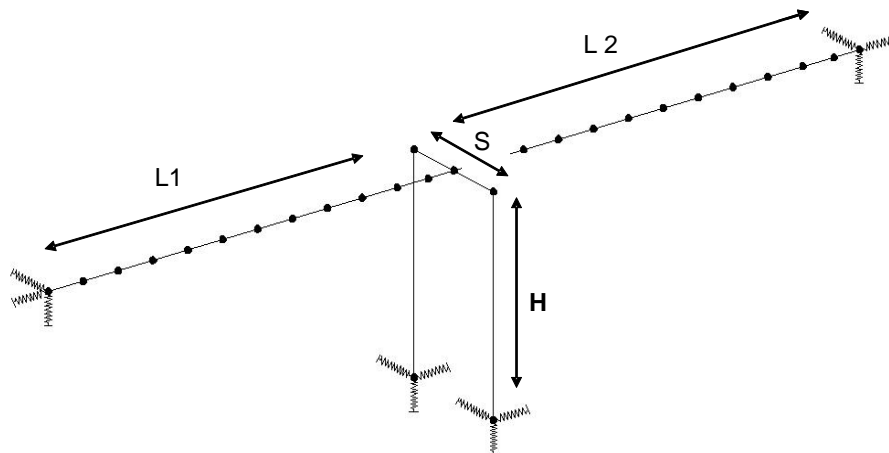


Figure 2 – Simulation model of typical two-span bridge

The end conditions both at the abutments and at the bottom of the columns were modeled using spring elements whose properties were determined using SDC (CalTrans 2006) guidelines. The superstructure was modeled both as elastic elements in the initial phase of the study and later as inelastic elements to examine the effects of inelasticity on reinforcement yielding. Potential inelastic regions of the columns were modeled using fiber hinge elements with prescribed plastic hinge lengths. Axial force – moment interaction was therefore included in the simulations. Additional details of the bridge and the simulation models are reported in Kunnath et al. (2007). In order to investigate the effect of vertical accelerations on a wider range of vertical frequencies, different bridge configurations were created by modifying the span lengths, L1 and L2. Table 1 presents the fundamental dynamic properties of the selected configurations.

Table 1 – Properties and periods of bridge configurations

Simulation Model #	$T_V$ (s)	$T_L$ (s)	$T_T$ (s)
1	0.19	0.32	0.55
2	0.12	0.27	0.46
3	0.30	0.43	0.64
4	0.37	0.53	0.68
5	0.45	0.62	0.75
6	0.24	0.35	0.59

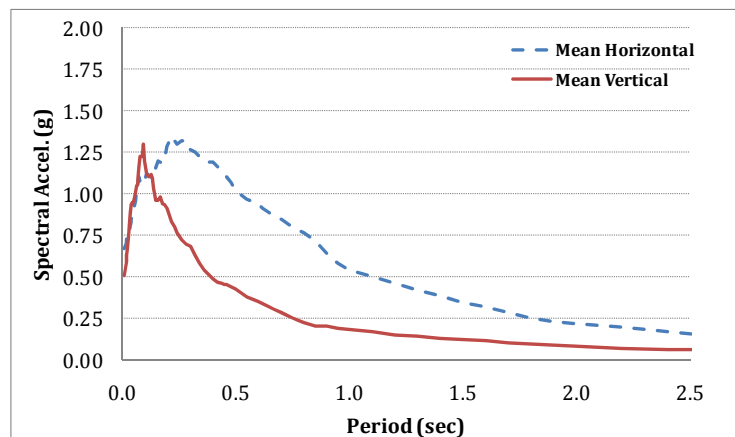


Figure 3 – Spectra of the horizontal component of ground motions scaled to match the ARS curve (Magnitude 8.0, PGA 0.5 g and site class D) at fundamental longitudinal period of base configuration, and corresponding vertical spectra

### Ground Motions

Following a preliminary set of analyses, a reduced subset of 29 near-fault records that produced the largest demands on the bridge was selected for detailed evaluation. All ground motions were scaled to match the ARS spectrum (CalTrans 2006) at the longitudinal period of each bridge configuration. Figure 3 displays typical

spectra of the horizontal component of the ground motions scaled to match the ARS curve for ground motions with a PGA 0.5g and site class C together with the corresponding vertical spectra.

**Effect of Vertical Acceleration on Column Axial Force**

Figure 4 summarizes the variation of the normalized axial load as a function of the vertical fundamental period. Both the maximum and minimum axial force experienced by the column in each simulation is recorded. The amplification of the axial load in the column is not a source for concern since the nominal axial load capacity of the columns is adequate to resist these forces without damage. However, the variation in the axial force on the column may result in significant changes in the moment and shear capacity of the column.

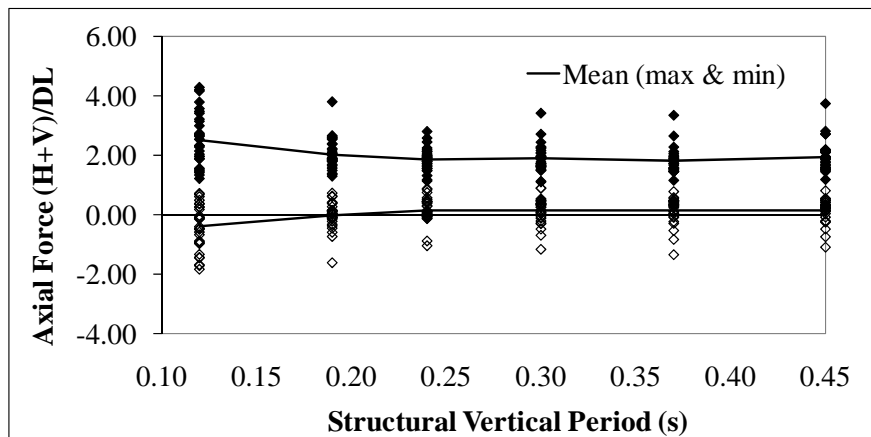


Figure 4 – Variation of column axial force demands with vertical period for unscaled ground motions

**Effect of Vertical Acceleration on Span Moment**

Figure 5 shows the variation of the normalized moment demand (ratio of moment demand to the moment demand due to dead load only) at mid-span of the left girder as a function of the fundamental vertical period. The results highlight the significant effects of vertical motions on the moment demands in the longitudinal girders. It should be pointed out that the girders were modeled as elastic elements in these simulations. Since the negative moments far exceed the available capacity, the simulations were repeated using inelastic elements for the girder. Peak strains were found to vary up to 12 times the yield strain.

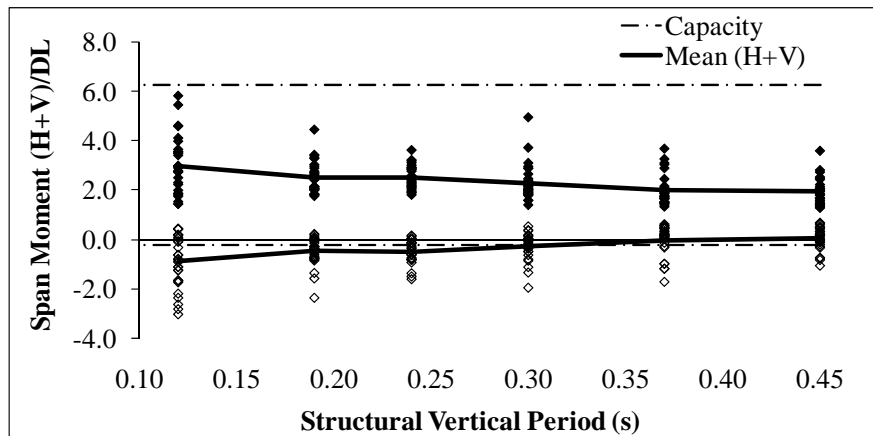


Figure 5 - Variation of moment demand at the mid-span with vertical period for unscaled ground motions

### **Effect of Vertical Acceleration on Column Moment**

The large increases in the axial compression in columns due to vertical accelerations (Figure 4) can lead to significant increases in the column moment capacity. Although this may suggest conservatism in the design, it may result in the shifting of the potential plastic hinge zone from the top of the column to the girder which is an undesirable situation that is supposed to be avoided by the requirements of SDC-2006.

### **Phase II Results**

In reviewing some of the earlier work on the effects of vertical motions on structures, some investigators have raised the issue of shear demand and capacity in bridge columns due to changes in the axial force demands. Since the bridge configurations used in the Phase I study consisted of two-column bents and single columns with very large shear span ratios, shear demands were generally not critical. Hence a new study was initiated to identify critical bridge configurations that might be prone to shear damage due to vertical effects.

The typical configuration selected for this phase of the work is the Plumas Bridge in California which is a three-span bridge with span lengths of 40.5m, 58.0m and 40.5m. The heights of the as-built columns are approx 9 m each. In order to study shear demands under strong near-fault motions, the column heights were varied to generate a range of aspect ratios. A nonlinear simulation model, as displayed in Figure 6, was developed in OpenSees (2009). To ensure proper modeling of the torsional properties of the deck, a three dimensional shell model of the bridge was created in SAP-2000 and a series of elastic modal analyses were carried out on both systems to calibrate the inertial properties of the superstructure of the line model.

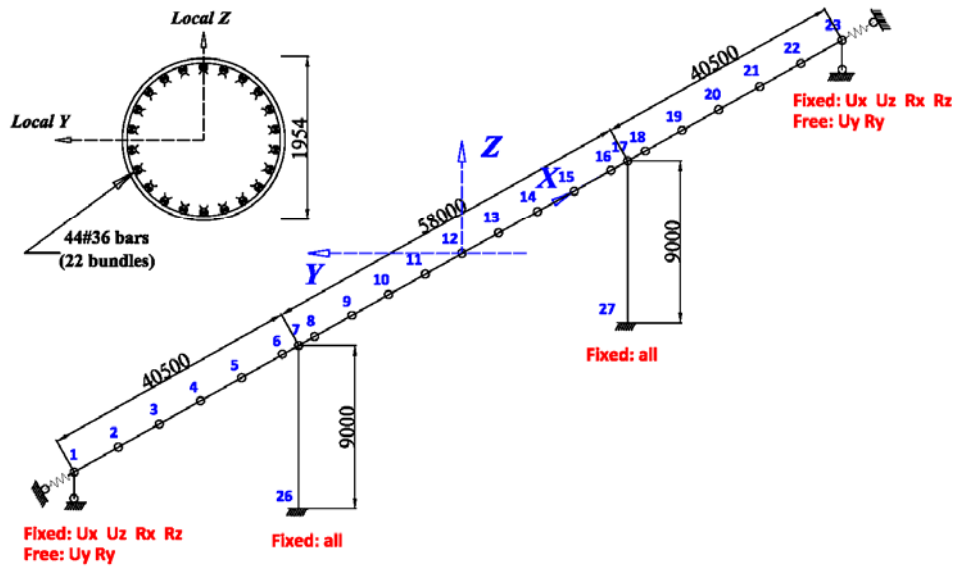


Figure 6 – Simulation model of the Plumas Bridge used in Phase II Study

The model was subjected to a series of combined horizontal and vertical near-fault motions. The earthquake records used in the simulations are listed in Table 2. Each set of records was scaled to match the SDC-ARS spectra (corresponding to a magnitude 8 event with PGA of 0.6g) at the fundamental transverse period of the bridge (which was estimated at 0.8 seconds). Scale factors were established for the larger of the two horizontal components and this factor was used to scale the remaining two components. A plot showing the mean spectra for all scaled records is summarized in Figure 7.

Table 2 – Characteristics of selected near-fault records

Earthquake	Year	Station	Distance* (km)	PGA-H <sub>MAX</sub> (g)	PGA-H <sub>MIN</sub> (g)	PGA-Vert (g)
1. Gazli (USSR)	1976	Karakyr	5.46	0.718	0.608	1.264
2. Imperial Valley	1979	Bonds Corner	2.68	0.755	0.588	0.425
3. Morgan Hill	1984	Coyote Lake Dam	0.30	1.298	0.711	0.388
4. Erzincan (Turkey)	1992	Erzincan	4.38	0.515	0.496	0.248
5. Landers	1992	Lucerne	2.19	0.785	0.721	0.818
6. Northridge	1994	Rinaldi Rec Stn	6.50	0.838	0.472	0.852
7. Kobe (Japan)	1995	KJMA	0.96	0.821	0.599	0.343

\* Closest fault distance

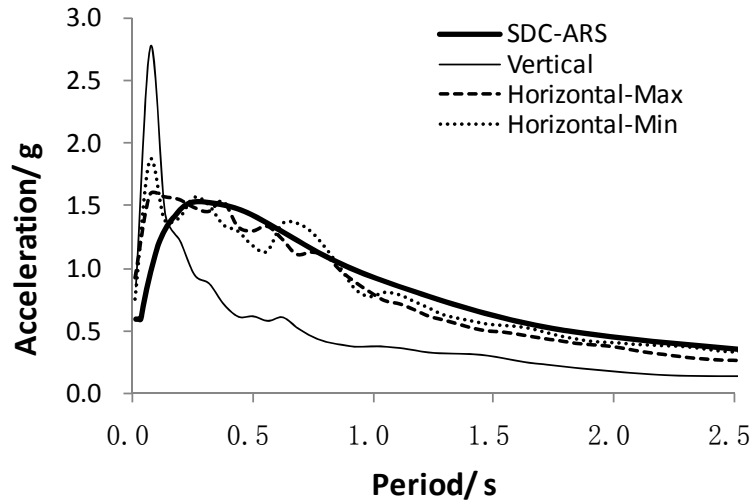


Figure 7 – Spectra of ground motions used in Phase II study

For each simulation, the axial force, shear demand and shear capacity in the column was monitored. Shear capacity at any instant in time was evaluated using ACI-318 (2007) expressions:

$$V_n = V_c + V_s \quad (1)$$

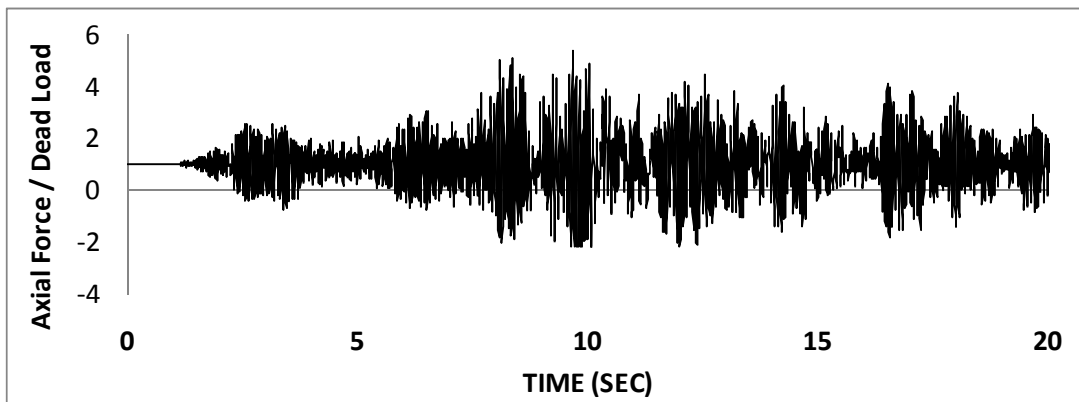
In the above equation,  $V_c$  is shear strength provided by concrete, and  $V_s$  is shear strength provided by shear reinforcement.

$$V_c = \begin{cases} 2 \left( 1 + \frac{N_u}{2000A_g} \right) \sqrt{f'_c} b_w d, & \text{when } N_u > 0 \text{ (axial compression)} \\ 2 \left( 1 + \frac{N_u}{500A_g} \right) \sqrt{f'_c} b_w d, & \text{when } N_u \leq 0 \text{ (tension)} \end{cases} \quad (2)$$

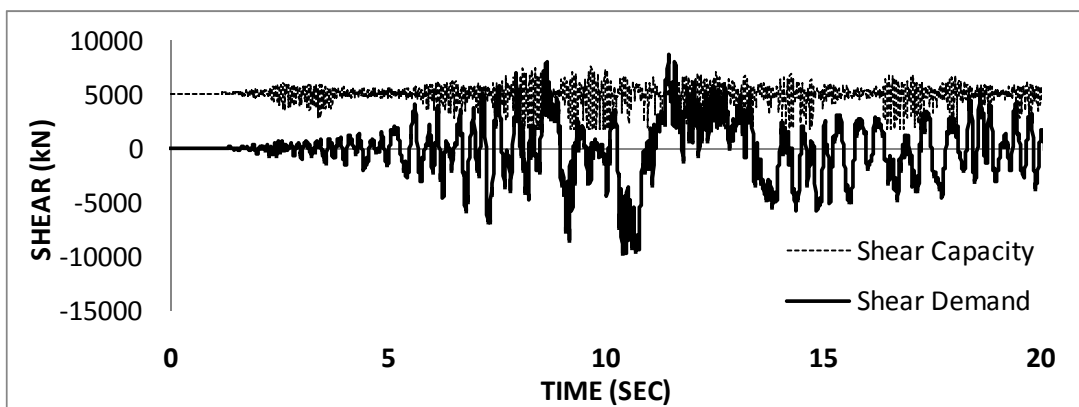
$$V_s = \frac{A_v f_y d}{s} \quad (3)$$

$N_u$  : factored axial force normal to the cross section

Figure 8 shows a typical response of the bridge column. The computed axial force is normalized by the dead load which means that values below 1.0 indicate a state of axial tension in the column. The shear capacity (which is a function of the axial force) is superimposed on the demand plot so that the demand to capacity ratio (DCR) can be ascertained. The particular case study presented in Figure 8 is for the Landers record set which provided the maximum DCR among all ground motions considered.



(a)



(b)

Figure 8 – Response of the bridge column with aspect ratio of 3.0 subjected to the Landers (1992) record: (a) Axial force variation; (b) Shear demand vs. available shear capacity.

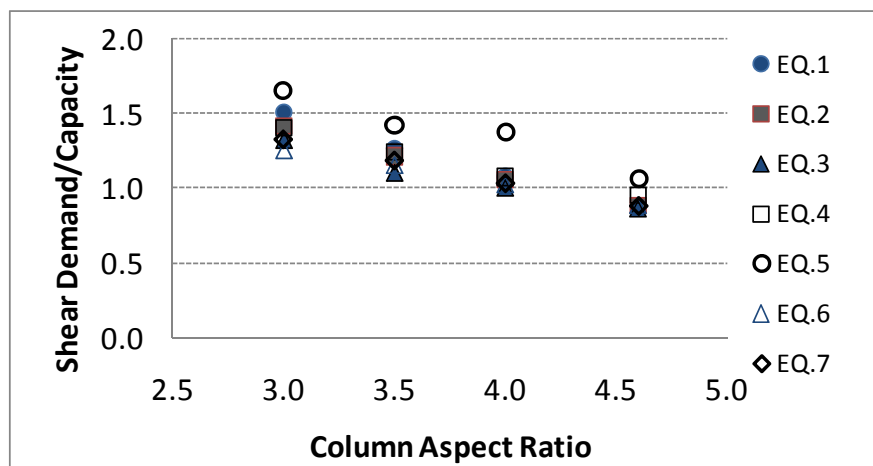


Figure 9 – Effect of aspect ratio (column height/diameter) on shear DCR

Finally, a summary of the shear DCR for all simulations is presented in Figure 9. The record numbers correspond to the list identified in Table 2. It is evident that shear damage is likely only for aspect ratios below 4.5. Given the fact that the expressions used to estimate shear capacity are generally conservative, it is reasonable to conclude that only columns with aspect ratios below 4.0 need further investigation.

### **Concluding Remarks**

The main objective of the present study is to assess current provisions in SDC-2006 for incorporating vertical effects of ground motions in seismic design of ordinary highway bridges. Results of the investigation suggest that highway over-crossings with vertical periods close to the predominant period of the vertical component of the motion are more vulnerable to vertical effects.

Findings also indicate that vertical ground motions significantly affect the axial force demand in columns which in turn have an effect on moment demands at the middle of the span. A separate study on the effects of vertical motions on shear demands and shear capacity in the columns reveal that the aspect ratio (column height to diameter) is a significant parameter that influences potential shear damage to the column. It should also be noted that axial forces vary at much higher frequencies than lateral forces. Hence the sudden shifts in shear capacity as the column goes from compression to tension may require further investigation. A shaking table test program on this issue is the subject of an ongoing investigation funded by Caltrans and being carried out collaboratively between UC Berkeley and UC Davis.

### **Acknowledgements**

Funding for this study provided by the California Department of Transportation (Caltrans) under Contracts No.59A0434 and No. 59A0688 is gratefully acknowledged. The contributions of Li-Hong Sheng (Project Manager), Mark Yashinsky and several Caltrans engineers throughout the project duration are also appreciated.

### **References**

- Bozorgnia, Y., M. Niazi. (1993). "Distance Scaling of Vertical and Horizontal Response Spectra of the Loma Prieta Earthquake." *Earthquake Engineering and Structural Dynamics*, Vol 22, pp.695-707.
- Bozorgnia, Y. M. and Campbell, K. W. (2004). The vertical-to-horizontal response spectral ratio and tentative procedures for developing simplified V/H and vertical design spectra, *J. Earthquake Engineering*, Vol. 8, pp. 175-207.
- Broekhuizen, D. S. (1996). "Effects of vertical acceleration on prestressed concrete bridges." MS Thesis, University of Texas at Austin, Texas.
- Button, M.R., Cronin, C.J. and Mayes, R.L. (2002). "Effect of Vertical Motions on Seismic Response of Bridges." *ASCE Journal of Structural Engineering*, Vol.128 (12), 1551-1564.

- CalTrans (2006), “Seismic Design Criteria”, California Department of Transportation Sacramento, CA.
- Collier, C.J. and Elnashai, A.S. (2001). “A Procedure for Combining Vertical and Horizontal Seismic Action Effects.” *Journal of Earthquake Engineering*, Vol. 5, No. 4, 521-539.
- Gloyd, S. (1997). “Design of ordinary bridges for vertical seismic acceleration.” *Proc., FHWA/NCEER Workshop on the National Representation of Seismic Ground Motion for New and Existing Highway Facilities, Tech. Rep. No. NCEER-97-0010*, National Center for Earthquake Engineering Research, State Univ. of New York at Buffalo, N.Y., pp.277–290.
- Kunnath, S.K., Erduran, E., Chai, Y.H. and Yashinsky, M. (2007). “Near-Fault Vertical Ground Motions on Seismic Response of Highway Overcrossings.” *ASCE Journal of Bridge Engineering*, Vol.13, No.3, 282-290.
- Papazoglou, A.J. and Elnashai, A.S. (1996). “Analytical and Field Evidence of the Damaging Effect of Vertical Earthquake Ground Motion.” *Earthquake Engineering and Structural Dynamics*, Vol. 25, No.10, 1109 – 1137.
- Saadeghvaziri, M. A., and Foutch, D. A. (1991). “Dynamic behavior of R/C highway bridges under the combined effect of vertical and horizontal earthquake motions.” *Earthquake Engineering and Structural Dynamics*, Vol 20, pp.535–549.
- Silva, W. J. (1997). “Characteristics of vertical ground motions for applications to engineering design.” *Proc., FHWA/NCEER Workshop on the National Representation of Seismic Ground Motion for New and Existing Highway Facilities, Tech. Rep. No. NCEER-97-0010*, National Center for Earthquake Engineering Research, State Univ. of New York at Buffalo, N.Y., pp.205–252.
- Yu, C-P., Broekhuizen, D. S., Roesset, J. M., Breen, J. E., and Kreger, M. E. (1997). “Effect of vertical ground motion on bridge deck response.” *Proc., Workshop on Earthquake Engineering Frontiers in Transportation Facilities, Tech. Rep. No. NCEER-97-0005*, National Center for Earthquake Engineering Research, State Univ. of New York at Buffalo, N.Y., pp.249–263.

**SEISMIC DESIGN OF MULTI SPAN CONTINUOUS RIGID-FRAME  
BRIDGE WITH PRESTRESSED CONCRETE BOX GIRDER  
—NEW-TOMEI GUNKAI-GAWA BRIDGE—**

Chiaki NAGAO<sup>1</sup> Yasushi KAMIHIGASHI<sup>2</sup> Akio KASUGA<sup>3</sup> Kenichi NAKATSUMI<sup>4</sup>

**Abstract**

The Gunkai-gawa Bridge is a seven-span continuous rigid frame box girder bridge made of prestressed reinforced concrete, which will be 740 m long and located near the Toyota-higashi Junction of the New Tomei Expressway. It was designed to have strong earthquake-resisting capacity and simple maintenance, by means of rigid-coupling construction between all piers and main girders. There are three techniques: first, lightweight upper structure, second below-grade footings for short piers, and the last horizontal stress application for displacement adjustment during closure of the main girders. This paper presents an overview of each process for the seismic design and the approach to construction of the bridge.

**1. Introduction**

The Gunkai-gawa Bridge will be located 3 km east of the Toyota-higashi junction on the New Tomei Expressway. The bridge will be 740 m long, a seven-span continuous rigid frame box girder bridge made of prestressed reinforced concrete. The building construction work of this bridge was ordered including designing and planning to construction. This ordering system enables us to require structural feasibility, of course, simple maintenance, consideration for surrounding environment, and what is more, shortened work schedule. The selected design was the bridge emphasized simple maintenance having no supports due to achieving a rigid-coupled prestressed reinforced concrete structure between all of the piers and main girders. Generally it is difficult to have rigid-frame bridge because the height of the bridge piers are lower in comparison to a span of 740 m long bridge. Here, there are three methods enabling the structure feasible:

- (1) Lightweight superstructure
- (2) Below-grade footings applied to short piers
- (3) Horizontal stress application method for displacement adjustment during closure of the main girders

This paper presents an overview of the process and its each issue through which the structural form of the Gunkai-gawa Bridge was determined. It also treats the

---

<sup>1</sup> Engineer, Planning and Design Team Nagoya Branch, Central Nippon Expressway Company Limited

<sup>2</sup> Director, Planning and Design Team Nagoya Branch, Central Nippon Expressway Company Limited

<sup>3</sup> Chief Engineer, Civil Engineering Designing Department, Sumitomo Mitsui Construction

<sup>4</sup> Engineer, Civil Engineering Designing Department, Sumitomo Mitsui Construction

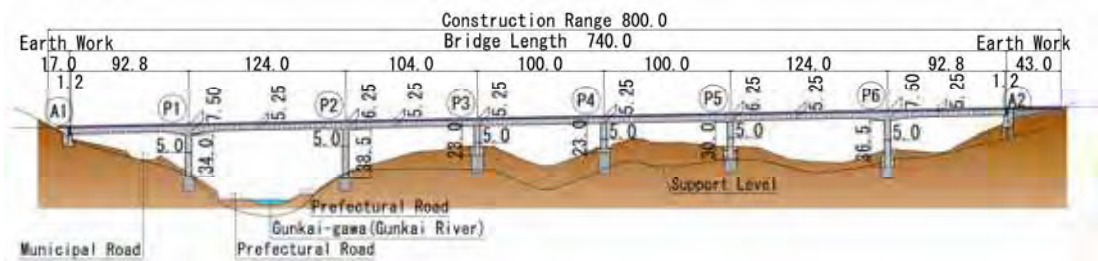
approach to construction of the bridge.

## 2. Overview of Gunkai-gawa Bridge

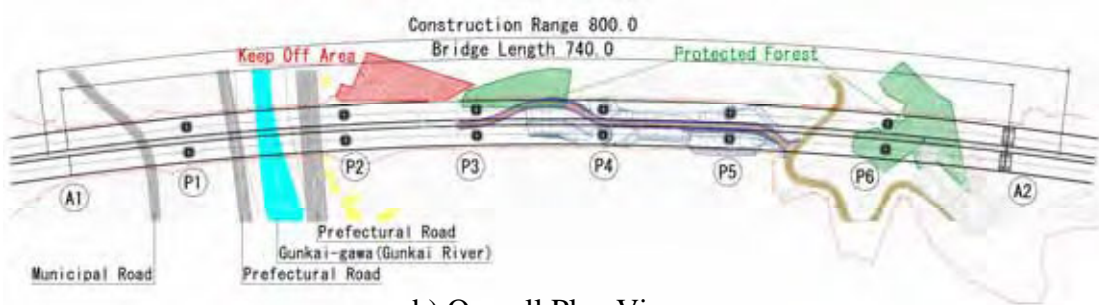
The control points of the Gunkai-gawa Bridge are the Gunkai-gawa (Gunkai River) and two prefectural roads, located along each bank of the river. Trying to save the span crossing these control points 100 m level, a bridge pier would need to be placed between them and the A1 abutment. Accordingly, the length of the span crossing the river was made 124 m in order to reduce the number of bridge piers. It was also determined that using 100 m spans for the other sections would further reduce the number of bridge piers. Consequently, a seven-span structure is confirmed optimal. Since simple maintenance was also required as a designing performance, concrete girders were used throughout the construction, and a rigid frame structure was used for all bridge piers in order to reduce the number of bearings.

As a result of the establishment of these constraints and the determination of the bridge pier and abutment positions based on further consideration of economy, simple maintenance and high construction performance, the bridge structure was finalized as a prestressed concrete seven-span continuous rigid frame box girder bridge measuring 740 m long. (Fig. 1)

The ratio of fixed span length to bridge pier height of this bridge is approximately 8:1. Considering the ratio in an ordinary rigid frame bridge is 5:1 or less, the bridge piers will be affected a major impact from the expansion and the contraction of the main girders. Therefore, the structure was achieved through the incorporation of measures such as a lightweight superstructure, below-grade footings for short piers, and horizontal stress application for displacement adjustment prior to closure of the



a) Side View



b) Overall Plan View

Fig.1 General View of Gunkai-gawa Bridge

cantilever erection for the outermost piers.

As shown in Fig. 2, the main girders have a wide sectional shape, so a single-cell box girder section with an extended slab reinforced with struts was adopted. Moreover, the use of a diagonal web enabled the main girder weight to be reduced by 18% as compared to a conventional single-cell box girder section. Long sections with the same girder height were provided and struts of the same length were used, greatly increasing the ease of construction. Moreover, to reduce the number of external tendons within the narrow box girders, high-strength prestressing strands were used. The main girders were designed using the limit state design method, and concrete with a design standard strength of  $\sigma_{ck} = 50 \text{ N/mm}^2$  was used in places to reduce the weight.

The design strength of the bridge pier concrete was  $\sigma_{ck} = 30 \text{ N/mm}^2$  ( $40 \text{ N/mm}^2$  in some sections), and SD 345 was used for the reinforcements. The types of foundation used were a large diameter caisson foundation for all bridge piers, a spread foundation for the A1 bridge abutment, and a caisson pile foundation for the A2 abutment. As shown in Fig. 3, shapes of all bridge piers were  $5.0 \times 5.0 \text{ m}$  hollow section, in which D51 (SD 345) in two planes at a maximum as axial reinforcements and D29 hoop ties were provided.

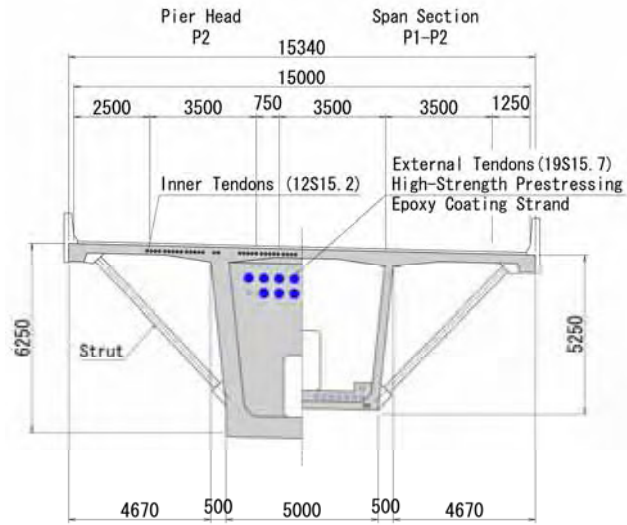


Fig.2 Main Girder Cross Section

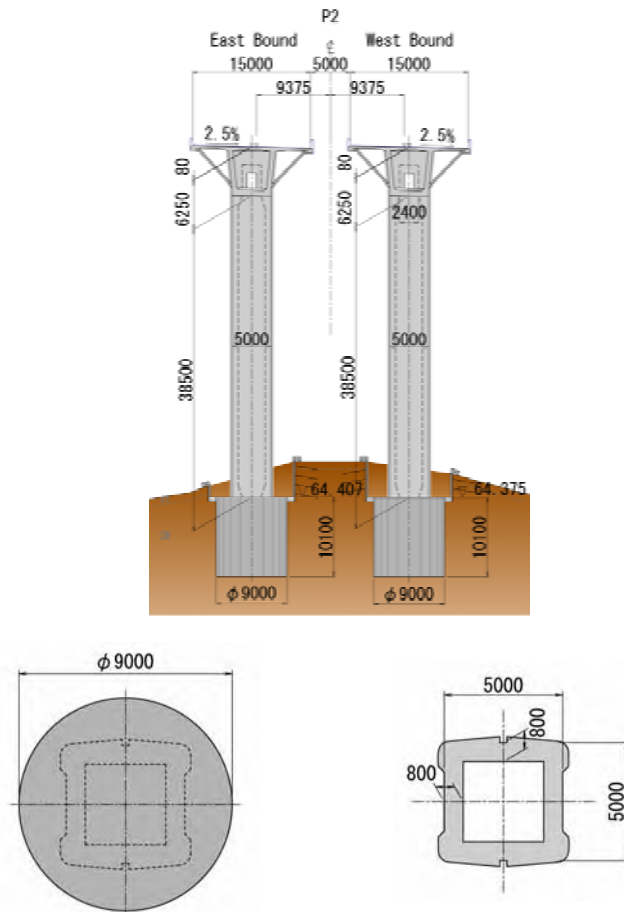


Fig.3 Pier Cross Section

### **3. Seismic design**

Two stages of ground motion, Level 1 and Level 2, were considered in the seismic design of the bridge. As the bridge was a continuous rigid frame bridge and the 1st vibration mode would be dominant, the static check method was used as the method of checking earthquake-resisting capacity with respect to a Level 1 ground motion. As adequate study has not been conducted for the applicability of the equal energy assumption based on the non-linear hysteretic behavior of the structural members and the bridge as a whole, the active check method was used for the Level 2 ground motion.

#### **3-1. Analysis model and analysis method**

A three-dimensional framework model created by modeling the bridge piers and main girders as bar elements was used as the analysis model. The A1 and A2 ends are support structures, so spring support was used for the bridge axial direction (X direction) and vertical direction (Z direction). As a displacement limit structure was employed for the perpendicular direction (Y direction), fixed support was used for this direction. For the bottom end of each bridge pier, a spring constant was considered for the large diameter caisson foundation. The analysis took into account material non-linearity for all members (M- $\phi$  model).

#### **3-2. Eigenvalue analysis**

Fig. 4 shows the major natural periods and vibration modes for the bridge. For the bridge axial direction, the 1st mode was dominant, and the natural period was 0.948 seconds. In the direction perpendicular to the bridge axis, the 1st and 2nd modes were dominant. In each of these modes, the main girder with the longest span length (124

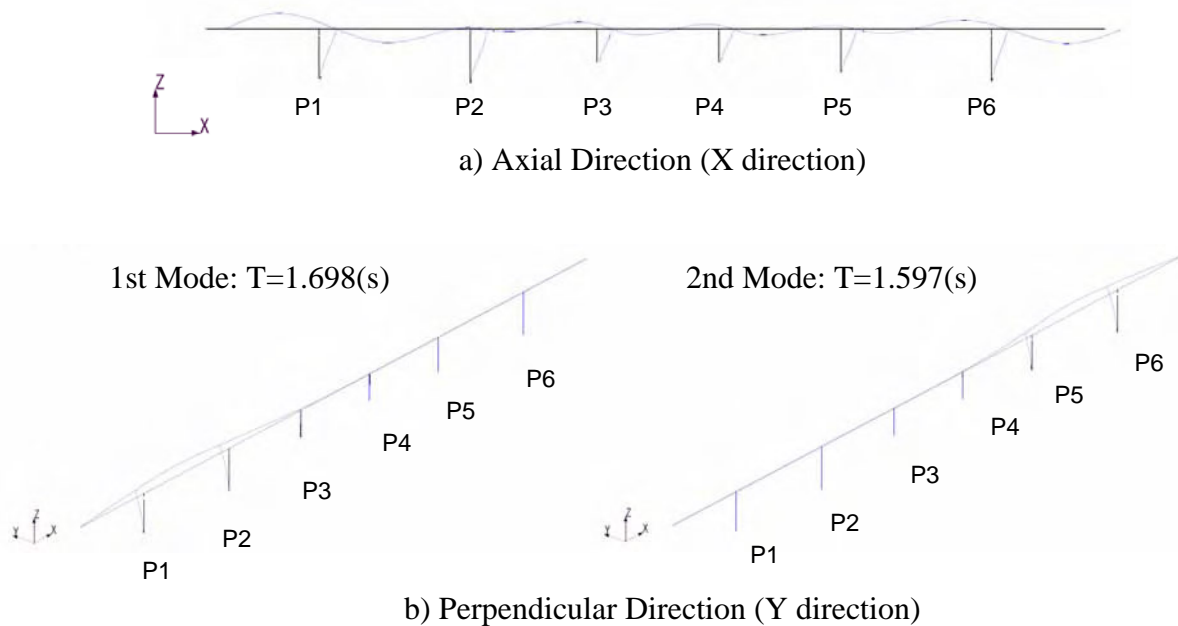


Fig.4 Vibration Mode

m) was deformed in the direction perpendicular to the bridge axis. The natural periods were 1.698 and 1.597 seconds, respectively.

### **3-3. Check of Level 1 ground motion**

Under Level 1 ground motion, the design horizontal seismic coefficient was determined by the static check method. That is, the value was  $kH=0.2$  calculated from its own natural period  $T=0.948(s)$  in the bridge axial direction, and the value was  $kH=0.15$  with natural period  $T = 1.698 (s)$  in the direction perpendicular to the bridge axis.

Table 1 shows the results of the check for the bridge piers for the bridge axial direction and the direction perpendicular to the bridge axis. In the bridge axial direction, piers P3 and P4 in the center had a lower height than the other bridge piers. The section force during an earthquake will be concentrated on these lower piers, which will be subjected to the most intense reinforcement stress.

In the direction perpendicular to the bridge axis, as noted in the former section about natural period modes, the dominant mode was the one in which the main girder with the longest span length of 124 m was deformed in the direction perpendicular to the bridge axis. Hence the bridge pier supporting this span, P2 and P3, will be subjected to substantial reinforcement stress.

Table1. Pier Check of Level 1 Ground Motion

		P1	P2	P3	P4	P5	P6
Design Strength of Concrete		40N/mm <sup>2</sup>	30N/mm <sup>2</sup>	30N/mm <sup>2</sup>	30N/mm <sup>2</sup>	30N/mm <sup>2</sup>	40N/mm <sup>2</sup>
Axial Reinforcing Bar	Axial Direction	SD345 D51@150 2 line	SD345 D51@150 2 line	SD345 D51@150 2 line	SD345 D51@150 1.5 line	SD345 D51@150 2 line	SD345 D51@150 2 line
	perpendicular direction	SD345 D51@150 2 line	SD345 D51@150 2 line	SD345 D51@150 1 line	SD345 D51@150 1 line	SD345 D51@150 2 line	SD345 D51@150 2 line
Hoop tie	Axial Direction	D29@150	D29@150	D29@125	D29@150	D29@150	D29@150
	perpendicular direction	D29@150	D29@150	D29@125	D29@150	D29@150	D29@150
Axial Direcion	$\sigma_c(N/mm^2)$	13.2	11.9	14.1	13.3	11.8	13.7
	$\sigma_a(N/mm^2)$	19.5	15.0				19.5
		O.K.	O.K.	O.K.	O.K.	O.K.	O.K.
	$\sigma_s(N/mm^2)$	214	189	284	270	194	228
	$\sigma_a(N/mm^2)$	300					
Perpendicular Direcion	$\sigma_c(N/mm^2)$	11.7	11.3	10.2	8.8	11.0	10.5
	$\sigma_a(N/mm^2)$	19.5	15.0				19.5
		O.K.	O.K.	O.K.	O.K.	O.K.	O.K.
	$\sigma_s(N/mm^2)$	177	172	176	142	171	145
	$\sigma_a(N/mm^2)$	300					
	O.K.	O.K.	O.K.	O.K.	O.K.	O.K.	

$\sigma_c$ :Concrete Stress  
 $\sigma_s$ :Reinforcing Bar Stress  
 $\sigma_a$ :Limit

### **3-4. Check of Level 2 ground motion**

The required earthquake-resisting capacity with respect to a Level 2 ground motion was based on Specifications for Highway Bridges (Part V: Seismic Design). The seismic design was conducted so as to satisfy earthquake-resisting capacity 2 (which means to be in limited damage resulting from an earthquake Level 2 which can be restored temporary bridge performance quickly). The input ground motion used for

the check was an acceleration waveform based on Specifications for Highway Bridges (Part V: Seismic Design).

**(1) Check of bridge piers**

The bridge piers were figured out to have enough performance by checking in three items in the bridge axial direction and the direction perpendicular to the bridge axis: (1) maximum response curvature at top and bottom ends (2) shear capacity, and (3) residual displacement. The results are shown in Table 2. The values for each check item satisfied the requirements for allowable limits.

Table2. Pier Check of Level 2 Ground Motion

			Unit	P1	P2	P3	P4	P5	P6	
(1)Maximum Respons Curvature	Axial Direcion	Type	response	(rad)	1.5E-03	1.7E-03	3.7E-03	4.0E-03	2.0E-03	1.5E-03
			limit	(rad)	4.4E-03	4.3E-03	4.9E-03	4.8E-03	4.4E-03	4.0E-03
			ratio		35%	39%	76%	84%	47%	37%
				OK	OK	OK	OK	OK	OK	
		Type	response	(rad)	2.0E-03	2.0E-03	6.2E-03	5.9E-03	2.7E-03	1.7E-03
			limit	(rad)	1.3E-02	1.2E-02	1.7E-02	1.6E-02	1.3E-02	1.0E-02
	ratio			16%	16%	36%	36%	21%	16%	
				OK	OK	OK	OK	OK	OK	
	Perpendicular Direcion	Type	response	(rad)	3.1E-03	3.8E-03	1.6E-03	1.7E-03	4.3E-03	3.3E-03
			limit	(rad)	4.5E-03	4.4E-03	4.2E-03	4.4E-03	4.5E-03	4.1E-03
			ratio		68%	87%	38%	38%	95%	82%
				OK	OK	OK	OK	OK	OK	
Type		response	(rad)	1.5E-03	1.7E-03	1.4E-03	1.5E-03	2.1E-03	1.6E-03	
		limit	(rad)	1.3E-02	1.3E-02	1.3E-02	1.4E-02	1.3E-02	1.1E-02	
	ratio		11%	13%	11%	11%	16%	15%		
			OK	OK	OK	OK	OK	OK		
(2)Shestr Capacity	Axial Direcion	Type	response	(kN)	2.7E+04	2.6E+04	3.6E+04	3.4E+04	3.4E+04	2.5E+04
			capacity	(kN)	3.7E+04	3.7E+04	4.4E+04	3.7E+04	3.7E+04	3.0E+04
			ratio		72%	71%	80%	92%	92%	83%
				OK	OK	OK	OK	OK	OK	
		Type	response	(kN)	3.1E+04	2.8E+04	3.8E+04	3.6E+04	3.6E+04	2.7E+04
			capacity	(kN)	3.8E+04	3.8E+04	4.5E+04	3.8E+04	3.8E+04	3.0E+04
	ratio			81%	74%	84%	96%	95%	89%	
				OK	OK	OK	OK	OK	OK	
	Perpendicular Direcion	Type	response	(kN)	1.9E+04	1.8E+04	1.7E+04	1.8E+04	1.8E+04	1.9E+04
			capacity	(kN)	3.7E+04	3.7E+04	4.4E+04	3.7E+04	3.7E+04	3.0E+04
			ratio		51%	47%	39%	48%	56%	63%
				OK	OK	OK	OK	OK	OK	
Type		response	(kN)	1.5E+04	1.5E+04	1.6E+04	1.8E+04	2.0E+04	1.7E+04	
		capacity	(kN)	3.8E+04	3.8E+04	4.5E+04	3.8E+04	3.8E+04	3.0E+04	
	ratio		40%	40%	35%	48%	53%	55%		
			OK	OK	OK	OK	OK	OK		
(3)Residual Displacement	Axial Direcion	Type	response	(m)	0.033	0.030	0.026	0.025	0.026	0.028
			limit	(m)	0.400	0.432	0.267	0.267	0.347	0.425
					OK	OK	OK	OK	OK	OK
		Type	response	(m)	0.052	0.049	0.044	0.041	0.042	0.044
			limit	(m)	0.400	0.432	0.267	0.267	0.347	0.425
					OK	OK	OK	OK	OK	OK
	Perpendicular Direcion	Type	response	(m)	0.060	0.064	0.015	0.016	0.082	0.063
			limit	(m)	0.400	0.432	0.267	0.267	0.347	0.425
					OK	OK	OK	OK	OK	OK
		Type	response	(m)	0.000	0.000	0.003	0.010	0.020	0.000
			limit	(m)	0.400	0.432	0.267	0.267	0.347	0.425
					OK	OK	OK	OK	OK	OK

**(2) Check of main girders**

In the check conducted for the bridge axial direction, it was confirmed that the

response bending moment in the in-plane direction acting on the main girder was within the initial yield moment of the axial direction reinforcements in both the top of the upper slab and the bottom of the lower slab (Fig. 5). To resist positive bending, the axial direction reinforcements in the bottom slab were upgraded throughout the entire length of the bridge, which were replaced up to D25 at 125 mm pitch. In addition, negative bending was increased at side spans according to vibration mode in Fig.4 a). That is due to the great length of the side spans at both ends (92.8 m) and the fact that the ends were supported by bearings. So the axial direction reinforcements for the top slab near the center of the span were also upgraded to D25 at intervals of 125 mm.

The check conducted for the direction perpendicular to the bridge axis confirmed that the response bending moment in the out-of-plane direction acting on the main girder was within the initial yield moment of the axial direction reinforcements on the outside of the web.

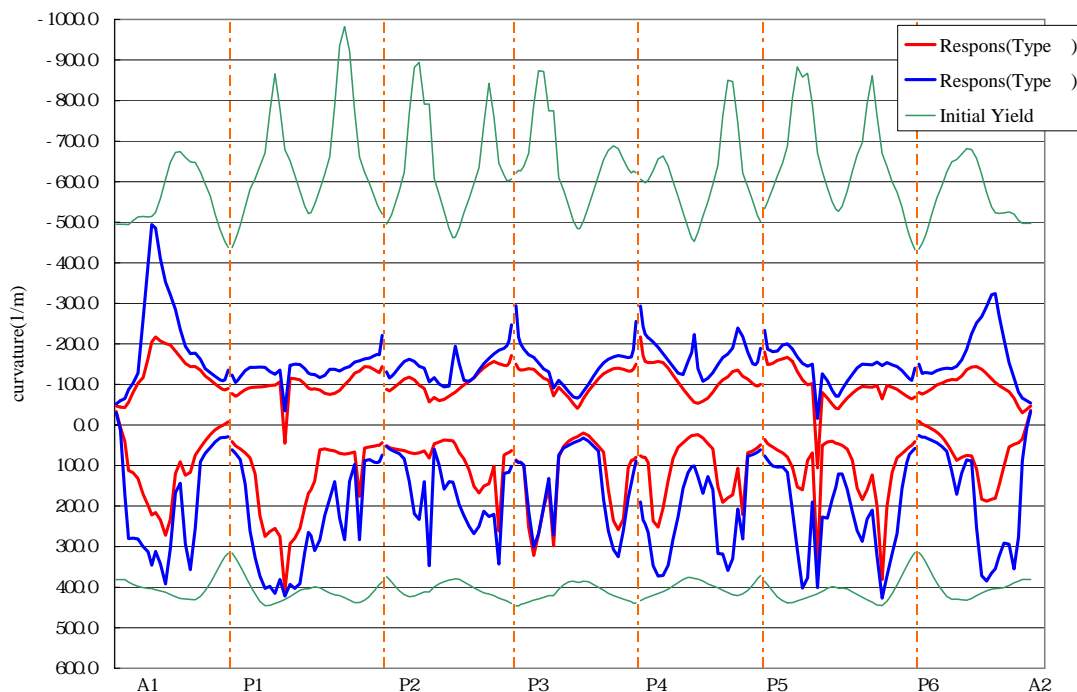


Fig.5 Maximum Response Curvature on the Main Girder of Level 2 Ground Motion

#### **4. Approach to future construction**

On this bridge, the eastbound and westbound lines are separated, but as access is restricted in some areas, the eastbound lanes will be constructed first. The major overall processes for the construction are as follows:

1. Ground leveling for construction road and work yard
2. Caisson foundation construction
3. Bridge pier construction
4. Pier caps

5. Cantilever erection work
6. Bridge surfacing

The cantilever erections of the main girders will be built up at once for all bridge piers to shorten the construction time.

Below is a description of the below-grade footings for short piers and the horizontal stress application method for displacement adjustment during closure of the main girders, methods that were adopted to achieve the characteristic rigid frame structure of the bridge.

**(1) Below-grade footings for short piers**

Below-grade footings are used for short piers to achieve the continuous rigid frame structure. On lower piers P3 and P4, the top surfaces of the foundations are placed below the surface of the ground to adjust the pier height. There are kept hollow with covers without backfilling between these piers and ground to prevent the pier from being subjected to ground resistance in the event of an earthquake. The cover can be removed and steps are hung to enables us to descent to the base of the pier for inspection after an earthquake. (see Fig. 6).

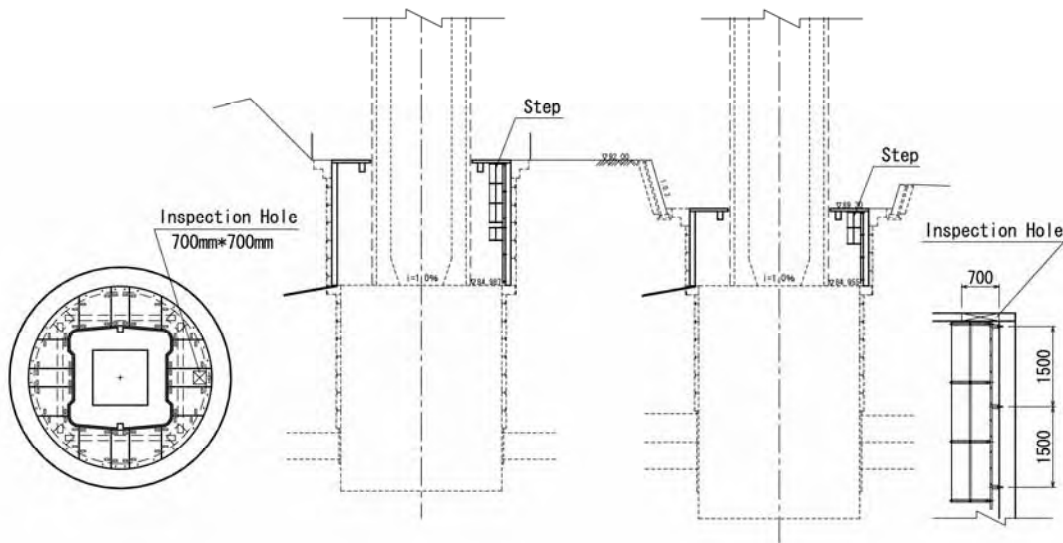


Fig.6 Below-Grade Footings for Short Piers

**(2) Horizontal stress application for displacement adjustment**

As this bridge has a long fixed span, the creep and dry shrinkage of concrete that may be large after the main girders have been completed will increase the bending moment applied to the end piers. Normally, under the condition of the bridge being subjected to dead load and temperature fluctuations, the section at the base of the end piers must be larger than those of the other bridge piers. As a result, the foundation structure of the end piers must also be larger.

In order to avoid this, before the main girders between end piers P1, P6 and the next pier P2, P5 are closed, horizontal force is applied to reduce the bending moment

that acts on the end piers. It enables to reduce the section force about 28% and to keep the reinforcement stress within the acceptable limit. Fig. 7 shows a conceptual diagram of the adjustment method.

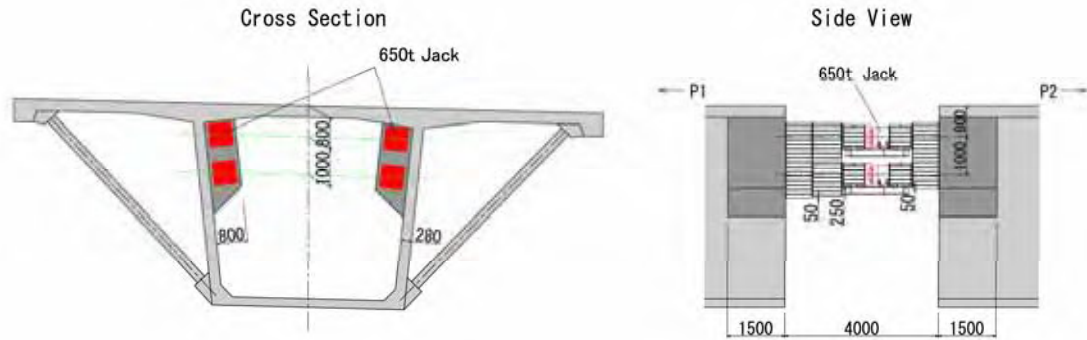


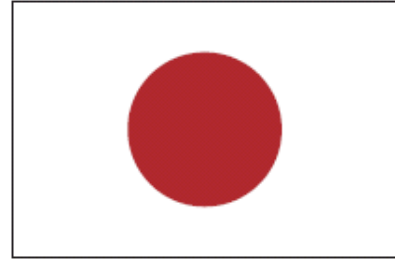
Fig.7 Horizontal Stress Application

## **5. Conclusion**

This paper has described the structural form adopted for the Gunkai-gawa Bridge, which was ordered as a design and build package project. There were three methods used to achieve the structure of this bridge. An overview of the seismic design of the structure was also presented. There are few examples of the construction of long, continuous rigid frame structures such as this bridge that also has a low bridge pier height. It was confirmed that the bridge which has a rigid-coupled structure that emphasizes simple maintenance also provides excellent earthquake-resisting capacity.

As of September 2009, construction of the Gunkai-gawa Bridge was at the stage of leveling the land for the construction road, so the work has just begun. A detailed construction plan will be drafted for the completion of the bridge, and thorough attention will be given to quality control and safety management.

blank



# **25<sup>th</sup> US-Japan Bridge Engineering Workshop**

## **Session 7**

### **Seismic Retrofit**

Seismic Retrofit Study of CABLE-STAYED Bridge on TOKYO-GAIKAN EXPRESSWAY

By Tsutomu Yoshioka, Yoshinori Kawahira, and Kouichirou Shitou

Repair of High Shear Standard Reinforced Concrete Bridge Columns Using Cfrp

By M. "Saiid" Saiidi and Ashkan Vosooghi

Seismic Retrofit Techniques for Reinforced Concrete Bridge Columns with Combination of FRP Sheet and Steel Jacketing

By Guangfeng Zhang, Shigeki Unjoh, Jun-ichi Hoshikum, and Junichi Sakai

Development and Refinement of Illinois' Earthquake Resisting System Strategy

By Daniel H. Tobias, Jerome F. Hajjar, Ralph E. Anderson,

James M. LaFave, Chad E. Hodel, Larry A. Fahnestock, William M. Kramer,

Joshua S. Steelman, Patrik D. Claussen, Kevin L. Riechers, and Mark D. Shaffer

Page Left Blank

# SEISMIC RETROFIT STUDY OF CABLE-STAYED BRIDGE ON TOKYO-GAIKAN EXPRESSWAY

Yoshinori Kawahira<sup>1</sup>, Kouichirou Shitou<sup>2</sup> and Tsutomu Yoshioka<sup>3</sup>

## **Abstract**

This paper describes the seismic performance verification and retrofit method examination of a cable-stayed bridge in the Sakitama Bridge. First, the input earthquake motion was specified for use in both the target seismic performance and the bridge verification, while the parts and members of the latter were verified by seismic response analysis. The main tower and caisson foundation that were difficult to evaluate were verified by a nonlinear finite element analysis. Based on the verification results, regions requiring a seismic retrofit were identified, and the retrofit methods were examined.

## **Introduction**

The imminence of large-scale earthquakes, namely the Tokai, Tonankai and Nankai Earthquakes has been pointed out in Japan in the near future. During the three-year period from FY 2005 to FY 2007, the Ministry of Land, Infrastructure, Transport and Tourism has focused on the seismic retrofit of bridges on emergency routes that would play important roles during earthquakes [1]. Under this Three-Year Program, in addition to bridges built before the 1980 edition of the Design Specifications for Highway Bridges was established, special structures and long-span bridges were also designated as targets of the seismic retrofit.

As the emergency transportation route, the Tokyo-Gaikan Expressway would assume vital roles in rescue and relief activities and emergency transportation during a large-scale earthquake (Fig. 1). The Sakitama Bridge on this Tokyo-Gaikan Expressway is located in Bijogi, Toda City, Saitama Prefecture, and crosses the Arakawa River (Fig. 2). The cable-stayed bridge in Sakitama Bridge has a special structure, and was therefore selected for the examination of a seismic retrofit under this Three-Year Program. This paper describes both the seismic performance verification and retrofit method of the cable-stayed bridge in Sakitama Bridge.

## **The Outline of the Studied Bridge**

Figure 3 shows a general view of a cable-stayed bridge in the Sakitama Bridge. This cable-stayed bridge is carrying both the expressway and general road (National Highway Route 298) of the Tokyo-Gaikan Expressway. The two bridges are arranged in a parallel for inbound and outbound routes.

This cable-stayed bridge lays the cables in a multi-fan type in a single plane. It

---

<sup>1</sup> Head Manager Management Section, Kitashuto National Highway Office

<sup>2</sup> Deputy director, Misato management office, East Nippon Expressway Co.,Ltd.

<sup>3</sup> Chief, Maintenance Engineering Research Institute, Nippon Engineering Consultants Co., Ltd.



Fig.1 Location of Sakitama Bridge



Fig.2 Photo of Sakitama Bridge

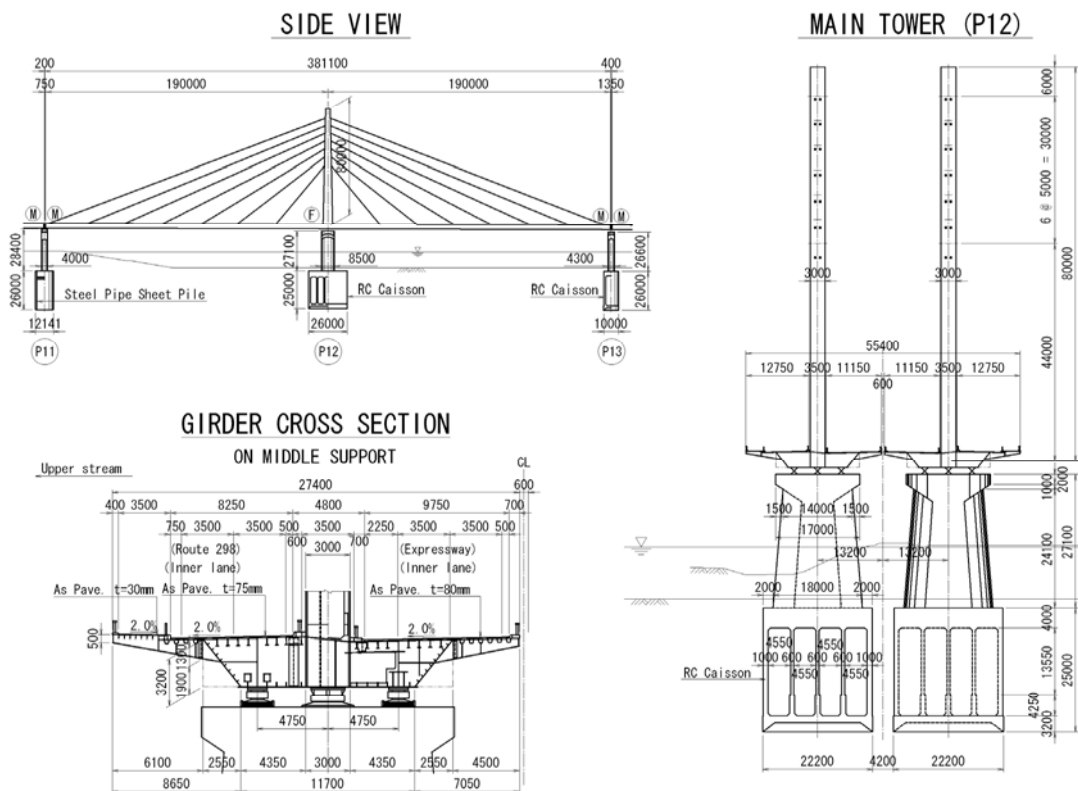


Fig.3 General view of Sakitama Bridge

is 2-span continuous steel cable-stayed bridge with a span length of 190m. The main tower is a single post type and made of steel. The main girder is a steel box girder with 3-cell, with a total width of 26m. The main tower and main girder are rigidly connected, and connected to the pier via the bearing support. The piers from P11 to P13 are all of the RC wall type. The bearing support condition in the longitudinal direction is fixed only on P12 pier, the middle support. A pivot bearing is installed on P12 and pivot roller bearings are installed on P11 and P13, which are the end supports. The bearing support condition in the transverse direction is all fixed, and wind bearings to be used

for fixing the transverse direction are installed on P11 and P13, which are the edge supports. Rocking bearings for controlling uplift are also installed on P11 and P 13. The ground is predominantly soft to a depth of about 25m from the surface; mainly comprising a cohesive soil layer, the N value of which is around 3 to 11. The primary natural period of the surface ground is 0.68 to 1.08 sec., and the ground is specified as Ground Type III in the Design Specifications for Highway Bridges. The foundation type of P11 is a steel-pipe-sheet pile foundation, and those of P12 and P13 are pneumatic caisson foundations.

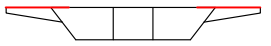
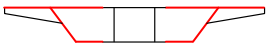
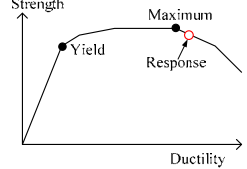
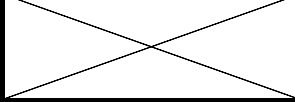
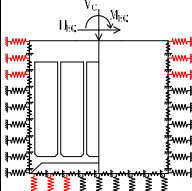
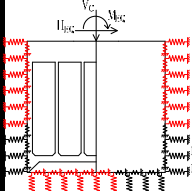
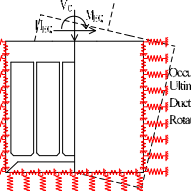
This bridge is based on the design standard specified in the Design Specifications for Highway Bridges of 1980 that was issued before the seismic design standards on highway bridges were revised in 1996, following the Hyogo-ken Nanbu Earthquake in 1995. Therefore, this bridge is designed to ensure seismic performance only for earthquakes (level 1 earthquake motion) highly likely to occur during the service life, and may not potentially satisfy the seismic performance for earthquakes (level 2 earthquake motion) not likely to occur but of high intensity. The cable-stayed bridge for the inbound route has been in service since 1992, and that for the outbound route since 1998.

### **Seismic Retrofit Basic Policy**

Based on the Seismic Design Edition of the Design Specifications for Highway Bridges [2] and the Three-Year Program of Seismic Retrofit of Bridges on Emergency Routes [1], the target seismic performance for the level 2 earthquake motion incurred by the cable-stayed bridge in Sakitama Bridge requires that it should sustain only limited damage from level 2 earthquake motion, and be capable of swiftly reverting to its main function as an emergency road. The performance is intended to ensure safety against the risk of the bridge collapsing, and facilitate the traffic of emergency vehicles for disaster recovery activities after earthquakes. The performance is also intended to allow ordinary vehicles to use the road only with emergency repairs, and allow permanent repairs to be made while the bridge is in service.

To meet the above-mentioned requirements of the target seismic performance, the critical state of the structural elements comprising the bridge must be set. Table 1 shows the division of the damage level of each member and the required performance for level 2 earthquake motion. The main girder is intended to avoid local buckling on the deck plates in the driving lanes of emergency vehicles, and the floor system that supports the deck plates is intended to yield only slightly and remain strong enough to bear the load of the emergency traffic. The main tower is intended not to succumb to local buckling, but to yield slightly in its marginal section, and remain strong enough to bear the load of emergency traffic. The cables are intended neither to succumb to falling away due to loss of cable tension, nor break when subject to tensile force. The bearing is intended to maintain the force applied to the component parts below the maximum strength. The pier is intended to tolerate major ductility but to confine it to an extent facilitating prompt repairs. The foundation is intended to tolerate ductility provided the ductility limits deformation to a level that is not destructive to the overall safety of the bridge system.

Table.1 Classification of damage level of bridge members for level 2 earthquake

Bridge members		Degree of damage for structure		
		← Slight damage		→ Severe damage
		Damage level I	Damage level II	Damage level III
Main girder	In plane derection	A state that occurrence stress degree slightly exceeded a yield stress degree	A state in the domain that was stable as for the strength and the ductility although the plasticity spread	A state that a strength as the main beam system has begun to deteriorate
	Out plane derection	A state that the deck plate which stretched caused local buckling, and the box girder inside slightly yield 	A state that local buckling and plasticity progressed to the box girder inside 	A state that a strength as the main beam system has begun to deteriorate 
Main tower	A state that occurrence stress degree slightly exceeded a yield stress degree, But local buckling at the elastic level does not occur	A state in the domain that was stable as for the strength and the ductility although the plasticity spread	A state that a strength as the main tower system has begun to deteriorate	
stay cable	A state that tensile stress degree exceeded a yield stress degree (0.7% elongation strength) in one cable $\sigma > \sigma_y (= \sigma_u / 1.4)$	A state that tensile stress degree exceeded a yield stress degree (0.7% elongation strength) in plural cables $\sigma > \sigma_y (= \sigma_u / 1.4)$	A state that a cable was falling away by tension loss in plural cables, and tensile stress degree exceeded break strength $\sigma > \sigma_u$	
Bearing support	A state that occurrence horizontal force exceeded the smallest yield strength in their component parts $P_v < P \leq P_u$		A state that occurrence horizontal force exceeded the smallest maximum strength in their component parts $P > P_u$	
RC pier	A state that cracking of the concrete and yield of the reinforcement occur, but have still redundancy for maximum strength $1.0 < \mu_r \leq 1.2$	A state that cracking of the concrete and yield of the reinforcement spread, but have stability for the strength and the ductility $1.0 < \mu_r \leq \mu_a$	A state that a strength as the pier system has begun to deteriorate $\mu_r > \mu_a$ $S > P_s$ $\delta_R > \delta_{Ra}$	
Foundation (P12,13 : caisson) (P11 : Steel pipe sheet pile)	A state that plasticity of the around ground and foundation slightly float 	A state that foundation yield, and foundation floating and plasticity of the around ground spread through 	A state that foundation strength deteriorated and lost stability of the superstructure 	

\* The bold frames show that it is a limit state to satisfy required performance.

Figure 4 shows an outline of the seismic retrofit examination on the cable-stayed bridge. After specifying the target seismic performance for level 2 earthquake motion, the seismic performance verification of the current structural system is performed via seismic response analysis. Regarding the input earthquake motion, we initially examined the need to prepare site waves taking regional characteristics into consideration. Consequently, it emerged that there was no information concerning the active fault near the Sakitama Bridge that required realistic consideration of an earthquake. Therefore, we decided to use the standard waves (type II of level 2 earthquake motion) in the Design Specifications for Highway Bridges established based on the Hyogo-ken Nanbu Earthquake of 1995. For plate-boundary earthquakes, we also decided to use the standard waves (type I of level 2 earthquake motion) in the Design Specifications for Highway Bridges because we considered that this bridge would be affected mainly by an inland direct strike type earthquake, and that no effect

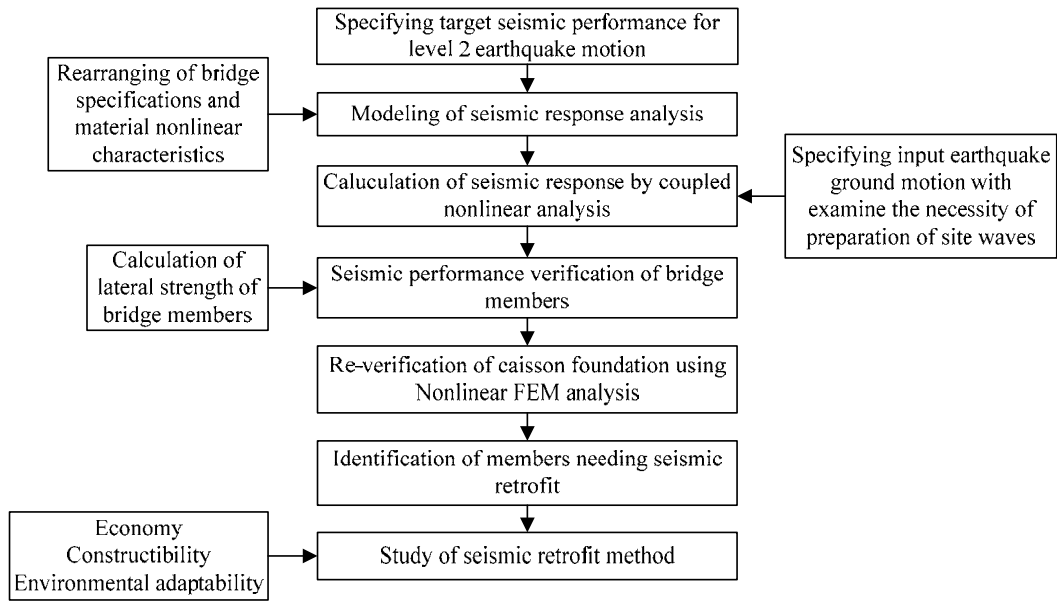


Fig.4 Flow of seismic retrofit design

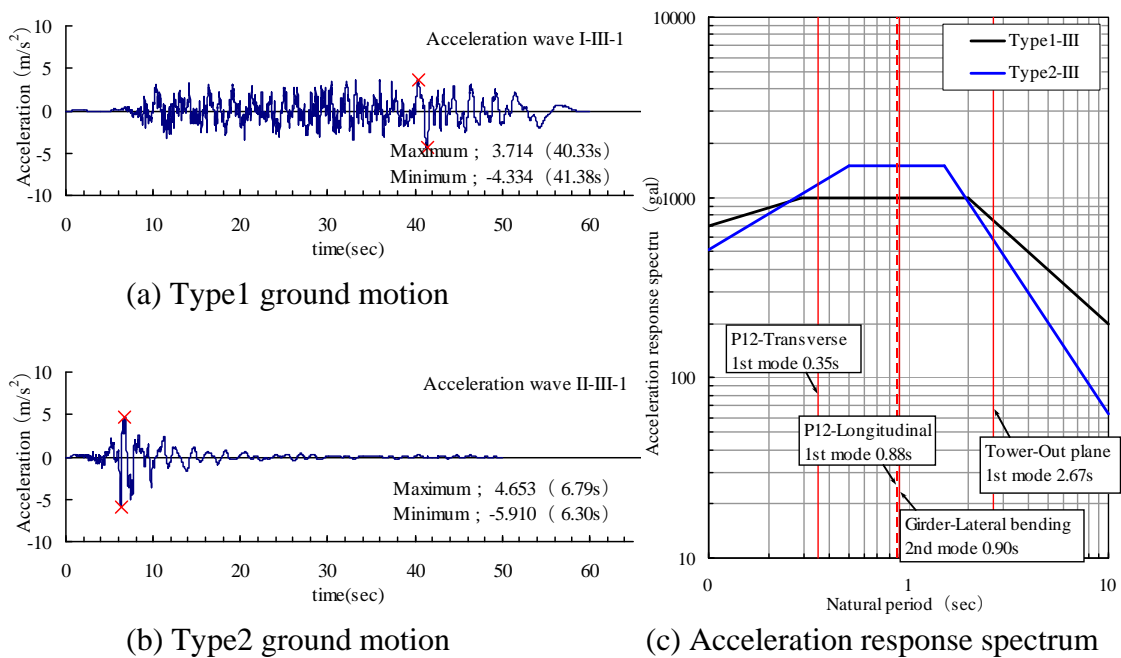


Fig.5 Design earthquake ground motion

could be expected from the preparation of site waves. Figure 5 shows the time history response waveform and acceleration response spectrum of the representative 1 wave of types I and II.

### Seismic Response Analysis Model

Before performing a seismic response analysis, we calculated the lateral strength of the bearing support, pier and foundation, and estimated the damage sequence. As shown in Fig. 6, the lateral strength of the caisson foundation of P13 in

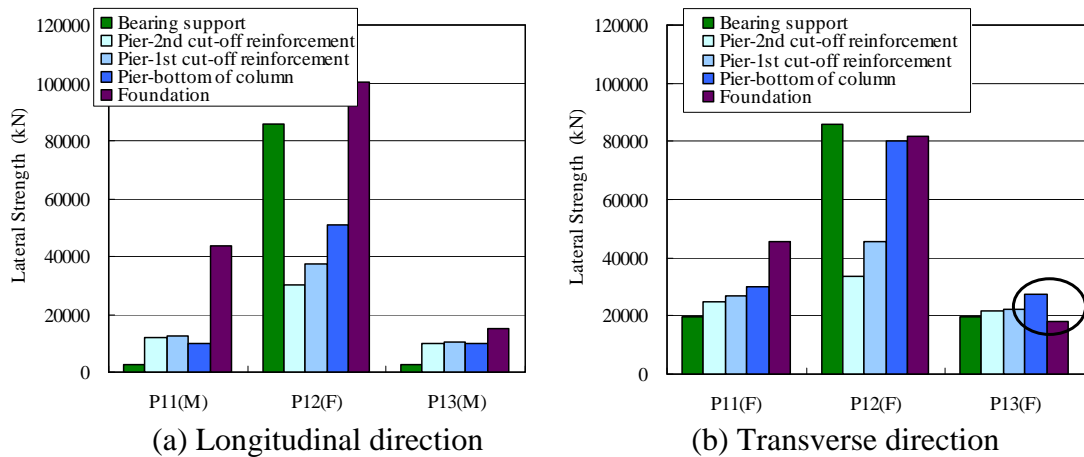


Fig.6 Comparison of lateral strength capacity of each member

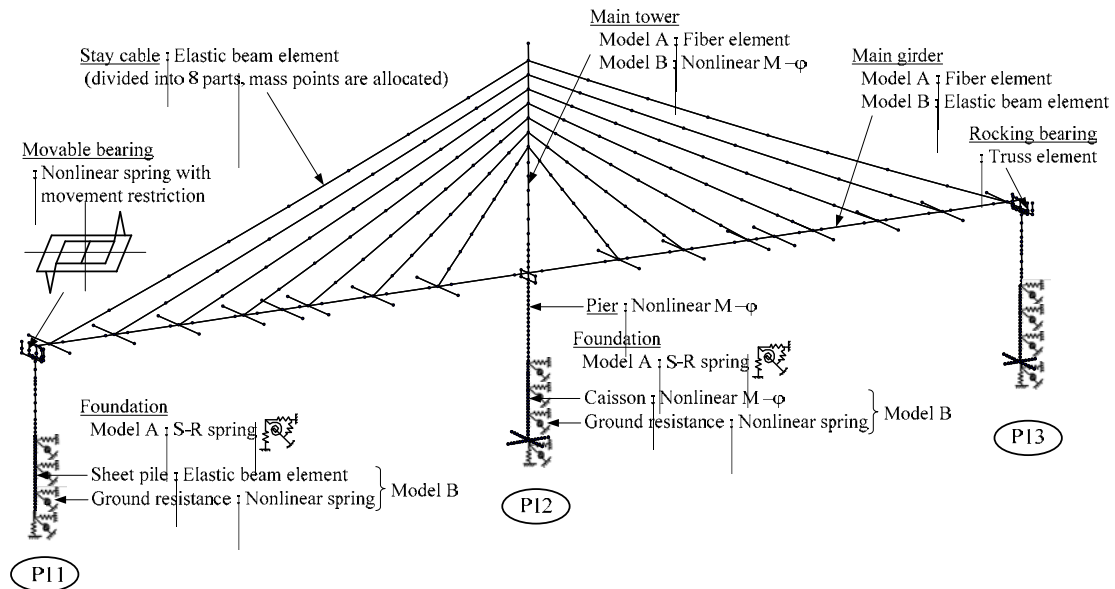


Fig.7 Analytical model

the transverse direction is lower than that of the pier, and the surface ground is soft. Accordingly, it is necessary to perform seismic performance verification of each part and member via seismic response analysis that takes account of the ductility of the foundation. As for the main girder made of orthotropic steel deck 1-box girder, the overhang of the deck is long, and number of ribs of the sidewalk is small. It is therefore highly probably that the main girder will buckle by an earthquake in the transverse direction, and it is advisable to use fiber elements that allow us to properly consider the nonlinearity of the material in complicated sectional form. However, the calculation load of the analysis that takes account of the plasticity of both the foundation and main girder is significant, and the calculation result is complicated. As shown in Fig. 7, we therefore decided to perform seismic response analyses on two cases; one for the case where the foundation is assumed to cause no ductility (Model A), and the other case where the ductility of the foundation is taken into consideration (Model B).

In Model A, the foundation is replaced with a sway-rocking spring, and the main girder is modeled with a fiber element; likewise the main tower and pier. Each

cable is subdivided into 8 parts, and mass allocated to take into account the vibration of cable itself. The rocking bearing is modeled with a truss element, and resistance in the longitudinal direction is taken into account. To take ductility of the foundation in Model B into consideration, the caisson foundation is a nonlinear girder element  $M-\phi$  model, and ground resistance is modeled with a nonlinear spring. The main tower and pier are also  $M-\phi$  models and thus the same as the foundation. To restore their force characteristics, the main tower is a movement hardening type tri-linear model, and the pier and caisson foundation are degrading type tri-linear models, while the main girder is an elastic beam element. The movable bearings on P11 and P13 are nonlinear springs that take account of both frictional resistance and movement restriction.

The material and geometrical nonlinear dynamic analysis of these Models A and B was performed using input seismic motion shown in Fig. 5. Rayleigh damping is used for viscous damping in a dynamic analysis. Rayleigh damping is set to include main modes by the natural vibration analysis performed in advance (Fig. 8). The Newmark- $\beta$  ( $\beta=0.25$ ) method is used as the numerical integration. The computation time interval is 0.002 seconds.

The main girder, and the cable significantly affected by the ductility of the main girder are verified using the result of Model A, while other parts are verified using that of Model B.

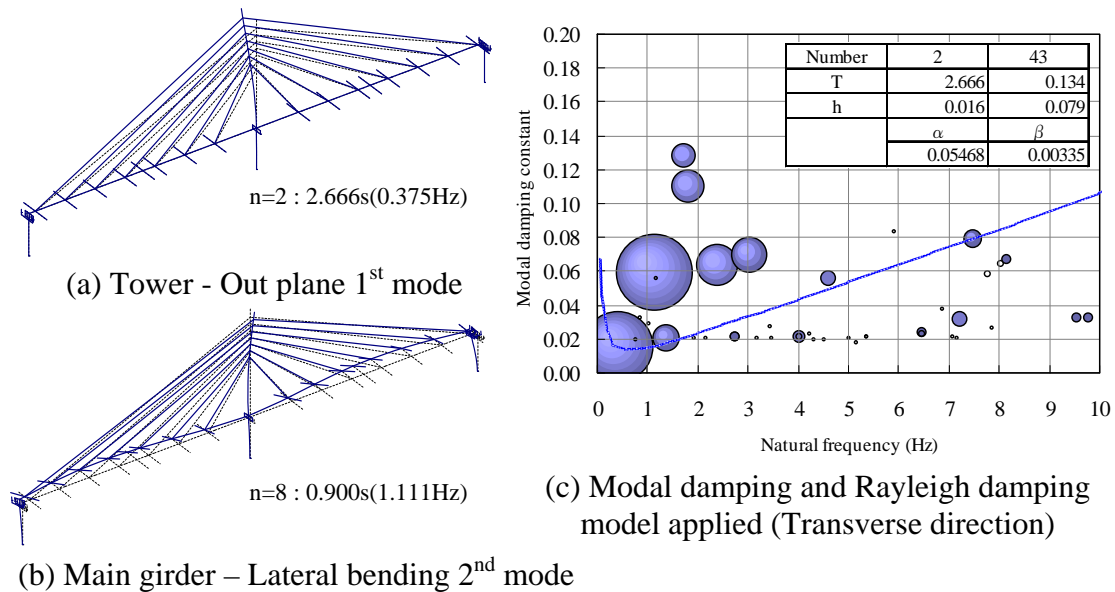


Fig.8 Natural vibration modes and modal damping (Model A)

### Seismic Performance Verification of Members

This section describes the details of the seismic performance verification performed using the seismic response that was calculated by material and geometrical nonlinear analysis, and also using either the load-carrying capacity or deformation performance of the bridge members.

The main girder was significantly affected by the earthquake in the transverse direction. The result of Model A that used fiber elements showed local ductility in both the sidewalk deck plate and the box girder, up to about  $4\epsilon_y$ , and  $2.5\epsilon_y$  respectively (Fig. 9). However, the nonlinear finite element analysis results suggested that the undulation

of the road surface after local buckling was so small that the serviceability of the road could be ensured after earthquake (Fig. 10). Consequently, the damage level was evaluated as I, and no retrofit was deemed necessary.

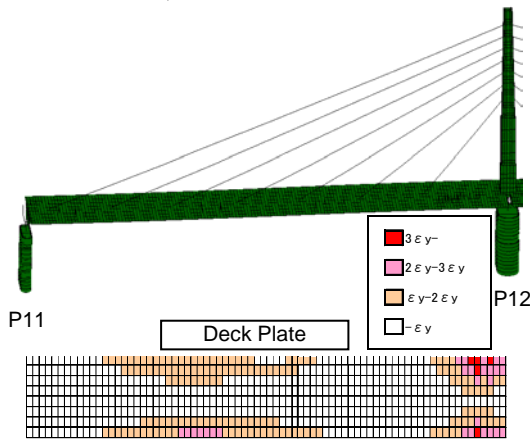


Fig.9 Strain distribution of deck plate (Dynamic analysis result by Model A)

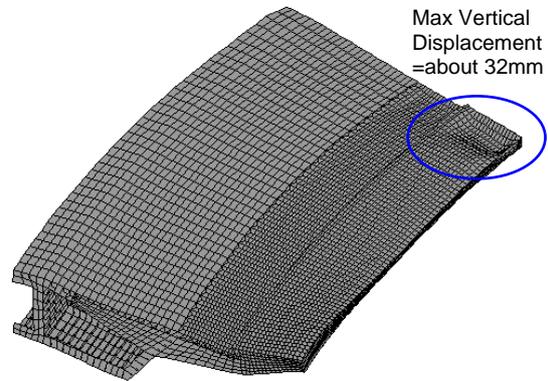


Fig.10 Deformation of deck plate (Nonlinear FEM analysis result)

The cables were affected predominantly by an earthquake in the longitudinal direction, however, the maximum tensile stress caused by earthquake was  $773\text{N/mm}^2$ , namely well below the 0.7% elongation strength  $\sigma_y (=1160\text{N/mm}^2)$  (Fig. 11). The minimum tensile stress was  $151\text{N/mm}^2$ , and the cable has no tension loss. Accordingly, there is no damage.

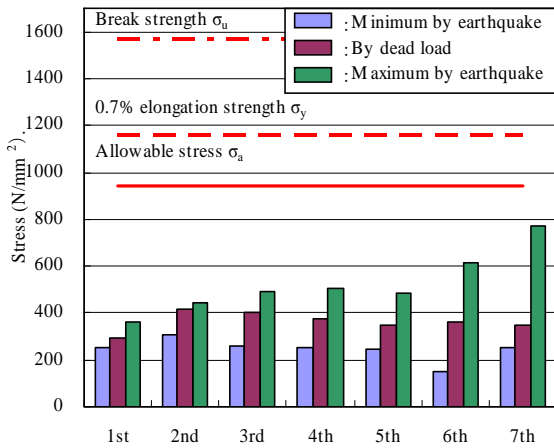


Fig.11 Performance verification result of stay cables (Longitudinal direction, Type2 earthquakes)

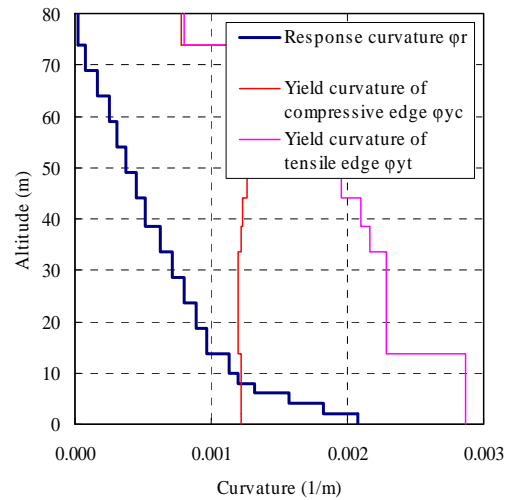


Fig.12 Curvature distribution of tower (Transverse direction, Type1 earthquakes)

The main tower was affected by a type I Earthquake in the transverse direction such that it caused local buckling in the elastic region within the range of about 26m from the foundation. For this reason, longitudinal ribs are added to control the width-thickness ratio parameter and keep it within the limiting value specified in the Design Specifications for Highway Bridges. Assuming that the parameter was

improved, the post-yielding behavior was observed, whereupon the tower was seen to show slight ductility within a range of about 8m from the foundation (response plasticity rate  $\mu_r=1.38$ ) as shown in Fig. 12. The P- $\delta$  curve of the main tower was calculated by nonlinear finite element analysis. The results showed that the tower lacked toughness of the SM570 high strength steel, and that its ductility capacity was evaluated as around 1.79 (Fig. 13). It was so close to the response value and difficult to evaluate the damage as level I, consequently, ductility enhancement measures were deemed necessary to reduce the deformation.

Table 2 shows the result of verification of the bearing supports. The maximum response horizontal force of the pivot bearing on P12 exceeded the yield strength, however, it was lower than the maximum strength. Consequently, the damage level was evaluated as level I, and the pivot bearing was deemed to satisfy the required performance. The maximum horizontal displacement of the pivot roller bearings on P11 and P13 exceeded the movement capacity, and the upper bearing collided with the stopper. However, the maximum horizontal force generated on the stopper was less than the maximum strength, hence no retrofit was deemed necessary. The maximum tensile force generated on the rocking bearing was less than the yield strength, hence the rocking bearing was to cause no damage. The maximum horizontal force generated on the wind bearing exceeded the maximum strength, hence suggest the potential for

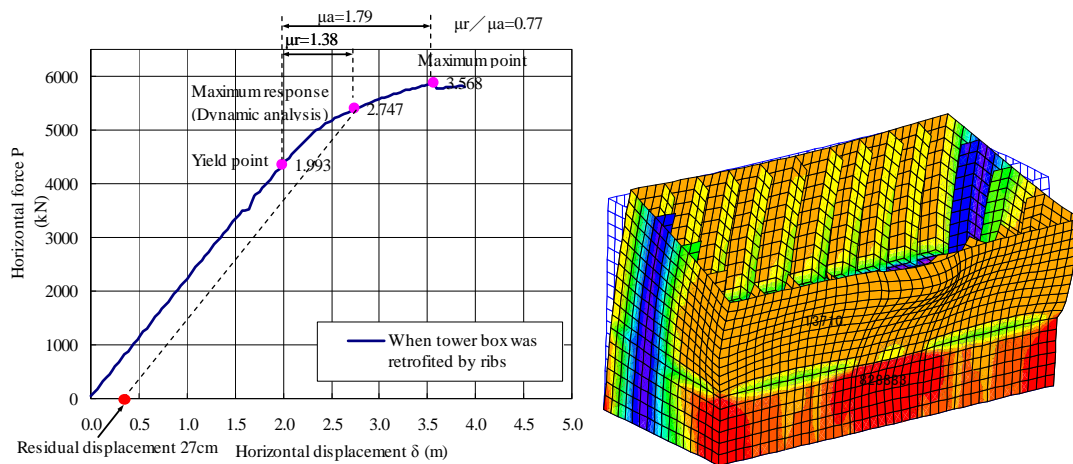


Fig.13 Nonlinear FEM analysis result of tower (Transverse direction, Type1 earthquakes)

Table.2 Performance verification result of bearing supports

Bearing support	Support No.	Response quantity	Seismic direction	Maximum response	Capacity		Damage level
					Yield strength	Maximum strength	
Pivot bearing	P12	Force (kN)	LG	56737	50460	85782	I
			TR	53935			I
Pivot roller bearing	P11	Displacement (mm)	LG	110	110	230	I
		Force (kN)	LG	2565	1512	2570	
	P13	Displacement (mm)	LG	106	110	230	0
		Force (kN)	LG	0	1512	2570	
Rocking bearing	P11	Tension (kN)	LG	14476	20937	27561	0
	P13		LG	6035			0
Wind bearing	P11	Force (kN)	TR	19822	11520	19584	III
	P13		TR	17621			III

the components to be broken and moved laterally. If the main girder slides laterally, loads carried by the rocking bearing sharply increases, thus causing the rocking bearing to break. Then, uplift of the main girder may be occurred, and the bridge would not be used for emergency vehicles. For these reasons, the damage level of the wind bearing was evaluated as level III, and a retrofit was deemed necessary.

Figure 14 shows the maximum response force distribution of the pier that corresponds to its failure mode. This figure shows the response distribution of both Models A and B together with that of the foundation. In an earthquake in the longitudinal direction, piers P 11 and P 13 caused ductility to their bases solely by the inertia force of their own weight. In an earthquake in the transverse direction, the maximum shear force of the entire pier, including the cut-off of longitudinal reinforcement at mid-height, exceeded the shear strength, hence the high potential for the piers to succumb to shear failure. Meanwhile, P12 experienced shear failure mode in both longitudinal and transverse directions, with the shear force exceeded its

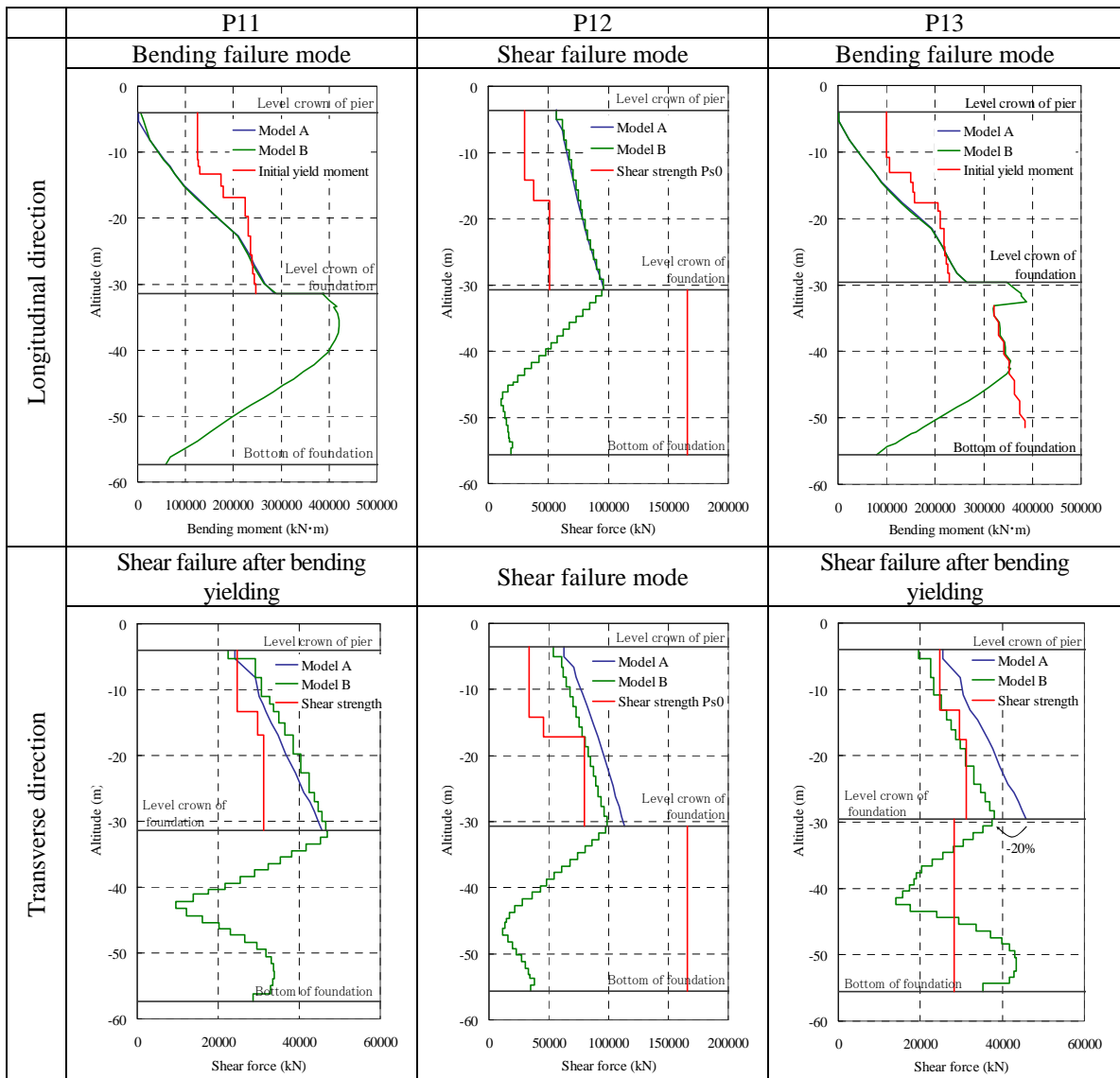


Fig.14 Maximum section force distribution of pier (Type2 earthquakes)

maximum shear capacity in both directions. Based on these results, all piers were evaluated as level III, and some retrofits were deemed necessary. As shown in the shear force distribution in the transverse direction of P13, the maximum horizontal force acting on the crest of the foundation diminished by around 20% in cases where the ductility of the foundation was taken into account. Consequently, such latter cases were considered to be closer to the actual behavior. It was decided to use the value of this case as the acting force to be used to verify the foundation.

Table 3 shows the verification result of the caisson foundation. The verification was performed by a lateral strength approach; using the acting force of the crest of the foundation obtained by a dynamic analysis. The verification of the caisson foundation of P12 showed that the shear force of its members exceeded the shear capacity, although satisfying the stability verification as the foundation. During the verification of the caisson foundation of P13, the shear force exceeded the shear capacity, and its ductility demand of about 27.0 substantially exceeded the ductility capacity of 5.9. The circumferential rebar of the sidewall of the caisson foundation of P13 is the main reinforcement, and bars are arranged using D19@300, while the reinforcement D16@300 in the longitudinal direction is very low. The verification of hollow RC section with low reinforcement based on the beam theory is simple, however, this verification may become over conservative. Therefore, the verification was repeated using nonlinear finite element analysis (see the subsequent section). Meanwhile, the steel-pipe-sheet-pile function of P11 satisfied both the stability and member verifications.

Table.3 Performance verification result of caisson foundations (Transverse direction, Type2 earthquakes)

Performance verification item				P12 caisson		P13 caisson			
				Response	Capacity	Response	Capacity		
Stability verification	Ductility demand of foundation			3.022	<	6.000	26.956	>	5.900
	Plasticity domain rate of foundation front			54.0	<	60.0	55.8	<	60.0
	Float area rate of foundation bottom			35.8	<	60.0	0.0	<	60.0
	Rotation angle of level crown of foundation			0.012	<	0.020	0.039	>	0.020
Verification of members	Vertical section of side wall	Shear	kN	77912	<	162837	52817	>	28727
	Horizontal section of side wall	Bending	kN·m	1277	>	1239	1709	>	1212
		Shear	kN	1153	<	1331	1153	>	411

Figure 15 shows a summary of the verification results showing both the evaluation results of the damage levels of this bridge, and the locations where the required performance were not met when exposed to an earthquake in the transverse direction

### **Seismic Performance Re-verification of the Caisson Foundation**

Figure 16 (a) shows the FE model of the caisson foundation of P13 that was verified in detail using nonlinear finite element analysis. On the FE model, the caisson foundation was modeled with a solid element, and the reinforcement was modeled with a rebar element. The surrounding soil was modeled with a nonlinear spring element, which was arranged at each joint on the peripheral surface. To reduce the computation,

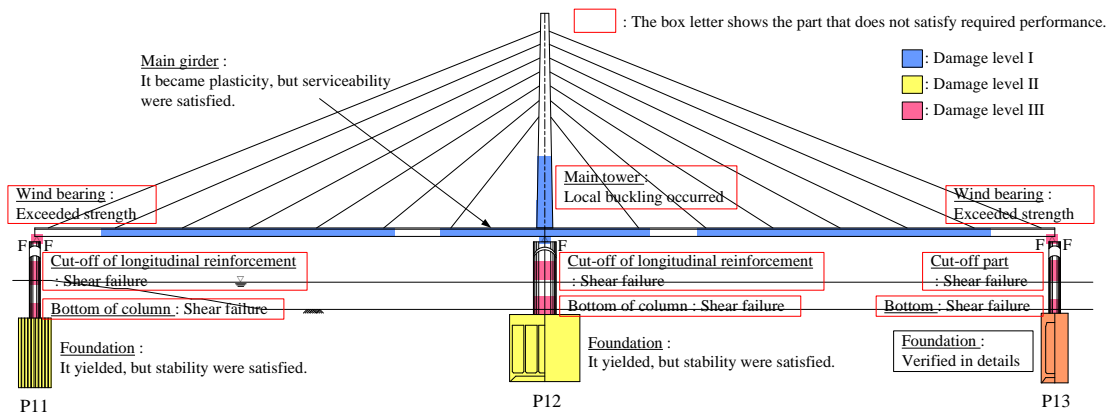


Fig.15 Summary of performance verification result (Transverse direction)

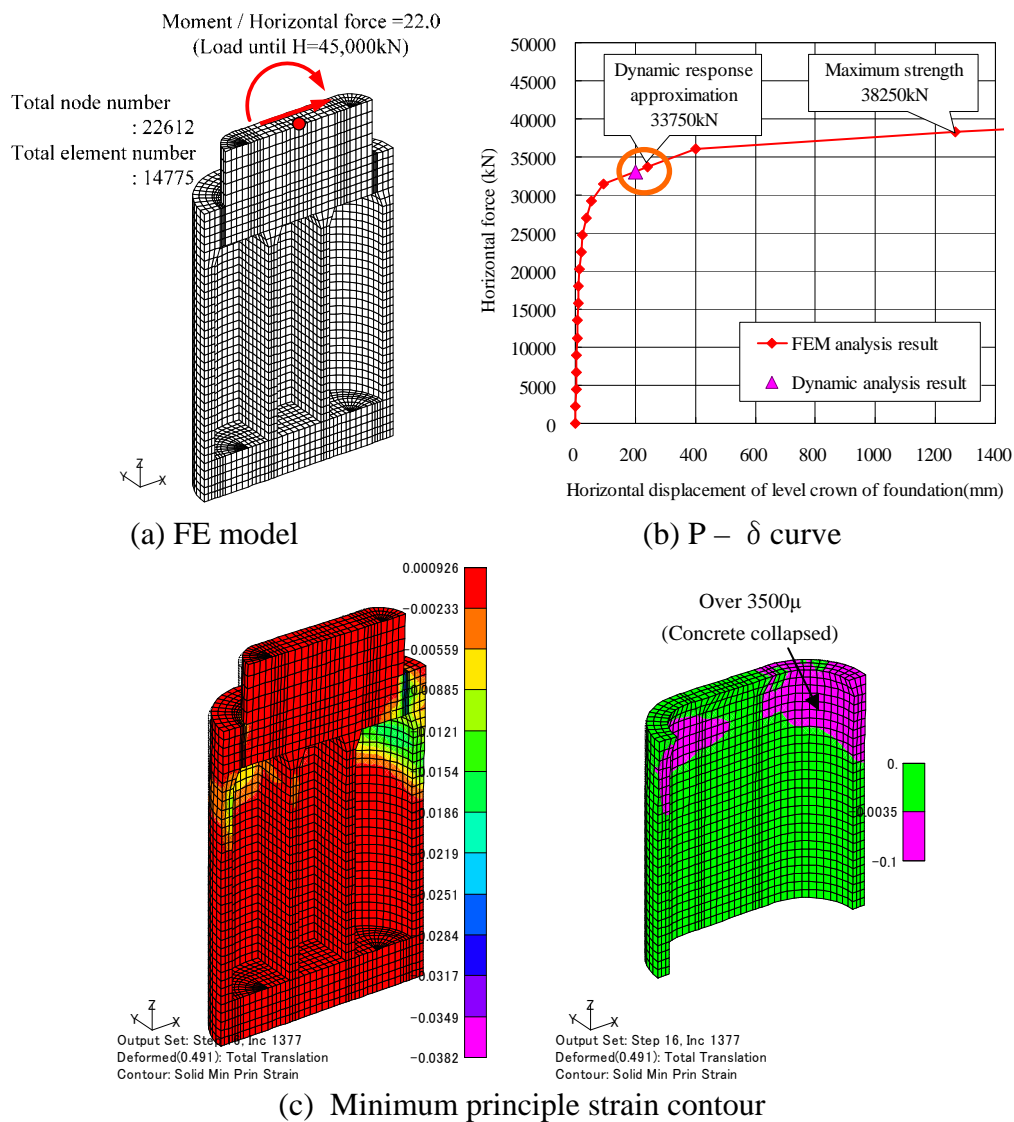


Fig.16 Nonlinear FEM analysis result of P13 caisson (Transverse direction, Type2 earthquakes)

a half model was used for the longitudinal direction. The model used in the analysis involved a 5m portion of the pier and the rigid surface on top of the pier, and the force obtained from the dynamic analysis was applied gradually to the center. The analysis software used for this analysis is the general-purpose finite element program ABAQUS Ver. 6.5.

Figure 16 (b) shows the P- $\delta$  curve obtained from the analysis. Stability verification was performed at the loading step corresponding to the dynamic analysis response of approximately 200mm, the horizontal displacement of the foundation crest. The result showed that the ductility demand of 6.4, although slightly exceeding the ductility capacity of 5.9 that included a safety factor of 1.8, did not reach the ultimate ductility factor of 9.8. The dynamic analysis response value was on the upward gradient region, and assuming that the horizontal strength of 38,250kN were considered, there is 13% margin remained until the strength. Therefore, although the foundation caused plasticity, it was considered the safety was maintained.

The members were checked for the loading steps that corresponded to the dynamic analysis response value. As shown in Fig. 16 (c), stress concentration associated with bending in the upper corner of the sidewall occurred. The right figure shows the minimum principal strain of the concrete expressed with the contour in two colors, when the ultimate strain was 3,500 $\mu\epsilon$ . This stress concentration exceeded the ultimate strain, and there was a possibility of causing spalling of cover concrete, and buckling and expansion of reinforcement. However, the dead load analysis performed on a model with no members in the circular area of the sidewall revealed that the stresses on the linear section of the side and partition walls were approximately half the allowable stress. Based on this result, it was considered that the members were able to support the dead load caused by the level 2 earthquake motion.

As described above, the caisson foundation was reevaluated by nonlinear finite element analysis, and the result showed that it was able to satisfy the stability requirements. However, the validity of this analysis method has not yet been confirmed by experiments. PWRI is now conducting experimental research into the caisson foundation of low steel reinforcement.

### **Areas Requiring Retrofit and Retrofit Details**

Based on the seismic performance verification results described above, Fig. 17 shows a summary of the areas requiring retrofit and the details.

As for the main tower, its width-thickness ratio parameter had to be improved, and increasing flexural strength at its tower base is necessary. For these reasons, we adopted a strengthening method involving installing stiffing ribs bolted on the exterior surface and these be continuous at cross ribs and diaphragms.

For the wind bearing, two methods were compared: 1) replacing the bearing, and 2) installing a structure limiting excessive displacement. Finally the method involving the replacement of only the upper bearing was adopted from an economic reason.

Regarding the piers, P11 and P13 incurred bending damage solely due to the inertia force due to their own weight, making it difficult to adopt retrofit methods by making use of dispersion of inertia force and seismic isolation. Consequently, the RC piling method was adopted for all three piers. For its construction method, a

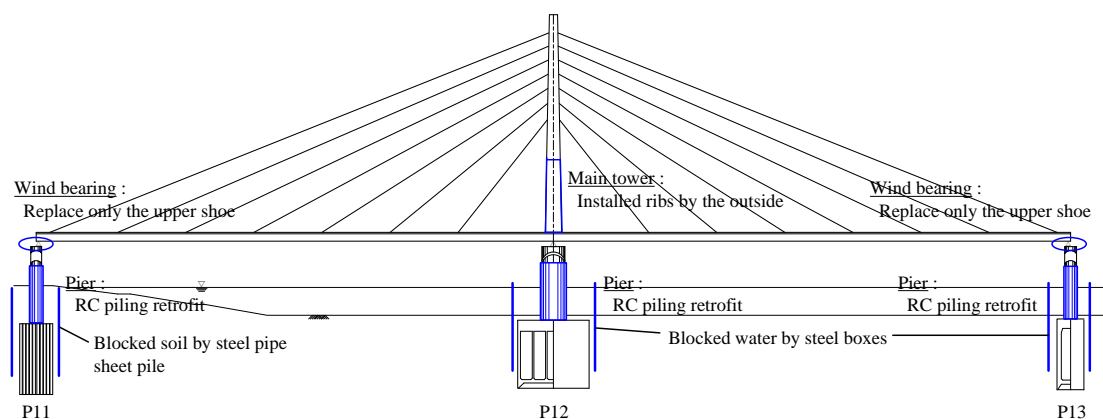


Fig.17 Seismic retrofit measures

comparative investigation was conducted between the PC confined method that allowed underwater placement, and the method involving blocking of water by steel casings to allow work to be performed in a dry condition. The latter method was adopted because of the significant advantages in terms of both construction period and cost and low impact on water quality.

### **Conclusion**

The seismic performance of the cable-stayed bridge in Sakitama Bridge was examined. Retrofit was deemed necessary for the tower, wind bearing, and piers to ensure the target seismic performance. For the caisson foundation, however, the necessity of the retrofit will be re-examined after the results of experimental research now conducted by PWRI becomes available.

### **Acknowledgments**

We highly appreciate "Sakitama Bridge Seismic Retrofit Examination Committee (Chair, Shigeki Unjou, Earthquake Disaster Researcher, NILIM)" for their valuable opinion and comments.

### **References**

- [1] Ministry of Land, Infrastructure, Transport and Tourism: Three-Year Program of Seismic Retrofit of Bridges on Emergency Routes, June 2005 (in Japanese).
- [2] Japan Road Association: Design Specifications for Highway Bridges, Part V Seismic Design Edition, Maruzen, March 2002.

# REPAIR OF HIGH SHEAR STANDARD REINFORCED CONCRETE BRIDGE COLUMNS USING CFRP

Ashkan Vosooghi<sup>1</sup> and M. Saiid Saiidi<sup>2</sup>

## Abstract

Two circular, high shear RC columns were designed identically using current bridge seismic codes. They were damaged to near failure using one of the shake tables at the University of Nevada, Reno. The columns were repaired using unidirectional carbon fiber reinforced polymer (CFRP) jacketing and retested to evaluate the repair performance. The loose concrete was removed and the spalled area was repaired using a fast-set non-shrink mortar. The cracks were epoxy injected. Different number of CFRP layers and different repair mortar and application method were used for the columns. The results indicate that the strength and drift capacity of the columns were fully restored. In addition, it was found that spirals maintain approximately 50% of their capacity even when the column damage is severe.

## Introduction

Past effort in seismic design of concrete bridges has been on detailing of bridges to prevent collapse. During earthquakes, reinforced concrete bridge columns are designed to undergo cracking, spalling, and yielding of steel and provide significant rotational capacity at plastic hinges so that the integrity of the overall structure is maintained. With proper design and construction, this objective can be met. However, the serviceability of the bridge after the earthquake is in question. Rapid and effective repair methods are needed to enable quick opening of the bridge to minimize impact on the community.

As part of this study, two 1/3 scale high shear standard RC bridge columns, which were damaged to the highest repairable level in the previous tests, were repaired using CFRP wrapping. At this level of the damage, many spirals and longitudinal bars are visible, some of the longitudinal bars are beginning to buckle, and the edge of concrete core is damaged. No bar is ruptured.

## Column Models

NHS1 and NHS2, New-design High Shear, were the two identical double-curvature column models that were studied. The double-curvature configuration allows for the application of a relatively high shear, resulting in extensive shear cracks

---

<sup>1</sup> PhD Candidate and Research Assistant, University of Nevada, Reno, US

<sup>2</sup> Professor, Department of Civil Engineering, University of Nevada, Reno, US

in concrete that induced high demand in the transverse steel, in addition to flexural cracks and plastic hinging. Note that the columns were flexure dominated and expected to be ductile. The latest Caltrans Seismic Design Criteria, SDC version 1.4 (2006), was used to design the column. Scale factor of 1/3 was selected based on the typical cross section dimensions of bridge columns. The scale factor was applied in a way that stresses would not be scaled and real concrete and steel could be used. NHS1 and NHS2 were repaired using fast set non-shrink concrete, epoxy injection, and CFRP wrapping. Different concrete repair methods and jacket layers were applied for NHS1 and NHS2. The former repaired column and the latter one are called NHS1-R and NHS2-R, respectively. The column specifications are listed in **Table 1**. The test setup and column section are shown in **Fig. 1**. The primary test variable was the number of CFRP wraps. The objective was to determine if by reducing the number of wraps and counting on partial contribution of the column spiral to shear would lead to satisfactory performance.

### **Repair Design**

The repair system was designed with the objective of restoring confinement and shear strength of the columns by using unidirectional CFRP jacketing.

### **Restoring confinement**

Because there are no seismic *repair* design guidelines available, seismic *retrofit* guidelines in the California Department of Transportation (Caltrans) provisions for RC columns were used to restore confinement using FRP jacketing. Based on the provisions, for regions inside a plastic hinge region, without a lap splice, it is necessary to provide a minimum confinement stress of 300 psi (2.07 MPa) at a radial dilating strain of 0.004. For regions outside the plastic hinge region, the criteria may be reduced to a minimum confining stress of 150 psi (1.03 MPa) at a radial dilating strain of 0.004. The length of the plastic hinge zone is defined as 1.5 times the cross sectional dimension in the direction of bending.

The required jacket thickness is calculated as follows:

$$t_j = \frac{f_l D}{2E_j \varepsilon_j} \quad (1)$$

Where  $t_j$  is jacket thickness,  $f_l$  is confinement stress,  $D$  is column diameter,  $E_j$  is CFRP modulus of elasticity, and  $\varepsilon_j$  is dilating strain as defined above.

### **Restoring shear strength**

Priestley (1996) recommended that in calculating the shear resistance contributed by the FRP, the stress in the FRP shall be limited to  $0.004E_j$  for a strain limit of 0.004 to avoid degradation in concrete aggregate interlock. Combining the recommendation and the Caltrans criteria for seismic shear design for ductile concrete members, the required thickness for the jacketing,  $t_j$ , is determined as:

$$t_j = \frac{V_o / \phi - (V_c + V_s)}{\pi / 2 \times 0.004 \times E_j \times D} \quad (2)$$

Where,  $V_o$  is over strength shear,  $V_c$  is the concrete shear capacity,  $V_s$  is the shear strength provided by spirals, and  $\phi$  is 0.85. Other parameters were defined previously.  $V_o$  was assumed to be associated with the maximum moment achieved in the NHS1 and NHS2 tests. Different assumptions were made for inside and outside the plastic hinge zone to calculate  $V_c$  and  $V_s$ :

#### ***Inside the plastic hinge***

Since some of the thin cracks are not repairable inside the core,  $V_c$  was neglected in the both columns. The spirals for NHS1 experienced a strain greater than 1.75 yield strain. As a result,  $V_s$  was assumed to be zero for NHS1-R. Testing NHS1-R on a shake table and calculating the contribution of the spirals to shear showed that spirals resisted approximately 50% of the shear even though they were neglected in design. In NHS2-R this led to a smaller number of CFRP Layers.

#### ***Outside the plastic hinge***

Since the spirals do not yield outside the plastic hinge, a 100% credit was given to spirals in both columns. Although shear cracks occurred outside the plastic hinge too, the level of damage was much lower than that of the plastic hinge. As a result, 50% credit was also given to the concrete outside the plastic hinges. A jacket system with a thickness of 0.04 in (1.0 mm) per layer was used.

### **Repair Process**

Neglecting the unexpected delays, the entire repair process can be conducted in one day. The repair process is shown in **Fig. 2** for one of the plastic hinges. The repair process consisted of the following steps:

#### **Straightening the column**

By adjusting the shake table, the column was returned to the initial vertical position.

#### **Removing loose concrete**

The loose concrete was removed by an impact hammer with a chisel point. Mostly, the loose concrete was removed from the compression dominant side of the column.

#### **Concrete repair**

Two different types of mortars and mortar placement were used for NHS1-R and NHS2-R. In NHS1-R, a one component, micro silica and latex modified, and non sag repair mortar was used. The specified 3-day compressive strength of the mortar in NHS1-R was 4000 psi (27.6 MPa). In NHSR-2, a rapid repair mortar was used. The

mortar was low-shrinkage, microsilica-modified, cement-based mortar for structural repair or overlays. The specified 3-hour and 1-day compressive strengths of the mortar used for NHS2-R were 3000 psi (20.7 MPa) and 4000 psi (27.6 MPa), respectively.

### **Pressurized epoxy injection of the cracks**

The epoxy was injected into shear cracks and flexural cracks on the tension dominant side of the column. To inject the epoxy, an inlet was put at one end of a crack and an outlet was put at the other end. Then the surface of the crack was covered by removable glue. Epoxy was injected with a standard pressure of 40 psi (0.28 MPa) from the inlet until it bled from the outlet to ensure that the crack was completely filled with epoxy.

### **Surface preparation for CFRP wrapping**

Column surface was roughened slightly by a grinder. A layer of epoxy was applied to prime the columns surfaces. After that, a thickened epoxy was applied directly to the columns to smooth out imperfections.

### **CFRP wrapping**

After preparing the surface, the epoxy was applied to CFRP layers using a paint roller. CFRP layers were wrapped around the columns manually.

### **Curing**

The entire curing took less than 48 hours which was composed of first half of accelerated curing, followed by curing under the lab ambient condition. During accelerated curing, the temperature was elevated to  $100^{\circ} F$  to  $112^{\circ} F$ , and the relative humidity was reduced to 10% to 15% .

### **Test Protocol**

The Sylmar ground motion record was applied in shake table testing of the columns. The record was applied to the columns with amplitudes increasing gradually. The objective of NHS-1 and NHS-2 testing was to reach to the imminent failure state. In this damage state, the column is approaching failure and damage has begun to penetrate the confined core. No bar rupture is desired in this damage state. To evaluate the repair performance, the repaired columns were subjected to identical increasing motions as original columns with additional motions having higher amplitudes applied to the repaired columns until failure.

### **Shake Table Tests Results**

The columns were tested on one of the shake tables for University of Nevada, Reno. The failure mode for NHS1-R was fracture of two longitudinal bars at the base (**Fig. 3**). In NHS2-R failure was due to the CFRP rupture at the column base on the compression dominant side along with rupture in two longitudinal bars at the base (**Fig. 4**). In both columns, bar ruptures were noted by removing the CFRP jacket.

The cumulative force-displacement hysteresis and back bone curves for NHS1-R and NHS2-R are shown in the upper graphs in **Fig. 5**. In the lower left graph, back bone curves for NHS1 and NHS1-R are plotted. Those of NHS2 and NHS2-R are plotted in the lower right graph.

Strength, stiffness, and deformability are the main characteristics of a structure. To compare the performance of the original columns and repaired ones, the following non-dimensional response indices were developed. These indices can also be used among repaired columns to compare the performance of different repair methods.

### **Strength Index (STRI)**

The lateral strength of a column is defined as the peak measured base shear. The ratio between the lateral strength of the repaired column and the original one is defined as strength index:

$$STRI = \frac{V_R}{V_O} \quad (3)$$

Where,  $V_R$  and  $V_O$  are the peak base shears for the repaired column and the original one, respectively.

### **Stiffness Index (STFI)**

The serviceability of a repaired structure also needs to be considered. The stiffness of the structure under low amplitude lateral loads is an important parameter for quantification the serviceability. Assuming a point on the push over curve with one-half of the peak base shear as the elastic limit, the chord service stiffness of the column is calculated by dividing the one-half of the peak base shear by the corresponding displacement. Having the chord service stiffness for the original column and the repaired one, the stiffness index is found as follow:

$$STFI = \frac{K_R}{K_O}$$

Where,  $K_R$  and  $K_O$  are the chord service stiffness for the repaired column and the original one, respectively. It should be noted that the elastic limit of the repaired column is not taken larger than that of the original column.

### **Deformability Index (DI)**

This index is defined as the ratio between the drift capacity of the repaired column ( $D_R$ ) and that of the original column ( $D_O$ ). Deformability index is determined as follows:

$$DI = \frac{D_R}{D_O} \quad (4)$$

Since the original columns were not tested to failure, their drift capacity is larger than the maximum measured drift. Past failure test data have shown that for well designed columns under high shear, the ratio of ultimate displacement to displacement at imminent failure is approximately 1.2. As a result, to calculate *DI*, the maximum measured drifts for NHS1 and NHS2 were increased by 20%.

The peak base shear, maximum drift, and service stiffness for the columns are listed in **Table 2**. These parameters were used to calculate the response indices. Although the strength of NHS2 was less than that of NHS1, the repaired columns had equal strengths. NHS2-R had considerably higher service stiffness than that of NHS1-R, however those of NHS1 and NHS2 were almost the same. The table also shows that the maximum drift for both repaired column was nearly the same.

The response indices are plotted in **Fig. 6**. In general, all the response indices for NHS2-R are higher than those of NHS1-R. It implies that the repair procedure in terms of quality and application method of the repair mortar has significant role in the performance of the repaired column. In addition, the number of CFRP layers in NHS1-R was not optimized and giving 50% credit to the spirals for NHS2-R was a reasonable assumption. **Fig. 6** shows that the strength and deformability of both columns were fully restored. Although the service stiffness was not fully restored in both columns, but the stiffness reduction in NHS2-R was 2/3 of that of NHS1-R. The reason is that the higher quality repair mortar and better application method, pouring and vibrating instead of patching, were used in NHS2-R.

## **Conclusions**

Based on the observations and the measured data from the testing of the original and the repaired columns, the following conclusions are made:

- The repair design method was rapid, and effective because it restored the lateral load and drift capacity of the columns.
- The repair process was practical and may be used for rapid emergency repair of earthquake damaged concrete columns.
- Giving 50% credit to the spirals capacity and neglecting the concrete strength inside the plastic hinges is a reasonable assumption in the repair design.
- Giving full credit to the spirals capacity and 50% credit to the concrete strength outside the plastic hinges is a reasonable assumption in the repair design.

## **References**

1- Ang Beng Ghee, M. J. N. Priestley, and T. Paulay, "Seismic Shear Strength of Circular Reinforced Concrete Columns," ACI Structural Journal, January-February 1989, pp. 45-59.

**2-** California Department of Transportation, “Memo to Designers 20-4 attachment B,” California, USA: Engineering service center, earthquake engineering branch, 2007.

**3-** California Department of Transportation, “Seismic Design Criteria, version 1.4,” California, USA: Engineering service center, earthquake engineering branch, 2006.

**4-** California Department of Transportation, “Bridge Design Specifications,” California, USA: Engineering service center, earthquake engineering branch, 2003.

**5-** Johnson, N., M. Saiidi, A. Itani, and S. Ladhany, “Seismic Retrofit of Octagonal Columns with Pedestal and One-Way Hinge at Base,” *ACI Structural Journal*, Vol. 102, No. 5, 2005, pp. 699-708.

**6-** Laplace, P. N., D. H. Sanders, M. Saiidi, B. M. Douglas, and S. El-Azazy, “Retrofitted Concrete Bridge Columns Under Shake Table Excitation,” *ACI Structural Journal*, Vol. 102, No. 4, 2005, pp. 622-628.

**7-** Li, Y. F. and Y. Y. Sung, “Seismic Repair and Rehabilitation of a Shear-Failure Damaged Circular Bridge Column Using Carbon Fiber Reinforced Plastic Jacketing,” *Canadian Journal of Civil Engineering*, No. 30, 2003, pp. 819-829.

**8-** Priestley, M. J. N., F. Seible, and G. M. Calvi, “Seismic Design and Retrofit of Bridges,” New York, USA: John Wiley & Sons, 1996.

**9-** Saiidi, M. and Z. Cheng, “Effectiveness of Composites in Earthquake Damage Repair of Reinforced Concrete Flared Columns,” *Journal of Composites for Construction* © ASCE Vol. 8, No. 4, 2004, pp. 306-314.

**10-** Saiidi, M., K. Sureshkumar, and C. Pulido, “A Simple Model for CFRP Confined Concrete,” *Journal of Composites for Construction*, ASCE, Vol. 9, No. 1, 2005, pp. 101-104.

**11-** Teng, J. G., J. F. Chen, S. T. Smith, and L. Lam, “FRP Strengthened RC Structures,” Sussex, England: John Wiley & Sons, Ltd., 2002.

**12-** Vosooghi, A., M. Saiidi, and J. Guitierrez, “Rapid Repair of RC Bridge Columns Subjected to Earthquakes,” 2nd International Conference on Concrete Repair, Rehabilitation, and Retrofitting, Cape Town, S. Africa, November 2008, pp. 1113-1119.

**Table 1.** Specifications for NHS1 and NHS2

H in (mm)	D in (mm)	Long. Steel Ratio	Trans. Steel Ratio	Aspect Ratio	Axial Load, kips (kN)
80 (2032)	16 (406)	3.08%	1.34%	2.5	100 (444.8)

**Table 2.** Main responses of the columns

	Peak base shear, Kips (kN)	Maximum drift	Service stiffness, Kips/in (kN/mm)
NHS1	94.1 (418.6)	9% [1.2*7.5%]	73.2 (12.8)
NHS1-R	95.2 (423.6)	13.1%	28.3 (5.0)
NHS2	78.9 (350.9)	7.7% [1.2*6.4%]	71.0 (12.4)
NHS2-R	92.1 (409.7)	13.3%	44.0 (7.70)

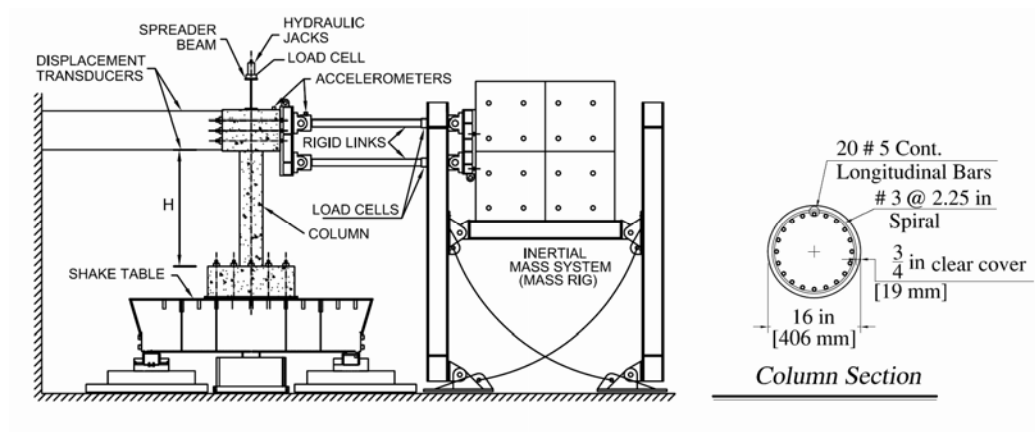


**Fig 1.** Test setup and section properties for NHS1 and NHS2



2a) Before repair



2b) Concrete Chipping



2c) Concrete patching (NHS1-R)



2d) Smoothing (NHS-R)



2e) Conc. pouring, vibrating (NHS-R)



2f) After concrete repair



2g) Epoxy injection



2h) Surface preparing



2i) CFRP wrapping

**Fig 2.** Repair process for NHS1 and NHS2



**Fig 3.** Bar ruptures in NHS1-R. (CFRP was removed after shake table tests.)

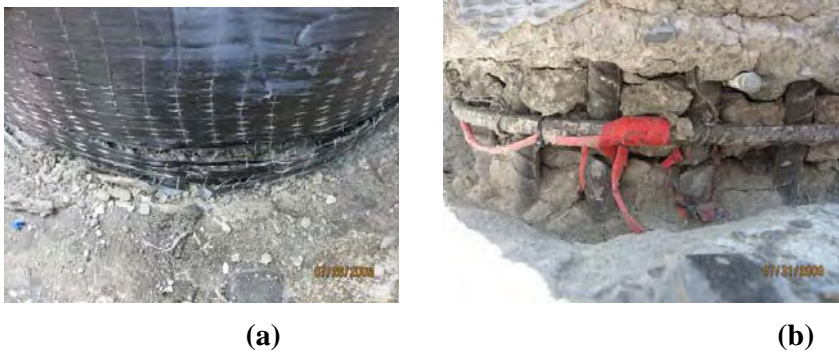


**Fig 4.** Failure in NHS2-R; a) CFRP rupture; b) bar rupture (CFRP was removed after shake table tests.)

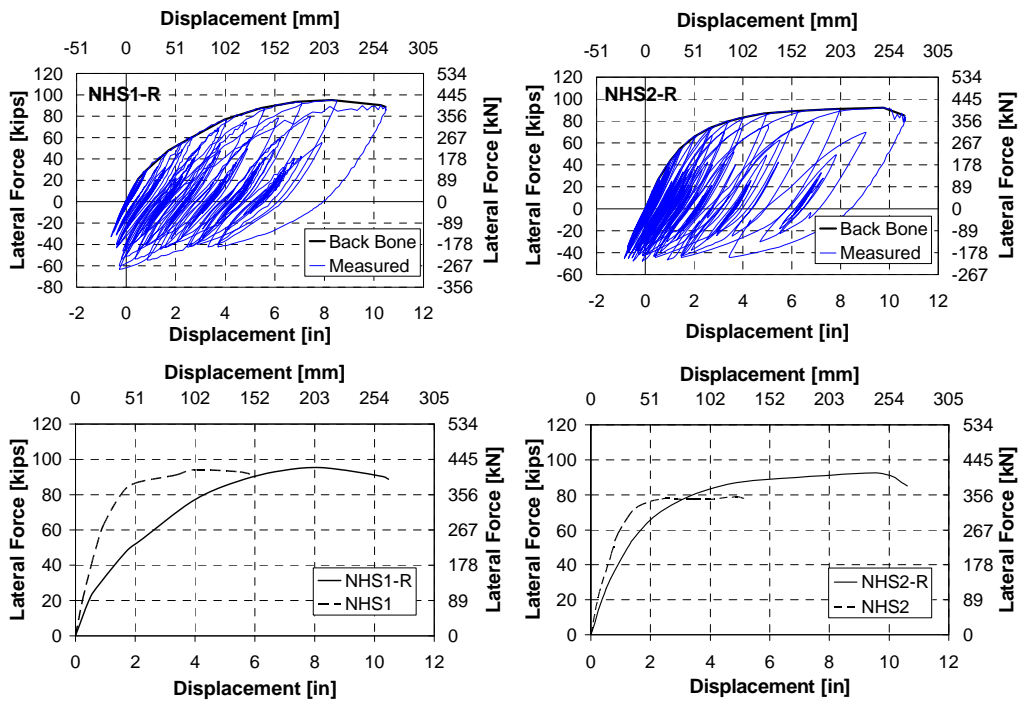


**Fig 5.** Lateral force-displacement relationships for the columns

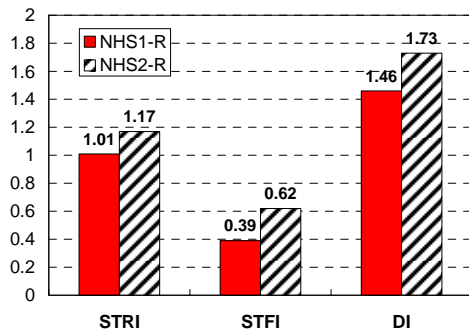


**Fig 6.** Response indices for the repaired columns

# SEISMIC RETROFIT TECHNIQUES FOR REINFORCED CONCRETE BRIDGE COLUMNS WITH COMBINATION OF FRP SHEET AND STEEL JACKETING

Guangfeng Zhang<sup>1</sup>, Shigeki Unjoh<sup>2</sup>, Jun-ichi Hoshikuma<sup>3</sup> and Junichi Sakai<sup>4</sup>

## Abstract

With the purpose to provide a seismic retrofit method with good workability for reinforced concrete (RC) highway bridge columns under severe construction work conditions, a retrofit method with combination of carbon fiber reinforced polymer (CFRP) sheet and steel jacketing has been proposed in the previous researches of this research project. In this research, bonding behavior between CFRP sheet and steel plate was investigated experimentally in order to establish a rational design method for the CFRP-steel bonded connection. This paper provide an introduction of the proposed seismic retrofit method companying with descriptions of the tests on CFRP-steel bonded connection and test on RC bridge column specimen for examining the retrofit effectiveness of the proposed retrofit method.

## Introduction

Attributing to the merits of high strength, light-weight and outstanding workability, fiber reinforced polymer (FRP) sheet has been widely used in repairing or strengthening reinforced concrete (RC) members in the recent decades. As for seismic retrofit of RC highway bridge columns in Japan, FRP sheet is usually used to retrofit columns with premature termination of longitudinal reinforcements without enough development length at the midheight. Figure 1 shows an example of RC bridge being under retrofitted with Carbon FRP (CFRP) sheet. CFRP sheet was jacketed around the termination sections of the longitudinal reinforcements in the longitudinal direction and circumferential direction to reinforce flexural and shear strength. In some other cases, FRP sheet is also used to reinforce ductility of the columns by jacketing around the plastic hinge in the circumferential direction.

However, it is not an effective method to reinforce the flexural strength of the column base by jacketing FRP sheet in the longitudinal direction. Generally, high elongation is required locally in both of the longitudinal and circumferential directions at the base. Enhancement of ductility capacity of the base can not be obtained because elongation of the FRP sheet is rather lower before breaking. From the point of view, a

---

<sup>1</sup> Researcher, Bridge and Structural Technology Research Group, Public Works Research Institute, Japan

<sup>2</sup> Research Coordinator for Earthquake Disaster Prevention, Research Center for Disaster Risk Management, National Institute for Land and Infrastructure Management, Japan

<sup>3</sup> Chief Researcher, Bridge and Structural Technology Research Group, Public Works Research Institute, Japan

<sup>4</sup> Senior Researcher, Ditto

method with using combination of CFRP sheet and steel jacketing has been proposed in the previous researches (Zhang and Unjoh, 2009). It should be noted for the retrofit method that bonding behavior between CFRP sheet and steel plate is a key issue, because the longitudinal force induced from the additional anchor bolts must be transmitted to CFRP sheet and thus the steel plate should be bonded with CFRP sheet in the inelastic response of the column.

This paper provide an introduction of the proposed seismic retrofit method accompanying with descriptions of the tests on CFRP-steel bonded connection and test on RC bridge column specimen for examining the retrofit effectiveness of the proposed retrofit method.



**Fig. 1** Retrofit of RC bridge columns with CFRP sheet

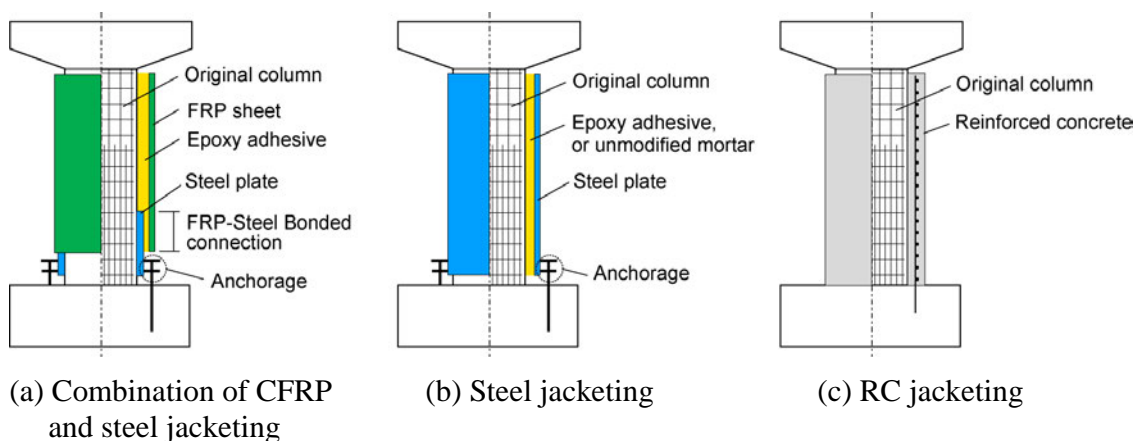
### **Overview of Seismic Retrofit methods**

Figure 2(a) shows schematic of the proposed retrofit method. It adopted a combination of CFRP sheet jacketing and steel plate jacketing (hereinafter, combination of CFRP and steel jacketing) taking advantage of the merits of both of the CFRP and steel. Considerations of this technique are to use different methods to retrofit the base and the other parts of a column. A method same as the normal steel jacketing is used to retrofit the base where upgrading of the strength and the ductility are required. A FRP jacketing is used to retrofit the other parts to provide high strength. Transmit of force between the steel plate and the CFRP sheet is accomplished by FRP-steel bonded connection with a certain bond length.

Comparing to the normal steel jacketing and RC jacketing as shown in figure 2(b)

and (c), the proposed method is complicated because it needs to design the details of the bonded connection. The merits of the proposed method are the high performance of construction and that increasing of the death weight after retrofit is very limited. The proposed method be suitable for the situations such as the followings: 1) bridges located in a place where no enough construction space can be ensured for building a large scale scaffolding or for the working of the construction machines and equipments; 2) bridges crossing a river or bridges located in a heavy snows region where construction period is short, etc.

Because this method employs a FRP-steel bonded connection to transfer the strength upgraded by the anchor bolts to the CFRP sheet, it is important to ensure the bonding capacity and certainty of the bonded connection. In this research, bonding behavior between CFRP sheet and steel plate was investigated intensively with shear bond tests in order to establish a rational design method for the bonded connection. Furthermore, a RC bridge column specimen was tested under cyclic loading method to inspect the retrofit effectiveness of the proposed retrofit method.



**Fig. 2** Schematics of seismic retrofit methods for RC bridge columns

### **Tests on Bonding Behavior between CFRP Sheet and Steel Plate**

Four series of double-lap shear bond tests were carried out taking the bonded layers of CFRP sheet as parameter. Three specimens were tested for each series. Table 1 shows a list of the specimens.

Figure 3 shows the details of the double-lap shear specimens. CFRP sheet of  $600 \text{ g/m}^2$  and ss400 steel plates were used. A long bond length of 600 mm was set in the tests in order to inspect the progress of debonding between CFRP sheet and steel plate. Surface of steel plate to be bonded with CFRP sheet was grinded with disc sanding machine. All

the specimens were cured for 7 days at ambient temperature. The tests were performed using a universal testing machine with a loading speed of 0.5-1.0 mm per minute.

Table 2 shows the test results of material properties of CFRP sheet and epoxy adhesive.

Table 1 List of Specimens

Series	Bond length (mm)	Bonded layers of CFRP	Numbers of specimens for each series
1-layer	600	1	3 (No.1, No.2, No.3)
2-layer	600	2	3 (No.1, No.2, No.3)
3-layer	600	3	3 (No.1, No.2, No.3)
4-layer	600	4	3 (No.1, No.2, No.3)

Table 2 Material Properties

Materials	Items	Values
CFRP sheet	Mass per area ( $\text{g}/\text{m}^2$ )	600
	Design thickness (mm)	0.333
	Young's modulus ( $\text{N}/\text{mm}^2$ )	$2.60 \times 10^5$
	Tensile strength ( $\text{N}/\text{mm}^2$ )	3,400
Epoxy adhesive	Young's modulus ( $\text{N}/\text{mm}^2$ )	$2.202 \times 10^3$
	Compressive strength ( $\text{N}/\text{mm}^2$ )	71.8
	Tensile strength ( $\text{N}/\text{mm}^2$ )	47.0
	Tensile shear strength ( $\text{N}/\text{mm}^2$ )	17.6

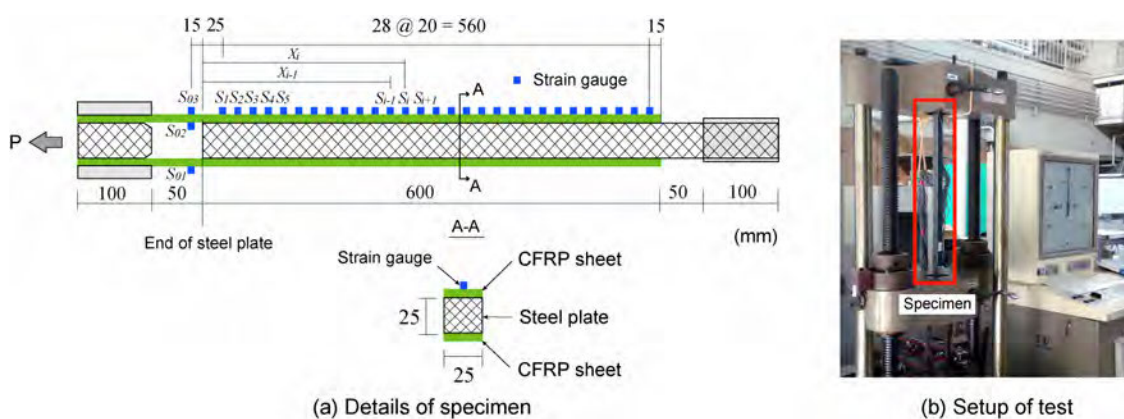
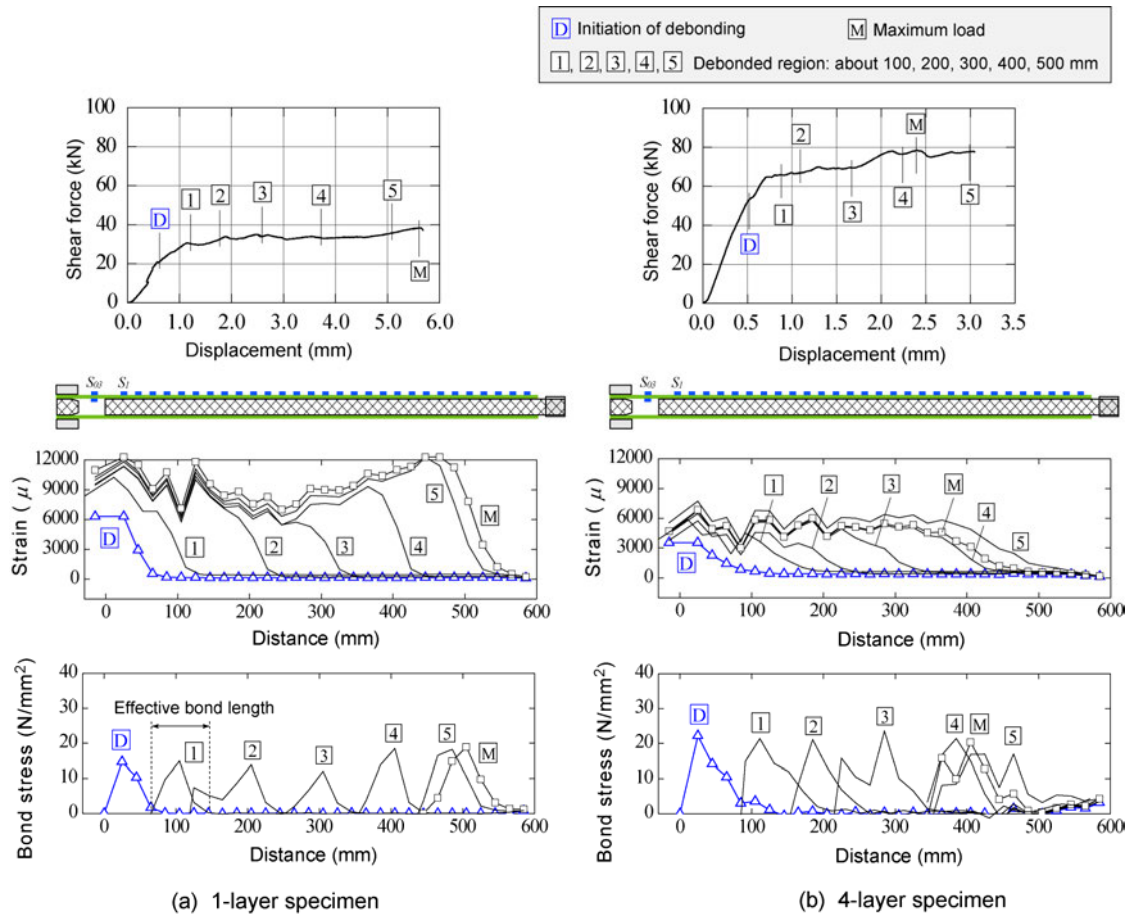


Fig. 3 Details of specimens and setup of test



**Fig. 4** Examples of test results on bonding behavior between CFRP sheet and steel plate

Test results were summarized with the items of relationship between shear force and displacement of CFRP at the end of steel plate, distribution of strain in CFRP and interfacial bond stress along the bond length. Here, bond stress was calculated from the strain using the relationship  $\tau = d\varepsilon(x)/dx \cdot E_f \cdot t_f$ , where,  $E_f$  and  $t_f$  are the Young's modulus and thickness of CFRP sheet. Figure 4 shows test results of a 1-layer specimen and a 4-layer specimen for examples.

The value of strain at the point of debonding initiated and the length of effective bond length were discussed. The value of strain at the point of debonding initiated will become lower with increasing of the bonded layers. The lowest value was confirmed as about 3,500 microstrain for 3-layer specimen and 4-layer specimen. The length of effective bond length is about 80-100mm for 1-layer specimens, 100-160mm for 2-layer specimens, 120-180mm for 3-layer specimens and 140-200mm for 4-layer specimens. From the view of design, it can be said from these results that bond length and strain of CFRP sheet used in design should be considered carefully to ensure the design strength.

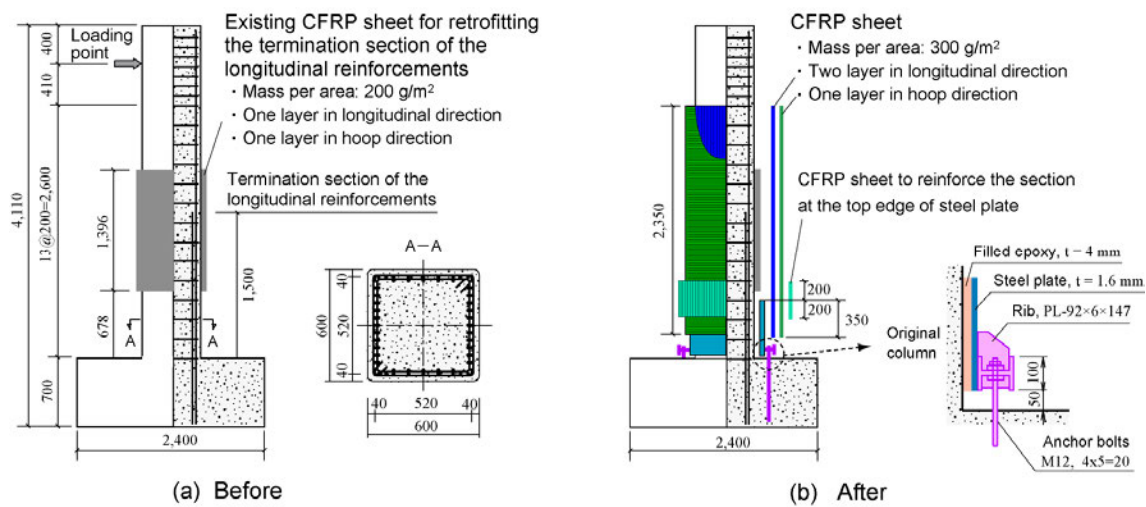


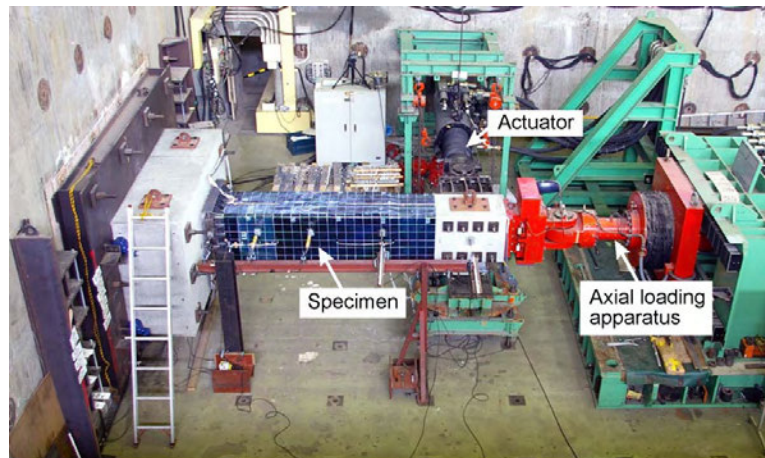
**Fig. 5** Details of RC bridge column specimen before and after retrofit with combination of CFRP and steel jacketing

### **Cyclic Loading Test on RC Bridge Column Specimen**

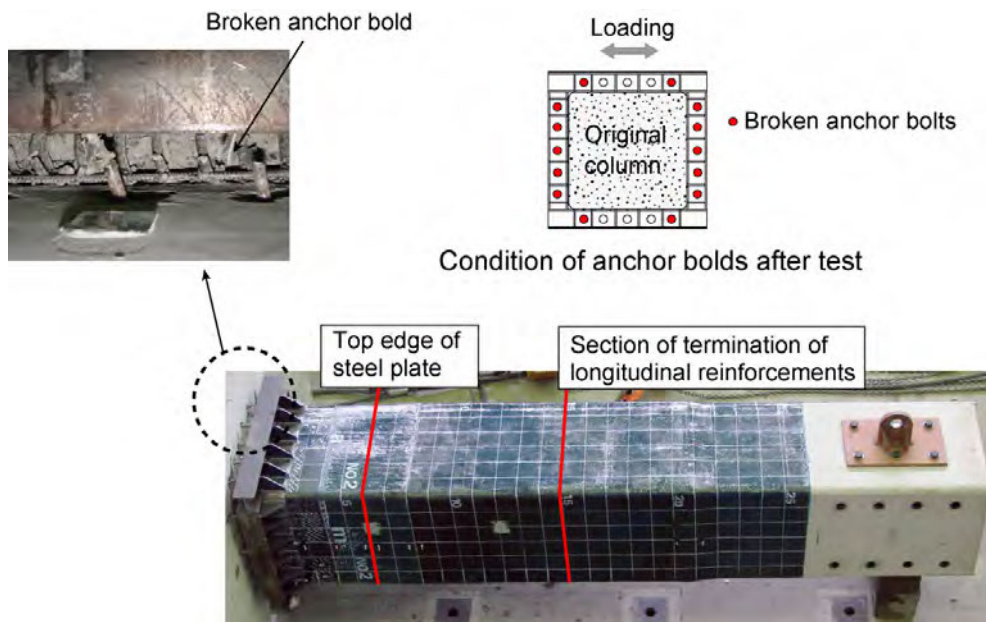
A RC bridge column specimen was tested under cyclic loading method to inspect the retrofit effectiveness of the proposed combination of CFRP and steel jacketing method. The specimen was a scaled model of a RC bridge column with premature termination of longitudinal reinforcements at the midheight but retrofit of the termination section of the longitudinal reinforcements was already performed. Retrofit of the termination section of the longitudinal reinforcements was designed to prevent failure at this section period to flexural failure of the base. Therefore, it can be considered that the specimen before retrofitted with the proposed method is equivalent to a column with a failure mode of flexural failure of the base.

Figure 5 shows the details of the specimen. Cross section of the original column was 600×600 mm. The height of the loading point was 3,100 mm with an aspect ratio of 5.0. SD295-D10 and SD295-D3 was used as longitudinal reinforcements and hoop ties, respectively. Reinforcement ratio was 1.58%. Retrofit with the proposed retrofit method was designed to upgrade the flexural strength with an increase of 30 percent. Bond length of 350 mm was applied between CFRP sheet and steel plate.

Figure 6 shows setup of the cyclic loading test. Axial force of 539 kN was applied during the loading to provide an axial stress of about 1.5MPa. Loading was performed under displacement control and the loading speed was 10 mm/sec. Cyclic number was 3 for each loading step.



**Fig. 6** Setup of cyclic loading test



**Fig. 7** Conditions of specimen after test

Cyclic loading was surcharged until a loading step of  $9\delta_y$  with yield displacement  $\delta_y$  of 12.7 mm. Initiation of cracks at the base, breaking of anchor bolts, remarkable compressive failure of core concrete and breaking of longitudinal reinforcements were confirmed at a loading step of  $3\delta_y$ ,  $6\delta_y$ ,  $7\delta_y$  and  $8\delta_y$ , respectively. Bonding condition between CFRP sheet and steel plate was checked after each loading step by tapping the CFRP surface with a small hammer to detect voids. It is noted that no debonding area was detected till the test finished. Figure 7 shows the conditions of specimen after test.

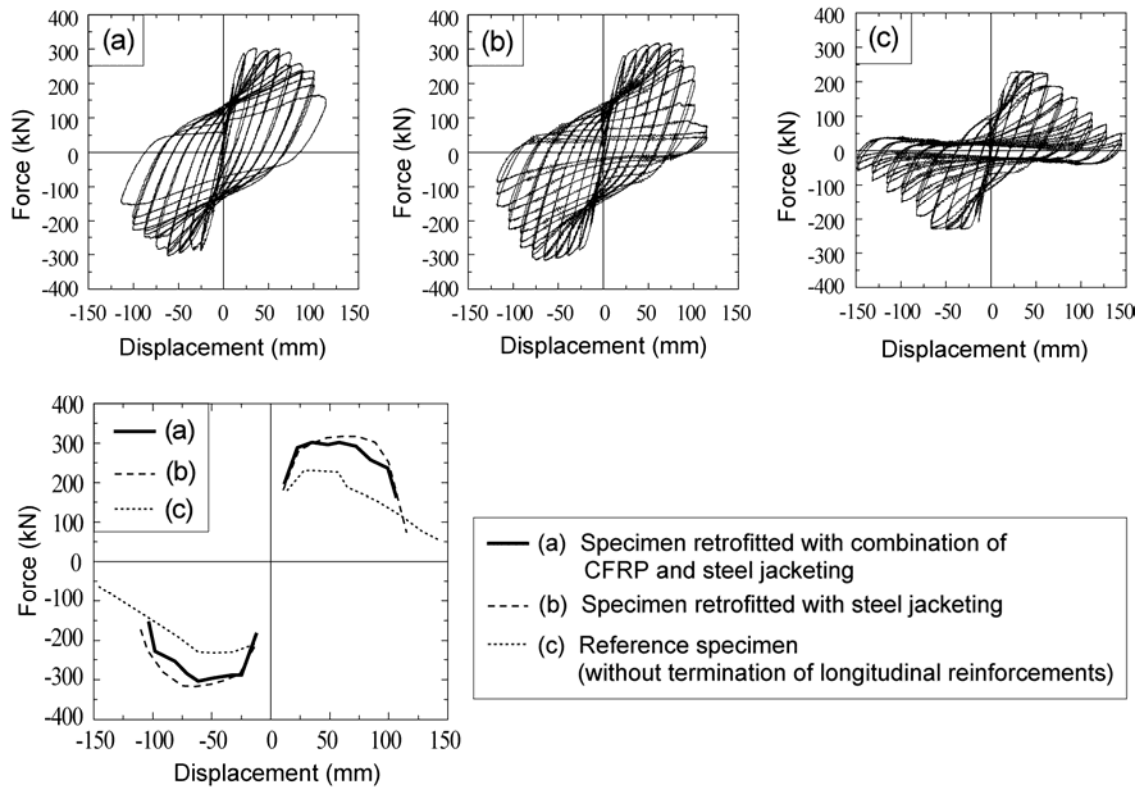


**Fig. 8** Lateral force-displacement

Retrofit effectiveness of the proposed retrofit method was discussed by comparing the flexural strength and ductility with that of a specimen retrofitted with normal steel jacketing and that of a reference specimen (Hoshikuma, J. and Unjoh, S.). Here, design of the base section of the original column was the same for each of the three specimens. And design of the anchorage was the same for each of the two retrofitted specimen. Figure 8 shows lateral force-displacement hysteresees and envelope curves of the three specimens. It can be seen that retrofit effect of the proposed retrofit method was similar with the normal steel jacketing.

### **Conclusions**

Retrofit method with using a combination of CFRP sheet jacketing and steel jacketing was proposed in this research project with the purpose to provide a seismic retrofit method for RC bridge columns under severe construction work conditions. Bonding behavior between the CFRP sheet and steel plate was investigated experimentally in order to establish a rational design method for the bonded connection. It is found that the proposed retrofit method with necessary bonding connection details can provide a retrofit effect similar with the normal steel jacketing.

## **References**

Zhang, G.F. and Unjoh, S.: “A Retrofit Method for Upgrading Seismic Performance of RC Columns with Termination of Main Reinforcements”, *Proceedings of the 12th Symposium on Ductility Design Method for Bridges, JSCE*, pp.47-52, 2009.1 (in Japanese)

Hoshikuma, J. and Unjoh, S.: “Seismic Retrofit of Existing Reinforced Concrete Columns by Steel jacketing”, *Proceedings of the Second Italy-Japan Workshop on Seismic Design and Retrofit of Bridges*, Rome, Italy, February 27-28, 1997, pp.413-428.

blank

## DEVELOPMENT AND REFINEMENT OF ILLINOIS' EARTHQUAKE RESISTING SYSTEM STRATEGY

Daniel H. Tobias<sup>1</sup>, Jerome F. Hajjar<sup>2</sup>, Ralph E. Anderson<sup>1</sup>, James M. LaFave<sup>2</sup>, Chad E. Hodel<sup>3</sup>, Larry A. Fahnestock<sup>2</sup>, William M. Kramer<sup>1</sup>, Joshua S. Steelman<sup>2</sup>, Patrik D. Claussen<sup>1</sup>, Kevin L. Riechers<sup>1</sup>, and Mark D. Shaffer<sup>1</sup>

### **Abstract**

An important aspect of newly adopted American Association of State Highway and Transportation Officials (AASHTO) bridge design code provisions is a design earthquake with significantly increased accelerations. The Illinois Department of Transportation (IDOT) has recently developed and implemented an Earthquake Resisting System (ERS) strategy for all bridges in the state in order to accommodate the increased AASHTO seismic design hazard. This paper provides a short history of the development of IDOT's ERS strategy as well as an overview of a recently established research program aimed at refinement and calibration at the University of Illinois at Urbana-Champaign (UIUC).

### **Introduction**

#### **Background**

In 2008 and 2009, the American Association of State Highway and Transportation Officials (AASHTO) published modernized codified standards for the design of highway bridges to resist earthquake loadings. The revised and updated provisions are contained in the *AASHTO Load and Resistance Factor Design Bridge Design Specifications (LRFD Code)* (AASHTO 2009b) and the 1<sup>st</sup> edition of the *AASHTO Guide Specifications for LRFD Seismic Bridge Design (LRFD Seismic Guide Specifications)* (AASHTO 2009a). These two documents reflect the culmination of several years of effort by the bridge engineering community in the United States (MCEER/ATC 2003; NCHRP 2006). Both the *LRFD Code* and the *LRFD Seismic Guide Specifications* have incorporated a design earthquake with a 1000 yr. return period (Leyendecker et al. 2007). Prior to 2008, the codified design return period earthquake was 500 yrs. (FEMA 1988; AASHTO 2002). The methods and soil parameters used to determine design earthquake response spectra (BSSC 1995) along with numerous other aspects of seismic bridge design philosophy were also modernized in the recently published AASHTO documents.

Traditionally, the philosophies and need to address typical bridge configurations in western states within the United States have driven advancements and codified provisions for seismic design of highway bridges nationwide. Seismic considerations have been a primary concern in these states for many years due to the

---

<sup>1</sup>Illinois Department of Transportation, Springfield, Illinois, USA.

<sup>2</sup>University of Illinois at Urbana-Champaign, Urbana, Illinois, USA.

<sup>3</sup>WHKS & Company, Springfield, Illinois, USA.

region's widely recognized high risk for large damaging earthquakes. With the advent of the newly adopted 1000 yr. design return period earthquake, though, there is a keener recognition of the risk for a large seismic event happening in some mid-western and eastern states. Significant earthquakes in these regions of the United States are known to have occurred, but the frequency of recurrence can be quite long. In the last several years, many states east of the Rocky Mountains, including Illinois, have made significant strides with regards to seismic design, retrofitting and construction methods for highway bridges. The modernization efforts in Illinois have focused on seismic design philosophies and methods that are the most appropriate for typical bridge configurations constructed in the state.

### **Scope of Increased Design Hazard**

Designing bridges for a 1000 yr. earthquake, which primarily affects approximately the southern half of Illinois, represents a significant increase in design accelerations from the 500 yr. event. Fig. 1 presents an approximate 1000 yr. spectral acceleration map for Illinois at a period of 1.0 sec. assuming all the soil is classified as Soil Site Class D according to the definitions contained in the *LRFD Code* and the *LRFD Seismic Guide Specifications*. Site Class D is a common soil type in southern regions of Illinois. The figure gives a generalized idea of the seismicity of Illinois for the 1000 yr. design seismic event. Spectral accelerations at 1.0 sec. are used to delineate between Seismic Performance Zones (SPZ) in the *LRFD Code* and Seismic Design Categories (SDC) in the *LRFD Seismic Guide Specifications*. As the SPZ (and SDC) increases in number (letter), so do the seismic design requirements. For the 500 yr. design earthquake, there were no parts of Illinois in SPZ 4 and only a small portion was in SPZ 3. Furthermore, the design accelerations within each SPZ are significantly greater for the 1000 yr. earthquake as compared to the 500 yr. earthquake.

### **Development and Refinement**

In late 2006 and mid 2008, after several years of development, the Illinois Department of Transportation (IDOT) published and implemented initial versions of a comprehensive strategy or framework for the design, retrofit and construction of bridges to resist seismic loadings in the *IDOT Bridge Manual* (IDOT 2008a) and the *IDOT Seismic Design Guide* (IDOT 2008b). The strategy is comprised of a set of core concepts and structural details which, when implemented together, form a generalized Earthquake Resisting System (ERS). Illinois' ERS strategy is flexible enough to be applicable to all common bridge types built in the state, and for any past or future codified hazard level. Pertinent aspects of recently adopted seismic provisions in the *LRFD Code*, the *LRFD Seismic Guide Specifications*, the *Federal Highway Administration Seismic Retrofitting Manual for Highway Bridges (FHWA Retrofit Manual)* (FHWA 2006), and several other sources (ICC 2000; AASHTO 2000) were used to formulate and tailor a viable ERS framework for the state. R-factor or forced based concepts (from the *LRFD Code*) are used as a primary basis for design.

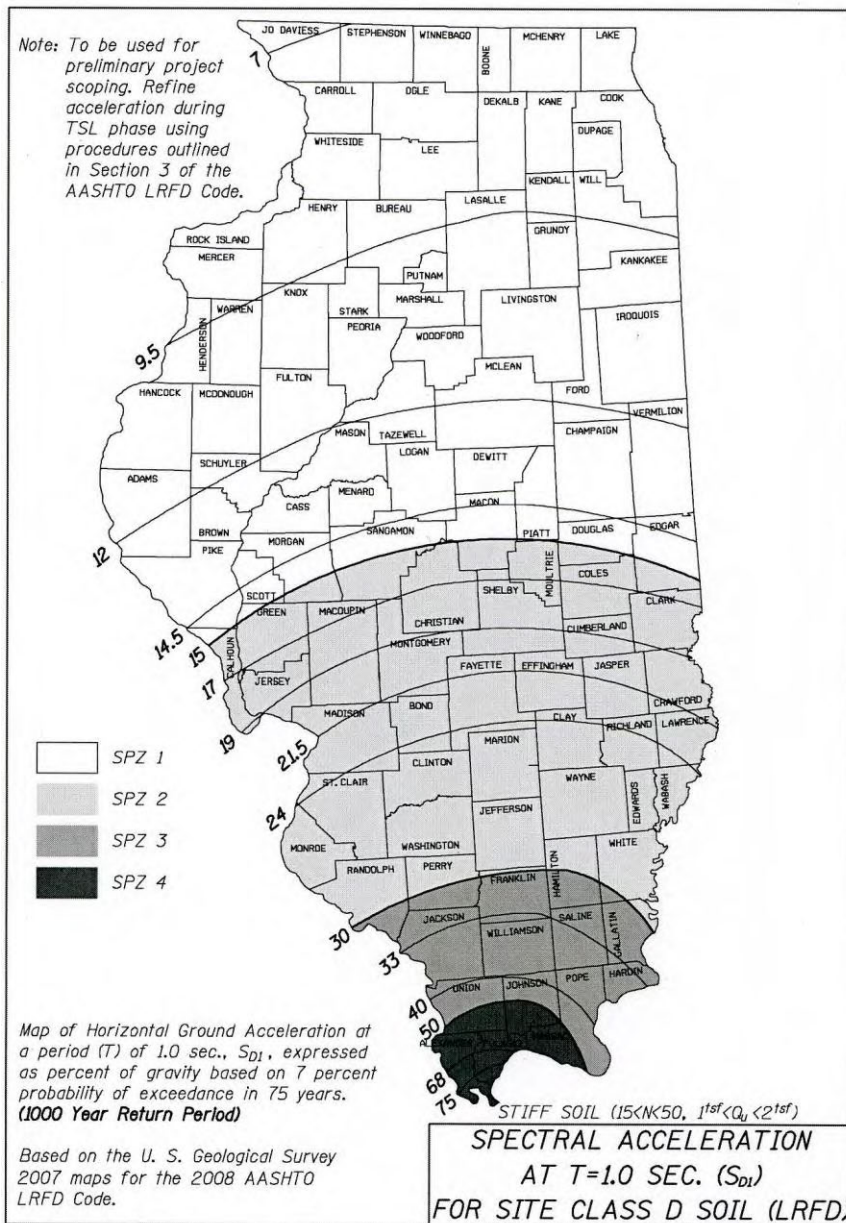


FIG. 1. APPROXIMATE SPECTRAL ACCELERATIONS AT A PERIOD OF 1.0 SEC. FOR SITE CLASS D SOIL IN ILLINOIS

Initial modernization and improvement efforts by IDOT in the state coincided with those of AASHTO over the last several years (Hodel et al. 2004; Tobias et al. 2006a; Tobias et al. 2006b; Tobias, et al. 2008a; Tobias, et al. 2008b). The processes of updating the *LRFD Code* and formulating the *LRFD Seismic Guide Specifications* were undertakings in which Illinois played an important role as a contributing member of the AASHTO Technical Subcommittee on Seismic Bridge Design (T-3). The involvement by IDOT at the national level helped to greatly enhance the locally developed Illinois ERS strategy. IDOT had the opportunity to garner experience and expertise from other contributing states, and also played a role in crafting some of the

key provisions that pertain to states with typical bridge configurations and seismicities which are similar to Illinois.

A research program initiated in early 2009 by IDOT at the University of Illinois at Urbana-Champaign is primarily focused on refinement and calibration of the currently implemented forced based approach for areas in Illinois with moderate to moderately high seismicity. In time, for areas in Illinois with higher seismicity, additional aspects of the recently developed displacement based approach (from the *LRFD Seismic Guide Specifications*) are also anticipated to be incorporated into Illinois' ERS strategy through the results of the ongoing research effort.

The first part of this paper provides a brief overview of the initial development of Illinois' ERS strategy over the last 5 to 6 years, while the second part provides a description of the ongoing research program aimed at calibration and refinement.

## **ERS Strategy**

### **Range of Applicability**

Illinois' ERS strategy is primarily intended for common bridge types built in the state that normally can be designed assuming the first mode of vibration is the dominant response to a seismic loading (i.e., are regular as defined by the *LRFD Code* and the *LRFD Seismic Guide Specifications*). Superstructures of these bridge configurations generally include those with a concrete deck on steel or precast prestressed I-beams, or a wearing surface on precast prestressed deck beams (box beams). The abutments include non-integral and integral stub. The piers can be of various types including multiple column concrete bents, several variations of drilled shaft bents, and solid walls. Foundation types include spread footings, HP and metal shell piling, and drilled shafts. Various combinations of these elements make up the vast majority of Illinois' inventory at present and for the foreseeable future. For bridges that are irregular, the general principles of the Illinois ERS strategy are also applicable, and required to be followed. Irregular bridges typically require multi-modal design and analysis methods.

### **Seismic Structural Redundancy Levels**

The underlying philosophy of Illinois' ERS strategy is to allow certain levels of damage during a seismic event at planned locations in a structure such that loss of span is prevented. Loss of span directly impacts critical public transportation facilities, and can potentially lead to loss of life. Optimally, prevention of span loss is achieved through what can be termed "levels or tiers of seismic structural redundancy" that dissipate energy from an earthquake in key components of bridges in succession as they fail (fuse) or engage, and alter the response of a structure. These key bridge components include weak or fuse-like connections between superstructures and substructures of bridges, conservative beam seat widths (support lengths) on substructures, an allowance for plastic deformation in superstructure components such as steel diaphragms, an allowance for plastic embankment

deformation at abutments, and an allowance for plastic hinging in selected parts of substructures and foundations (when necessary).

The first tier or level of seismic structural redundancy, and theoretically weakest fuse in Illinois' ERS strategy, is the connections between superstructures and substructures. These connections are designed to fail at a nominal level of dynamic excitation while still meeting the strength requirements for normal or service loads (non-extreme event). Fig. 2 presents a typical fusible elastomeric bearing and superstructure-to-substructure connection with side retainers for steel I-beams used in Illinois, and Fig. 3 illustrates the details of the side retainer design. Most non-integral connections between superstructures and substructures for typical bridges in Illinois are designed to nominally carry 20% of the tributary dead weight of a superstructure in the restrained direction regardless of the Seismic Performance Zone of the structure. In 2008, AASHTO updated and clarified the provisions for the seismic design of connections between superstructures and substructures. The notion that, at the discretion of owner, bearings and their connections may be designed as sacrificial elements (i.e. fusible) is now fully endorsed alongside the historical concept which required connections between superstructures and substructures always be designed to stay elastic during a design seismic event.

For Illinois, it is much more economical and logical to embrace the fuse concept between superstructures and substructures in order to adapt to increased design accelerations. The benefits of energy dissipation and an increased chance of substructure/foundation survival (possibly beyond the 1000 yr. seismic design event) outweigh the cost of modifications to typical bridge configurations in Illinois that would be required to keep these connections elastic during a large seismic event.

Once superstructure-to-substructure connections have fused during an earthquake, adequate seat widths for beams on substructures are provided such that superstructures can "ride out" the remainder of a design seismic event (or possibly greater). Conservatively designed seat widths are the second tier of seismic structural redundancy in Illinois' ERS strategy. The empirical relationship for determining required support length,  $N$  (m), used by Illinois is given by Eq. 1.

$$N = \left[ 0.10 + 0.0017 L + 0.007 H + 0.05 \sqrt{H} \sqrt{1 + \left( \frac{B}{L} \right)^2} \right] \frac{1 + 1.25 F_v S_1}{\cos \alpha} \quad (1)$$

where  $L$  = typically length between expansion bearings (m);  $H$  = tallest pier between expansion bearings (m);  $B$  = out-to-out width of superstructure (m);  $B/L$  = ratio not to be taken greater than  $\frac{3}{8}$ ;  $\alpha$  = skew angle ( $^\circ$ ); and  $F_v S_1$  = one second period spectral response coefficient modified for Site Class. The required seat widths calculated using Eq. 1 are typically about 25 to 30% greater than that required by the *LRFD Code* and the *LRFD Seismic Guide Specifications*.

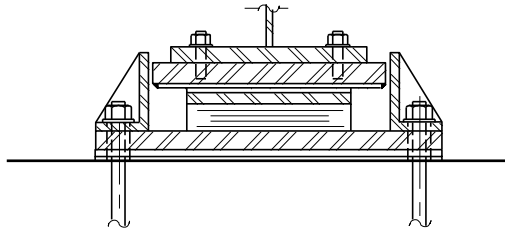
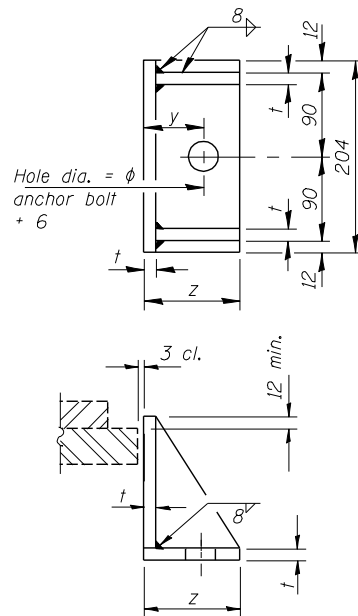


FIG. 2. TYPICAL FUSIBLE ELASTOMERIC BEARING AND CONNECTION DETAIL WITH SIDE RETAINERS FOR STEEL I-BEAMS

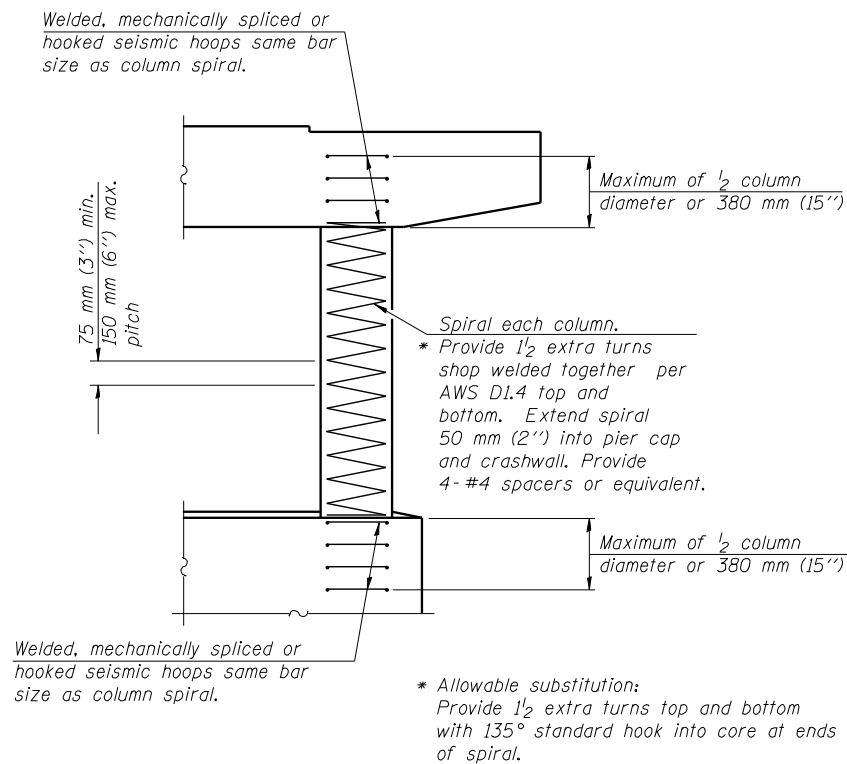


Dimensions in mm.  
(Note: 25.4 mm = 1")

FIG. 3. TYPICAL FUSIBLE SIDE RETAINER DESIGN FOR STEEL I-BEAMS

The third tier of seismic redundancy in Illinois' ERS strategy generally encompasses plastic hinging of elements in substructures such as reinforced concrete columns and, when necessary due to a bridge's configuration, substructure/foundational elements such as piles and drilled shafts. Figs. 4 and 5 provide some typical seismic details used in Illinois for multiple round columns piers and drilled shafts. Embankments at abutments are generally considered sacrificial elements as part of the third tier of seismic structural redundancy. The "amperage level" for fuses in substructures and foundations is generally somewhat greater than those of the first tier of seismic redundancy. Failure of the connections between superstructures and substructures along with plastic deformations in superstructure

diaphragm elements helps to provide an enhanced probability that the third tier of redundancy may not become fully engaged or fuse during a moderate to significant seismic event (but probably will during a major seismic event without causing span loss). The concept is analogous to comparing the primary electrical fuse for an entire house to the many secondary individual fuses that are connected to it.



### ELEVATION

FIG. 4. SEISMIC CONFINEMENT DETAILING OPTIONS FOR CIRCULAR COLUMNS

### $\phi$ and R-factors

Depending on the specific situation, varying degrees of isolation between superstructures and substructures are likely provided after fusing occurs primarily because friction may be the only mechanism of seismic force transfer at these interfaces. If elastomeric bearings are employed on a structure, some isolation is also provided before fusing. Since there are several sources of seismic energy attenuation in the load path from superstructures down to their interfaces with substructures, IDOT permits an increase in some  $\phi$  or strength reduction factors for the 1000 yr. design return period seismic event from those prescribed by the *LRFD Code*. These increases primarily apply to reinforced concrete pier construction (usually from 0.9 to 1.0) for combined moment and axial force resistance. R-factors are primarily used in the design of substructures/foundations to promote ductile structural response during an earthquake by reducing design moments. The recommended R-factors in Illinois'

ERS strategy for substructure and foundation design generally follow the guidance and bounds of the *LFRD Code*. However, interpretation and judgment was required to develop and clarify for practitioners values that should be used for design which are applicable to specific pier and abutment types built in Illinois. Refinement and calibration of the  $\phi$  and R-factors currently used in Illinois' ERS strategy are one of the primary focuses of the research effort that is currently ongoing at the University of Illinois at Urbana-Champaign.

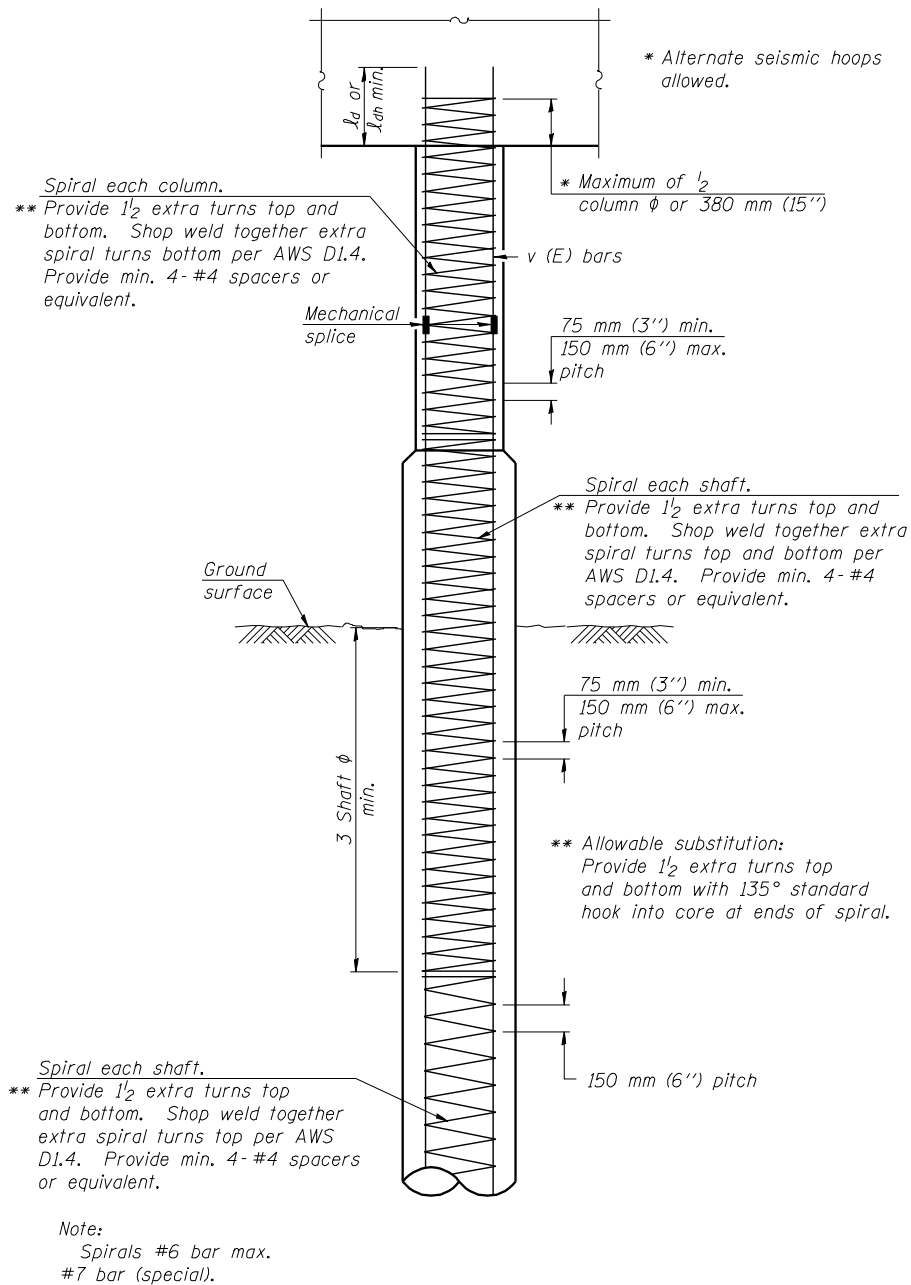


FIG. 5. SEISMIC DETAILS FOR INDIVIDUAL COLUMN DRILLED SHAFT PIERS

## **Calibration and Refinement of ERS Strategy**

### **General**

IDOT has teamed with the University of Illinois at Urbana-Champaign to obtain assistance with furthering the enhancement of Illinois' ERS strategy. There are some theoretical methods and assumptions embedded in the strategy that lack full verification as well as significant areas which can be targeted for refinement and calibration. An experimental university testing program that also includes the employment of sophisticated analytical computer models can provide each of these to IDOT. In recognition of the variability and uncertainty inherent in seismic design, Illinois' ERS strategy was initially formulated as a fairly conservative framework of relatively straightforward design and detailing methods primarily intended to economically streamline seismic bridge design efforts. The changes to the AASHTO bridge design provisions (primarily the adoption of the 1000 yr. design return period earthquake) have substantially increased the population of structures in Illinois requiring seismic analysis and design. In order to fully realize the economic benefits of Illinois' recently established ERS strategy, it is in the state's best interest to make improvements such that it will be less costly and time consuming to obtain a similar and heightened level of seismic resistance for new bridges. In the long term, it will also be much more economical for Illinois to achieve some level of uniformity in seismic resistance for its full population of bridges (new and retrofitted).

University of Illinois researchers are employing the current documentation of Illinois' ERS strategy, an oversight panel comprised of IDOT and Federal Highway Administration engineers, information from prior research on bridge behavior in Mid-America, as well as any other ongoing national and international initiatives related to seismic analysis and design to provide key background for the project. It is expected that the research effort will lead to a more rational and consistent bridge design approach that balances structural safety with design methodologies, construction practices, and construction costs appropriate for Illinois. In addition to more realistic analytical models, static and dynamic testing of bridge components and foundation elements should provide IDOT with a clearer picture of how to refine its ERS strategy. The aspects of the strategy that are probably somewhat more conservative than required should be able to be refined because the uncertainty surrounding the differences between actual behavior under seismic loading and that assumed in the current simplified design models can be better quantified.

### **Stage 1: Refinement and Calibration of Seismic Structural Redundancy Level 1**

A series of laboratory tests are in the planning stages, and computational simulations are ongoing. The tests and simulations are planned to document the force-deformation relationship, cyclic energy dissipation, and deformation capacity during loading of bearing assemblies that are commonly used in the areas of Illinois which are prone to seismic activity. These bearings are intended to constitute a seismic fuse, so they are desired to be the first primary elements to fail (i.e. are sacrificial elements) within the structural system. Horizontal shearing combined with

the effects from gravity load on side retainers and other bearing elements are under investigation. The experimental and computational results are expected to produce better quantified “fuse capacities”, as well as provide information for assessing the response of the superstructures and substructures as the fuses breach their capacities.

The computational work in this stage includes a two-tiered analysis approach for simulating the local structural response of bridge bearing fuse assemblies. The first set of analyses is using component modeling concepts to characterize the likely range of response of the bridge bearings. The formulation utilizes a combination of coarse-mesh continuum elements and beam or spring elements that allows for parametric bracketing of the likely variables which govern the response of bridge bearing assemblies and neighboring components of a bridge’s superstructure. These parametric studies are helping to highlight the details of what needs to be assessed in the experimental study. The second set are more detailed continuum type analyses of the test specimens that allow for both prediction and corroboration of the experiments, and to enable exploration of a wide range of parametric variables than can be assessed in the tests. Both types of analyses include nonlinear constitutive response of the bearing and, as needed, the bridge superstructure, geometric nonlinearity based on the anticipated deformations, and gap/contact/friction response (where appropriate).

The experiments in this research stage are planned to focus on the three bridge bearing types most commonly used in current IDOT design and construction practice:

1. Standard Illinois “Low-profile” fixed bearings
2. Standard Illinois “Type I” steel reinforced elastomeric expansion bearings
3. Standard Illinois “Type II” steel reinforced elastomeric expansion bearings with a slider surface

All bearing types are planned to be experimentally evaluated at full-scale for longitudinal, transverse and bi-directional (skew) horizontal loading conditions. Figs. 6, 7 and 8 illustrate the preliminary rig configuration for the testing of bearing fuse capacities at the University of Illinois’ Newmark Structural Engineering Laboratory. Fig. 6 presents a plan view, and Figs. 7 and 8 present elevation views.

## **Stage 2: Computational Simulation of Response of Bridge Systems**

Based on calibrations of the fuse responses determined from Stage 1, a series of parametric computational analyses are planned for a suite of typical bridge systems in order to investigate the response of the superstructure and substructure to appropriate seismic excitations. Specific issues to be addressed in these analyses include: a) Documentation of the progression of damage (sequence of fusing) in the bridge, to ensure that proper fuses typically fail first (rather than other portions of the superstructure or substructure); b) Investigation of the required seat widths to ensure adequate bridge performance; c) Documentation of anticipated peak forces that will be transmitted to the substructure, and; d) Evaluation of changes in stiffness or strength characteristics (such as period) after a seismic event. Fig. 9 illustrates a typical preliminary bridge system model. Parameters that will be varied in the global

bridge system modeling include: bearing type; superstructure type (steel girder and prestressed concrete girder); single vs. multi-span (with the strong focus being especially on continuous multi-span systems); and selected, common substructure types (including pier and wall assemblies, integral abutments, appropriate soil and embankment conditions, and related parameters). Of particular interest in these system studies is addressing concern about vertical accelerations unseating the girders on the pintles of low profile fixed bearings in construction typical to Illinois, as well as assessing appropriate seat-widths for damage due to dynamic loading.

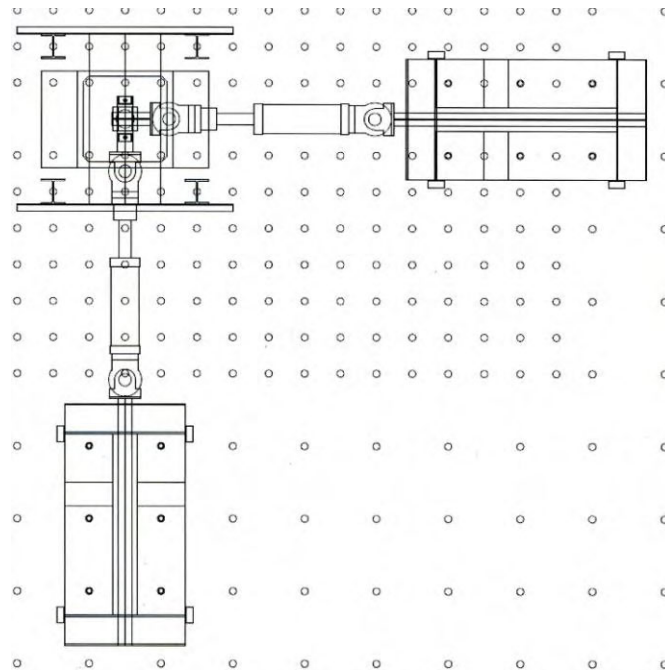


FIG. 6. PRELIMINARY PLAN VIEW OF BEARING TEST SETUP

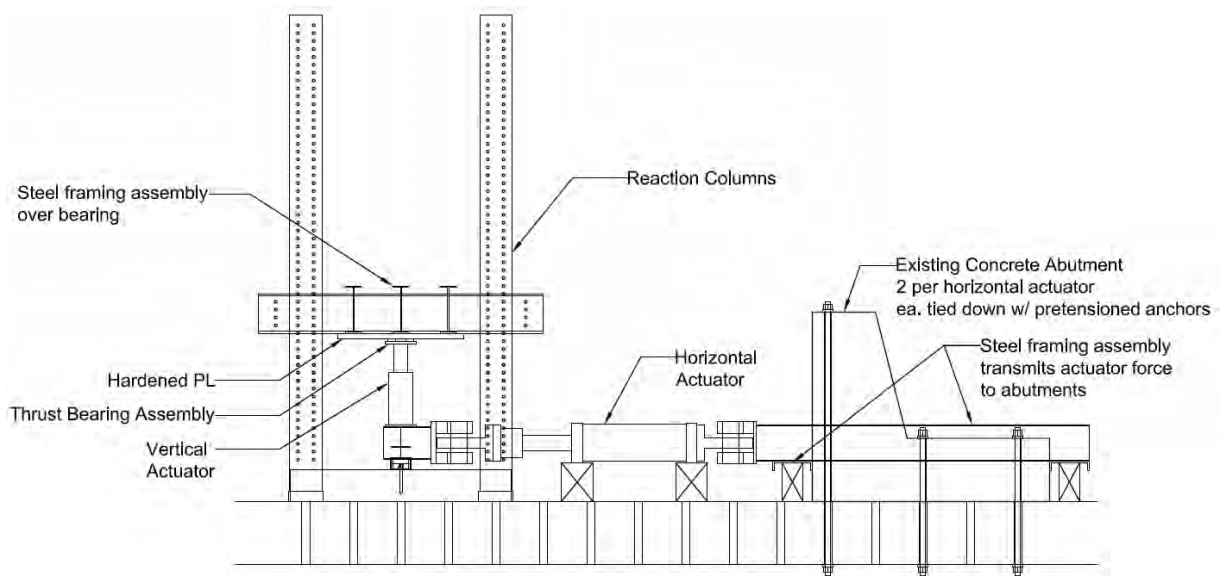


FIG. 7. PRELIMINARY ELEVATION VIEW #1 OF BEARING TEST SETUP

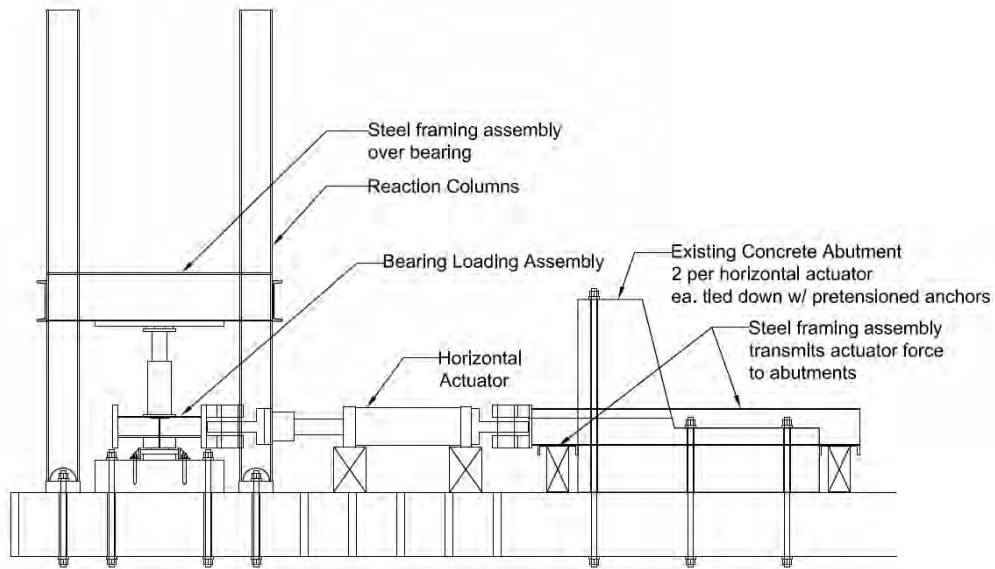


FIG. 8. PRELIMINARY ELEVATION VIEW #2 OF BEARING TEST SETUP

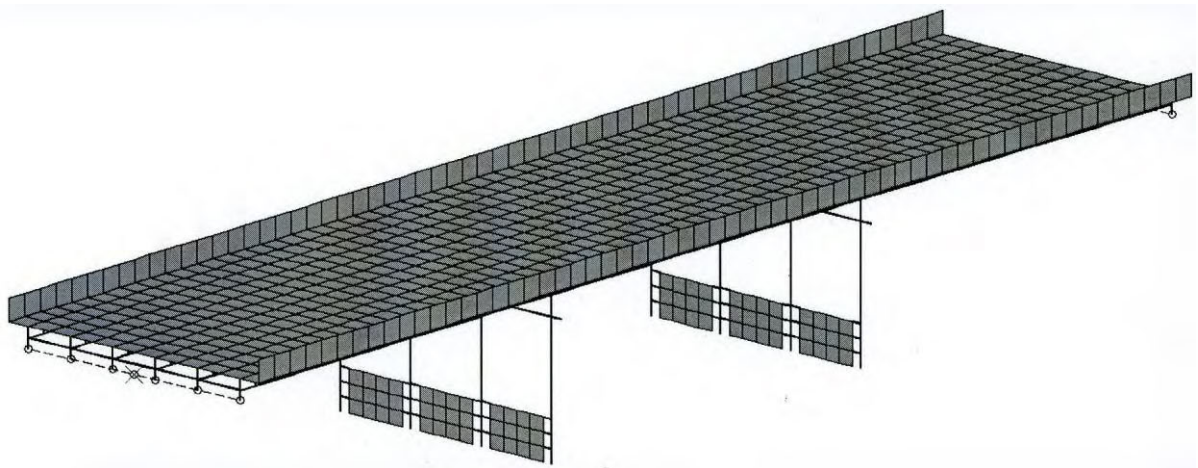


FIG. 9. PRELIMINARY TYPICAL SYSTEM ANALYSIS MODEL

The modeling strategies will typically include detailed macro-level component models of the bridge, where the girders, deck, bearings, and substructure components are modeled explicitly. Model components outside the scope of testing in this research will be calibrated in part based on existing seismic experimental studies of appropriate components available in the literature. Both equivalent static and dynamic analyses will be included in these studies. The equivalent static (pushover) will be used to assess monotonic strengths (system capacity), whereas the dynamic analyses will be used to corroborate the monotonic strengths as well as to determine estimated seismic demands. Seismic records appropriate for Mid-America have been reported in the literature and will be utilized for this study.

### **Stage 3: Refinement of Strength Reduction Factors ( $\phi$ ) and R-factors**

Plans for the final stage of the project include adequately processing the system analyses from Stage 2 in order to assess appropriate and calibrated seismic strength reduction factors ( $\phi$ ) and design values for R-factors, and to begin development of an appropriate simplified method for pushover analysis for use as part of the typical design procedure in highly seismic regions of Illinois. Simplified pushover analysis in the *LRFD Seismic Guide Specifications* is not well developed for many typical bridge systems used in Illinois.

### **Acknowledgements**

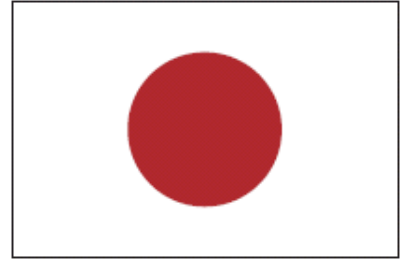
The funding for the ongoing research project described in this paper, *ICT R27-70: Calibration and Refinement of Illinois' Earthquake Resisting System Bridge Design Methodology*, provided by the Illinois Center for Transportation (ICT), is gratefully acknowledged.

The authors also acknowledge the contributions of Mr. Thomas J. Domagalski, Mr. Michael A. Mossman, Mr. Greg D. Farmer, and Ms. Rebecca M. Leach. Mr. Domagalski, Unit Chief of Design in the Bureau of Bridges and Structures at IDOT, contributed valuable advice and guidance during development of the IDOT ERS strategy. Mr. Mossman, Mr. Farmer, and Ms. Leach produced the detailed drawings in the initial part of this paper.

### **References**

- American Association of State Highway and Transportation Officials (AASHTO). (2000). *Guide specifications for seismic isolation design with interims*, Washington, D.C.
- AASHTO. (2002). *Standard specifications for highway bridges*, Washington, D.C.
- AASHTO. (2009a). *Guide specifications for LRFD seismic bridge design*, Washington, D.C.
- AASHTO. (2009b). *LRFD bridge design specifications and interim specifications*, Washington, D.C.
- Building Seismic Safety Council (BSSC). (1995). "1994 edition NEHRP recommended provisions for seismic regulations for new buildings and other structures." *Rep. Nos. FEMA-222a and FEMA-223a*, prepared by BSSC for Federal Emergency Management Agency (FEMA), Washington, D.C.
- Federal Emergency Management Agency (FEMA). (1988). "NEHRP recommended provisions for the development of seismic regulations for new buildings." *Rep. Nos. FEMA-95 Part 1: Provisions and FEMA-96 Part 2: Commentary*, FEMA, Washington, D.C.

- Federal Highway Administration (FHWA). (2006). "Seismic retrofitting manual for highway structures, Part 1 – Bridges." *Pub. No. FHWA-HRT-06-032*, FHWA, Washington, D.C.
- Hodel, C. E., Trello, M. J., and Tobias, D. H. (2004). "Seismic retrofitting in Illinois: bridge population implementation." *Proc., 4<sup>th</sup> Nat. Seismic Conf. and Workshop on Bridges and Highways*, Federal Highway Administration, Washington, D.C.
- Illinois Department of Transportation (IDOT). (2008a). *Bridge Manual*, Springfield, IL.
- IDOT. (2008b). *Seismic Design Guide*, Springfield, IL.
- International Code Council (ICC). (2000). *International Building Code*, Birmingham, AL.
- Leyendecker, E., Frankel, A., and Rukstales, K. (2007). "AASHTO guide specifications for LRFD seismic bridge design." AASHTO, Washington, D.C.
- Multidisciplinary Center for Earthquake Engineering Research (MCEER)/Applied Technology Council(ATC). (2003). "Recommended LRFD guidelines for the seismic design of highway bridges." *Special Pub. No. MCEER-03-SP03*, MCEER, Buffalo, NY.
- National Cooperative Highway Research Program (NCHRP). (2006). "Recommended LRFD guidelines for the seismic design of highway bridges." *Draft Rep. NCHRP 20-07 Task 193*, TRC Imbsen and Associates, Sacramento, CA.
- Tobias, D. H., Anderson, R. E., Hodel, C. E., Kramer, W. M., and Wahab, R. M. (2006a). "Implications of future seismic bridge design provisions for Illinois." *Proc., 5<sup>th</sup> Nat. Seismic Conf. and Workshop on Bridges and Highways*, Federal Highway Administration, Washington, D.C.
- Tobias, D. H., Anderson, R. E., Kramer, W. M., Hodel, C. E., and Wahab, R. M. (2006b). "Standardized seismic bridge design in Illinois." *Proc., ASCE Structures Congress 2006*, American Society of Civil Engineers, Reston, VA, 1-8.
- Tobias, D. H., Anderson, R. E., Hodel, C. E., Kramer, W. M., Wahab, R. M., and Chaput, R. J. (2008a). "Implementation of 2008 AASHTO Seismic Bridge Design Provisions for Illinois." *Proc., 6<sup>th</sup> Nat. Seismic Conf. and Workshop on Bridges and Highways*, Federal Highway Administration, Washington, D.C.
- Tobias, D. H., Anderson, R. E., Hodel, C. E., Kramer, W. M., Wahab, R. M., and Chaput, R. J. (2008b). "Overview of Earthquake Resisting System Design and Retrofit Strategy for Bridges in Illinois." *Pract. Per. on Structural Design and Constr.*, American Society of Civil Engineers, Reston, VA, Vol. 13, No. 3, 147-158.



**25<sup>th</sup> US-Japan  
Bridge Engineering Workshop**

**Resolution**

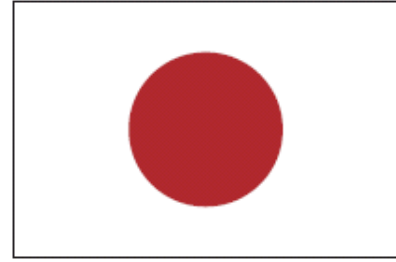
Page Left Blank

RESOLUTIONS  
OF THE TWENTY-FIFTH U.S.-JAPAN BRIDGE ENGINEERING  
WORKSHOP (Draft)  
TASK COMMITTEE G, TRANSPORTATION SYSTEM  
U.S.-JAPAN PANEL ON WIND AND SEISMIC EFFECTS (UJNR)  
Tsukuba, Japan  
19-21 October 2009

The following resolutions are hereby adopted:

1. The Twenty-fifth U.S.-Japan Bridge Engineering Workshop provided valuable exchange of technical information that was beneficial to both countries. Thirteen U.S. side participants and thirty-one Japan-side participants discussed the subjects of Seismic Engineering and Management of highway bridges. In view of the importance of cooperative programs on the subjects of bridge engineering, the continuation of the Workshop is considered essential.
2. Because of the importance and benefits of the Workshop, it is recommended to hold the Twenty-sixth U.S.-Japan Bridge Engineering Workshop in the autumn of 2010 in the United States. Dates, location, themes, program and itinerary will be proposed by the U.S.-side Task Committee G with the concurrence of the Japan-side Task Committee G.

Page Left Blank



# **25<sup>th</sup> US-Japan Bridge Engineering Workshop**

## **Appendix 1:**

### **Japan Participants**

Taro Awamoto

Taku Hanai

Jun-ichi Hoshikuma

Koichi Ikuta

Kazuhiko Kawashima

Takayoshi Kodama

Yuji Mishima

Chiaki Nagao

Takao Okada

Shinya Omote

Junichi Sakai

Masahiro Sirato

Yoshihiko Taira

Yoshiki Tanaka

Hiroshi Watanabe

Eiki Yamaguchi

Koichi Yokoyama

Atsushi Yoshioka

Tsutomu Yoshioka

Shinsuke Yumoto

Guangfeng Zhang

Page Left Blank

**Taro Awamoto**

Senior Staff Member  
Maintenance Section  
Road and Street Administration Division  
Bureau of Construction  
Tokyo Metropolitan Government  
2-8-1 Nishi-shinjuku Shinjuku-ku Tokyo, 163-8001, Japan  
Phone: +81-3-5320-5366  
Fax: +81-3-5388-1529  
E-mail: Tarou\_Awamoto@member.metro.tokyo.jp

**Taku Hanail**

Senior Researcher  
Bridge and Structural Technology Research Group  
Center for Advanced Engineering Structural Assessment and Research  
Public Works Research Institute  
1-6, Minamihara, Tsukuba, Ibaraki, 305-8516, Japan  
Phone: +81-29-879-6773  
Fax: +81-29-879-6739  
E-mail: hanai@pwri.go.jp

**Jun-ichi Hoshikuma, Dr.Eng.**

Chief Researcher  
Bridge and Structural Technology Research Group  
Center for Advanced Engineering Structural Assessment and Research  
Public Works Research Institute  
1-6, Minamihara, Tsukuba, Ibaraki, 305-8516, Japan  
Phone: +81-29-879-6793  
Fax: +81-29-879-6739  
E-mail: hosikuma@pwri.go.jp

**Koichi Ikuta**

Researcher  
Bridge and Structures Division, Road Department,  
National Institute for Land and Infrastructure Management  
Ministry of Land, Infrastructure, Transport and Tourism  
1 Asahi, Tsukuba, Ibaraki, 305-0804 Japan  
Phone: +81-29-864-4919  
Fax: +81-29-864-4917  
E-mail: ikuta-k8810@nilim.go.jp

**Kazuhiko Kawashima, Dr.Eng.**

Professor  
Department of Civil Engineering  
Tokyo Institute of Technology  
M1-10, O-Okayama, Meguro, Tokyo, 152-8552, Japan  
Phone: +81-3-5734-2922  
Fax: +81-3-5734-3810  
E-mail: kawashima.k.ae@m.titech.ac.jp

**Takayoshi Kodama**

Manager of Technology Department  
Kajima road company, Tokyo  
7-27, 1cho-me Kouraku, Bunkyo-city, Tokyo, Japan  
Phone: +81-3-5802-8014  
Fax: +81-3-5802-8045  
E-mail: kodama@kajimaroad.co.jp

**Yuji Mishima**

Manager, Infrastructure Technology Development Dept.,  
Hitachi Zosen Corporation  
7-89, Nanko-kita 1-chome, Suminoe-ku, Osaka, Japan  
Phone: +81-6-6569-0051  
Fax: +81-6-6569-0055  
E-mail: mishima\_y@hitachizosen.co.jp

**Chiaki Nagao**

Engineer  
Central Nippon Expressway Company Limited  
Planning and Design Team Nagoya Branch Central  
Nippon Expressway Company Limited;  
Mitsui-Sumitomo Bank Nagoya Building, 2-18-19, Nishiki, Naka-ku, Nagoya, 460-0003  
Phone: +81-52-222-1594  
Fax: +81-52-232-3718  
E-mail: c.nagao.aa@c-nexco.co.jp

**Takao Okada**

Researcher  
Bridge and Structural Technology Research Group  
Center for Advanced Engineering Structural Assessment and Research  
Public Works Research Institute  
1-6, Minamihara, Tsukuba, Ibaraki, 305-8516, Japan  
Phone: +81-29-879-6773  
Fax: +81-29-879-6739  
E-mail: okada@pwri.go.jp

**Shin-ya Omote**

Researcher  
Structures Research Team  
Civil Engineering Research Institute for Cold Region  
Public Works Research Institute  
Hiragishi 1-3-1-34, Toyohira-ku, Sapporo, 062-8602, Japan  
Phone: +81-11-841-1698  
Fax: +81-11-841-3502  
E-mail: omote@ceri.go.jp

**Junichi Sakai, Dr.Eng.**

Senior Researcher  
Bridge and Structural Technology Research Group  
Center for Advanced Engineering Structural Assessment and Research  
Public Works Research Institute  
1-6, Minamihara, Tsukuba, Ibaraki, 305-8516, Japan  
Phone: +81-29-879-6773  
Fax: +81-29-879-6739  
E-mail: sakai55@pwri.go.jp

**Masahiro Shirato, Dr.Eng.**

Senior Researcher  
Bridge and Structural Technology Research Group  
Center for Advanced Engineering Structural Assessment and Research  
Public Works Research Institute  
1-6, Minamihara, Tsukuba, Ibaraki, 305-8516, Japan  
Phone: +81-29-879-6773  
Fax: +81-29-879-6739  
E-mail: shirato@pwri.go.jp

**Yoshihiko Taira**

Senior Structural Engineer  
Sumitomo Mitsui Construction Co., Ltd.  
1-38-1 Chuo Nakano-ku, Tokyo, 164-0011, Japan  
Phone: +81-3-5337-2134  
Fax: +81-6-3367-4763  
E-mail: ytaira@smcon.co.jp

**Yoshiki Tanaka**

Senior Research Engineer  
Bridge and Structural Technology Research Group  
Center for Advanced Engineering Structural Assessment and Research  
Public Works Research Institute  
1-6, Minamihara, Tsukuba, Ibaraki, 305-8516, Japan  
Phone: +81-29-879-6773  
Fax: +81-29-879-6739  
E-mail: tanakay@pwri.go.jp

**Hiroshi Watanabe**

Leader of Construction Material Team  
Material and Geotechnical Engineering Research Group  
1-6, Minamihara, Tsukuba, Ibaraki, 305-8516, Japan  
Phone: +81-29-879-6760  
Fax: +81-29-879-6736  
E-mail: hwatana@pwri.go.jp

**Eiki Yamaguchi, Ph.D.**

Professor of Civil Engineering  
Dept. of Civil Engineering  
Kyushu Institute of Technology  
Kitakyushu, 804-8550, Japan  
Phone: +81-93-884-3110  
Fax: +81-93-884-3100  
E-mail: yamaguch@civil.kyutech.ac.jp

**Atsushi Yoshioka**

Director  
Bridge and Structural Technology Research Group  
Center for Advanced Engineering Structural Assessment and Research  
Public Works Research Institute  
1-6, Minamihara, Tsukuba, Ibaraki, 305-8516, Japan  
Phone: +81-29-879-6726  
Fax: +81-29-879-6739  
E-mail: yoshioka@pwri.go.jp

**Tsutomu Yoshioka**

Chief of Maintenance Engineering  
Nippon Engineering Consultants Co., Ltd  
3-23-1 Komagome Toshimaku Tokyo, Japan, 170-0003  
Phone: +81-3-5394-7604  
Fax: +81-3-5394-7606  
E-mail: yoshioka@ne-con.co.jp

**Shinsuke Yumoto**

Staff of Bridges Department  
Public Works Division, Public Works Bureau  
Osaka City Government  
WTC-building 12F, 1-14-16 Nankokita Suminoe-Ku Osaka City, 559-0034, Japan  
Phone: +81-6-6615-6818  
Fax: +81-6-6615-6583  
E-mail: s-yumoto@city.osaka.lg.jp

**Guangfeng Zhang**

Researcher

Bridge and Structural Technology Research Group

Center for Advanced Engineering Structural Assessment and Research

Public Works Research Institute

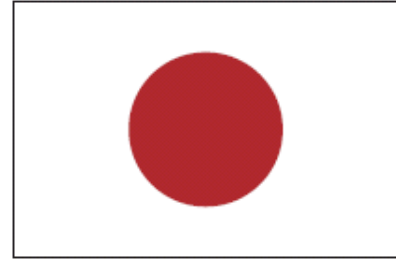
1-6, Minamihara, Tsukuba, Ibaraki, 305-8516, Japan

Phone: +81-29-879-6773

Fax: +81-29-879-6739

E-mail: [tyou44@pwri.go.jp](mailto:tyou44@pwri.go.jp)

blank



## **25<sup>th</sup> US-Japan Bridge Engineering Workshop**

### **Appendix 2:**

#### **US Participants**

Abdeldjelil "DJ" Belarbi

X. Hannah Cheng

Catherine French

Jugesh Kapur

Sashi Kunnath

Manos Maragakis

Barney T. MartinJr.

Barton Newton

M. "Saiid" Saiidi

David H. Sanders

Daniel H. Tobias

Bojidar Yanev

W. Phillip Yen

Page Left Blank

**Abdeldjelil "DJ" Belarbi**

Distinguished Professor  
Department of Civil, Architectural and Environmental Engineering  
Missouri University of Science and Technology (Missouri S&T)  
323 Butler-Carlton Hall 1401 North Pine Street Rolla, MO 65409-0030  
Phone: 573-341-4478  
Fax: 573-202-2117  
E-mail: belarbi@mst.edu

**X. Hannah Cheng**

Civil Engineer, Bureau of Structural Engineering,  
New Jersey Department of Transportation  
1035 Parkway Ave., Trenton, NJ 08625  
Phone: 609- 530-2464  
Fax: 609-530-5777  
E-mail: Xiaohua.Cheng@dot.state.nj.us

**Catherine French**

Institute of Technology Distinguished Professor Department of Civil  
Engineering University of Minnesota  
122 CivE Bldg.  
500 Pillsbury Dr. S.E.  
Minneapolis, MN 55455-0220  
Phone: 612-625-3877  
Fax: 612-626-7750  
E-mail: cfrench@umn.edu

**Jugesh Kapur**

Washington State DOT  
State Bridge & Structures Engineer  
WSDOT Bridge and Structures Office  
P O Box 47340 Olympia, WA 98504-7340  
Phone: 360-705-7207  
Fax: 360-705-6814  
E-mail: KapurJu@wsdot.wa.gov

**Sashi Kunnath**

Professor & Chair  
Department of Civil & Environmental Engineering  
University of California  
Davis CA 95616  
Phone: 530-754-6428  
Fax: 530-752-7872  
E-mail: skkunnath@ucdavis.edu

**Barney T. Martin, Jr.**

President  
Modjeski and Masters, Inc.  
301 Manchester Road, Suite 102  
Poughkeepsie, New York 12603  
Phone: 845-471-2630  
Fax: 845-471-4259  
E-mail: btmartin@modjeski.com

**Barton Newton**

State Bridge Maintenance Engineer  
California Department of Transportation (Caltrans)  
1801 30th Street, MS 9-1/9i  
Sacramento, California 95816  
Phone: 916-227-8841  
Fax: 916-227-8357  
E-mail: barton.newton@dot.ca.gov

**M. "Saiid" Saiidi**

Professor  
Civil and Environmental Engineering Department (258)  
University of Nevada  
Reno, NV 89509  
Phone: 775-784-4839  
Fax: 775-784-1390  
E-mail: Saiidi@unr.edu

**David H. Sanders**

Professor  
Department of Civil and Environmental Engineering  
University of Nevada, Reno  
1664 North Virginia Street-MS 258  
Reno, NV 89557-0258  
Phone: 775-784-4288  
Fax: 775-784-1390  
E-mail: sanders@unr.edu

**Daniel H. Tobias**

Bureau of Materials and Physical Research  
Illinois Department of Transportation  
126 East Ash Street  
Springfield, IL 62704-4766  
Phone: 217-782-2912  
Fax: 217-782-2572  
E-Mail: Daniel.Tobias@illinois.gov

**Bojidar Yanev**

Executive Director, Bridge Inspection & Management,  
Department of Transportation, New York City  
55 Water St., New York, NY10038  
Phone: 212 839 4181  
Fax:  
E-mail: byanev@dot.nyc.gov

**W. Phillip Yen**

Seismic Research Program Manager  
Office of Infrastructure, R&D  
Federal Highway Administration  
6300 Georgetown Pike  
McLean, VA 22101  
Phone: 202-493-3056  
Fax: 202-493-3442  
E-mail: Wen-huei.Yen@fhwa.dot.gov